# Draft ASME Boiler and Pressure Vessel Code Cases and Technical Bases for Use of Alloy 617 for Constructions of Nuclear Component Under Section III, Division 5

December 2021

Richard Wright

INL Idaho National Laboratory

Draft ASME Boiler and Pressure Vessel Code Cases and Technical Bases for Use of Alloy 617 for Constructions of Nuclear Component Under Section III, Division 5

Richard Wright

December 2021

**Idaho National Laboratory
Advanced Reactor Technologies
Idaho Falls, Idaho 83415**

http://www.art.inl.gov

INL ART Program

Draft ASME Boiler and Pressure Vessel Code Cases and Technical Bases for Use of Alloy 617 for Construction of Nuclear Components Under Section III, Division 5

INL/EXT-15-36305 Rev 2

December 2021

Technical Reviewer:

(signature: Ting-Leung Sham)   November 22, 2021

Ting-Leung Sham   Date
NST Directorate Fellow

Approved by:

(signature: M. Davenport)   11/22/2021

Michael E. Davenport   Date
INL ART Project Manager

(signature: Gerhard Strydom)   11/22/2021

Gerhard Strydom   Date
INL ART Co-National Technical Director

(signature: Michelle Sharp)   12/15/21

Michelle T. Sharp   Date
INL Quality Assurance

Note

This report is based on a report entitled, "Draft ASME Boiler and Pressure Vessel Code Case for Use of Alloy 617 for Construction of Nuclear Components Under Section III Division 5," INL report INL/ EXT-15-36305, Revision 1, September 2016, by J.K. Wright. The 2016 report was prepared under DOE sponsorship in support of the development of the ASME Alloy 617 Code Cases. It was issued by the INL Advanced Reactor Technologies (ART), Technology Development Office under the "Project Controlled Information" designation. The 2016 report contains the two draft Alloy 617 code cases, one for low temperature applications and the other for high temperatures. Technical bases for the two code cases were included in the report.

Approval has been obtained on November 10, 2021 from the INL ART Program to remove the "Project Controlled Information" designation from the 2016 report in preparation for public release.

In addition to the removal of the "Project Controlled Information" marking from the 2016 report, the "Draft - for committee use only" marking was also removed as it is no longer necessary. The draft Alloy 617 high temperature code case contained in the 2016 report has been replaced by an updated draft proposal in this report. Technical bases of some sections of the Alloy 617 high temperature code case were missing from the 2016 report. They are now herein included in this report.

Furthermore, editorial corrections to the 2016 report were made to the Appendix IV Data Compilation of Creep-Rupture Tests for Alloy 617 of the background of Record 16-994. These corrections include the Rupture Life (hrs) for rows 277-295, and 323-348, as well as the Creep Strain (%) for rows 323-348. These errors were due to a transcribing error when copying the values from the original data tables. The correct values were used in the original Larson-Miller Parameter calculations and plots within the Swindeman Spreadsheet, the errors corrected were editorial corrections within the Appendix IV Table that did not affect the time-dependent allowable stresses in the high temperature code case. These corrections are highlighted in yellow in the Appendix IV Table of the background of Record 16-994 in this report.

This report documents the state of the background files in 2016. Subsequent to this time, two ASME Section III, Division 5 Code Cases for Alloy 617 have been fully approved:

- Case N-872, Use of 52Ni–22Cr–13Co–9Mo Alloy 617 (UNS N06617) for Low Temperature Service Construction

- Case N-898, Use of Alloy 617 (UNS N06617) for Class A Elevated Temperature Service Construction

It is finally noted that the background files were developed for the sub-tier records and the overall records of the code cases to support the balloting workflow. Thus each has its own numbering system for figures, tables, equations, appendices, etc.

Page intentionally left blank

ABSTRACT

The American Society of Mechanical Engineers (ASME) Boiler and Pressure Vessel Code currently only allows five materials for use in construction of nuclear components for high temperature service. These are: 2.25Cr-1Mo and V-modified 9Cr-1Mo steels, Types 304 and 316 stainless steels and the high nickel Alloy 800H. Since 2005, the US high temperature gas-cooled reactor program has been characterizing elevated temperature mechanical properties of Alloy 617 as the leading candidate construction material for the intermediate heat exchanger. After analysis of these experimental results, along with historical data and additional results available through the Generation IV International Forum, Very High Temperature Reactor, Materials Program Management Board Materials Handbook, a draft ASME Code Case to allow nuclear construction with Alloy 617 for temperatures up to 1750°F (954°C) has been developed.

This report contains the Code Case for Low Temperature Service Construction of Section III, Division 5, Subsection HB, Subpart A, Class A and Subsection HC, Subpart A, Class B components, which has been approved in Section II, *Materials*, and Section III, *Rules for Construction of Nuclear Facility Components.* Supporting technical justification for the low temperature Code Case is also included. This Code Case allows use of Alloy 617 up to 800°F (425°C).

This report also contains an updated draft of a Section III, Division 5, Subsection HB, Subpart B, Class A Code Case for Alloy 617 to qualify it for use in construction of nuclear components up to 1750°F (954°C) for service life up to 100,000 hours. The draft contained in Appendix 4, subject to editorial revision and approval by the ASME Special Task Group on Alloy 617 Code Qualification, will be submitted for approval by letter ballot by the appropriate ASME Committees. The technical justification supporting the Code Case is presented in Appendix 5 of this report. This background document is part of the information package that will be submitted with the Code Case for ballot.

Page intentionally left blank

ACKNOWLEDGEMENTS

Page intentionally left blank

CONTENTS

Page intentionally left blank

ACRONYMS

ART	Advanced Reactor Technologies
ASME	American Society of Mechanical Engineers
BPV	Boiler and Pressure Vessel
INL	Idaho National Laboratory
SG-D	Subgroup Design
SG-ETD	Subgroup Elevated Temperature Design
SG-ExtPress	Subgroup External Pressure
SG-HTR	Subgroup High Temperature Reactors
SG-MF&E	Subgroup Materials, Fabrication and Evaluation
SG-PhysProp	Subgroup Physical Properties
SG-NFA	Subgroup Nonferrous Alloys
SG-StrengthWeld	Subgroup Strength of Weldments
VHTR	Very High Temperature Reactor
WG-AM	Working Group Analysis Methods
WG-ASC	Working Group Allowable Stress Criteria
WG-CFNC	Working Group Creep-Fatigue and Negligible Creep

Page intentionally left blank

Draft ASME Boiler and Pressure Vessel Code Case for Use of Alloy 617 for Construction of Nuclear Components Under Section III Division 5

Early in the US very high temperature reactor (VHTR) program several candidate nickel alloys were considered for use in construction of the intermediate heat exchanger. Based primarily on technical maturity, a downselection was made to focus on Alloy 617. After this downselection, the primary goal of the research and development program was to develop sufficient information on the high temperature properties of the material to qualify it for construction of high temperature nuclear components in the ASME Boiler and Pressure Vessel (BPV) Code.

Alloy 617 is a solid-solution strengthened material with nominal Ni-Cr-Co-Mo composition. The alloy was originally developed for aerospace applications such as burner can liners for turbine engines by Huntington Alloys. (Huntington Alloys is now Special Metals Division of Precision Castparts, Inc.). The ASME BPV Code allows use of Alloy 617 for construction of non-nuclear pressure vessels, and Alloy 617 is used in fossil fired power plants. It was the subject of substantial characterization activity in the US, German and Japanese high temperature gas reactor programs in the 1980s.

Section III, Division 1, Subsection NB of the ASME BPV Code was developed for construction of nuclear components in light water reactors and allows use of ferritic materials up to 700°F and austenitic alloys up to 800°F. Subsection NH of Section III Division 1 was written to allow higher temperature construction with a primary focus on sodium cooled reactors. Recently, a new Division 5 of Section III was published specifically for high temperature reactors (regardless of the primary working fluid) and incorporates both Subsections NB and NH.

There are only five alloys currently allowed for use in high temperature nuclear components 2.25Cr-1Mo and V-modified 9Cr-1Mo steels, Types 304 and 316 stainless steels and the high nickel austenitic Alloy 800H. This very sparse set of allowed materials is in contrast with the collection of more than 150 materials that are allowed for use in non-nuclear pressure vessel construction. A draft Code Case to add Alloy 617 to the list of qualified alloys for use in high temperature nuclear design was submitted to ASME in the early 1990s but it was withdrawn prior to formal Code action.

In general, the Code Committees will not take action on a new material without a request from a vendor stating the need to qualify the material. A letter from AREVA requesting Code action on Alloy 617 is attached to this report as Appendix 1.

A great deal of experimental characterization of high temperature mechanical properties is required for Code qualification. An appendix to Section III, Division 5 of the Code "Appendix HBB-Y Guidelines for Design Data Needs for New Materials" provides a roadmap for qualifying new materials. There are several additional requirements for qualification of materials for use in high temperature nuclear construction, compared to conventional pressure vessels. For non-nuclear pressure vessel construction, creep rupture data for 10,000 hours can be used to support qualification up to 100,000 hours of service. For high temperature nuclear construction, extrapolation of rupture life beyond the longest experimental rupture lives is restricted to a factor of 3 to 5. High temperature nuclear construction is also the only area of the Code which requires creep-fatigue characterization.

For Alloy 617, there are data from Huntington Alloys, and from the historical records and literature that resulted from previous US, German and Japanese gas cooled high temperature reactor programs. In addition, there has been a significant amount of characterization of contemporary heats of Alloy 617 since about 2005, as part of the US Advanced Reactor Technologies research and development program (formerly the Next Generation Nuclear Plant Program). Further data are also available from French and Korean programs as part of the Generation IV International Forum VHTR Materials Program Management Board.

A Code Case to qualify Alloy 617 for use in nuclear construction under Section III, Division 5, Subsection HB, Subpart A, Class A and Subsection HC, Subpart A, Class B for components designed for use up to 800°F (427°C) has been approved by Section II, *Materials*, and Section III, *Rules for Construction of Nuclear Facility Components*. Final approval is pending by the Board of Nuclear Codes and Standards. This Code Case for Low Temperature Service Construction is presented in Appendix 2 and the background document with supporting technical justification is presented in Appendix 3.

Appendix 4 contains the updated draft of a Section III, Division 5, Subsection HB, Subpart B, Code Case for Alloy 617 to qualify it for use in construction of nuclear components up to 1750°F (954°C) for service life up to 100,000 hours. This draft, subject to editorial revision and approval by the ASME Special Task Group on Alloy 617 Code Qualification, will be submitted for approval by letter ballot by the appropriate Committees.

A detailed balloting plan has been developed for the high temperature Alloy 617 Code Case. Record numbers have been established in the ASME information managements system, C&S Connect, for sections of the Code Case that are related topically, as shown in Fig. 1. These records will contain detailed background files and related data tables to enable working groups and subgroups to evaluate those sections of the Code Case that are relevant to their area of expertise. For example, Record 16-994 contains details of eight sections of the Draft Code Case that relate to allowable stresses. This record will be balloted within Section III first by the Working Group Allowable Stress Criteria (WG-ASC). After the record is approved by the working group, it will be sent (with revisions as required) to the Subgroup Elevated Temperature Design (SG-ETD). Upon passage by this subgroup, the record will next be balloted concurrently by the Subgroups High Temperature Reactors (SG-HTR), and Materials, Fabrication and Evaluation (SG-MF&E). Record 16-994 also requires approval by Section II Subgroups Nonferrous Alloys (SG-NFA) and Strength of Weldments (SG-StrengthWeld). After approval by the subgroups, the draft will be balloted by the Section II Committee (BPV II). In addition to this specific record, each of the working groups and subgroups that are balloted in both Section II and Section III will receive the entire Draft Code Case (Record 16-1001) for review and comment. After Records 16-994 through 16-1000 are approved by the lower tier committees and BPV II, the complete Draft Code Case will be balloted by the Section III Committee (BPV III).

The technical justification documents supporting the High Temperature Code Case are shown in Appendix 5 of this report. This background documentation is part of the information package that will be submitted with the Code Case for ballot, and is therefore split into individual documents, indicated by the colors in Fig. 1, to denote the areas of expertise and accommodate the ASME C&S Connect document management system. When the color is comprised of multiple item numbers (first column of Fig. 1), the document is divided into sections, each containing their own subsections such as "Scope," "Data Sources" and "References." Many of these sections (numbered items in the first column of Fig. 1) also include tabulations of data presented in appendices.

Note that the Code considers values in customary units to be the governing quantities; values in SI units are provided in some cases for convenience.

No.	Record/ Project Manager	Alloy 617 Code Case Topics (dry run presentations in TG-A617CC)	Section III, for approval (order of balloting indicated by numbers)	Section II, for approval (order of balloting indicated by numbers)	Review and Comment, accompanying each sub-record
1	RC16-994, R. Wright	Permissible base materials	1. WG-ASC 2. SG-ETD 3. (SG-HTR, SG-MF&E)	4. (SG-NFA, SG-StrengthWeld) 5. BPV II	RC-16-1001
2		Permissible weld materials			
3		Yield and ultimate (SS_{yy}, SS_{uu})			
4		Allowable stresses (SS_{O}, SS_{mm}, SS_{rr}, SS_{tt}, SS_{mmtt})			
5		Stress rupture factor			
6		Relaxation cracking			
7		Aging factor			
8		Cold work and annealing			
9	RC16-995 R. Wright	Extension of modulus values to higher temperatures	1. WG-ASC 2. SG-ETD 3. (SG-HTR, SG-MF&E)	4. (SG-PhyProp, SG-NFA) 5. BPV II	RC-16-1001
10		Thermophysical properties (CTE, diffusivity, conductivity)			
11	RC16-996 Jetter	Temperature/time limits for buckling charts	1. WG-AM 2. SG-ETD 3. (SG-HTR, SG-MF&E)	4. (SG-ExtPress, SG-NFA) 5. BPV II	RC-16-1001
12	RC16-997 Jetter	Huddleston parameters	1. WG-ASC 2. SG-ETD 3. (SG-HTR, SC-D)		RC-16-1001
13		Isochronous stress-strain curves			
14	RC16-998 Jetter	Negligible creep	1. WG-CFNC 2. SG-ETD 3. (SG-HTR, SC-D)		RC-16-1001
15		Creep-fatigue D-diagram			
16		EPP creep-fatigue damage evaluations			
17	RC16-999 Jetter	EPP strain limits evaluations	1. WG-AM 2. SG-ETD 3. (SG-HTR, SC-D)		RC-16-1001
18	RC16-1000 Jetter	Fatigue curves	1. (WG-FS, WG-CFNC) 2. SG-ETD 3. (SG-HTR, SG-MF&E, SC-D)		RC-16-1001
19	RC16-1001 Jetter	Overall Alloy 617 Code Case	1. BPV III		

Fig. 1. Balloting Plan for approval of the high temperature Alloy 617 Code Case.

Page intentionally left blank

APPENDIX 1
LETTER FROM AREVA REQUESTING CODE ACTION
ON ALLOY 617

Page intentionally left blank

LETTER FROM AREVA REQUESTING CODE ACTION ON ALLOY 617

AREVA

June 22, 2015

Mr. Joseph Brzuszkiewicz
Project Engineering Administrator
ASME
2 Park Avenue
New York, NY 10016-5990
brzuszkiewiczj@asme.org

Dear Mr. Brzuszkiewicz,

AREVA Inc. requests a Section III Division 5 Code Case for 52Ni–22Cr–13Co–9Mo Alloy 617 (UNS N06617) to allow for its use in construction of high temperature reactor systems. This alloy is currently allowed for construction under Sections I and VIII. Because of the superior creep resistance of this alloy, the proposed Code Case would extend the temperature range for nuclear components such as intermediate heat exchangers from the current 760 to 950°C. This is necessary for the development of future very high temperature reactor concepts which could provide very high temperature process heat for a variety of industrial applications. Moreover, while this capability is not essential for high temperature gas-cooled reactors being designed for the 700-800°C range, it would also provide significantly increased design flexibility for such concepts. At temperatures in the range of interest for steam cycle HTGRs, its higher creep strength compared to other austenitic materials would allow more efficient designs providing increased performance and lower cost.

A data package and associated analysis supporting the draft Code Case has been assembled through an extensive effort supported by the US Department of Energy and partners in the Generation IV International Forum. The draft Code Case and background documentation will be posted on C&S Connect, and it is expected that this item will be placed on the agenda of appropriate committees during the August 2015 Code Week.

Sincerely,

Finis Southworth

Chief Technology Officer
AREVA Inc.
3315 Old Forest Road
Lynchburg, VA 24501
Finis.Southworth@areva.com

c: Allyson Byk
         S&C Project Engineer
         Nuclear Codes and Standards
         ASME
         2 Park Avenue
         New York, NY 10016-5990
         byka@asme.org

APPENDIX 2
CASE N-XXX: USE OF ALLOY 617 (UNS N06617) FOR LOW TEMPERATURE SERVICE CONSTRUCTION SECTION III, DIVISION 5

Page intentionally left blank

Case N-XXX: Use of 52Ni–22Cr–13Co–9Mo, Alloy 617 (UNS N06617) for Low Temperature Service Construction Section III, Division 5

Inquiry: May 52Ni–22Cr–13Co–9Mo Alloy 617 (UNS N06617) in the solution annealed condition be used in the construction of components conforming to the requirements of Section III, Division 5, Subsection HB, Subpart A, Class A and Subsection HC, Subpart A, Class B?

Reply: It is the opinion of the Committee that 52Ni–22Cr–13Co–9Mo Alloy 617 (UNS N06617) conforming to the product specifications shown in Table 1 may be used in the construction of Section III, Division 5, Subsection HB, Subpart A, Class A and Subsection HC, Subpart A, Class B components provided the following requirements are met:

    (a) The maximum use temperature shall not exceed 800°F (425°C).
    (b) The design stress intensity values and yield and tensile strength values for Class A shall be as shown in Table 2.
    (c) The maximum allowable stress values and yield and tensile strength values for Class B shall be as shown in Table 3.
    (d) The moduli of elasticity shown in Section II, Part D, Table TM-4 shall apply.
    (e) The values of Poisson's ratio and density shown in Section II, Part D, Table PRD shall apply.
    (f) The coefficients of thermal expansion shown in Table 4 shall apply.
    (g) The nominal coefficients of thermal conductivity and thermal diffusivity shown in Table 5 shall apply.
    (h) All other requirements of Section III, Division 5, Subsection HB, Subpart A for Class A components, and Subsection HC, Subpart A for Class B components shall be met.
    (i) The design fatigue curve shown in Section III Appendices, Mandatory Appendix I, Figure I-9.5 and Table I-9.5 shall apply.
    (j) External pressure chart Figure NFN-4 and values in Table NFN-4 of Section II, Part D shall apply.
    (k) This Case number shall be listed on the Data Report Form for the component.

Table 1. Product Specifications

Product Form	Spec. No.
Rod, bar and wire	SB-166
Seamless pipe and tube	SB-167
Plate, sheet and strip	SB-168
Forgings	SB-564

For Metal Temperature Not Exceeding, °F	Design Stress Intensity S_m, ksi [NOTE 1]	Yield Strength S_y, ksi	Tensile Strength S_u, ksi
100	23.3	35.0	95.0
200	23.3	31.1	95.0
300	23.3	28.9	95.0
400	23.3	27.1	95.0
500	23.3	25.9	95.0
600	22.5	25.0	93.2
650	22.1	24.6	92.3
700	21.9	24.3	91.4
750	21.7	24.1	90.6
800	21.5	23.8	89.9

[NOTE 1]   Due to the relatively low yield strength of this material, the higher stress values were established at temperatures where the short-time tensile properties govern to permit the use of these alloys where slightly greater deformation is acceptable. The stress values in this range exceed 66⅔% but do not exceed 90% of the yield strength at temperature. Use of these stresses may result in dimensional changes due to permanent strain. These stress values are not recommended for the flanges of gasketed joints or other applications where slight amounts of distortion can cause leakage or malfunction. For Section III applications, Table Y-2 lists multiplying factors that, when applied to the yield strength values shown in Table 2 above, will give allowable stress values that will result in lower levels of permanent strain.

For Metal Temperature Not Exceeding, °C	Design Stress Intensity S_m, MPa [NOTE 1]	Yield Strength S_y, MPa	Tensile Strength S_u, MPa
40	161	241	655
65	161	227	655
100	161	212	655
125	161	205	655
150	161	199	655
175	161	193	655
200	161	188	655
225	161	183	655
250	161	180	655
275	160	177	651
300	157	174	647
325	154	171	640
350	152	169	635
375	151	167	629
400	150	166	624
425	148	164	620

[NOTE 1]   Due to the relatively low yield strength of this material, the higher stress values were established at temperatures where the short-time tensile properties govern to permit the use of these alloys where slightly greater deformation is acceptable. The stress values in this range exceed 66⅔% but do not exceed 90% of the yield strength at temperature. Use of these stresses may result in dimensional changes due to permanent strain. These stress values are not recommended for the flanges of gasketed joints or other applications where slight amounts of distortion can cause leakage or malfunction. For Section III applications, Table Y-2 lists multiplying factors that, when applied to the yield strength values shown in Table 2M above, will give allowable stress values that will result in lower levels of permanent strain.

For Metal Temperature Not Exceeding, °F	Maximum Allowable Stress S, ksi [NOTE 1]		Yield Strength S_y, ksi	Tensile Strength S_u, ksi
100	23.3	23.3	35.0	95.0
200	20.8	23.3	31.1	95.0
300	19.2	23.3	28.9	95.0
400	18.1	23.3	27.1	95.0
500	17.2	23.3	25.9	95.0
600	16.6	22.5	25.0	93.2
650	16.4	22.1	24.6	92.3
700	16.2	21.9	24.3	91.4
750	16.0	21.7	24.1	90.6
800	15.9	21.5	23.8	89.9

[NOTE 1]   Due to the relatively low yield strength of this material, the higher stress values were established at temperatures where the short-time tensile properties govern to permit the use of these alloys where slightly greater deformation is acceptable. The stress values in this range exceed 66⅔% but do not exceed 90% of the yield strength at temperature. Use of these stresses may result in dimensional changes due to permanent strain. These stress values are not recommended for the flanges of gasketed joints or other applications where slight amounts of distortion can cause leakage or malfunction. For Section III applications, Table Y-2 lists multiplying factors that, when applied to the yield strength values shown in Table 3 above, will give allowable stress values that will result in lower levels of permanent strain.

For Metal Temperature Not Exceeding, °C	Maximum Allowable Stress S, MPa [NOTE 1]		Yield Strength S_y, MPa	Tensile Strength S_u, MPa
40	161	161	241	655
65	152	161	227	655
100	142	161	212	655
125	136	161	205	655
150	132	161	199	655
175	129	161	193	655
200	125	161	188	655
225	122	161	183	655
250	120	161	180	655
275	117	160	177	651
300	115	157	174	647
325	114	154	171	640
350	113	152	169	635
375	111	151	167	629
400	110	150	166	624
425	110	148	164	620

[NOTE 1]   Due to the relatively low yield strength of this material, the higher stress values were established at temperatures where the short-time tensile properties govern to permit the use of these alloys where slightly greater deformation is acceptable. The stress values in this range exceed 66⅔% but do not exceed 90% of the yield strength at temperature. Use of these stresses may result in dimensional changes due to permanent strain. These stress values are not recommended for the flanges of gasketed joints or other applications where slight amounts of distortion can cause leakage or malfunction. For Section III applications, Table Y-2 lists multiplying factors that, when applied to the yield strength values shown in Table 3M above, will give allowable stress values that will result in lower levels of permanent strain.

	Coefficients for N06617		
Temperature, °F	A	B	C
70	7.0	7.0	0
100	7.1	7.0	0.3
150	7.1	7.1	0.7
200	7.2	7.1	1.1
250	7.3	7.1	1.6
300	7.4	7.2	2.0
350	7.5	7.2	2.4
400	7.6	7.3	2.9
450	7.7	7.3	3.4
500	7.8	7.4	3.8
550	7.9	7.4	4.3
600	8.0	7.5	4.8
650	8.2	7.5	5.3
700	8.3	7.6	5.8
750	8.4	7.6	6.3
800	8.6	7.7	6.8

GENERAL NOTE: Coefficient A is the instantaneous coefficient of thermal expansion $\times 10^{-6}$ (in./in./°F). Coefficient B is the mean coefficient of thermal expansion $\times 10^{-6}$ (in./in./°F) in going from 70°F to indicated temperature. Coefficient C is the linear thermal expansion (in./100 ft) in going from 70°F to indicated temperature.

Table 4M. Thermal Expansion for Alloy 617

	Coefficients for N06617		
Temperature, °C	A	B	C
20	12.6	12.6	0
50	12.8	12.7	0.4
75	12.9	12.7	0.7
100	13.0	12.8	1.0
125	13.2	12.9	1.4
150	13.3	12.9	1.7
175	13.5	13.0	2.0
200	13.6	13.1	2.4
225	13.8	13.2	2.7
250	14.0	13.2	3.0
275	14.2	13.3	3.4
300	14.4	13.4	3.8
325	14.6	13.5	4.1
350	14.8	13.6	4.5
375	15.0	13.7	4.9
400	15.2	13.8	5.2
425	15.4	13.9	5.6

GENERAL NOTE: Coefficient A is the instantaneous coefficient of thermal expansion $\times 10^{-6}$ (mm/mm/°C). Coefficient B is the mean coefficient of thermal expansion $\times 10^{-6}$ (mm/mm/°C) in going from 20°C to indicated temperature. Coefficient C is the linear thermal expansion (mm/m) in going from 20°C to indicated temperature.

Table 5. Nominal Coefficients of Thermal Conductivity and Thermal Diffusivity for Alloy 617

Temperature °F	Thermal Conductivity Btu/hr-ft-°F	Thermal Diffusivity ft²/hr
70	6.0	0.112
100	6.2	0.114
150	6.6	0.118
200	6.9	0.122
250	7.2	0.125
300	7.5	0.129
350	7.8	0.132
400	8.1	0.136
450	8.4	0.139
500	8.7	0.142
550	9.0	0.145
600	9.3	0.149
650	9.5	0.152
700	9.8	0.155
750	10.0	0.158
800	10.3	0.161

Table 5M. Nominal Coefficients of Thermal Conductivity and Thermal Diffusivity for Alloy 617

Temperature °C	Thermal Conductivity W/(m·°C)	Thermal Diffusivity × 10⁻⁶ m²/sec
20	10.3	2.88
50	11.0	2.99
75	11.6	3.08
100	12.1	3.17
125	12.6	3.25
150	13.1	3.33
175	13.6	3.41
200	14.0	3.49
225	14.5	3.57
250	14.9	3.64
275	15.3	3.71
300	15.8	3.79
325	16.2	3.86
350	16.6	3.93
375	17.0	4.01
400	17.4	4.08
425	17.8	4.15

Page intentionally left blank

APPENDIX 3

BACKGROUND FOR DRAFT CODE CASE: USE OF ALLOY 617 (UNS N06617) FOR LOW TEMPERATURE SERVICE CONSTRUCTION

Page intentionally left blank

Introduction

The Task Group on Alloy 617 Qualification is requesting a Section III Division 5 Code Case for Alloy 617 (UNS N06617) 52Ni-22Cr-13Co-9Mo to allow construction of Section III, Division 5, Subsection HB, Subpart A, Class A and Subsection HC, Subpart A, Class B components. These subsections of Division 5 limit the temperature of components to 800°F.

Allowable stress and design stress intensity values are calculated from existing Section IID Tables Y-1 and U as described in the section below.

Thermal expansion, thermal diffusivity, and thermal conductivity are not currently contained in Section II for Alloy 617. Values for these properties have recently been determined and are detailed in this technical justification.

Alloy 617 Stress Values

The technical basis and a graphical representation of the proposed values for yield strength, S_y, tensile strength, S_u, allowable stress, S, and the design stress intensity, S_m, as a function of temperature are presented here. Alloy 617 is allowed for use in Section I and Section VIII Division 1 design; as a result, values for S_y, S_u and S are tabulated in Section II Part D. Design stress intensity values are presented here based on criteria evaluated below.

Yield and Tensile Strength

Alloy 617 yield and tensile strengths are tabulated as a function of temperature in Section IID Tables Y-1 and U, respectively. Yield and tensile strength are listed for the alloy in the annealed condition for several product forms. The strength at a given temperature is the same for all of the product forms. The proposed yield and tensile strength values for this code case are taken from Tables Y-1 and U and are shown in Figure 1and Figure 2, respectively.
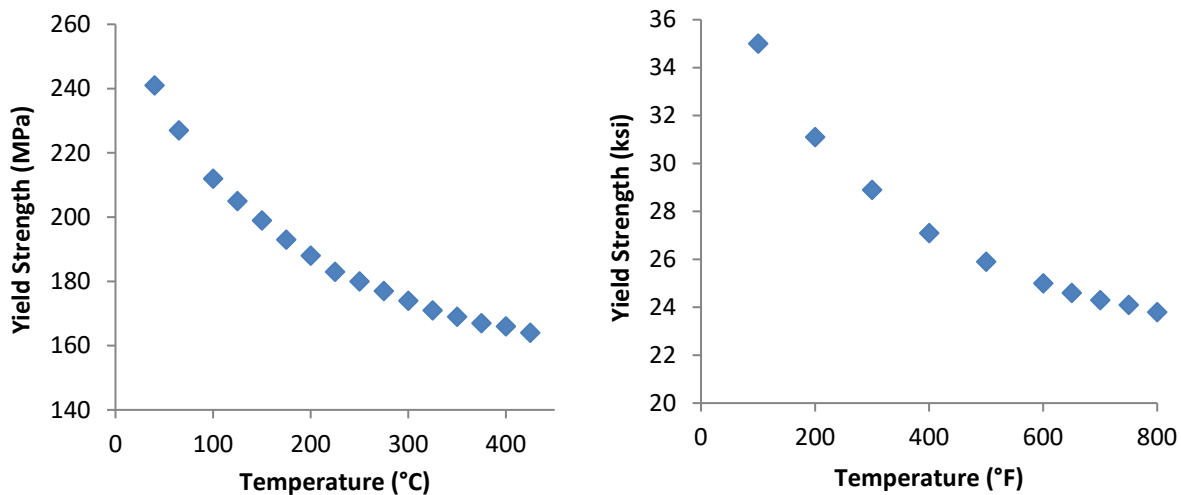
Figure 1. Alloy 617 yield strength values from Section II Part D Table Y-1 for a) SI and b) conventional units.
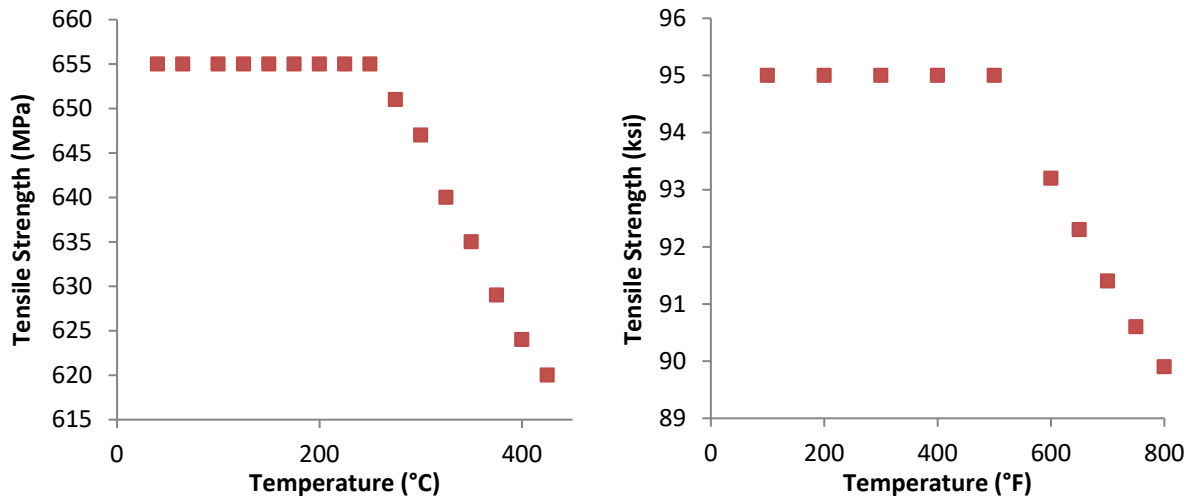
Figure 2. Alloy 617 tensile strength values from Section II Part D Table Y-1 for a) SI and b) conventional units.

Maximum Allowable Stress

The proposed maximum allowable stress values for this code case are taken from Section IID Table 1B. The allowable stress, S, is determined as the minimum of the values calculated using the criteria listed in Table 1-100 of Mandatory Appendix 1 of Section IID, reproduced here as Table 1. The note to Table 1-100 points out that for austenitic steels and some nickel alloys two sets of allowable stress values may be listed. The lower values are controlled by the $^2/_3 S_Y$ criteria, while if a small amount of deformation can be tolerated in the part, 0.9 S_Y can be used resulting in higher allowable stress. Alloy 617 is one of the nickel alloys with two sets of allowable stress in Table 1B, as shown in Figure 3. The higher values meet the 0.9 S_y criteria and is denoted by the footnote G5:

> Due to the relatively low yield strength of these materials, these higher stress values were established at temperatures where the short–time tensile properties govern to permit the use of these alloys where slightly greater deformation is acceptable. The stress values in this range exceed 66 $^2/_3$% but do not exceed 90% of the yield strength at temperature. Use of these stresses may result in dimensional changes due to permanent strain. These stress values are not recommended for the flanges of gasketed joints or other applications where slight amounts of distortion can cause leakage or malfunction. For Section III applications, Table Y–2 lists multiplying factors that, when applied to the yield strength values shown in Table Y–1, will give allowable stress values that will result in lower levels of permanent strain.

Table 1. Copy of Table 1-100 from ASME B&PV Code, Section IID and definitions of values.

<table>
<tr><td colspan="9" align="center">Table 1-100
Criteria for Establishing Allowable Stress Values for Tables 1A and 1B</td></tr>
<tr>
<td rowspan="3">Product/Material</td>
<td colspan="2" align="center">Room Temperature and Below</td>
<td colspan="6" align="center">Above Room Temperature</td>
</tr>
<tr>
<td rowspan="2" align="center">Tensile Strength</td>
<td rowspan="2" align="center">Yield Strength</td>
<td colspan="2" align="center">Tensile Strength</td>
<td align="center">Yield Strength</td>
<td align="center">Yield Strength</td>
<td colspan="2" align="center">Stress Rupture</td>
<td align="center">Creep Rate</td>
</tr>
<tr><td></td><td></td><td></td><td></td><td></td><td></td><td></td></tr>
<tr>
<td>Wrought or cast ferrous and nonferrous</td>
<td align="center">$\dfrac{S_T}{3.5}$</td>
<td align="center">$\tfrac{2}{3}\,S_Y$</td>
<td align="center">$\dfrac{S_T}{3.5}$</td>
<td align="center">$\dfrac{1.1}{3.5}\,S_T R_T$</td>
<td align="center">$\tfrac{2}{3}\,S_Y$</td>
<td align="center">$\tfrac{2}{3}\,S_Y R_Y$ or $0.9\,S_Y R_Y$ [Note (1)]</td>
<td align="center">$F_{avg}S_{R\ avg}$</td>
<td align="center">$0.8 S_{R\ min}$</td>
<td align="center">$1.0 S_c$</td>
</tr>
<tr>
<td>Welded pipe or tube, ferrous and nonferrous</td>
<td align="center">$\dfrac{0.85}{3.5}\,S_T$</td>
<td align="center">$\tfrac{2}{3}\times 0.85 S_Y$</td>
<td align="center">$\dfrac{0.85}{3.5}\,S_T$</td>
<td align="center">$\dfrac{(1.1\ \times\ 0.85)}{3.5}\,S_T R_T$</td>
<td align="center">$\tfrac{2}{3}\times 0.85 S_Y$</td>
<td align="center">$\tfrac{2}{3}\times 0.85 S_Y R_Y$ or $0.9\times 0.85 S_Y R_Y$ [Note (1)]</td>
<td align="center">$(F_{avg}\times 0.85)S_{R\ avg}$</td>
<td align="center">$(0.8\times 0.85)S_{R\ min}$</td>
<td align="center">$0.85 S_c$</td>
</tr>
</table>

NOTE:
(1) Two sets of allowable stress values may be provided in Table 1A for austenitic materials and in Table 1B for specific nonferrous alloys. The lower values are not specifically identified by a footnote. These lower values do not exceed two-thirds of the minimum yield strength at temperature. The higher alternative allowable stresses are identified by a footnote. These higher stresses may exceed two-thirds but do not exceed 90% of the minimum yield strength at temperature. The higher values should be used only where slightly higher deformation is not in itself objectionable. These higher stresses are not recommended for the design of flanges or for other strain sensitive applications.

S_T	Specified Minimum Tensile Strength at Room Temperature
S_Y	Specified Minimum Yield Strength at Room Temperature
R_T	Ratio of average temperature dependent trend curve to tensile strength to RT tensile strength
R_Y	Ratio of average temperature dependent trend curve to yield strength to RT yield strength
S_C	Average stress to produce a creep rate of 0.01%/1000 h
$S_{R\ avg}$	Average stress to cause rupture at the end of 100,000 h
$S_{R\ min}$	Minimum stress to cause rupture at the end of 100,000 h
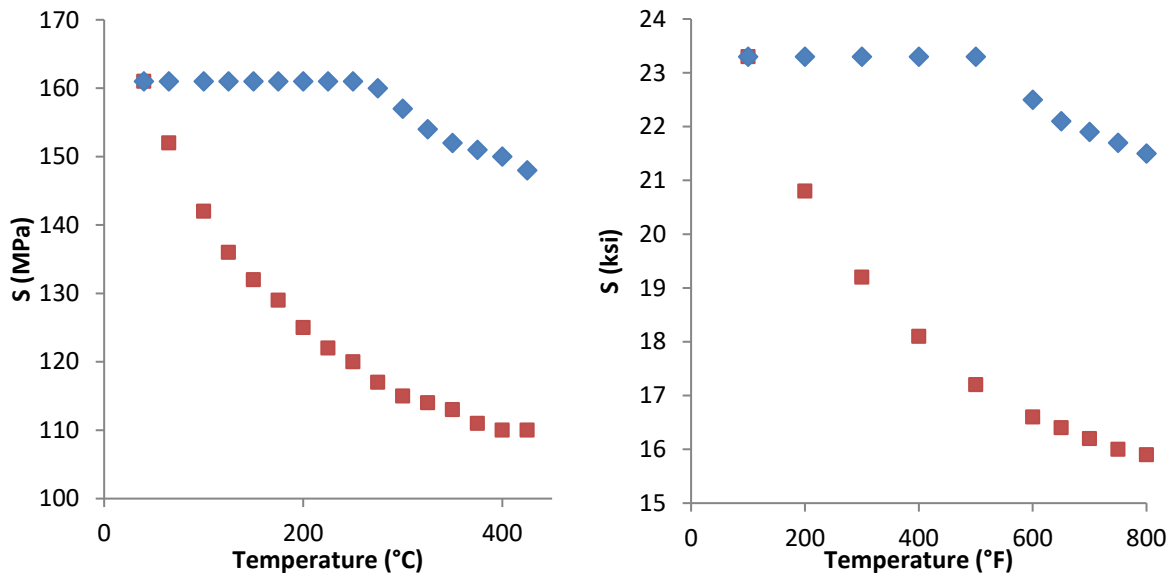
Figure 3. Alloy 617 maximum allowable stress values from Section II Part D Table Y-1 for a) SI and b) conventional units.

Design Stress Intensity

Design stress intensity values, S_m, are shown in Table 2B of Section IID of the Code for nonferrous alloys allowed for Section III design. Since Alloy 617 is not currently allowed for Section III use, S_m is not shown in Table 2B for this alloy and values must be determined. The process is very similar to that used to

determine S. The criteria to be evaluated to determine S_m are given in Table 2-100(a) of Mandatory Appendix 2 of Section IID (shown here in Table 2). As specified in Note (1) to Table 2-100(a), a yield strength multiplication factor of either $^2/_3$ or 0.9 must be selected for austenitic and nickel alloys when determining the yield strength criteria above room temperature. Examination of tabulated S_m values in Table 2A and B of the Code revealed that 0.9 was used for nickel alloys 600, 690 and 800 as well as Types 304 and 316 stainless steels. The factor of $^2/_3$ was used for Alloy 625 apparently because of its higher strength. The Board of Pressure Technology Codes and Standards recently approved Record 13-2008, which changed wording in Section II part D Appendices 1, 2 and 10 to specify that the high stress rules apply to austenitic stainless steel, nickel alloys and cobalt alloys whose yield to tensile strength ratio is less than 0.625. For Alloy 617 this ratio is less than 0.5 in the temperature range covered by Division 5.

Table 2. Copy of Table 2-100(a) from ASME B&PV Code, Section IID.

Table 2-100(a)
Criteria for Establishing Design Stress Intensity Values for Tables 2A and 2B

Product/Material	Room Temperature and Below		Above Room Temperature			
	Tensile Strength	Yield Strength	Tensile Strength		Yield Strength	
Wrought or cast, ferrous and nonferrous	$\dfrac{S_T}{3}$	$^2/_3 S_Y$	$\dfrac{S_T}{3}$	$\dfrac{1.1}{3} S_T R_T$	$^2/_3 S_Y$	$^2/_3 S_Y R_Y$ or $0.9 S_Y R_Y$ [Note (1)]
Welded pipe or tube, ferrous and nonferrous	$\dfrac{0.85}{3} S_T$	$^2/_3 \times 0.85 S_Y$	$\dfrac{0.85}{3} S_T$	$\dfrac{1.1 \times 0.85}{3} S_T R_T$	$^2/_3 \times 0.85 S_Y$	$^2/_3 \times 0.85 S_Y R_Y$ or $0.9 \times 0.85 S_Y R_Y$ [Note (1)]

NOTE:
(1) For austenitic materials in Table 2A and for specific nonferrous alloys in Table 2B, the design stress intensity values may exceed two-thirds and may be as high as 90% of the yield strength at temperature.

Numerical evaluation of the criteria for establishing the design stress intensity for Alloy 617 is presented in Table 3 for conventional units. S_m is the minimum value at each temperature (shaded in blue in Table 3). The S_m values based on the $0.9S_y$ criteria have been used, as discussed above. S_m values determined using this evaluation are tabulated in the draft Code Case. These values are plotted in Figure 4. To obtain S_m in SI units, the S_m values are interpolated from Table 3 for Celsius temperatures of interest and converted to SI units.

Table 3. Values used as criteria for establishing design stress intensity, S_m, for Alloy 617 in ksi.

T, °F	S_u	S_y	$S_T=35$ $R_T = S_u/S_T$	$S_Y=95$ $R_Y = S_y/S_Y$	Tensile Strength $S_T/3$	Yield Strength $2S_Y/3$	Tensile Strength $S_T/3$	Tensile Strength $1.1/3$ $S_T R_T$	Yield Strength $2/3$ S_Y	Yield Strength $2/3$ S_YR_Y	Yield Strength 0.9 S_YR_Y
70	95	35	1.00	1.00	31.7	23.3					
100	95	35	1.00	1.00			31.7	34.8	23.3	23.3	31.5
200	95	31.1	1.00	0.89			31.7	34.8	23.3	20.7	28.0
300	95	28.9	1.00	0.83			31.7	34.8	23.3	19.3	26.0
400	95	27.1	1.00	0.77			31.7	34.8	23.3	18.1	24.4
500	95	25.9	1.00	0.74			31.7	34.8	23.3	17.3	23.3
600	93.2	25.0	0.98	0.71			31.7	34.2	23.3	16.7	22.5
650	92.3	24.6	0.97	0.70			31.7	33.8	23.3	16.4	22.1
700	91.4	24.3	0.96	0.69			31.7	33.5	23.3	16.2	21.9
750	90.6	24.1	0.95	0.69			31.7	33.2	23.3	16.1	21.7
800	89.9	23.8	0.95	0.68			31.7	33.0	23.3	15.9	21.4
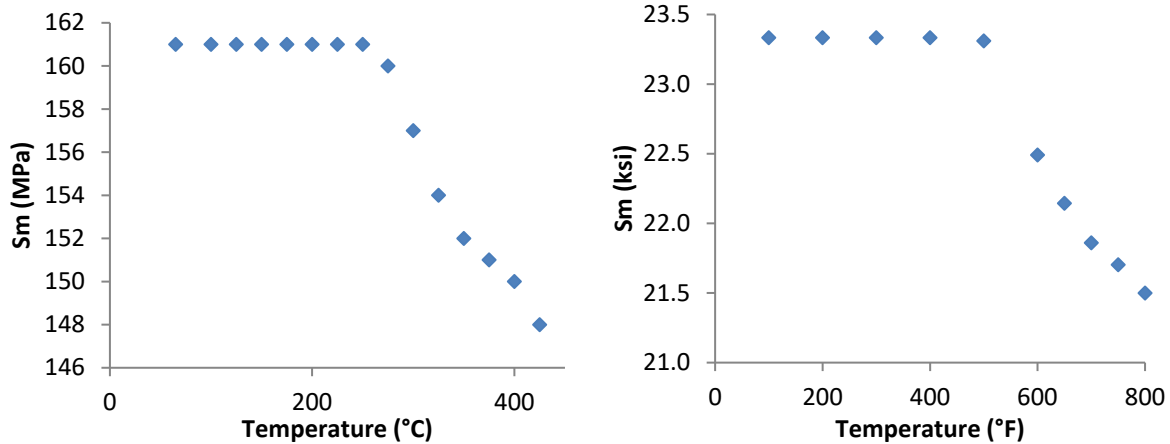
Figure 4. Alloy 617 design stress intensity values for a) SI and b) conventional units.

Alloy 617 Thermal Properties

Proposed values for Coefficient of Thermal Expansion (CTE), thermal diffusivity and thermal conductivity for Alloy 617 based on new experimental measurements of four heats of material are discussed in this section. A complete tabulation of proposed values is given in an appendix for temperatures up to 1800°F and 1000°C; only the values up to 800°F are included in the Division 5 draft Code Case. Where possible we have shown comparison between the proposed values from the current work and literature values for Alloy 617, or Section II D values for comparable nickel based solid solution alloys. All of the measurements reported here were made under a NQA-1 quality program. A discussion of the physical properties of Alloy 617 has also been published in the peer reviewed literature in the paper "Thermophysical Properties of Alloy 617 from 25 to 1000°C", B. H. Rabin, W. D. Swank and R. N. Wright, *Nuclear Engineering and Design Journal,* vol. 262, p. 72, 2013.

Experimental measurements were made using SI units. The method used to convert each of the proposed physical properties from SI to conventional units will be discussed in the sections below. Graphical representation of the physical properties will generally be shown first in SI units and then in conventional units.

Thermal Expansion

Thermal expansion of four heats of Alloy 617 was measured using a Netzsch dilatometer over the temperature range 20 to 1000°C. Measured $\Delta l/l_0$ values are shown in Figure 4. It can be seen in the figure that the values are very similar for the four materials (three Alloy 617 plates and one sample from a GTAW weld made with Alloy 617 wire) and the data are well represented by a third order polynomial fit. The polynomial expression for $\Delta l/l_0$ in SI units was used to calculate the corresponding $\Delta l/l_0$ values in conventional units.

The equations for thermal expansion in SI and conventional units are:

$$\frac{\Delta l}{l_0} = 1.93151E - 09T^3 + 2.20191E - 06\,T^2 + 0.012521582T + -0.251327866 \text{ mm/m}$$

and

$$\frac{\Delta l}{l_0} = 3.97430782830011E - 10\,T^3 + 7.77368917626926E - 07\,T^2 + 0.0082967491323776\,T + -0.567898459832691 \quad \text{in./(100 ft)}.$$
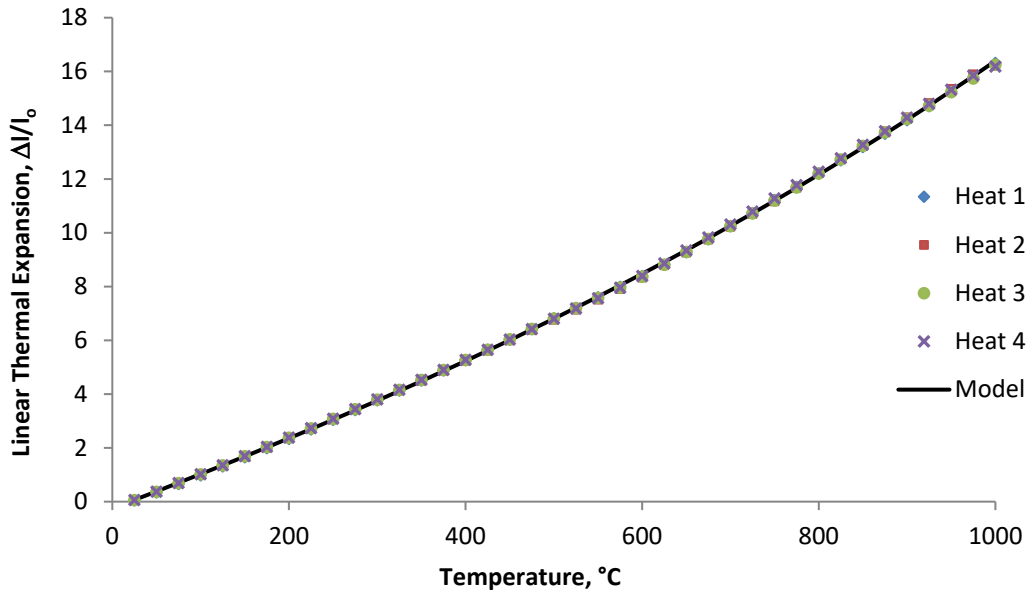
Figure 5. Change in length/initial length (mm/m) for four heats of Alloy 617 measured in current work. Third order polynomial fit is shown.

We have been unable to find comparable data in the literature for Alloy 617 for comparison. There are values currently in Section II Part D Table TE-4 for similar nickel based solid solution alloys. In Figure 6 the $\Delta l/l_0$ values determined in the current work (in conventional units) are compared to values from Table

TE-4 for Haynes 230 and Hastelloy X. It can be seen that the values are very comparable. Figure 7 shows the equivalent figure in conventional units.
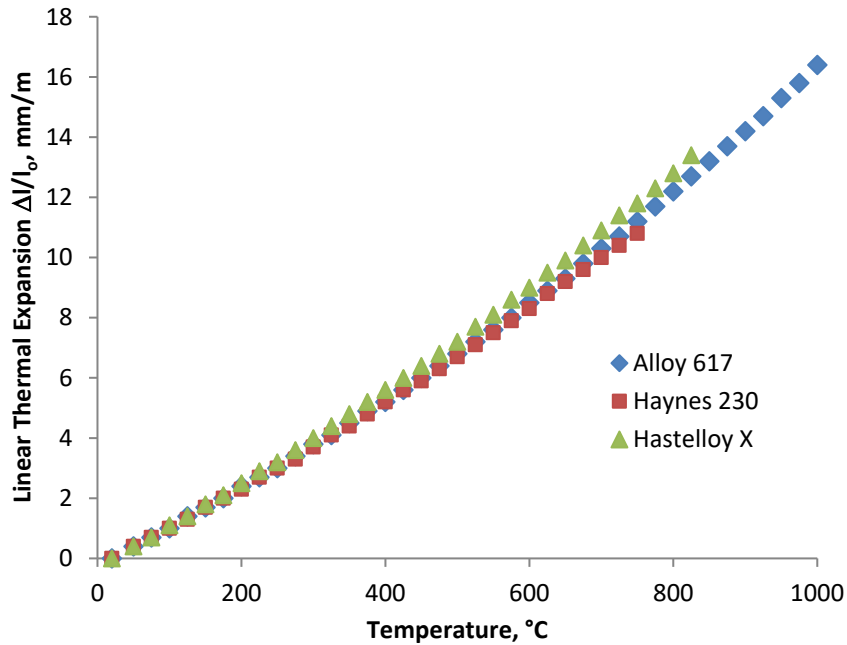
Figure 6. Alloy 617 $\Delta l/l_0$ behavior in SI units (mm/m) calculated from the polynomial fit to experimental data compared to Code values for similar solid solution Ni based alloys.
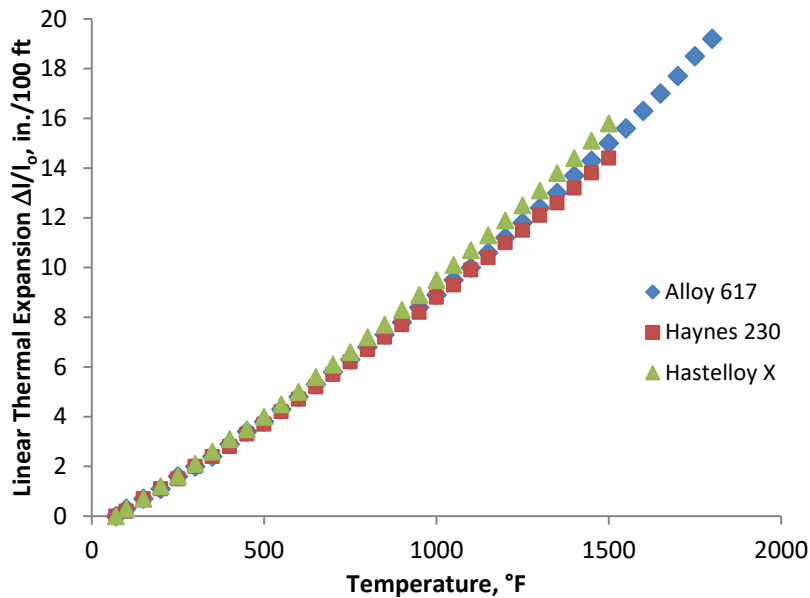
Figure 7. Alloy 617 $\Delta l/l_0$ behavior in conventional units (inches in 100 feet) calculated from the polynomial fit to experimental data compared to Code values for similar solid solution Ni based alloys.

Mean CTE values from 20°C (70°F) were calculated from the $\Delta l/l_0$ polynomial fit. There are comparable values in vendor data sheets that appear to have been determined by Huntington Alloys (now Special Metals) during development of the alloy. There also exists a draft ASME Alloy 617 Code Case submitted

in 1992 (and withdrawn before final approval) that has mean CTE values, although the origin of the data in the draft Code Case is not clear. A comparison of values from the current work and historical values is shown in Figure 8. For this comparison only values for conventional units are shown, since it is believed that the original experiments were carried out using conventional units and the method for subsequent conversion to SI units is not specified.
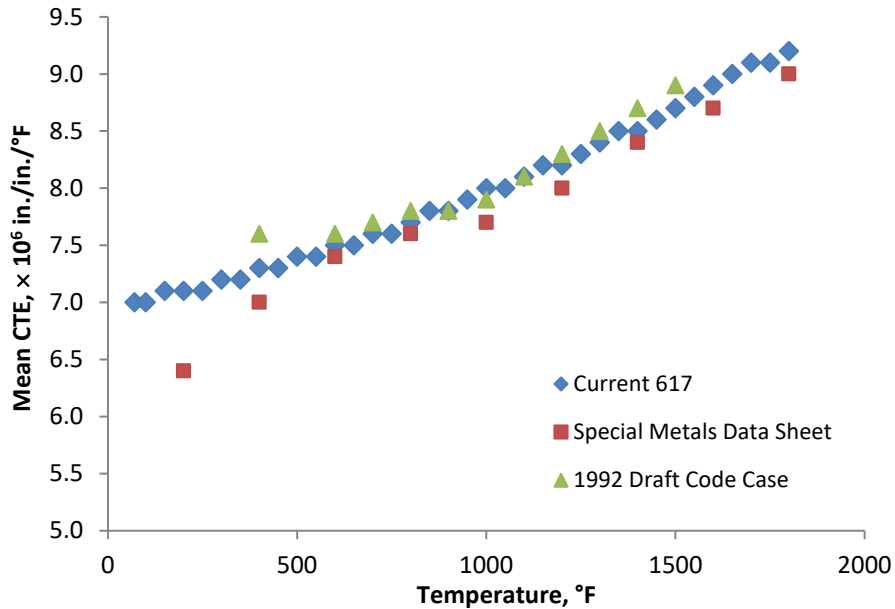
Figure 8. Mean CTE (linear expansion from 70°F to temperature of interest) for current experiments compared to values from vendor data sheet and from 1992 draft Alloy 617 code Case.

A comparison to Section II D Table TE-4 values for the nickel based solid solutions Haynes 230 and Hastelloy X is shown in Figure 9 and Figure 10. There is reasonable agreement between these alloys and Alloy 617.
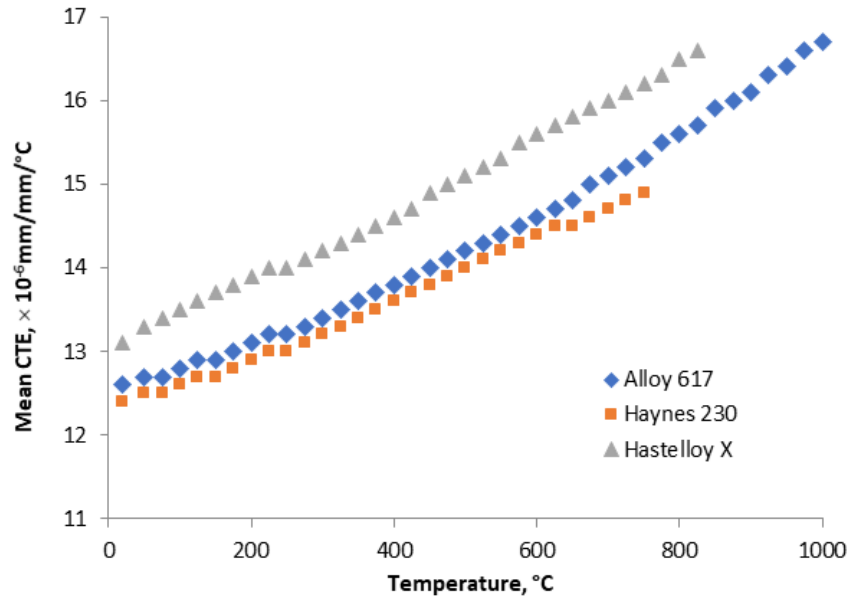
Figure 9. Mean CTE (linear expansion from 20°C to temperature of interest) for current experiments compared to Code values for two similar solid solution Ni based alloys from Section II D Table TE-4.
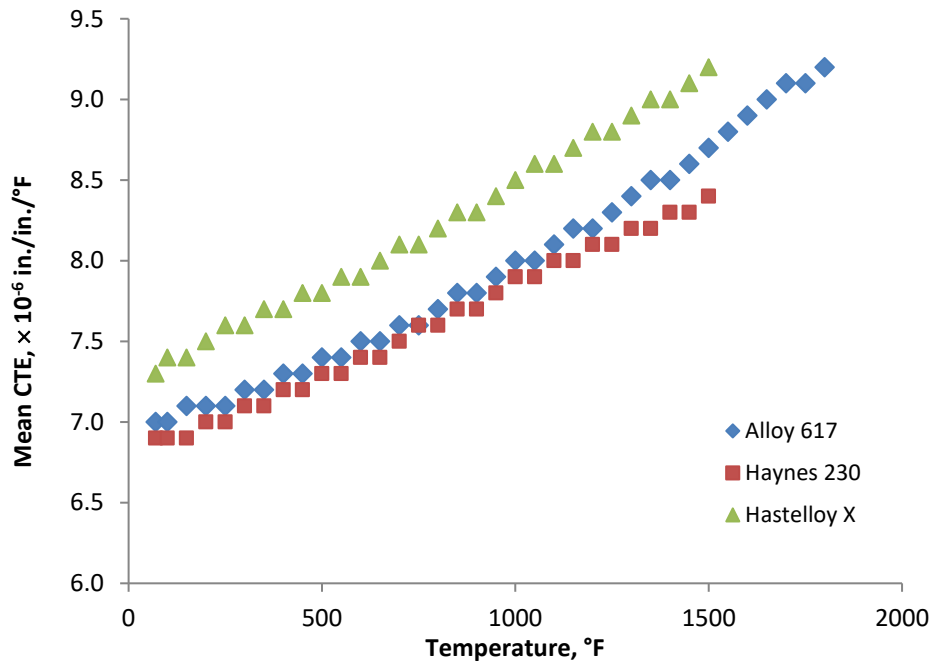
Figure 10. Mean CTE (linear expansion from 70°F to temperature of interest) for current experiments compared to Code values for two similar solid solution Ni based alloys from Section II D Table TE-4.

The instantaneous CTE was calculated using the derivative of the polynomial fit to the $\Delta l/l_0$ data from 20 to 1000°C (70 to 1800°F). Independent measurements for this alloy have not been found in the literature. Figure 11 and Figure 12 show Instantaneous CTE for current experiments using the fit to data shown in Figure 5 compared to Section II D Table TE-4 values for two similar solid solution Ni based alloys in SI and conventional units, respectively. As was shown above for mean CTE values, the agreement is quite good. The values for mean and instantaneous CTE for Alloy 617 determined in the current work are shown together in Figure 13 and Figure 14 for visual comparison.
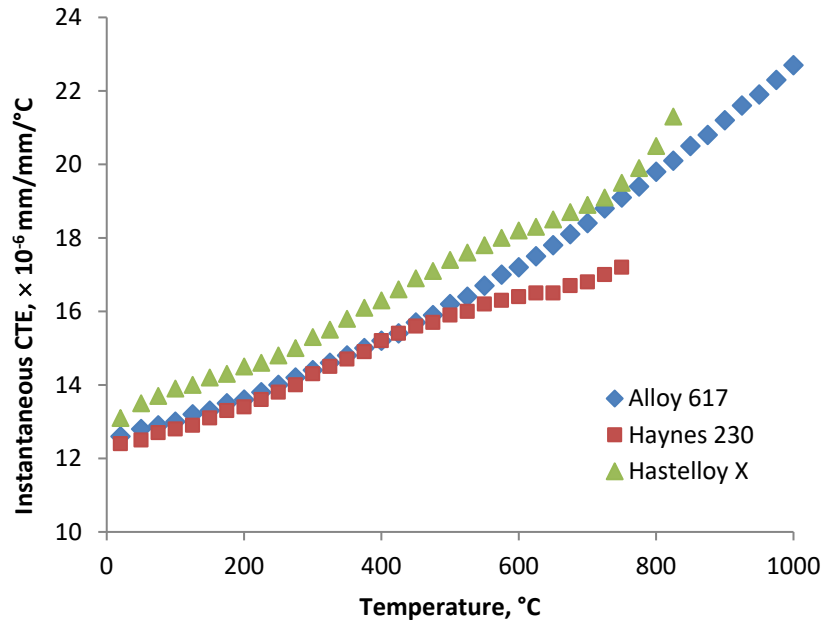
Figure 11. Instantaneous CTE in SI units for current experiments using fit to data shown in Figure 5 compared to Code values for two similar solid solution Ni based alloys.
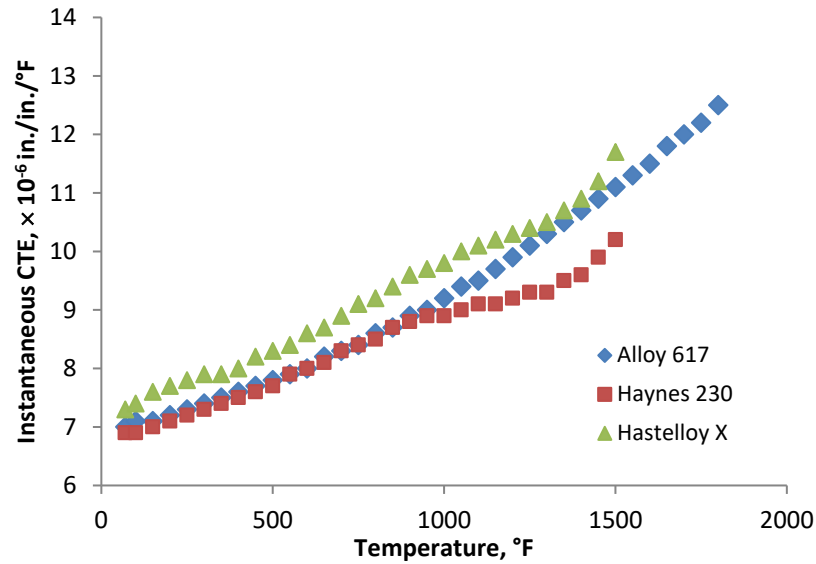
Figure 12. Instantaneous CTE in conventional units for current experiments using fit to data shown in Figure 5 compared to Code values for two similar solid solution Ni based alloys.
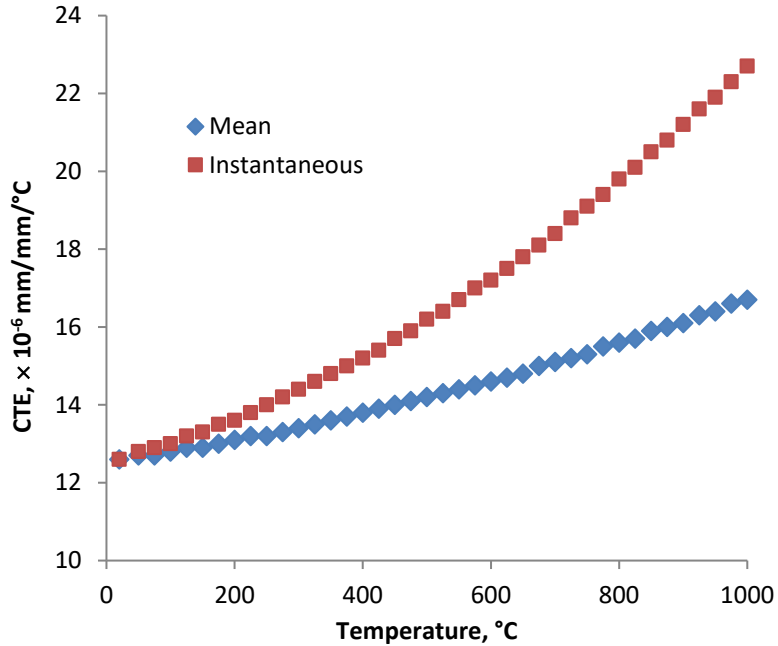
Figure 13. Mean and instantaneous CTE in SI units for Alloy 617 from the current work.
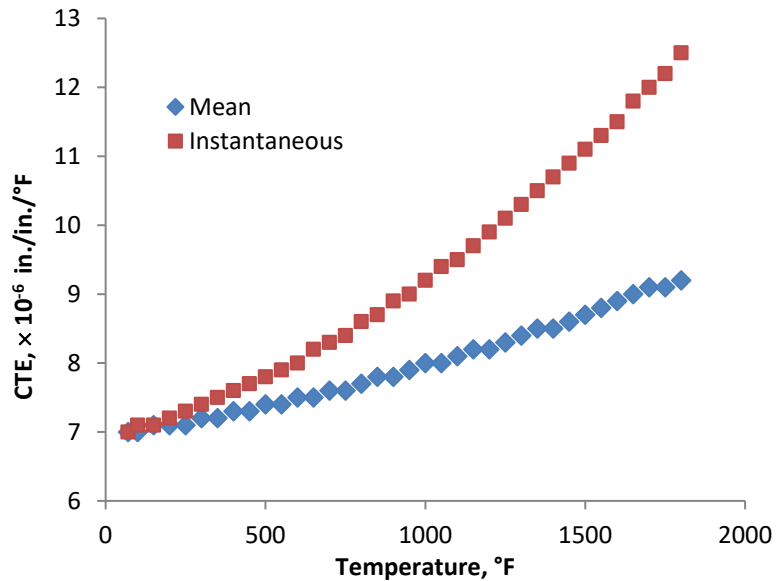
Figure 14. Mean and instantaneous CTE in conventional units for Alloy 617 from the current work.

Thermal Diffusivity and Conductivity

Thermal diffusivity was measured for the same Alloy 617 materials noted above from 20 to 1000°C using a Netzsch laser flash system. The experimental values are shown in Figure 15. A two piece third order polynomial fit is used to describe the experimental data due to the deviation from monotonic behavior in the region of 750°C. This local maximum appears to be the result of Ni-Cr clustering. This is discussed at some length in our publication "Thermophysical Properties of Alloy 617 from 25 to 1000°C", B. H. Rabin, W. D. Swank and R. N. Wright, *Nuclear Engineering and Design Journal,* vol. 262, p. 72, 2013.

The polynomial fit to the diffusivity data in SI units was used to calculate the values in conventional units, shown in Figure 16. The equations describing the thermal diffusivity in SI and conventional units are given by:

$Diffusivity * 10\text{^}6$

$$= \begin{cases} 2.38191E - 09T^3 + -2.62275E - 06T^2 + 0.003850314T + \quad 2.804066484 & T \leq 700°C \\ -4.77014E - 08T^3 + 0.000132652T^2 + -0.119993352T + 40.38858886 & T > 700°C \end{cases}$$

Diffusivity units are m^2/sec

$Diffusivity * 10\text{^}6$

$$= \begin{cases} 1.58E - 11T^3 + -3.28872E - 08\ T^2 + 8.4945E - 05T + 0.10597 & T \leq 1292°F \\ -3.16947E - 10T^3 + 1.61693E - 06T^2 + -0.002685705\ T + 1.649358103 & T > 1292°F \end{cases}$$

Diffusivity units are ft^2/hr
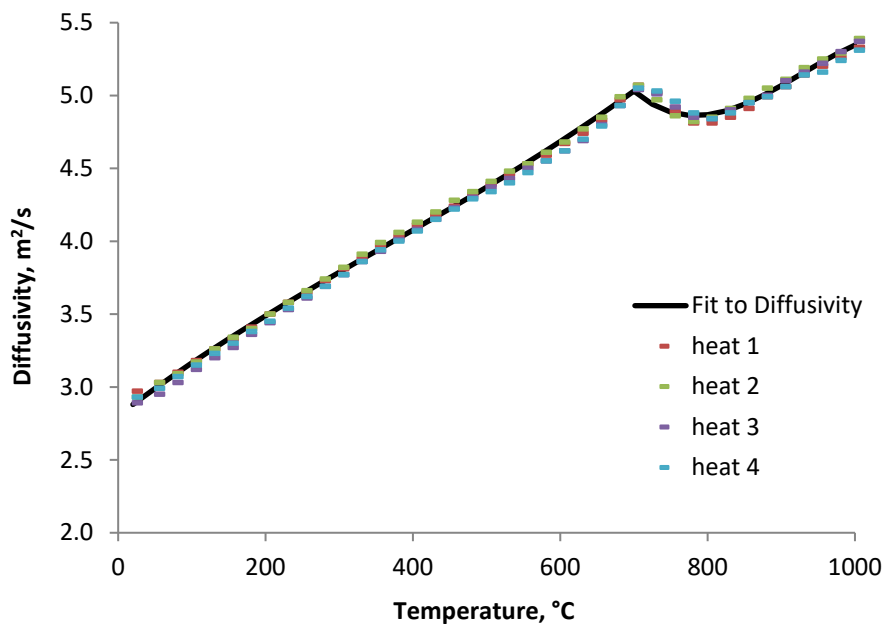
Figure 15. Thermal diffusivity for four heats of Alloy 617 from current work showing two-piece cubic fit.
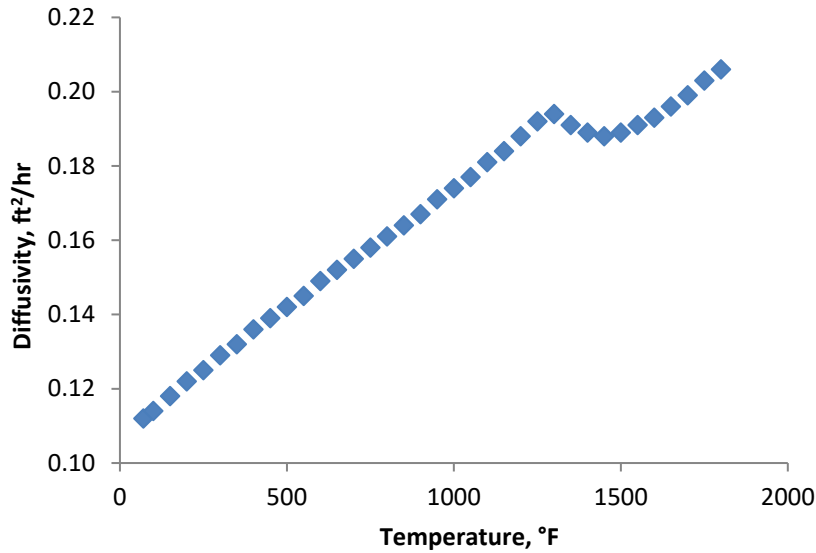
Figure 16. Thermal diffusivity for Alloy 617 in conventional units calculated from polynomial fit to experimental data in SI units.

The heat capacity of the four Alloy 617 materials was measured using a Netzsch calorimeter, and the temperature corrected density can be calculated from the Section III D Table PRD density and the thermal expansion data shown above. The thermal conductivity is the product of the diffusivity, temperature corrected density, and heat capacity. Values calculated for Alloy 617 by this means are shown in Figure 17 in SI units along with data from the Special Metals vendor data sheet for comparison. Note that while there is a reasonable correlation to the two sets of values a footnote on the vendor datasheet notes thermal conductivity is calculated from electrical resistivity. It is not clear if that is the sole reason why the vendor data do not include the perturbation from monotonic behavior in the region of 750°C. Thermal conductivity values in conventional units are shown in Figure 18. Fitting the thermal conductivity required a three piece second order polynomial. The equations in SI and conventional units are:

$$Conductivity = \begin{cases} -6.2655E - 06T^2 + 0.020902839T + \quad 10.04848217 & T \leq 550°C \\ -0.000322895T^2 + 0.444196901T + \; -126.982849 & 550 < T \leq 700°C \\ 7.99813E - 05\,T^2 + \; -0.125490253T + \quad 74.38879386 & T > 700°C \end{cases}$$

Conductivity units are W/(m·°C)

$$Conductivity = \begin{cases} -1.11733E - 06T^2 + \; 0.006781195T + \; 5.590050435 & T \leq 1022°F \\ -5.75819E - 05T^2 + 0.14626978T \quad - 77.99098851 & 1022 < T \leq 1292°F \\ 1.42631E - 05T^2 + \; -0.041194455T + 44.28465926 & T > 1292°F \end{cases}$$

Conductivity units are BTU/(hr·ft·°F)

34
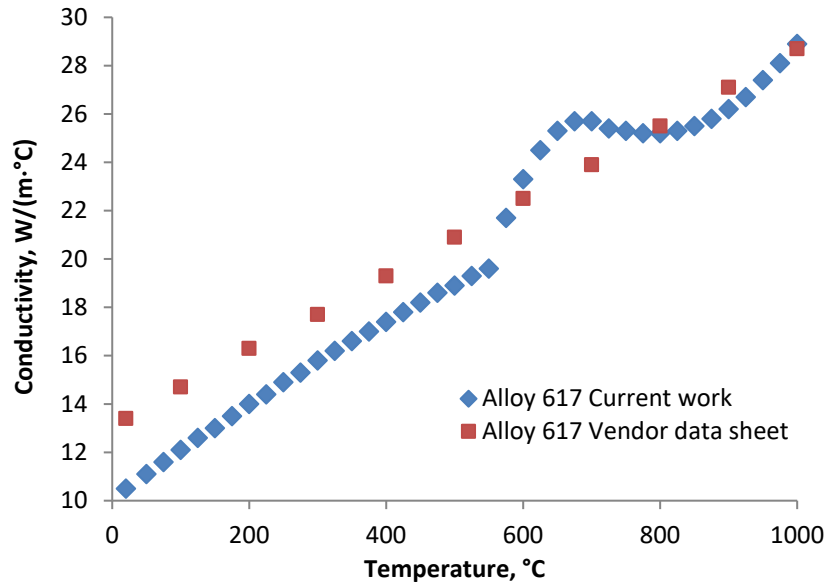
Figure 17. Thermal conductivity for Alloy 617 from the current work from a three-piece fit to data for four heats of material compared to data from Alloy 617 vendor datasheet. Note that thermal conductivity for the current work is calculated using experimental values for thermal diffusivity, temperature compensated density, and heat capacity; footnote on vendor datasheet notes thermal conductivity is calculated from electrical resistivity.
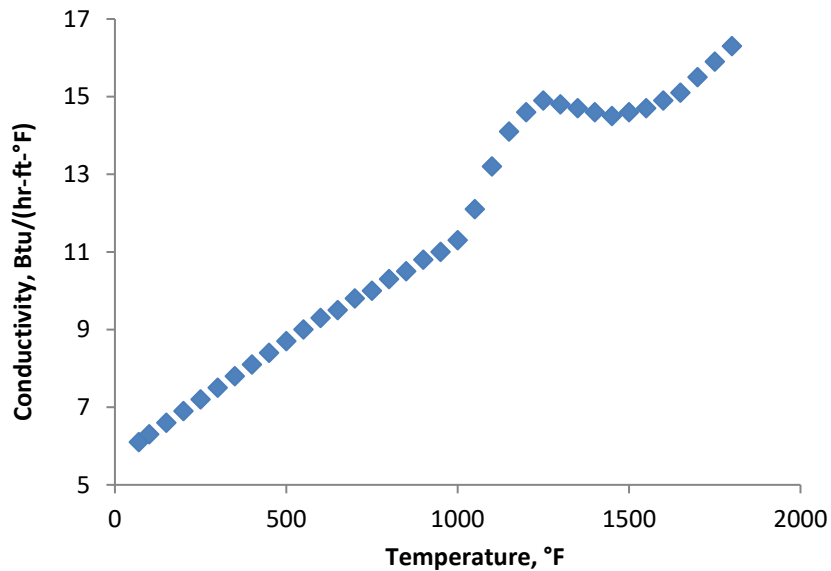
Figure 18. Thermal conductivity for Alloy 617 in conventional units.

The Special Metals vendor data sheet was the only source of historical information on thermal conductivity available in the literature specifically for Alloy 617. In Figure 19 we show a comparison between the thermal conductivity determined in the current work and values in Section IID Table TCD for comparable nickel solid solution alloys. While there is reasonable agreement for many temperatures, it is again not clear why the vendor data do not include the perturbation from monotonic behavior in the region of 750°C. Note that the heat capacity also exhibits a deviation from monotonic behavior, but over a

slightly different temperature range compared to that for the thermal diffusivity. As a result the temperature range of non-monotonic behavior shown by the thermal conductivity extends over approximately 200°C. Although the deviation is not shown in either the vendor data sheet for Alloy 617 or in Section II D for the other nickel solid solutions, the magnitude of the local peak in conductivity is nearly 20% compared to a monotonic curve, and the local peak lies within the temperature range where it is anticipated that Alloy 617 will be used for nuclear heat exchanger design. As noted in "Thermophysical Properties of Alloy 617 from 25 to 1000°C", B. H. Rabin, W. D. Swank and R. N. Wright, *Nuclear Engineering and Design Journal,* vol. 262, p. 72, 2013, other investigators have observed this behavior and ascribed it to Ni-Cr clustering. It therefore seems reasonable to include the non-monotonic behavior in the proposed thermal properties.
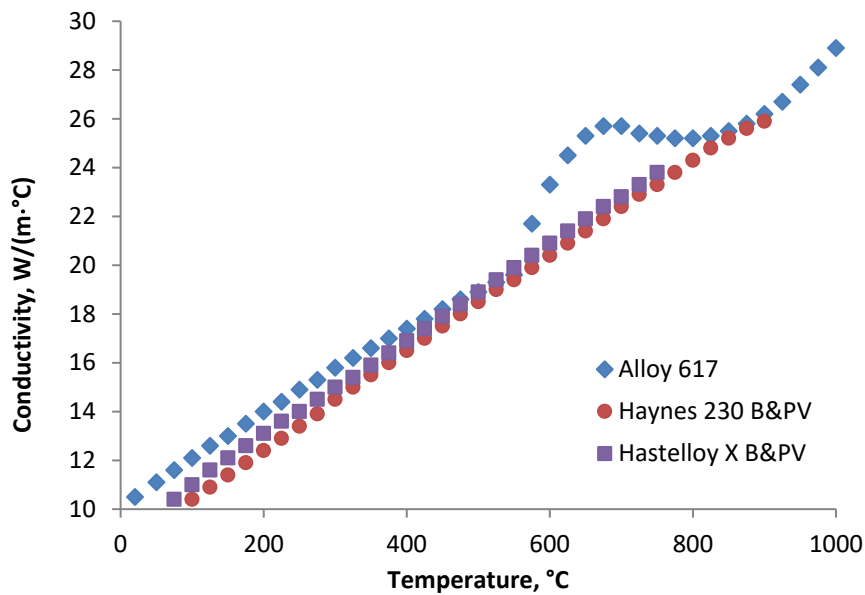
Figure 19. Thermal conductivity of Alloy 617 from the current work compared to values from Section II D Table TCD for Haynes 230 and Hastelloy X.

APPENDIX

Proposed Values of CTE, Thermal Diffusivity and Thermal Conductivity for Alloy 617

Thermal Expansion for Alloy 617

Temp., °F	Coefficients for N06617		
	A	B	C
70	7.0	7.0	0.0
100	7.1	7.0	0.3
150	7.1	7.1	0.7
200	7.2	7.1	1.1
250	7.3	7.1	1.6
300	7.4	7.2	2.0
350	7.5	7.2	2.4
400	7.6	7.3	2.9
450	7.7	7.3	3.4
500	7.8	7.4	3.8
550	7.9	7.4	4.3
600	8.0	7.5	4.8
650	8.2	7.5	5.3
700	8.3	7.6	5.8
750	8.4	7.6	6.3
800	8.6	7.7	6.8
850	8.7	7.8	7.3
900	8.9	7.8	7.8
950	9.0	7.9	8.4
1000	9.2	8.0	8.9
1050	9.4	8.0	9.5
1100	9.5	8.1	10.0
1150	9.7	8.2	10.6
1200	9.9	8.2	11.2
1250	10.1	8.3	11.8
1300	10.3	8.4	12.4
1350	10.5	8.5	13.0
1400	10.7	8.5	13.7
1450	10.9	8.6	14.3
1500	11.1	8.7	15.0
1550	11.3	8.8	15.6
1600	11.5	8.9	16.3
1650	11.8	9.0	17.0
1700	12.0	9.1	17.7
1750	12.2	9.1	18.5
1800	12.5	9.2	19.2

GENERAL NOTE: Coefficient A is the instantaneous coefficient of thermal expansion $\times 10^{-6}$ (in./in./°F). Coefficient B is the mean coefficient of thermal expansion $\times 10^{-6}$ (in./in./°F) in going from 70°F to indicated temperature. Coefficient C is the linear thermal expansion (in./100 ft) in going from 70°F to indicated temperature.

Thermal Expansion for Alloy 617

Temp., °C	Coefficients for N06617		
	A	B	C
20	12.6	12.6	0.0
50	12.8	12.7	0.4
75	12.9	12.7	0.7
100	13.0	12.8	1.0
125	13.2	12.9	1.4
150	13.3	12.9	1.7
175	13.5	13.0	2.0
200	13.6	13.1	2.4
225	13.8	13.2	2.7
250	14.0	13.2	3.0
275	14.2	13.3	3.4
300	14.4	13.4	3.8
325	14.6	13.5	4.1
350	14.8	13.6	4.5
375	15.0	13.7	4.9
400	15.2	13.8	5.2
425	15.4	13.9	5.6
450	15.7	14.0	6.0
475	15.9	14.1	6.4
500	16.2	14.2	6.8
525	16.4	14.3	7.2
550	16.7	14.4	7.6
575	17.0	14.5	8.0
600	17.2	14.6	8.5
625	17.5	14.7	8.9
650	17.8	14.8	9.3
675	18.1	15.0	9.8
700	18.4	15.1	10.3
725	18.8	15.2	10.7
750	19.1	15.3	11.2
775	19.4	15.5	11.7
800	19.8	15.6	12.2
825	20.1	15.7	12.7
850	20.5	15.9	13.2
875	20.8	16.0	13.7
900	21.2	16.1	14.2
925	21.6	16.3	14.7
950	21.9	16.4	15.3
975	22.3	16.6	15.8
1000	22.7	16.7	16.4

GENERAL NOTE: Coefficient A is the instantaneous coefficient of thermal expansion $\times 10^{-6}$ (mm/mm/°C). Coefficient B is the mean coefficient of thermal expansion $\times 10^{-6}$ (mm/mm/°C) in going from 20°C to indicated temperature. Coefficient C is the linear thermal expansion (mm/m) in going from 20°C to indicated temperature.

Nominal Coefficients of Thermal Conductivity (TC) and Thermal Diffusivity (TD) for Alloy 617

Temp., □F	N06617 TC	TD
70	6.1	0.112
100	6.3	0.114
150	6.6	0.118
200	6.9	0.122
250	7.2	0.125
300	7.5	0.129
350	7.8	0.132
400	8.1	0.136
450	8.4	0.139
500	8.7	0.142
550	9.0	0.145
600	9.3	0.149
650	9.5	0.152
700	9.8	0.155
750	10.0	0.158
800	10.3	0.161
850	10.5	0.164
900	10.8	0.167
950	11.0	0.171
1000	11.3	0.174
1050	12.1	0.177
1100	13.2	0.181
1150	14.1	0.184
1200	14.6	0.188
1250	14.9	0.192
1300	14.8	0.194
1350	14.7	0.191
1400	14.6	0.189
1450	14.5	0.188
1500	14.6	0.189
1550	14.7	0.191
1600	14.9	0.193
1650	15.1	0.196
1700	15.5	0.199
1750	15.9	0.203
1800	16.3	0.206

GENERAL NOTES:

(a) TC is the thermal conductivity, Btu/(hr-ft-°F), and TD is the thermal diffusivity, ft²/hr:

$$TD = \frac{TC[\text{Btu/hr} \cdot \text{ ft} \cdot {}^\circ F\,]}{\text{density (lb/ft}^3) \times [\text{specific heat (Btu/lb} \cdot {}^\circ F)]}$$

Nominal Coefficients of Thermal Conductivity (TC) and Thermal Diffusivity (TD) for Alloy 617

Temp., °C	N06617	
	TC	TD
20	10.5	2.88
50	11.1	2.99
75	11.6	3.08
100	12.1	3.17
125	12.6	3.25
150	13.0	3.33
175	13.5	3.41
200	14.0	3.49
225	14.4	3.57
250	14.9	3.64
275	15.3	3.71
300	15.8	3.79
325	16.2	3.86
350	16.6	3.93
375	17.0	4.01
400	17.4	4.08
425	17.8	4.15
450	18.2	4.22
475	18.6	4.30
500	18.9	4.37
525	19.3	4.45
550	19.6	4.53
575	21.7	4.60
600	23.3	4.69
625	24.5	4.77
650	25.3	4.85
675	25.7	4.94
700	25.7	5.03
725	25.4	4.94
750	25.3	4.89
775	25.2	4.86
800	25.2	4.87
825	25.3	4.90
850	25.5	4.94
875	25.8	5.00
900	26.2	5.07
925	26.7	5.14
950	27.4	5.22
975	28.1	5.29
1000	28.9	5.35

GENERAL NOTES:

(a) TC is the thermal conductivity, W/(m·°C), and TD is the thermal diffusivity, 10^{-6} m²/sec:

$$TD = \frac{TC[W/(m \cdot °C)]}{\text{density} \left(\frac{kg}{m^3}\right) \times \left[\text{specific heat} \left(\frac{J}{kg \cdot °C}\right)\right]}$$

Page intentionally left blank

APPENDIX 4
CASE N-XXX: USE OF ALLOY 617 (UNS N06617) FOR CLASS A ELEVATED TEMPERATURE SERVICE CONSTRUCTION, SECTION III, DIVISION 5

Page intentionally left blank

CASE N-XXX: USE OF ALLOY 617 (UNS N06617) FOR CLASS A ELEVATED TEMPERATURE SERVICE CONSTRUCTION
SECTION III, DIVISION 5

Inquiry: May 52Ni-22Cr-13Co-9Mo, Alloy 617 (UNS N06617) be used at elevated temperatures in the construction of components conforming to the requirements of Section III, Division 5, Subsection HB, Subpart B "Elevated Temperature Service"?

Reply: It is the opinion of the Committee that 52Ni-22Cr-13Co-9Mo, Alloy 617 (UNS N06617) may be used in the construction of components conforming to the requirements of Section III, Division 5, Subsection HB, Subpart B "Elevated Temperature Service" providing the following requirements are met:

(a) The modifications and additions to the rules provided in Subsection HB, Subpart B defined in this Code Case shall be met.

(b) The service temperature shall be limited to 1,750°F (954°C)[1] and below.

(c) Service time shall be limited to 100,000 hours.

(d) All other applicable requirements of Section III, Division 5, Subsection HB, Subpart B shall be met.

(e) This Case number shall be listed on the Data Report Form for the component.

This Code Case was written to be used in conjunction with Section III, Division 5, Subsection HB, Subpart B. All requirements of Subsection HB, Subpart B shall be met except:

- when these requirements are modified by the corresponding numbered paragraphs of this Code Case, or
- when new requirements are added with new numbered paragraphs of this Code Case.

Since this Code Case was written in conjunction with Subsection HB, Subpart B, it is important that the Code Case and Subsection HB, Subpart B be used together to ensure that all the elevated temperature service requirements for Alloy 617 are satisfied. All general notes contained in Section III, Division 5 shall apply to the corresponding figures and tables in this Code Case. References within Section III, Division 5 to figures and tables in Appendix HBB-I-14, design fatigue curves or isochronous stress-strain curves should be extended to include corresponding figures and tables for Alloy 617 within this Code Case.

Thermal expansion, thermal diffusivity, and thermal conductivity are not currently contained in Section II for Alloy 617 (UNS N06617). Values for these properties are shown in Tables TE-4 and TCD of this Code Case. Elastic modulus values for Alloy 617 are currently included in Section II Part D (Table TM-4) in US Customary units for temperatures up to 1,500°F and in SI units for temperatures up to 850°C, but the temperature range must be increased to 1,750°F (954°C) to cover the maximum service temperature of this Code Case. Elastic modulus values are shown in Table TM-4 of this Code Case.

---

[1] For those Alloy 617 tables presented herein that list material properties or allowable stresses in SI units only to 950°C, a conversion from the US Customary units values at 1750°F may be used to obtain 954°C values.

ARTICLE HBB-2000
MATERIAL

HBB-2100

HBB-2160   DETERIORATION OF MATERIAL IN SERVICE

(d) Long−time, elevated temperature service may result in the reduction of the subsequent yield and ultimate tensile strengths.

    (3) When the yield and ultimate tensile strengths are reduced by the elevated temperature service, it is necessary to appropriately reduce the values of S_{mt} and S_m. To reflect the effects of long-time elevated temperature service, the S_{mt} values of Tables HBB-I-14.3A through HBB-I-14.3F shall be redefined as the lower of *(-a)* through *(-g)* below, and the values of S_m shall be defined as the lower of *(-b)* through *(-g)* below:

        (-g) for Alloy 617, the product of the yield strength at temperature (Table HBB-I-14.5) and the yield strength reduction factor (Table HBB-3225-2).

ARTICLE HBB-3000
DESIGN

HBB-3200   DESIGN BY ANALYSIS

HBB-3210   DESIGN CRITERIA

HBB-3212   Basis for Determining Stress, Strain, and Deformation Quantities

(d) An additional material of this Subsection, Alloy 617, has several unique characteristics that should be recognized and reflected in multiaxial stress-strain relationships. These include the following:

(1) There is not a clear distinction between time-independent elastic-plastic behavior and time-dependent creep behavior.

(2) Flow stresses are strongly strain-rate sensitive at elevated temperatures.

HBB-3214   Stress Analysis

HBB-3214.2   Inelastic Analysis

[Note: Add the following paragraph as a new last paragraph to HBB-3214.2]

For Alloy 617, decoupling of plastic and creep strains in the classical constitutive framework is generally a poor representation of the true material behavior. Unified constitutive equations, which do not distinguish between rate-dependent plasticity and time-dependent creep, represent the rate dependence and softening that occur, particularly at higher temperatures.

HBB-3220   DESIGN RULES AND LIMITS FOR LOAD-CONTROLLED STRESSES IN STRUCTURES OTHER THAN BOLTS

HBB-3225   Level D Service Limits

The following temperature-dependent tensile strength values, S_u, for Alloy 617 are added in Table HBB-3225-1 of this Code Case.

The following tensile and yield strength reduction factors due to long-time prior elevated temperature service for Alloy 617 are added in Table HBB-3225-2 of this Code Case.

Table HBB-3225-1
Tensile Strength Values, S_u

U.S. Customary Units, ksi	
	See Section II, Part D, Subpart 1, Table U for Values up to 1,000°F
For Metal Temperature Not Exceeding, °F	UNS N06617
1,050	85.2
1,100	83.4
1,150	81.2
1,200	78.4
1,250	75.2
1,300	71.3
1,350	66.9
1,400	62.0
1,450	56.6
1,500	50.8
1,550	44.7
1,600	38.5
1,650	32.4
1,700	26.4
1,750	21.0

SI Units, MPa	
	See Section II, Part D, Subpart 1, Table U for Values up to 538°C
For Metal Temperature Not Exceeding, °C	UNS N06617
550	593
575	584
600	572
625	557
650	540
675	520
700	496
725	470
750	440
775	408
800	373
825	336
850	298
875	260
900	221
925	185
950	151

GENERAL NOTES:

(a) The tabulated values of tensile strength and yield strength are those which the Committee believes are suitable for use in design calculations required by this Subsection. At temperatures above room temperature, the values of tensile strength tend toward an average or expected value which may be as much as 10% above the tensile strength trend curve adjusted to the minimum specified room temperature tensile strength. At temperatures above room temperature, the yield strength values correspond to the yield strength trend curve adjusted to the minimum specified room temperature yield strength. Neither the tensile strength nor the yield strength values correspond exactly to either *average* or *minimum* as these terms are applied to a statistical treatment of a homogeneous set of data.

(b) Neither the ASME Material Specifications nor the rules of this Subsection required elevated temperature testing for tensile or yield strengths of production material for use in Code components. It is not intended that results of such tests, if performed, be compared with these tabulated tensile and yield strength values for ASME Code acceptance/rejection purposes for materials. If some elevated temperature test results on production material appear lower than the tabulated values by a large amount (more than the typical variability of material and suggesting the possibility of some error), further investigation by retest or other means should be considered.

Table HBB-3225-2
Tensile and Yield Strength Reduction Factor Due to Long-Time Prior Elevated Temperature Service

Material	Temp. °F (°C)	YS Reduction Factor	TS Reduction Factor
617	≥ 800 (427)	1.0	1.0

GENERAL NOTE: No reduction factor required for service below the indicated temperature.

ARTICLE HBB-4000
FABRICATION AND INSTALLATION

HBB-4200

HBB-4210

HBB-4212   Effects of Forming and Bending Processes

(a) Post fabrication heat treatment [in accordance with *(b)* below] of materials that have been formed during fabrication, shall be required for fabrication induced strains greater than 5%.

(b) When required, the post fabrication heat treatment shall be in accordance with the following:

    (3) For Alloy 617, the post fabrication heat treatment shall consist of the heat treatment specified in the base material specification.

HBB-4800   RELAXATION CRACKING

Components that will see service between 932°F (500°C) and 1436°F (780°C) shall be given a heat treatment of three hours at 1796°F (980°C) to eliminate relaxation cracking after post fabrication heat treatment, if needed according to HBB-4212. This heat treatment is required for material in either a welded or solution annealed condition.

MANDATORY APPENDIX HBB-I-14
TABLES AND FIGURES

The following Tables and Figures have Alloy 617 data added as indicated.

Table HBB-I-14.1(a)
Permissible Base Materials for Structures Other Than Bolting

Base Material	Spec. No.	Product Form	Types, Grades or Classes
Alloy 617	SB-166	Bar, rod	UNS N06617
[Note (7)]	SB-167	Smls. pipe & tube	UNS N06617
	SB-168	Plate, sheet, strip	UNS N06617
	SB-564	Forgings	UNS N06617

NOTE:
(7) The minimum material thickness shall be 0.125 inches (3.175 mm).

Table HBB-I-14.1(b)
Permissible Weld Materials

Base Material	Spec. No. [Note (1)]	Class
Alloy 617	SFA-5.14	ERNiCrCoMo-1

NOTE:
(1) Only Gas Tungsten Arc Welding (GTAW) is permitted.

Table HBB-I-14.2
S_o – Maximum Allowable Stress Intensity, ksi (MPa), for Design Condition Calculations

U.S. Customary Units	
For Metal Temperature Not Exceeding, °F	**N06617**
700	---
750	---
800	21.5
850	21.3
900	21.2
950	21.0
1,000	20.9
1,050	20.9
1,100	20.8
1,150	20.7
1,200	18.1
1,250	14.5
1,300	11.2
1,350	8.7
1,400	6.6
1,450	5.1
1,500	3.9
1,550	3.0
1,600	2.3
1,650	1.8
1,700	1.4
1,750	1.1

SI Units		
For Metal Temperature Not Exceeding, °C	**N06617**	
375	---	
400	---	
425	148	
450	147	
475	146	
500	145	
525	144	
550	144	
575	144	
600	143	
625	142	
650	124	
675	101	
700	81	
725	64	
750	50	
775	40	
800	31	
825	25	
850	19	
875	15	
900	12	
925	10	[Note (5)]
950	7.9	[Note (5)]

NOTE:
(5) Interpolated from values given in Note G29 of Section II, Part D, Subpart 1, Table 1B.

Figure HBB-I-14.3F
S_{mt} − Alloy 617
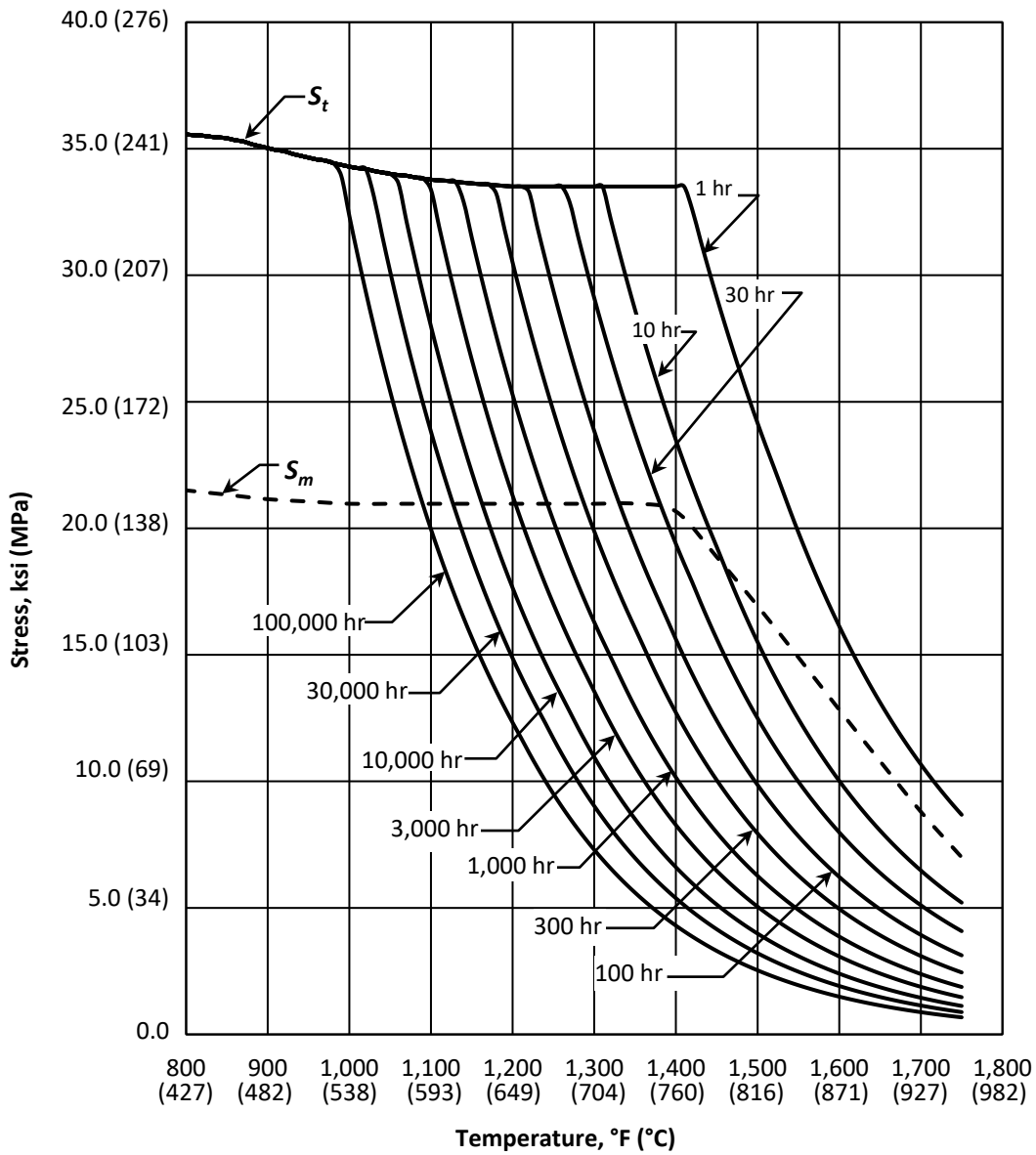
Table HBB-I-14.3F
S_{mt} – Allowable Stress Intensity Values, ksi (MPa), Alloy 617

U.S. Customary Units

Temp., °F	1 hr	10 hr	30 hr	100 hr	300 hr	1,000 hr	3,000 hr	10,000 hr	30,000 hr	100,000 hr
800	21.5	21.5	21.5	21.5	21.5	21.5	21.5	21.5	21.5	21.5
850	21.3	21.3	21.3	21.3	21.3	21.3	21.3	21.3	21.3	21.3
900	21.2	21.2	21.2	21.2	21.2	21.2	21.2	21.2	21.2	21.2
950	21.1	21.1	21.1	21.1	21.1	21.1	21.1	21.1	21.1	21.1
1,000	21.0	21.0	21.0	21.0	21.0	21.0	21.0	21.0	21.0	21.0
1,050	21.0	21.0	21.0	21.0	21.0	21.0	21.0	21.0	21.0	21.0
1,100	21.0	21.0	21.0	21.0	21.0	21.0	21.0	21.0	21.0	20.0
1,150	21.0	21.0	21.0	21.0	21.0	21.0	21.0	21.0	18.8	15.7
1,200	21.0	21.0	21.0	21.0	21.0	21.0	21.0	17.6	14.9	12.3
1,250	21.0	21.0	21.0	21.0	21.0	20.3	17.0	14.0	11.7	9.5
1,300	21.0	21.0	21.0	21.0	19.9	16.3	13.6	11.0	9.0	7.3
1,350	21.0	21.0	21.0	19.3	16.0	12.9	10.6	8.5	7.0	5.6
1,400	21.0	20.7	19.4	15.6	12.7	10.2	8.3	6.6	5.4	4.3
1,450	19.3	18.9	15.6	12.4	10.0	8.0	6.5	5.1	4.2	3.3
1,500	16.9	15.5	12.5	9.9	7.9	6.3	5.0	4.0	3.2	2.5
1,550	14.9	12.5	10.0	7.8	6.3	4.9	3.9	3.1	2.5	1.9
1,600	12.8	10.0	8.0	6.2	5.0	3.9	3.1	2.4	1.9	1.5
1,650	10.8	8.1	6.4	4.9	3.9	3.0	2.4	1.9	1.5	1.1
1,700	8.8	6.5	5.1	3.9	3.1	2.4	1.9	1.4	1.1	0.9
1,750	7.0	5.2	4.1	3.1	2.4	1.9	1.5	1.1	0.9	0.7

SI Units

Temp., °C	1 h	10 h	30 h	100 h	300 h	1,000 h	3,000 h	10,000 h	30,000 h	100,000 h
425	148	148	148	148	148	148	148	148	148	148
450	148	148	148	148	148	148	148	148	148	148
475	146	146	146	146	146	146	146	146	146	146
500	146	146	146	146	146	146	146	146	146	146
525	145	145	145	145	145	145	145	145	145	145
550	145	145	145	145	145	145	145	145	145	145
575	145	145	145	145	145	145	145	145	145	145
600	145	145	145	145	145	145	145	145	145	130
625	145	145	145	145	145	145	145	145	125	105
650	145	145	145	145	145	145	145	121	102	84
675	145	145	145	145	145	142	119	98	82	67
700	145	145	145	145	142	116	97	79	65	52
725	145	145	145	141	117	95	78	63	51	41
750	145	145	144	117	95	76	62	50	41	33
775	136	136	119	95	77	61	50	40	32	26
800	124	121	98	77	62	49	40	32	26	20
825	112	99	80	63	51	40	32	25	20	16
850	99	82	65	51	41	32	26	20	16	13
875	87	67	53	42	33	26	21	16	13	10
900	74	55	44	34	27	21	16	13	10	8
925	62	45	36	27	22	17	13	10	8	6
950	50	37	29	22	18	13	11	8	6	5

GENERAL NOTE: As described in HBB-2160(d), it may be necessary to adjust the values of S_{mt} to account for the effects of long-time service at elevated temperature.

Figure HBB-I-14.4F
S_t — Alloy 617
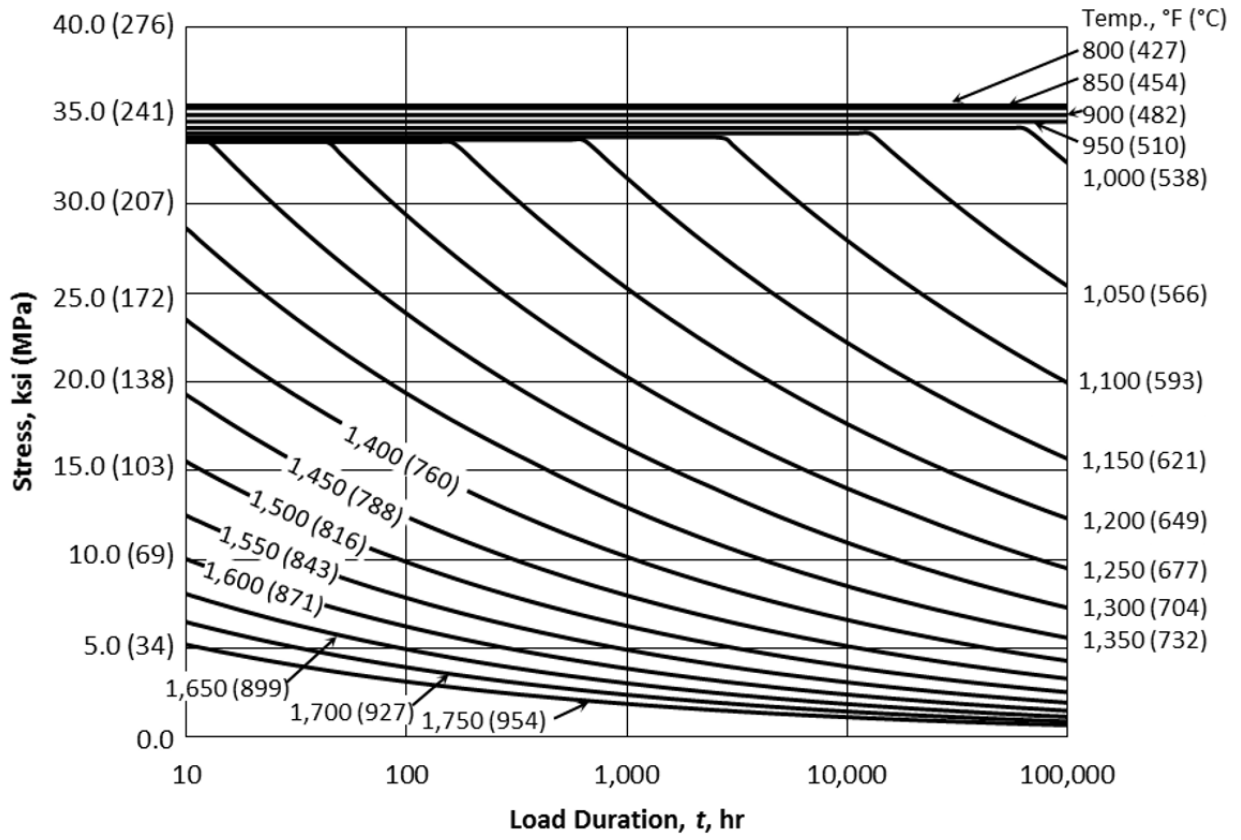
Table HBB-I-14.4F
S_t– Allowable Stress Intensity Values, ksi (MPa), Alloy 617

U.S. Customary Units										
Temp., °F	1 hr	10 hr	30 hr	100 hr	300 hr	1,000 hr	3,000 hr	10,000 hr	30,000 hr	100,000 hr
800	35.6	35.6	35.6	35.6	35.6	35.6	35.6	35.6	35.6	35.6
850	35.4	35.4	35.4	35.4	35.4	35.4	35.4	35.4	35.4	35.4
900	35.0	35.0	35.0	35.0	35.0	35.0	35.0	35.0	35.0	35.0
950	34.6	34.6	34.6	34.6	34.6	34.6	34.6	34.6	34.6	34.6
1,000	34.3	34.3	34.3	34.3	34.3	34.3	34.3	34.3	34.3	32.3
1,050	34.0	34.0	34.0	34.0	34.0	34.0	34.0	34.0	30.1	25.4
1,100	33.8	33.8	33.8	33.8	33.8	33.8	33.4	28.0	23.8	20.0
1,150	33.6	33.6	33.6	33.6	33.6	31.5	26.7	22.2	18.8	15.7
1,200	33.5	33.5	33.5	33.5	30.5	25.3	21.3	17.6	14.9	12.3
1,250	33.5	33.5	33.5	29.4	24.6	20.3	17.0	14.0	11.7	9.5
1,300	33.5	33.5	29.1	23.8	19.9	16.3	13.6	11.0	9.0	7.3
1,350	33.5	28.6	23.7	19.3	16.0	12.9	10.6	8.5	7.0	5.6
1,400	33.5	23.5	19.4	15.6	12.7	10.2	8.3	6.6	5.4	4.3
1,450	29.1	19.3	15.6	12.4	10.0	8.0	6.5	5.1	4.2	3.3
1,500	24.2	15.5	12.5	9.9	7.9	6.3	5.0	4.0	3.2	2.5
1,550	19.8	12.5	10.0	7.8	6.3	4.9	3.9	3.1	2.5	1.9
1,600	16.1	10.0	8.0	6.2	5.0	3.9	3.1	2.4	1.9	1.5
1,650	13.1	8.1	6.4	4.9	3.9	3.0	2.4	1.9	1.5	1.1
1,700	10.7	6.5	5.1	3.9	3.1	2.4	1.9	1.4	1.1	0.9
1,750	8.7	5.2	4.1	3.1	2.4	1.9	1.5	1.1	0.9	0.7
SI Units										
Temp., °C	1 h	10 h	30 h	100 h	300 h	1,000 h	3,000 h	10,000 h	30,000 h	100,000 h
425	245	245	245	245	245	245	245	245	245	245
450	245	245	245	245	245	245	245	245	245	245
475	242	242	242	242	242	242	242	242	242	242
500	240	240	240	240	240	240	240	240	240	240
525	238	238	238	238	238	238	238	238	238	238
550	235	235	235	235	235	235	235	235	235	200
575	234	234	234	234	234	234	234	225	192	161
600	233	233	233	233	233	233	218	182	155	130
625	232	232	232	232	232	210	178	148	125	105
650	231	231	231	231	208	173	145	121	102	84
675	231	231	231	205	172	142	119	98	82	67
700	231	231	207	170	142	116	97	79	65	52
725	231	208	173	141	117	95	78	63	51	41
750	231	174	144	117	95	76	62	50	41	33
775	219	146	119	95	77	61	50	40	32	26
800	185	121	98	77	62	49	40	32	26	20
825	156	99	80	63	51	40	32	25	20	16
850	130	82	65	51	41	32	26	20	16	13
875	108	67	53	42	33	26	21	16	13	10
900	90	55	44	34	27	21	16	13	10	8
925	75	45	36	27	22	17	13	10	8	6
950	62	37	29	22	18	13	11	8	6	5

Table HBB-I-14.5
Yield Strength Values, S_y, Versus Temperature

U.S. Customary Units	
	Stresses, ksi
Temp., °F	UNS N06617
RT : 1,000	See Section II, Part D, Subpart 1, Table Y-1 for Values up to 1,000°F
1,050	23.3
1,100	23.3
1,150	23.3
1,200	23.3
1,250	23.3
1,300	23.3
1,350	23.3
1,400	23.3
1,450	23.3
1,500	22.6
1,550	21.6
1,600	20.4
1,650	19.0
1,700	17.4
1,750	15.7

SI Units	
	Stresses, MPa
Temp., °C	UNS N06617
RT : 525	See Section II, Part D, Subpart 1, Table Y-1 for Values up to 538°C
550	161
575	161
600	161
625	161
650	161
675	161
700	161
725	161
750	161
775	161
800	159
825	153
850	147
875	139
900	131
925	121
950	110

Figure HBB-I-14.6G
Minimum Stress-to-Rupture - Alloy 617

58
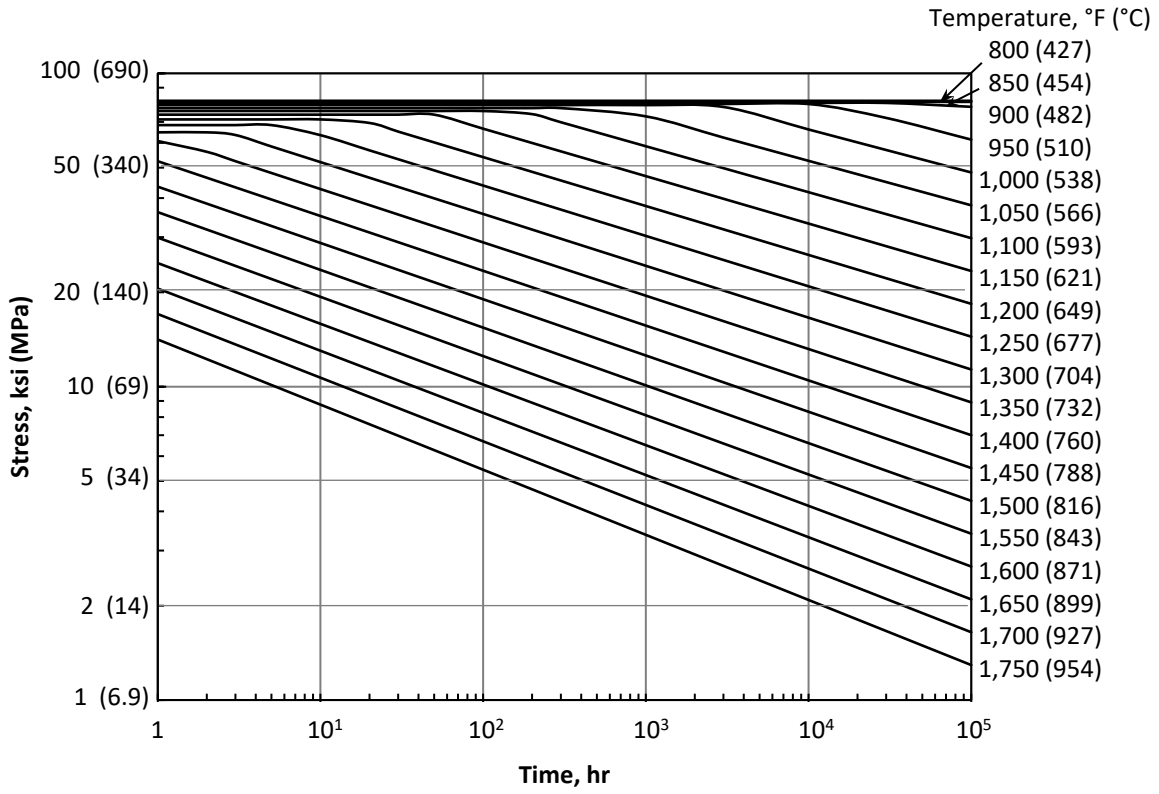
Table HBB-I-14.6G
Expected Minimum Stress-to-Rupture Values, ksi (MPa), Alloy 617

U.S. Customary Units

Temp., °F	1 hr	3 hr	10 hr	30 hr	100 hr	300 hr	1,000 hr	3,000 hr	10,000 hr	30,000 hr	100,000 hr
800	81.7	81.7	81.7	81.7	81.7	81.7	81.7	81.7	81.7	81.7	81.7
850	81.1	81.1	81.1	81.1	81.1	81.1	81.1	81.1	81.1	81.1	81.1
900	80.5	80.5	80.5	80.5	80.5	80.5	80.5	80.5	80.5	80.5	78.2
950	79.8	79.8	79.8	79.8	79.8	79.8	79.8	79.8	79.8	72.1	61.4
1,000	79.2	79.2	79.2	79.2	79.2	79.2	79.2	78.1	66.2	56.9	48.3
1,050	77.5	77.5	77.5	77.5	77.5	77.5	72.9	62.4	52.6	45.0	37.9
1,100	75.8	75.8	75.8	75.8	75.8	69.8	58.5	49.8	41.8	35.5	29.8
1,150	73.8	73.8	73.8	73.8	66.6	56.4	47.0	39.8	33.2	28.1	23.4
1,200	71.3	71.3	71.3	65.2	54.0	45.5	37.7	31.8	26.3	22.2	18.4
1,250	68.4	68.4	63.5	53.2	43.8	36.7	30.3	25.4	20.9	17.5	14.4
1,300	64.8	63.6	52.1	43.4	35.6	29.7	24.3	20.3	16.6	13.8	11.3
1,350	60.8	52.4	42.7	35.4	28.9	24.0	19.5	16.2	13.2	10.9	8.9
1,400	52.4	43.3	35.1	28.9	23.4	19.3	15.7	12.9	10.5	8.6	7.0
1,450	43.5	35.7	28.8	23.6	19.0	15.6	12.6	10.3	8.3	6.8	5.5
1,500	36.1	29.4	23.6	19.3	15.4	12.6	10.1	8.2	6.6	5.4	4.3
1,550	29.9	24.3	19.4	15.7	12.5	10.2	8.1	6.6	5.2	4.3	3.4
1,600	24.8	20.0	15.9	12.8	10.2	8.2	6.5	5.3	4.2	3.4	2.7
1,650	20.6	16.5	13.0	10.5	8.2	6.6	5.2	4.2	3.3	2.7	2.1
1,700	17.1	13.6	10.7	8.5	6.7	5.4	4.2	3.4	2.6	2.1	1.6
1,750	14.1	11.3	8.8	7.0	5.4	4.3	3.4	2.7	2.1	1.7	1.3

SI Units

Temp., °C	1 h	3 h	10 h	30 h	100 h	300 h	1,000 h	3,000 h	10,000 h	30,000 h	100,000 h
425	564	564	564	564	564	564	564	564	564	564	564
450	560	560	560	560	560	560	560	560	560	560	560
475	555	555	555	555	555	555	555	555	555	555	555
500	552	552	552	552	552	552	552	552	552	541	462
525	548	548	548	548	548	548	548	548	508	438	372
550	539	539	539	539	539	539	539	488	412	354	299
575	531	531	531	531	531	531	466	398	335	286	241
600	520	520	520	520	520	457	383	325	272	232	194
625	506	506	506	506	446	377	314	266	221	187	156
650	491	491	491	446	369	311	258	217	180	152	126
675	473	473	443	371	306	257	212	177	146	123	101
700	451	451	371	309	254	212	174	145	119	99	81
725	427	380	310	258	210	175	142	118	97	80	65
750	387	320	260	215	174	144	117	97	78	65	53
775	327	269	217	179	144	119	96	79	64	52	42
800	276	226	182	149	120	98	79	64	52	42	34
825	233	190	152	124	99	81	65	53	42	34	27
850	197	160	127	103	82	67	53	43	34	28	22
875	167	135	106	86	68	55	44	35	28	22	18
900	141	113	89	72	56	45	36	29	23	18	14
925	119	95	75	60	47	37	29	23	18	15	12
950	100	80	62	50	39	31	24	19	15	12	9

Table HBB-I-14.10F-1
Stress Rupture Factors for Alloy 617 Welded with ERNiCrCoMo-1

U.S. Customary Units		SI Units	
Temp., °F	Ratio	Temp., °C	Ratio
800	1.0	425	1.0
850	1.0	450	1.0
900	1.0	475	1.0
950	1.0	500	1.0
1,000	1.0	525	1.0
1,050	1.0	550	1.0
1,100	1.0	575	1.0
1,150	1.0	600	1.0
1,200	1.0	625	1.0
1,250	1.0	650	1.0
1,300	1.0	675	1.0
1,350	1.0	700	1.0
1,400	1.0	725	1.0
1,450	1.0	750	1.0
1,500	1.0	775	1.0
1,550	1.0	800	1.0
1,600	0.85	825	1.0
1,650	0.85	850	0.85
1,700	0.85	875	0.85
1,750	0.85	900	0.85
		925	0.85
		950	0.85

Table HBB-I-14.11
Permissible Materials for Bolting

Not applicable for Alloy 617.

NONMANDATORY APPENDIX HBB-T
RULES FOR STRAIN, DEFORMATION, AND FATIGUE LIMITS AT ELEVATED TEMPERATURES

HBB-T-1300 DEFORMATION AND STRAIN LIMITS FOR STRUCTURAL INTEGRITY

HBB-T-1320 SATISFACTION OF STRAIN LIMITS USING ELASTIC ANALYSIS

HBB-T-1321 General Requirements

(e) Paragraph HBB-T-1321, HBB-T-1322 and HBB-T-1323 are not applicable to Alloy 617 above 1200°F (650°C).

HBB-T-1323 Test No. A-2

The following data are added for Alloy 617 in Table HBB-T-1323 of this Code Case as indicated below.

Table HBB-T-1323	
Temperatures at Which $S_m = S_t$ at 10^5 hr	
Material	**Temp., °F (°C)**
Alloy 617	1090 (588)

HBB-T-1324 Test No. A-3

The following data are added for Alloy 617 in Table HBB-T-1324 of this Code Case as indicated below.

Table HBB-T-1324		
Values of the *r* and *s* Parameters		
Material	*r*	*s*
Alloy 617	1.0	1.5

The reference for determination of maximum allowable time, t_{id}, shall be revised to Figure HBB-I-14.6G of this Code Case for expected minimum stress-to-rupture.

HBB-T-1330 SATISFACTION OF STRAIN LIMITS USING SIMPLIFIED INELASTIC ANALYSIS

HBB-T-1331 General Requirements

(i) Paragraph HBB-T-1331 is not applicable to Alloy 617 above 1200°F (650°C).

HBB-T-1332 Tests No. B-1 and B-2

(e) Paragraph HBB-T-1332 is not applicable to Alloy 617 above 1200°F (650°C).

HBB-T-1333 Test No. B-3

(d) Paragraph HBB-T-1333 is not applicable to Alloy 617 above 1200°F (650°C).

HBB-T-1340   SATISFACTION OF STRAIN LIMITS USING ELASTIC-PERFECTLY PLASTIC ANALYSIS

HBB-T-1341   General Requirements

As an alternative to HBB-T-1320 and HBB-T-1330, the strain limits of HBB-T-1310 and HBB-T-1713 are considered satisfied if the requirements of this subsubarticle are satisfied.

The design methodology employed for evaluation of strain limits is based on ratcheting analyses using a small strain theory elastic-perfectly plastic material model where the yield stress is adjusted based on a pseudo-yield stress selected to bound accumulated inelastic strain. Guidance on ratcheting analysis is provided in HBB-T-1346. The term "pseudo-yield stress" refers to a temperature-dependent isochronous stress based on the total time duration of elevated temperature service and a target inelastic strain, not to exceed the yield strength of the material at temperature and is explicitly defined in HBB-T-1344.2.

(a) This design methodology is not applicable to skeletal structures, e.g., a constant diameter bar with uniform axial load throughout, nor to structures where geometrical nonlinearities exist, e.g., canopy or omega seals.

HBB-T-1342   Load Definition

Define all applicable loads and load cases per Section III, Division 5, HBB-3113.2, Service Loadings.

HBB-T-1342.1   Composite Cycle Definition. For the purpose of performing an elastic-perfectly plastic ratcheting analysis, an overall cycle must be defined that includes all relevant features from the individual Level A, B and C Service Loadings identified in the Design Specification. Relevant features include, as a minimum, the time-dependent sequence of thermal, mechanical and pressure loading, including starting and ending conditions. Such an overall cycle is defined herein as a composite cycle subject to the following requirements.

(a) An individual cycle, as defined in the Design Specification, cannot be further subdivided into individual cycles to satisfy these requirements.

(b) Except as described in paragraph *(c)* below, a single cycle from each Level A, B and C Service Loading cycle type shall be included in the composite cycle for evaluation of strain limits.

(c) Level C Service Loadings may be combined with the applicable Level A and B Service Loadings to define an additional composite cycle(s) to be evaluated separately from the composite cycle defined in paragraph *(b)* above. Multiple composite cycles that include Level C Service Loadings may be defined for separate evaluation. The total number of Level C Service Loading cycles shall not exceed 25.

HBB-T-1343   Numerical Model

Develop a numerical model of the component, including all relevant geometry characteristics. The model used for the analysis shall be selected to accurately represent the component geometry, boundary conditions, and applied loads. The model must also be accurate for small details, such as small holes, fillets, corner radii, and other stress risers. The local temperature history shall be determined from a thermal transient analysis based on the thermal boundary conditions determined from the loading conditions defined in HBB-T-1342.

HBB-T-1344   Requirements for Satisfaction of Strain Limits

Perform a ratcheting analysis for each of the composite cyclic histories defined in HBB-T-1342.1. Each of these cyclic histories must be shown to be free from ratcheting based on the pseudo-yield stress, S_{xT}, as defined in HBB-T-1344.2. In the following steps, inelastic strain for a particular stress, time and

temperature is obtained by subtracting the elastic strain from the total strain as given by the isochronous stress-strain curve at the same stress, time and temperature. Additional requirements for weldments are shown in HBB-T-1345.

HBB-T-1344.1   **Step 1.** Define t_{design} as the total time duration of elevated temperature service for all Level A, B, and C Service Loadings when the temperature is above 800°F (427°C).

HBB-T-1344.2   **Step 2.** Select a target inelastic strain, x, where $0 < x < \varepsilon_{avg}$ and ε_{avg} is equal to 0.01 for base metal or 0.005 for weldments. Define a pseudo-yield stress, S_{xT}, at each location,[2] using the temperature determined from the transient thermal analysis. This pseudo-yield stress is equal to the lesser of the quantities defined below in *(a)* and *(b)*.

(a) The yield strength, S_y, given in Table HBB-I-14.5 of this Code Case;

(b) The stress to cause x inelastic strain in time t_{design}, as determined from the isochronous stress-strain curves in HBB-T-1836 of this Code Case.

HBB-T-1344.3   **Step 3.** Perform a cyclic elastic-perfectly plastic analysis for each composite cycle defined in HBB-T-1342.1(b) above with temperature-dependent pseudo-yield stress, S_{xT}. If ratcheting does not occur, obtain the plastic strain distribution throughout the component. The plastic strain, ε_p, is evaluated according to

$$\varepsilon_p = \sqrt{\frac{2}{3}\left[\left(\varepsilon_x^p\right)^2 + \left(\varepsilon_y^p\right)^2 + \left(\varepsilon_z^p\right)^2 + 2\left(\varepsilon_{xy}^p\right)^2 + 2\left(\varepsilon_{yz}^p\right)^2 + 2\left(\varepsilon_{zx}^p\right)^2\right]}$$

(1)

where the plastic strain components, ε_x^p, ε_y^p, ε_z^p, ε_{xy}^p, ε_{yz}^p and ε_{zx}^p, are those strains accumulated at the end of the composite cycle.

HBB-T-1344.4   **Step 4.** Assess acceptability in accordance with *(a)* and *(b)* below by using the plastic strains, ε_p, from Step 3. If the requirements of both *(a)* and *(b)* are satisfied, then the strain limits of HBB-T-1310 for base metal and HBB-T-1713 for weldments are also considered satisfied. This condition is illustrated in Figure HBB-T-1344, sketch (a).

(a) The requirement $x + \varepsilon_p \leq \varepsilon_{avg}$ must be satisfied at least at one point for all through-thickness locations. As defined in Step 2, ε_{avg} is equal to 0.01 for base metal or 0.005 for weldments. Failure of this requirement is illustrated in Figure HBB-T-1344, sketch (b).

(b) The requirement $x + \varepsilon_p \leq \varepsilon_{local}$ must be satisfied at all points. The local strain limit, ε_{local}, is equal to 0.05 for base metal and 0.025 for weldments. Failure of this requirement is illustrated in Figure HBB-T-1344, sketch (c).

(c) In order to proceed if either of the requirements of *(a)* or *(b)* above are not satisfied, return to HBB-T-1344.2 and select a smaller value of the target inelastic strain, x. If it is not possible to find a value of x that does not ratchet and also satisfies the requirements of this paragraph HBB-T-1344.4, then the loading conditions of HBB-T-1342 applied to the component configuration defined in HBB-T-1343 do not meet the requirements of HBB-T-1340.

---

[2] "Each location" refers to nodal points or integration points in the finite element mesh where the calculations are performed.

Figure HBB-T-1344 Strain Limits Pass/Fail Criteria Illustrated

Pass

Fail

Fail

(a)

(b)

(c)

$x + \varepsilon_p \leq \varepsilon_{avg}$

$\varepsilon_{avg} < x + \varepsilon_p \leq \varepsilon_{local}$

$x + \varepsilon_p > \varepsilon_{local}$
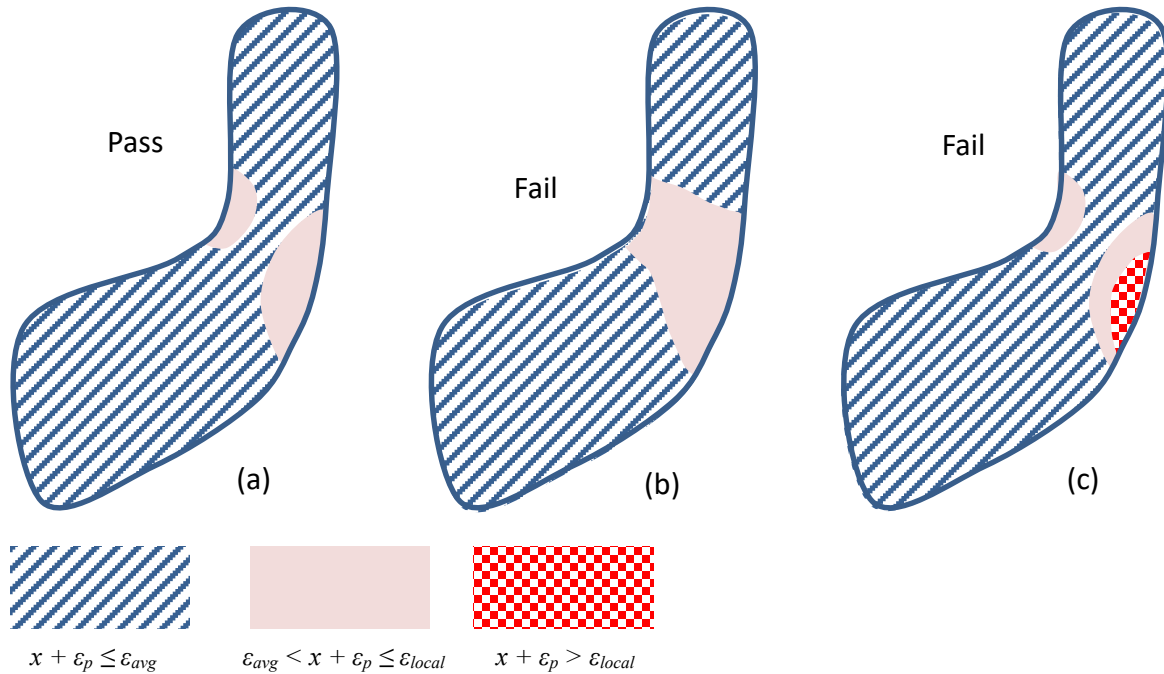
HBB-T-1345   Weldments

Implementation of the strain limits for weldments defined above in HBB-T-1344 requires additional consideration.

HBB-T-1345.1   Weld Region Model Boundaries. Figure HBB-T-1345 shows a full penetration butt weld as an example of the definition of a weld region. As shown, w_1 and w_2 are needed to define the weld region for use in this Code Case and are approximations consistent with the specified weld configuration and parameters. The specified weld region must include applicable stress concentrations in accordance with the requirements for analysis of geometry, HBB-T-1714, unless ground flush.

The weld shown in Figure HBB-T-1345 represents a full penetration butt weld in a shell. Other weld configurations may be needed for construction of an elevated temperature service component in accordance with Section III, Division 5, Subsection HB, Subpart B. Section III, Division 5, HBB-4200 refers to various Section III, Division 1, Article NB-4000 paragraphs for weld configurations and requirements. These NB-4000 weld configurations are represented by the shaded region.

Figure HBB-T-1345 Weld Region Model Boundaries

w_1

Flush ground (no stress concentration)

Effective modeling edges of the weld

Stress concentration if applicable per HBB-T-1714

w_2

64
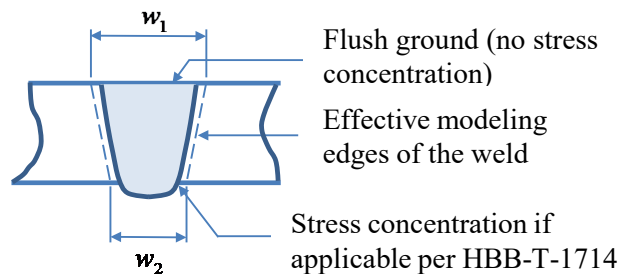
HBB-T-1345.2. Geometry. The requirements for analysis of geometry of Section III, Division 5, HBB-T-1714 are applicable for satisfaction of the requirements of this Code Case.

HBB-T-1345.3. Physical Properties. The thermal/physical properties of weldments shall be assumed to be the same as the corresponding base metal for the base metal-weld combinations listed in Table HBB-I-14.10F-1.

HBB-T-1345.4 Dissimilar Metal Welds. Requirements for dissimilar metal welds are in the course of preparation.

HBB-T-1346   Ratcheting Analysis

The steps to perform a ratcheting analysis to demonstrate compliance with strain limits are as follows:

(a) Define Composite Cycle Load Time-Histories and Analysis Step(s).

(1) It may consist of histories of mechanical loads, pressure loads, displacements, temperatures and thermal boundary conditions.

(2) Time-independent parts of the cycle may be truncated because the elastic-perfectly plastic analysis is not time-dependent.

(3) The cycle should not have discontinuities. Discontinuities arising from the selection of the specified cycles to form a composite cycle should be eliminated by a simple and reasonable transition from one operating state to the next.

(4) Subject to the requirements in *(b)* below, the composite cycle time does not affect the result of the ratcheting analysis.

(5) Temperatures, thermal boundary conditions, boundary displacements and mechanical loads over a cycle should be cyclic; that is, begin and end at the same value.

(6) A single analysis step may represent one cycle. Dividing a single cycle into more than one step to facilitate definition of the load cycle, and to ensure that maximum loads are analyzed, is often helpful.

(b) Define Analysis Types.

(1) A sequentially coupled thermal-mechanical analysis of the composite cycle may be performed. First, a thermal analysis is performed to generate temperature histories. Next, the mechanical analyses are performed using these temperature histories as inputs. Care must be taken that times in the mechanical analysis step and in the previous thermal analysis are the same or do not conflict, depending on the requirements of the analysis software.

(2) Alternatively, a coupled thermal-mechanical analysis may be performed. The composite temperature history to be used in the mechanical analysis should be cyclic; that is, the beginning and end temperature distributions should be the same.

(c) Define Material Properties.

(1) For the thermal analyses, density and temperature-dependent specific heat and conductivity will generally be required.

(2) For the mechanical analyses, the temperature-dependent properties required are elastic modulus, Poisson's ratio, and the mean expansion coefficient. Density may also be required.

(3) In addition, the mechanical analyses temperature-dependent yield stress will need to be adjusted based on the selected pseudo-yield stress, S_{xT}, defined in HBB-T-1344.2.

(d) Perform Analyses.

(1) Perform an elastic-perfectly plastic cyclic mechanical and thermal stress analysis using the temperature-dependent pseudo-yield stress defined above. Enough cycles are required to demonstrate ratcheting or the absence of ratcheting.

(2) Care must be taken to ensure that the analysis deals with all the changes within a cycle. Elastic-plastic analysis routines increase increment size where possible, and may miss a detail in the loading. A conservative limit to maximum increment size can address this problem, as can division of the cycle into more than one step, as discussed in *(a)(6)* above.

(e) Detect Ratcheting.

(1) Ratcheting is defined as repeated non-cyclic deflections; that is, between the beginning and end of a cycle, a repeated finite displacement change occurs somewhere in the structure.

(2) Detecting ratcheting is most easily done by plotting nodal deflections over time. Cyclic (repeated) behavior indicates non-ratcheting. History plots of equivalent plastic strains will also identify ratcheting.

HBB-T-1400   CREEP‑FATIGUE EVALUATION

HBB-T-1410   GENERAL REQUIREMENTS

HBB-T-1411   Damage Equation

The following entry, Alloy 617, C=0.24, is added to HBB-T-1411.

The following Alloy 617 data are added in Table HBB-T-1411-1 of this Code Case.

Table HBB-T-1411-1		
	K'	
Material	**Elastic Analysis**	**Inelastic Analysis**
Alloy 617	0.9	0.67

HBB-T-1420   LIMITS USING INELASTIC ANALYSIS

(b) The fatigue damage term of Equation HBB-T-1411(10) is evaluated by entering a design fatigue curve at the strain range ϵ_t. The strain range ϵ_t is defined as $\epsilon_t = \Delta\epsilon_{max}$; where $\Delta\epsilon_{max}$ is the value calculated in either HBB-T-1413 or HBB-T-1414. The appropriate design fatigue curve for Alloy 617 is Figure HBB-T-1420-1F and corresponds to the maximum metal temperature experienced during the cycle.

(c) The total damage, *D*, shall not exceed the creep-fatigue damage envelope in Figure HBB-T-1420-2 of this Code Case.

Figure HBB-T-1420-1F
Design Fatigue Strain Range, ϵ_t, for Alloy 617
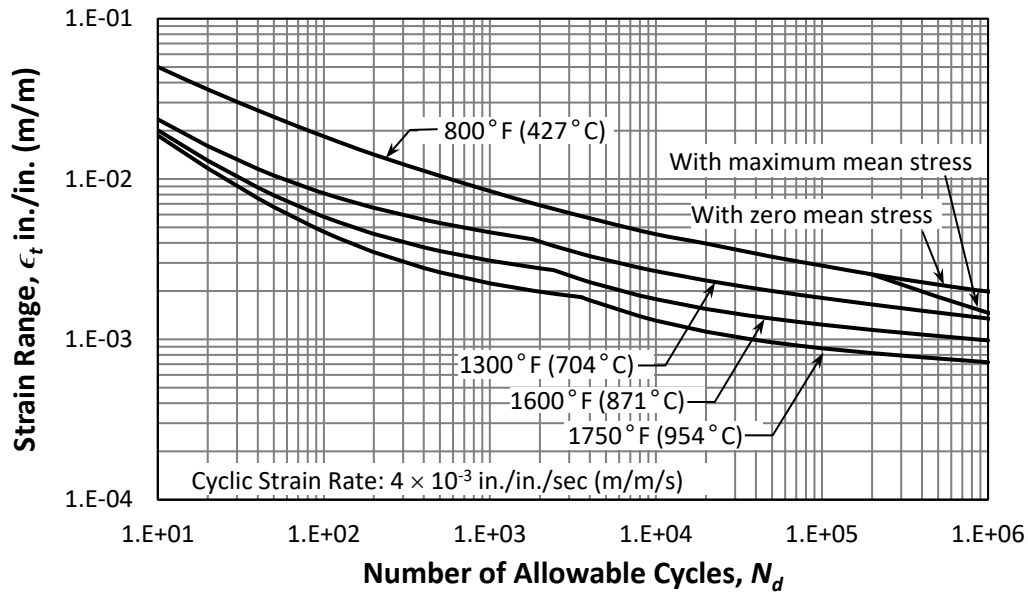
Number of Cycles, N_d [Note (1)]	U.S. Customary Units				
	Strain Range, ε_t, in./in. at Temperature				
	800°F Zero Mean Stress	**800°F** Maximum Mean Stress	**1,300°F**	**1,600°F**	**1,750°F**
1.E+01	0.05007	0.05007	0.02354	0.02015	0.01868
2.E+01	0.03621	0.03621	0.01606	0.01303	0.01166
4.E+01	0.02681	0.02681	0.01156	0.00885	0.00760
1.E+02	0.01846	0.01846	0.00815	0.00582	0.00469
2.E+02	0.01421	0.01421	0.00661	0.00455	0.00350
4.E+02	0.01123	0.01123	0.00558	0.00375	0.00279
1.E+03	0.00842	0.00842	0.00466	0.00310	0.00223
2.E+03	0.00686	0.00686	0.00407	0.00278	0.00198
4.E+03	0.00570	0.00570	0.00331	0.00227	0.00175
1.E+04	0.00453	0.00453	0.00266	0.00178	0.00131
2.E+04	0.00396	0.00396	0.00233	0.00155	0.00112
4.E+04	0.00340	0.00340	0.00207	0.00139	0.00099
1.E+05	0.00289	0.00289	0.00181	0.00124	0.00088
2.E+05	0.00254	0.00254	0.00165	0.00115	0.00082
4.E+05	0.00227	0.00199	0.00151	0.00107	0.00077
1.E+06	0.00199	0.00146	0.00135	0.00098	0.00072

Number of Cycles, N_d [Note (1)]	SI Units				
	Strain Range, ε_t, m/m at Temperature				
	427°C Zero Mean Stress	**427°C** Maximum Mean Stress	**704°C**	**871°C**	**954°C**
1.E+01	0.05007	0.05007	0.02354	0.02015	0.01868
2.E+01	0.03621	0.03621	0.01606	0.01303	0.01166
4.E+01	0.02681	0.02681	0.01156	0.00885	0.00760
1.E+02	0.01846	0.01846	0.00815	0.00582	0.00469
2.E+02	0.01421	0.01421	0.00661	0.00455	0.00350
4.E+02	0.01123	0.01123	0.00558	0.00375	0.00279
1.E+03	0.00842	0.00842	0.00466	0.00310	0.00223
2.E+03	0.00686	0.00686	0.00407	0.00278	0.00198
4.E+03	0.00570	0.00570	0.00331	0.00227	0.00175

Figure HBB-T-1420-1F
Design Fatigue Strain Range, ϵ_t, for Alloy 617 (Cont'd)

Number of Cycles, N_d [Note (1)]	SI Units				
	Strain Range, ε_t, m/m at Temperature				
	427°C Zero Mean Stress	427°C Maximum Mean Stress	704°C	871°C	954°C
1.E+04	0.00453	0.00453	0.00266	0.00178	0.00131
2.E+04	0.00396	0.00396	0.00233	0.00155	0.00112
4.E+04	0.00340	0.00340	0.00207	0.00139	0.00099
1.E+05	0.00289	0.00289	0.00181	0.00124	0.00088
2.E+05	0.00254	0.00254	0.00165	0.00115	0.00082
4.E+05	0.00227	0.00199	0.00151	0.00107	0.00077
1.E+06	0.00199	0.00146	0.00135	0.00098	0.00072

NOTE:

(1) Cyclic strain rate: 1×10^{-3} and 4×10^{-3} in./in./sec (m/m/s)

Figure HBB-T-1420-2
Creep-Fatigue Damage Envelope for Alloy 617

Figure HBB-T-1420-1F
Design Fatigue Strain Range, ϵ_t, for Alloy 617 (Cont'd)

Number of Cycles, N_d [Note (1)]	SI Units				
	Strain Range, ε_t, m/m at Temperature				
	427°C Zero Mean Stress	427°C Maximum Mean Stress	704°C	871°C	954°C
1.E+04	0.00453	0.00453	0.00266	0.00178	0.00131
2.E+04	0.00396	0.00396	0.00233	0.00155	0.00112
4.E+04	0.00340	0.00340	0.00207	0.00139	0.00099
1.E+05	0.00289	0.00289	0.00181	0.00124	0.00088
2.E+05	0.00254	0.00254	0.00165	0.00115	0.00082
4.E+05	0.00227	0.00199	0.00151	0.00107	0.00077
1.E+06	0.00199	0.00146	0.00135	0.00098	0.00072

NOTE:

(1) Cyclic strain rate: 1×10^{-3} and 4×10^{-3} in./in./sec (m/m/s)

Figure HBB-T-1420-2
Creep-Fatigue Damage Envelope for Alloy 617

Intersection (0.1, 0.1)

$\sum \dfrac{\Delta t}{T_d}$

$\sum \dfrac{n}{N_d}$

HBB-T-1430   LIMITS USING ELASTIC ANALYSIS

HBB-T-1431   General Requirements

(b) Revise the reference to the appropriate design fatigue curve to Figure HBB-T-1420-1F of this Code Case.

(d) The total damage, D, shall not exceed the creep- fatigue damage envelope of Figure HBB-T-1420-2 of this Code Case.

(e) Paragraph HBB-T-1431 is not applicable to Alloy 617 above 1200°F (650°C).

HBB-T-1432   Strain Range Determination

(c) Revise the references to the appropriate time -independent isochronous stress-strain curves to be Figures HBB-T-1836-1 through HBB-T-1836-20 of this Code Case.

(g) Revise the reference to the isochronous stress-strain curve to Figures HBB-T-1836-1 through HBB-T-1836-20 of this Code Case.

(h) Revise the reference to the design fatigue curves to Figure HBB-T-1420-1F of this Code Case.

HBB-T-1433   Creep Damage Evaluation

(a) In Step 4, revise the references to the time-independent isochronous stress-strain curves to be Figures HBB-T-1836-1 through HBB-T-1836-20 of this Code Case. In Step 5*(b)*, revise the references to the appropriate time-independent isochronous stress-strain curves to be Figures HBB-T-1836-1 through HBB-T-1836-20 of this Code Case. In Step 10, revise the reference to the expected minimum stress-to-rupture curve to Figure HBB-I-14.6G of this Code Case and K' is from Table HBB-T-1411-1 of this Code Case.

(b) Revise the reference to the expected minimum stress-to-rupture curve to Figure HBB-I-14.6G of this Code Case and K' is from Table HBB-T-1411-1 of this Code Case.

HBB-T-1435   Alternate Creep-Fatigue Evaluation

(a) The reference to Section III Appendices, Mandatory Appendix I is replaced by Figure HBB-T-1420-1F, where S_a is one-half the product of ϵ_t and Young's Modulus, E, is at the metal temperature of the cycle for the point under consideration.

HBB-T-1440 CREEP-FATIGUE DAMAGE LIMITS USING ELASTIC-PERFECTLY PLASTIC ANALYSIS

HBB-T-1441   General Requirements

Fatigue and creep damage may be evaluated using elastic-perfectly plastic material models instead of the procedures of HBB-T-1420, HBB-T-1430 and HBB-T-1715, when performed in accordance with the requirements of this subsubarticle.

The design methodology employed for evaluation of creep damage is based on elastic shakedown analyses using an elastic-perfectly plastic material model, small strain theory, and a pseudo-yield stress selected to bound creep damage. In this subsubarticle, "shakedown" refers to the achievement of cyclic elastic behavior throughout the part, based on real or pseudo-yield stress. In this Code Case, the term "pseudo-yield stress" refers to a temperature-dependent minimum stress-to-rupture value based on a selected trial time duration, not to exceed the yield strength of the material at temperature and is explicitly defined in HBB-T-1444.2. Guidance on shakedown analysis is provided in HBB-T-1447.

HBB-T-1441.1.   Allowable Damage Accumulation. The combination of Levels A, B, and C Service Loadings shall be evaluated for accumulated creep and fatigue damage, including hold time and strain rate effects. For a design to be acceptable, the creep and fatigue damage at each point in the component shall satisfy the following relation:

$$D_c + D_f \leq D \tag{2}$$

where

> D = total creep-fatigue damage, as limited by Figure HBB-T-1420-2 of this Code Case

> D_c = creep damage, as determined in paragraph HBB-T-1444, below

> D_f = fatigue damage, as determined in paragraph HBB-T-1445, below

This design methodology is not applicable to structures where geometrical nonlinearities exist, e.g., canopy and omega seals.

HBB-T-1442   Load Definition

Define all applicable loads and load cases per Section III, Division 5, HBB-3113.2, Service Loadings.

HBB-T-1442.1   Composite Cycle Definition. For the purpose of performing an elastic-perfectly plastic shakedown analysis, an overall cycle must be defined that includes all relevant features from the individual Level A, B and C Service Loadings identified in the Design Specification. Relevant features include, as a minimum, the time-dependent sequence of thermal, mechanical and pressure loading, including starting and ending conditions. Such an overall cycle is defined herein as a composite cycle subject to the following requirements:

(a) An individual cycle as defined in the Design Specification cannot be further subdivided into individual cycles to satisfy these requirements.

(b) Except as described in *(c)* below, a single cycle from each Level A, B and C Service Loading cycle type shall be included in the composite cycle for evaluation of creep-fatigue.

(c) Level C Service Loadings may be combined with the applicable Level A and B Service Loadings to define a composite cycle(s) to be evaluated separately from the composite cycle defined in *(b)* above. Multiple composite cycles that include Level C Service Loadings may be defined for separate evaluation. The total number of Level C Service Loading cycles shall not exceed 25.

HBB-T-1443   Numerical Model

Develop a numerical model of the component, including all relevant geometry characteristics. The model used for the analysis shall be selected to accurately represent the component geometry, boundary conditions, and applied loads. The model must also be accurate for small details, such as small holes, fillets, corner radii, and other stress risers. The local temperature history shall be determined from a thermal transient analysis based on the thermal boundary conditions determined from the loading conditions defined in paragraph HBB-T-1442.

HBB-T-1444   Calculation of Creep Damage

Perform a shakedown analysis for each of the composite cyclic histories defined in HBB-T-1442.1. Each of these cyclic histories must be shown to shakedown based on the pseudo-yield stress, $S_{Td'}$, as defined in HBB-T-1444.2. Additional requirements for welds are found in HBB-T-1446.

HBB-T-1444.1 **Step 1.** Define t_{design} as the total time duration of elevated temperature service for all Level A, B, and C Service Loadings when the temperature is above 800°F (427°C).

HBB-T-1444.2 **Step 2.** Select a trial time duration, T_d', in order to define a pseudo-yield stress, $S_{Td'}$, at each location, using the temperature determined from the transient thermal analysis. This pseudo-yield stress is equal to the lesser of the quantities defined in *(a)* and *(b)* below.

(a) The yield strength, S_y, given in Table HBB-I-14.5 of this Code Case;

(b) S_r, where S_r is the minimum stress to rupture in time, T_d', from Figure HBB-I-14.6G multiplied by the factor, K', from Table HBB-T-1411-1 of this Code Case, using the tabulated values for elastic analysis.

HBB-T-1444.3 **Step 3.** Perform a cyclic elastic-perfectly plastic analysis for each composite cycle defined in HBB-T-1442 above with temperature-dependent pseudo-yield stress, $S_{Td'}$. The assessment temperature shall be taken as the local instantaneous temperature at every location in the numerical model of the component. If shakedown occurs, that is, cycles with eventual elastic behavior everywhere, proceed to HBB-T-1444.4.

HBB-T-1444.4 **Step 4.** The maximum creep damage over the structure for the composite cycle under consideration is:

$$D_c = \frac{t_{design}}{T_d'}$$

(3)

The above value of D_c is used to evaluate total damage in Equation (2). If the pseudo-yield stress in HBB-T-1444.2 is governed by the yield strength as defined in HBB-T-1444.2(a), then the trial time duration for use in Equation (3) is given by the time at which the minimum stress to rupture is equal to the yield strength; $S_r = S_y$. Linear extrapolation of S_r values corresponding to the two longest tabulated times can be used to obtained the trial time duration, when necessary.

(a) HBB-T-1444.2 through HBB-T-1444.4 may be repeated to revise the value of D_c by selecting alternative values of the trial time duration, T_d'. Longer values of T_d' will reduce the calculated creep damage. However, these longer values will lead to lower values of the pseudo-yield stress, $S_{Td'}$, which will make shakedown more difficult to achieve. If it is not possible to achieve shakedown, then the loading conditions of HBB-T-1442 applied to the component configuration defined in HBB-T-1443 do not meet the requirements of HBB-T-1440.

HBB-T-1445   Calculation of Fatigue Damage

The fatigue damage summation, D_f, in Equation (2) is determined in accordance with HBB-T-1445.1 through HBB-T-1445.3 below. Additional requirements for welds are found in HBB-T-1446.

HBB-T-1445.1 **Step 1.** Determine all of the total (elastic plus plastic) strain components for the composite cycle at each point of interest from the shakedown analysis performed in HBB-T-1444.3 above.

HBB-T-1445.2 **Step 2.** Calculate the equivalent strain range in accordance with HBB-T-1413, or HBB-T-1414 when applicable, with Poisson's ratio $v* = 0.3$.

HBB-T-1445.3 **Step 3.** Determine the fatigue damage for each composite cycle from the expression:

$$D_f = \sum_j \frac{n_j}{(N_d)_j}$$

(4)

where

n_j = number of applied repetitions of cycle type, j

$(N_d)_j$ = number of design allowable cycles for cycle type, j, determined from Figure HBB-T-1420-1F, corresponding to the maximum metal temperature occurring during the cycle.

The value of D_f used to evaluate total damage in Equation (2) is the maximum value at any location in the numerical model.

HBB-T-1446   Weldments

Implementation of the evaluation of creep-fatigue damage in HBB-T-1444 and HBB-T-1445 above for weldments requires additional consideration.

HBB-T-1446.1   Pseudo-Yield Stress. In the weld region, the pseudo-yield stress value, $S_{Td'}$, defined by T_d' in HBB-1444.2(b) is reduced further by multiplying the value of S_r for the base metal by the applicable weld strength reduction factor from Table HBB-I-14.10F-1.

HBB-T-1446.2   Allowable Cycles. The number of allowable cycles, $(N_d)_j$, in the weld region is one-half the number of allowable cycles from Figure HBB-T-1420-1F for base metal.

HBB-T-1446.3   Geometry. The requirements for analysis of geometry of HBB-T-1714 are applicable for satisfaction of the requirements of this Code Case.

HBB-T-1446.4   Physical Properties. The thermal/physical properties of weldments shall be assumed to be the same as the corresponding base metal for the base metal-weld combinations listed in Table HBB-I-14.10F-1.

HBB-T-1446.5   Weld Region Model Boundaries. Figure HBB-T-1345 shows a full penetration butt weld as an example of the definition of a weld region. As shown, w_1 and w_2 are needed to define the weld region for use in this Code Case and are approximations consistent with the specified weld configuration and parameters. The specified weld region must include applicable stress concentrations in accordance with the requirements for analysis of geometry, HBB-T-1714, unless ground flush.

The weld shown in Figure HBB-T-1345 represents a full penetration butt weld in a shell. Other weld configurations may be needed for construction of an elevated temperature service component in accordance with Section III, Division 5, Subsection HB, Subpart B. Section III, Division 5, HBB-4200 refers to various Section III, Division 1, Article NB-4000 paragraphs for weld configurations and requirements. These NB-4000 weld configurations are represented by the shaded region.

HBB-T-1446.6   Dissimilar metal welds. The requirements for dissimilar metal welds are in the course of preparation.

HBB-T-1447   Shakedown Analysis

The steps to perform a shakedown analysis to calculate bounding creep damage are as follows:

(a) Define Composite Cycle Load Time-Histories and Analysis Step(s).

(1) It may consist of histories of mechanical loads, pressure loads, displacements, temperatures and thermal boundary conditions.

(2) Time-independent parts of the cycle may be truncated because the elastic-perfectly plastic analysis is not time-dependent.

(3) The cycle should not have discontinuities. Discontinuities arising from the selection of the specified cycles to form a composite cycle should be eliminated by a simple and reasonable transition from one operating state to the next.

(4) Subject to the requirements in *(b)* below, the composite cycle time does not affect the result of the shakedown analysis.

(5) Temperatures, thermal boundary conditions, boundary displacements and mechanical loads over a cycle should be cyclic; that is, begin and end at the same value.

(6) A single analysis step may represent one cycle. Dividing a single cycle into more than one step to facilitate definition of the load cycle, and to ensure that maximum loads are analyzed, is often helpful.

(b) Define Analysis Types.

(1) A sequentially coupled thermal-mechanical analysis of the composite cycle may be performed. First, a thermal analysis is performed to generate temperature histories. Next, the mechanical analyses are performed using these temperature histories as inputs. Care must be taken that times in the mechanical analysis step and in the previous thermal analysis are the same or do not conflict, depending on the requirements of the analysis software.

(2) Alternatively, a coupled thermal-mechanical analysis may be performed. The composite temperature history to be used in the mechanical analysis should be cyclic; that is, the beginning and end temperature distributions should be the same.

(c) Define Material Properties.

(1) For thermal analyses, density, temperature-dependent specific heat and conductivity will generally be required.

(2) For the mechanical analyses, the temperature-dependent properties required are elastic modulus, Poisson's ratio, and mean expansion coefficient. Density may also be required.

(d) Perform Analyses.

(1) Perform an elastic-perfectly plastic cyclic mechanical and thermal stress analysis using the temperature-dependent pseudo-yield stress defined above. Enough cycles are required to demonstrate shakedown or otherwise.

(2) Care must be taken to ensure that the analysis deals with all the changes within a cycle. Elastic-plastic analysis routines increase increment size where possible, and may miss a detail in the loading. A conservative limit to maximum increment size can address this problem, as can division of the cycle into more than one step, as discussed in *(a)(6)* above.

(e) Shakedown. Shakedown is defined in this Code Case as eventual elastic behavior everywhere in the model. Failure to achieve shakedown may be identified by plotting history plots of equivalent plastic strain.

HBB-T-1500 BUCKLING AND INSTABILITY

HBB-T-1510 GENERAL REQUIREMENTS

HBB-T-1510 *(g)* Add reference to the Alloy 617 hot tensile curves of Figures HBB-T-1836-1 through 20 and the tabulated yield strength in Table HBB-I-14.5 of this Code Case.

HBB-T-1520 BUCKLING LIMITS

HBB-T-1522 Time-Dependent Buckling

The following curves for Alloy 617 are added to Figures HBB-T-1522-1, HBB-T-1522-2, and HBB-T-1522-3.

Figure HBB-T-1522-1
Time-Temperature Limits for Application of Section II External Pressure Charts
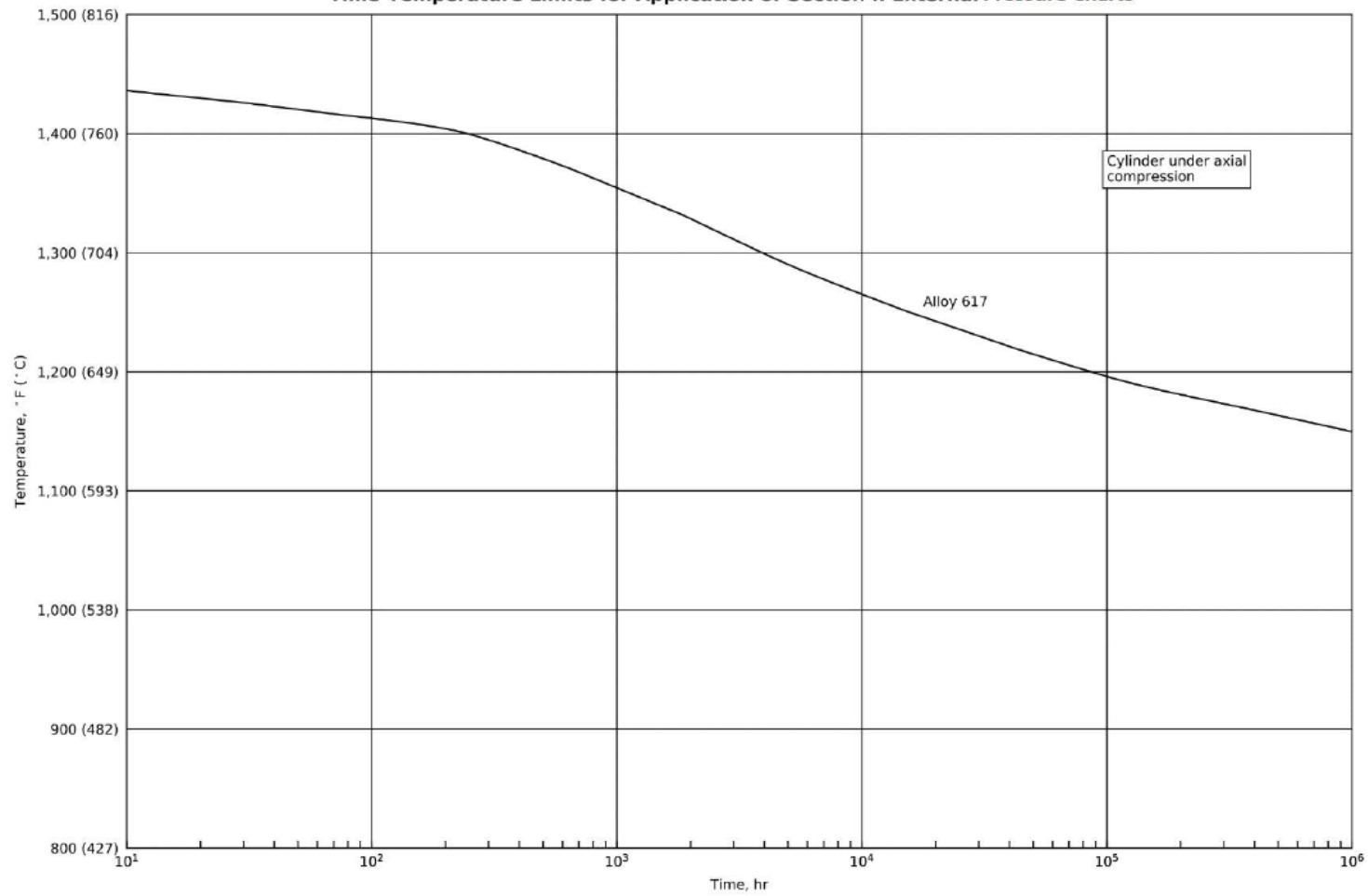
Figure HBB-T-1522-2
Time-Temperature Limits for Application of Section II External Pressure Charts
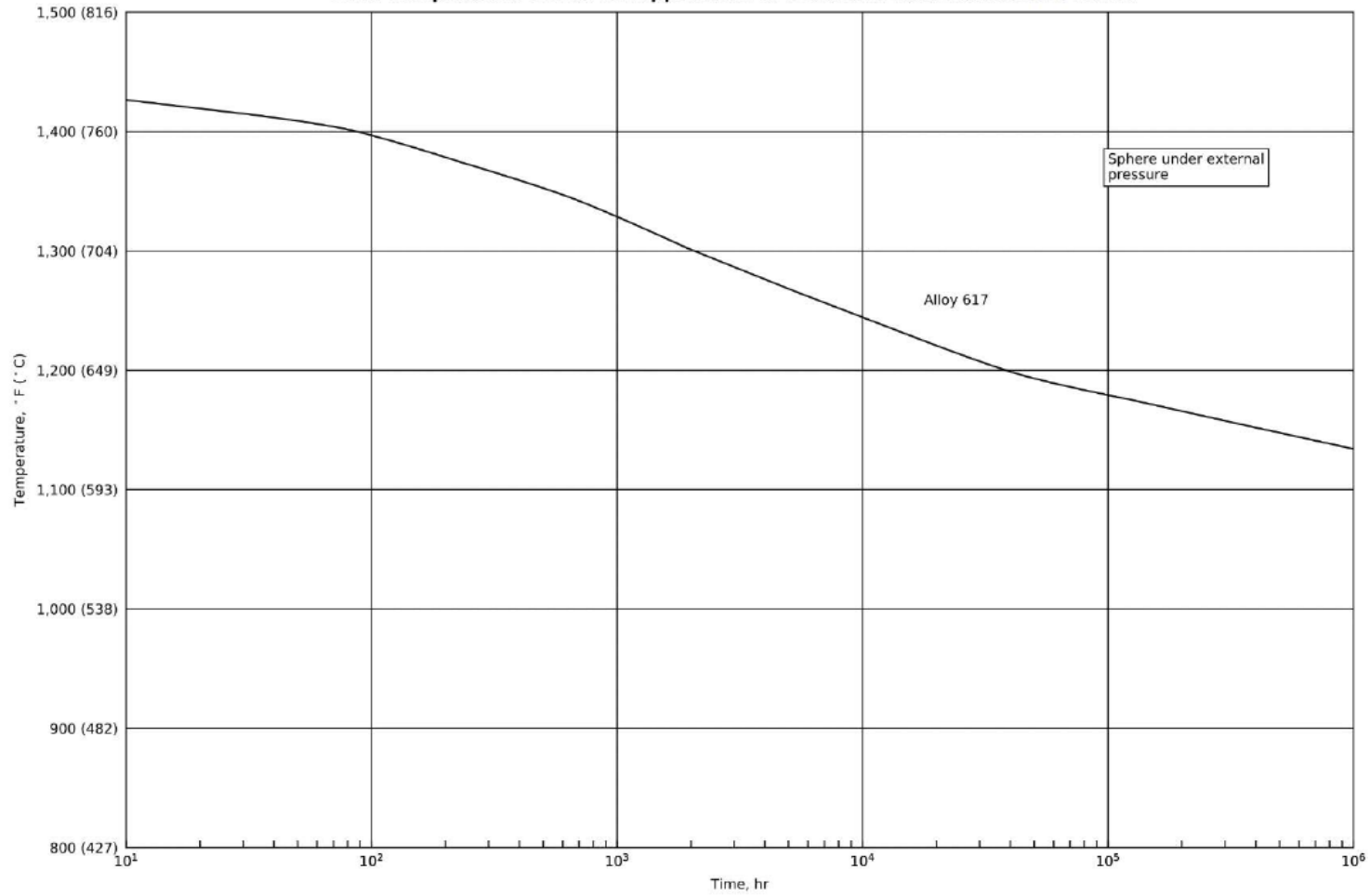
**Figure HBB-T-1522-3
Temperature Limits for Application of Section II External Pressure Charts**
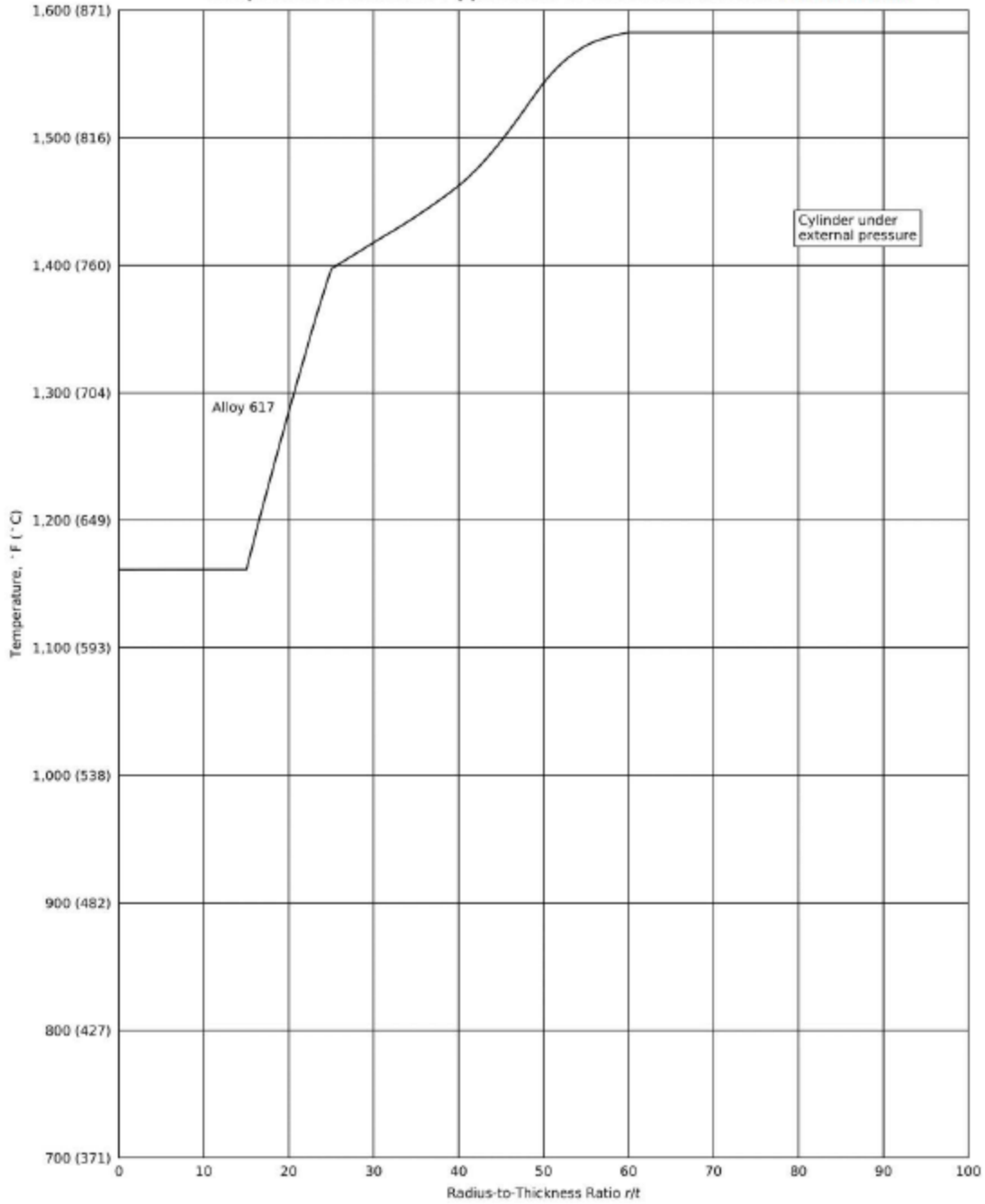
HBB-T-1700   SPECIAL REQUIREMENTS

HBB-T-1710   SPECIAL STRAIN REQUIREMENTS AT WELDS

HBB-T-1715   Creep-Fatigue Reduction Factors

Revise the reference for allowable number of design cycles, N_d, for parent material to Figure HBB-T-1420-1F of this Code Case. Revise the reference for the allowable time duration, T_d, based on parent material stress-to-rupture to HBB-I-14.6G of this Code Case and the reference for weld strength reduction factor to Table HBB-I-14.10F-1 of this Code Case. The factor K' is from Table HBB-T-1411-1 of this Code Case.

HBB-T-1800   ISOCHRONOUS STRESS‑STRAIN RELATIONS

HBB-T-1810   OBJECTIVE

HBB-T-1820 MATERIALS AND TEMPERATURE LIMITS

Data for Alloy 617 is added in Table HBB-T-1820-1 of this Code Case as indicated below.

Table HBB-T-1820-1

Material	Maximum Temp., °F (°C)	Temperature Increment, °F (°C)
Alloy 617	1750 (954)	50 (28)

HBB-T-1830 EQUATIONS FOR THE ISOCHRONOUS CURVES

The equations for determining the elastic strain, plastic strain and creep strain are expressed in terms of temperature and stress in SI units. When working in US Customary units or other local customary units, the temperature and stress values should first be converted to °C and MPa units, respectively, and then be entered into the equations to obtain the appropriate strain values.

HBB-T-1836   Alloy 617

(a) Elastic strain:

$$\varepsilon_e = \frac{\sigma}{E}$$

with E the temperature-dependent value of Young's modulus found in Table TM-4 (M) of this Code Case.

(b) Plastic strain:

$$\varepsilon_p = \begin{cases} \begin{cases} 0 & \sigma \leq \sigma_0 \\ K\left(\dfrac{\sigma - \sigma_0}{\sigma_0}\right)^n & \sigma > \sigma_0 \end{cases} & T \leq 750°C \\ \begin{cases} 0 & \sigma \leq \sigma_1 \\ \dfrac{1}{\delta}\ln\left(1 - \dfrac{\sigma - \sigma_1}{\sigma_p - \sigma_1}\right) & \sigma > \sigma_1 \end{cases} & T > 750°C \end{cases}$$

where Table HBB-T-1836-1gives the temperature-dependent values of the parameters σ_0, K, and n, and Table HBB-T-1836-2 gives the temperature-dependent values of σ_1, δ, and σ_p. The parameters may be linearly interpolated between temperature values in Tables HBB-T-1836-1 and HBB-T-1836-2.

Table HBB-T-1836-1

T (°C)	σ_0 (MPa)	K (-)	n (-)
427	175	0.056	1.96
450	170	0.053	1.97
500	166	0.050	2.01
550	165	0.052	1.84
600	178	0.067	1.50
650	209	0.13	2.13
700	206	0.12	2.29
750	205	0.093	1.55

Table HBB-T-1836-2

T (°C)	σ_1 (MPa)	σ_p (MPa)	δ (-)
750	228	522	9.70
800	178	317	35.5
850	50	214	482
900	51	164	1250
954	54	122	1240

(c) Creep strain:

$$
\varepsilon_c = \begin{cases} \dot{\varepsilon}_0 e^{B_1 \mu b^3/(AkT_k)} \left(\dfrac{\sigma}{\mu}\right)^{-\mu b^3/(AkT_k)} t & T \leq 775^\circ\ \mathrm{C} \\[2ex] \dot{\varepsilon}_0 e^{B_2 \mu b^3/(AkT_k)} \left(\dfrac{\sigma}{\mu}\right)^{-\mu b^3/(AkT_k)} t & T > 775^\circ\ \mathrm{C} \end{cases}
$$

where Table HBB-T-1836-3 gives the values of the parameters $\dot{\varepsilon}_0$, A, B_1, B_2, b, and k;

$$T_k = T + 273.15$$

and

$$\mu = \frac{E}{2(1 + \nu)}$$

where E is the temperature-dependent value of Young's modulus found in Table TM-4 (M) of this Code Case and ν is the temperature-dependent value of Poisson's ratio found in Section II, Part D (Metric) Table PRD for Alloy 617.

Table HBB-T-1836-3

Parameter	Value
$\dot{\varepsilon}_0$	1.656e7 hrs^{-1}
A	-4.480
B_1	-2.510
B_2	-3.174
b	2.019e-7 mm
k	1.38064e-20 mJ/K

Figure HBB-T-1836-1
Average Isochronous Stress-Strain Curves

Hot tensile to 100,000 hr

Material-Alloy 617
Temperature-800°F (427°C)

Stress, 1000 psi (MPa)
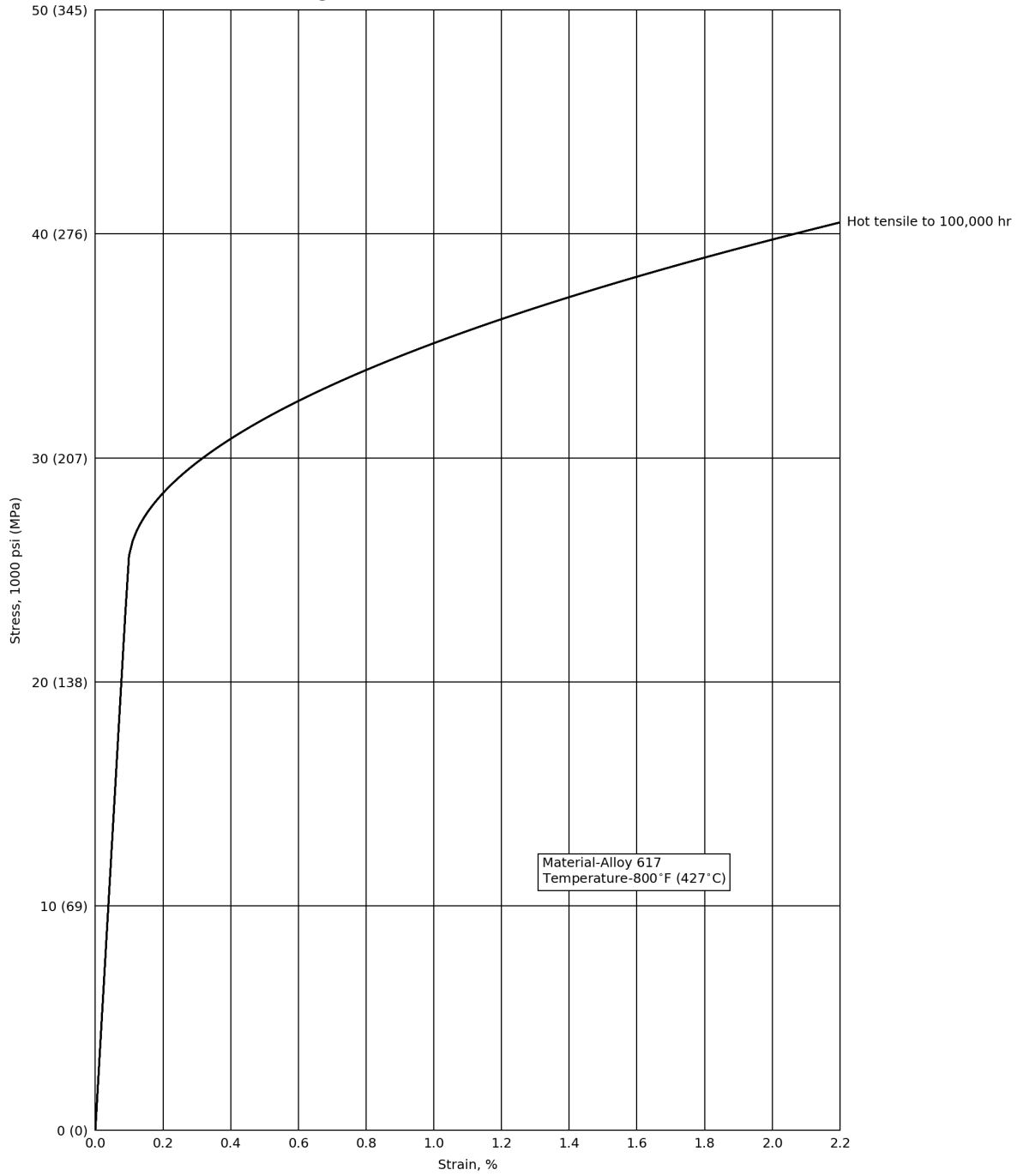
Strain, %

Figure HBB-T-1836-2
Average Isochronous Stress-Strain Curves

Hot tensile to 100,000 hr

Material-Alloy 617
Temperature-850°F (454°C)

Stress, 1000 psi (MPa)
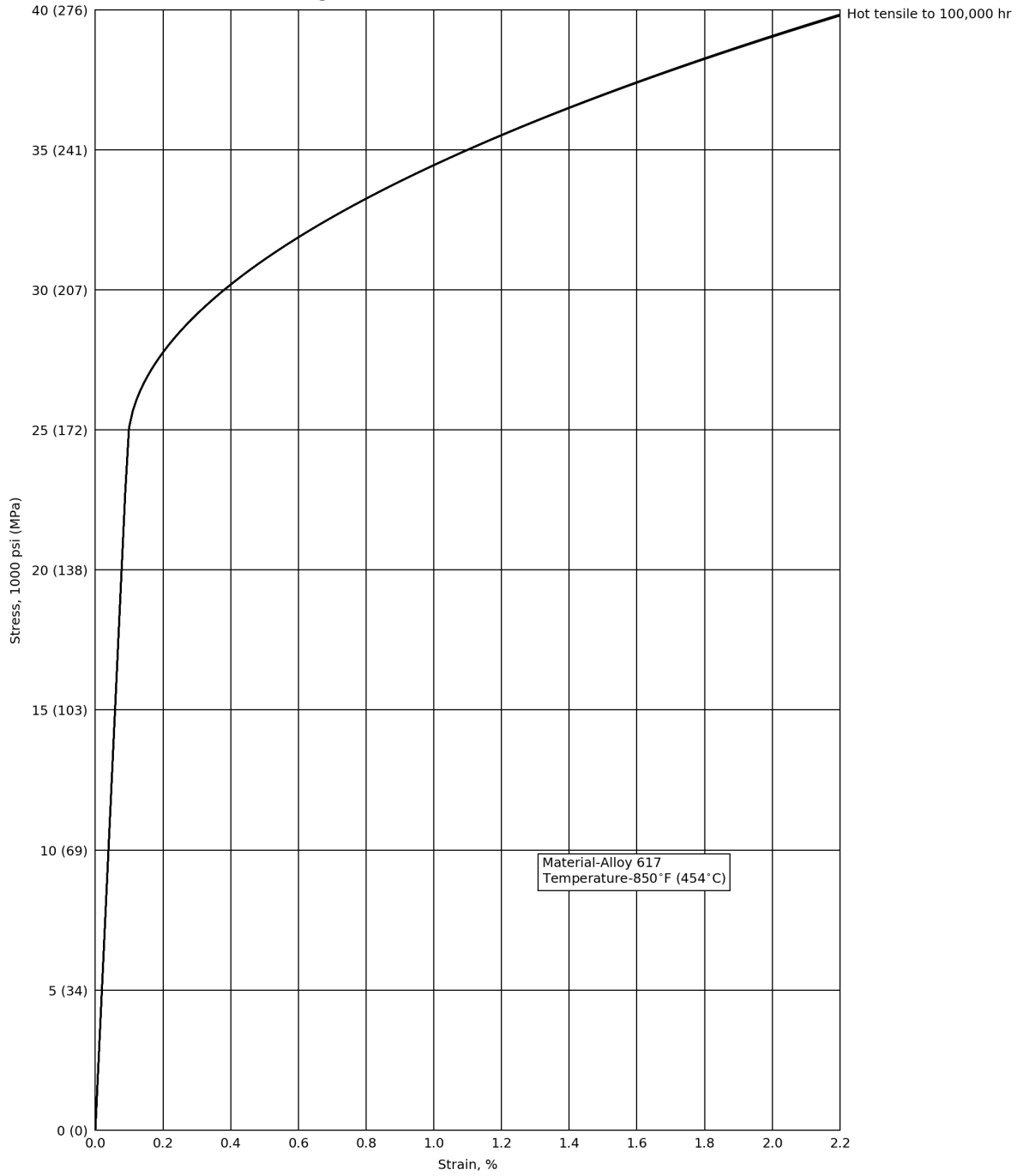
Strain, %

Figure HBB-T-1836-3
Average Isochronous Stress-Strain Curves

Hot tensile to 100,000 hr

Material-Alloy 617
Temperature-900°F (482°C)

Stress, 1000 psi (MPa)
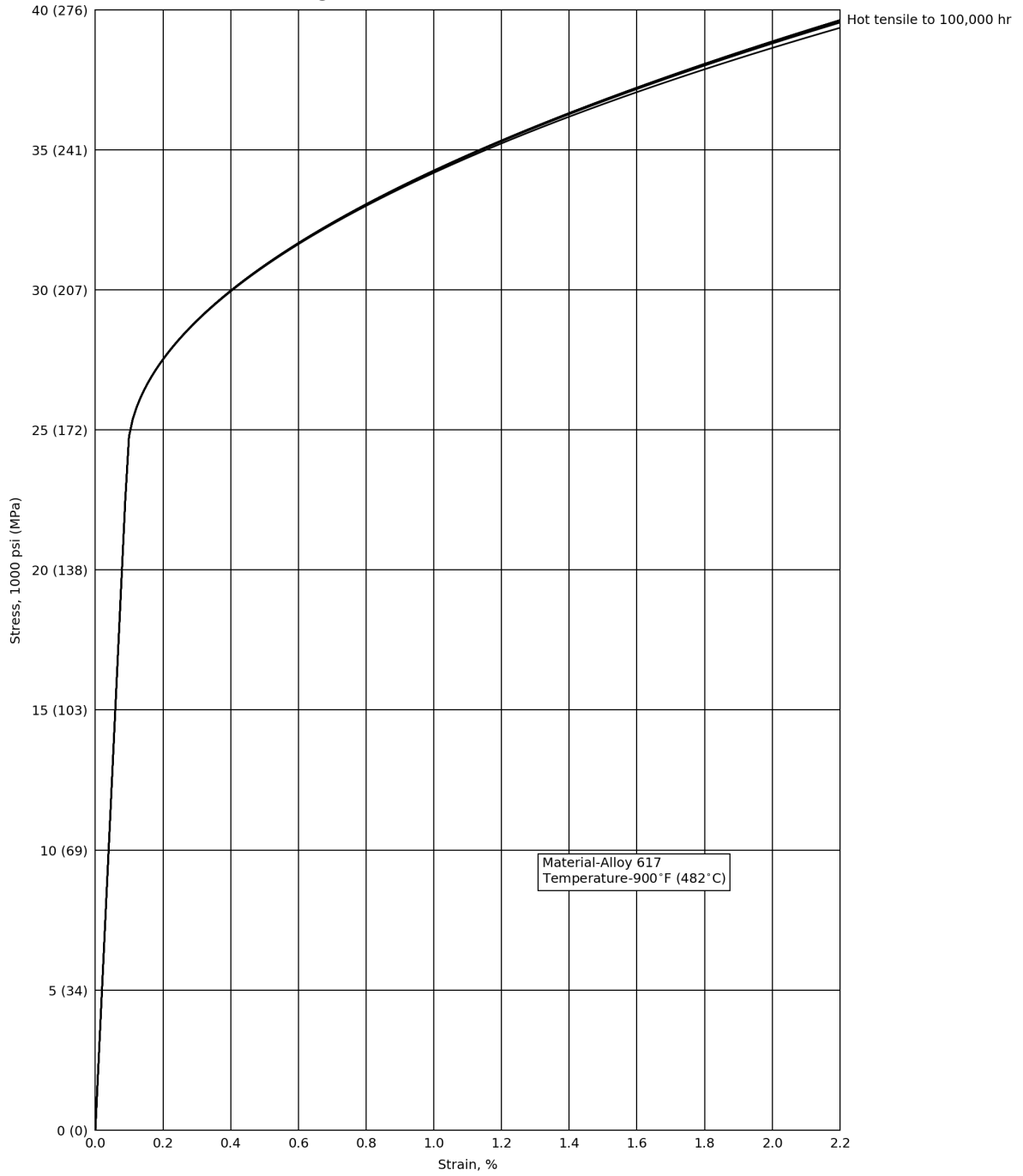
Strain, %

Figure HBB-T-1836-4
Average Isochronous Stress-Strain Curves

Hot tensile to 30,000 hr

100,000 hr

Material-Alloy 617
Temperature-950°F (510°C)

Stress, 1000 psi (MPa)
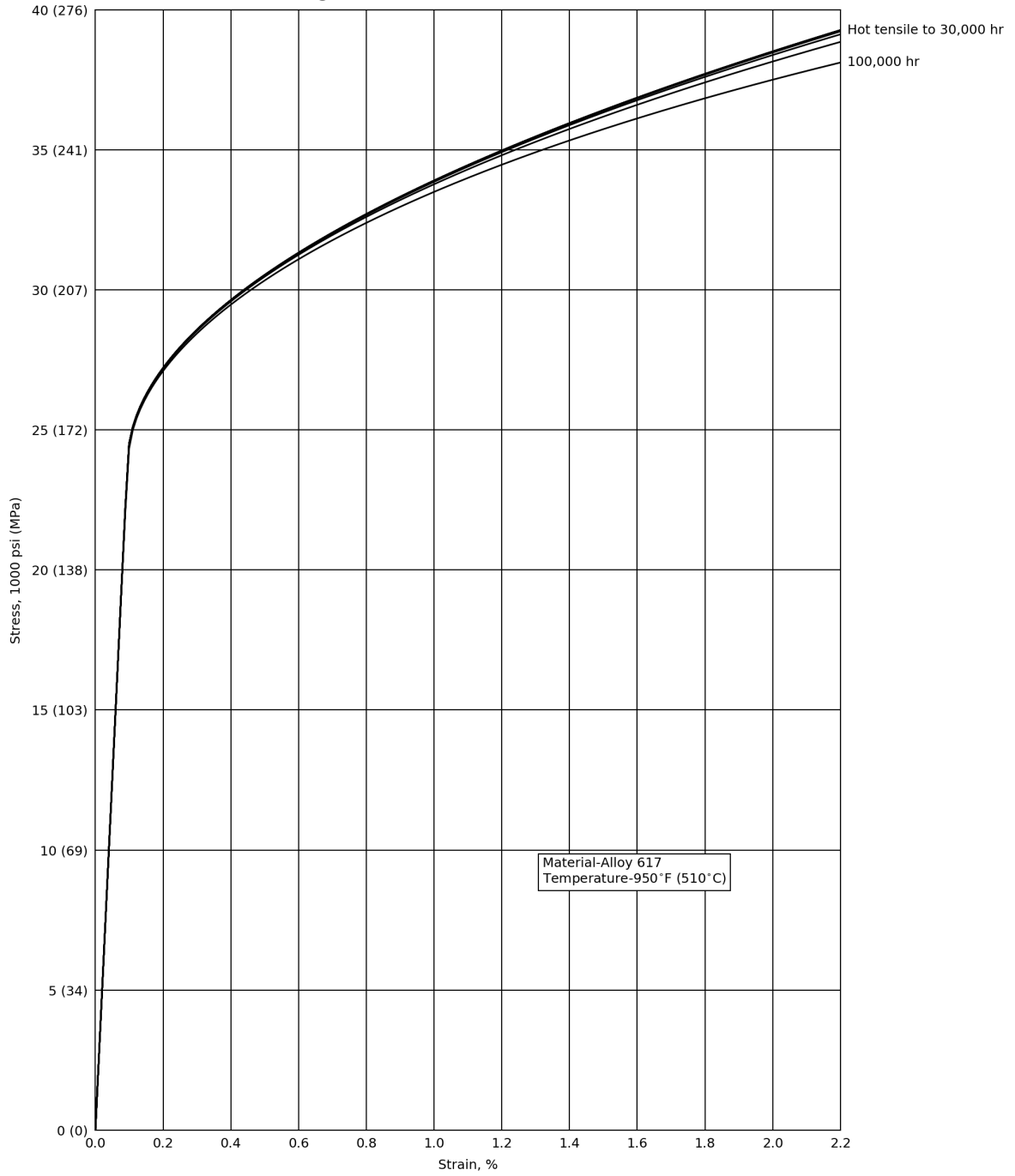
Strain, %

Figure HBB-T-1836-5
Average Isochronous Stress-Strain Curves

Hot tensile to 10,000 hr

30,000 hr

100,000 hr

Material-Alloy 617
Temperature-1000°F (538°C)

Stress, 1000 psi (MPa)
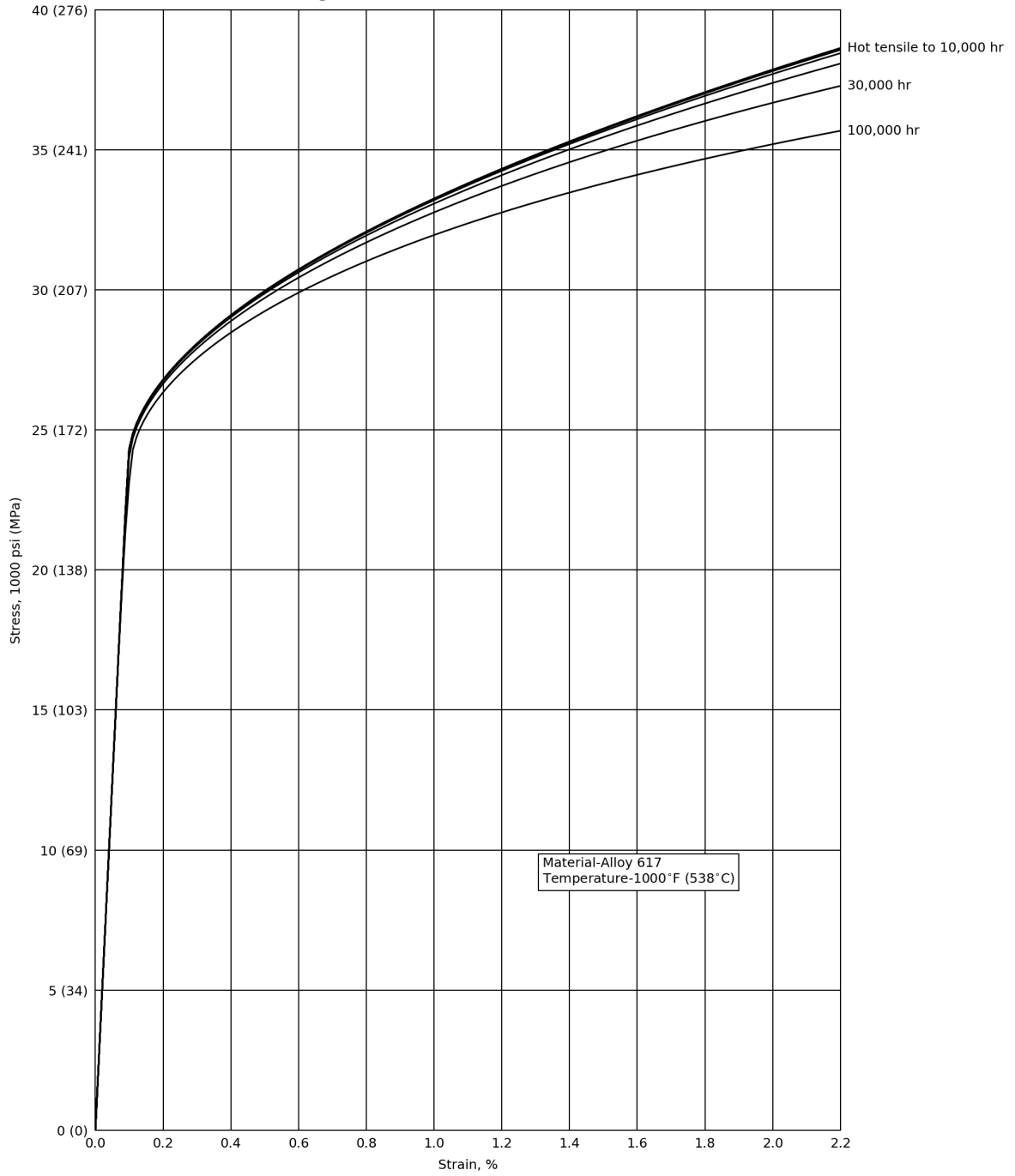
Strain, %

Figure HBB-T-1836-6
Average Isochronous Stress-Strain Curves

Hot tensile to 3,000 hr

10,000 hr

30,000 hr

100,000 hr

Material-Alloy 617
Temperature-1050°F (566°C)

Stress, 1000 psi (MPa)
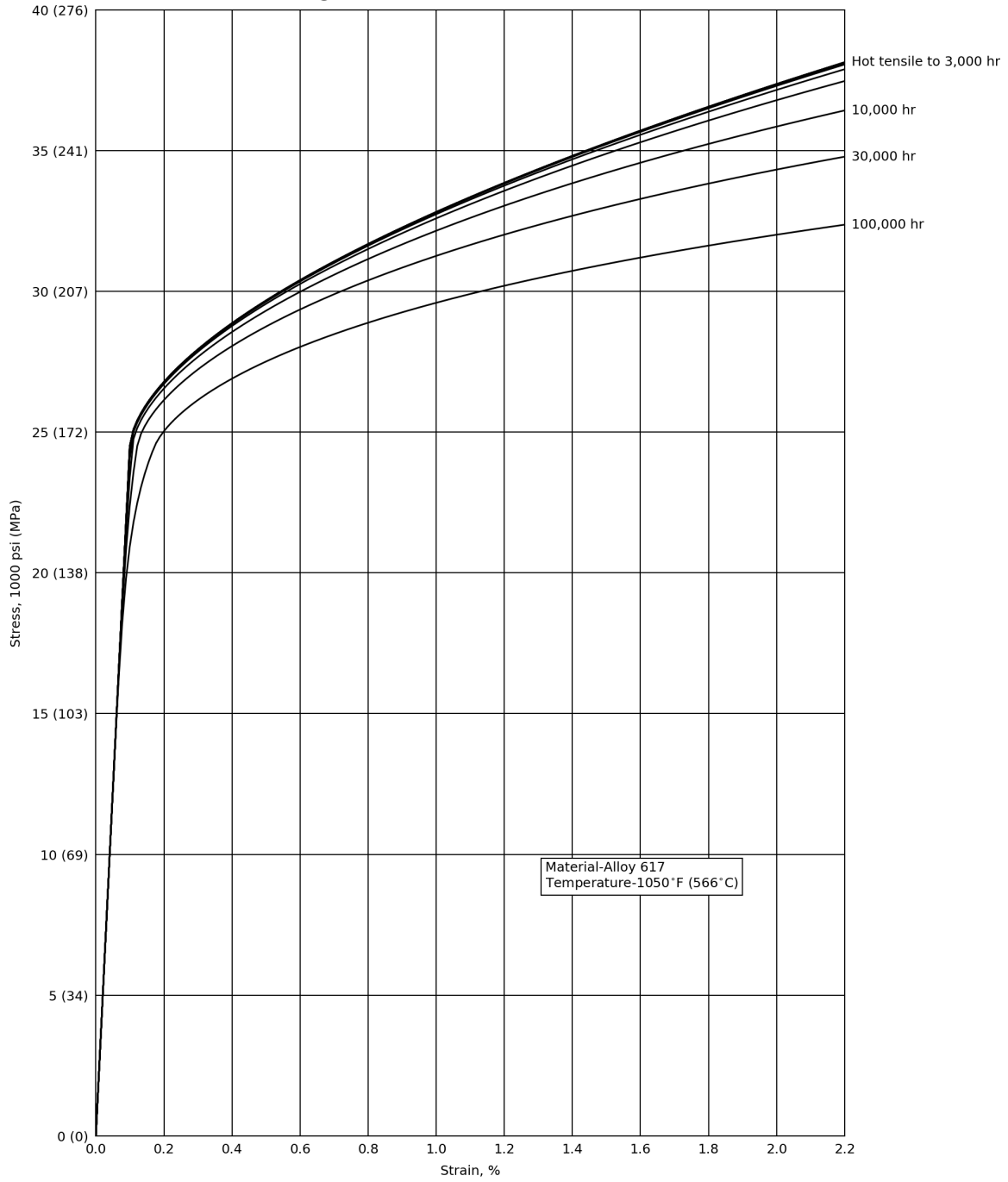
Strain, %

Figure HBB-T-1836-7
Average Isochronous Stress-Strain Curves

Hot tensile to 1,000 hr

3,000 hr

10,000 hr

30,000 hr

100,000 hr

Material-Alloy 617
Temperature-1100°F (593°C)

Stress, 1000 psi (MPa)
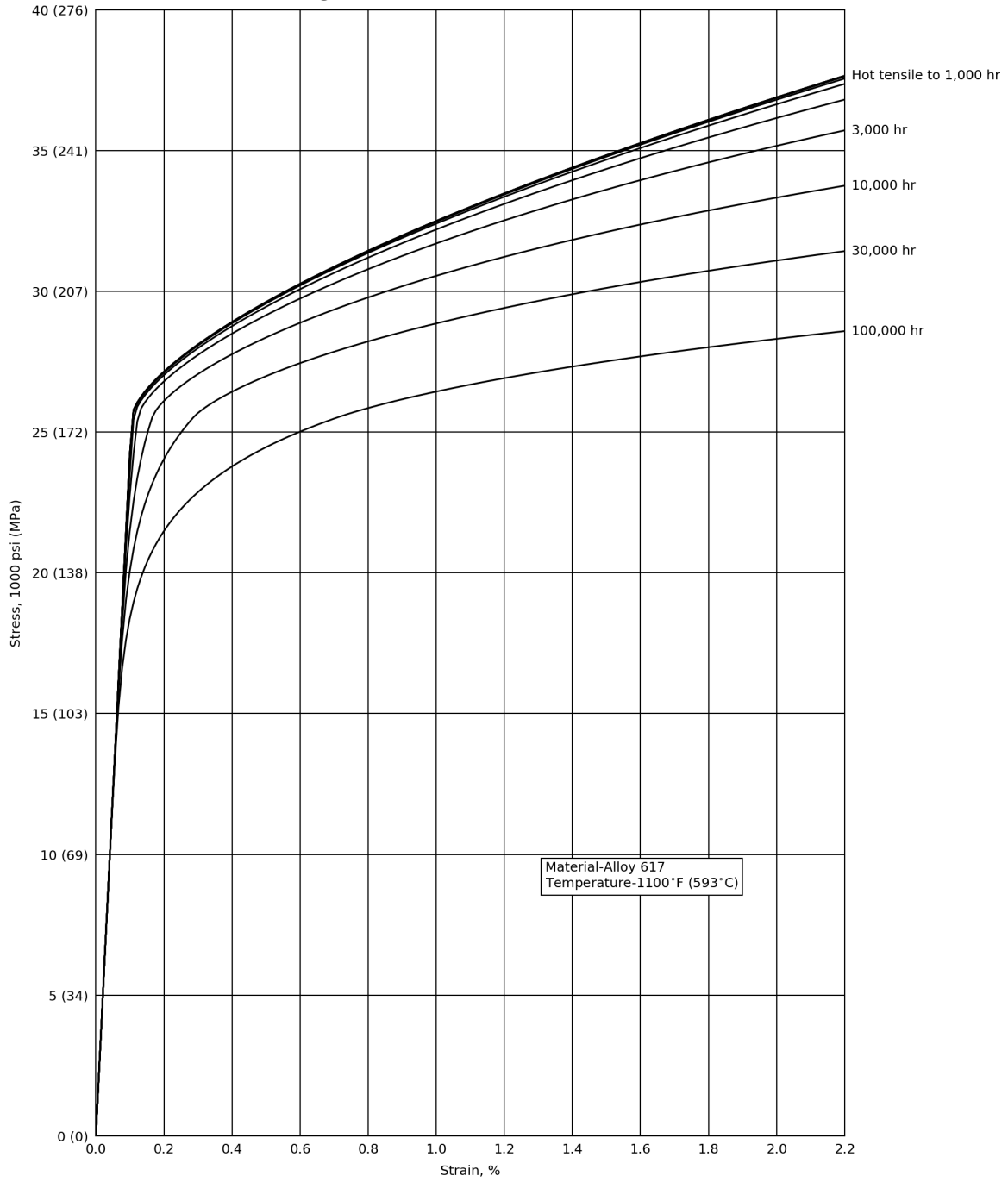
Strain, %

Figure HBB-T-1836-8
Average Isochronous Stress-Strain Curves

Hot tensile to 100 hr
300 hr
1,000 hr
3,000 hr
10,000 hr
30,000 hr
100,000 hr

Stress, 1000 psi (MPa)

40 (276)
35 (241)
30 (207)
25 (172)
20 (138)
15 (103)
10 (69)
5 (34)
0 (0)

0.0   0.2   0.4   0.6   0.8   1.0   1.2   1.4   1.6   1.8   2.0   2.2

Strain, %

Material-Alloy 617
Temperature-1150°F (621°C)
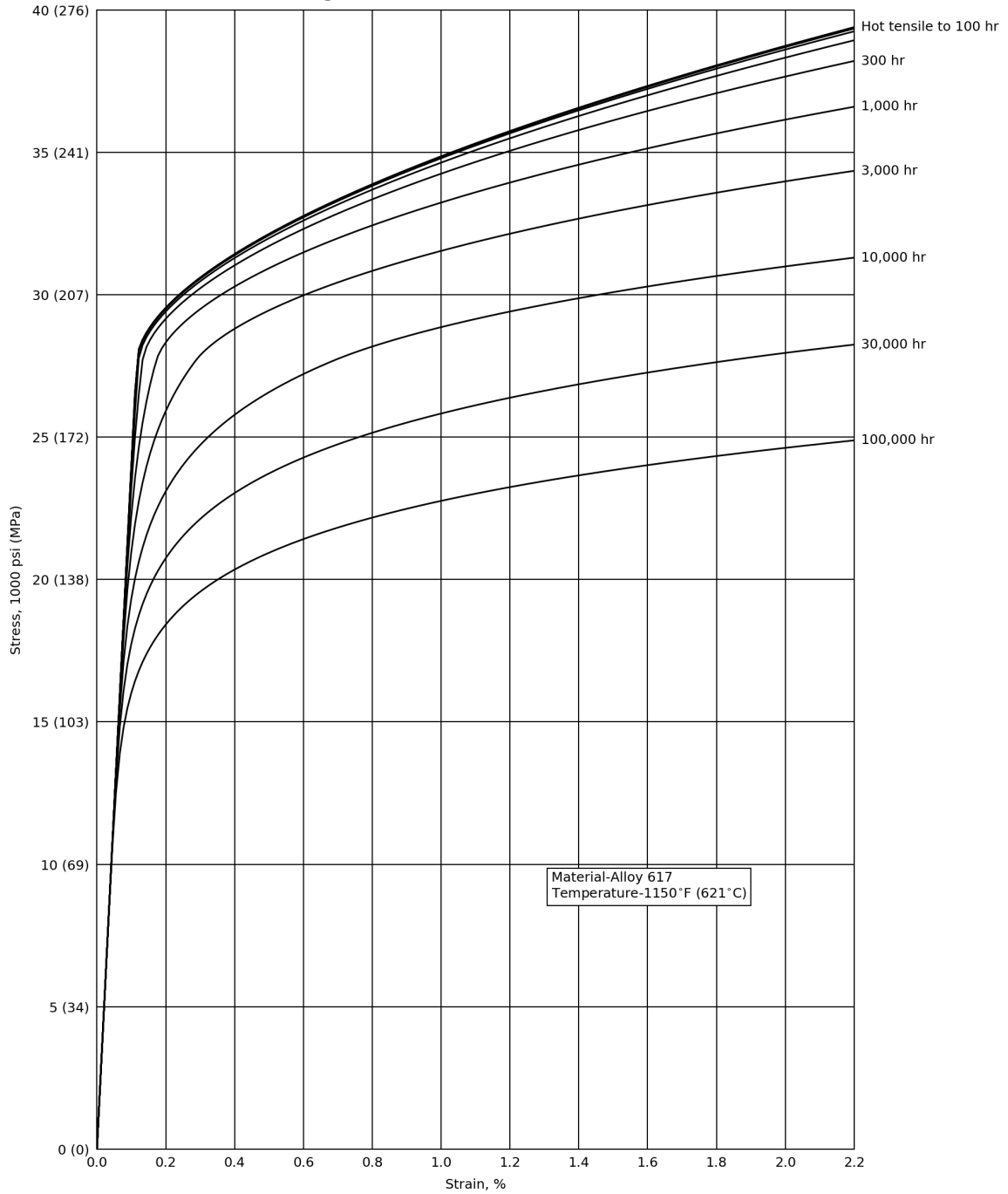
Figure HBB-T-1836-9
Average Isochronous Stress-Strain Curves

Hot tensile to 30 hr
100 hr
300 hr
1,000 hr
3,000 hr
10,000 hr
30,000 hr
100,000 hr

Stress, 1000 psi (MPa)

Strain, %

Material-Alloy 617
Temperature-1200°F (649°C)
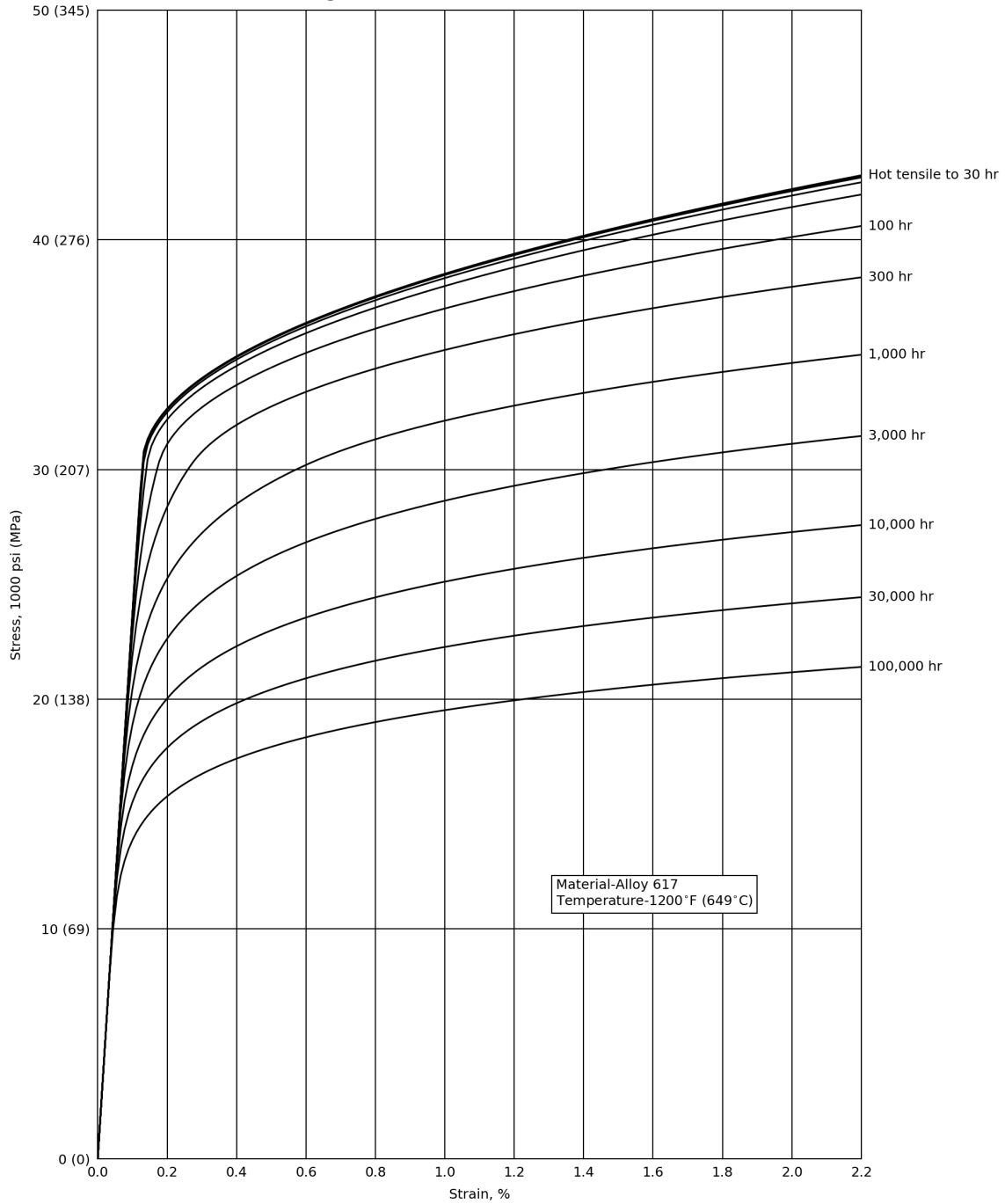
Figure HBB-T-1836-10
Average Isochronous Stress-Strain Curves

Hot tensile to 3 hr
10 hr
30 hr
100 hr
300 hr
1,000 hr
3,000 hr
10,000 hr
30,000 hr
100,000 hr

Material-Alloy 617
Temperature-1250°F (677°C)

Stress, 1000 psi (MPa)
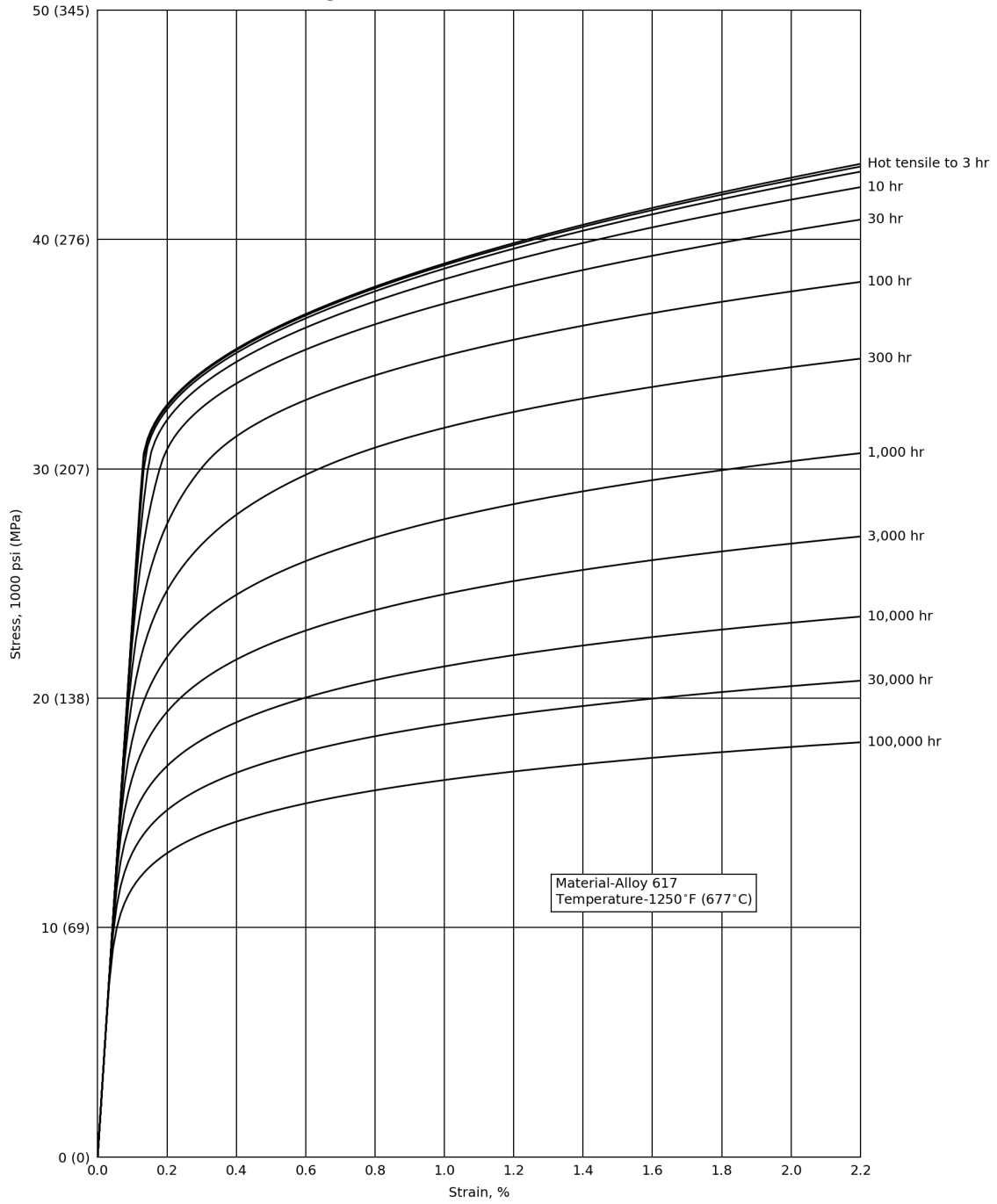
Strain, %

Figure HBB-T-1836-11
Average Isochronous Stress-Strain Curves

Material-Alloy 617
Temperature-1300°F (704°C)

Hot tensile to 3 hr
10 hr
30 hr
100 hr
300 hr
1,000 hr
3,000 hr
10,000 hr
30,000 hr
100,000 hr

Stress, 1000 psi (MPa)
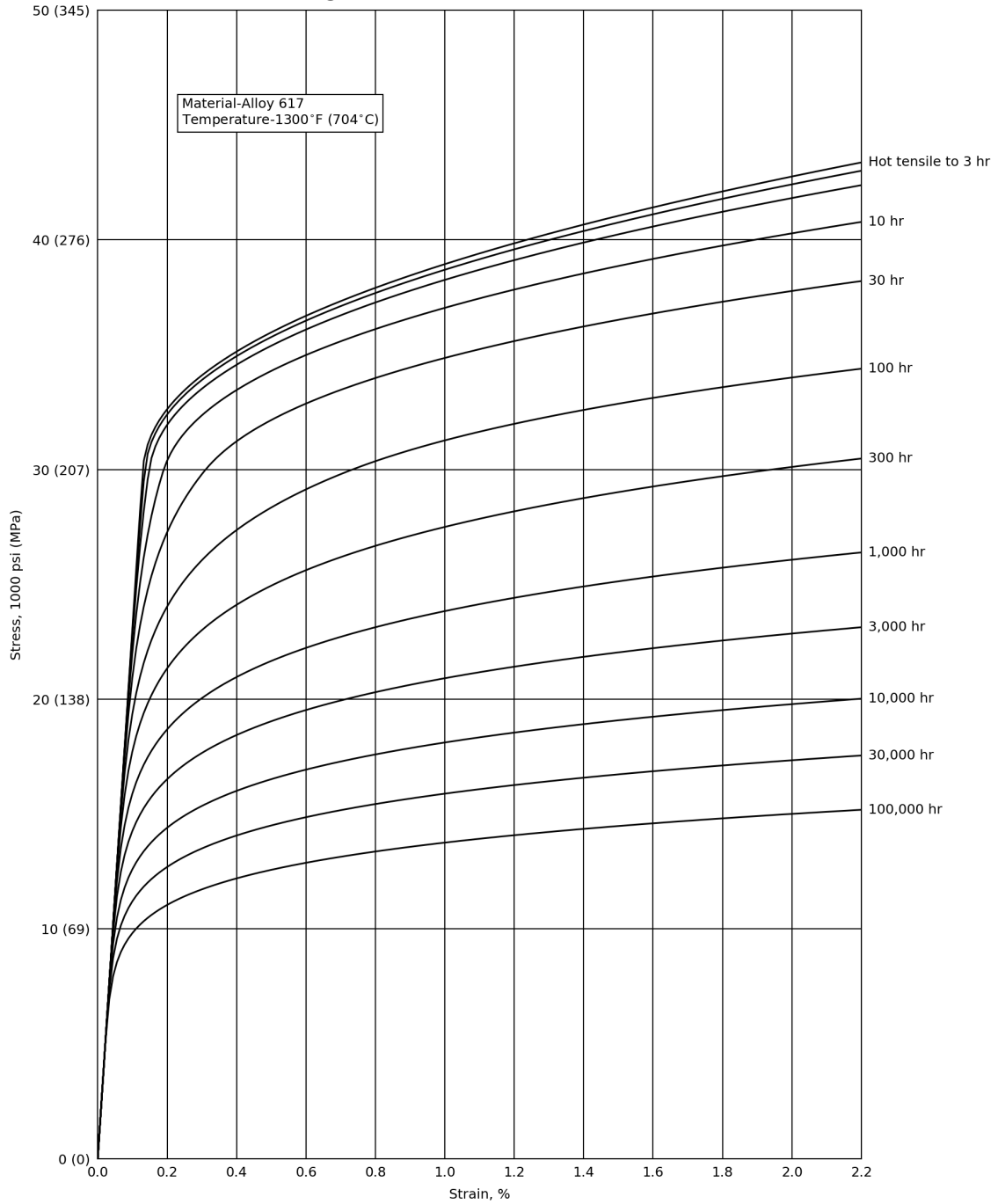
Strain, %

Figure HBB-T-1836-12
Average Isochronous Stress-Strain Curves

Material-Alloy 617
Temperature-1350°F (732°C)

Hot tensile to 1 hr
3 hr
10 hr
30 hr
100 hr
300 hr
1,000 hr
3,000 hr
10,000 hr
30,000 hr
100,000 hr

Stress, 1000 psi (MPa)
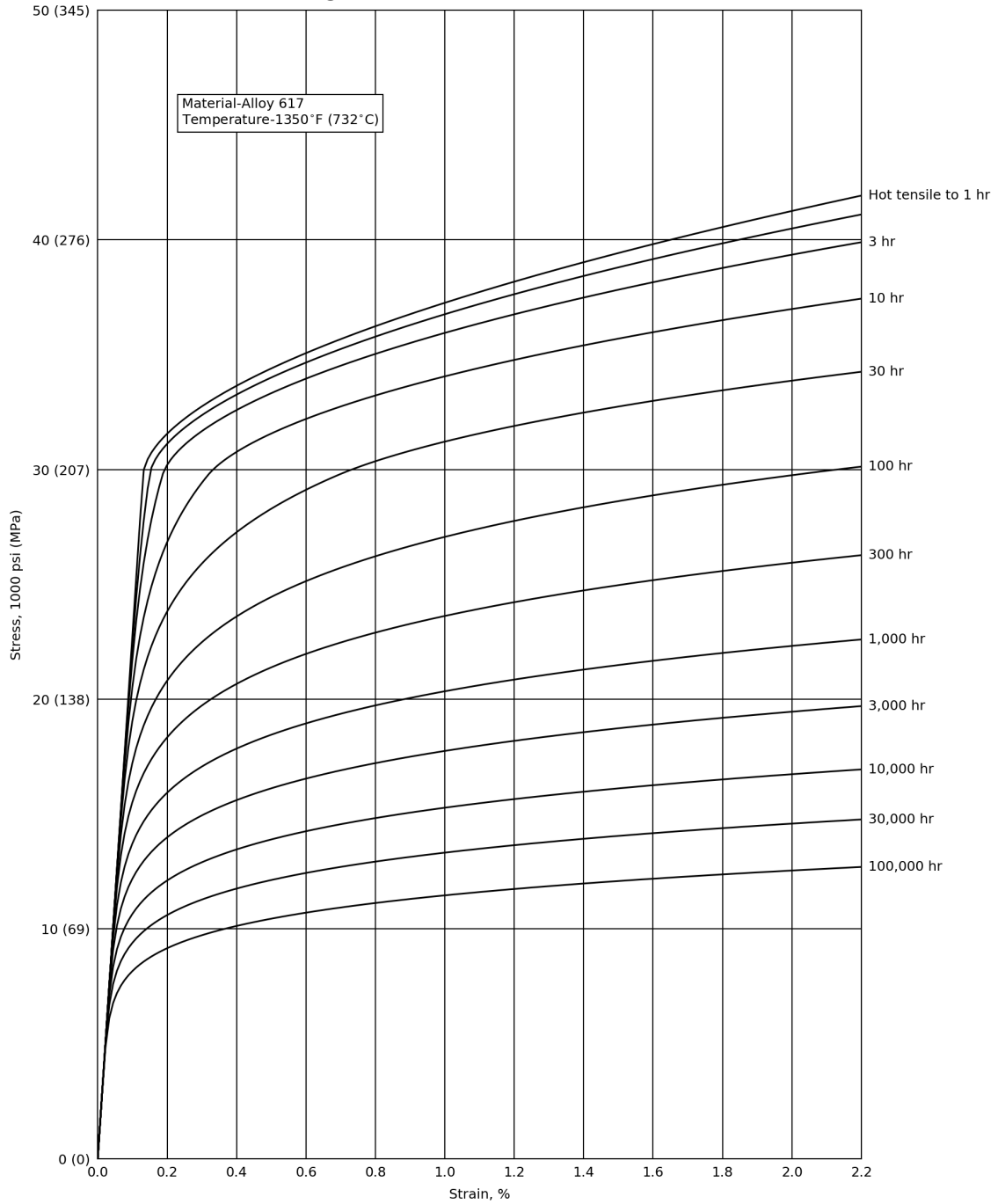
Strain, %

Figure HBB-T-1836-13
Average Isochronous Stress-Strain Curves

Material-Alloy 617
Temperature-1400°F (760°C)

Hot tensile
1 hr
3 hr
10 hr
30 hr
100 hr
300 hr
1,000 hr
3,000 hr
10,000 hr
30,000 hr
100,000 hr

Stress, 1000 psi (MPa)
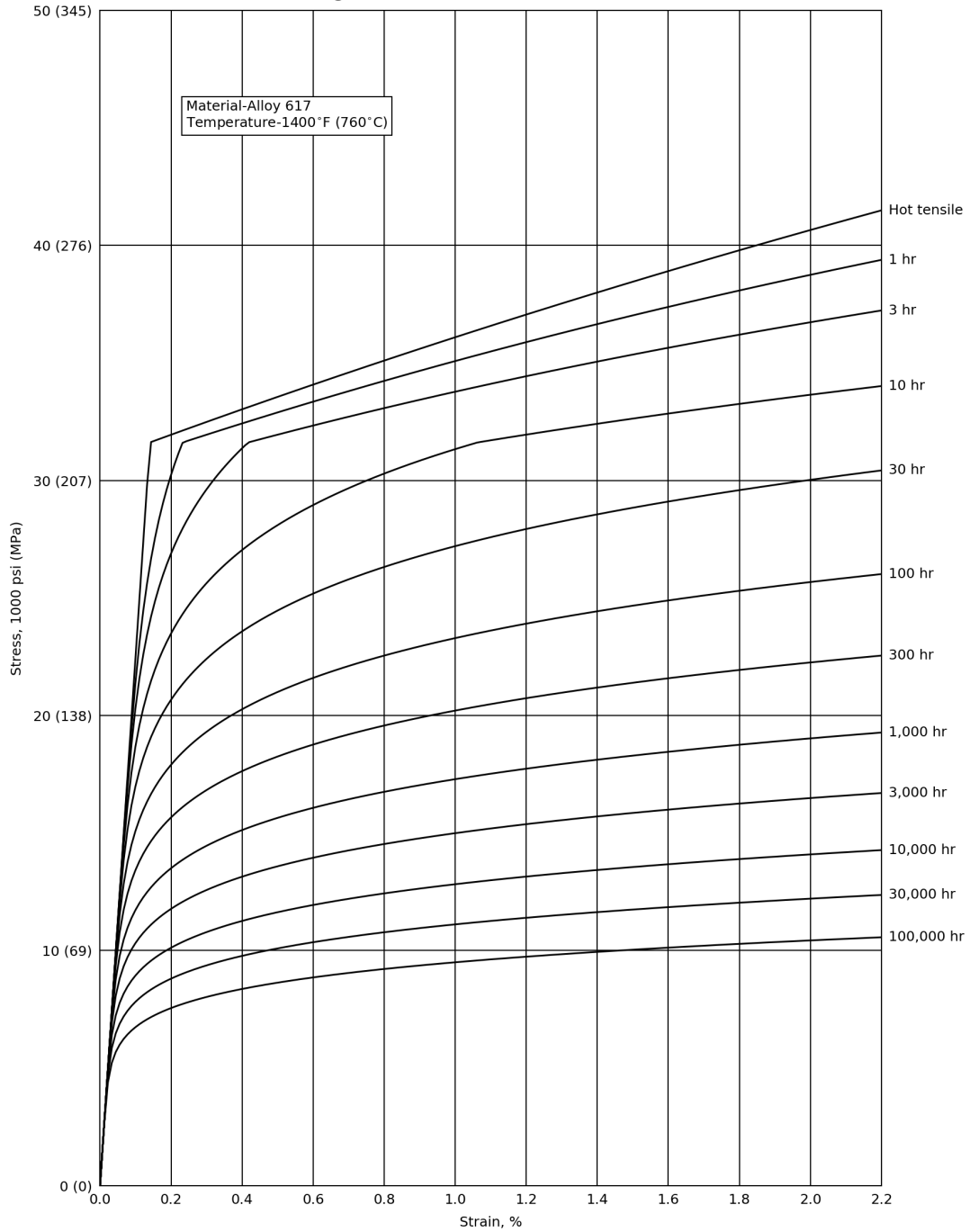
Strain, %

**Figure HBB-T-1836-14
Average Isochronous Stress-Strain Curves**

Material-Alloy 617
Temperature-1450°F (788°C)

Hot tensile
1 hr
3 hr
10 hr
30 hr
100 hr
300 hr
1,000 hr
3,000 hr
10,000 hr
30,000 hr
100,000 hr

Stress, 1000 psi (MPa)
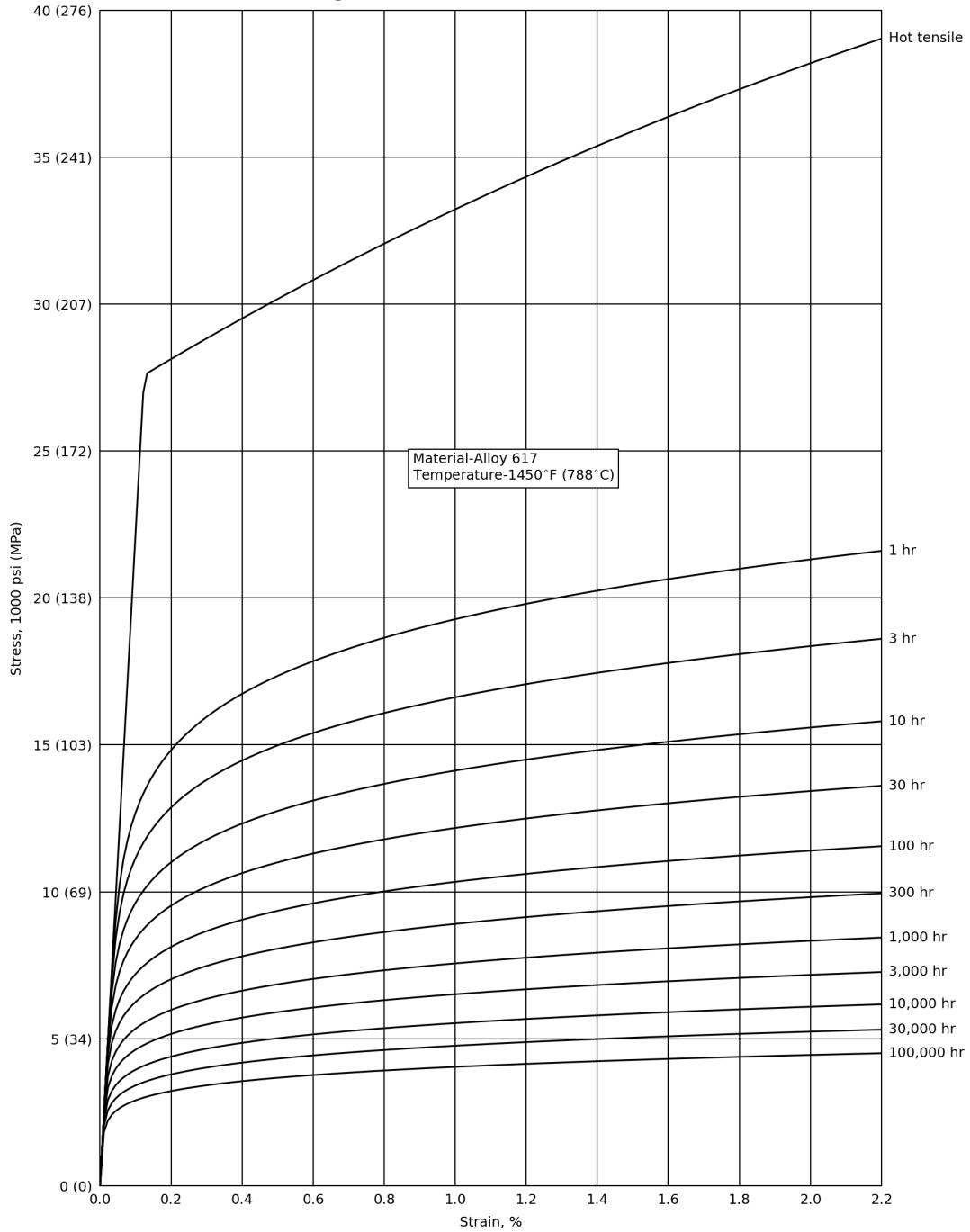
Strain, %

Figure HBB-T-1836-15
Average Isochronous Stress-Strain Curves

Material-Alloy 617
Temperature-1500°F (816°C)

Hot tensile

1 hr

3 hr

10 hr

30 hr

100 hr

300 hr

1,000 hr

3,000 hr

10,000 hr

30,000 hr to 100,000 hr

Stress, 1000 psi (MPa)
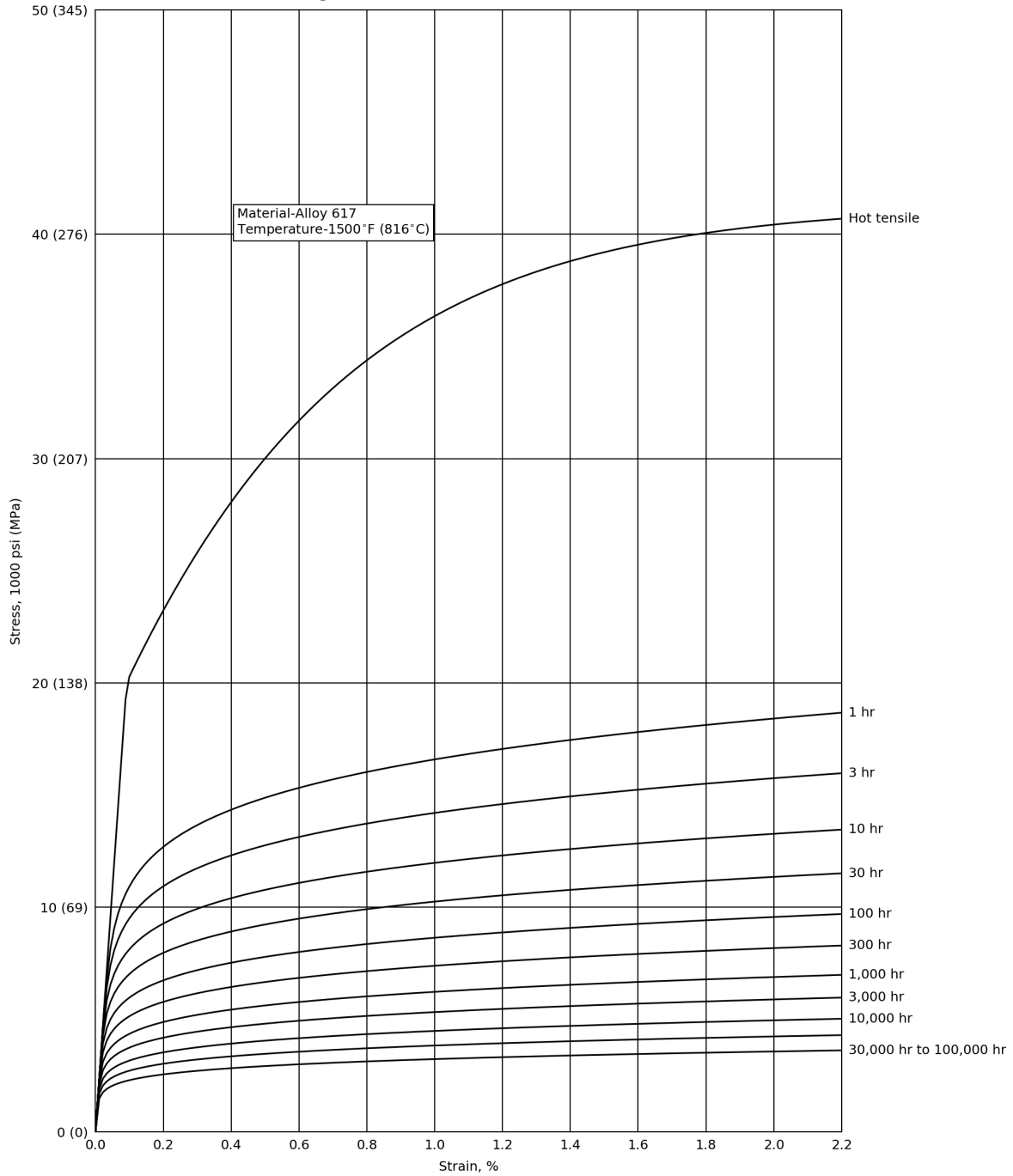
Strain, %

Figure HBB-T-1836-16
Average Isochronous Stress-Strain Curves

Material-Alloy 617
Temperature-1550°F (843°C)

Hot tensile

1 hr
3 hr
10 hr
30 hr
100 hr
300 hr
1,000 hr
3,000 hr
10,000 hr
30,000 hr to 100,000 hr

Stress, 1000 psi (MPa)
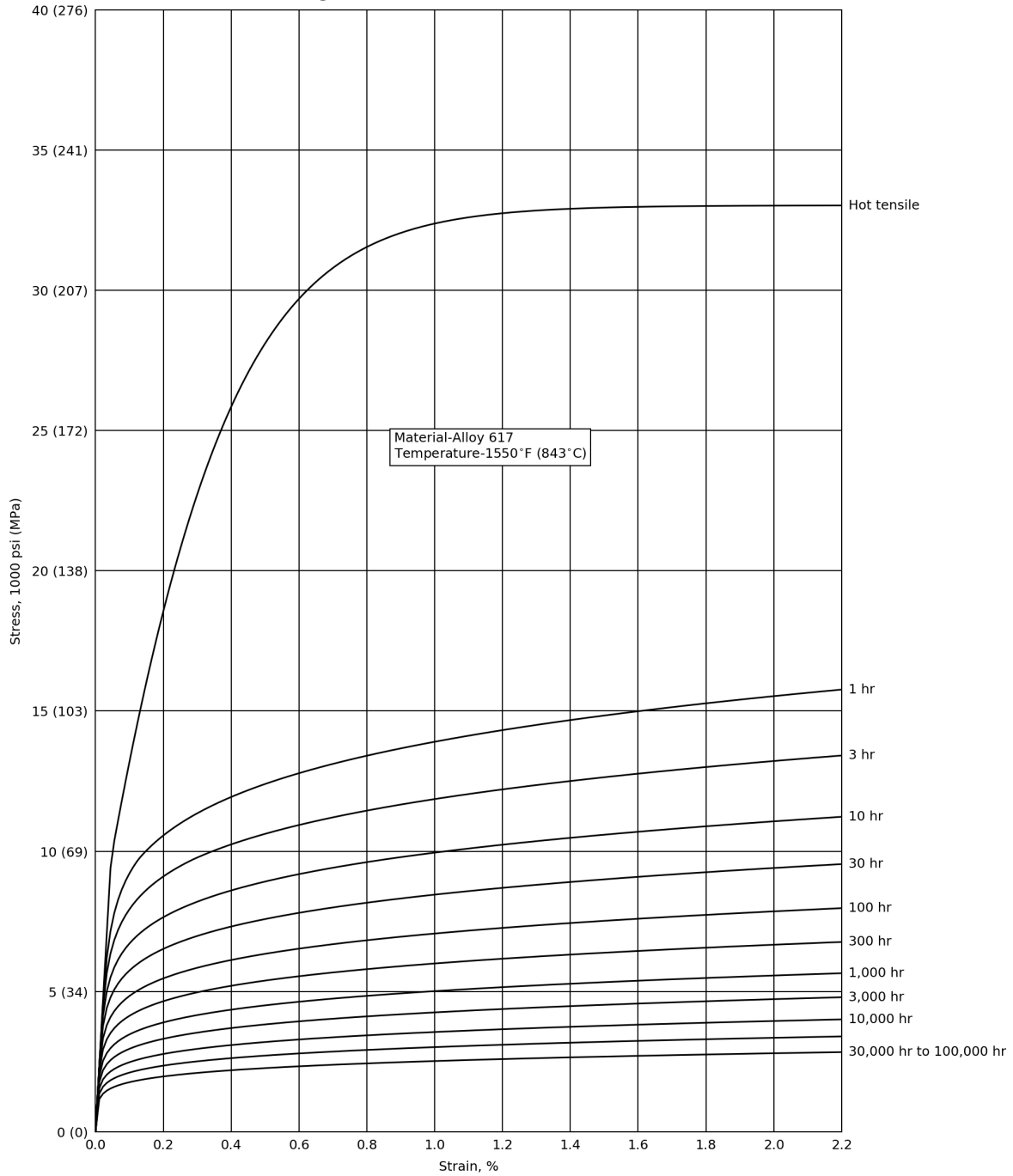
Strain, %

**Figure HBB-T-1836-17
Average Isochronous Stress-Strain Curves**

Material-Alloy 617
Temperature-1600°F (871°C)

Hot tensile

1 hr

3 hr

10 hr

30 hr

100 hr

300 hr

1,000 hr

3,000 hr

10,000 hr

30,000 hr to 100,000 hr

Stress, 1000 psi (MPa)
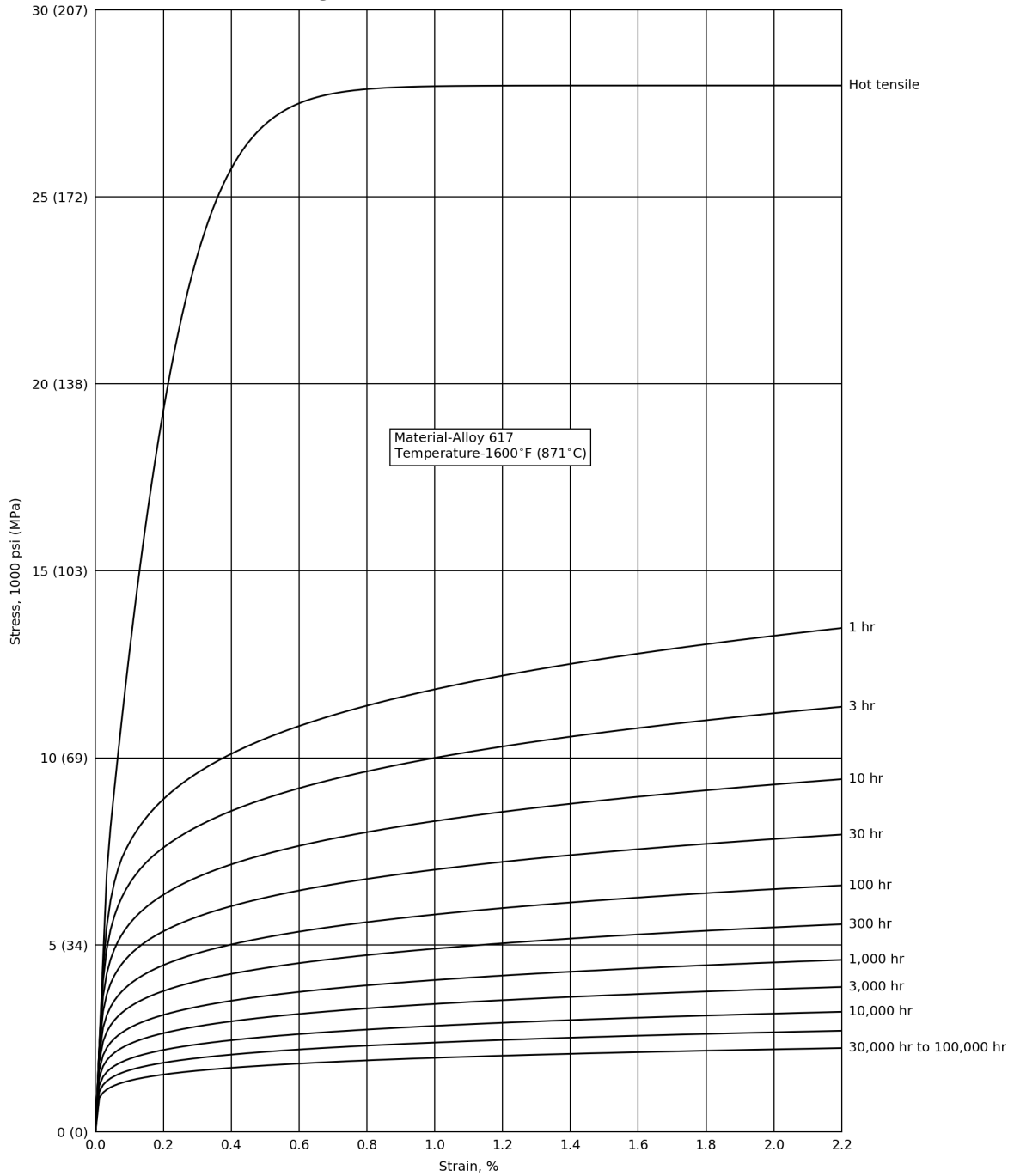
Strain, %

Figure HBB-T-1836-18
Average Isochronous Stress-Strain Curves

Material-Alloy 617
Temperature-1650°F (899°C)

Hot tensile

1 hr
3 hr
10 hr
30 hr
100 hr
300 hr
1,000 hr
3,000 hr
10,000 hr to 100,000 hr

Stress, 1000 psi (MPa)
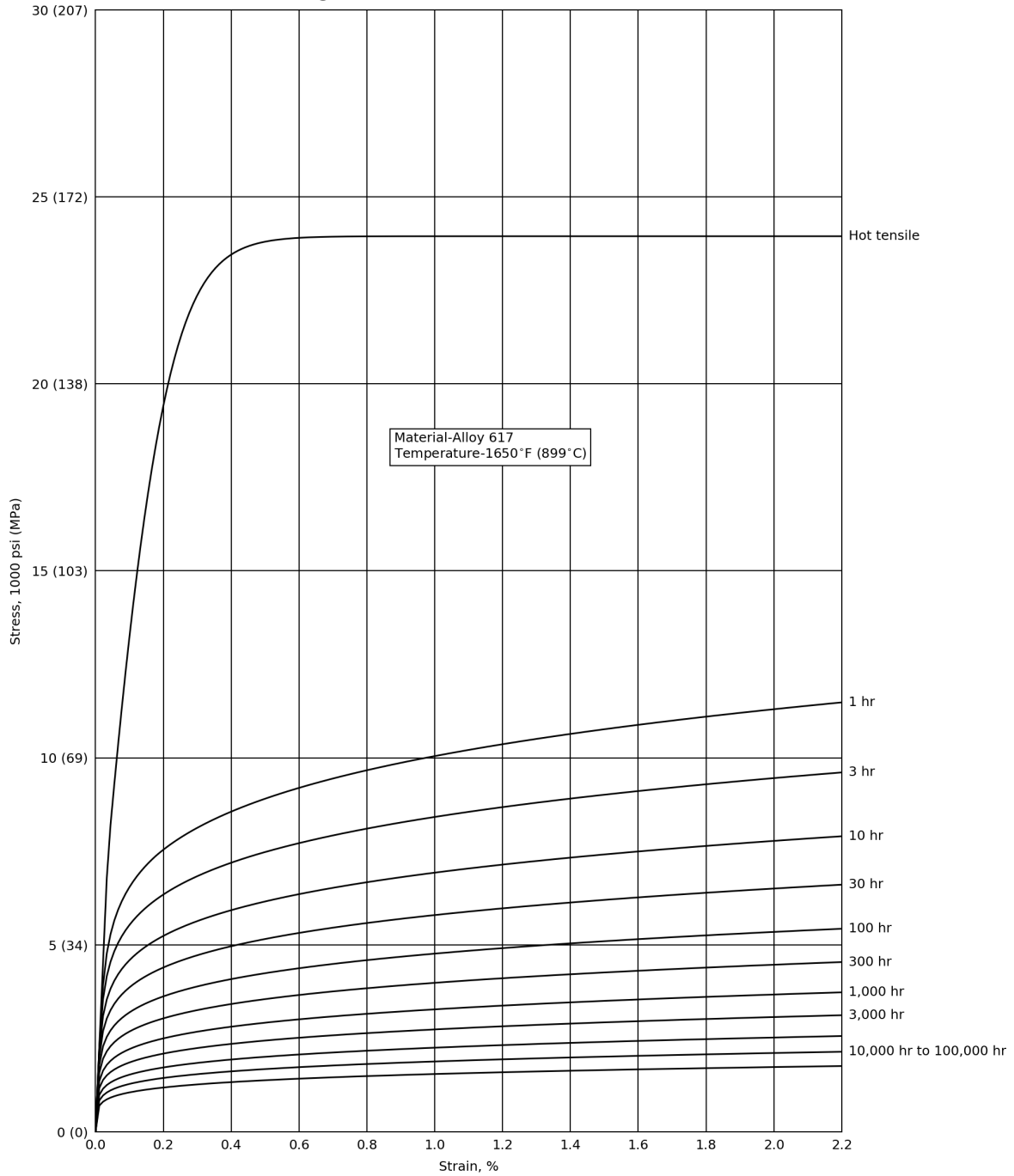
Strain, %

Figure HBB-T-1836-19
Average Isochronous Stress-Strain Curves

Material-Alloy 617
Temperature-1700°F (927°C)

Hot tensile

1 hr

3 hr

10 hr

30 hr

100 hr

300 hr

1,000 hr

3,000 hr to 100,000 hr

Stress, 1000 psi (MPa)
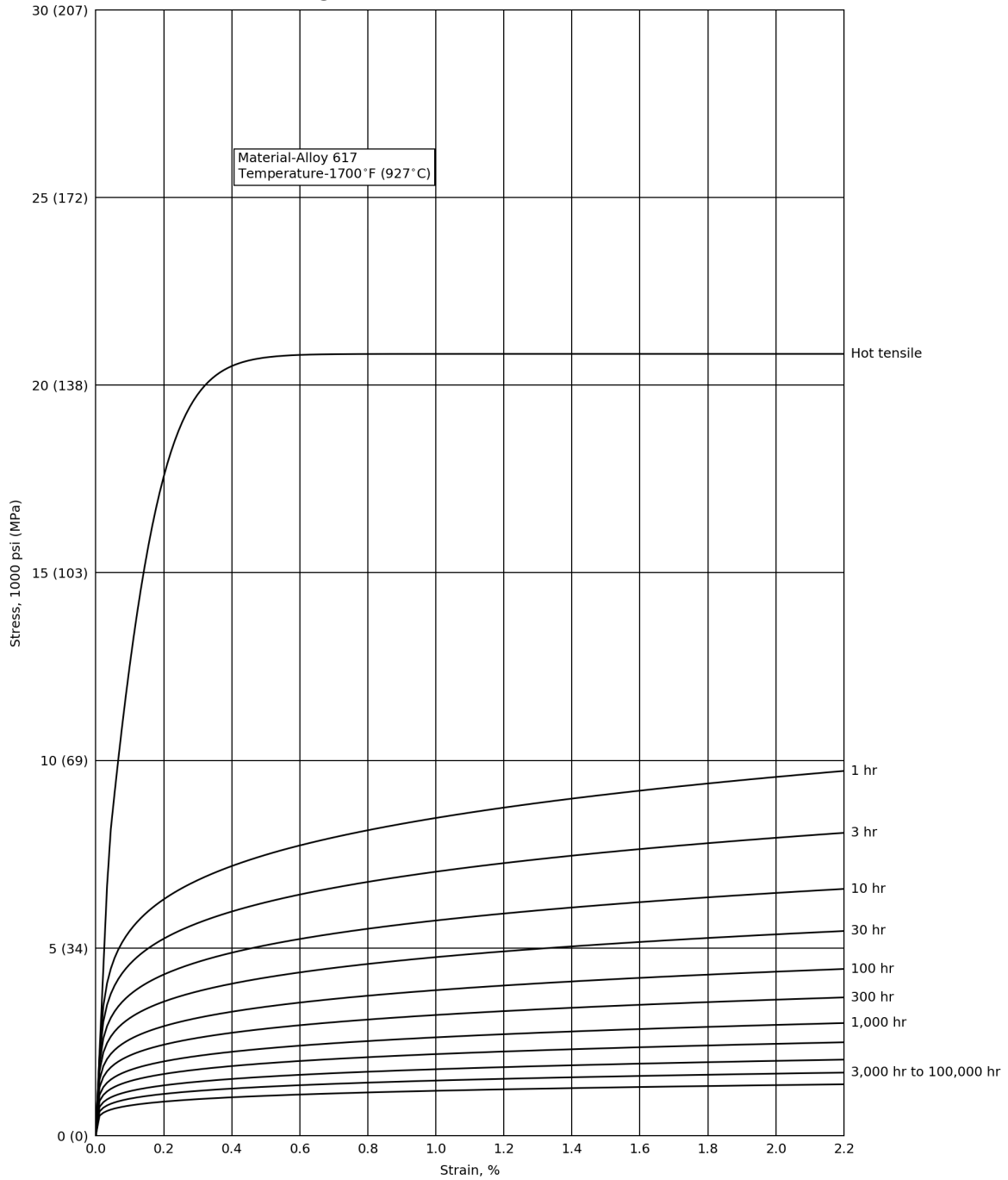
Strain, %

Figure HBB-T-1836-20
Average Isochronous Stress-Strain Curves

Hot tensile

Material-Alloy 617
Temperature-1750°F (954°C)

1 hr

3 hr

10 hr

30 hr

100 hr

300 hr

1,000 hr

3,000 hr

10,000 hr to 100,000 hr

Stress, 1000 psi (MPa)

Strain, %
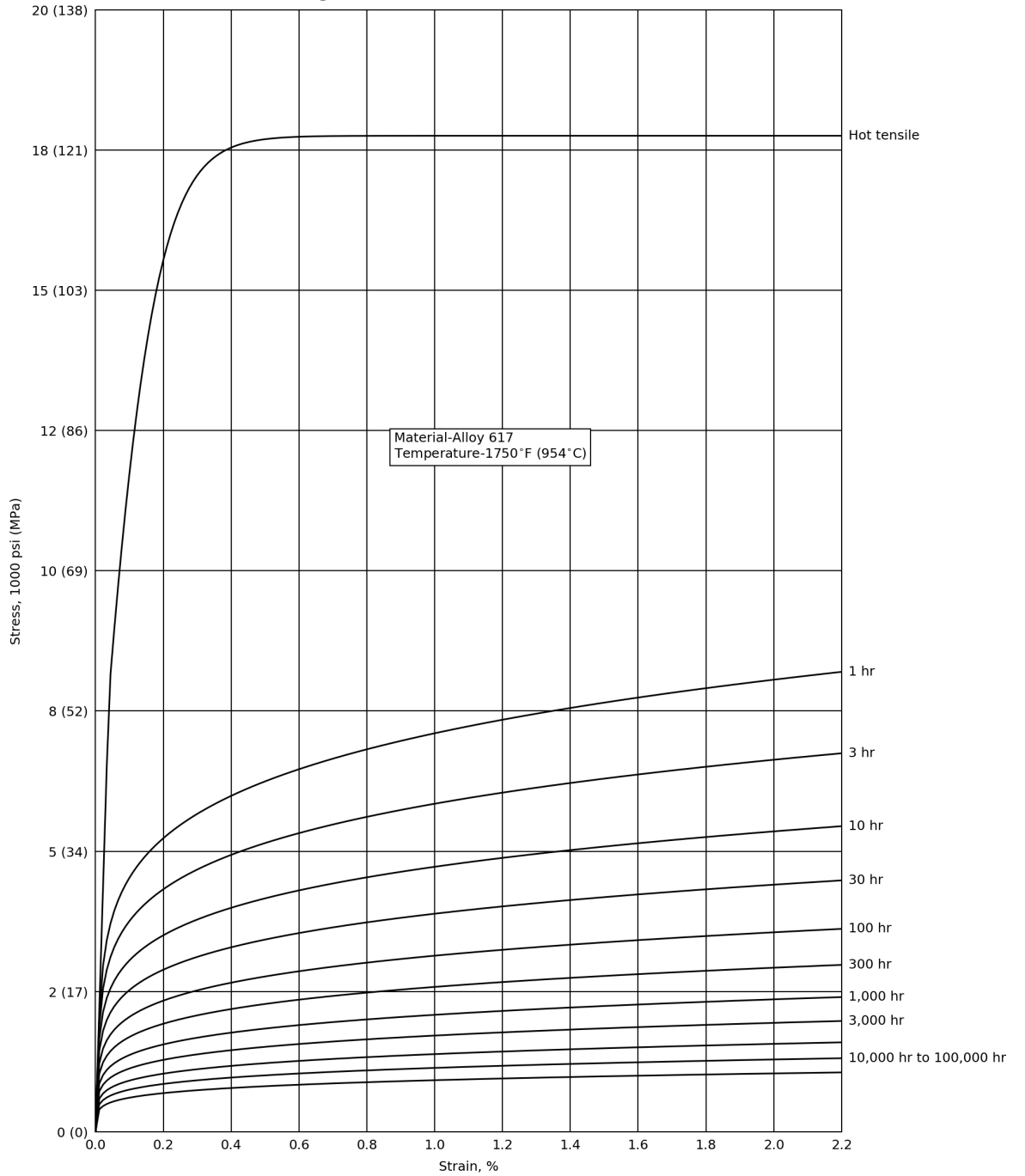
PHYSICAL PROPERTIES TABLES

THERMAL EXPANSION

Table TE-4
Thermal Expansion for Alloy 617

Temperature, °F	Coefficients for N06617		
	A	B	C
70	7.0	7.0	0.0
100	7.1	7.0	0.3
150	7.1	7.1	0.7
200	7.2	7.1	1.1
250	7.3	7.1	1.6
300	7.4	7.2	2.0
350	7.5	7.2	2.4
400	7.6	7.3	2.9
450	7.7	7.3	3.4
500	7.8	7.4	3.8
550	7.9	7.4	4.3
600	8.0	7.5	4.8
650	8.2	7.5	5.3
700	8.3	7.6	5.8
750	8.4	7.6	6.3
800	8.6	7.7	6.8
850	8.7	7.8	7.3
900	8.9	7.8	7.8
950	9.0	7.9	8.4
1,000	9.2	8.0	8.9
1,050	9.4	8.0	9.5
1,100	9.5	8.1	10.0
1,150	9.7	8.2	10.6
1,200	9.9	8.2	11.2
1,250	10.1	8.3	11.8
1,300	10.3	8.4	12.4
1,350	10.5	8.5	13.0
1,400	10.7	8.5	13.7
1,450	10.9	8.6	14.3
1,500	11.1	8.7	15.0
1,550	11.3	8.8	15.6
1,600	11.5	8.9	16.3
1,650	11.8	9.0	17.0
1,700	12.0	9.1	17.7
1,750	12.2	9.1	18.5

GENERAL NOTE: Coefficient A is the instantaneous coefficient of thermal expansion x 10^{-6} (in./in./°F). Coefficient B is the mean coefficient of thermal expansion x 10^{-6} (in./in./°F) in going from 70°F to indicated temperature. Coefficient C is the linear thermal expansion (in./100 ft) in going from 70°F to indicated temperature.

Table TE-4 (M)
Thermal Expansion for Alloy 617

Temperature, °C	Coefficients for N06617		
	A	B	C
20	12.6	12.6	0.0
50	12.8	12.7	0.4
75	12.9	12.7	0.7
100	13.0	12.8	1.0
125	13.2	12.9	1.4
150	13.3	12.9	1.7
175	13.5	13.0	2.0
200	13.6	13.1	2.4
225	13.8	13.2	2.7
250	14.0	13.2	3.0
275	14.2	13.3	3.4
300	14.4	13.4	3.8
325	14.6	13.5	4.1
350	14.8	13.6	4.5
375	15.0	13.7	4.9
400	15.2	13.8	5.2
425	15.4	13.9	5.6
450	15.7	14.0	6.0
475	15.9	14.1	6.4
500	16.2	14.2	6.8
525	16.4	14.3	7.2
550	16.7	14.4	7.6
575	17.0	14.5	8.0
600	17.2	14.6	8.5
625	17.5	14.7	8.9
650	17.8	14.8	9.3
675	18.1	15.0	9.8
700	18.4	15.1	10.3
725	18.8	15.2	10.7
750	19.1	15.3	11.2
775	19.4	15.5	11.7
800	19.8	15.6	12.2
825	20.1	15.7	12.7
850	20.5	15.9	13.2
875	20.8	16.0	13.7
900	21.2	16.1	14.2
925	21.6	16.3	14.7
950	21.9	16.4	15.3

GENERAL NOTE: Coefficient A is the instantaneous coefficient of thermal expansion x 10^{-6} (mm/mm/°C). Coefficient B is the mean coefficient of thermal expansion x 10^{-6} (mm/mm/°C) in going from 20°C to indicated temperature. Coefficient C is the linear thermal expansion (mm/m) in going from 20°C to indicated temperature.

THERMAL CONDUCTIVITY AND THERMAL DIFFUSIVITY

Table TCD
Nominal Coefficients of Thermal Conductivity (TC) and Thermal Diffusivity (TD)
for Alloy 617

	N06617	
Temp., °F	TC	TD
70	6.1	0.112
100	6.3	0.114
150	6.6	0.118
200	6.9	0.122
250	7.2	0.125
300	7.5	0.129
350	7.8	0.132
400	8.1	0.136
450	8.4	0.139
500	8.7	0.142
550	9.0	0.145
600	9.3	0.149
650	9.5	0.152
700	9.8	0.155
750	10.0	0.158
800	10.3	0.161
850	10.5	0.164
900	10.8	0.167
950	11.0	0.171
1,000	11.3	0.174
1,050	12.1	0.177
1,100	13.2	0.181
1,150	14.1	0.184
1,200	14.6	0.188
1,250	14.9	0.192
1,300	14.8	0.194
1,350	14.7	0.191
1,400	14.6	0.189
1,450	14.5	0.188
1,500	14.6	0.189
1,550	14.7	0.191
1,600	14.9	0.193
1,650	15.1	0.196
1,700	15.5	0.199
1,750	15.9	0.203

GENERAL NOTES:

(a) TC is the thermal conductivity, Btu/(hr-ft-°F), and TD is the thermal diffusivity, ft²/hr:

$$TD = \frac{TC[Btu/hr \cdot ft - °F]}{density\ (lb/ft^3) \times specific\ heat\ (Btu/lb - °F)}$$

(b) Values of thermal expansion and thermal diffusivity should be used with the understanding that there is an associated ±10% uncertainty. This uncertainty results from compositional variations and variables associated with original data acquisition and analysis.

Table TCD (M)
Nominal Coefficients of Thermal Conductivity (TC) and Thermal Diffusivity (TD)
for Alloy 617

Temp., °C	N06617 TC	N06617 TD
20	10.5	2.88
50	11.1	2.99
75	11.6	3.08
100	12.1	3.17
125	12.6	3.25
150	13.0	3.33
175	13.5	3.41
200	14.0	3.49
225	14.4	3.57
250	14.9	3.64
275	15.3	3.71
300	15.8	3.79
325	16.2	3.86
350	16.6	3.93
375	17.0	4.01
400	17.4	4.08
425	17.8	4.15
450	18.2	4.22
475	18.6	4.30
500	18.9	4.37
525	19.3	4.45
550	19.6	4.53
575	21.7	4.60
600	23.3	4.69
625	24.5	4.77
650	25.3	4.85
675	25.7	4.94
700	25.7	5.03
725	25.4	4.94
750	25.3	4.89
775	25.2	4.86
800	25.2	4.87
825	25.3	4.90
850	25.5	4.94
875	25.8	5.00
900	26.2	5.07
925	26.7	5.14
950	27.4	5.22

GENERAL NOTES:

(a) TC is the thermal conductivity, W/(m·°C), and TD is the thermal diffusivity, 10^{-6} m^2/sec:

$$TD = \frac{TC[W/(m\cdot°C)]}{\text{density (kg/m}^3) \times \text{specific heat [J/(kg·°C)]}}$$

(b) Values of thermal expansion and thermal diffusivity should be used with the understanding that there is an associated ±10% uncertainty. This uncertainty results from compositional variations and variables associated with original data acquisition and analysis.

Page intentionally left blank

MODULUS OF ELASTICITY

Table TM-4
Moduli of Elasticity *E* of Alloy 617 for Given Temperatures

Material	Modulus of Elasticity E = Value Given × 10^6 psi, for Temperature, °F, of

Material	-325	-200	-100	70	200	300	400	500	600	700	800	900	1,000	1,100	1,200	1,300	1,400	1,500	1,600	1,700	1,800
N06617	-	-	-	29.2	28.4	28.0	27.7	27.4	27.0	26.5	26.0	25.5	24.9	24.3	23.8	23.2	22.5	21.8	21.0	20.2	19.3

Table TM-4 (M)
Moduli of Elasticity *E* of Alloy 617 for Given Temperatures

Material	-200	-125	-75	25	100	150	200	250	300	350	400	450	500	550	600	650	700	750	800	850	900	950
N06617	-	-	-	201	196	193	191	189	187	184	181	178	174	171	167	164	160	156	152	146	141	136

The header spanning row for Table TM-4 (M) reads: Modulus of Elasticity E = Value Given × 10^3 MPa, for Temperature, °C, of

Page intentionally left blank

APPENDIX 5

BACKGROUND FOR DRAFT CODE CASE: USE OF ALLOY 617 (UNS N06617) FOR CLASS A ELEVATED TEMPERATURE SERVICE CONSTRUCTION

Page intentionally left blank

Background Document – Record No. 16-994

Contents

- Balloting Plan
- HBB-I-14.1(a) Permissible Base Materials
- HBB-I-14.1(b) Permissible Weld Materials
- Yield and Ultimate Strength
  - HBB-3225-1 Tensile Strength Values, S_u
  - HBB-I-14.5 Yield Strength Values, S_y
- Allowable Stress Values
  - HBB-I-14.2 S_o − Maximum Allowable Stress Intensity
  - HBB-I-14.3 S_{mt} – Allowable Stress Intensity Values
  - HBB-I-14.4 S_t – Allowable Stress Intensity Values
  - HBB-I-14.6 S_r - Minimum Stress-to-Rupture
- HBB-I-14.10 Stress Rupture Factors for Welded Alloy 617
- HBB-4800 Relaxation Cracking
- HBB-3225-2 Strength Reduction Factor Due to Long Time Prior Elevated Temperature Service
- HBB-4212 Effects of Forming and Bending Processes
- Appendices
  - Appendix I Data Compilation for Tensile Tests
  - Appendix II Data Compilation of Time to 1% Creep Strain
  - Appendix III Data Compilation of Time to Onset of Tertiary Creep
  - Appendix IV Data Compilation of Creep-Rupture Tests
  - Appendix V Data Compilation for Creep Tests of Weldments
  - Appendix VI Data Compilation for Tensile Tests of Aged Alloy 617

Page intentionally left blank

Alloy 617 Code Case Balloting Actions

RC #	Item	Section II and III Committees (See Color Key Below For Balloting Actions)								
16-994	Permissible base and weld materials, allowable stress values	WG-ASC	SG-ETD	SG-HTR	SG-MFE	II-SG-NFA	II-SG-SW	BPV-II		
16-995	Physical properties and extension of modulus values to higher temperatures	WG-ASC	SG-ETD	SG-HTR	SG-MFE	II-SG-NFA	II-SG-PP	BPV-II		
16-996	Temperature-time limits for NB buckling charts	WG-AM	SG-ETD	SG-HTR	SG-MFE	II-SG-EP	BPV-II	II-SG-NFA	SC-D	
16-997	Huddleston parameters, ISSCs	WG-ASC	SG-ETD	SG-HTR	II-SG-NFA	BPV-II	SC-D			
16-998	Negligible creep, Creep-Fatigue: D-diagram and EPP	WG-CFNC	SG-ETD	SG-HTR	SC-D					
16-999	EPP strain limits	WG-AM	SG-ETD	SG-HTR	SC-D					
16-1000	Fatigue design curves	WG-CFNC	WG-FS	SG-ETD	SG-HTR	SG-DM	SC-D			
16-1001	Alloy 617 Overall Code Case	WG-ASC	WG-AM	WG-CFNC	WG-FS	SG-ETD	SG-HTR	SG-MFE	SC-D	BPV-II
		BPV-III								

Color Key	Balloting Action
	For Review and Approval
	For Review and Comment

Page intentionally left blank

BACKGROUND

TABLE HBB-I-14.1(a)

PERMISSIBLE BASE MATERIALS FOR STRUCTURES OTHER THAN BOLTING

Scope

This document provides the background/technical basis in support of the recommendation for the permissible base materials for structures other than bolting for Alloy 617 specified in Table HBB-I-14.1(a).

Background

HBB-2121, Permitted Material Specifications, stipulates that material specifications in Table HBB-I-14.1(a) are considered extensions of Section II, Part D, Subpart 1. Table HBB-I-14.1(a) is also referenced in HBB-3221 General Requirements for HBB-3220, Design Rules and Limits for Load-controlled Stresses in Structures other than Bolts.

Determination of Permissible Base Materials for Structures other than Bolting

All of the specification numbers that are permitted in Table HBB-I-14.1(a) represent wrought and solution annealed material. All wrought product forms with a minimum material thickness of at least 0.125 inches are permitted. The creep data set that has been used to generate the time dependent allowable stresses in this Code Case includes specimens from plate, sheet, rod, tube and forgings. Significant differences in creep properties have not been observed with varying product form. It is therefore reasonable to use these values for all wrought product forms.

The solution treatment required by these specifications produces a large grain size that contributes to the creep resistance of the alloy. The minimum thickness is specified to prevent sections with too few grains through the cross-section, to ensure that material selected for construction is well represented by the bulk properties used in developing allowable stresses for this Code Case. It is commonly thought that a minimum of approximately ten grains are required in the cross-section before section size effects become negligible. The grain size of wrought Alloy 617 is typically in the range of 100-300 μm after solution annealing. A thickness of 0.125 inches represents approximately 10 grains of the maximum observed diameter.

Page intentionally left blank

BACKGROUND

TABLE HBB-I-14.1(b)

PERMISSIBLE WELD MATERIALS

Scope

This document provides the background/technical basis in support of the recommendation for the permissible weld materials for Alloy 617 specified in Table HBB-I-14.1(b).

Background

HBB-2121, Permitted Material Specifications, stipulates that weld material specifications in Table HBB-I-14.1(b) are considered extensions of Section II, Part D, Subpart 1. Table HBB-I-14.1(b) is also referenced in HBB-2539, Repair by Welding.

Only one filler metal, ERNiCrCoMo-1 (Alloy 617), is allowed in Section IX of the Code for Gas Tungsten Arc Welding (GTAW) of Alloy 617.

Materials and Welding

A qualified weld was constructed from the INL Alloy 617 reference plate, a 37 mm thick solution annealed plate (heat 314626), with an average grain size of 150 µm produced by ThyssenKrupp VDM. The INL has performed extensive property characterization on specimens machined from this reference material. The weld wire was ERNiCrCoMo-1 (Alloy 617), (heat XX3703UK) produced by Oxford Alloys. The chemical composition for the base metal and weld wire are shown in Table 1, along with the ASTM specified chemistry. Welding was performed using an automated tungsten gas arc process with multiple passes to fill a v-notch weld preparation.

Quality Statement

Weldment properties from Alloy 617 heat 314626, reported by the Idaho National Laboratory (INL) through the Next Generation Nuclear Plant (NGNP) or Advanced Reactor Technologies (ART) programs were determined under an NQA-1 quality program. Details of the quality program implementation are given in INL document PLN-2690 "Idaho National Laboratory Advanced Reactor Technologies Technology Development Office Quality Assurance Program Plan." Testing on heat XX3824UK predated implementation of the NQA-1 quality program.

Weld Qualification

The GTAW process was qualified for 1.5 inch thick plate using the ERNiCrCoMo-1 (Alloy 617) filler metal and the ASME Section IX qualification process through the INL Welding Procedure Specification I5.0. The INL Procedure Qualification Record sheets are shown in Figure 1. The properties of the weld were qualified using tensile and bend testing, the results of which are reported on page 2 of the Procedure Qualification Record. No post-weld heat treatment is required for Alloy 617, and all characterization was done in the as-welded condition.

A macrograph showing the completed weld is shown in Figure 2. Micrographs of a polished and etched cross-section of the weld are shown in Figure 3. It can be seen in the micrographs that there is no heat affected zone associated with this GTAW weldment, as would be expected for a solid solution austenitic alloy.

Welds that were produced using this procedure for subsequent creep and rupture testing passed examination using the criteria in Section III Division 5 HBB-5210 (b), including radiographic examination using two different angles. Only GTAW weldments have been characterized, so the Code Case is limited to GTAW.

Table 1. Source and chemical composition of the Alloy 617 materials (weight percent).

Heat ID	Source	Form	Ni	Cr	Co	Mo	Fe	Mn	Al	C	Cu	Si	S	Ti	B
	ASME		44.5 min	20.0-24.0	10.0-15.0	8.0-10.0	3.0 max	1.0 max	0.8-1.5	0.05-0.15	0.5 max	1.0 max	0.015 max	0.6 max	0.006 max
314626	VDM	plate	54.1	22.2	11.6	8.6	1.6	0.1	1.1	0.05	0.04	0.1	<0.002	0.4	<0.001
XX3703UK	Oxford	weld wire	53.91	22.41	11.49	8.98	1.37	0.11	1.10	0.089	0.04	0.04	0.001	0.34	NR

CODE: ASME IX-QW
PQR NO.: WPD 656

IDAHO NATIONAL LABORATORY
PROCEDURE QUALIFICATION RECORD

Page 1 of 2
REV NO.: 0

COMPANY NAME: INL   DATE: 8/5/09
PQR NUMBER: WPD 656   REVISION: 0
WELDING PROCESS: GTAW   TYPES: Machine

JOINT (QW-402)

Surface finish as-received for these surfaces
.188"±.01"
15°±2°
R.125"
0.25"±.02"
1.5" nom.
w
plate width "w" varies; groove centered

POST WELD HEAT TREATMENT (QW-407)
TEMPERATURE: NA
TIME: NA

GAS (QW-408)
SHIELDING: Helium/Argon
COMPOSITION: 75% / 25% Welding Grade
FLOW RATE: 30 cfh
PURGING: NA
COMPOSITION: NA
FLOW RATE: NA
TRAILING: NA
COMPOSITION: NA
FLOW RATE: NA

BASE METALS
SPECIFICATION: ASME SB 168
TYPE OR GRADE: Alloy 617 UNS NO6617
P NO. FROM: 43   TO P NO.: 43
THICKNESS: 1.500 in.   DIAMETER: NA
OTHER: NA

FILLER METALS
SPECIFICATION: SFA 5.9
CLASSIFICATION: ERNiCrCoMo-1
F NO.: 6   A NO.: None
SOLID/TUBULAR/FLUX/COVERED(GTAW): Solid
SIZE: 0.045 in.
CHEMICAL COMPOSITION: NA
OTHER: NA

POSITION (QW-405)
POSITION: 1G
PROGRESSION: NA

PREHEAT (QW-406)
PREHEAT TEMP. (MIN): 50° F
INTERPASS TEM. (MAX): 200° F

ELECTRICAL CHARACTERISTICS (QW-409)
CURRENT: Direct
POLARITY: Straight
AMPS: 200 to 355
VOLTS: 9 to 13
TUNGSTEN TYPE: EWTh-2
TUNGSTEN SIZE: 0.125 in.

TECHNIQUE (QW-410)
TRAVEL SPEED: 3.5 to 5 ipm
STRING OR WEAVE BEAD: Stringer and weave
OSCILLATION: Slight
SINGLE/MULTIPLE PASS: Multiple
SINGLE/MULTIPLE ELEC.: Single
TRANSFER MODE(GMAW): NA

CODE: ASME IX-QW
PQR NO.: WPD 656

IDAHO NATIONAL LABORATORY
PROCEDURE QUALIFICATION RECORD

Page 2 of 2
REV NO.: 0

TENSIL TEST (QW-150)

SPECIMEN NUMBER	WIDTH (mm)	THICK. (mm)	AREA (mm²)	LOAD (Kn)	UTS (ksi)	TYPE OF FAILURE AND LOCATION
A-0-1	18.99	11.71	222.4	181.2	118	Ductile / BM
A-O-2	18.63	11.79	219.7	175.7	116	Ductile / BM
A-MID	19.01	11.47	218.0	170.2	113	Ductile / BM
B-O-1	18.56	11.42	212.0	174.5	119	Ductile / Weld
B-0-2	18.95	11.49	217.7	175.1	117	Ductile/ BM
B-MID	18.62	10.98	204.5	166.3	118	Ductile / BM

GUIDED BEND TESTS (QW-160)

TYPE AND FIGURE NUMBER	RESULTS
Side bends 4 EA. Figure QW 462.2	Pass

NOTES:

WELDER'S NAME: Denis Clark   IDENTIFICATION: KI

TEST BY: Kyle Kofford

WE CERTIFY THAT THE STATEMENTS IN THIS RECORD ARE CORRECT AND THAT THE TEST WELDS WERE PREPARED, WELDED, AND TESTED IN ACCORDANCE WITH THE REQUIREMENTS OF SECTION IX OF THE ASME 2007 CODE.

CERTIFIED BY: *[signature]*

COMPANY: INL

DATE: 9/2/09

Figure 1. INL Procedure Qualification Record sheets for Alloy 617 GTAW weld.

Figure 2. Macrograph of completed weld of Alloy 617 plate.
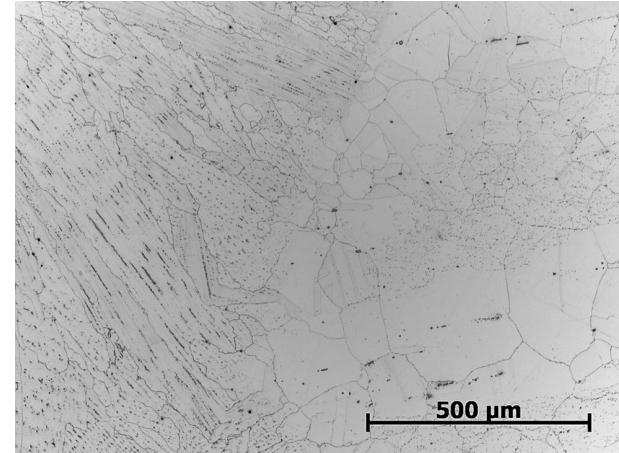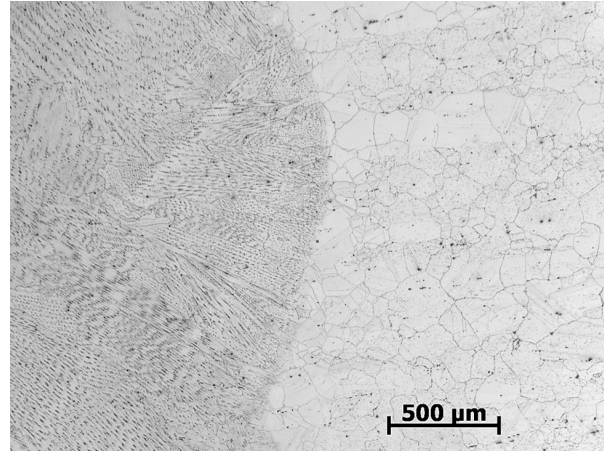
Figure 3. Micrographs of the qualified weld metal and adjacent base metal.

Page intentionally left blank

BACKGROUND

HBB-3225-1 TENSILE STRENGTH VALUES, S_u, FOR ALLOY 617

AND HBB-I-14.5 YIELD STRENGTH VALUES, S_y, FOR ALLOY 617

Scope

This document provides the background/technical basis in support of the recommendation for the tensile strength values, S_u, in Table HBB-3225-1, and the yield strength values, S_y, in Table HBB-I-14.5 of the Alloy 617 Code Case.

Background

The tensile and yield strength values, S_u, and S_y, are derived from tensile tests at various temperatures. These time-independent values are used to determine the maximum allowable value of general primary membrane stress to be used as a reference for stress calculations under design loadings, S_0, and the lowest time-independent stress intensity values S_m, as discussed in HBB-3221. Tensile properties are also used in determining the hot tensile curves in HBB-T-1800-F-1 through HBB-T-1800-F-20.

Data Sources

Tensile data has been compiled from testing of modern heats of Alloy 617 plate in current or recent VHTR programs, historical data from previous high-temperature reactor programs, and data originally generated by the vendor developing Alloy 617. The data set has been limited to specimens with known chemistry that were tested in air, and represents multiple product forms and heats.[1] A tabulation of the tensile data can be found in Appendix I.

The Generation IV International Forum (GIF) VHTR Materials Program Management Board has agreed to compile data from earlier testing programs and share data generated from current member test programs in the GIF Materials Handbook.[2] Past tensile data include those generated at Huntington Alloys (the original producer of Inconel 617 and now part of Special Metals Corporation (SMC)),[3] as well as Oak Ridge National Laboratory (ORNL)[4] as part of the Department of Energy High-Temperature Gas-Cooled Reactor Research Program of the 1980s and 1990s. Recent tensile data have been contributed by Idaho National Laboratory (INL).[5] Additional data have been reported as part of an International Nuclear Energy Research Initiative with INL and France's Commissariat a l'energie atomique (CEA).[6]

Materials

The INL has performed extensive property characterization on specimens machined from an Alloy 617 reference material plate.[5] The reference plate is a 37 mm thick solution annealed plate, labeled as heat 314626, with an average grain size of 150 µm and the composition given in Table 1. The microstructure of the plate is shown in Figure 1. Tensile testing was performed at INL on specimens machined from this reference plate. Additional tensile testing was done on specimens machined from 51-mm diameter rod, labeled as heat 188155 with an average grain size of 150 µm and the composition given in Table 1. The microstructure of the rod is shown in Figure 2. Both product forms were produced by ThyssenKrupp VDM and provided in the solution-annealed condition, consisting of holding at 2150°F (1175°C) followed by rapid cooling to room temperature, according to standards SB166 and SB168.[7,8]

Chemistries for the CEA, Huntington and ORNL heats are included in Table 1.
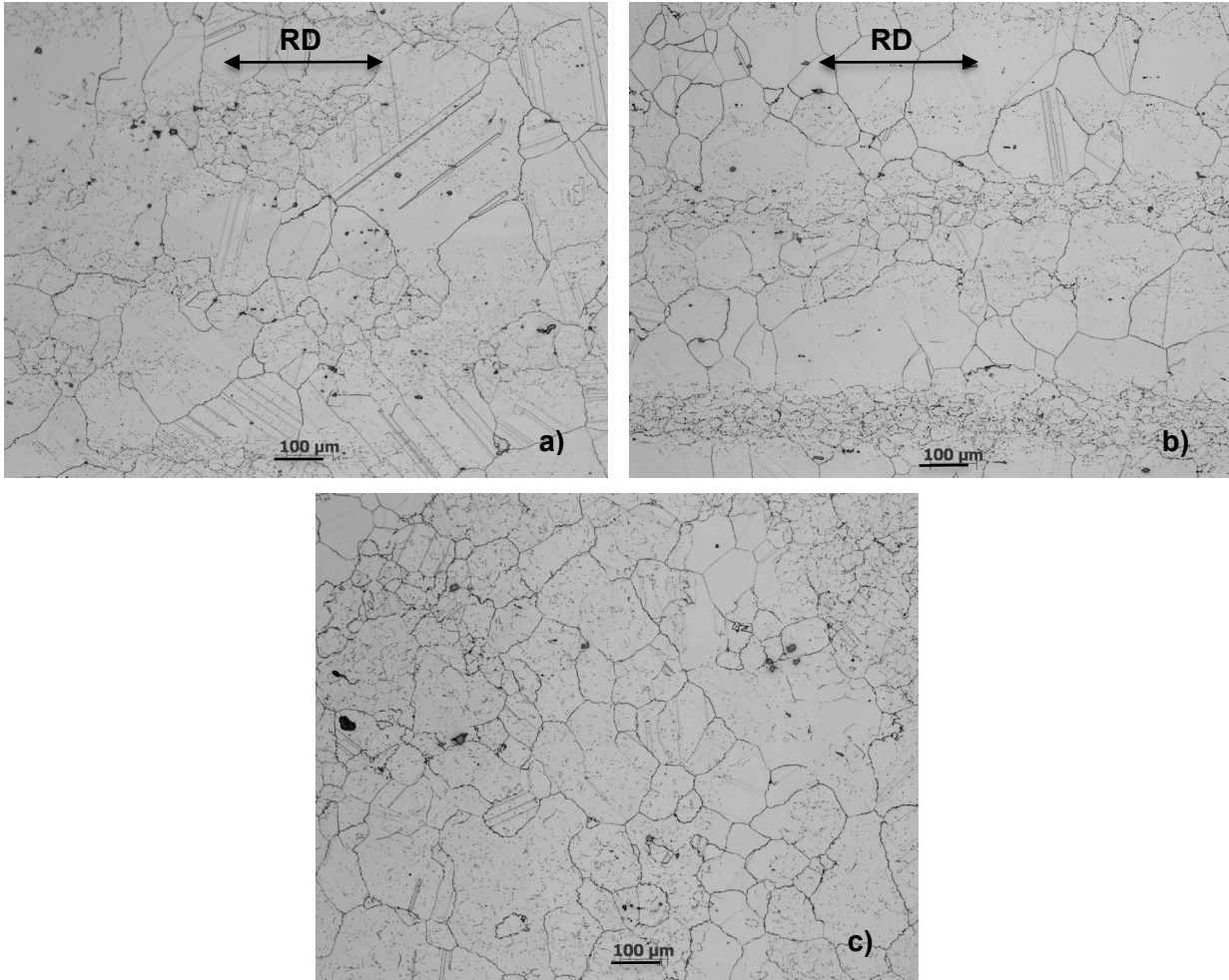
Figure 1. Optical metallography of plate product form for a) parallel to plate surface, b) through-thickness, parallel to rolling direction and c) through-thickness, perpendicular to rolling direction.
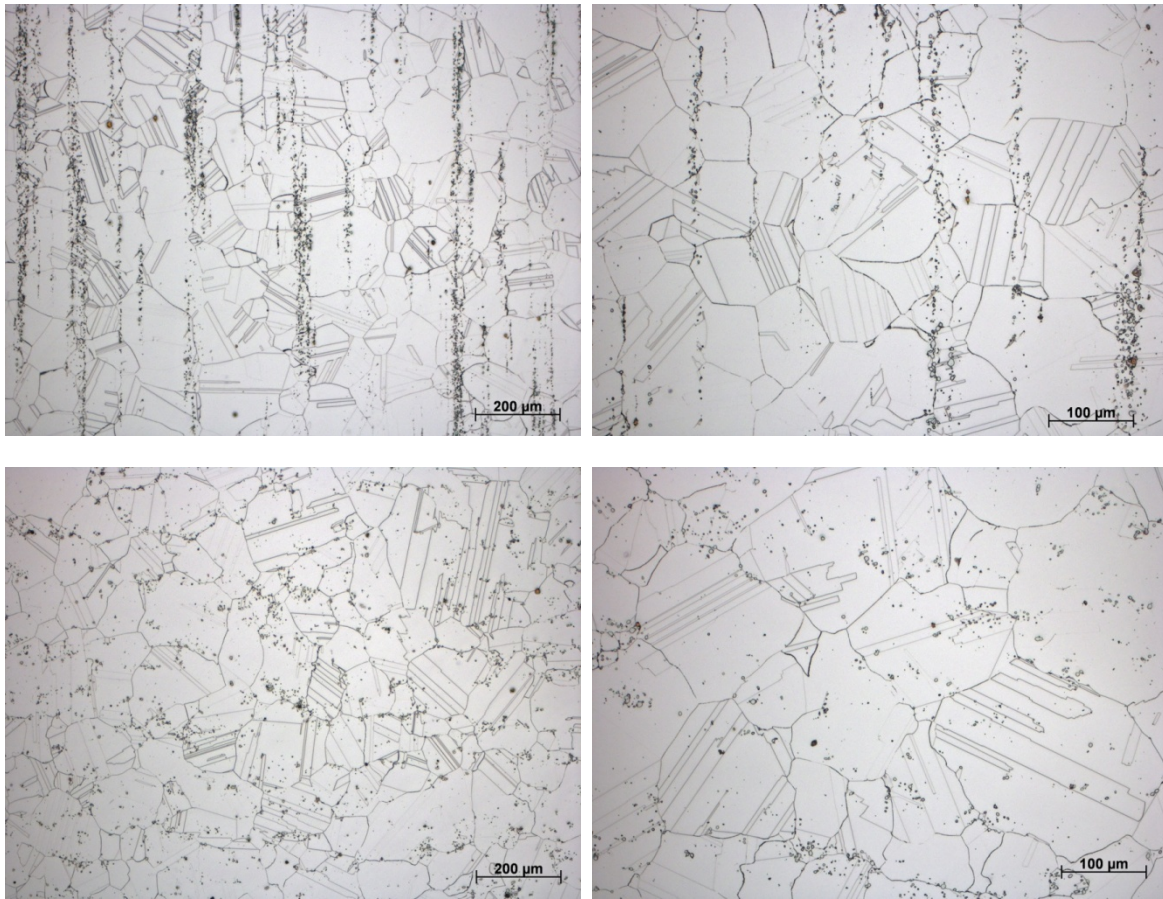
Figure 2. Optical metallography of rod product form at two magnifications for longitudinal (top) and transverse orientations.

Quality Statement

Tensile properties of Alloy 617 reported by the Idaho National Laboratory (INL) through the Next Generation Nuclear Plant (NGNP) or Advanced Reactor Technologies (ART) programs were determined under an NQA-1 quality program. Details of the quality program implementation are given in INL document PLN-2690 "Idaho National Laboratory Advanced Reactor Technologies Technology Development Office Quality Assurance Program Plan".

Values from other sources that are used in the assessment of S_y and S_u were generally obtained from tabulations of properties. Those values have only been included when the chemistry of the heat was reported

.

Page intentionally left blank

Table 1. Chemical composition of the Alloy 617 materials (weight percent).

Heat ID	Product Forms	Source	Ni	Cr	Co	Mo	Al	Ti	Fe	Mn	Cu	Si	C	S	B
min		ASME	44.5	20.0	10.0	8.0	0.8	--	--	--	--	--	0.05	--	--
max			--	24.0	15.0	10.0	1.5	0.6	3.0	1.0	0.5	1.0	0.15	0.015	0.006
314626	plate	INL	54.1	22.2	11.6	8.6	1.1	0.4	1.6	0.1	0.04	0.1	0.05	<0.002	<0.001
188155	rod	INL	53.27	22.02	11.91	9.38	1.1	0.32	1.46	0.23	0.02	0.2	0.08	0.001	0.002
DLH4168		CEA	bal.	21.6	12.0	9.2	1.0	0.4	1.0	0.1	0.1	0.2	0.06		0.002
XX00A1US	rod, sheet	Huntington	53.91	22.51	12.67	8.91	1.05	0.41	0.13	0.04	0.23	0.04	0.07	0.007	0.0051
XX00A3US	plate, forgings	Huntington	54.76	22.64	12.5	8.82	1.01	0.39	0.09	0.03	0.01	0.06	0.06	0.007	0.004
XX00A4US	rod	Huntington	54.73	22.31	12.46	9.09	1.06	0.35	0.15	0.02	0.01	0.08	0.07	0.007	0.0043
XX00A5US	rod, sheet	Huntington	55.91	21.77	12.24	8.71	0.99	0.46	0.19	0.03	0.02	0.06	0.07	0.007	0.0059
XX05A4UK	rod	Huntington	54.97	22.04	12.46	9.00	1.08	0.43	0.24	0.02	0.07	0.12	0.07	0.002	0.002
XX07A7UK	rod	Huntington	55.12	21.99	12.3	8.52	1.31	0.43	0.52	0.02	0.09	0.14	0.08	0.003	0.001
XX20A5UK	plate	Huntington	55.61	21.32	12.67	8.85	1.05	0.27	0.28	0.01	0.1	0.15	0.06	0.001	0.002
XX26A8UK	sheet	Huntington	54.54	21.89	12.48	9.00	1.17	0.26	0.48	0.03		0.09	0.06	0.001	0.002
XX01A3US	plate	ORNL	57.35	20.30	11.72	8.58	0.76		1.01	0.05		0.16	0.07	0.004	
XX09A4UK	plate	ORNL	55.11	21.83	12.55	8.79	1.15		0.38	0.02		0.1	0.07	0.001	

Blank cells indicate a composition that was not reported.

Page intentionally left blank

Tensile Testing

INL tensile testing is performed in conformance with ASTM E 8[9] and E 21,[10] for room temperature and elevated temperature tests, respectively. Tensile specimens conformed to ASTM E21, with a 6.35 mm diameter reduced section and a reduced section length of 32 mm (Figure 3) cut from material in the as-received condition with the axis of the specimen parallel to the direction of fabrication. The length and diameter of the test specimens were measured using calibrated micrometers. For INL testing, final dimensions, such as diameter and gauge length, were measured on the fractured specimen with ends fit carefully together, and the ductility and percent reduction in area calculated. For tabulated data from other sources it is not known if the elongation is measured from fractured specimens or the final crosshead displacement. The two values are typically similar and elongation is not a Code value; it is reported only to provide assurance that there is no elevated temperature embrittlement. Yield strengths are reported at an offset of 0.2% strain.
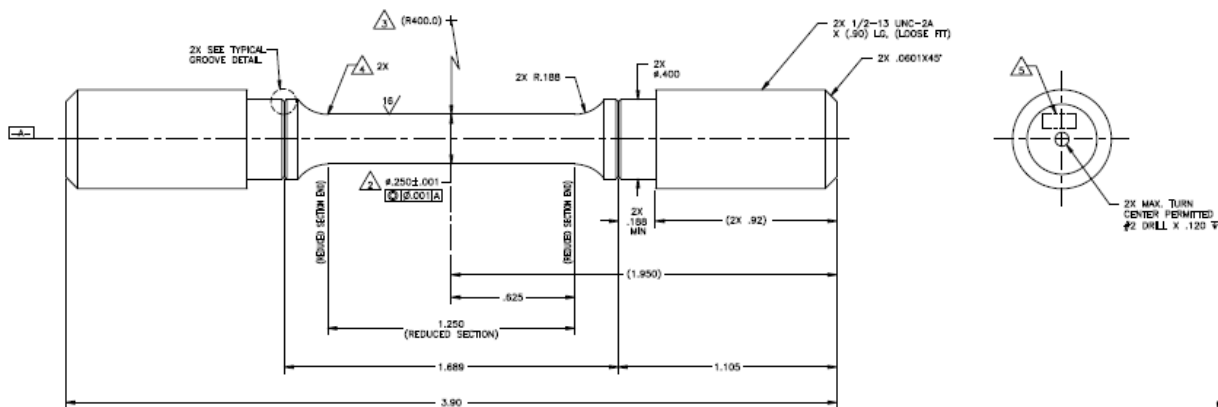
Figure 3. Tensile specimen used for testing at INL.

Tensile tests on rod were conducted at room temperature, 427°C (800°F, the cutoff of ASME Subsection NB), and at 200-400°C and 650-1000°C at 50°C intervals. Two replicate tests were performed at each temperature to assess the reproducibility of results. The test machine was a screw driven electro-mechanical machine with a resistance heated box furnace. Extensometers were direct mounted to the reduced section of the specimens and used from 0-20% strain for each test. Strain data after removal of the extensometers are a displacement-estimated strain based on the beginning and ending strain values and the crosshead displacement. For room temperature testing the crosshead speed was generally ~1.25 mm/minute to achieve a stress rate between 1.15-11.5 MPa/sec. For elevated temperature testing, tensile tests were carried out at constant crosshead-displacement rate of ~0.2 mm/minute corresponding with a strain rate of approximately 0.5%/min at yield. The temperature was monitored by thermocouples attached to the specimen and the gage section was held within 3°C of the specified test temperature.

Tensile properties on the plate were measured at room temperature, 425°C, and at 50°C intervals in the temperature range of 450-1000°C. Testing at 425-650°C followed the procedure described above for tests on the rod product form. Other tests at 650-1000°C were performed using dual averaging LVDT transducers to monitor the strain during testing to a resolution of better than 0.01% strain.

Details of the testing procedure are not known for the CEA, Huntington and ORNL tensile tests. It is believed that the existing values in Section II, Part D for S_u and S_y for temperatures up to 1000°F are largely based on the Huntington data included here.

The NDMA Spreadsheet

The New Material Data Analysis (NDMA) Spreadsheet[11] was used to calculate S_u and S_y for T > 525°C. The following description of the curve-fitting process appears in the user's guide for the software:

> "An Excel™-based software program was written to calculate allowable stress values consistent with the time-independent criteria specified in Appendix 1 and 2 of ASME BPV II Part D for Tables 1 through 5. The software produced a fit to the ratio values of elevated temperature to room temperature values for the yield and ultimate strengths, R_Y and R_T. The ratios were represented by a polynomial in terms of (T-T_{RT}) where T is temperature and T_{RT} is room temperature, both in °F or °C. Based on the minimum specified yield strength, S_Y, and ultimate strength, S_T, the *Y-1*, *U*, and allowable stresses (or stress intensity values) were recommended."

HBB-3225-1
S_u, Tensile Strength Values

Tensile strength values (S_u) from Section II, Part D, Table U for Alloy 617 are used up to 1000°F (525°C).

The New Material Data Analysis (NDMA) Excel spreadsheet for time-independent material properties[11] was used to determine S_u for T > 525°C. Tensile data from the sources detailed above were used as input. A fifth-order polynomial was fit to the tensile ratio. The plot of the fit to the R_T ratios of the entered values is shown in Figure 4. Proposed values of S_u are shown in Figure 5. The open square shows the values calculated by the NDMA spreadsheet at 1000°F and 525°C (86.6 ksi and 600.3 MPa vs the current ASME Code values of 87.1 ksi and 603 MPa). The calculated and current values are similar and both fall between the S_u values at the adjacent temperatures. The current Code values at 1000°F and 525°C are used in Table HBB-3225-1 of the Code Case; above that temperature new values based on this analysis are proposed.
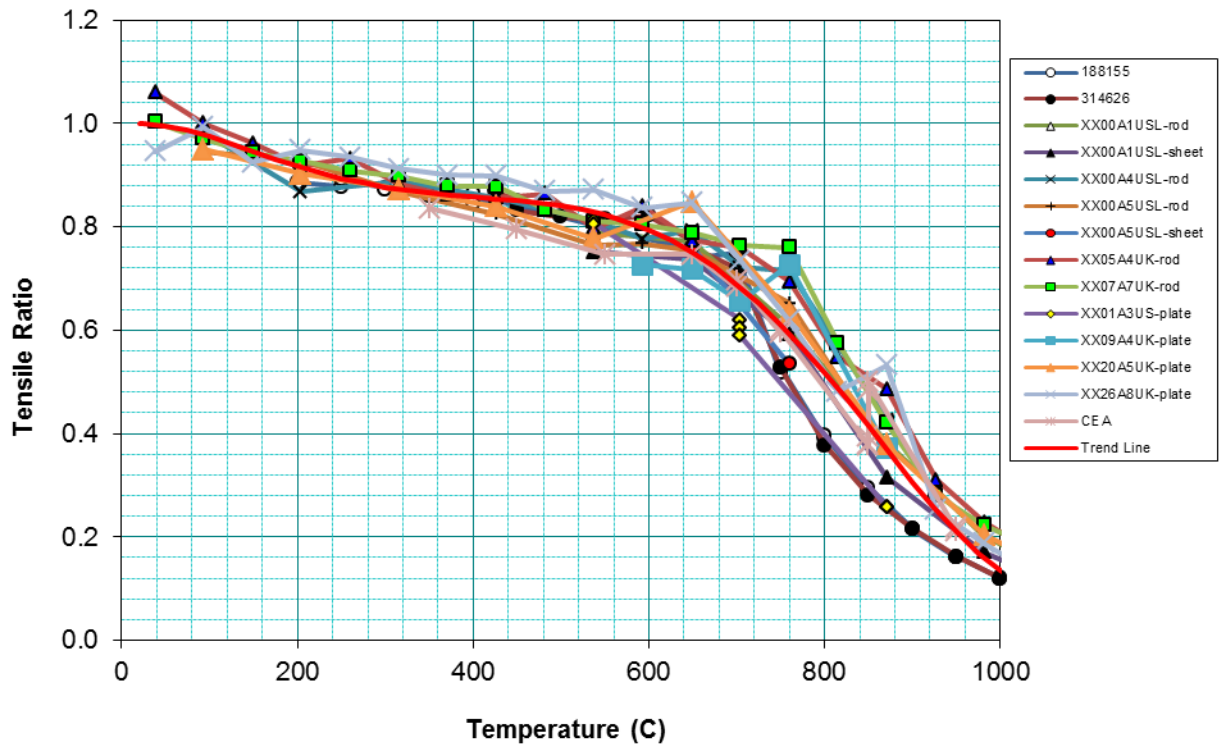
Figure 4. Plot produced by the NDMA spreadsheet for the fit to the tensile ratio, R_T.
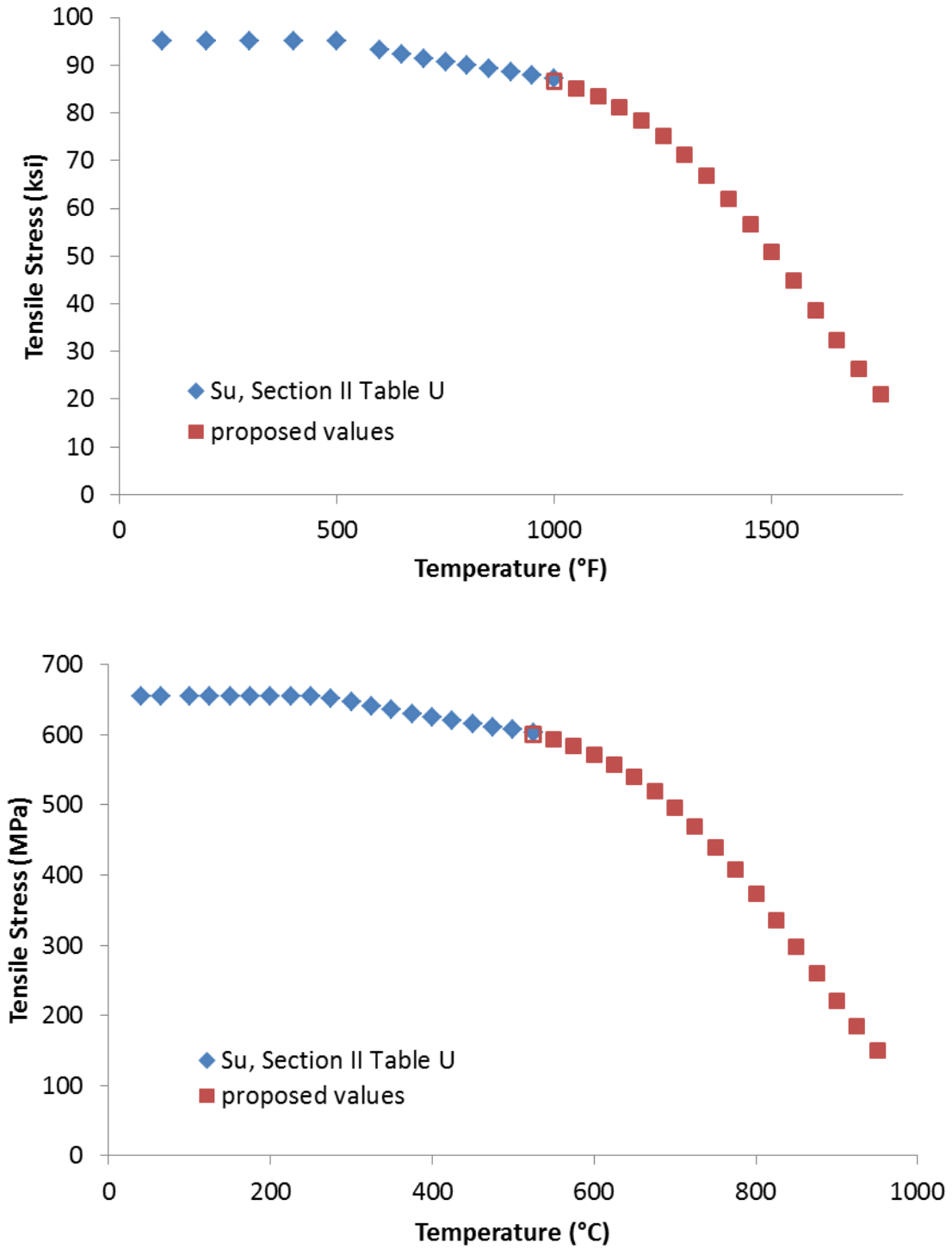
Figure 5. *S_u* for Alloy 617 in customary and SI units.

HBB-I-14.5
S_y, Yield Strength Values

Yield strength values (S_y) from Section II, Part D, Table Y-1 for Alloy 617 are used up to 1000°F (525°C).

The New Material Data Analysis (NDMA) Excel spreadsheet for time-independent material properties[11] was used to determine S_y for T > 525°C. Yield strength data from the sources detailed above were used as input. A fifth-order polynomial was fit to the yield strength ratio. The plot of the fit to the R_Y ratios of the entered values is shown in Figure 6. Note that the red trend line in Figure 6 reaches a minimum of 0.686 at about 450°C. The minimum R_Y ratio corresponds to an S_y value of 23.9 ksi or 164.8 MPa. The ASME Code value is not permitted to increase with increasing temperature, so the minimum S_y value is held constant with temperature until it decreases further at higher temperatures, rather than increasing as the polynomial would dictate. However the minimum value calculated by the polynomial is slightly greater than the current Code values of 23.3 ksi and 161 MPa at 1000°F and 525°C. The current Code values are used at 1000°F and 525°C in Table HBB-I-14.2 of the Code Case, and the value is held constant until 1500°F or 800°C, as shown in Figure 7. Above that temperature, new values based on this analysis are proposed.
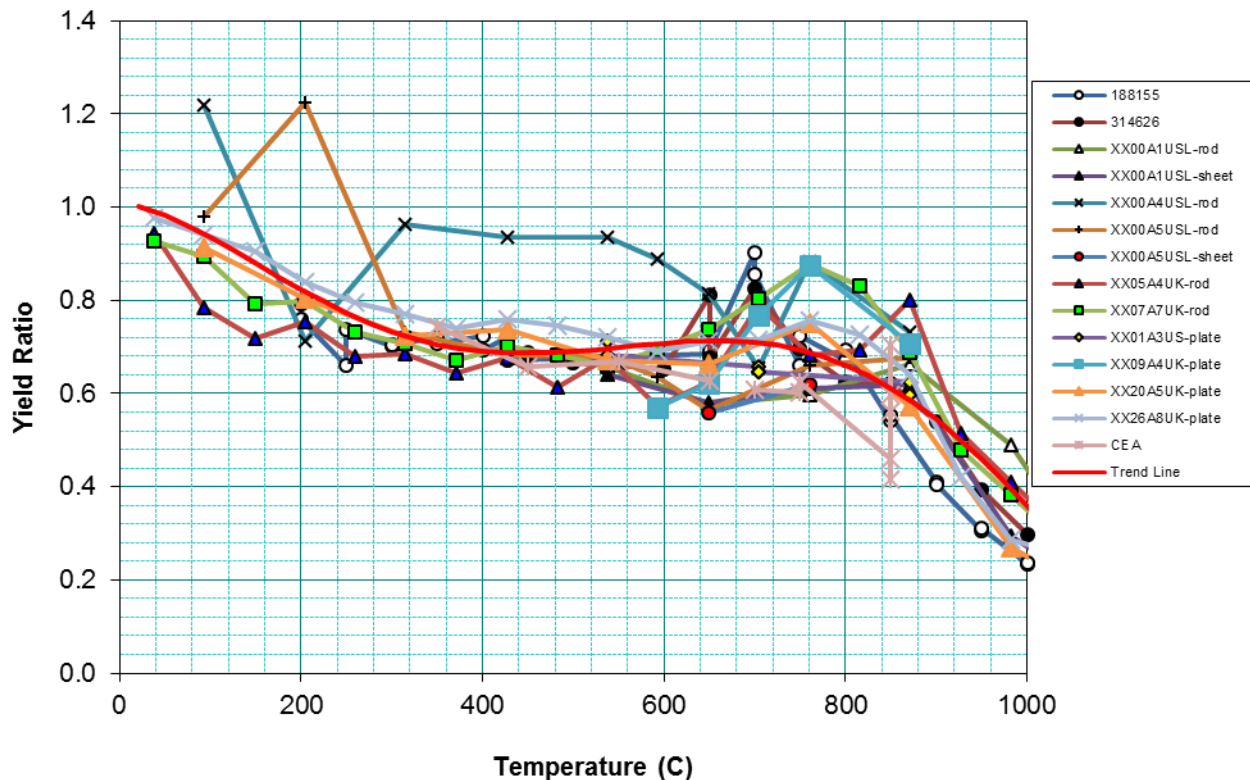
Figure 6. Plot produced by the NDMA spreadsheet for the fit to the yield ratio, R_Y.
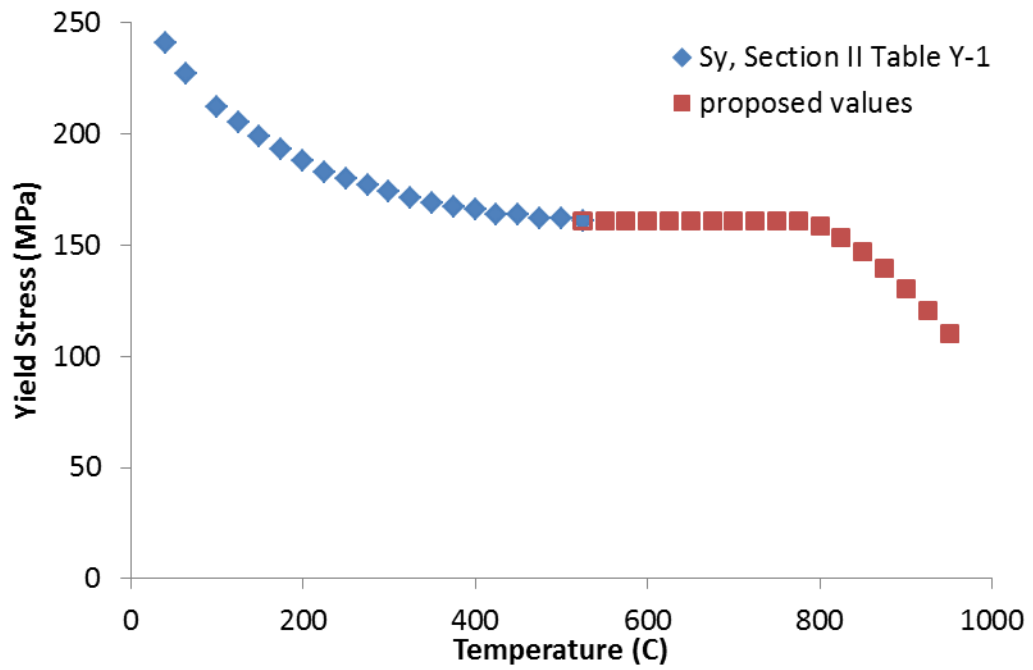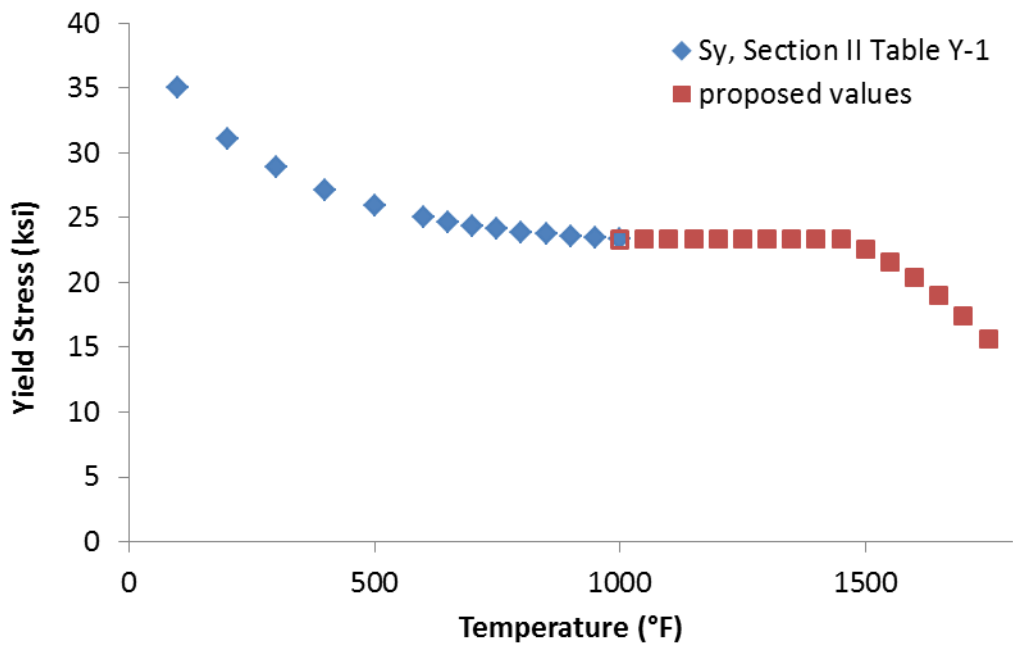
Figure 7. S_y for Alloy 617 in customary and SI units.

References

[1] J. K. Wright and T. M. Lillo (Idaho National Laboratory), *Progress Report on Alloy 617 time-Dependent Allowable Stresses*, INL/EXT-15-35640, Revision 1, July 2015.

[2] R. Weiju, 2009, "Gen IV Materials Handbook Functionalities and Operation," ORNL/TM-2009/285, U.S. Department of Energy Office of Nuclear Energy, December 2, 2009.

[3] Huntington Alloys Data Package of Inconel 617.

[4] H. E. McCoy, J. F. King (Oak Ridge National Laboratory), *Mechanical Properties of Inconel 617 and 618*, ORNL/TM-9337, February 1985.

[5] J. K. Wright, L. J. Carroll, C. Cabet, T. M. Lillo, J. K. Benz, J. A. Simpson, W. R. Lloyd, J. A. Chapman, and R. N. Wright, "Characterization of elevated temperature properties of heat exchanger and steam generator alloys," *Nuclear Engineering Design*, Vol. 251, 2012, pp. 252–260.

[6] C. Cabet, *High-Temperature Nickel-Based Alloys for VHTR Application: Mechanical and corrosion Testing*, International Nuclear Energy Research Initiative (INERI) with INL and CEA, Project Number 2006-002-F.

[7] ASTM B166 Standard specification for Nickel-Chromium-Iron Alloys (UNS N06600, N06601, N06603, N06690, N06025, N06046, N06696), Nickel-Chromium-Cobalt-Molybenum Alloy (UNS N06617), and Nickel-Iron-Chromium-Tungsten Alloy (UNS N06674) Rod, Bar, and Wire, ASTM International, 100 Barr Harbor Drive, PO Box C700, West Conshohocken, PA, 2011.

[8] ASTM B168 Standard specification for Nickel-Chromium-Iron Alloys (UNS N06600, N06601, N06603, N06690, N06025, N06046, N06696), Nickel-Chromium-Cobalt-Molybenum Alloy (UNS N06617), and Nickel-Iron-Chromium-Tungsten Alloy (UNS N06674) Plate, Sheet and Strip, ASTM International, 100 Barr Harbor Drive, PO Box C700, West Conshohocken, PA, 2011.

[9] ASTM E-8-11, Standard Test Methods for Tension Testing of Metallic Materials, ASTM International, 100 Barr Harbor Drive, PO Box C700, West Conshohocken, PA, 2011.

[10] ASTM E-21-09, Standard Test Methods for Elevated Temperature Tension Tests of Metallic Materials, ASTM International, 100 Barr Harbor Drive, PO Box C700, West Conshohocken, PA, 2009.

[11] R. W. Swindeman and M. J. Swindeman, *Analysis of Time-Independent Materials Properties Data,* ASME Standards Technology, LLC, 2009.

Page intentionally left blank

BACKGROUND

ALLOWABLE STRESS VALUES

Scope

This document provides the background/technical basis in support of the recommendation for the Maximum Allowable Stress Intensity, S_o, in Table HBB-I-14.2; Allowable Stress Intensity Value, S_{mt}, in Figure HBB-I-14.3F and Table HBB-I-14.3F; Allowable Stress Intensity Values, S_t, in Figure HBB-I-14.4F and Table HBB-I-14.4F; and Minimum Stress-to-Rupture Values, S_r, in Figure HBB-I-14.6G and Table HBB-I-14.6G.

Background

The maximum allowable value of general primary membrane stress intensity, S_o, are given in Table HBB-I-14.2 and correspond to the S values given in Section II, Part D, Subpart 1, Table 1A. They are used as a reference for stress calculations under Design Loadings and are determined from tensile values.

Allowable Stress Intensity Value, S_{mt}, is used as a reference for stress calculations for the actual service life and under the Level A and B Service Loadings. S_{mt} is the lower of two stress intensity values, S_m (time-independent) and S_t (time-dependent).

The Expected Minimum Stress-to-rupture values, S_r, are obtained from creep rupture tests at various temperature and stress levels. The minimum stress-to-rupture values given in Figure HBB-I-14.6G are used to determine the maximum allowed time values required in articles HBB-3225, HBB-T-1324, HBB-T-1411, HBB-T-1433, and HBB-T-1715 of Section III, Division 5, Subsection HB, Subpart B.

The temperature and time-dependent stress intensity, S_t, are also obtained from creep rupture tests at various temperature and stress levels. S_t is defined as the lesser of three quantities: 100% of the average stress required to obtain a total (elastic, plastic, primary and secondary creep) strain of 1%, 67% of the minimum stress to cause rupture, and 80% of the minimum stress to cause the initiation of tertiary creep. The load stress intensity values given in Figure HBB-I-14.4G are used to determine the maximum allowed time value required in article HBB-3224 of Section III, Division 5, Subsection HB, Subpart B.

The S_{mt}, S_o, S_r, and S_t values are used along with S_m and S_y, in determining the allowable stress intensity values in the subarticles under HBB-3220 of Section III, Division 5, Subsection HB, Subpart B.

Data Sources

Creep and tensile data have been compiled from three general sources: testing of modern heats of Alloy 617 plate in current VHTR programs, historical data from previous high-temperature reactor programs, and data originally generated by the vendor developing Alloy 617. The data set has been limited to specimens with known chemistry that were tested in air, and represents multiple product forms and heats. A tabulation of the creep data can be found in the Appendices of this background document. Tensile data can be found in Appendix I.

The Generation IV International Forum (GIF) VHTR Materials Program Management Board has agreed to compile data from earlier testing programs and share data generated from current member test programs in the GIF Materials Handbook.[1] Past data include those generated at Huntington Alloys (the original producer of Inconel 617 and now part of Special Metals Corporation (SMC)),[2] as well as General Electric (GE)[3] and Oak Ridge National Laboratory (ORNL)[4] as part of the Department of Energy High-

Temperature Gas−Cooled Reactor Research Program of the 1980s and 1990s. Additionally, creep data have recently been released by SMC[5] and by Japan's National Institute for Materials Science (NIMS).[6] Creep curves (i.e., strain vs. time) are not available for all of these creep tests, and the inclusion of other details (e.g., creep rate) varies among and within the laboratories. Similarly, tensile curves (stress vs. strain) are generally not available. Some details of the testing procedure are also unknown.

More recently, creep data have been contributed by INL,[7] ANL,[8] and the Korean Atomic Energy Research Institute (KAERI).[9-12] Somewhat more is known regarding creep test procedures of these organizations. Detailed tensile data from INL is also presented.[13]

Additional data have been published in scientific literature. Discussion with members of the ASME Section III Working Group on Allowable Stress Criteria suggested that a subset of these data could be incorporated into the data set used to determine allowable stresses for Alloy 617 provided there was known chemistry for the material. Two sources of creep data met this condition. Cook[14] reports data from creep tests conducted in air at temperatures from 800 to 950°C at 50°C increments. Data are reported in graphical form and required digitization to obtain rupture time and stress. CEA[15] reports data from five specimens tested in air at 850 or 950°C. The source tabulates stress, temperature, and rupture time for each test.

Materials

The Idaho National Laboratory (INL) has performed extensive property characterization on specimens machined from an Alloy 617 reference material plate.[16] The reference plate is a 37 mm thick solution annealed plate labeled as heat 314626, with an average grain size of 150 μm and the composition given in Table 1. Creep and tensile testing has been performed at INL and creep testing has been performed at Argonne National Laboratory (ANL)[8] on specimens machined from this reference plate. Additional tensile testing was done at INL on specimens machined from 51-mm diameter rod, labeled as heat 188155 with an average grain size of 150 μm and the composition given in Table 1. Both product forms were produced by ThyssenKrupp VDM and provided in the solution−annealed condition, consisting of holding at 2150°F (1175°C) followed by rapid cooling to room temperature, according to standards SB166 and SB168.[17,18] The microstructures of both the plate and the rod product forms can be found in the background section for HBB-3225-1, S_u, and HBB-I-14.5, S_y.

KAERI creep specimens tested at 850, 900, and 950°C were machined from commercial−grade Alloy 617 solution annealed hot−rolled plate produced by SMC,[9, 10] with a thickness of 16 mm and a grain size of approximately 300 μm. The chemical composition is shown in Table 1. Specimens tested at 800°C came from an approximately 16 mm thick plate produced by Haynes,[11] also shown in Table 1.

The Cook[14] creep specimens were primarily machined from a 25 mm bar (designated as C in the source), but include a few specimens from a 12 mm bar (A) and one from a 12 mm plate (B). The grain sizes are reported as ASTM grain numbers of 4, 2.5, and 1.5, respectively. CEA[15] creep specimens were machined from a single heat of 50 mm diameter bar stock produced by SMC with a grain size of 280 μm. Chemistries from these sources as well as the NIMS, Huntington/SMC, ORNL and GE heats are included in Table 1.

Table 1. Chemical composition of the Alloy 617 materials (weight percent).

Heat ID	Source	Ni	Cr	Co	Mo	Al	Ti	Fe	Mn	Cu	Si	C	S	B
min	ASTM	44.5	20.0	10.0	8.0	0.8	--	--	--	--	--	0.05	--	--
max		--	24.0	15.0	10.0	1.5	0.6	3.0	1.0	0.5	1.0	0.15	0.015	0.006
314626	INL	54.1	22.2	11.6	8.6	1.1	0.4	1.6	0.1	0.04	0.1	0.05	<0.002	<0.001
188155	INL	53.27	22.02	11.91	9.38	1.1	0.32	1.46	0.23	0.02	0.2	0.08	0.001	0.002
93351	KAERI	bal	22.16	11.58	9.8	1.12	0.35	1.5	0.1	0.08	0.06	0.08	0.001	0.002
Haynes	KAERI	bal	22.2	12.3	9.5	1.06	0.41	0.949	0.029	0.027	0.084	0.08	<0.002	<0.002
A	Cook	bal	22.31	12.46	9.09	1.06	0.35	0.15	0.02		0.08	0.07	0.007	
B	Cook	bal	20.30	11.72	8.58	0.76	0.56	1.01	0.05		0.16	0.07	0.004	
C	Cook	bal	21.15	12.44	9.35	0.82	0.55	1.43	0.03		0.23	0.08	0.002	
DLH 6003	CEA (creep)	54.2	21.45	12	9.3	0.9		1.27	0.12		0.14	0.06		0.001
DLH 4168	CEA (tensile)	bal	21.6	12.0	9.2	1.0	0.4	1.0	0.1	0.1	0.2	0.06		0.002
NIMS	NIMS	bal	20.31	11.71	8.64	0.72	0.57	1.02	0.05		0.19	0.069	0.03	
XX00A1US	Huntington	53.91	22.51	12.67	8.91	1.05	0.41	0.13	0.04	0.23	0.04	0.07	0.007	0.0051
XX00A2US	Huntington	54.6	22.77	12.72	8.59	0.98	0.25	0.18	0.02	0.01	0.04	0.07	0.008	0.005
XX00A3US	Huntington	54.76	22.64	12.5	8.82	1.01	0.39	0.09	0.03	0.01	0.06	0.06	0.007	0.004
XX00A4US	Huntington	54.73	22.31	12.46	9.09	1.06	0.35	0.15	0.02	0.01	0.08	0.07	0.007	0.0043
XX00A5US	Huntington	55.91	21.77	12.24	8.71	0.99	0.46	0.19	0.03	0.02	0.06	0.07	0.007	0.0059
XX05A4UK	Huntington	54.97	22.04	12.46	9.00	1.08	0.43	0.24	0.02	0.07	0.12	0.07	0.002	0.002
XX05A7UK	Huntington	55.02	21.77	12.57	9.15	1.07	0.51	0.21	0.01	0.07	0.14	0.06	0.004	0.002
XX07A7UK	Huntington	55.12	21.99	12.3	8.52	1.31	0.43	0.52	0.02	0.09	0.14	0.08	0.003	0.001
XX10A3UK	Huntington	54.16	22.17	12.7	9.29	1.04	0.32	0.33	0.04	0.19	0.18	0.09	0.003	0.001
XX18A4UK	Huntington	54.22	21.86	12.35	8.95	1.03	0.28	0.72	0.01	0.09	0.17	0.051	0.006	0.003
XX20A5UK	Huntington	55.61	21.32	12.67	8.85	1.05	0.27	0.28	0.01	0.1	0.15	0.06	0.001	0.002
XX26A8UK	Huntington	54.54	21.89	12.48	9.00	1.17	0.26	0.48	0.03		0.09	0.06	0.001	0.002
XX41A7UK	Huntington	54.01	21.42	12.9	8.83	0.92	0.3	1.35	0.02	0.04	0.19	0.06	0.001	0.001
XX0529UK	SMC	52.12	21.98	12.47	9.74	1.17	0.28	1.61	0.06	0.07	0.15	0.085	<0.001	0.002
XX0574UK	SMC	52.52	21.54	12.45	9.71	1.22	0.27	1.72	0.08	0.06	0.15	0.088	<0.001	0.002
XX0684UK	SMC	52.45	21.94	12.57	9.49	1.09	0.31	1.61	0.05	0.17	0.13	0.082	<0.001	0.005
XX0688UK	SMC	52.33	21.56	12.54	9.87	1.12	0.32	1.32	0.05	0.51	0.12	0.080	<0.001	0.006
XX0693UK	SMC	52.82	22.00	12.69	9.70	1.06	0.32	0.99	0.03	0.12	0.12	0.079	<0.001	0.001
XX01A3US	ORNL	57.35	20.30	11.72	8.58	0.76		1.01	0.05		0.16	0.07	0.004	
XX09A4UK	ORNL	55.11	21.83	12.55	8.79	1.15		0.38	0.02		0.1	0.07	0.001	
XX14A6UK	GE	bal	21.74	12.32	8.91	1.11	0.3	0.53	0.02	0.11	0.18	0.06	0.002	0.003
XX63A8UK	GE	bal	22.3	12.1	9.27	1.07	0.37	1.02	0.06	0.09	0.19	0.07	0.001	0.003

Blank cells indicate an elemental composition that was not reported.

Page intentionally left blank

Quality Statement

Creep and tensile properties of Alloy 617 reported by INL and ANL were conducted through the Next Generation Nuclear Plant (NGNP) or Advanced Reactor Technologies (ART) programs and were determined under an NQA-1 quality program. Details of the quality program implementation are given in INL document PLN-2690 "Idaho National Laboratory Advanced Reactor Technologies Technology Development Office Quality Assurance Program Plan".

Values from other sources that are used in the assessment of the allowable stress values were generally obtained from tabulations of properties. Those values have only been included when the chemistry of the heat was reported.

Tensile Testing

Details of the tensile testing and associated data analysis along with methods for determining Tensile Strength (S_u) and Yield Strength (S_y) values for the Alloy 617 Code Case are given in the previous section of this background document.

Creep Testing

Information on the details of creep testing for the CEA, NIMS, Huntington/SMC, ORNL and GE heats is limited. Information on more recent testing is given below.

ANL

The creep test specimens used in the ANL testing are a button−head design that meets the ASTM E8[19] specification as shown in Figure 1.
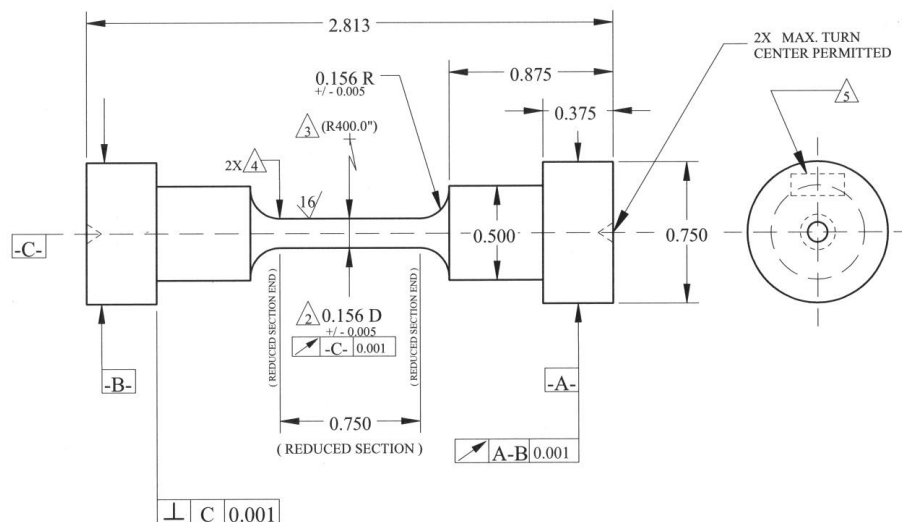
Figure 1. Creep specimen used for testing at ANL.

Direct−load creep frames were used to test the specimens. A three-zone furnace was used to heat to the test temperature set point over a 3−hour ramp time. The test specimen was centered in the middle furnace zone and the specimen temperature profile was maintained within ±1°C of the desired test temperature. Calibrated thermocouples were spot welded to the specimen outer transition radius shoulder edge so as not to introduce defects into the gage length area. The creep test was completed when the specimen

ruptured and the system provided automatic cooldown. An LVDT extensometer was used to monitor strain during the test.[8]

INL

Cylindrical creep specimens, with nominal 6.35 mm reduced section diameter and gage length of 32 mm (Figure 2), were machined in conformance with ASTM E 139.[20] Testing was performed using direct loaded creep frames with dead weight loading, with the exception of a 750°C test which utilized a 20:1 lever arm. The temperature of the gage section of the creep specimen was measured with type K thermocouples for tests at temperatures of 750 °C and type R thermocouples for tests at temperatures of 900 °C or above. The specimen temperature was controlled to within ±3°C of the target test temperature. Dual averaging LVDT transducers or Heidenheim linear encoded photoelectric gauges were used to monitor creep strain during the creep tests to a resolution of better than 0.01% strain. Most tests culminated in creep−rupture; however, in some cases creep tests were interrupted at a pre−determined strain for purposes of microstructural analysis.
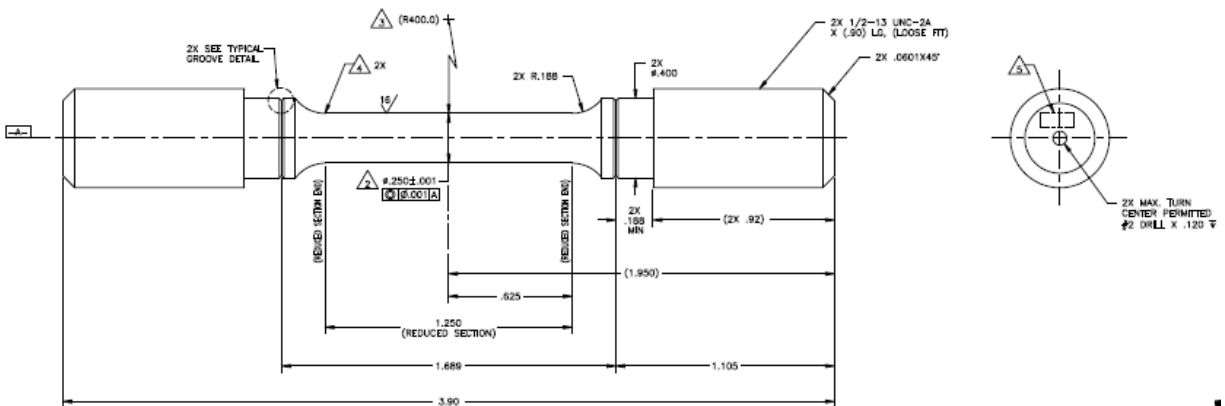
Figure 2. Creep specimen used for testing at INL.

KAERI

Cylindrical creep specimens had a 30 mm gauge length and a 6 mm diameter, with the axis aligned with the rolling direction. Creep tests were controlled to ±2°C during testing. A range of stress levels was tested; however, stress levels of 30 and 35 MPa were tested for each temperature. Strain was measured using an extensometer. Stress levels of 60−100 MPa were tested in air, using Type−K thermocouples to monitor the temperature within the split three−zone furnace used for heating the specimen.

HBB-I-14.2
S_o− Maximum Allowable Stress Intensity

S_o values correspond to the S values given in ASME Code Section II, Part D, Subpart 1, Table 1B. S is the lowest of the time-independent and time-dependent criteria defined in ASME Code Section II, Part D, Table 1-100. The SI version of Table 1B only includes values up to 900°C, but additional values are given in Note G29 that were used to interpolate the values proposed for 925 and 950°C.

HBB-I-14.3
S_{mt} – Allowable Stress Intensity Values

S_{mt}, the allowable limit of general primary membrane stress intensity is the lower of two stress intensity values, S_m (time−independent) and S_t (time−dependent).

142

At each temperature, S_m is the lowest of the stress intensity values obtained from the time−independent strength criteria given in ASME Code Section II, Part D, Table 2-100(a). In Section III, Division 5, Subsection HB, Subpart B, S_m values are extended to elevated temperatures using the same criteria.

Since Alloy 617 is not currently allowed for Section III use, values of S_m for Alloy 617 do not appear in Table 2B of Section II, Part D. Below the maximum temperature of 800°F (427°C) for Section III, Division 5, Subsection HB, Subpart A, the yield criteria govern. The yield criteria for S_m from Table 2-100(a) are the same as for S from Table 1-100 therefore, S_m is the same as S and S_o for this temperature range.

As specified in Note (1) to Table 2-100(a), a yield strength multiplication factor of either $^2/_3$ or 0.9 must be selected for austenitic and nickel alloys when determining the yield strength criteria above room temperature. Section II, Part D Appendices 1 and 2 specify that the high stress rules apply to austenitic stainless steel, nickel alloys and cobalt alloys whose yield to tensile strength ratio is less than 0.625. For Alloy 617 this ratio is less than 0.5 in the temperature range where this yield criterion governs, thus the yield strength multiplication factor of 0.9 applies.

Above 800°F (427°C), S_m is governed by $0.9S_YR_Y$ up to 1400°F (775°C), and by $1.1/3*S_TR_T$ at higher temperatures, where $S_y = S_YR_Y$, and $S_u = 1.1*S_TR_T$, from Section II, Part D, Appendix 2, article 2-110 and $S_Y = 240$ MPa, and $S_T = 655$ MPa from Table 1B and the values for S_y and S_u are tabulated in this Code Case. S_m and S are plotted as a function of temperature in Figure 3. (S values are governed by time-dependent criteria above 1150°F (625°C) and are therefore much lower than S_m.)

S_t is presented in detail in Section HBB-I-14.4 of this background document.

An abbreviated tabulation of S_{mt} values is shown in Table 2. Yellow is used in Table 2 to illustrate which time/temperature combinations are governed by the time−dependent allowable (S_t); white cells are governed by the time−independent allowable (S_m).
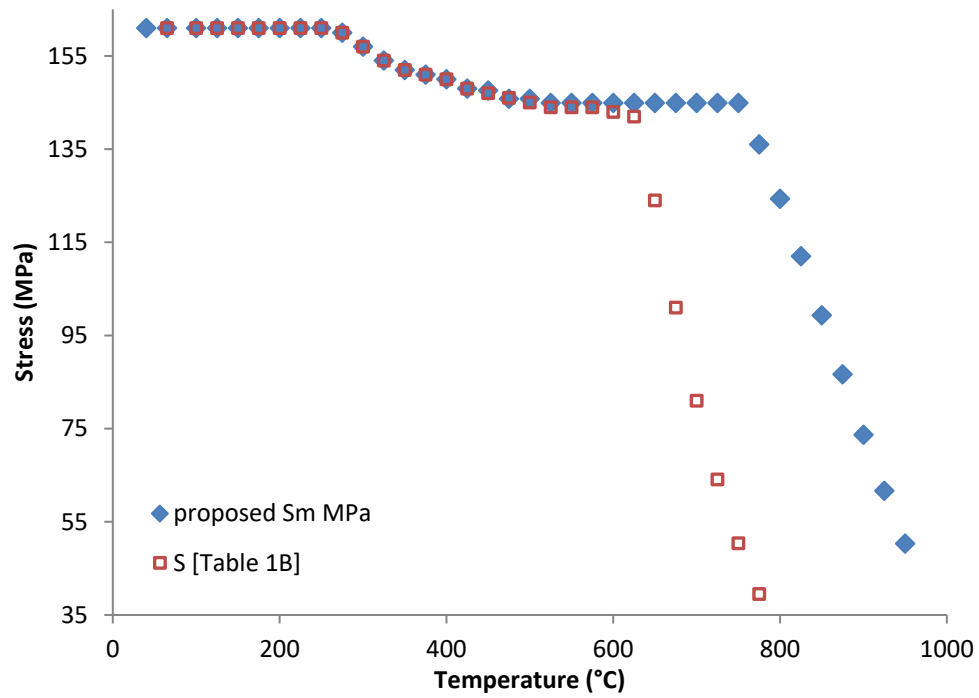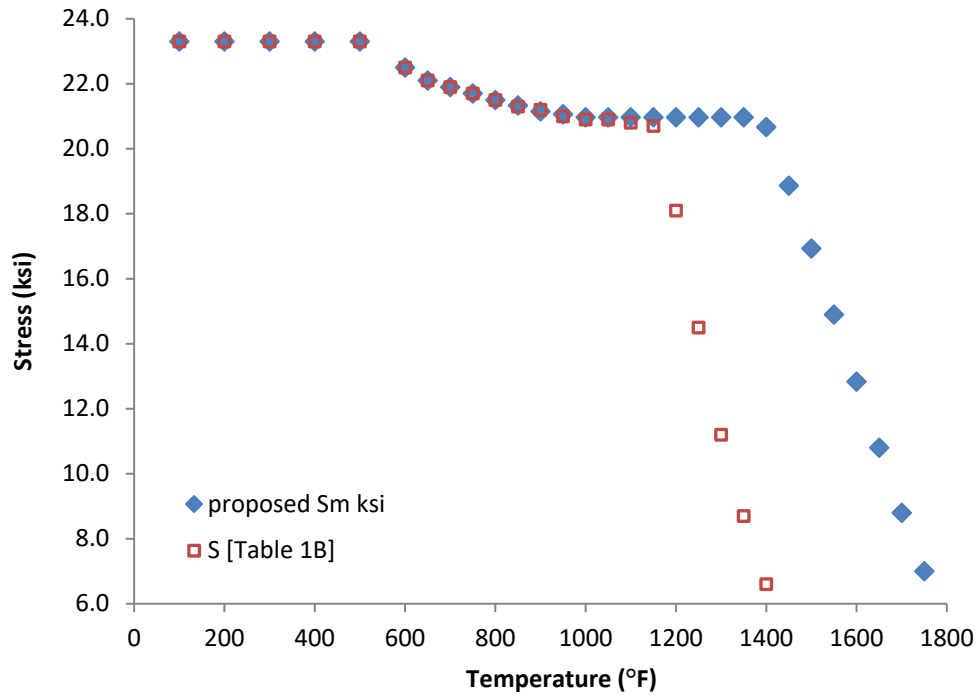
Figure 3. S_m for Alloy 617 in customary and SI units.

Table 2. Sampling of allowable stress intensity values, S_{mt}, in SI units, showing time–dependent (S_t) values in yellow.

Time (h)→	Stress (MPa)									
	1	10	30	100	300	1000	3000	10000	30000	100000
Temperature (°C) ↓	S_{mt}									
425	148	148	148	148	148	148	148	148	148	148
450	147	147	147	147	147	147	147	147	147	147
500	146	146	146	146	146	146	146	146	146	146
550	145	145	145	145	145	145	145	145	145	145
600	145	145	145	145	145	145	145	145	145	130
650	145	145	145	145	145	145	145	121	102	84
700	145	145	145	145	142	116	97	79	65	52
750	145	145	144	117	95	76	62	50	41	33
800	124	121	98	77	62	49	40	32	26	20
850	99	82	65	51	41	32	26	20	16	13
900	74	55	44	34	27	21	16	13	10	8
950	50	37	29	22	18	13	11	8	6	5

HBB-I-14.4
S_t – Allowable Stress Intensity Values (Time-Dependent)

S_t is defined as the lesser of three quantities: 100% of the average stress required to obtain a total (elastic, plastic, primary and secondary creep) strain of 1%, 67% of the minimum stress to cause rupture, and 80% of the minimum stress to cause the initiation of tertiary creep. In order to determine S_t, each of the three criteria must be calculated for the matrix of times and temperatures. This is achieved by using the Larson–Miller plots to all acceptable creep data, combined with information from the hot tensile curves.

The Larson–Miller Equation

The most common method for comparing creep–rupture tests performed at various temperatures and stress levels is by plotting stress against the Larson–Miller parameter (LMP):

$$LMP = T(C + log_{10}(t)) \qquad [1]$$

where T is absolute temperature, C is the Larson–Miller constant and t is time, which is typically time to rupture, but can also be time to 1% total strain or time to onset of tertiary creep.[21] For Alloy 617 a linear equation in log stress describes the creep data well.

$$LMP = a_0 + a_1 log_{10}(\sigma) \qquad [2]$$

where a_0 and a_1 are the fitting parameters, and σ is stress (MPa). For the purposes of the regression analysis, the stress function is rewritten so that log t is the dependent variable and T and log σ are the independent variables:

$$log_{10}(t) = \left[\frac{a_0 + a_1 \, log_{10} \, \sigma}{T}\right] - C \qquad [3]$$

Using a least squares fitting method, the optimum values for C, a_0, and a_1 are determined. A "lot–centering" procedure developed by Sjodahl[22] was employed that calculates the lot constant (C_{lot}) for each heat of material, along with the Larson–Miller constant, C, which is the average of the lot constants. A spreadsheet developed for ASME for the analysis of time–dependent materials properties[23] was used to generate the Larson–Miller plots.

Time to 1% Strain

A Larson−Miller plot was created using time to 1% total strain measured during creep tests (Figure 4).[21] Time to 1% total strain was not reported for all creep−rupture tests, but was available for many of the INL interrupted creep tests. Specimens with a time to 1% strain or rupture time of less than 10 hours were excluded, resulting in a data set of 220 specimens, shown in Appendix II. Regression analysis for a linear fit produced $C = 16.70735830$ in Equation [1] and $a_0 = 30489.71670$ and $a_1 = -5232.632763$ in Equation [2] when SI units are used. A linear fit was used rather than a higher order polynomial to prevent the calculated *LMP* line from curving up, thus ensuring that extrapolation to long time/higher temperature is conservative.
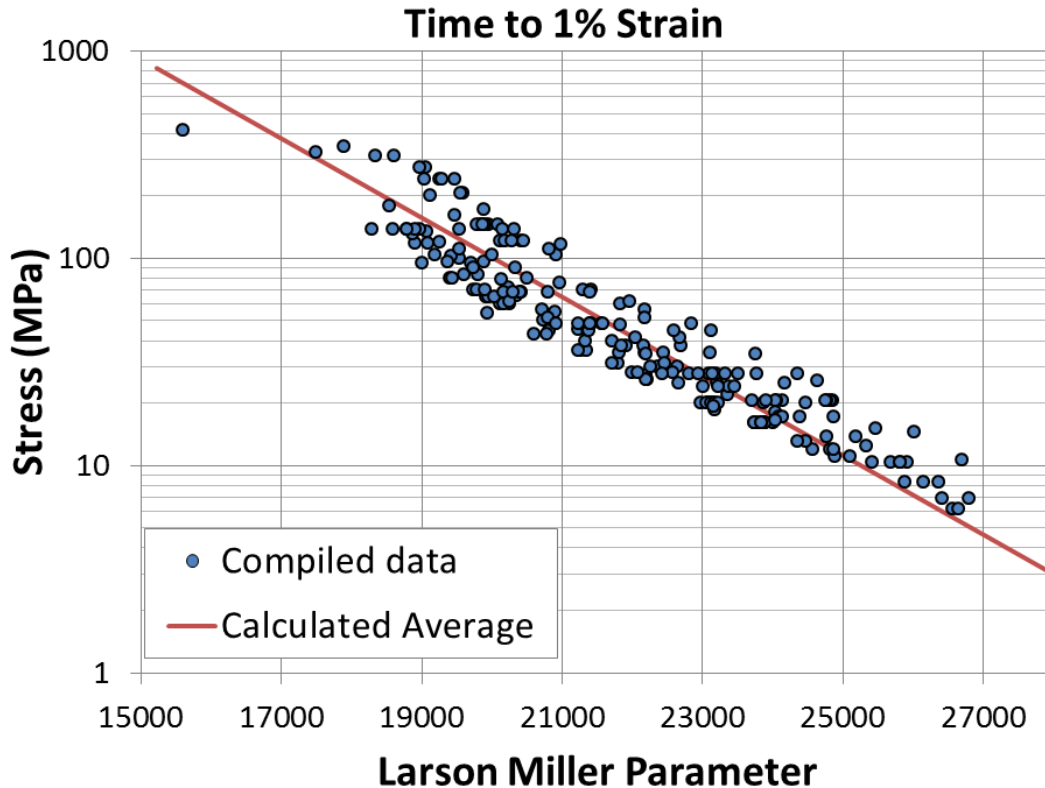
Figure 4. Larson−Miller plot with a linear fit (red line) for time to 1% creep strain for Alloy 617.

The stress at 1% total strain from creep tests is determined from the Larson−Miller plots; however, the stress at 1% plastic + elastic strain must be obtained from the hot tensile curves. The average hot tensile curves are plotted along with isochronous stress−strain curves in Section HBB-T-1800 of this Code Case. Previously the minimum hot tensile curves were used to determine these plastic stress values. However, the average hot tensile curves have been recently used for Type 316 stainless steel after discussion within the ASME Subgroup on Elevated Temperature Design.[24] Table 3 gives stress at 1% total strain from the average hot tensile curves, used as the upper limit for S_t. Note that the value in the range of 650–750°C is held constant at 231 MPa, although the values from the hot tensile curves increase slightly in this temperature range because of the anomalous yield behavior of Alloy 617 (increasing yield strength in this temperature range with increasing temperature due to formation of the γ' phase). The total stress at a strain of 1% will be the minimum of the hot tensile stress from Table 3 and the stress from the 1% Larson−Miller plot for a given temperature.

Table 3. Stress at 1% total strain as a function of temperature obtained from the average hot tensile curves.

Temperature (°C)	Stress 1% (MPa)
425	245.3
450	244.6
475	242.2
500	239.8
525	237.6
550	235.4
575	233.9
600	232.5
625	231.8
650	231.0
675	231.0
700	231.0
725	231.0
750	231.0
775	230.9
800	228.3
825	215.9
850	202.9
875	184.9
900	167.0
925	154.9
950	142.9

Time to Onset of Tertiary Creep

A Larson−Miller plot was also created using time to onset of tertiary creep.[21] This value was not reported for all creep−rupture tests. The historical creep data (Huntington, ORNL, GE) is available in tabular form, and creep curves (strain as a function of time) are not available. In many cases creep strain was not measured continuously during the test as is typically done today. Tests were periodically suspended, the specimen removed from the load frame and measured to determine strain, and the test resumed. In these cases creep curves may not have had the resolution to determine onset of tertiary creep.

The recommended method of determining the onset of tertiary creep involves determining the minimum creep rate, shown as the solid black line in Figure 5, drawing a parallel line offset by 0.2% strain, and finding the intersection of the offset line (dashed in Figure 5) with the creep curve (red), labeled as B. This method is used for tests where a creep curve is available, and is reported in a few cases for historical data. In other cases, the deviation from linearity, labeled as A, is reported, and in others it is not clear if the value reported represents A or B. Furthermore, in some cases creep curves for Alloy 617 do not follow the classical shape shown in Figure 5. They may have either an inflection point rather than a linear secondary creep portion, have two linear portions, or have no discernable primary or secondary creep.
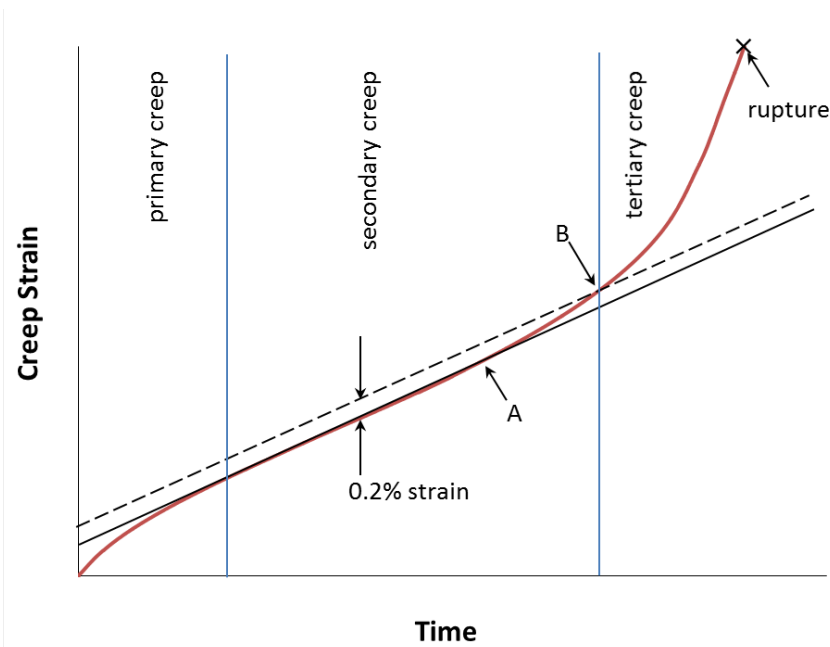
Figure 5. Typical creep curve showing the three stages of creep, minimum creep rate, and 0.2% offset to onset of tertiary creep.

For this data set, the offset value (B in Figure 5) was used where possible, and if a tabulated value was reported, it was included even if it was not offset (A in Figure 5) or unknown, as A values are more conservative. If the curve had an inflection point or short linear portion, a value could generally be determined, but for curves where the onset of tertiary creep was ambiguous, the curve was not included in the tertiary creep data set. If the time to onset of tertiary creep was less than 10% of the creep−rupture time it was assumed that the creep curve did not have a classical shape enabling analysis as shown in Figure 5. Leyda and Rowe analyzed 760 creep curves from 18 alloys and found the ratio of time to tertiary creep to time to rupture ranged from 0.158 to 0.546, well above the cut−off used for this analysis.[25]

Specimens with a time to onset of tertiary creep or rupture time of less than 10 hours were excluded from the data set in addition to those with non−classical creep curves as discussed above. The final data set contained 183 specimens, given in Appendix III. Regression analysis for a linear fit (Figure 6) produced $C = 17.15722823$ in Equation [1] and $a_0 = 32{,}317.18475$ and $a_1 = -5533.123186$ in Equation [2] when SI units are used. The linear regression for time to onset of tertiary creep results in a better fit and higher stress values for larger Larson−Miller parameters, but lower stress values for intermediate Larson−Miller parameters.

In order to determine the time to onset of tertiary creep criterion, the *LMP* is calculated for each time and temperature increment. However, the minimum stress is needed rather than the average. This is accomplished by creating a line that is displaced by 1.65 multiplied by the standard error of estimate (*SEE*) in log time from the average time to tertiary strain line (shown on Figure 6). In order to accomplish this, Equation [1] must be replaced by:

$$LMP = T\,(C + \log_{10} t + 1.65\;SEE) \qquad [4]$$

SEE, calculated as 0.4375148215, is included in the output of the spreadsheet used to calculate and plot the Larson−Miller relationships.[23] Finally, Equation [2] is used to solve for stress, σ; 80% of σ is used for the tertiary creep criterion (also shown on Figure 6).
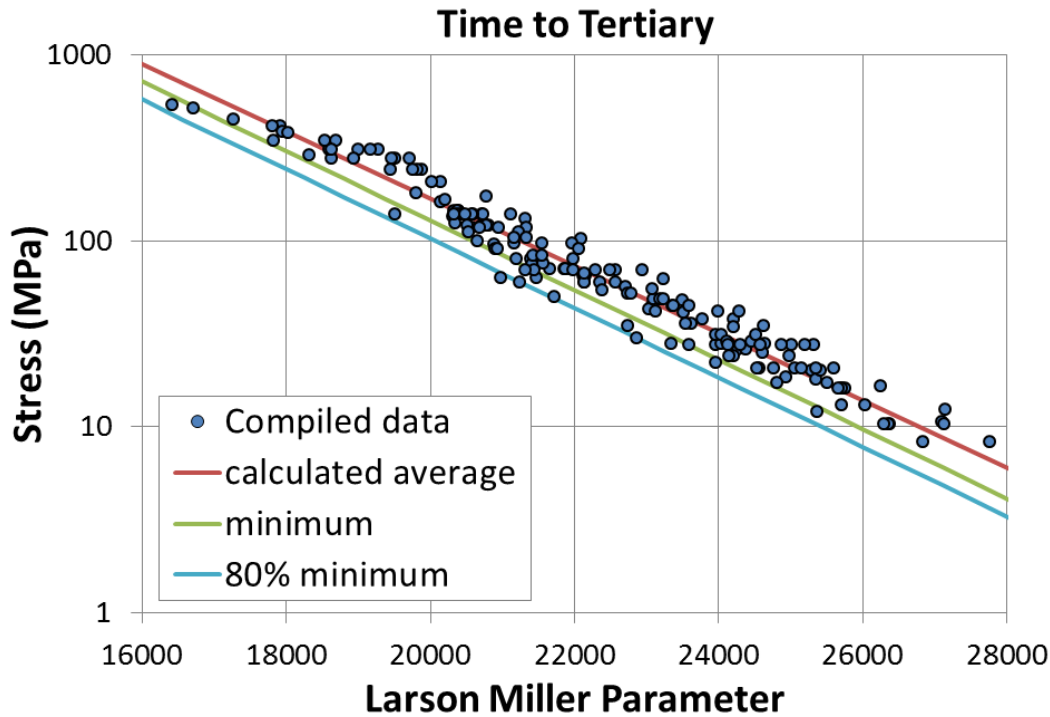
Figure 6. Larson−Miller plot for time to tertiary creep strain for Alloy 617 with linear fit (red line), minimum based on 1.65 SEE (green line) and 80% of the minimum (blue line).

Stress−Rupture

The calculation of minimum stress to rupture, S_r, is discussed in Section HBB-I-14.6 of this background document, including the Larson Miller plot (Figure 7) and details of the data set used. The stress−rupture criterion is defined as 67% of S_r.

Determining S_t

To determine S_t the minimum of the three criteria is determined for each time/temperature combination.[21] Table 4 presents the S_t (minimum) value with colors used to illustrate which criterion is governing for each time/temperature combination. While the tertiary creep criterion governs the creep behavior in most cases; the 1% total strain criterion is governing when the behavior is primarily plastic (little or no creep).

The strain to 1% and rupture criteria are used to limit the overall deformation of a component and actual failure, respectively. ASME adopted the tertiary creep criterion after it was observed experimentally that internally−pressurized tubes of austenitic stainless steel leaked due to creep damage at times less than those predicted using analysis based on uniaxial rupture data. In the absence of extensive experimental tube failure data over a range of relevant temperatures, this criterion was developed based on the logic that the onset of tertiary creep during uniaxial testing of austenitic stainless steels is associated with extensive creep induced cavitation. Eliminating tertiary creep, and the associated cavitation, was presumed to represent a conservative indirect limit to minimize the potential for premature failure of tubes under multi−axial loading. For many temperatures and stresses, Alloy 617 exhibits extensive tertiary creep prior to rupture, without evidence of measurable cavitation. This has raised questions regarding the validity of the tertiary creep criterion for the S_t value for Alloy 617 as well as some other alloys that exhibit similar creep behavior. S_t would be increased over a wide range of time and temperatures by eliminating the tertiary creep criterion.

149

Table 4. Minimum value used to determine S_t, in SI units, with colors used to illustrate which criterion is governing for each time/temperature combination.

1% Strain	Tertiary Creep	Rupture

	Stress (MPa)										
Time (h)→	1	3	10	30	100	300	1000	3000	10000	30000	100000
Temperature (C) ↓	Minimum, All Criteria										
425	245	245	245	245	245	245	245	245	245	245	245
450	245	245	245	245	245	245	245	245	245	245	245
475	242	242	242	242	242	242	242	242	242	242	242
500	240	240	240	240	240	240	240	240	240	240	240
525	238	238	238	238	238	238	238	238	238	238	238
550	235	235	235	235	235	235	235	235	235	235	200
575	234	234	234	234	234	234	234	234	225	192	161
600	233	233	233	233	233	233	233	218	182	155	130
625	232	232	232	232	232	232	210	178	148	125	105
650	231	231	231	231	231	208	173	145	121	102	84
675	231	231	231	231	205	172	142	119	98	82	67
700	231	231	231	207	170	142	116	97	79	65	52
725	231	231	208	173	141	117	95	78	63	51	41
750	231	214	174	144	117	95	76	62	50	41	33
775	219	180	146	119	95	77	61	50	40	32	26
800	185	152	121	98	77	62	49	40	32	26	20
825	156	126	99	80	63	51	40	32	25	20	16
850	130	104	82	65	51	41	32	26	20	16	13
875	108	86	67	53	42	33	26	21	16	13	9.9
900	90	71	55	44	34	27	21	16	13	10	7.8
925	75	59	45	36	27	22	17	13	10	8.0	6.2
950	62	49	37	29	22	18	13	11	8.1	6.3	4.9

HBB-I-14.6
S_r – Minimum Stress–to–Rupture

The Larson-Miller Relation

A Larson−Miller plot was created using time to rupture as described above in section HBB-I-14.4 (Figure 7).[21] The creep−rupture data set, given in Appendix IV, is comprised of information from 348 creep specimens from multiple heats and product forms with known chemistry. A linear equation in log stress describes the average creep−rupture data well. Regression analysis produced values of a_0 = 32976.41125, a_1 = −5908.103107 and C = 16.73049602. For the Code Case, the minimum stress is needed rather than the average. This is accomplished by creating a line that is displaced by 1.65 multiplied by the standard error of estimate (*SEE*) in log time from the average time−to−rupture line (shown on Figure 7) according to Equation [4] as described above in section HBB-I-14.4. For this data set *SEE* has a value of 0.3389336430. In order to determine the allowable stress intensity values, S_t, 67% of the minimum stress−to−rupture is required, which is also shown on Figure 7.
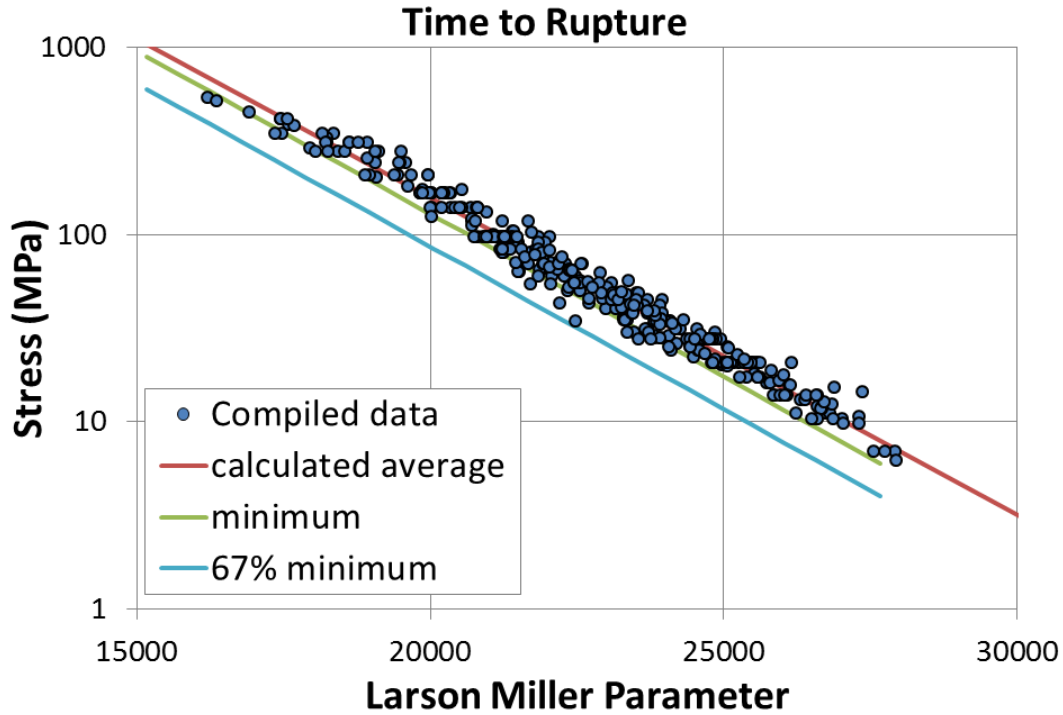
Figure 7. Larson−Miller plot for time to creep rupture of Alloy 617 with linear fit (red line), minimum based on 1.65 SEE (green line) and 67% of the minimum (blue line).

Setting the upper bound

The value of the rupture stress calculated from the above Larson−Miller correlation can exceed the ultimate strength of the material, which is not physically possible. Therefore an upper bound is placed on S_r that is controlled by the tensile strength, S_u. At temperatures above room temperature, values of S_u tend toward an average or expected value. Since S_r is the minimum stress to rupture, the upper bound has been set at $S_u/1.1$ to represent a minimum tensile stress (although not in a statistical sense), following the procedure recently applied to Types 304 and 316 stainless steel.[24] Values of S_u and $S_u/1.1$ are shown in Table 5. S_u can be found for Alloy 617 in Table U of ASME Code Section II, Part D up to 525°C. Higher temperature values for materials approved for use in elevated temperature nuclear applications appear in Table HBB-3225-1 of the Alloy 617 Code Case.

Table 5. Tensile strength proposed for Alloy 617 as a function of temperature.

T (°C)	S_u (MPa)	$S_u/1.1$ (MPa)
425	620	563.6
450	616	560.0
475	611	555.5
500	607	551.8
525	603	548.2
550	593	539.1
575	584	530.9
600	572	520.0
625	557	506.4
650	540	490.9
675	520	472.7
700	496	450.9
725	470	427.3
750	440	400.0
775	408	370.9
800	373	339.1
825	336	305.5
850	298	270.9
875	260	236.4
900	221	200.9
925	185	168.2
950	151	137.3

Determining S_r

An abbreviated table of S_r values is shown in Table 6. Orange is used in Table 6 to illustrate which time/temperature combinations are governed by time−dependent behavior (creep); white cells are governed by the tensile strength.

Table 6. S_r, Sampling of minimum stress−to−rupture values, in SI units, showing time−dependent values in orange.

	Stress (MPa)										
Time (h)→	1	3	10	30	100	300	1000	3000	10000	30000	100000
Temperature (°C) ↓						Minimum S_r					
450	560	560	560	560	560	560	560	560	560	560	560
500	552	552	552	552	552	552	552	552	552	541	462
550	539	539	539	539	539	539	539	488	412	354	299
600	520	520	520	520	520	457	383	325	272	232	194
650	491	491	491	446	369	311	258	217	180	152	126
700	451	451	371	309	254	212	174	145	119	99	81
750	387	320	260	215	174	144	117	97	78	65	53
800	276	226	182	149	120	98	79	64	52	42	34
850	197	160	127	103	82	67	53	43	34	28	22
900	141	113	89	72	56	45	36	29	23	18	14
950	100	80	62	50	39	31	24	19	15	12	9

References

[1] R. Weiju, 2009, "Gen IV Materials Handbook Functionalities and Operation," ORNL/TM-2009/285, U.S. Department of Energy Office of Nuclear Energy, December 2, 2009.

[2] Huntington Alloys Data Package of Inconel 617.

[3] D. H. Baldwin, O. F. Kimball, R. A. Williams (General Electric), *Design Data for Reference Alloys: Inconel 617 and Alloy 800H*, US DOE file number HTGR-86-041, April 1986.

[4] H. E. McCoy, J. F. King (Oak Ridge National Laboratory), *Mechanical Properties of Inconel 617 and 618*, ORNL/TM-9337, February 1985.

[5] Debajyoti Maitra, Special Metals Corporation, private communication, 2015.

[6] NIMS Inconel 617 Stress Rupture Data, Japan, 1975.

[7] J. K. Wright and T. M. Lillo (Idaho National Laboratory), *Progress Report on Alloy 617 Time-Dependent Allowable Stresses*, INL/EXT-15-35640, Revision 1, July 2015.

[8] K. Natesan, M. Li, W. K. Soppet, and D. L. Rink, "Creep Testing of Alloy 617 and A508/533 Base metals and Weldments," Argonne National Laboratory, ANL/EXT-12/36, Sep. 2012.

[9] W. G. Kim, S. N. Yin, G.-G. Lee, and Y.-W. Kim, "Creep Behavior for Alloy 617 in Air at 950 C," Mater. Sci. Forum, vol. 654–656, pp. 508–511, 2010.

[10] W.-G. Kim, Song-Nan Yin, Y.-W. Kim, and W.-S. Ryu, "Creep behaviour and long-term creep life extrapolation of alloy 617 for a very high temperature gas-cooled reactor," Trans. Indian Inst. Met., vol. 63, no. 2–3, pp. 145–150, 2010.

[11] W.-G. Kim, I. M. W. Ekaputra, J.-Y. Park, M.-H. Kim, and Y.-W. Kim, "Investigation of Creep Rupture Properties in Air and He Environments of Alloy 617 at 800 C," in Proceedings of HTR 2014, Weihai, China, 2014.

[12] W.-G. Kim, S.-N. Yin, G.-G. Lee, Y.-W. Kim, and Seon-Jin Kim, "Creep oxidation behaviour and creep strength prediction for Alloy 617," Int. J. Press. Vessels Pip., vol. 87, pp. 289–295, 2010.

[13] INL, unpublished research.

[14] Cook, "Creep Properties of INCONEL-617 in Air and Helium at 800 to 1000 C," Nucl. Technol., vol. 66, pp. 283–288, 1984.

[15] J. M. Gentzbittel, D. Vincent, N. Scheer, *Results of Mechanical and Microstructural Characterizations of Alloys 617 and 230. Mechanical Properties of TIG Welded 617*, CEA DTH/DL/2007/80, 2007.

[16] J. K. Wright, L. J. Carroll, C. Cabet, T. M. Lillo, J. K. Benz, J. A. Simpson, W. R. Lloyd, J. A. Chapman, and R. N. Wright, "Characterization of elevated temperature properties of heat exchanger and steam generator alloys," *Nuclear Engineering Design*, Vol. 251, 2012, pp. 252–260.

[17] ASTM B166 Standard specification for Nickel-Chromium-Iron Alloys (UNS N06600, N06601, N06603, N06690, N06025, N06046, N06696), Nickel-Chromium-Cobalt-Molybenum Alloy (UNS N06617), and Nickel-Iron-Chromium-Tungsten Alloy (UNS N06674) Rod, Bar, and Wire, ASTM International, 100 Barr Harbor Drive, PO Box C700, West Conshohocken, PA, 2011.

[18] ASTM B168 Standard specification for Nickel-Chromium-Iron Alloys (UNS N06600, N06601, N06603, N06690, N06025, N06046, N06696), Nickel-Chromium-Cobalt-Molybenum Alloy (UNS N06617), and Nickel-Iron-Chromium-Tungsten Alloy (UNS N06674) Plate, Sheet and Strip, ASTM International, 100 Barr Harbor Drive, PO Box C700, West Conshohocken, PA, 2011.

[19] ASTM E 8, "Standard Test Methods for Tension Testing of Metallic Materials," ASTM International.

[20] ASTM E 139, "Standard Test Methods for Conducting Creep, Creep-Rupture, and Stress Rupture Tests of Metallic Materials," ASTM International.

[21] F. R. Larson and J. Miller, "A Time-Temperature Relationship for Rupture and Creep Stresses," *Trans. ASME*, Vol. 74, 1952, pp. 765−775.

[22] L. H. Sjodahl, "A Comprehensive Method of Rupture Data Analysis With Simplified Models," in *Characterization of Materials for Service at Elevated Temperatures*, New York, NY: American Society of Mechanical Engineers, 1978, pp. 501–516.

[23]R. W. Swindeman and M. J. Swindeman, *Analysis of Time-Dependent Materials Properties Data,* ASME Standards Technology, LLC, 2014.

[24]M. Sengupta and J. E. Nestell, "Task 14a – Correct and Extend Allowable Stress Values for 304 and 316 Stainless Steel," MPR-3813, Revision 2, ASME Standards Technology, LLC, October, 2013.

[25] W. E. Leyda and J. P. Rowe (American Society for Metals), *A Study of Time for Departure from Secondary Creep for Eighteen Steels*, ASM Technical Report P9-6.1, Metals Park Ohio, 1969.

BACKGROUND

HBB-I-14.10F-1

STRESS RUPTURE FACTORS FOR WELDED ALLOY 617

Scope

This document provides the background/technical basis in support of the recommendation for the Stress Rupture Factors in Table HBB-I-14.10F-1.

Background

The Stress Rupture Factor (SRF) is defined as the ratio of the weld metal creep-rupture strength to the base metal creep-rupture strength. This value is labeled "R" in articles HBB-3221, and HBB-3225, and is also used in article HBB-T-1715 of Section III, Division 5, Subsection HB, Subpart B "Elevated Temperature Service". The factor is used in conjunction with the minimum stress−to−rupture values given in Figure HBB-I-14.6G and Table HBB-I-14.6G. Only gas tungsten arc (GTA) welding is permitted using weld wire Class ERNiCr CoMo-1, Spec. No. SFA-5.14, according to HBB-I-14.1(b) in the Alloy 617 Code Case.

Data Sources

Creep testing was performed at Argonne National Laboratory (ANL) and at Idaho National Laboratory (INL) on specimens machined from the welded reference plate described below. Additional weldment creep data has been compiled from three other sources: a report from CEA of GTAW welded plate,[1] an Outokumpu VDM 2013 data sheet for Alloy 617B GTAW weldments,[2] and an older Huntington Alloys report[3] represented in the current SMC vendor datasheet.[4] All are transverse GTAW welds using Alloy 617 weld wire, except for the Huntington/SMC source, which includes Gas Metal Arc−spray and Pulsed Arc−Gas Metal Arc welding processes. Huntington also reported longitudinal[3] creep results (also labeled as weld−metal−only[4]).

Materials and Welding

The Alloy 617 material used in this study is a 37 mm thick solution annealed plate produced by ThyssenKrupp VDM, identified as heat 314626. The plate has an average grain size of 150 μm and the composition is given in Table 1. The majority of INL property characterization has been performed on specimens machined from this reference material plate.[5]

Table 1. Chemical composition of the Alloy 617 plate 314626 (weight percent).

Heat ID	Ni	Cr	Co	Mo	Al	Ti	Fe	Mn	Cu	Si	C	S	B
314626	54.1	22.2	11.6	8.6	1.1	0.4	1.6	0.1	0.04	0.1	0.05	<0.002	<0.001
XX3703UK	53.91	22.41	11.49	8.98	1.10	0.34	1.37	0.11	0.04	0.04	0.089	0.001	NR

Welding was performed using an automated tungsten gas arc process with multiple passes to fill a v-notch weld preparation.[6] Alloy 617 filler wire was supplied by Oxford Alloys, Inc., identified as Heat No. XX3703UK. The process was qualified by INL Welding Procedure Specification I5.0, which meets the requirements of ASME Boiler and Pressure Vessel Code Section IX.[7] A cross section of the weld is

shown in Figure 1. Further details of the weld qualification can be found in the background section for HBB-I-14.1 (b), Permissible Weld Materials.
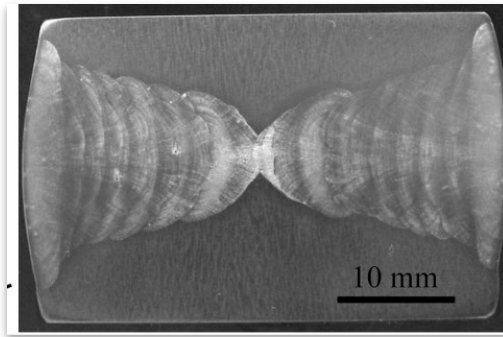
Figure 1. Cross section of weld in Alloy 617 plate.

Creep Testing of Welds

All creep–rupture testing was performed in conformance with ASTM E 139.[8] All weldment creep testing utilized transverse weld specimens, with the weld direction perpendicular to the axis of the specimen.[9, 6]

ANL

The creep test specimens used in the ANL testing are a button–head design that meets the ASTM E8[10] specification as shown in Figure 2. A schematic illustrating the v–weld location within the creep specimen gage length is shown in Figure 3. Figure 4 is a photograph of two representative specimens containing weldments. The size of the weldment (and location within the creep specimen) varied somewhat, depending upon its location with respect to the weld in the plate as can be seen in Figure 4.
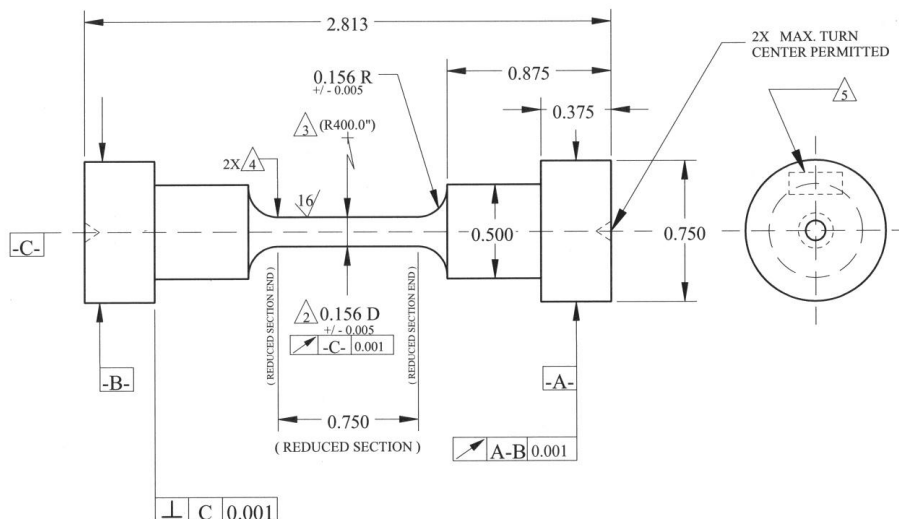
Figure 2. Creep specimen used for testing at ANL (units in inches).
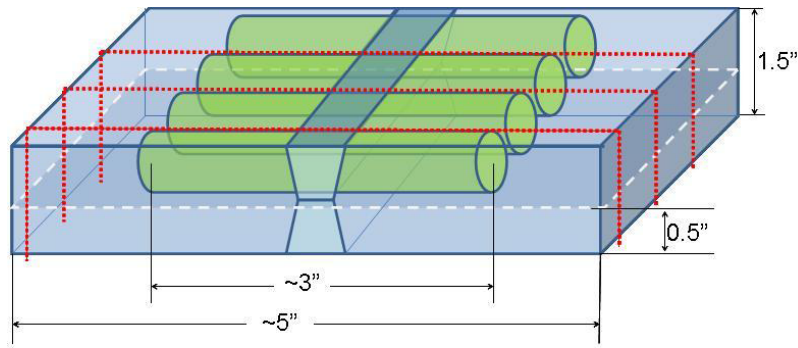
Center button head specimens on weld.

Figure 3. Schematic illustrating the v–weld location within the ANL creep specimen gage length.
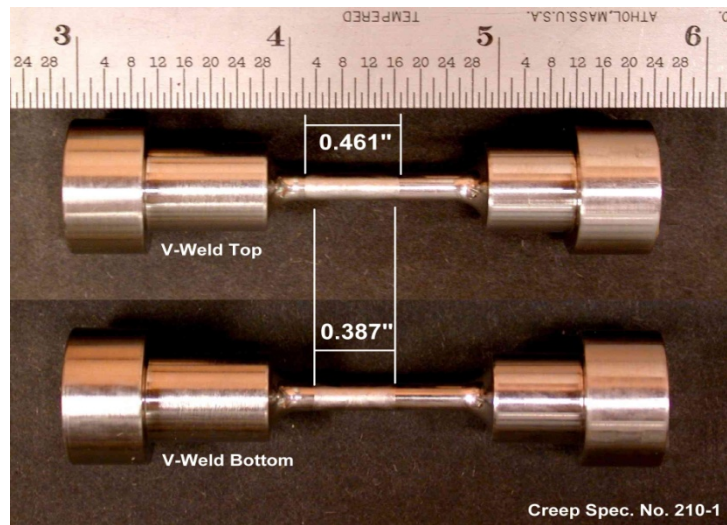
Figure 4. Creep specimen No. 210-1 weld region dimensions.

Direct–load creep frames were used to test the specimens. A three–zone furnace was used to heat to the test temperature set point over a 3–hour ramp time. The test specimen was centered in the middle furnace zone and the specimen temperature profile was maintained within ±1°C of the desired test temperature. Calibrated thermocouples were spot welded to the specimen outer transition radius shoulder edge so as not to introduce defects into the gage length area. The creep test was completed when the specimen ruptured and the system provided automatic cooldown. An LVDT extensometer was used to monitor strain during the test.

INL

Cylindrical creep specimens, with nominal 6.35 mm reduced section diameter and gage length of 34.2 mm (Figure 5), were machined in conformance with ASTM E139.[8] The weld was centered within the specimen as shown schematically in Figure 6, where the smaller rectangular blocks were used to machine creep specimens. Testing was performed using direct loaded creep frames with dead weight loading, with the exception of a 750°C test which utilized a 20:1 lever arm. The temperature of the gage section of the creep specimen was measured with type K thermocouples for tests at temperatures of 750°C and type R thermocouples for tests at temperatures of 900°C or above. The specimen temperature was controlled to within ±3°C of the target test temperature. Dual averaging LVDT transducers or Heidenheim linear encoded photoelectric gauges were used to monitor creep strain during the creep tests to a resolution of better than 0.01% strain.[6]

Figure 5. Creep specimen used for testing at INL (units in inches).
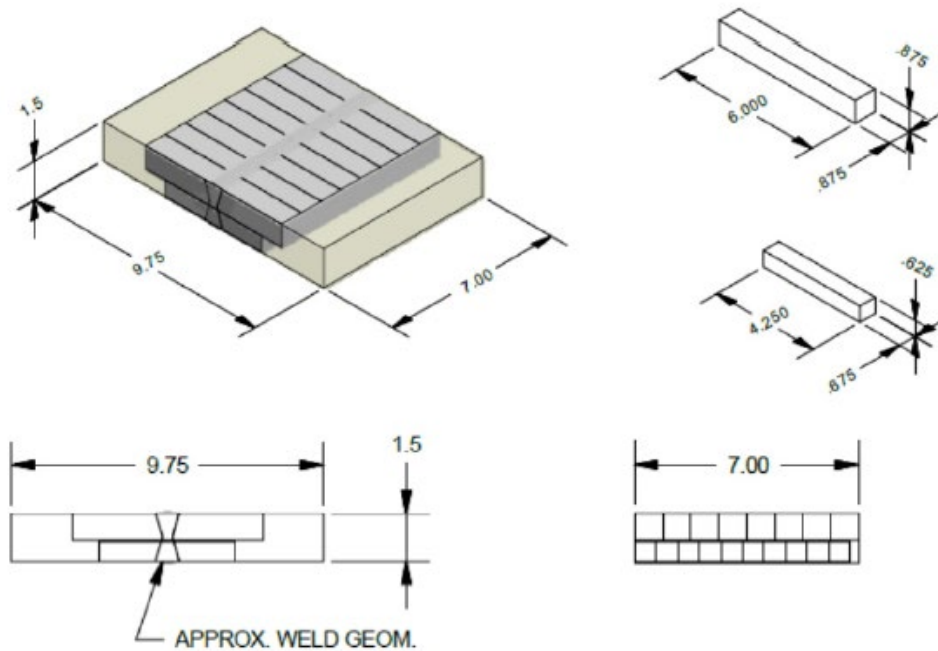
Figure 6. Schematic illustrating the centered v−weld location within the INL creep specimen blank. Creep specimens were machined from the smaller blanks (bottom).

Stress Rupture Factor Analysis Method

The SRF is defined as Stress$_{weld}$/Stress$_{base}$, where Stress$_{weld}$ is the applied stress which causes creep rupture in time t, and Stress$_{base}$ is the rupture stress of the base metal in the same time and at the same temperature. Ideally, the heat of the base metal is the same as that used to fabricate the weldment. In practice, the data base does not include base metal creep specimens with rupture times that match those of the weld specimens, and often does not include specimens of the same heat. Instead, an average base metal rupture stress is calculated for the time to rupture of the weldment using a Larson–Miller relation for a large, multi−heat compilation of Alloy 617 creep−rupture data. The result is one data point for the SRF of each weldment creep−rupture test.

The Larson–Miller Relation

A spreadsheet developed for ASME[11] for the analysis of time−dependent materials properties was used to generate the Larson–Miller relation for creep rupture (Figure 7) in Section HBB-I-14.6. The data set is comprised of information from 348 creep specimens from multiple heats and product forms with known chemistry.

Time to Rupture
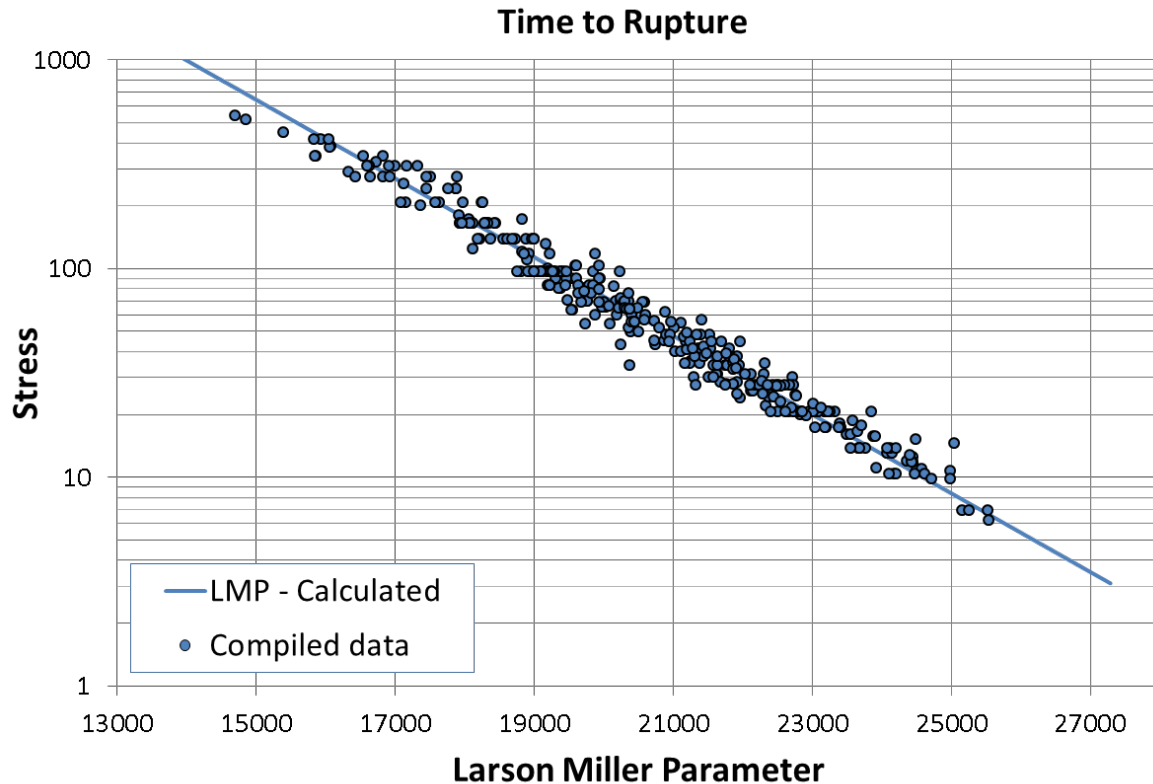
Figure 7. Larson−Miller plot with linear fit to compiled creep−rupture dataset for Alloy 617.

The Larson−Miller parameter (LMP) is defined as

$$LMP = T(C + log_{10}(t))$$

where T is the temperature in Kelvin, C is the Larson−Miller constant, and t is time in hours. A linear equation in log stress describes the creep data well.

$$LMP = a_0 + a_1 log_{10}(\sigma)$$

where a_0 and a_1 are the fitting parameters, and σ is stress (MPa). Regression analysis produced values of a_0 = 32976.41125, a_1 = −5908.103107 and C = 16.73049602. Consistent with the definition of the stress rupture factor, best−estimate average values of the base metal rupture stress are determined.

Stress Rupture Factor Calculation and Discussion

Results of creep-rupture tests of weldments are given in Appendix V, including test conditions, time−to−rupture and rupture location. Experimentally determined values for SRF are also tabulated in Appendix V and shown in Figure 8. Only tests on transverse GTAW weldments have been included on the figure,

although other weld methods and longitudinal specimens tested by Huntington Alloys are included in Appendix V. Based on the information presented above, it was concluded that a factor of 1.0 adequately described the experimentally determined behavior for GTAW weldments up to 850°C (1562°F). At a temperature of 850° and above, a factor of 0.85 provides a more conservative representation of the experimental data. The recommended values of the SRF are shown as solid lines, and the Code Case maximum allowable temperature of 950°C is shown as a dotted line on Figure 8.
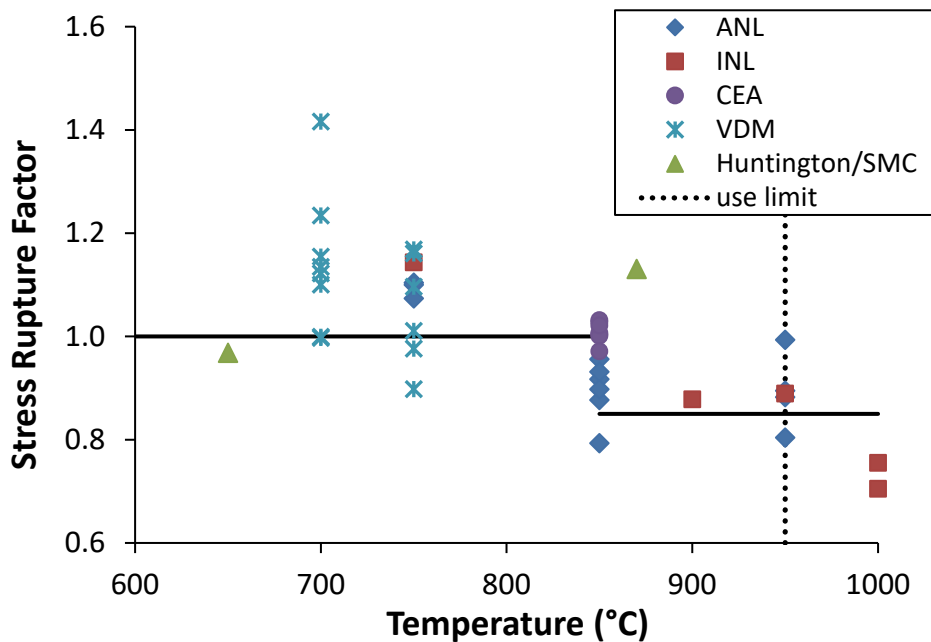
Figure 8. Weldment stress reduction factors (solid lines) determined from experiments on Alloy 617 transverse GTAW weldments from multiple sources. The maximum temperature limit of 950°C for the Code Case is shown as a dotted line on the plot.

The INL reference heat used as the base metal of the INL and ANL weldment specimens tends to have creep−rupture strengths at the low end of the overall database shown in Figure 7. If the SRF for the INL and ANL data points are calculated by using a Larson Miller relation based on only creep data for the INL reference heat (Figure 9), the SRF values increase, as shown in Figure 10. It is not possible to apply this method to the Huntington data because the welded specimens have base metal from a heat that is not represented in the overall creep−rupture data base, and the heats of the VDM specimens are not specified.
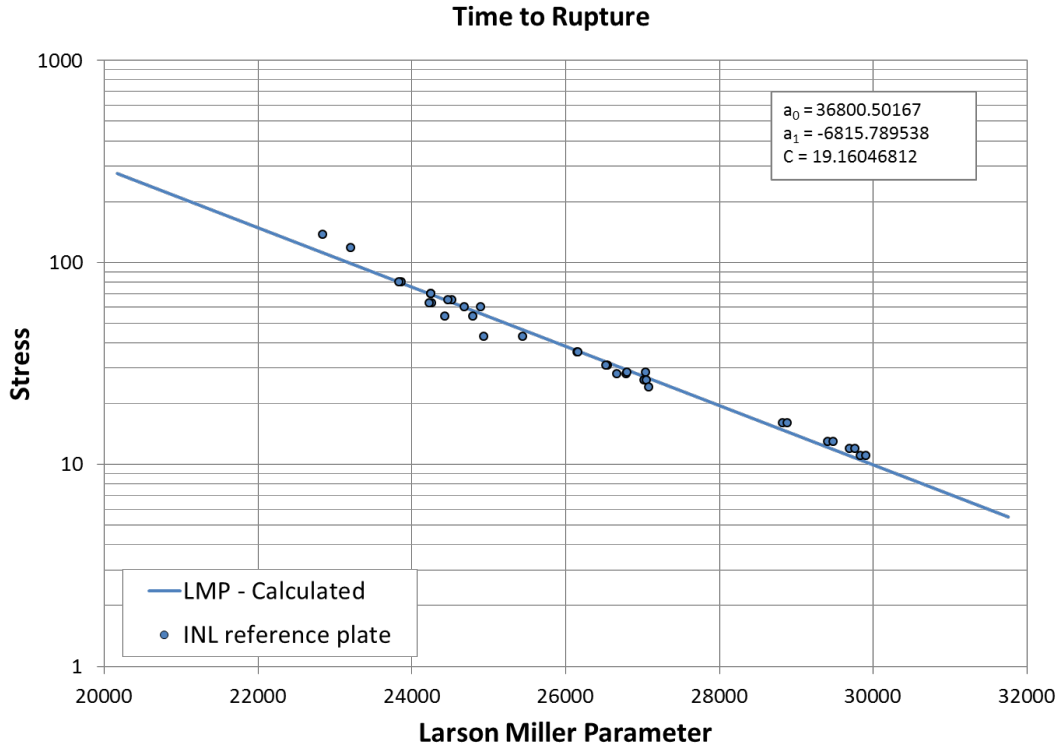
Figure 9. Larson−Miller plot with linear fit to compiled creep−rupture dataset for Alloy 617.
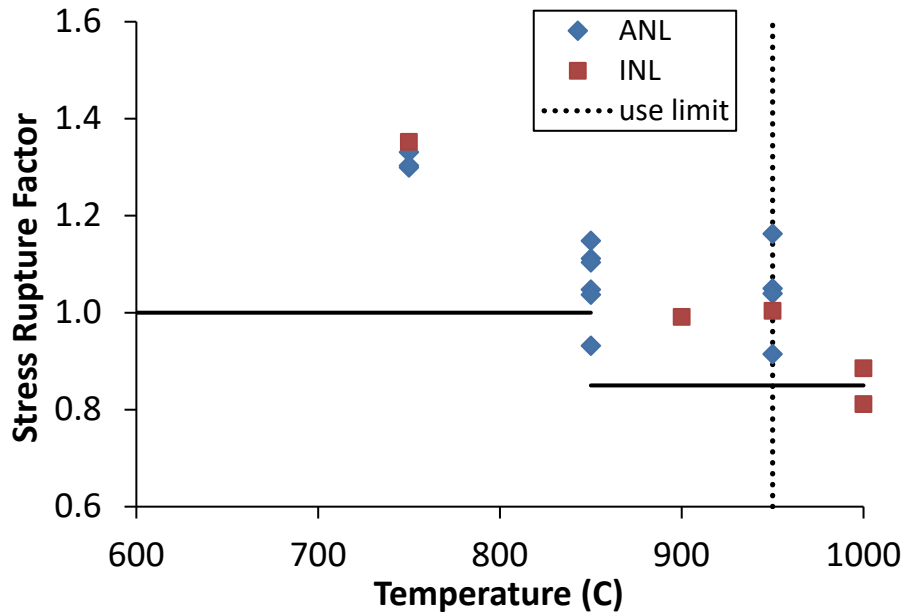
Figure 10. SRF calculated using only INL base metal heat data in the Larson−Miller plot used to calculate the denominator values. The recommended SRF values are shown as solid lines and the maximum temperature limit of 950°C for the Code Case is shown as a dotted line on the plot.

Plotting the SRF data from all sources, for temperatures up to and including the 950°C use temperature as a function of creep−rupture time, shows that there is no downward trend within the range of times represented in the weldment creep dataset (Figure 11). The recommended SRF values of 1.0 and 0.85 are shown as solid and dashed lines, respectively.
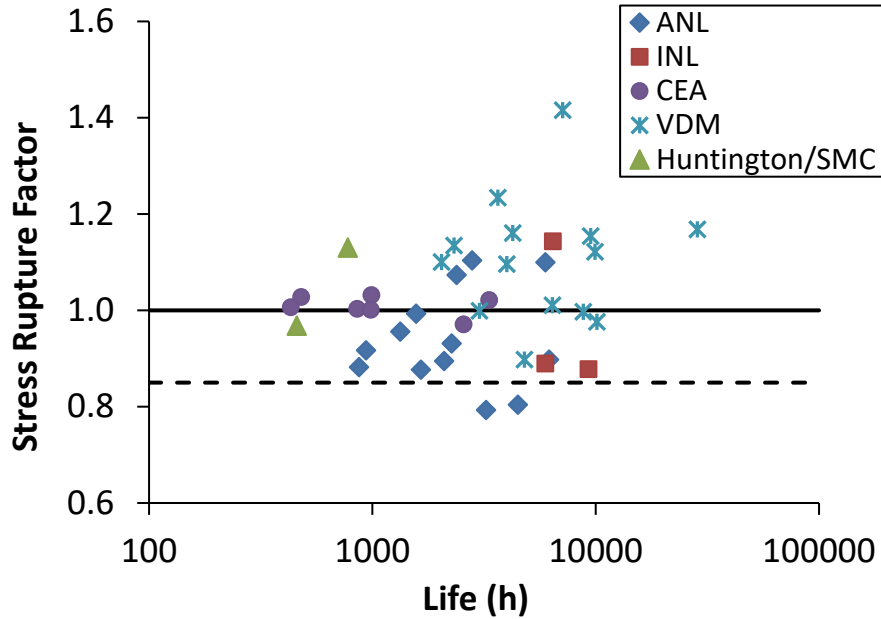
Figure 11. SRF determined from experiments on Alloy 617 transverse GTAW weldments multiple sources as a function of creep−rupture life for temperatures ≤ 950°C. The recommended SRF values of 1.0 and 0.85 are shown as solid and dashed lines, respectively.

A separate analysis of reduction factors for welds of CCA617 (also known as 617B) has been prepared for ASME Code Section I by the Electric Power Research Institute (EPRI).[12] Those data are shown in Figure 12 and include GTAW welding as well as other processes. For GTAW welds, a reduction factor of 1.0 has also been proposed for Section I up to 850°C.

Figure 12. Weldment stress reduction factors for Alloy 617 welded by several processes, compiled by EPRI.

Summary

The background and technical basis in support of the recommendation for the Stress Rupture Factors in Table HBB-I-14.10F-1 has been presented. Creep−rupture testing and analysis methods are detailed and a complete compilation of data is tabulated in Appendix V. Figures are shown that support an SRF of 1.0 for temperatures < 850°C, and 0.85 for temperatures ≥ 850°C.

References

[1] J. M. Gentzbittel, D. Vincent, N. Scheer, *Results of Mechanical and Microstructural Characterizations of Alloys 617 and 230. Mechanical Properties of TIG Welded 617*, DTH/DL/2007/80, 2007.

[2] M. Spiegel, R. Krein (Salzgitter Mannesmann Forschung), J. Klöwer (Outokumpu VDM), T. Kremser, P. Schraven (Salzgitter Mannesmann Stainless Tubes), V. Knezevic, I. Steller (Vallourec & Mannesmann Tubes), *Alloy 617B Metallurgy, Properties, Fabrication and Welding*, 2013.

[3] *INCONEL Welding Electrode 177 INCONEL Filler Metal 617*, Huntington Alloys, Inc., Huntington, WV.

[4] INCONEL® Alloy 617 Datasheet, Special Metals Corp., Publication No. SMC-029 Huntington, WV, 2005.

[5] J. K. Wright, L. J. Carroll, C. Cabet, T. M. Lillo, J. K. Benz, J. A. Simpson, W. R. Lloyd, J. A. Chapman, and R. N. Wright, "Characterization of elevated temperature properties of heat exchanger and steam generator alloys," *Nuclear Engineering Design*, Vol. 251, 2012, pp. 252–260.

[6] J. K. Wright, L. J. Carroll, and R. N. Wright (Idaho National Laboratory), *Creep and Creep−Fatigue of Alloy 617 Weldments*, INL/EXT-14-32966, August 2014.

[7] INL Welding Procedure Specification (WPS) I5.0.

[8] ASTM E 139, "Standard Test Methods for Conducting Creep, Creep−Rupture, and Stress Rupture Tests of Metallic Materials," ASTM International.

[9] K. Natesan, M. Li, W. K. Soppet, and D. L. Rink, *Creep Testing of Alloy 617 and A508/533 Base Metals and Weldments*, Argonne National Laboratory, ANL/EXT-12/36, September, 2012.

[10] ASTM E 8, "Standard Test Methods for Tension Testing of Metallic Materials," ASTM International.

[11] R. W. Swindeman and M. J. Swindeman, *Analysis of Time−Dependent Materials Properties Data,* ASME Standards Technology, LLC, 2014.

[12] J. Shingledecker, J. Siefert, M. Santella, P. Tortorelli, "Creep−Rupture Analysis of Alloy CCA617 Base Metal and Weldments," *7th International Conference on Advanced Material Technology for Fossil Power Plants, Hawaii, Oct. 23, 2013*.

BACKGROUND

HBB-4800 RELAXATION CRACKING

Scope

This document provides the background/technical basis in support of the recommendation for Relaxation Cracking in HB-4800 of the Alloy 617 Code Case.

Background

Relaxation cracking is a mode of delayed intergranular failure defined in Section II, Part D, Appendix A, Subsection A-206:

> *"Relaxation cracking is a condition that may develop in cold-worked or warm-worked austenitic materials when temper-resistant particles precipitate at excess defect sites generated by the cold or warm working operations; these precipitates act to "pin" the defects, which results in a substantial increase in the material's creep strength and hardness. The bulk of the strengthening occurs within the individual grains, while the grain boundaries remain comparatively weak, so that when the material is heated to intermediate temperatures ... any strains that develop ... concentrate in the grain boundaries. This can lead to rapid creep crack growth and ultimately failure of the component in a nonductile fashion... In the nickel-base alloys titanium and aluminum contribute to the formation of gamma prime or gamma double-prime precipitates. The rate of crack growth can be quite rapid if the amount of working and the temperature of exposure are unfavorable."*

Relaxation cracking in Alloy 617 is usually observed in association with welds or in cold worked material, but is also observed in solution annealed material.[1,2] It is most prevalent from 550 to 700°C. It occurs after extended periods of exposure (typically on the order of one to two years) in the range where carbide precipitation occurs and/or the ordered γ' (Ni_3Al) phase forms. Relaxation cracking has been observed in cold worked nickel alloys even in the absence of weldments.[3]

The rules contained in PG-19 (BPVC Section I) and UHA-44 (Section VIII, Division 1) were developed, in part, to minimize the risk of relaxation cracking.

Vendor Recommendations

Special Metals, and VDM Alloy 617 datasheets make specific mention of the potential susceptibility of the alloy to relaxation cracking.[4,5] VDM notes that the temperature range of susceptibility to cracking is 550 to 780°C for solution annealed and welded semi-finished products and 500 to 780°C on products which have already seen service and have been repair welded.[5] Vendors recommend that components for service in these temperature ranges be given a heat treatment of three hours at 980°C to eliminate relaxation cracking.

Post-Fabrication Heat Treatment

This issue is closely related to recommendations for allowable cold work and post-fabrication heat treatments discussed in BPVC Section III, Division 5, Subsection HB, Subpart B paragraph HBB-4212, "Effects of Forming and Bending Processes." A post-fabrication solution heat treatment of 1150°C for 20 minutes/25 mm of thickness or 10 minutes, whichever is greater, has been recommended for all cases

where fabrication strains are greater than 5% are incurred for Alloy 617, as discussed in the background section for HBB-4212, Effects of Forming and Bending Processes.

HBB- 4800

It is recommended that components that will see service between 500 and 780°C be given a heat treatment of three hours at 980°C to eliminate relaxation cracking. This recommendation applies regardless of whether the material is in a welded or solution annealed condition, and is consistent with recommendations in datasheets for the major vendors of this alloy. This heat treatment must be performed after the post-fabrication solution annealing if post-fabrication heat treatment was also required.

References

[1] Louis E. Shoemaker, Gaylord D. Smith, Brian A. Baker and Jon M. Poole, "Fabricating Nickel Alloys to Avoid Relaxation Cracking" Proc. Corrosion 2007, NACE International, Paper No. 07421.

[2] Hans van Wortel, "Control of Relaxation Cracking in Austenitic High Temperature Components" Proc. Corrosion 2007, NACE International, Paper No. 07423.

[3] J. C. van Wortel, "Relaxation cracking in the process industry, an underestimated problem", unpublished industry working group report (shared with ASME) 1998.

[4] INCONEL Alloy 617 Data Sheet, Special Metals Corp., Publication No. SMC-029 Huntington, WV, 2005.

[5] Nicrofer 5520 Co – Alloy 617 Material Data Sheet, ThyssenKrupp VDM, Datasheet 4019, 2005.

HBB-3225-2 TENSILE AND YIELD STRENGTH REDUCTION FACTOR DUE TO LONG TIME PRIOR ELEVATED TEMPERATURE SERVICE

Scope

This document provides the background/technical basis in support of the recommendation for the Tensile and Yield Strength Reduction Factor Due to Long Time Prior Elevated Temperature Service in Table HBB-3225-2 of the Alloy 617 Code Case.

Background

ASME Code Section III, Division 5, Subsection HB, Subpart B Table HBB-3225-2 lists tensile and yield strength factors due to long time prior elevated temperature service. Although "long time" is not defined, a reduction factor is required for service at and above a given temperature for the three austenitic materials permitted in Subsection HB, Subpart B.

Data Sources

The Generation IV International Forum (GIF) VHTR Materials Program Management Board has agreed to compile data from earlier testing programs and share data generated from current member test programs in the GIF Materials Handbook.[1] Past aged tensile data include those generated at Oak Ridge National Laboratory (ORNL)[2] as part of the Department of Energy High-Temperature Gas-Cooled Reactor Research Program of the 1980s and 1990s. Additional data has been obtained from the Special Metals Corporation (SMC)) materials data sheet,[3] formerly Huntington Alloys (the original producer of Inconel 617). Recent tensile data have been contributed by Idaho National Laboratory (INL). Tensile data of aged Alloy 617 has been compiled from these three sources and can be found in Appendix VI.

Materials

The INL has performed extensive property characterization on specimens machined from an Alloy 617 reference material plate.[4] The reference plate is a 37 mm thick solution annealed plate (heat 314626), with an average grain size of 150 μm. Tensile testing was performed at INL on specimens machined from this reference plate. Additional tensile testing was done on specimens machined from 51-mm diameter rod (heat 188155), with an average grain size of 150 μm. Both product forms were produced by ThyssenKrupp VDM. Additional tensile tests were performed on specimens machined from a 20 mm thick plate of Alloy 617 (heat XX2834UK) procured from Special Metals Corporation.[5] The microstructure of the plate is heavily banded with stringers of coarse carbide precipitates and associated coarse and fine grains aligned in the rolling direction. Grains in the coarse bands are approximately 100 μm in diameter and the finer grains range from approximately 10 to 30 μm in diameter.

The microstructure of the ORNL material is reported as fairly coarse grained with inhomogeneous stringers in the longitudinal direction.[2] The specific chemistry or heat ID was not reported in the SMC data sheet. Chemistries for the INL and ORNL heats are listed in Table 1.

Page intentionally left blank

Table 1. Chemical composition of the Alloy 617 materials (weight percent).

Heat ID	Product Forms	Source	Ni	Cr	Co	Mo	Al	Ti	Fe	Mn	Cu	Si	C	S	B
min		ASME	44.5	20.0	10.0	8.0	0.8	--	--	--	--	--	0.05	--	--
max			--	24.0	15.0	10.0	1.5	0.6	3.0	1.0	0.5	1.0	0.15	0.015	0.006
314626	plate	INL	54.1	22.2	11.6	8.6	1.1	0.4	1.6	0.1	0.04	0.1	0.05	<0.002	<0.001
188155	rod	INL	53.27	22.02	11.91	9.38	1.1	0.32	1.46	0.23	0.02	0.2	0.08	0.001	0.002
XX2834UK	plate	INL	bal.	21.91	11.42	9.78	0.96	0.34	1.69	0.11		0.12		0.001	0.002
XX01A3US	plate	ORNL	57.35	20.30	11.72	8.58	0.76		1.01	0.05		0.16	0.07	0.004	

Blank cells indicate a composition that was not reported.

Page intentionally left blank

All unaged specimens were tested in the solution-annealed condition, consisting of holding at 2150°F (1175°C) followed by rapid cooling to room temperature, according to standards SB166 and SB168.[6,7] INL material from heats 314626 and 188155 were aged in air at temperatures of 650 and 750°C for times of 200, 650, 2000, 5300, 20,000 and 32,000 h. Heat XX2834UK was aged at 800 and 1000°C for times of 100, 1000 and 10,000 h. The ORNL plate was aged at temperatures of 538, 704, and 871°C (1000, 1300 and 1600°F) in static air for times of 2500, 10,000 and 20,000 h.[2] SMC material was aged at temperatures of 595, 650, 705, and 760°C (1100, 1200, 1300 and 1400°F) for times of 100, 1000, 4000, 8000, and 12,000.[3] INL and ORNL specimens were machined after aging.

Tensile Testing

INL testing on heats 314626 and 188155, as-received and aged at 650 and 750°C

Tensile testing is performed in conformance with ASTM E 8[8] and E 21,[9] for room temperature and elevated temperature tests, respectively. Tensile specimens conformed to ASTM E21, cut from material in the heat treated condition (as-received condition for baseline specimens) with the axis of the specimen parallel to the direction of fabrication. Care was taken to ensure any surface effects resulting from the aging were removed during machining of the specimens. Specimens had a 6.35 mm diameter, 32 mm long reduced section (Figure 1). Final dimensions, such as diameter and gauge length, were measured using a calibrated micrometer on the fractured specimen with ends fit carefully together, and the ductility and percent reduction in area calculated. Yield strengths are reported at an offset of 0.2% strain.
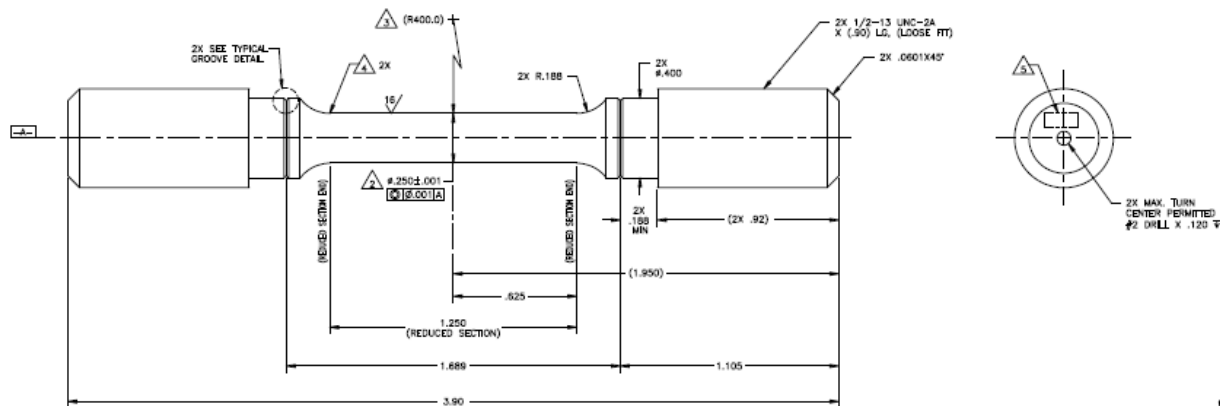
Figure 1. Tensile specimen used for testing at INL.

The tests were conducted on screw driven electro-mechanical machines with resistance heated box furnaces. In most cases extensometers were direct mounted to the reduced section of the specimens and used from 0-20% strain for each test. Strain data after removal of the extensometers are a displacement-estimated strain based on the beginning and ending strain values and the crosshead displacement. Elevated temperature testing on the as-received plate material was performed using dual averaging LVDT transducers to monitor the strain during testing to a resolution of better than 0.01% strain.

For room temperature testing the crosshead speed was generally ~1.25 mm/minute to achieve a stress rate between 1.15-11.5 MPa/sec. For elevated temperature testing, tensile tests were carried out at constant crosshead-displacement rate of ~0.2 mm/minute corresponding with an initial strain rate of approximately 0.5%/min. The temperature was monitored by thermocouples attached to the specimen and the gage section was held within 3°C of the specified test temperature. In some cases two replicate tests were performed to assess the reproducibility of results.

Tensile tests on aged INL rod were conducted only at room temperature. Tensile properties on the INL reference plate were measured at room temperature, and at 50°C intervals in the temperature range of 650-1000°C.

INL testing on heats XX3824UK, as-received and aged at 800 and 1000°C

Specimens aged at 800 and 1000 from heat XX2834UK pre-dated the lower temperature aged material described above by several years. Test procedures were similar, but with the following notable exceptions. Specimens were smaller with a reduced section of 4.15 mm diameter and 17.5 mm length. The initial cross-head speed was 1 mm/min resulting in an initial strain rate of ~6%/min. Testing was performed at room temperature and the aging temperature. Two specimens were tested for each aging/test temperature combination.

Other testing

Properties are reported for the ORNL plate at room temperature, 538, 704, and 871°C (1000, 1300 and 1600°F).[2] ORNL specimens had a 6.35 mm gage diameter were oriented with the axis parallel to the rolling direction, and strain was measured with an extensometer.[2] Further details of the testing procedure are unknown.

SMC testing was conducted only at room temperature. No tensile testing details are given.[3]

Quality

Tensile properties from Alloy 617 heats 314626 and 188155, reported by the Idaho National Laboratory (INL) through the Next Generation Nuclear Plant (NGNP) or Advanced Reactor Technologies (ART) programs were determined under an NQA-1 quality program. Details of the quality program implementation are given in INL document PLN-2690 "Idaho National Laboratory Advanced Reactor Technologies Technology Development Office Quality Assurance Program Plan." Testing on heat XX3824UK predated implementation of the NQA-1 quality program.

HBB-3225-2

Room temperature tensile properties for alloy 617 aged at temperatures up to 800°C show that the yield and ultimate tensile strengths actually increase slightly after aging in the range of 100 to 10,000 hours. Data from SMC[3] as plotted by Ren and Swindeman[10] for 593, 649, 704, and 760°C are shown in Figure 2. These data are confirmed by INL data for plate aged at 650, 750 and 800°C for up to 32,000 hours (also plotted in Figure 2). All data show a slight increase in room temperature yield and ultimate tensile strength upon aging. Tensile properties of material from a component that has seen service for 101,500 hours at an estimated temperature of 800°C[11] are in the range of those for long aging times in Figure 2.
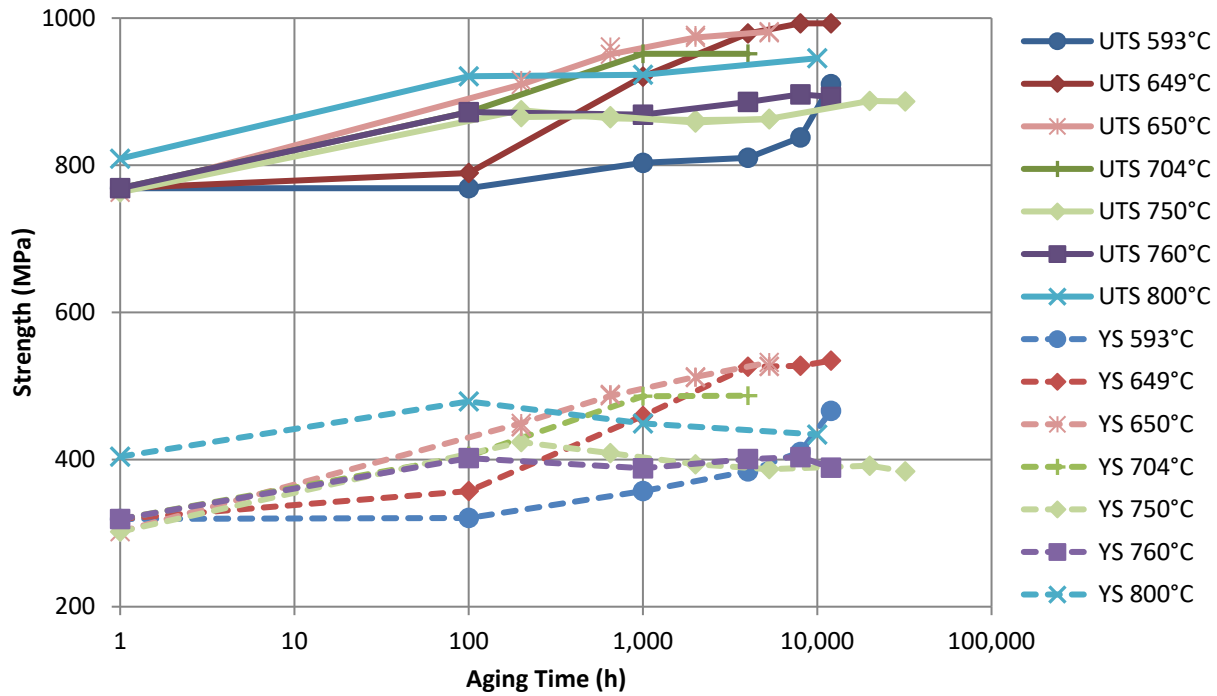
Figure 2. Room temperature tensile strength as a function of aging time for aging temperatures up to 800°C.

Tensile properties for Alloy 617 aged at a range of temperatures up to 871°C for times up to 20,000 hours are shown in Figure 3 (SMC[3] and ORNL[2] data, reproduced from Ren and Swindeman[10]). The peak associated with aging at intermediate temperatures is evident in the figure. For aging at 871°C there may be a small decrease in tensile strength.
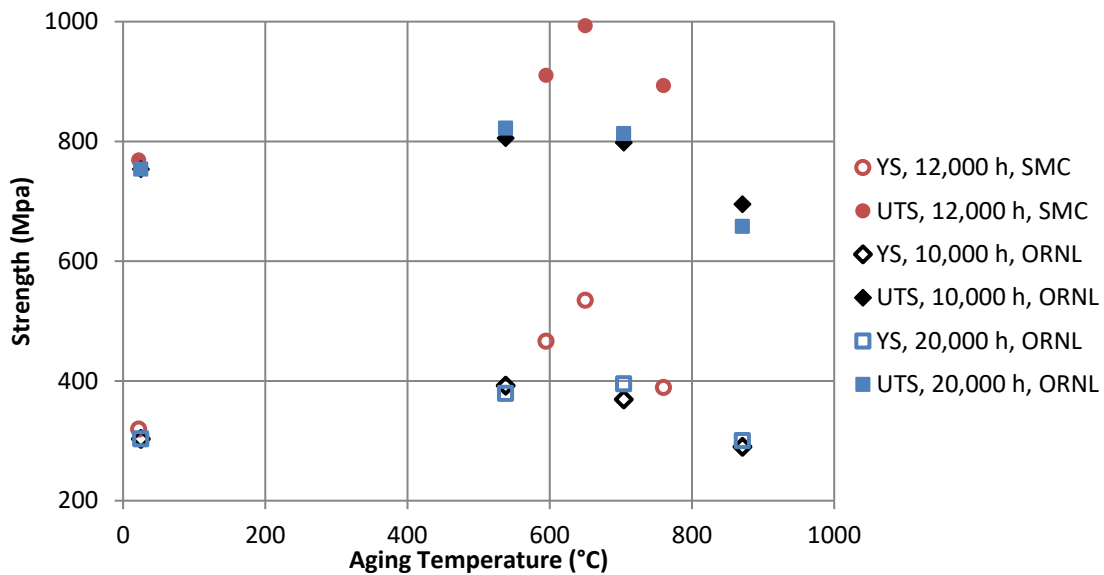
Figure 3. Room temperature tensile strength as a function of aging temperature for aging times ≥ 10,000 hours.

Room temperature tensile properties after aging for shorter times are available at temperatures above the 871°C temperature where long time data are available, and are presented in Figure 4, with data from the INL Alloy 617 research program, as well as from the literature.[2,3,10,12] For aging times of 100 and 1000h, the aged strengths are similar to the solution annealed properties. The nearly constant value up to 1000°C and the T-T-T diagram for this material[13] both indicate that it is highly unlikely that a new aging phenomenon is operative at this temperature compared to those at lower temperature.
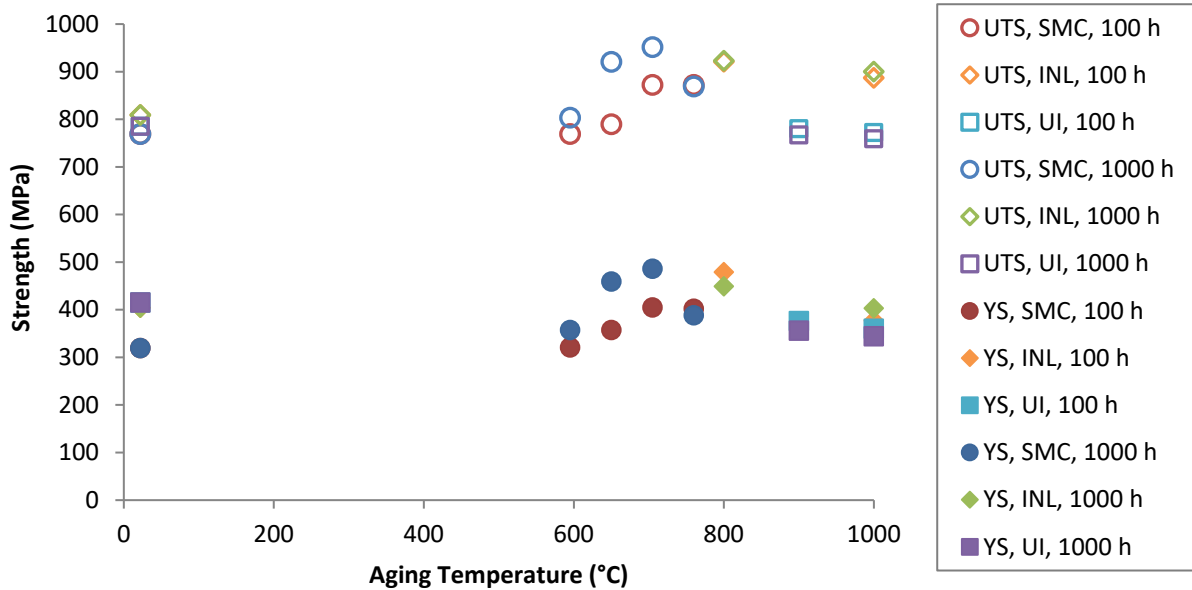
Figure 4. Room temperature tensile properties as a function of aging temperature after aging for 100 and 1000 hours. (UI refers to work done at University of Illinois at Urbana-Champaign.[12])
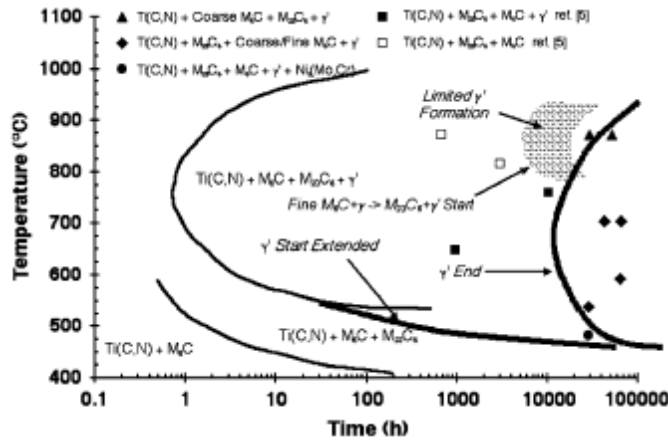
Figure 5. T-T-T diagram for Alloy 617 presented by Wu et al.[13]

Tensile properties measured at the aging temperature are shown in Figure 6, with the unaged properties shown as filled symbols. Yield and tensile strength are about the same or higher for the aged material for all aging/test temperatures. Similarly, material aged at 650 and 750°C and tested at higher temperatures showed no decrease in strength as a function of aging.

In some cases ductility is decreased after aging, however all specimens had total elongations of at least 20%. Total elongation is reported in Appendix VI for each specimen.
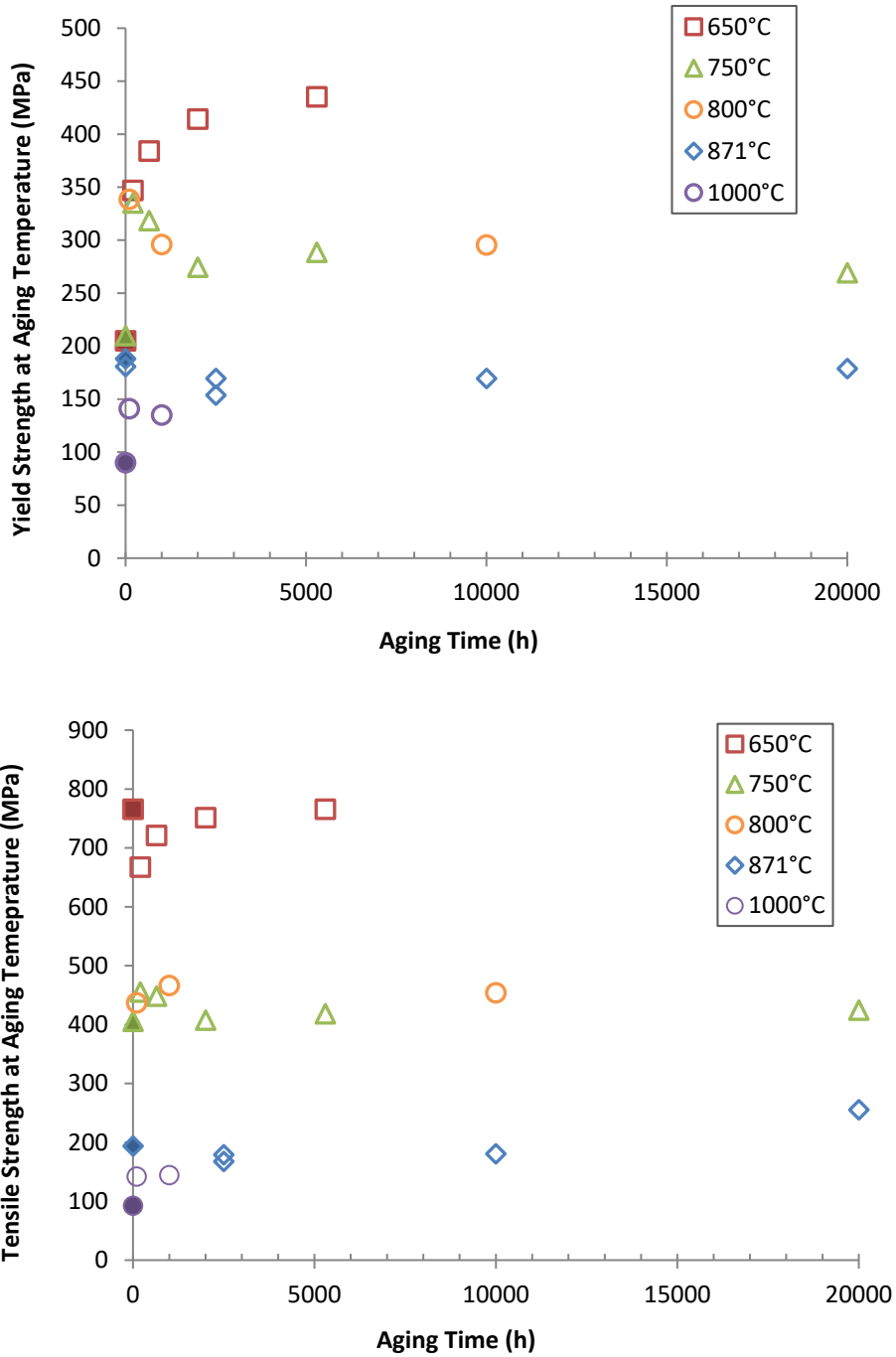
Figure 6. a) Yield strength and b) tensile strength measured at aging temperature as a function of aging time. Filled symbols indicate unaged properties.

Based on the discussion and data shown in this section, it is proposed that the Table HBB-3225-2 values for Alloy 617 be listed as 1.0 for both the yield strength reduction factor and tensile reduction factor for temperatures ≥425°C (800°F) up to and including 950°C (1750°F).

References

[1] W. Ren, 2009, "Gen IV Materials Handbook Functionalities and Operation," ORNL/TM-2009/285, U.S. Department of Energy Office of Nuclear Energy, December 2, 2009.

[2] H. E. McCoy and J. F. King (Oak Ridge National Laboratory), *Mechanical Properties of Inconel 617 and 618*, ORNL/TM-9337, February 1985.

[3] Special Metals Corporation, "Inconel Alloy 617" Publication Number SMC-029, 2005.

[4] J. K. Wright, L. J. Carroll, C. Cabet, T. M. Lillo, J. K. Benz, J. A. Simpson, W. R. Lloyd, J. A. Chapman, and R. N. Wright, "Characterization of elevated temperature properties of heat exchanger and steam generator alloys," *Nuclear Engineering Design*, Vol. 251, 2012, pp. 252–260.

[5] R. N. Wright, "Summary of Studies of Aging and Environmental Effects on Inconel 617 and Haynes 230, INL/EXT-06-11750, September 2006.

[6] ASTM B166 Standard specification for Nickel-Chromium-Iron Alloys (UNS N06600, N06601, N06603, N06690, N06025, N06046, N06696), Nickel-Chromium-Cobalt-Molybenum Alloy (UNS N06617), and Nickel-Iron-Chromium-Tungsten Alloy (UNS N06674) Rod, Bar, and Wire, ASTM International, 100 Barr Harbor Drive, PO Box C700, West Conshohocken, PA, 2011.

[7] ASTM B168 Standard specification for Nickel-Chromium-Iron Alloys (UNS N06600, N06601, N06603, N06690, N06025, N06046, N06696), Nickel-Chromium-Cobalt-Molybenum Alloy (UNS N06617), and Nickel-Iron-Chromium-Tungsten Alloy (UNS N06674) Plate, Sheet and Strip, ASTM International, 100 Barr Harbor Drive, PO Box C700, West Conshohocken, PA, 2011.

[8] ASTM E-8-11, Standard Test Methods for Tension Testing of Metallic Materials, ASTM International, 100 Barr Harbor Drive, PO Box C700, West Conshohocken, PA, 2011.

[9] ASTM E-21-09, Standard Test Methods for Elevated Temperature Tension Tests of Metallic Materials, ASTM International, 100 Barr Harbor Drive, PO Box C700, West Conshohocken, PA, 2009.

[10] W. Ren and R. Swindeman, "A Review Paper on Aging Effects in Alloy 617 for Gen IV Nuclear Reactor Applications", *Journal of Pressure Vessel Technology*, Vol. 131, 2009.

[11] M. Akbari-Garakani and M. Mehdizadeh, "Effect of long-term service exposure on microstructure and mechanical properties of Alloy 617," *Material and Design*, Vol. 32, 2011, pp. 2695-2700.

[12] K. Mo, G. Lovicu, H.-M. Tung, X. Chen and J. F. Stubbins, "High Temperature Aging and Corrosion Study on Alloy 617 and Alloy 230," *Journal of Engineering for Gas Turbines and Power*, Vol. 133, 2011.

[13] Q. Wu, H. Song, R. W. Swindeman, J. P. Shingledecker, and V. K. Vasudevan, "Microstructure of Long-Term Aged IN617 Ni-Base Superalloy," *Metallurgical Transactions*, Vol. 39A, 2008, pp. 2569-2585.

BACKGROUND

HBB-4212 EFFECTS OF FORMING AND BENDING PROCESSES

Scope

This document provides the background/technical basis in support of the recommendation for post-fabrication heat treatment for fabrication induced strains greater than 5% in the Alloy 617 Code Case.

Background

ASME Code Section III, Division 5, Subsection HB, Subpart B, Subarticle HBB-4212, "Effects of Forming and Bending Processes" describes the requirements for post-fabrication heat treatment for fabrication induced strains. For qualified materials in Section III, Division 5, a post-fabrication heat treatment is not required for materials that have experienced strains of 5% or less. Austenitic materials that have been subjected to strains greater than 20% are not permitted. HBB-4212, and Table HBB-4212-1, define the allowable temperature limits for short-time exposure of material cold worked more than 5 and less than 20% for which heat treatment is not required. For exposure greater than these time/temperature limits, the allowed materials are required to be heat treated to the solution annealing conditions specified in the appropriate standard for solution annealed material.

Cold work alters the creep rupture behavior of Alloy 617 for strains as low as 5%. Specific changes to the creep and rupture behavior depend on the amount of cold work and the creep temperature; in general the time and strain to rupture are reduced.

For fabrication strains greater than 5%, a post-fabrication solution heat treatment of 1150°C for 20 minutes/25 mm of thickness or 10 minutes, whichever is greater, is currently required in ASME Code Section VIII, Division 1. This requirement is also adopted for this Code Case.

Data Sources

Recent creep data have been contributed by Idaho National Laboratory (INL).[1] Creep data of cold-worked Alloy 617 has also been compiled from the literature.[2,3]

Materials

The INL has performed extensive property characterization on specimens machined from an Alloy 617 reference material plate.[4] The reference plate is a 37 mm thick solution annealed plate, labeled as heat 314626 produced by ThyssenKrupp VDM, with the chemistry given in Table 1. Creep testing and pre-straining was performed at INL on specimens machined from this reference plate. All specimens were tested in the solution-annealed condition, consisting of holding at 2150°F (1175°C) followed by rapid cooling to room temperature, according to standards SB166 and SB168.

Thermomechanical processing, i.e. hot rolling and solution anneal, has the potential to develop different microstructures in the three orthogonal directions in the plate. Therefore, samples were cut from the plate with orientations of each of the three faces shown in Figure 1. The samples were mechanically polished (3 μm Al_2O_3 final polishing step) and then electropolished for ~7 seconds in an electrolyte of ethanol-10% ethylene glycol monobutyl ether-10% water-6.7% perchloric acid at 17°C and 14 volts in the Stuers LectroPol-5 to remove artifacts produced by mechanical polishing. Orientation Imaging Microscopy (OIM) was performed on all three faces with the labeling convention shown in Figure 1.

Page intentionally left blank

Table 1. Chemical composition of the Alloy 617 materials (weight percent).

Heat ID	Product Form	Source	Ni	Cr	Co	Mo	Al	Ti	Fe	Mn	Cu	Si	C	S	B
min		ASME	44.5	20.0	10.0	8.0	0.8	--	--	--	--	--	0.05	--	--
max			--	24.0	15.0	10.0	1.5	0.6	3.0	1.0	0.5	1.0	0.15	0.015	0.006
314626	plate	INL	54.1	22.2	11.6	8.6	1.1	0.4	1.6	0.1	0.04	0.1	0.05	<0.002	<0.001

Page intentionally left blank
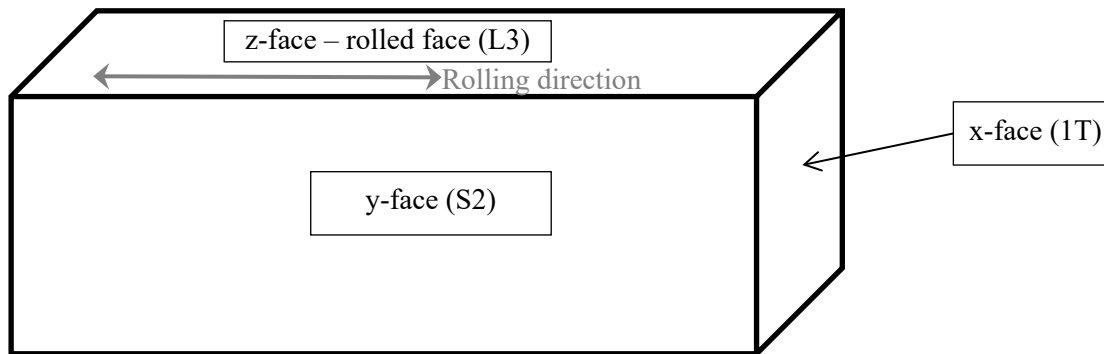
Figure 1. Schematic illustration of the three faces of the rolled I-617 plate (QA # 151053) that were analyzed for grain size.

Three areas on the x-face and z-face were analyzed for grain size while two areas on the y-face were analyzed. Each area was approximately 1.3 mm by 3 mm and a step size of 2 microns was used for OIM data collection to produce a dataset for each area containing over 1 million points. Twin boundaries were removed from the calculations of grain size. This included not only $\Sigma 3$ twins but also higher order twins, as well, e.g. $\Sigma 9$ and $\Sigma 27$. The fraction of these higher order twins is much lower than the fraction of the $\Sigma 3$ twin boundaries and their removal did not significantly affect the calculated grain size. Grains touching the edge of the analysis area were also excluded from the grain size calculation. Only high angle grain boundaries (>15° mis-orientation) were included in the grain size determination.

OIM images of each face are shown in Figure 2 and a plot of the range of observed grain sizes for the Y face is shown in Figure 3. The minimum grain size in the analysis of the OIM data was set to approximately 10 microns in diameter, so grains smaller than this were not included in the average grain size calculation. It is clear that there is a population of very small grains in the solution annealed as-received plate. The presence of bands of fine grains in the solution annealed material could complicate post-test analysis of recrystallization in the microstructures; the possible contribution of fine grains to the rupture life is also already incorporated at least in part in measurements of the solution annealed material.
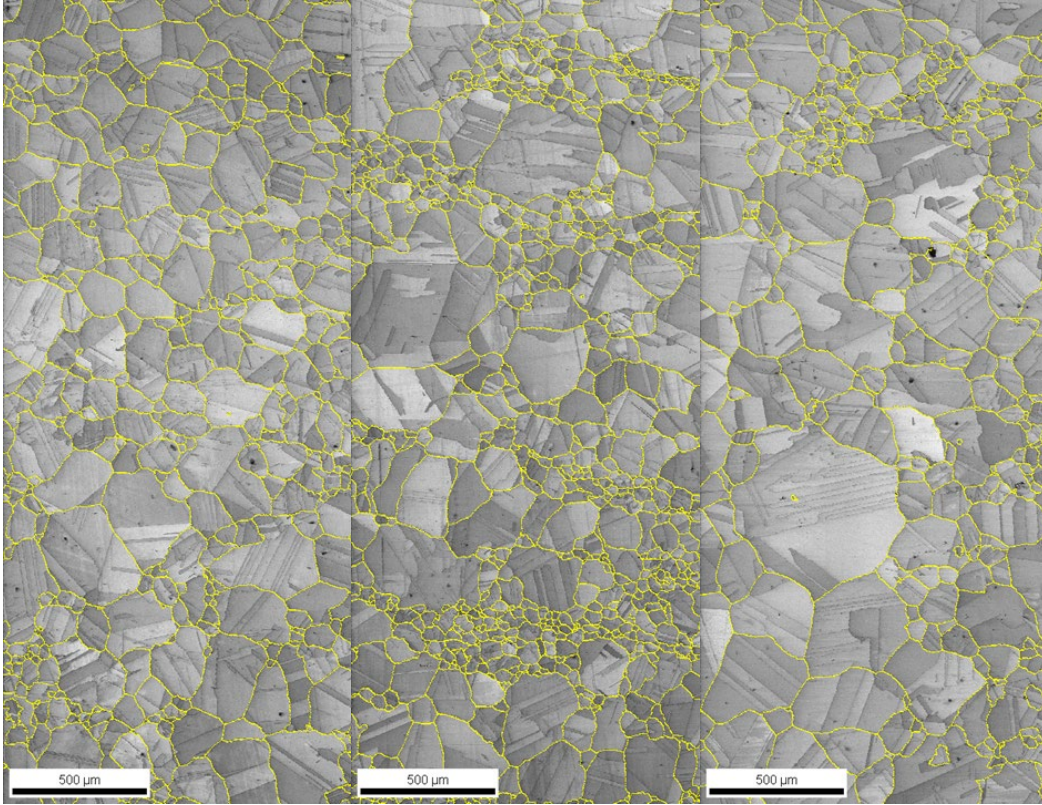
Figure 2. OIM images showing the wide range of grain sizes in solution annealed Alloy 617 plate on the X, Y and Z faces as defined in Figure 1.
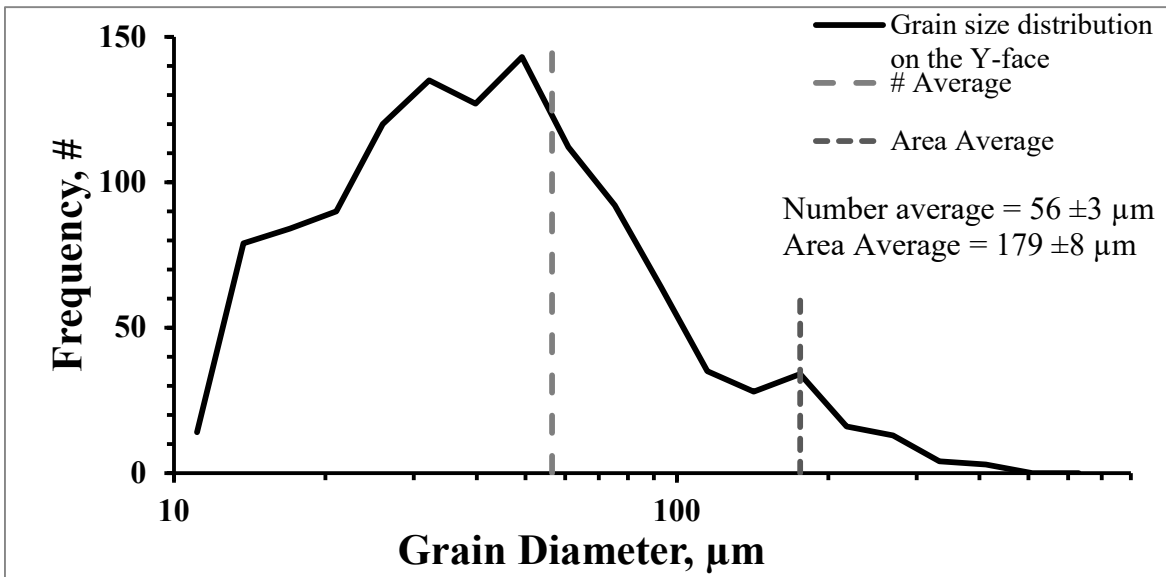
Figure 3. Grain size distribution from OIM images on the y-face of the solution annealed Alloy 617 plate.

Creep Testing

Creep specimens conformed to ASTM E139,[5] with a 6.35 mm diameter reduced section and a reduced section length of 32 mm (Figure 4) cut from material in the as-received condition with the axis of the specimen parallel to the direction of fabrication. The length and diameter of the test specimens were measured using calibrated micrometers.
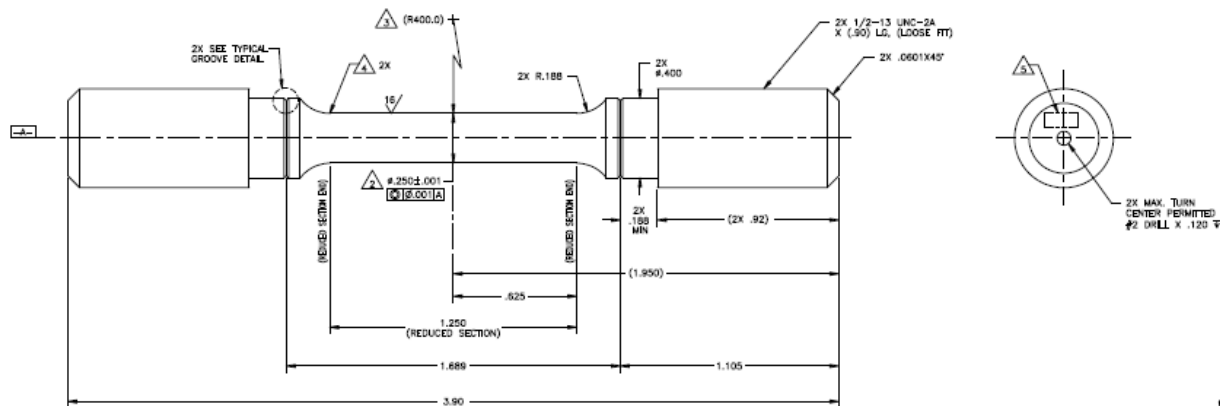
Figure 4. Tensile specimen used for testing at INL.

Creep testing was performed using direct loaded creep frames with dead weight loading. The temperature of the gage section of the creep specimen was measured with type R thermocouples and was controlled to within ±3ºC of the target test temperature. Dual averaging LVDT transducers or Heidenheim linear encoded photoelectric gauges were used to monitor creep strain during the creep tests to a resolution of better than 0.01% strain. Selected specimens were strained in tension at room temperature to a total strain of 10 or 15% prior to creep testing.

Quality

Creep properties of Alloy 617 reported by the Idaho National Laboratory (INL) through the Next Generation Nuclear Plant (NGNP) or Advanced Reactor Technologies (ART) programs were determined under an NQA-1 quality program. Details of the quality program implementation are given in INL document PLN-2690 "Idaho National Laboratory Advanced Reactor Technologies Technology Development Office Quality Assurance Program Plan".

Results

Creep-Rupture

The most significant potential effect of cold work on Alloy 617 properties at VHTR heat exchanger inlet temperatures is reduced creep-rupture life. Several reports on this effect have been published with a range of temperatures and pre-strain levels.[1-3] Creep curves for creep-rupture tests at 900 and 1000°C are shown in Figure 5 and Figure 6, respectively. For these tests the specimen was strained in tension at room temperature to the indicated strain prior to creep testing. Rupture life and strain to rupture are given in Table 2. At 900°C the initial creep rate, strain to failure and the time to rupture are significantly reduced in the cold worked material compared to comparable creep-rupture tests on solution annealed material. Creep testing the cold worked material at 1000°C showed increased creep rate compared to solution annealed material, however, the time to failure is significantly reduced as seen at the lower temperature.

Table 2. Data Compilation for INL Creep Tests of Alloy 617

ID	Tensile Pre-strain (%)	Temperature (°C)	Stress (MPa)	Rupture Life (h)	Creep Strain (%)
G-63	0	900	36	1373	27.6
G-22	0	900	36	1380	29.3
P-21	10	900	36	777.6	11.7
P-24	15	900	36	361.5	22.3
G-51	0	1000	13	9900	56.5
G-30	0	1000	13	8768	53.5
P-22*	10	1000	13	2969	44.1
P-25	15	1000	13	1934	59.5

* Testing anomaly occurred at ~17% strain, 1218 h. Reported rupture life and creep strain are upper limit approximations for this specimen.
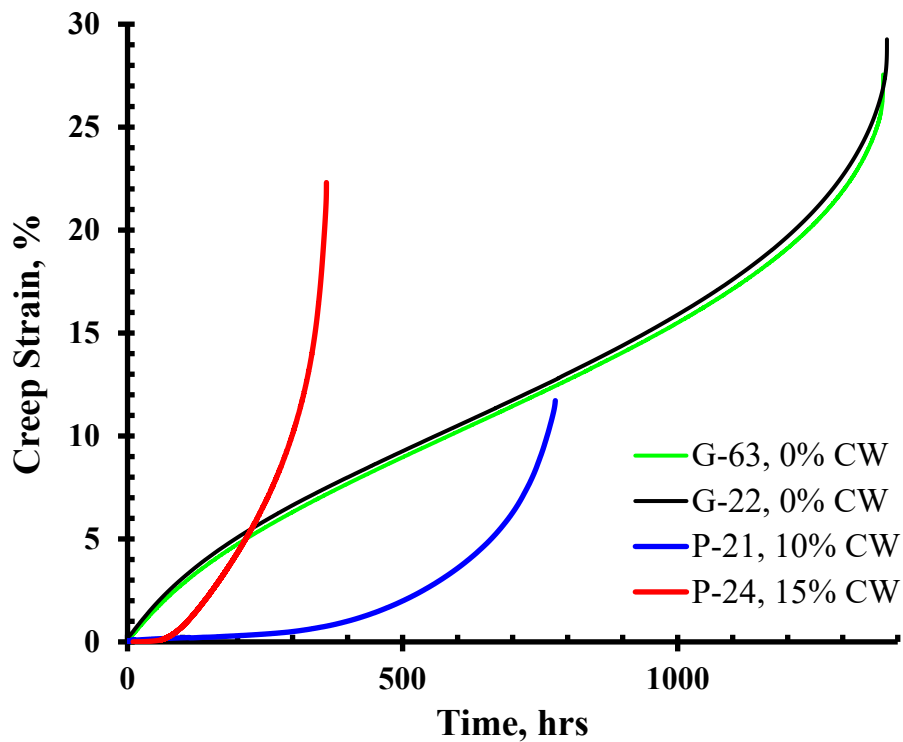
Figure 5. Creep curves for Alloy 617 in the as-received (solution annealed) condition and after 10% and 15% cold working at room temperature for a test temperature of 900°C and stress of 36 MPa.
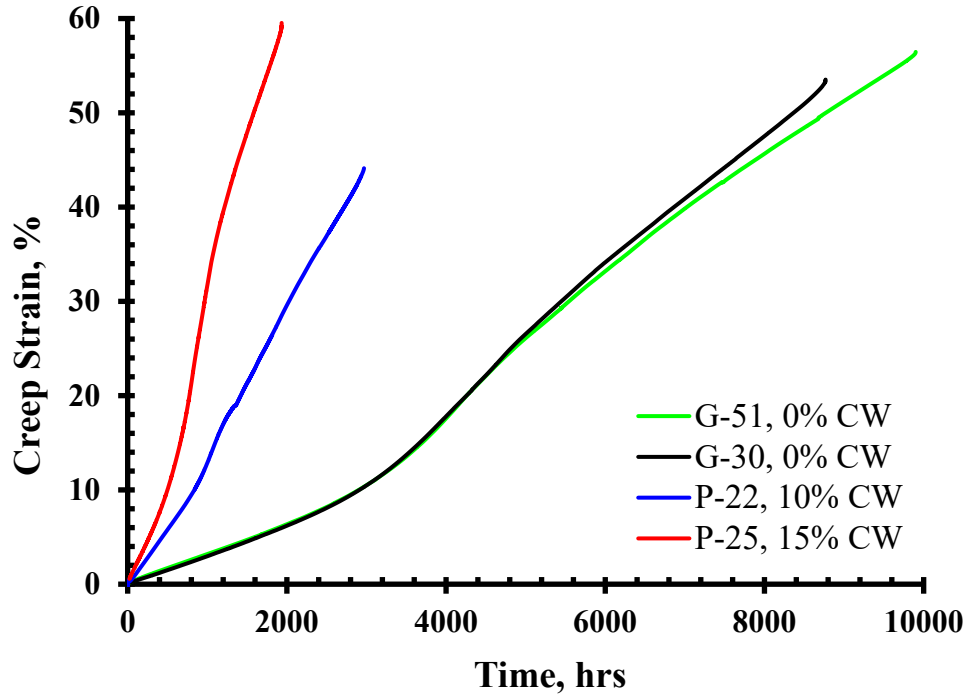
Figure 6. Creep curves for Alloy 617 in the as-received (solution annealed) condition and after 10% and 15% cold working at room temperature for a test temperature of 1000°C and stress of 13 MPa. A testing anomaly occurred at ~17% strain, 1218 h. Results up to this point are accurate, but the curve is a best estimate after this point.

Results reported in the literature for several cold worked specimens creep tested at 850°C are shown in Figure 7 and Figure 8.[2,3] The total tensile pre-strain for the rupture test shown in Figure 7 was 20%, however, the specimen exhibited similar qualitative behavior as the cold work specimens tested at INL. The creep rate, and strain to failure are reduced compared to solution annealed material as a result of the prior cold work, although the rupture time is longer. It can be seen from Figure 8 for tests interrupted after 3000 h that the creep rate is not greatly influenced by the amount of cold work over the range of 5 to 20%, but is much reduced compared to solution annealed material.

Figure 9 shows rupture curves from the literature for Alloy 617 in the solution annealed, aged and 20% cold worked condition for testing at 950°C and a stress of 30 MPa.[2] The creep-rupture behavior of cold worked material at this temperature is qualitatively similar to that shown in Figure 6 tested at 1000°C. The creep rate is significantly increased compared to solution annealed material and the time and strain to rupture are significantly reduced.
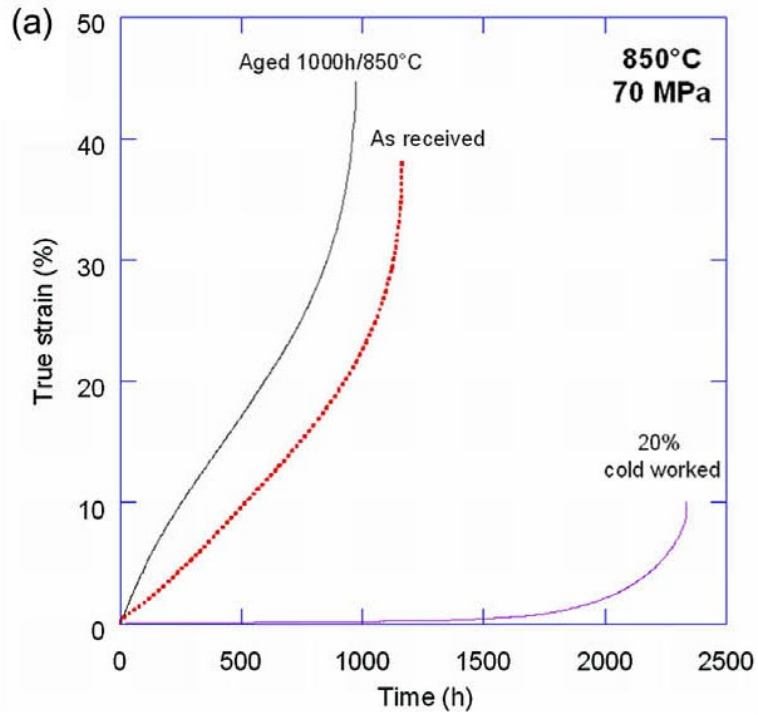
Figure 7. Creep-rupture curves for Alloy 617 in the solution annealed, statically aged and cold worked condition at 850°C and a stress of 70 MPa from Chomette et al.[2]

(a) Creep Results, 850°C, 36 MPa, Helium
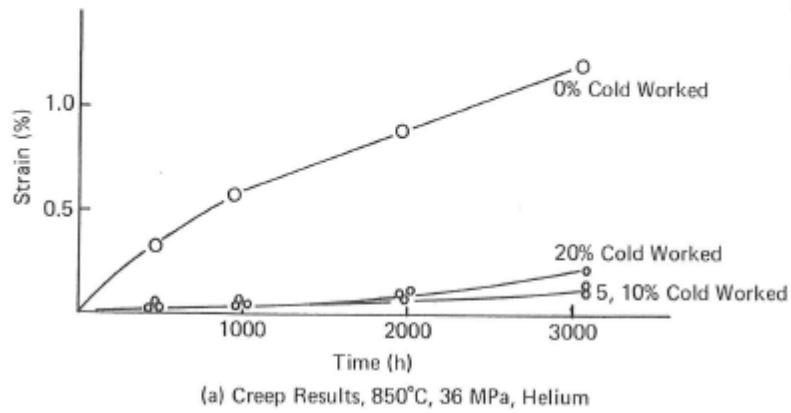
Figure 8. Creep curves for interrupted tests at 850°C and 36 MPa on solution annealed Alloy 617 and specimens pre-strained to three different levels of cold work from Cook.[3]
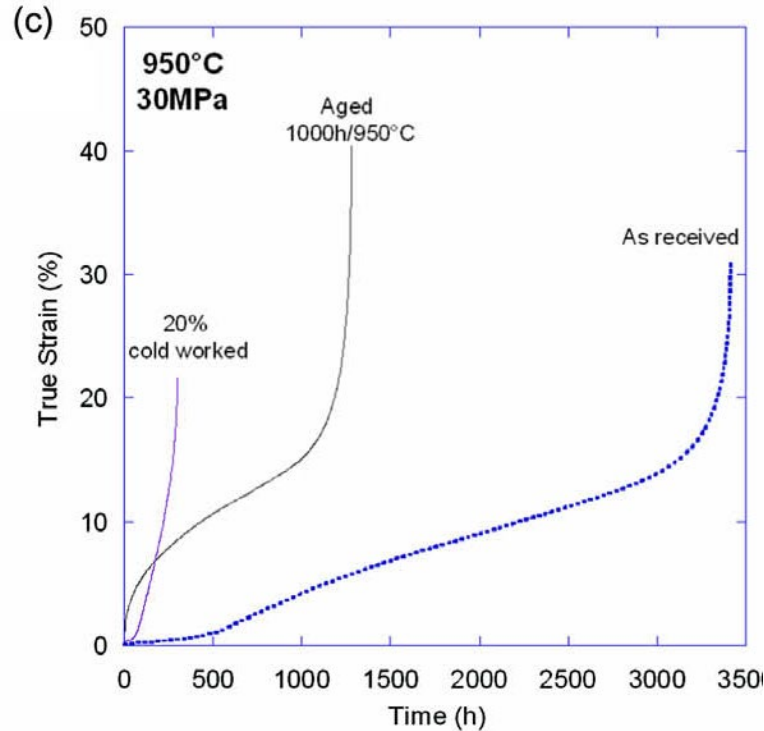
Figure 9. Creep-rupture curves for Alloy 617 in the solution annealed, statically aged and cold worked condition at 950°C and a stress of 30 MPa from Chomette et al.[2]

Recrystallization

Recrystallization of Alloy 617 is very difficult to characterize using optical metallography. Unpublished collaborative research between INL and Boise State University characterized recrystallization of Alloy 617 that had been cold rolled to 50% reduction. It was found that conventional polishing and chemical etching revealed only the carbides associated with solution annealed grain boundaries even in material that hardness measurements indicated was fully recrystallized. The most certain method for showing the recrystallization was using OIM, Figure 10(a). Figure 10(b) shows an OIM image from near the fracture surface from the 10% cold work sample tested to rupture at 900ºC at a stress of 36 MPa. It is obvious from visual comparison of the images that bulk recrystallization did not occur under these rupture conditions.

Chomette et al. found that extensive recrystallization appears to be driven by localized deformation associated with necking in creep-rupture specimens even in the absence of bulk cold working prior to creep testing.[2] Furthermore, bulk recrystallization does not occur in cold worked material for all rupture conditions. The total strain to rupture for the INL sample shown in Figure 10(b) was approximately 5%, whereas the strain to failure in the sample for which Chomette et al., report recrystallization near the fracture was on the order of 40%.[2] These combined results suggest that recrystallization to a fine grain size is probably not a dominant mechanism for the generally observed reduction in creep properties resulting from cold work. Efforts to confirm this observation are hindered by the uncertainty of identifying recrystallization in some of the literature where only optical micrographs are shown.
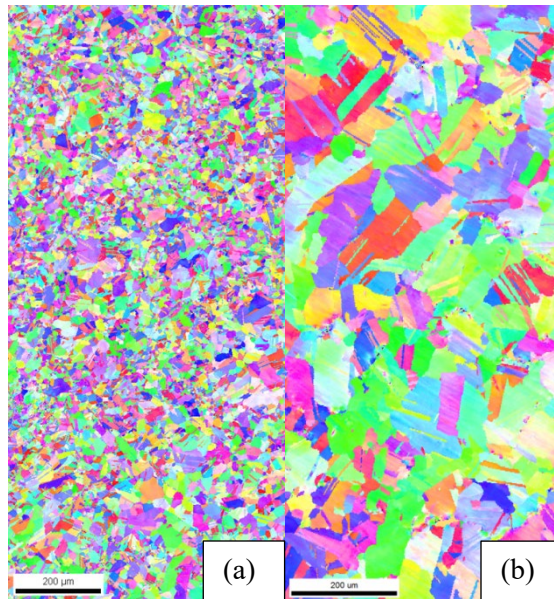
Figure 10. OIM images of (a) sample recrystallized at 1000ºC after bulk deformation to 50% by rolling and (b) region near the fracture surface of a specimen tested to rupture in creep at a temperature of 900°C and stress of 36 MPa.

ASME Code Considerations

HBB-4212

ASME Code Section III, Division 5, Subsection HB, Subpart B allows use of only three austenitic structural materials, Type 304 and 316 stainless steel, and Alloy 800H. Section III, Division 5, does not require a post-fabrication heat treatment for materials that have experienced strains of 5% or less. Austenitic materials that have been subjected to strains greater than 20% are not permitted. Figure HBB-4212-1, and Table HBB-4212-1, define the allowable temperature limits for short-time exposure of material cold worked more than 5 and less than 20% for which heat treatment is not required. For exposure greater than these time/temperature limits, the allowed materials are required to be heat treated to the solution annealing conditions specified in the appropriate standard for solution annealed material. For Alloy 617 this temperature is 1150°C.

It has not been possible to recover the background for Figure HBB-4212-1, however, it is reasonable to assume that the limits on Alloy 617 would be similar to those for Alloy 800H. For the desired 100,000 hour life for temperatures up to 950ºC, this material would be limited to 5% or less cold work without post-fabrication solution anneal.

Section VIII Division 1

Alloy 617 is allowed for design of non-nuclear pressure vessels in Section VIII Division 1 of the ASME Code. Requirements for post-fabrication heat treatment of cold worked alloys, including Alloy 617, are given in Table UNF-79 of Section VIII Division 1. The limits for permissible strain shown in the table for Alloy 617 are 15% in the design temperature range 540 to 675°C and 10% in the temperature range exceeding 675°C. If these strain limits are exceeded for cold working, defined as "the finishing-forming temperature is below the minimum heat-treating temperature given in Table UNF-79", a post-fabrication solution treatment is required. This heat treatment is specified as heating to the temperature in Table UNF-79 (1150°C for Alloy 617) for 20 minutes/25 mm of thickness or 10 minutes, whichever is greater.

Vendor Recommendations on Fabrication Strains

Special Metals, the original developer of Alloy 617, as well as Haynes International and VDM all caution against imposing small amounts of cold work, generally less than 10%, to any of the solid solution nickel based alloys.[6-9] Depending on the particular alloy, this limited amount of cold work can result in abnormal grain growth during prolonged exposure to elevated service temperatures. In a study specific to Alloy 617 Special Metals examined the effect of abnormal grain growth on low cycle fatigue properties and found degraded properties.[6] Haynes International presents data in their fabrication guide for Hastelloy X and Haynes 230 (both solid solution nickel alloys that are frequently compared to Alloy 617) that do not show any change in the grain size after annealing at temperatures up to 1120°C for short times after tensile pre-straining from 1 to 10%.[9] Given that coarse grains are generally desirable for creep resistance, it is not evident that a change in microstructure resulting from abnormal grain growth would be deleterious to creep-rupture behavior.

Code Case Recommendation

It is clear that cold work alters the creep rupture behavior of Alloy 617 for strains as low as 5%. Although specific changes depend on the amount of cold work and the creep temperature; the time and strain to rupture are both generally reduced. The mechanism by which these changes occur is not clear. It does not appear that bulk recrystallization occurs; local recrystallization in the highly deformed region near the fracture surface of ruptured specimens has been reported even in the absence of prior cold work.

Limiting the fabrication strain to 5% in components which are not given a post-fabrication solution treatment, is recommended. This limited amount of allowed cold work allows incidental deformation associated with fit-up and installation without deleterious effect on properties. It is also consistent with requirements for Alloy 800H, a similar solid solution alloy in the current Section III, Subsection NB rules.

For fabrication strains greater than 5 % a post-fabrication solution heat treatment of 1150°C for 20 minutes/25 mm of thickness or 10 minutes, whichever is greater as currently required in ASME Section VIII Division 1 is recommended. This heat treatment will likely recrystallize the material and allow grain growth that is required for creep-rupture resistance.

References

[1] R. N. Wright, "The Effect of cold work on Properties of Alloy 617, INL/EXT-14-32965, August 2014.

[2] S. Chomette, J.-M. Gentzbittel, B. Viguier, "Creep behavior of as-received, aged and cold worked Inconel 617 at 850 and 950°C", Journal of Nuclear Materials, Vol. 399, 2010, pp. 266-274.

[3] Roger H. Cook, "Creep properties of Inconel 617 in air and helium at 800 to 1000°C", Nuclear Technology, vol. 66, 1984, pp. 283-288.

[4] J. K. Wright, L. J. Carroll, C. Cabet, T. M. Lillo, J. K. Benz, J. A. Simpson, W. R. Lloyd, J. A. Chapman, and R. N. Wright, "Characterization of elevated temperature properties of heat exchanger and steam generator alloys," *Nuclear Engineering Design*, Vol. 251, 2012, pp. 252–260.

[5] ASTM E 139, "Standard Test Methods for Conducting Creep, Creep-Rupture, and Stress Rupture Tests of Metallic Materials," ASTM International.

[6] Special Metals Fabricating Guide, Special Metals Corp., Huntington, WV, 2008.

[7] Nicrofer 5520 Co – Alloy 617 Material Data Sheet, ThyssenKrupp VDM, Datasheet 4019, 2005.

[8] INCONEL Alloy 617 Data Sheet, Special Metals Corp., Publication No. SMC-029 Huntington, WV, 2005.

[9] Fabrication of Haynes and Hastelloy Solid-Solution Strengthened High-Temperature Alloys, Haynes International, Kokomo, IN, 2002.

Appendix I

Data Compilation for Tensile Tests of Alloy 617

	Heat/Lot ID	Product Form	Temp. (°C)	Yield Strength (MPa)	Tensile Strength (MPa)	Elongation (%)	Reduction in Area (%)	Source
1	188155	Rod	22	402	811	64	63	INL
2	188155	Rod	22	413	808	63	64	INL
3	188155	Rod	200	323	719	63	61	INL
4	188155	Rod	200	309	717	65	64	INL
5	188155	Rod	250	269	711	65	58	INL
6	188155	Rod	250	301	722	66	59	INL
7	188155	Rod	300	286	709	64	56	INL
8	188155	Rod	300	287	706	65	55	INL
9	188155	Rod	350	294	700	69	56	INL
10	188155	Rod	350	288	696	67	58	INL
11	188155	Rod	400	295	701	68	52	INL
12	188155	Rod	400	283	683	69	57	INL
13	188155	Rod	427	294	692	66	58	INL
14	188155	Rod	427	273	689	64	59	INL
15	188155	Rod	650	279	610	46	34	INL
16	188155	Rod	650	282	598	46	36	INL
17	188155	Rod	700	368	607	31	26	INL
18	188155	Rod	700	349	605	33	27	INL
19	188155	Rod	750	269	420	81	61	INL
20	188155	Rod	750	295	428	76	61	INL
21	188155	Rod	800	273	316	117	71	INL
22	188155	Rod	800	282	320	113	73	INL
23	188155	Rod	850	221	235	131	79	INL
24	188155	Rod	850	225	239	116	78	INL
25	188155	Rod	900	167	175	128	80	INL
26	188155	Rod	900	165	174	142	82	INL
27	188155	Rod	950	125	130	103	97	INL
28	188155	Rod	950	127	131	115	95	INL
29	188155	Rod	1000	95	97	117	96	INL
30	188155	Rod	1000	97	99	101	97	INL
31	314626	Plate	20	302	768	63	62	INL
32	314626	Plate	425	209	667	65	51	INL
33	314626	Plate	450	205	653	68	52	INL
34	314626	Plate	450	208	639	66	53	INL
35	314626	Plate	500	201	629	65	49	INL
36	314626	Plate	550	199	626	68	47	INL
37	314626	Plate	600	197	631	72	45	INL
38	314626	Plate	650	245	593	72	43	INL
39	314626	Plate	650	204	584	69	51	INL
40	314626	Plate	700	249	553	61	46	INL
41	314626	Plate	750	210	406	65	62	INL
42	314626	Plate	800	189	290	94	80	INL
43	314626	Plate	850	188	216	119	80	INL
44	314626	Plate	900	163	166	103	81	INL
45	314626	Plate	950	119	124	96	86	INL
46	314626	Plate	1000	90	92	99	87	INL
47	CEA		25	333	728			CEA
48	CEA		25	373	791			CEA
49	CEA		25	342	730			CEA
50	CEA		25	344	734			CEA

	Heat/Lot ID	Product Form	Temp. (°C)	Yield Strength (MPa)	Tensile Strength (MPa)	Elongation (%)	Reduction in Area (%)	Source
51	CEA		25	349	739			CEA
52	CEA		350	259	622			CEA
53	CEA		450	229	592			CEA
54	CEA		550	233	556			CEA
55	CEA		650	218	556			CEA
56	CEA		700		509			CEA
57	CEA		700	212	519			CEA
58	CEA		750	210	443			CEA
59	CEA		750	217	448			CEA
60	CEA		850	160	282			CEA
61	CEA		850	195	293			CEA
62	CEA		850	208	359			CEA
63	CEA		850	145	280			CEA
64	CEA		850	245	372			CEA
65	CEA		950		157			CEA
66	CEA		950		163			CEA
67	XX00A1USL	Bar	21	296	735	70	57	Huntington
68	XX00A1USL	Bar	538	195	580	69	58	Huntington
69	XX00A1USL	Bar	649	171	568	75	55	Huntington
70	XX00A1USL	Bar	760	177	447	84	65	Huntington
71	XX00A1USL	Bar	871	196	281	120	93	Huntington
72	XX00A1USL	Bar	982	145	148	124	94	Huntington
73	XX00A1USL	Bar	1093	51	79	90	78	Huntington
74	XX00A1USL	CR Sheet	21	324	765	54		Huntington
75	XX00A1USL	CR Sheet	21	354	805	56		Huntington
76	XX00A1USL	CR Sheet	538	217	590	56		Huntington
77	XX00A1USL	CR Sheet	649	197	579	62		Huntington
78	XX00A1USL	CR Sheet	760	207	465	76		Huntington
79	XX00A1USL	CR Sheet	871	210	248	92		Huntington
80	XX00A1USL	CR Sheet	982	100	134	58		Huntington
81	XX00A1USL	CR Sheet	1093	52	72	58		Huntington
82	XX00A3USL	Forging	21	348	803	60	58	Huntington
83	XX00A3USL	Forging	21	307	725	68	58	Huntington
84	XX00A3USL	Forging	21	321	767	66	58	Huntington
85	XX00A3USL	Forging	21	310	708	62	46	Huntington
86	XX00A3USL	Plate	21	309	741	66	58	Huntington
87	XX00A3USL	Plate	21	306	743	70	62	Huntington
88	XX00A3USL	Plate	21	309	736	66	59	Huntington
89	XX00A3USL	Plate	21	308	741	68	61	Huntington
90	XX00A4USL	Bar	21	387	785	58	50	Huntington
91	XX00A4USL	Bar	21	356	769	61	54	Huntington
92	XX00A4USL	Bar	93	453	763	55	49	Huntington
93	XX00A4USL	Bar	204	265	674	64	51	Huntington
94	XX00A4USL	Bar	315	358	690	60	53	Huntington
95	XX00A4USL	Bar	427	347	665	61	54	Huntington
96	XX00A4USL	Bar	538	347	630	63	52	Huntington
97	XX00A4USL	Bar	593	330	603	62	54	Huntington
98	XX00A4USL	Bar	649	303	617	61	47	Huntington
99	XX00A4USL	Bar	704	243	561	64	48	Huntington
100	XX00A4USL	Bar	760	328	556	58	51	Huntington
101	XX00A4USL	Bar	871	272	332	74	69	Huntington
102	XX00A5USL	Bar	21	321	767	64	55	Huntington
103	XX00A5USL	Bar	93	314	725	60	49	Huntington
104	XX00A5USL	Bar	204	393	712	57	53	Huntington

	Heat/Lot ID	Product Form	Temp. (°C)	Yield Strength (MPa)	Tensile Strength (MPa)	Elongation (%)	Reduction in Area (%)	Source
105	XX00A5USL	Bar	315	235	667	64	56	Huntington
106	XX00A5USL	Bar	427	219	632	68	53	Huntington
107	XX00A5USL	Bar	538	218	587	66	53	Huntington
108	XX00A5USL	Bar	593	204	589	65	56	Huntington
109	XX00A5USL	Bar	649	181	578	64	53	Huntington
110	XX00A5USL	Bar	760	212	500	72	54	Huntington
111	XX00A5USL	Bar	871	217	279	99	86	Huntington
112	XX00A5USL	CR Sheet	21	346	820	50		Huntington
113	XX00A5USL	CR Sheet	649	193	624	65		Huntington
114	XX00A5USL	CR Sheet	760	214	438	84		Huntington
115	XX05A4UK	Bar	21	330	738	61	53	Huntington
116	XX05A4UK	Bar	21	349	730	64	53	Huntington
117	XX05A4UK	Bar	38	320	778	46	52	Huntington
118	XX05A4UK	Bar	93	266	734	59	54	Huntington
119	XX05A4UK	Bar	149	244	706	60	54	Huntington
120	XX05A4UK	Bar	204	256	674	63	58	Huntington
121	XX05A4UK	Bar	260	231	684	60	54	Huntington
122	XX05A4UK	Bar	315	233	648	65	61	Huntington
123	XX05A4UK	Bar	371	219	632	66	58	Huntington
124	XX05A4UK	Bar	427	230	629	68	59	Huntington
125	XX05A4UK	Bar	482	208	634	63	56	Huntington
126	XX05A4UK	Bar	538	230	585	64	64	Huntington
127	XX05A4UK	Bar	593	194	616	62	46	Huntington
128	XX05A4UK	Bar	649	212	568	66	56	Huntington
129	XX05A4UK	Bar	704	268	558	53	42	Huntington
130	XX05A4UK	Bar	760	232	510	52	48	Huntington
131	XX05A4UK	Bar	815	235	402	47	53	Huntington
132	XX05A4UK	Bar	871	272	357	43	52	Huntington
133	XX05A4UK	Bar	927	175	228	63	80	Huntington
134	XX05A4UK	Bar	982	139	168	72	73	Huntington
135	XX05A4UK	Bar	1038	105	125	79	74	Huntington
136	XX05A4UK	Bar	1093	74	87	71	61	Huntington
137	XX07A7UK	Bar	21	371	764	59	50	Huntington
138	XX07A7UK	Bar	21	367	776	56	49	Huntington
139	XX07A7UK	Bar	38	342	772	54	47	Huntington
140	XX07A7UK	Bar	93	330	747	56	52	Huntington
141	XX07A7UK	Bar	149	292	726	57	51	Huntington
142	XX07A7UK	Bar	204	294	714	56	55	Huntington
143	XX07A7UK	Bar	260	270	700	57	54	Huntington
144	XX07A7UK	Bar	315	261	692	59	55	Huntington
145	XX07A7UK	Bar	371	248	677	60	54	Huntington
146	XX07A7UK	Bar	427	259	676	62	56	Huntington
147	XX07A7UK	Bar	482	252	642	56	45	Huntington
148	XX07A7UK	Bar	538	244	624	58	50	Huntington
149	XX07A7UK	Bar	593	256	620	57	43	Huntington
150	XX07A7UK	Bar	649	272	607	55	48	Huntington
151	XX07A7UK	Bar	704	296	588	48	43	Huntington
152	XX07A7UK	Bar	760	324	585	37	34	Huntington
153	XX07A7UK	Bar	815	307	443	34	38	Huntington
154	XX07A7UK	Bar	871	254	324	42	48	Huntington
155	XX07A7UK	Bar	927	177	216	61	60	Huntington
156	XX07A7UK	Bar	982	141	171	69	65	Huntington
157	XX07A7UK	Bar	1038	105	141	61	55	Huntington
158	XX07A7UK	Bar	1093	82	108	60	62	Huntington

	Heat/Lot ID	Product Form	Temp. (°C)	Yield Strength (MPa)	Tensile Strength (MPa)	Elongation (%)	Reduction in Area (%)	Source
159	XX20A5UK	CR Sheet	21	338	731	62		Huntington
160	XX20A5UK	CR Sheet	21	341	722	64		Huntington
161	XX20A5UK	CR Sheet	93	310	690	65		Huntington
162	XX20A5UK	CR Sheet	204	273	656	64		Huntington
163	XX20A5UK	CR Sheet	315	246	634	71		Huntington
164	XX20A5UK	CR Sheet	427	250	610	70		Huntington
165	XX20A5UK	CR Sheet	538	228	565	72		Huntington
166	XX20A5UK	CR Sheet	649	225	616	52		Huntington
167	XX20A5UK	CR Sheet	760	255	461	59		Huntington
168	XX20A5UK	CR Sheet	871	194	275	73		Huntington
169	XX20A5UK	CR Sheet	982	92	148	93		Huntington
170	XX20A5UK	CR Sheet	1093	51	80	76		Huntington
171	XX26A8UK	CR Sheet	21	359	811	53		Huntington
172	XX26A8UK	CR Sheet	38	351	767	34		Huntington
173	XX26A8UK	CR Sheet	93	338	805			Huntington
174	XX26A8UK	CR Sheet	149	325	750	21		Huntington
175	XX26A8UK	CR Sheet	204	301	769	58		Huntington
176	XX26A8UK	CR Sheet	260	285	758	53		Huntington
177	XX26A8UK	CR Sheet	315	277	740	58		Huntington
178	XX26A8UK	CR Sheet	371	266	730	62		Huntington
179	XX26A8UK	CR Sheet	427	273	729	60		Huntington
180	XX26A8UK	CR Sheet	482	268	705	55		Huntington
181	XX26A8UK	CR Sheet	538	259	707	59		Huntington
182	XX26A8UK	CR Sheet	593	248	679	57		Huntington
183	XX26A8UK	CR Sheet	649	256	687	62		Huntington
184	XX26A8UK	CR Sheet	704	257	595	47		Huntington
185	XX26A8UK	CR Sheet	760	272	502	42		Huntington
186	XX26A8UK	CR Sheet	815	261	390	61		Huntington
187	XX26A8UK	CR Sheet	871	230	432	68		Huntington
188	XX26A8UK	CR Sheet	927	151	205	52		Huntington
189	XX26A8UK	CR Sheet	982	103	152	61		Huntington
190	XX26A8UK	CR Sheet	1038	92	105	39		Huntington
191	XX26A8UK	CR Sheet	1093	66	82	59		Huntington
192	XX01A3US	Plate	23	303	747	54	36	ORNL
193	XX01A3US	Plate	23	301	757	61	41	ORNL
194	XX01A3US	Plate	23	305	754	58	32	ORNL
195	XX01A3US	Plate	538	216	610	67	50	ORNL
196	XX01A3US	Plate	538	207	606	64	46	ORNL
197	XX01A3US	Plate	704	199	466	68	49	ORNL
198	XX01A3US	Plate	704	196	454	75	53	ORNL
199	XX01A3US	Plate	704	196	443	70	53	ORNL
200	XX01A3US	Plate	871	189	194	92	86	ORNL
201	XX01A3US	Plate	871	181	194	88	88	ORNL
202	XX09A4UK	Plate	23	394	765	57	63	ORNL
203	XX09A4UK	Plate	23	363	765	50	54	ORNL
204	XX09A4UK	Plate	593	216	556	52	49	ORNL
205	XX09A4UK	Plate	649	235	549	48	45	ORNL
206	XX09A4UK	Plate	704	290	502	34	40	ORNL
207	XX09A4UK	Plate	760	331	556	20	17	ORNL
208	XX09A4UK	Plate	871	268	284	20	26	ORNL

Appendix II

Data Compilation of Time to 1% Creep Strain for Alloy 617

	Heat/Lot ID	Product Form	Temperature (°C)	Stress (MPa)	Time to 1% Strain (hrs)	Source
1	314626	plate	750	95.0	361	ANL
2	314626	plate	750	118.0	60	ANL
3	314626	plate	750	118.0	88	ANL
4	314626	plate	750	135.1	86	ANL
5	314626	plate	750	137.8	30	ANL
6	314626	plate	850	43.0	44	ANL
7	314626	plate	850	43.1	64	ANL
8	314626	plate	850	54.0	11	ANL
9	314626	plate	950	18.5	175	ANL
10	314626	plate	750	121.0	903	INL
11	314626	plate	750	121.0	1,042	INL
12	314626	plate	750	121.0	1,810	INL
13	314626	plate	750	121.0	1,929	INL
14	314626	plate	750	121.0	1,316	INL
15	314626	plate	750	145.0	632	INL
16	314626	plate	750	145.0	475	INL
17	314626	plate	750	145.0	566	INL
18	314626	plate	750	145.0	428	INL
19	314626	plate	750	145.0	515	INL
20	314626	plate	750	145.0	843	INL
21	314626	plate	750	161.5	211	INL
22	314626	plate	800	60.0	109	INL
23	314626	plate	800	60.0	147	INL
24	314626	plate	800	65.0	73	INL
25	314626	plate	800	65.0	77	INL
26	314626	plate	800	70.0	49	INL
27	314626	plate	800	70.0	53	INL
28	314626	plate	800	80.0	24	INL
29	314626	plate	800	80.0	26	INL
30	314626	plate	800	94.2	10	INL
31	314626	plate	850	27.5	1,147	INL
32	314626	plate	900	26.0	170	INL
33	314626	plate	900	26.0	164	INL
34	314626	plate	900	28.0	109	INL
35	314626	plate	900	28.0	129	INL
36	314626	plate	900	31.0	75	INL
37	314626	plate	900	31.0	63	INL
38	314626	plate	900	36.0	26	INL
39	314626	plate	900	36.0	31	INL
40	314626	plate	900	36.0	25	INL
41	314626	plate	900	44.7	11	INL
42	314626	plate	950	12.0	3,844	INL
43	314626	plate	1000	11.0	701	INL
44	314626	plate	1000	11.0	1,023	INL
45	314626	plate	1000	12.0	390	INL
46	314626	plate	1000	12.0	680	INL
47	314626	plate	1000	13.0	331	INL
48	314626	plate	1000	13.0	266	INL
49	314626	plate	1000	16.0	88	INL

	Heat/Lot ID	Product Form	Temperature (°C)	Stress (MPa)	Time to 1% Strain (hrs)	Source
50	314626	plate	1000	16.0	115	INL
51	314626	plate	1000	16.0	113	INL
52	314626	plate	1000	16.0	142	INL
53	314626	plate	1000	16.0	115	INL
54	314626	plate	1000	16.0	96	INL
55	314626	plate	1000	16.0	87	INL
56	314626	plate	1000	16.0	104	INL
57	314626	plate	1000	16.0	104	INL
58	314626	plate	1000	20.0	22	INL
59	314626	plate	1000	20.0	27	INL
60	314626	plate	1000	20.0	28	INL
61	314626	plate	1000	20.0	26	INL
62	314626	plate	1000	20.0	31	INL
63	314626	plate	1000	20.0	29	INL
64	314626	plate	1000	20.0	32	INL
65	314626	plate	1000	20.0	35	INL
66	XX14A6UK	plate	750	200.0	97	GE
67	XX14A6UK	plate	850	56.6	1,100	GE
68	XX14A6UK	plate	850	64.8	14	GE
69	XX14A6UK	plate	850	72.4	21	GE
70	XX14A6UK	plate	850	79.3	17	GE
71	XX14A6UK	plate	950	25.5	2,750	GE
72	XX14A6UK	plate	950	37.9	70	GE
73	XX14A6UK	plate	1049	10.7	3,100	GE
74	XX14A6UK	plate	1049	14.5	950	GE
75	XX14A6UK	plate	1049	20.7	125	GE
76	XX14A6UK	plate	1100	15.2	70	GE
77	XX63A8UK	plate	850	44.8	218	GE
78	XX63A8UK	plate	850	48.3	160	GE
79	XX63A8UK	plate	850	56.6	55	GE
80	XX63A8UK	plate	850	66.2	26	GE
81	XX63A8UK	plate	950	20.7	475	GE
82	XX63A8UK	plate	950	24.1	255	GE
83	XX63A8UK	plate	950	31.0	45	GE
84	XX63A8UK	plate	950	37.9	17	GE
85	XX00A1US	rod	760	103.4	75	Huntington
86	XX00A1US	rod	816	69.0	105	Huntington
87	XX00A1US	rod	816	89.6	26	Huntington
88	XX00A1US	rod	871	27.6	780	Huntington
89	XX00A1US	rod	871	34.5	503	Huntington
90	XX00A1US	rod	871	48.3	102	Huntington
91	XX00A1US	rod	871	48.3	38	Huntington
92	XX00A1US	rod	871	62.1	10	Huntington
93	XX00A1US	rod	982	19.3	56	Huntington
94	XX00A1US	rod	982	20.7	335	Huntington
95	XX00A1US	rod	982	20.7	285	Huntington
96	XX00A1US	rod	982	24.1	42	Huntington
97	XX00A1US	rod	1038	13.8	320	Huntington
98	XX00A1US	rod	1038	16.5	43	Huntington
99	XX00A1US	rod	1093	6.2	625	Huntington
100	XX00A1US	rod	1093	8.3	395	Huntington
101	XX00A1US	rod	1093	8.3	175	Huntington
102	XX00A1US	rod	1093	10.3	154	Huntington

	Heat/Lot ID	Product Form	Temperature (°C)	Stress (MPa)	Time to 1% Strain (hrs)	Source
103	XX00A1US	sheet	871	48.3	99	Huntington
104	XX00A1US	sheet	871	48.3	144	Huntington
105	XX00A1US	sheet	871	69.0	11	Huntington
106	XX00A1US	sheet	982	13.8	1,080	Huntington
107	XX00A1US	sheet	982	20.7	290	Huntington
108	XX00A1US	sheet	982	27.6	38	Huntington
109	XX00A1US	sheet	1093	6.2	545	Huntington
110	XX00A1US	sheet	1093	8.3	272	Huntington
111	XX00A1US	sheet	1093	10.3	80	Huntington
112	XX00A2US	rod	871	48.3	100	Huntington
113	XX00A2US	rod	982	20.7	218	Huntington
114	XX00A2US	rod	982	24.1	97	Huntington
115	XX00A2US	rod	1093	10.3	154	Huntington
116	XX00A4US	rod	650	275.8	7,200	Huntington
117	XX00A4US	rod	650	310.3	2,860	Huntington
118	XX00A4US	rod	760	110.3	2,800	Huntington
119	XX00A4US	rod	760	117.2	4,100	Huntington
120	XX00A4US	rod	760	137.9	162	Huntington
121	XX00A4US	rod	760	137.9	30	Huntington
122	XX00A4US	rod	871	24.8	26,600	Huntington
123	XX00A4US	rod	871	44.8	3,250	Huntington
124	XX00A4US	rod	871	44.8	1,100	Huntington
125	XX00A4US	rod	871	51.7	477	Huntington
126	XX00A4US	rod	871	69.0	100	Huntington
127	XX00A4US	rod	871	69.0	30	Huntington
128	XX00A4US	rod	982	12.4	3,050	Huntington
129	XX00A4US	rod	982	17.2	1,300	Huntington
130	XX00A4US	rod	1000	20.0	331	Huntington
131	XX00A4US	rod	1000	27.6	263	Huntington
132	XX00A5US	rod	593	324.1	3,160	Huntington
133	XX00A5US	rod	760	62.1	35,600	Huntington
134	XX00A5US	rod	760	75.8	3,950	Huntington
135	XX00A5US	rod	760	96.5	350	Huntington
136	XX00A5US	rod	760	96.5	110	Huntington
137	XX00A5US	rod	760	131.0	36	Huntington
138	XX00A5US	rod	871	27.6	3,700	Huntington
139	XX00A5US	rod	871	37.9	471	Huntington
140	XX00A5US	rod	871	48.3	137	Huntington
141	XX00A5US	rod	871	69.0	14	Huntington
142	XX00A5US	rod	982	17.2	540	Huntington
143	XX00A5US	rod	982	27.6	49	Huntington
144	XX05A4UK	rod	704	206.9	2,070	Huntington
145	XX05A4UK	rod	704	241.3	1,080	Huntington
146	XX05A4UK	rod	760	103.4	446	Huntington
147	XX05A4UK	rod	760	137.9	40	Huntington
148	XX05A4UK	rod	816	55.2	310	Huntington
149	XX05A4UK	rod	816	69.0	65	Huntington
150	XX05A4UK	rod	816	82.7	20	Huntington
151	XX05A4UK	rod	871	41.4	369	Huntington
152	XX05A4UK	rod	871	69.0	13	Huntington
153	XX05A4UK	rod	982	20.7	1,060	Huntington
154	XX05A4UK	rod	982	27.6	105	Huntington
155	XX05A4UK	rod	1000	20.7	543	Huntington

	Heat/Lot ID	Product Form	Temperature (°C)	Stress (MPa)	Time to 1% Strain (hrs)	Source
156	XX05A4UK	rod	1093	6.9	817	Huntington
157	XX05A7UK	tube	760	137.9	30	Huntington
158	XX05A7UK	tube	871	27.6	1,700	Huntington
159	XX05A7UK	tube	871	37.9	242	Huntington
160	XX05A7UK	tube	871	51.7	30	Huntington
161	XX05A7UK	tube	982	17.2	309	Huntington
162	XX05A7UK	tube	982	24.1	63	Huntington
163	XX05A7UK	tube	1000	17.2	182	Huntington
164	XX07A7UK	rod	650	241.3	24,500	Huntington
165	XX07A7UK	rod	650	310.3	1,450	Huntington
166	XX07A7UK	rod	704	172.4	4,400	Huntington
167	XX07A7UK	rod	704	206.9	2,180	Huntington
168	XX07A7UK	rod	704	241.3	990	Huntington
169	XX07A7UK	rod	760	103.4	3,420	Huntington
170	XX07A7UK	rod	760	137.9	928	Huntington
171	XX07A7UK	rod	816	82.7	30	Huntington
172	XX07A7UK	rod	871	27.6	3,280	Huntington
173	XX07A7UK	rod	871	41.4	1,300	Huntington
174	XX07A7UK	rod	982	27.6	175	Huntington
175	XX07A7UK	rod	1093	6.9	425	Huntington
176	XX07A7UK	rod	1093	10.3	183	Huntington
177	XX10A3UK	tube	650	344.8	480	Huntington
178	XX10A3UK	tube	760	137.9	630	Huntington
179	XX10A3UK	tube	982	20.7	1,170	Huntington
180	XX10A3UK	tube	1093	10.3	125	Huntington
181	XX20A5UK	sheet	650	241.3	8,400	Huntington
182	XX20A5UK	sheet	704	179.3	185	Huntington
183	XX20A5UK	sheet	760	110.3	160	Huntington
184	XX20A5UK	sheet	760	137.9	45	Huntington
185	XX20A5UK	sheet	871	48.3	1,820	Huntington
186	XX20A5UK	sheet	927	34.5	1,240	Huntington
187	XX41A7UK	sheet	982	27.6	75	Huntington
188	Haynes	plate	800	60.0	4,384	KAERI
189	Haynes	plate	800	70.0	1,800	KAERI
190	Haynes	plate	800	70.0	1,404	KAERI
191	Haynes	plate	800	80.0	255	KAERI
192	Haynes	plate	800	90.0	179	KAERI
193	Haynes	plate	800	100.0	32	KAERI
194	Haynes	plate	800	120.0	18	KAERI
195	93351	plate	850	30.0	2,826	KAERI
196	93351	plate	850	35.0	1,878	KAERI
197	93351	plate	850	40.0	193	KAERI
198	93351	plate	850	45.0	157	KAERI
199	93351	plate	850	50.0	58	KAERI
200	93351	plate	850	60.0	18	KAERI
201	93351	plate	850	70.3	10	KAERI
202	93351	plate	900	25.0	1,216	KAERI
203	93351	plate	900	28.0	345	KAERI
204	93351	plate	900	30.0	229	KAERI
205	93351	plate	900	35.0	161	KAERI
206	93351	plate	900	40.0	64	KAERI
207	93351	plate	900	45.0	32	KAERI
208	93351	plate	900	50.0	12	KAERI

	Heat/Lot ID	Product Form	Temperature (°C)	Stress (MPa)	Time to 1% Strain (hrs)	Source
209	93351	plate	950	18.0	879	KAERI
210	93351	plate	950	20.0	652	KAERI
211	93351	plate	950	22.0	248	KAERI
212	93351	plate	950	25.0	66	KAERI
213	93351	plate	950	30.0	31	KAERI
214	93351	plate	950	35.0	14	KAERI
215	XX01A3US	plate	593	413.7	20	ORNL
216	XX01A3US	plate	650	275.8	8,850	ORNL
217	XX01A3US	plate	760	102.7	125	ORNL
218	XX01A3US	plate	760	137.9	10	ORNL
219	XX01A3US	plate	871	35.0	3,100	ORNL
220	XX01A3US	plate	871	48.0	240	ORNL

Page intentionally left blank

Appendix III

Data Compilation of Time to Onset of Tertiary Creep for Alloy 617

	Heat/Lot ID	Product Form	Temperature (°C)	Stress (MPa)	Time to Tertiary (hrs)	Source
1	314626	plate	750	95.0	1,805	ANL
2	314626	plate	750	118.0	921	ANL
3	314626	plate	750	118.0	1,163	ANL
4	314626	plate	750	135.1	504	ANL
5	314626	plate	750	137.8	632	ANL
6	314626	plate	850	43.0	2,253	ANL
7	314626	plate	850	54.0	593	ANL
8	314626	plate	850	63.0	92	ANL
9	314626	plate	850	63.1	33	ANL
10	314626	plate	950	18.5	1,718	ANL
11	314626	plate	950	24.1	430	ANL
12	314626	plate	950	28.6	360	ANL
13	314626	plate	950	28.6	696	ANL
14	314626	plate	750	121.0	1,233	INL
15	314626	plate	750	121.0	1,326	INL
16	314626	plate	750	121.0	1,555	INL
17	314626	plate	750	121.0	1,402	INL
18	314626	plate	750	121.0	1,413	INL
19	314626	plate	750	145.0	603	INL
20	314626	plate	750	145.0	520	INL
21	314626	plate	750	145.0	598	INL
22	314626	plate	750	145.0	575	INL
23	314626	plate	750	161.5	346	INL
24	314626	plate	800	60.0	4,736	INL
25	314626	plate	800	60.0	7,506	INL
26	314626	plate	800	65.0	2,928	INL
27	314626	plate	800	65.0	3,069	INL
28	314626	plate	800	70.0	1,932	INL
29	314626	plate	800	70.0	1,673	INL
30	314626	plate	800	80.0	676	INL
31	314626	plate	800	80.0	615	INL
32	314626	plate	850	27.5	15,058	INL
33	314626	plate	900	26.0	3,470	INL
34	314626	plate	900	26.0	4,210	INL
35	314626	plate	900	28.0	2,153	INL
36	314626	plate	900	28.0	2,694	INL
37	314626	plate	900	31.0	1,839	INL
38	314626	plate	900	31.0	2,145	INL
39	314626	plate	900	36.0	964	INL
40	314626	plate	900	36.0	832	INL
41	314626	plate	900	44.7	336	INL
42	314626	plate	900	59.6	52	INL
43	314626	plate	900	74.5	13	INL
44	314626	plate	950	12.0	3,829	INL
45	314626	plate	1000	13.0	1,099	INL
46	314626	plate	1000	13.0	1,957	INL
47	314626	plate	1000	16.0	1,101	INL
48	314626	plate	1000	16.0	1,203	INL
49	314626	plate	1000	16.0	1,094	INL

	Heat/Lot ID	Product Form	Temperature (°C)	Stress (MPa)	Time to Tertiary (hrs)	Source
50	314626	plate	1000	16.0	1,014	INL
51	314626	plate	1000	20.0	506	INL
52	314626	plate	1000	28.0	159	INL
53	314626	plate	1000	41.0	21	INL
54	XX14A6UK	plate	850	79.3	260	GE
55	XX14A6UK	plate	1050	10.7	2,140	GE
56	XX63A8UK	plate	850	44.8	4,400	GE
57	XX63A8UK	plate	850	48.3	2,540	GE
58	XX63A8UK	plate	850	56.6	1,150	GE
59	XX63A8UK	plate	850	66.2	358	GE
60	XX63A8UK	plate	850	75.8	110	GE
61	XX63A8UK	plate	950	31.0	788	GE
62	XX00A1US	rod	650	310.3	1,080	Huntington
63	XX00A1US	rod	760	137.9	340	Huntington
64	XX00A1US	rod	816	89.6	1,250	Huntington
65	XX00A1US	rod	816	117.2	120	Huntington
66	XX00A1US	rod	816	165.5	25	Huntington
67	XX00A1US	rod	871	62.1	1,440	Huntington
68	XX00A1US	rod	871	96.5	48	Huntington
69	XX00A1US	rod	927	41.4	1,220	Huntington
70	XX00A1US	rod	982	20.7	1,760	Huntington
71	XX00A1US	rod	982	20.7	379	Huntington
72	XX00A1US	rod	982	27.6	1,040	Huntington
73	XX00A1US	sheet	982	20.7	260	Huntington
74	XX00A1US	sheet	982	27.6	118	Huntington
75	XX00A1US	rod	1038	16.5	735	Huntington
76	XX00A1US	rod	1038	27.6	115	Huntington
77	XX00A1US	rod	1093	8.3	305	Huntington
78	XX00A1US	rod	1093	8.3	1,460	Huntington
79	XX00A1US	rod	1093	10.3	137	Huntington
80	XX00A1US	rod	1093	12.4	525	Huntington
81	XX00A2US	rod	982	20.7	246	Huntington
82	XX00A2US	rod	982	24.1	120	Huntington
83	XX00A2US	rod	1093	10.3	124	Huntington
84	XX00A4US	rod	593	344.8	26,800	Huntington
85	XX00A4US	rod	593	413.7	2,610	Huntington
86	XX00A4US	rod	593	537.8	63	Huntington
87	XX00A4US	rod	650	310.3	5,500	Huntington
88	XX00A4US	rod	760	110.3	2,450	Huntington
89	XX00A4US	rod	760	117.2	3,100	Huntington
90	XX00A4US	rod	760	137.9	365	Huntington
91	XX00A4US	rod	760	137.9	1,920	Huntington
92	XX00A4US	rod	871	24.8	22,500	Huntington
93	XX00A4US	rod	871	44.8	2,950	Huntington
94	XX00A4US	rod	871	44.8	1,900	Huntington
95	XX00A4US	rod	871	51.7	535	Huntington
96	XX00A4US	rod	871	69.0	320	Huntington
97	XX00A4US	rod	871	69.0	785	Huntington
98	XX00A4US	rod	982	17.2	1,450	Huntington
99	XX00A4US	rod	1000	20.0	640	Huntington
100	XX00A4US	rod	1000	27.6	240	Huntington
101	XX00A5US	rod	593	324.1	21,000	Huntington
102	XX00A5US	rod	593	386.1	3,800	Huntington

	Heat/Lot ID	Product Form	Temperature (°C)	Stress (MPa)	Time to Tertiary (hrs)	Source
103	XX00A5US	rod	593	448.2	615	Huntington
104	XX00A5US	rod	593	517.1	140	Huntington
105	XX00A5US	rod	650	275.8	9,600	Huntington
106	XX00A5US	rod	650	310.3	2,680	Huntington
107	XX00A5US	rod	650	379.2	240	Huntington
108	XX00A5US	rod	760	96.5	13,000	Huntington
109	XX00A5US	rod	760	131.0	3,000	Huntington
110	XX00A5US	rod	871	37.9	10,100	Huntington
111	XX00A5US	rod	871	48.3	1,290	Huntington
112	XX00A5US	rod	871	69.0	375	Huntington
113	XX00A5US	rod	982	27.6	600	Huntington
114	XX05A4UK	rod	650	275.8	2,300	Huntington
115	XX05A4UK	rod	650	310.3	995	Huntington
116	XX05A4UK	rod	704	206.9	2,200	Huntington
117	XX05A4UK	rod	704	241.3	1,160	Huntington
118	XX05A4UK	rod	760	103.4	2,130	Huntington
119	XX05A4UK	rod	760	137.9	595	Huntington
120	XX05A4UK	rod	816	55.2	10,800	Huntington
121	XX05A4UK	rod	816	69.0	1,070	Huntington
122	XX05A4UK	rod	816	82.7	425	Huntington
123	XX05A4UK	rod	871	41.4	6,480	Huntington
124	XX05A4UK	rod	871	69.0	30	Huntington
125	XX05A4UK	rod	982	20.7	640	Huntington
126	XX05A4UK	rod	982	27.6	265	Huntington
127	XX05A4UK	rod	1000	20.7	400	Huntington
128	XX05A7UK	tube	760	137.9	475	Huntington
129	XX05A7UK	tube	871	37.9	4,240	Huntington
130	XX05A7UK	tube	871	51.7	575	Huntington
131	XX05A7UK	tube	982	24.1	560	Huntington
132	XX05A7UK	tube	1000	17.2	217	Huntington
133	XX07A7UK	rod	650	241.3	24,200	Huntington
134	XX07A7UK	rod	650	275.8	8,560	Huntington
135	XX07A7UK	rod	650	310.3	4,190	Huntington
136	XX07A7UK	rod	704	172.4	12,800	Huntington
137	XX07A7UK	rod	704	206.9	2,950	Huntington
138	XX07A7UK	rod	704	241.3	1,350	Huntington
139	XX07A7UK	rod	760	103.4	3,100	Huntington
140	XX07A7UK	rod	760	137.9	825	Huntington
141	XX07A7UK	rod	816	82.7	330	Huntington
142	XX07A7UK	rod	816	96.5	190	Huntington
143	XX07A7UK	rod	816	124.1	34	Huntington
144	XX07A7UK	rod	871	27.6	2,880	Huntington
145	XX07A7UK	rod	871	41.4	1,140	Huntington
146	XX07A7UK	rod	871	69.0	39	Huntington
147	XX07A7UK	rod	982	27.6	160	Huntington
148	XX07A7UK	rod	1093	10.3	140	Huntington
149	XX10A3UK	tube	650	344.8	855	Huntington
150	XX10A3UK	tube	760	137.9	590	Huntington
151	XX10A3UK	tube	982	20.7	1,100	Huntington
152	XX10A3UK	tube	1093	10.3	500	Huntington
153	XX20A5UK	sheet	650	241.3	8,400	Huntington
154	XX20A5UK	sheet	650	289.6	500	Huntington
155	XX20A5UK	sheet	650	344.8	143	Huntington

	Heat/Lot ID	Product Form	Temperature (°C)	Stress (MPa)	Time to Tertiary (hrs)	Source
156	XX20A5UK	sheet	704	179.3	1,320	Huntington
157	XX20A5UK	sheet	760	110.3	520	Huntington
158	XX20A5UK	sheet	760	137.9	54	Huntington
159	XX20A5UK	sheet	871	48.3	1,430	Huntington
160	XX20A5UK	sheet	927	34.5	1,040	Huntington
161	XX41A7UK	sheet	650	275.8	1,070	Huntington
162	Haynes	plate	800	60.0	2,951	KAERI
163	Haynes	plate	800	70.0	1,726	KAERI
164	Haynes	plate	800	70.0	1,065	KAERI
165	Haynes	plate	800	80.0	401	KAERI
166	Haynes	plate	800	90.0	211	KAERI
167	Haynes	plate	800	90.0	224	KAERI
168	Haynes	plate	800	100.0	122	KAERI
169	Haynes	plate	800	120.0	91	KAERI
170	93351	plate	850	50.0	153	KAERI
171	93351	plate	850	60.0	58	KAERI
172	93351	plate	900	28.0	549	KAERI
173	93351	plate	900	30.0	218	KAERI
174	93351	plate	900	35.0	169	KAERI
175	93351	plate	950	18.0	3,744	KAERI
176	93351	plate	950	22.0	273	KAERI
177	XX01A3US	plate	593	413.7	3,450	ORNL
178	XX01A3US	plate	650	275.8	16,000	ORNL
179	XX01A3US	plate	760	102.7	17,000	ORNL
180	XX01A3US	plate	760	137.9	780	ORNL
181	XX01A3US	plate	871	35.0	23,200	ORNL
182	XX01A3US	plate	871	48.0	2,400	ORNL
183	XX01A3US	plate	871	69.0	212	ORNL

Appendix IV

Data Compilation of Creep-Rupture Tests for Alloy 617

	Heat/Lot ID	Product Form	Temperature (°C)	Stress (MPa)	Rupture Life (hrs)	Creep Strain (%)	Source
1	314626	plate	800	60.0	6,949	34.4	INL
2	314626	plate	800	60.0	11,045	33.3	INL
3	314626	plate	800	65.0	4,896	41.3	INL
4	314626	plate	800	65.0	4,404	41.3	INL
5	314626	plate	800	70.0	2,738	45.2	INL
6	314626	plate	800	70.0	2,751	48.6	INL
7	314626	plate	800	80.0	1,208	53.7	INL
8	314626	plate	800	80.0	1,138	54.4	INL
9	314626	plate	900	26.0	7,567	36.4	INL
10	314626	plate	900	26.0	7,983	28.7	INL
11	314626	plate	900	28.0	3,788	24.6	INL
12	314626	plate	900	28.0	4,731	33.7	INL
13	314626	plate	900	31.0	2,960	31.1	INL
14	314626	plate	900	31.0	2,846	21.1	INL
15	314626	plate	900	36.0	1,372	29.0	INL
16	314626	plate	900	36.0	1,380	32.9	INL
17	314626	plate	1000	16.0	3,034	48.3	INL
18	314626	plate	1000	16.0	3,367	49.1	INL
19	314626	plate	1000	13.0	8,768	54.8	INL
20	314626	plate	1000	13.0	9,998	56.7	INL
21	314626	plate	1000	12.0	14,506	62.7	INL
22	314626	plate	1000	12.0	16,696	64.9	INL
23	314626	plate	1000	11.0	18,923	57.5	INL
24	314626	plate	1000	11.0	21,303	51.8	INL
25	Haynes	plate	800	120.0	369	67.9	KAERI
26	Haynes	plate	800	100.0	830	71.8	KAERI
27	Haynes	plate	800	90.0	1,694	48.1	KAERI
28	Haynes	plate	800	90.0	1,996	51.8	KAERI
29	Haynes	plate	800	80.0	3,508	46.6	KAERI
30	Haynes	plate	800	70.0	6,801	53.2	KAERI
31	Haynes	plate	800	70.0	9,857	46.5	KAERI
32	Haynes	plate	800	60.0	16,777	35.8	KAERI
33	93351	plate	850	30.0	14,900	47.2	KAERI
34	93351	plate	850	35.0	11,700	31.7	KAERI
35	93351	plate	850	40.0	5,530	43.5	KAERI
36	93351	plate	850	45.0	3,080	43.6	KAERI
37	93351	plate	850	50.0	1,490	46.5	KAERI
38	93351	plate	850	60.0	534	70.0	KAERI
39	93351	plate	850	70.3	237	74.7	KAERI
40	93351	plate	900	25.0	12,700	48.2	KAERI
41	93351	plate	900	28.0	4,620	41.2	KAERI
42	93351	plate	900	30.0	1,510	27.0	KAERI
43	93351	plate	900	35.0	1,370	31.9	KAERI
44	93351	plate	900	40.0	1,060	34.4	KAERI
45	93351	plate	900	45.0	660	43.8	KAERI
46	93351	plate	900	50.0	314	44.4	KAERI
47	93351	plate	950	18.0	14,100	28.0	KAERI
48	93351	plate	950	20.0	4,940	19.5	KAERI
49	93351	plate	950	22.0	1,950	40.5	KAERI
50	93351	plate	950	25.0	888	24.3	KAERI

	Heat/Lot ID	Product Form	Temperature (°C)	Stress (MPa)	Rupture Life (hrs)	Creep Strain (%)	Source
51	93351	plate	950	30.0	465	22.3	KAERI
52	93351	plate	950	35.0	218	46.0	KAERI
53	314626	plate	750	137.8	1,470	27.0	ANL
54	314626	plate	750	118.0	3,345	21.3	ANL
55	314626	plate	850	63.1	275	46.0	ANL
56	314626	plate	850	63.0	261	52.3	ANL
57	314626	plate	850	54.1	394	41.5	ANL
58	314626	plate	850	54.0	826	45.2	ANL
59	314626	plate	850	43.1	1,115	38.7	ANL
60	314626	plate	850	43.0	3,105	31.0	ANL
61	314626	plate	950	28.6	562	32.3	ANL
62	314626	plate	950	28.6	893	30.3	ANL
63	314626	plate	950	24.1	957	56.9	ANL
64	SMC	bar	850	80.0	396	49	CEA
65	SMC	bar	850	80.0	398	60	CEA
66	SMC	bar	850	70.0	1,139	59	CEA
67	SMC	bar	850	55.0	6,677	33	CEA
68	SMC	bar	950	30.0	3,946	34	CEA
69	XX00A4US	rod	593	537.8	98	45.5	Huntington
70	XX00A4US	rod	593	413.7	2,670	13.2	Huntington
71	XX00A4US	rod	593	344.8	28,700	5.5	Huntington
72	XX00A5US	rod	593	517.1	148	42.0	Huntington
73	XX00A5US	rod	593	448.2	639	29.2	Huntington
74	XX00A5US	rod	593	386.1	3,810	20.0	Huntington
75	XX00A5US	rod	593	324.1	21,400	8.9	Huntington
76	XX20A5UK	sheet	650	344.8	159	13.8	Huntington
77	XX20A5UK	sheet	650	289.6	520	6.3	Huntington
78	XX20A5UK	sheet	650	241.3	8,410	1.5	Huntington
79	XX41A7UK	sheet	650	275.8	1,770	5.0	Huntington
80	XX10A3UK	tube	650	344.8	887	2.6	Huntington
81	XX00A1US	rod	650	413.7	149	31.0	Huntington
82	XX00A1US	rod	650	310.3	1,090	11.5	Huntington
83	XX00A4US	rod	650	310.3	6,150	1.9	Huntington
84	XX00A5US	rod	650	379.2	265	18.7	Huntington
85	XX00A5US	rod	650	310.3	2,780	10.0	Huntington
86	XX00A5US	rod	650	275.8	9,700	6.7	Huntington
87	XX05A4UK	rod	650	310.3	1,030	8.3	Huntington
88	XX05A4UK	rod	650	275.8	2,300	6.9	Huntington
89	XX07A7UK	rod	650	310.3	4,200	2.7	Huntington
90	XX07A7UK	rod	650	275.8	8,560	0.6	Huntington
91	XX07A7UK	rod	650	241.3	24,500	1.0	Huntington
92	XX20A5UK	sheet	704	179.3	2,280	8.9	Huntington
93	XX05A4UK	rod	704	310.3	218	7.3	Huntington
94	XX05A4UK	rod	704	241.3	2,110	4.6	Huntington
95	XX05A4UK	rod	704	206.9	4,990	6.9	Huntington
96	XX07A7UK	rod	704	241.3	1,610	4.6	Huntington
97	XX07A7UK	rod	704	206.9	5,180	5.3	Huntington
98	XX07A7UK	rod	704	172.4	20,000	9.7	Huntington
99	XX05A7UK	tube	760	137.9	651	22.7	Huntington
100	XX20A5UK	sheet	760	137.9	450	43.9	Huntington
101	XX20A5UK	sheet	760	110.3	2,110	43.4	Huntington
102	XX10A3UK	tube	760	137.9	1,430	15.8	Huntington
103	XX00A1US	rod	760	255.1	40	54.0	Huntington
104	XX00A1US	rod	760	206.9	124	98.5	Huntington

	Heat/Lot ID	Product Form	Temperature (°C)	Stress (MPa)	Rupture Life (hrs)	Creep Strain (%)	Source
105	XX00A1US	rod	760	172.4	321	84.0	Huntington
106	XX00A1US	rod	760	137.9	425	38.2	Huntington
107	XX00A4US	rod	760	137.9	2,580	46.2	Huntington
108	XX00A4US	rod	760	137.9	2,020	20.0	Huntington
109	XX00A4US	rod	760	117.2	18,200	38.5	Huntington
110	XX00A5US	rod	760	131.0	3,750	27.3	Huntington
111	XX00A5US	rod	760	96.5	40,100	23.5	Huntington
112	XX05A4UK	rod	760	137.9	1,100	23.3	Huntington
113	XX05A4UK	rod	760	103.4	9,880	38.3	Huntington
114	XX07A7UK	rod	760	137.9	2,470	27.1	Huntington
115	XX07A7UK	rod	760	103.4	10,200	28.1	Huntington
116	XX00A1US	sheet	816	165.5	31	102	Huntington
117	XX00A1US	sheet	816	165.5	45	107	Huntington
118	XX00A3US	shapes	816	165.5	46	92	Huntington
119	XX00A3US	shapes	816	165.5	67	94	Huntington
120	XX00A3US	shapes	816	165.5	41	100	Huntington
121	XX00A3US	shapes	816	165.5	41	106	Huntington
122	XX00A3US	shapes	816	165.5	72	89	Huntington
123	XX00A3US	shapes	816	165.5	31	87	Huntington
124	XX00A3US	plate	816	165.5	73	101	Huntington
125	XX00A3US	plate	816	165.5	33	83	Huntington
126	XX00A3US	plate	816	165.5	89	98	Huntington
127	XX00A3US	plate	816	165.5	72	97	Huntington
128	XX00A1US	rod	816	165.5	93	91	Huntington
129	XX00A1US	rod	816	117.2	217	101	Huntington
130	XX00A1US	rod	816	89.6	2,150	52.5	Huntington
131	XX00A2US	rod	816	165.5	65	86	Huntington
132	XX00A2US	rod	816	165.5	65	110	Huntington
133	XX05A4UK	rod	816	82.7	1,150	54.6	Huntington
134	XX05A4UK	rod	816	69.0	2,500	37.9	Huntington
135	XX05A4UK	rod	816	55.2	19,100	33.8	Huntington
136	XX07A7UK	rod	816	124.1	46	51.2	Huntington
137	XX07A7UK	rod	816	96.5	293	47.4	Huntington
138	XX07A7UK	rod	816	82.7	777	43.2	Huntington
139	XX05A7UK	tube	871	96.5	43	62.5	Huntington
140	XX05A7UK	tube	871	51.7	657	31.5	Huntington
141	XX05A7UK	tube	871	37.9	5,750	25.9	Huntington
142	XX00A1US	sheet	871	96.5	66	68	Huntington
143	XX00A1US	sheet	871	96.5	61	72	Huntington
144	XX00A5US	sheet	871	96.5	77	35	Huntington
145	XX18A4UK	sheet	871	96.5	36	82	Huntington
146	XX20A5UK	sheet	871	96.5	54	44	Huntington
147	XX20A5UK	sheet	871	89.6	111	51.6	Huntington
148	XX20A5UK	sheet	871	48.3	6,800	69.2	Huntington
149	XX10A3UK	tube	871	96.5	237	40.6	Huntington
150	XX10A3UK	tube	871	89.6	293	42.9	Huntington
151	XX00A3US	shapes	871	96.5	95	78	Huntington
152	XX00A3US	shapes	871	96.5	54	128	Huntington
153	XX00A3US	shapes	871	96.5	68	115	Huntington
154	XX00A3US	shapes	871	96.5	48	100	Huntington
155	XX00A3US	shapes	871	96.5	91	98	Huntington
156	XX00A3US	shapes	871	96.5	52	104	Huntington
157	XX00A3US	plate	871	96.5	70	84	Huntington
158	XX00A3US	plate	871	96.5	26	86	Huntington

	Heat/Lot ID	Product Form	Temperature (°C)	Stress (MPa)	Rupture Life (hrs)	Creep Strain (%)	Source
159	XX00A3US	plate	871	96.5	78	99	Huntington
160	XX00A3US	plate	871	96.5	75	102	Huntington
161	XX00A1US	rod	871	117.2	67	85	Huntington
162	XX00A1US	rod	871	96.5	101	120	Huntington
163	XX00A1US	rod	871	82.7	234	69.5	Huntington
164	XX00A1US	rod	871	62.1	1,930	45.5	Huntington
165	XX00A2US	rod	871	96.5	111	70.0	Huntington
166	XX00A2US	rod	871	96.5	74	83.1	Huntington
167	XX00A4US	rod	871	82.7	212	60.8	Huntington
168	XX00A4US	rod	871	69.0	1,040	30.3	Huntington
169	XX00A4US	rod	871	69.0	993	29.9	Huntington
170	XX00A4US	rod	871	51.7	2,460	15.5	Huntington
171	XX00A4US	rod	871	44.8	9,670	15.7	Huntington
172	XX00A4US	rod	871	44.8	16,500	17.4	Huntington
173	XX00A5US	rod	871	69.0	545	26.2	Huntington
174	XX00A5US	rod	871	48.3	3,560	25.4	Huntington
175	XX00A5US	rod	871	37.9	15,200	37.5	Huntington
176	XX05A4UK	rod	871	96.5	39	82.7	Huntington
177	XX05A4UK	rod	871	69.0	280	57.8	Huntington
178	XX05A4UK	rod	871	41.4	7,010	43.1	Huntington
179	XX07A7UK	rod	871	96.5	29	42.7	Huntington
180	XX07A7UK	rod	871	69.0	167	46.5	Huntington
181	XX07A7UK	rod	871	41.4	5,390	45.0	Huntington
182	XX07A7UK	rod	871	27.6	11,000	25.0	Huntington
183	XX20A5UK	sheet	927	34.5	2,040	4.8	Huntington
184	XX10A3UK	tube	927	34.5	100	0.1	Huntington
185	XX00A1US	rod	927	89.6	13	80.5	Huntington
186	XX00A1US	rod	927	75.8	35	67.0	Huntington
187	XX00A1US	rod	927	41.4	1,590	40.0	Huntington
188	XX05A7UK	tube	982	24.1	714	23.8	Huntington
189	XX05A7UK	tube	982	17.2	3,160	34.3	Huntington
190	XX41A7UK	sheet	982	27.6	493	25.1	Huntington
191	XX10A3UK	tube	982	20.7	2,520	8.8	Huntington
192	XX00A1US	rod	982	48.3	48	74.0	Huntington
193	XX00A1US	rod	982	34.5	225	47.5	Huntington
194	XX00A1US	rod	982	27.6	1,230	50.0	Huntington
195	XX00A1US	rod	982	20.7	3,330	41.5	Huntington
196	XX00A4US	rod	982	17.2	4,790	17.3	Huntington
197	XX00A5US	rod	982	27.6	868	33.3	Huntington
198	XX00A5US	rod	982	17.2	4,560	22.5	Huntington
199	XX05A4UK	rod	982	27.6	1,090	32.5	Huntington
200	XX05A4UK	rod	982	20.7	4,050	27.4	Huntington
201	XX07A7UK	rod	982	27.6	545	15.8	Huntington
202	XX05A7UK	tube	1000	34.5	157	37.4	Huntington
203	XX05A7UK	tube	1000	17.2	1,340	18.8	Huntington
204	XX00A2US	rod	1000	34.5	104	58.4	Huntington
205	XX00A2US	rod	1000	34.5	137	53.2	Huntington
206	XX00A2US	rod	1000	31.0	353	42.2	Huntington
207	XX00A4US	rod	1000	27.6	750	31.1	Huntington
208	XX00A5US	rod	1000	27.6	445	38.0	Huntington
209	XX00A5US	rod	1000	27.6	60	31.4	Huntington
210	XX05A4UK	rod	1000	34.5	157	37.6	Huntington
211	XX05A4UK	rod	1000	20.7	1,980	23.6	Huntington
212	XX07A7UK	rod	1000	34.5	95	19.3	Huntington

	Heat/Lot ID	Product Form	Temperature (°C)	Stress (MPa)	Rupture Life (hrs)	Creep Strain (%)	Source
213	XX00A1US	rod	1038	13.8	2,620	41.0	Huntington
214	XX00A1US	rod	1038	16.5	1,170	26.5	Huntington
215	XX00A1US	rod	1038	24.8	242	44.3	Huntington
216	XX00A1US	rod	1038	27.6	157	54.2	Huntington
217	XX00A1US	rod	1038	41.4	20	66.0	Huntington
218	XX00A1US	sheet	1093	20.7	41	40	Huntington
219	XX00A1US	sheet	1093	20.7	49	42	Huntington
220	XX00A5US	sheet	1093	20.7	48	18.5	Huntington
221	XX10A3UK	tube	1093	10.3	1,120	40	Huntington
222	XX00A3US	shapes	1093	20.7	80	32	Huntington
223	XX00A3US	shapes	1093	20.7	71	113	Huntington
224	XX00A3US	shapes	1093	20.7	67	114	Huntington
225	XX00A3US	shapes	1093	20.7	98	NA	Huntington
226	XX00A3US	shapes	1093	20.7	27	74	Huntington
227	XX00A3US	shapes	1093	20.7	46	56	Huntington
228	XX00A3US	plate	1093	20.7	99	43	Huntington
229	XX00A3US	plate	1093	20.7	106	50	Huntington
230	XX00A3US	plate	1093	20.7	84	72	Huntington
231	XX00A3US	plate	1093	20.7	78	42	Huntington
232	XX00A2US	rod	1093	10.3	865	44.8	Huntington
233	XX07A7UK	rod	1093	10.3	530	20.4	Huntington
234	XX00A1US	rod	1093	12.4	835	41.5	Huntington
235	XX00A1US	rod	1093	17.2	101	102	Huntington
236	XX00A1US	rod	1093	20.7	31	87.5	Huntington
237	XX00A2US	rod	1093	20.7	83	84	Huntington
238	XX00A2US	rod	1093	20.7	75	70	Huntington
239	XX00A2US	rod	1093	6.2	5,320	57.0	Huntington
240	XX05A4UK	rod	1093	6.9	5,100	39.5	Huntington
241	XX07A7UK	rod	1093	6.9	2,770	40.2	Huntington
242	XX14A6UK	plate	704	200.0	625	19.6	GE
243	XX14A6UK	plate	850	56.6	12,200	43.1	GE
244	XX63A8UK	plate	850	56.6	2,300	66.8	GE
245	XX63A8UK	plate	850	66.2	791	42.1	GE
246	XX14A6UK	plate	850	72.4	1,130	58.3	GE
247	XX63A8UK	plate	850	75.8	326	78.1	GE
248	XX63A8UK	plate	850	44.8	7,720	41.7	GE
249	XX63A8UK	plate	850	48.3	4,820	40.3	GE
250	XX14A6UK	plate	850	64.8	1,050	68.7	GE
251	XX14A6UK	plate	850	79.3	596	56.7	GE
252	XX63A8UK	plate	850	96.5	86	81.2	GE
253	XX63A8UK	plate	950	20.7	5,020	36.4	GE
254	XX63A8UK	plate	950	24.1	2,390	40.5	GE
255	XX63A8UK	plate	950	31.0	1,280	41.4	GE
256	XX63A8UK	plate	950	31.0	1,110	31.5	GE
257	XX14A6UK	plate	950	37.9	723	34.9	GE
258	XX63A8UK	plate	950	37.9	282	38.8	GE
259	XX63A8UK	plate	950	44.8	140	55.4	GE
260	XX63A8UK	plate	950	55.2	51	56.0	GE
261	XX14A6UK	plate	950	48.3	334	46.9	GE
262	XX14A6UK	plate	1049	10.7	8,510	14.5	GE
263	XX14A6UK	plate	1049	14.5	9,290	33.0	GE
264	XX14A6UK	plate	1049	20.7	1,150	23.2	GE
265	XX14A6UK	plate	1100	15.2	723	34.9	GE
266	XX09A4UK	plate	593	344.8	2,110	3.4	ORNL

	Heat/Lot ID	Product Form	Temperature (°C)	Stress (MPa)	Rupture Life (hrs)	Creep Strain (%)	Source
267	XX01A3US	plate	593	413.7	3,570	6.9	ORNL
268	XX01A3US	plate	650	275.8	25,600	6.4	ORNL
269	XX09A4UK	plate	650	275.8	1,120	1.4	ORNL
270	XX09A4UK	plate	650	275.8	667	1.9	ORNL
271	XX09A4UK	plate	704	206.9	2,620	1.2	ORNL
272	XX01A3US	plate	760	102.7	20,700	28.0	ORNL
273	XX01A3US	plate	760	137.9	1,310	48.5	ORNL
274	XX01A3US	plate	871	35.0	34,200	30.3	ORNL
275	XX01A3US	plate	871	48.0	4,800	26.2	ORNL
276	XX01A3US	plate	871	69.0	576	45.1	ORNL
277	C	bar	800	81.6	6,358	NA	Cook
278	C	bar	800	69.7	8,859	NA	Cook
279	C	bar	800	75.8	10,121	NA	Cook
280	C	bar	800	64.8	13,308	NA	Cook
281	C	bar	850	56.0	3,022	NA	Cook
282	C	bar	850	52.0	3,465	NA	Cook
283	C	bar	850	47.2	7,230	NA	Cook
284	C	bar	850	44.7	8,613	NA	Cook
285	A	bar	850	42.5	13,183	NA	Cook
286	B	plate	850	44.5	16,282	NA	Cook
287	A	bar	850	36.6	32,134	NA	Cook
288	C	bar	900	40.8	1,253	NA	Cook
289	C	bar	900	37.7	2,992	NA	Cook
290	C	bar	900	35.4	4,670	NA	Cook
291	C	bar	900	32.8	4,589	NA	Cook
292	C	bar	950	24.9	1,760	NA	Cook
293	C	bar	950	23.0	2,856	NA	Cook
294	C	bar	950	21.4	3,896	NA	Cook
295	C	bar	950	19.8	5,741	NA	Cook
296	NIMS 1975	unknown	900	78.0	69	88	NIMS
297	NIMS 1975	unknown	900	64.7	217	72	NIMS
298	NIMS 1975	unknown	900	63.7	229	59	NIMS
299	NIMS 1975	unknown	900	63.7	245	61	NIMS
300	NIMS 1975	unknown	900	63.7	244	77	NIMS
301	NIMS 1975	unknown	900	49.0	1,248	42	NIMS
302	NIMS 1975	unknown	900	39.0	3,830	34	NIMS
303	NIMS 1975	unknown	1000	39.0	79	73	NIMS
304	XX01A3US	unknown	1000	33.3	170	55	NIMS
305	NIMS 1975	unknown	1000	27.5	526	36	NIMS
306	NIMS 1975	unknown	1000	27.5	499	38	NIMS
307	NIMS 1975	unknown	1000	27.5	529	40	NIMS
308	NIMS 1975	unknown	1000	27.5	538	36	NIMS
309	NIMS 1975	unknown	1000	27.5	495	38	NIMS
310	NIMS 1975	unknown	1000	22.6	1,254	32	NIMS
311	NIMS 1975	unknown	1000	21.6	1,544	32	NIMS
312	NIMS 1975	unknown	1000	18.6	3,533	27	NIMS
313	NIMS 1975	unknown	1000	15.7	6,125	27	NIMS
314	NIMS 1975	unknown	1000	15.7	6,451	22	NIMS
315	NIMS 1975	unknown	1000	11.8	17,091	30	NIMS
316	NIMS 1975	unknown	1000	11.8	16,448	32	NIMS
317	NIMS 1975	unknown	1050	29.0	73	68	NIMS
318	NIMS 1975	unknown	1050	24.5	172	47	NIMS
319	NIMS 1975	unknown	1050	17.7	876	35	NIMS
320	NIMS 1975	unknown	1050	12.7	2,940	33	NIMS

	Heat/Lot ID	Product Form	Temperature (°C)	Stress (MPa)	Rupture Life (hrs)	Creep Strain (%)	Source
321	NIMS 1975	unknown	1050	9.8	5,055	31	NIMS
322	NIMS 1975	unknown	1050	9.8	8,116	45	NIMS
323	XX0529UK14	plate	760	206.9	43	18	SMC
324	XX0529UK14	plate	760	206.9	37	18.2	SMC
325	XX0547UK11	plate	760	137.9	2,580	16.1	SMC
326	XX0547UK11	plate	760	206.9	110	9.9	SMC
327	XX0529UK14	plate	871	55.2	796	35.6	SMC
328	XX0529UK14	plate	871	82.7	64	34.2	SMC
329	XX0529UK14	plate	871	82.7	68	37.3	SMC
330	XX0547UK11	plate	871	55.2	796	35.6	SMC
331	XX0547UK11	plate	871	82.7	67	53.0	SMC
332	XX0529UK14	plate	982	41.4	96	20.6	SMC
333	XX0684UK21	plate	982	13.8	7,529	51	SMC
334	XX0684UK21	plate	982	20.7	1,674	41.2	SMC
335	XX0688UK11	plate	982	13.8	9,063	27	SMC
336	XX0688UK11	plate	982	20.7	1,735	30	SMC
337	XX0693UK17	plate	982	13.8	7,723	32	SMC
338	XX0693UK17	plate	982	20.7	1,113	17	SMC
339	XX0693UK17	plate	1038	11.0	1,887	21	SMC
340	XX0529UK14	plate	1093	13.8	229	29.2	SMC
341	XX0529UK14	plate	1093	27.6	16	25.9	SMC
342	XX0547UK11	plate	1093	13.8	558	19.0	SMC
343	XX0547UK11	plate	1093	27.6	25	22.6	SMC
344	XX0529UK14	plate	1149	6.9	611	35.5	SMC
345	XX0529UK14	plate	1149	13.8	39	28.2	SMC
346	XX0547UK11	plate	1149	13.8	91	24.7	SMC
347	XX0684UK21	plate	1093	10.3	474	43	SMC
348	XX0693UK17	plate	1093	10.3	561	31	SMC

NA – not available

Page intentionally left blank

Appendix V

Data Compilation for Creep Tests of Weldments Using Alloy 617 Weld Wire

Source	Weld Process[†]	Specimen Weld Orientation	Temp (°C)	Applied Weld Stress (MPa)	Rupture time (h)	L-M Parameter, Base Metal	Base Stress[*] (MPa)	SRF	Rupture Location
INL	GTAW	transverse	750	171.0	6,436	21014.3	105.8	1.616	Weld
INL	GTAW	transverse	900	26.0	9,298	24282.6	29.6	0.878	Weld
INL	GTAW	transverse	950	19.3	5948.4	25080.2	21.7	0.889	Weld
INL	GTAW	transverse	1000	16.0	1040.6	25141.6	21.2	0.755	Weld
INL	GTAW	transverse	1000	13.0	1982.8	25498.0	18.4	0.705	Weld
INL/ANL	GTAW	transverse	750	135.0	2794.9	20643.7	122.3	1.104	Base
INL/ANL	GTAW	transverse	750	135.0	2381.4	20572.5	125.7	1.074	Base
INL/ANL	GTAW	transverse	750	118.0	5953.4	20979.7	107.3	1.100	Base
INL/ANL	GTAW	transverse	850	61.3	1332.4	22300.0	64.1	0.956	Base
INL/ANL	GTAW	transverse	850	62.9	936.4	22128.0	68.6	0.917	Base
INL/ANL	GTAW	transverse	850	54.0	1648.6	22403.9	61.6	0.877	Base
INL/ANL	GTAW	transverse	850	54.0	2264.9	22558.8	58.0	0.931	Base
INL/ANL	GTAW	transverse	850	43.0	3226.3	22731.4	54.2	0.793	Base
INL/ANL	GTAW	transverse	850	43.0	6184.4	23048.8	47.9	0.898	Base
INL/ANL	GTAW	transverse	950	28.5	871.1	24059.7	32.3	0.882	Base
INL/ANL	GTAW	transverse	950	28.4	1569.3	24372.4	28.6	0.993	Base
INL/ANL	GTAW	transverse	950	24.1	2093.8	24525.6	26.9	0.895	Base
INL/ANL	GTAW	transverse	950	18.5	4484.5	24930.2	23.0	0.804	Weld
CEA	GTAW	transverse	850	80	480.5	21802.5	77.8	1.028	Base
CEA	GTAW	transverse	850	80	431	21749.5	79.5	1.007	Base
CEA	GTAW	transverse	850	70	855	22083.6	69.8	1.003	Base
CEA	GTAW	transverse	850	70	990	22155.1	67.9	1.032	Base
CEA	GTAW	transverse	850	68	984	22152.1	67.9	1.001	Base
CEA	GTAW	transverse	850	55	2560	22618.5	56.6	0.971	Base
CEA	GTAW	transverse	850	55	3338	22748.0	53.9	1.021	Base
VDM 617B	GTAW	transverse	700	171.0	9,500	20152.0	148.1	1.155	not reported
VDM 617B	GTAW	transverse	700	210.0	2,040	19501.8	190.8	1.100	not reported
VDM 617B	GTAW	transverse	700	214.0	3,648	19747.5	173.4	1.234	not reported
VDM 617B	GTAW	transverse	700	212.0	2,320	19556.2	186.8	1.135	not reported
VDM 617B	GTAW	transverse	750	95.5	28,543	21676.2	81.8	1.168	not reported
VDM 617B	GTAW	transverse	750	95.5	10,121	21215.5	97.9	0.976	not reported
VDM 617B	GTAW	transverse	750	107.1	6,402	21011.9	105.9	1.011	not reported
VDM 617B	GTAW	transverse	750	126.0	4,000	20803.0	114.9	1.096	not reported

Source	Weld Process[†]	Specimen Weld Orientation	Temp (°C)	Applied Weld Stress (MPa)	Rupture time (h)	L-M Parameter, Base Metal	Base Stress[*] (MPa)	SRF	Rupture Location
VDM 617B	GTAW	transverse	750	132.0	4,250	20829.9	113.7	1.161	not reported
VDM 617B	GTAW-o	transverse	700	149.5	8,807	20119.9	150.0	0.997	not reported
VDM 617B	GTAW-o	transverse	700	165.0	9,921	20170.3	147.1	1.122	not reported
VDM 617B	GTAW-o	transverse	700	178.8	3,015	19666.9	178.9	0.999	not reported
VDM 617B	GTAW-o	transverse	700	220.0	7,108	20029.3	155.4	1.416	not reported
VDM 617B	GTAW-o	transverse	750	100.0	4,793	20883.4	111.4	0.898	not reported
Huntington/SMC	PA	transverse	650	344.8	416.7	17863.0	361.4	0.954	not reported
Huntington/SMC	GMA	transverse	650	344.8	393.2	17839.7	364.7	0.945	not reported
Huntington/SMC	GTAW	transverse	650	344.8	458.7	17901.5	356.1	0.968	not reported
Huntington/SMC	PA	transverse	760	165.5	936.1	20354.7	136.9	1.209	not reported
Huntington/SMC	PA	transverse	870	69.0	881.2	22491.8	59.5	1.159	not reported
Huntington/SMC	GMA	transverse	870	69.0	576.1	22280.8	64.6	1.067	not reported
Huntington/SMC	GTAW	transverse	870	69.0	776.1	22428.8	61.0	1.131	not reported
Huntington/SMC	PA	transverse	980	30.3	455.6	24297.1	29.4	1.030	not reported
Huntington/SMC	PA	longitudinal	650	399.9	119.9	17363.6	439.1	0.911	not reported
Huntington/SMC	PA	longitudinal	650	275.8	3510.7	18717.4	259.1	1.065	not reported
Huntington/SMC	PA	longitudinal	760	206.9	189.7	19638.4	180.9	1.143	not reported
Huntington/SMC	PA	longitudinal	760	117.2	8232.2	21330.2	93.6	1.253	not reported
Huntington/SMC	PA	longitudinal	870	89.6	140.7	21581.0	84.9	1.056	not reported
Huntington/SMC	PA	longitudinal	870	41.4	14448.8	23880.5	34.6	1.194	not reported
Huntington/SMC	PA	longitudinal	980	41.4	155.1	23710.7	37.0	1.118	not reported
Huntington/SMC	PA	longitudinal	980	17.2	3770.3	25447.2	18.8	0.917	not reported
Huntington/SMC	GTA	longitudinal	1093	12.4	747.9	26782.1	11.2	1.110	not reported

[†] GTAW – Gas Tungsten Arc Weld

  GTAW-o – Gas Tungsten Arc Weld-orbital

  PA – Pulsed Arc Gas Metal Arc

  GMA – Gas Metal Arc

[*] Base Stress is determined from a Larson-Miller correlation of base metal rupture stress values from all available heats

Appendix VI

Data Compilation for Tensile Tests of Aged Alloy 617

	Heat/Lot ID	Product Form	Test Temp. (°C)	Aging Temp. (°C)	Aging Time (h)	Yield Strength (MPa)	Tensile Strength (MPa)	Total Elongation (%)	Source
1	XX01A3US	Plate	21	none	0	303	747	54	ORNL
2	XX01A3US	Plate	21	none	0	301	757	61	ORNL
3	XX01A3US	Plate	21	none	0	305	754	58	ORNL
4	NR	NR	21	none	0	319	769	68	SMC
5	314626	Plate	21	none	0	302	768	63	INL
6	188155	Rod	21	none	0	402	811	64	INL
7	188155	Rod	21	none	0	413	808	63	INL
8	XX2834UK	Plate	21	none	0	404	809	50	INL
9	XX01A3US	Plate	21	538	2500	358	794	68	ORNL
10	XX01A3US	Plate	21	538	2500	360	796	70	ORNL
11	XX01A3US	Plate	21	538	10000	392	805	53	ORNL
12	XX01A3US	Plate	21	538	20000	379	822	63	ORNL
13	NR	NR	21	595	100	321	769	69	SMC
14	NR	NR	21	595	1000	357	803	67	SMC
15	NR	NR	21	595	4000	384	810	67	SMC
16	NR	NR	21	595	8000	410	838	61	SMC
17	NR	NR	21	595	12000	466	910	34	SMC
18	NR	NR	21	650	100	357	789	69	SMC
19	314626	Plate	21	650	200	449	910	48	INL
20	314626	Plate	21	650	200	445	915	49	INL
21	188155	Rod	21	650	200	588	1005	36	INL
22	314626	Plate	21	650	650	487	951	41	INL
23	314626	Plate	21	650	650	488	961	43	INL
24	188155	Rod	21	650	650	591	1052	35	INL
25	NR	NR	21	650	1000	459	920	37	SMC
26	314626	Plate	21	650	2000	512	974	41	INL
27	314626	Plate	21	650	2000	512	977	41	INL
28	188155	Rod	21	650	2000	634	1079	33	INL
29	NR	NR	21	650	3640	526	979	33	SMC
30	314626	Plate	21	650	5300	532	982	39	INL
31	314626	Plate	21	650	5300	527	980	40	INL
32	188155	Rod	21	650	5300	638	1078	32	INL
33	NR	NR	21	650	8000	527	993	28	SMC
34	NR	NR	21	650	12000	534	993	32	SMC
35	XX01A3US	Plate	21	704	2500	371	847	39	ORNL
36	XX01A3US	Plate	21	704	2500	372	849	44	ORNL
37	XX01A3US	Plate	21	704	10000	369	798	30	ORNL
38	XX01A3US	Plate	21	704	20000	395	813	21	ORNL
39	NR	NR	21	705	100	405	872	38	SMC
40	NR	NR	21	705	1000	486	952	33	SMC
41	NR	NR	21	705	4000	487	952	36	SMC
42	314626	Plate	21	750	200	425	875	56	INL
43	314626	Plate	21	750	200	416	865	55	INL
44	188155	Rod	21	750	200	562	1020	36	INL
45	314626	Plate	21	750	650	410	864	58	INL
46	314626	Plate	21	750	650	414	867	53	INL
47	188155	Rod	21	750	650	543	1019	35	INL
48	314626	Plate	21	750	2000	396	861	56	INL
49	314626	Plate	21	750	2000	391	858	55	INL
50	188155	Rod	21	750	2000	487	972	27	INL

	Heat/Lot ID	Product Form	Test Temp. (°C)	Aging Temp. (°C)	Aging Time (h)	Yield Strength (MPa)	Tensile Strength (MPa)	Total Elongation (%)	Source
51	314626	Plate	21	750	5300	388	862	56	INL
52	314626	Plate	21	750	5300	388	863	53	INL
53	188155	Rod	21	750	5300	442	882	20	INL
54	314626	Plate	21	750	20000	392	887	39	INL
55	314626	Plate	21	750	32000	384	887	33	INL
56	NR	NR	21	760	100	402	872	35	SMC
57	NR	NR	21	760	1000	388	869	37	SMC
58	NR	NR	21	760	4000	401	886	38	SMC
59	NR	NR	21	760	8000	403	896	40	SMC
60	NR	NR	21	760	12000	389	893	38	SMC
61	XX2834UK	Plate	21	800	100	472	922	41	INL
62	XX2834UK	Plate	21	800	100	488	932	41	INL
63	XX2834UK	Plate	21	800	1000	475	943	40	INL
64	XX2834UK	Plate	21	800	1000	422	905	41	INL
65	XX2834UK	Plate	21	800	10000	428	944	33	INL
66	XX2834UK	Plate	21	800	10000	440	947	32	INL
67	XX01A3US	Plate	21	871	2500	331	797	30	ORNL
68	XX01A3US	Plate	21	871	2500	334	822	35	ORNL
69	XX01A3US	Plate	21	871	10000	290	695	28	ORNL
70	XX01A3US	Plate	21	871	20000	300	658	20	ORNL
71	XX2834UK	Plate	21	1000	100	370	886	47	INL
72	XX2834UK	Plate	21	1000	100	385	889	50	INL
73	XX2834UK	Plate	21	1000	1000	408	904	48	INL
74	XX2834UK	Plate	21	1000	1000	399	896	48	INL
75	XX01A3US	Plate	538	none	0	216	610	67	ORNL
76	XX01A3US	Plate	538	none	0	207	606	64	ORNL
77	XX01A3US	Plate	538	538	2500	260	638	69	ORNL
78	XX01A3US	Plate	538	538	2500	259	638	69	ORNL
79	XX01A3US	Plate	538	538	10000	222	669	37	ORNL
80	XX01A3US	Plate	538	538	20000	281	621	66	ORNL
81	XX01A3US	Plate	538	704	10000	274	629	59	ORNL
82	314626	Plate	650	none	0	204	584	69	INL
83	314626	Plate	650	650	200	347	668	50	INL
84	314626	Plate	650	650	650	384	721	48	INL
85	314626	Plate	650	650	2000	414	751	48	INL
86	314626	Plate	650	650	5300	435	766	49	INL
87	314626	Plate	700	none	0	249	553	61	INL
88	314626	Plate	700	650	200	322	586	54	INL
89	314626	Plate	700	650	650	360	621	50	INL
90	314626	Plate	700	650	2000	388	617	52	INL
91	314626	Plate	700	650	5300	422	648	53	INL
92	314626	Plate	700	750	200	348	574	54	INL
93	314626	Plate	700	750	650	317	559	63	INL
94	314626	Plate	700	750	2000	275	517	67	INL
95	314626	Plate	700	750	5300	293	532	62	INL
96	314626	Plate	700	750	5300	279	533	65	INL
97	314626	Plate	700	750	32000	266	522	61	INL
98	XX01A3US	Plate	704	none	0	199	466	68	ORNL
99	XX01A3US	Plate	704	none	0	196	443	70	ORNL
100	XX01A3US	Plate	704	none	0	196	454	75	ORNL
101	XX01A3US	Plate	704	704	2500	257	502	75	ORNL
102	XX01A3US	Plate	704	704	2500	256	475		ORNL
103	XX01A3US	Plate	704	704	10000	211	461	69	ORNL
104	XX01A3US	Plate	704	704	20000	285	525	53	ORNL

	Heat/Lot ID	Product Form	Test Temp. (°C)	Aging Temp. (°C)	Aging Time (h)	Yield Strength (MPa)	Tensile Strength (MPa)	Total Elongation (%)	Source
105	314626	Plate	750	none	0	210	406	65	INL
106	314626	Plate	750	650	200	287	468	62	INL
107	314626	Plate	750	650	650	320	484	54	INL
108	314626	Plate	750	650	2000	343	496	57	INL
109	314626	Plate	750	650	5300	365	502	55	INL
110	314626	Plate	750	750	200	335	455	51	INL
111	314626	Plate	750	750	650	319	449	61	INL
112	314626	Plate	750	750	2000	275	408	68	INL
113	314626	Plate	750	750	5300	289	418	60	INL
114	314626	Plate	750	750	20000	269	425	64	INL
115	314626	Plate	750	750	32000	261	424	69	INL
116	314626	Plate	800	none	0	189	290	94	INL
117	314626	Plate	800	650	200	206	301	80	INL
118	314626	Plate	800	650	650	236	304	93	INL
119	314626	Plate	800	650	2000	216	281	93	INL
120	314626	Plate	800	650	5300	247	289	83	INL
121	314626	Plate	800	750	200	261	305	72	INL
122	314626	Plate	800	750	650	285	327	82	INL
123	314626	Plate	800	750	2000	267	323	74	INL
124	314626	Plate	800	750	5300	264	311	77	INL
125	314626	Plate	800	750	20000	258	318	76	INL
126	314626	Plate	800	750	32000	253	323	70	INL
127	XX2834UK	Plate	800	800	100	351	447	45	INL
128	XX2834UK	Plate	800	800	100	326	427	41	INL
129	XX2834UK	Plate	800	800	1000	300	471	41	INL
130	XX2834UK	Plate	800	800	1000	292	462	45	INL
131	XX2834UK	Plate	800	800	10000	312	460	43	INL
132	XX2834UK	Plate	800	800	10000	279	448	44	INL
133	XX2834UK	Plate	800	1000	100	259	434	47	INL
134	XX2834UK	Plate	800	1000	100	255	413	52	INL
135	XX2834UK	Plate	800	1000	1000	258	434	47	INL
136	XX2834UK	Plate	800	1000	1000	280	413	50	INL
137	314626	Plate	850	none	0	188	216	119	INL
138	314626	Plate	850	650	200	221	221	114	INL
139	314626	Plate	850	650	650	208	208	110	INL
140	314626	Plate	850	650	2000	209	207	105	INL
141	314626	Plate	850	650	5300	208	207	106	INL
142	314626	Plate	850	750	200	205	205	97	INL
143	314626	Plate	850	750	650	213	213	86	INL
144	314626	Plate	850	750	2000	213	215	88	INL
145	314626	Plate	850	750	5300	202	203	87	INL
146	314626	Plate	850	750	20000	201	203	112	INL
147	314626	Plate	850	750	32000	199	209	87	INL
148	XX01A3US	Plate	871	none	0	181	194	88	ORNL
149	XX01A3US	Plate	871	none	0	189	194	92	ORNL
150	XX01A3US	Plate	871	871	2500	154	168		ORNL
151	XX01A3US	Plate	871	871	2500	170	179	98	ORNL
152	XX01A3US	Plate	871	871	10000	170	181	91	ORNL
153	XX01A3US	Plate	871	871	20000	180	255	90	ORNL
154	314626	Plate	900	none	0	163	166	103	INL
155	314626	Plate	900	650	200	167	165	112	INL
156	314626	Plate	900	650	650	152	151	94	INL
157	314626	Plate	900	650	2000	152	153	106	INL
158	314626	Plate	900	650	5300	150	151	109	INL

	Heat/Lot ID	Product Form	Test Temp. (°C)	Aging Temp. (°C)	Aging Time (h)	Yield Strength (MPa)	Tensile Strength (MPa)	Total Elongation (%)	Source
159	314626	Plate	900	750	200	162	162	99	INL
160	314626	Plate	900	750	650	159	158	93	INL
161	314626	Plate	900	750	2000	159	159	77	INL
162	314626	Plate	900	750	5300	147	147	80	INL
163	314626	Plate	900	750	20000	147	147	105	INL
164	314626	Plate	900	750	32000	140	144	106	INL
165	314626	Plate	950	none	0	119	124	96	INL
166	314626	Plate	950	650	200	121	121	97	INL
167	314626	Plate	950	650	650	109	111	90	INL
168	314626	Plate	950	650	2000	111	112	92	INL
169	314626	Plate	950	650	5300	111	113	98	INL
170	314626	Plate	950	750	200	115	115	97	INL
171	314626	Plate	950	750	200	116	118	95	INL
172	314626	Plate	950	750	650	105	108	90	INL
173	314626	Plate	950	750	650	105	107	116	INL
174	314626	Plate	950	750	2000	116	116	81	INL
175	314626	Plate	950	750	5300	107	107	74	INL
176	314626	Plate	950	750	20000	107	107	92	INL
177	314626	Plate	950	750	32000	109	110	98	INL
178	314626	Plate	1000	none	0	90	92	99	INL
179	314626	Plate	1000	650	200	88	89	99	INL
180	314626	Plate	1000	650	650	87	89	84	INL
181	314626	Plate	1000	650	2000	82	83	88	INL
182	314626	Plate	1000	650	5300	82	84	78	INL
183	314626	Plate	1000	750	200	85	86	79	INL
184	314626	Plate	1000	750	650	86	87	89	INL
185	314626	Plate	1000	750	2000	86	87	89	INL
186	314626	Plate	1000	750	5300	80	81	80	INL
187	314626	Plate	1000	750	20000	79	80	99	INL
188	314626	Plate	1000	750	32000	81	82	103	INL
189	XX2834UK	Plate	1000	1000	100	142	144	58	INL
190	XX2834UK	Plate	1000	1000	100	141	141	59	INL
191	XX2834UK	Plate	1000	1000	1000	130	136	59	INL
192	XX2834UK	Plate	1000	1000	1000	140	153	60	INL

NR – not reported

Background Document – Record No. 16-995

Contents

- Balloting Plan
- Physical Property Tables for Alloy 617
  - TE – Thermal Expansion
  - TCD – Thermal Conductivity and Thermal Diffusivity
- Modulus of Elasticity Tables for Alloy 617
- Appendices
  - Appendix I. Data Compilation for Coefficient of Thermal Expansion of Alloy 617
  - Appendix II. Data Compilation for Thermal Diffusivity of Alloy 617
  - Appendix III. Data Compilation for Heat Capacity (C_p), Density and Thermal Conductivity of Alloy 617
  - Appendix IV. Data Compilation for Modulus of Elasticity for Alloy 617

Page intentionally left blank

Alloy 617 Code Case Balloting Actions

RC #	Item	Section II and III Committees (See Color Key Below For Balloting Actions)								
16-994	Permissible base and weld materials, allowable stress values	WG-ASC	SG-ETD	SG-HTR	SG-MFE	II-SG-NFA	II-SG-SW	BPV-II		
16-995	Physical properties and extension of modulus values to higher temperatures	WG-ASC	SG-ETD	SG-HTR	SG-MFE	II-SG-NFA	II-SG-PP	BPV-II		
16-996	Temperature-time limits for NB buckling charts	WG-AM	SG-ETD	SG-HTR	SG-MFE	II-SG-EP	BPV-II	II-SG-NFA	SC-D	
16-997	Huddleston parameters, ISSCs	WG-ASC	SG-ETD	SG-HTR	II-SG-NFA	BPV-II	SC-D			
16-998	Negligible creep, Creep-Fatigue: D-diagram and EPP	WG-CFNC	SG-ETD	SG-HTR	SC-D					
16-999	EPP strain limits	WG-AM	SG-ETD	SG-HTR	SC-D					
16-1000	Fatigue design curves	WG-CFNC	WG-FS	SG-ETD	SG-HTR	SG-DM	SC-D			
16-1001	Alloy 617 Overall Code Case	WG-ASC	WG-AM	WG-CFNC	WG-FS	SG-ETD	SG-HTR	SG-MFE	SC-D	BPV-II
		BPV-III								

Color Key	Balloting Action
	For Review and Approval
	For Review and Comment

Page intentionally left blank

BACKGROUND

PHYSICAL PROPERTY TABLES FOR ALLOY 617

Scope

This document provides the background/technical basis in support of the recommendation for Section II Part D, Subpart 2, Physical Properties Tables. This includes Table TE-4 Thermal Expansion for Nickel Alloys, Table TCD Nominal Coefficients of Thermal Conductivity (TC) and Thermal Diffusivity (TD). Alloy 617 is not currently included in these tables.

Background

The following is extracted from Section II Part D, Subpart 2, Physical Properties Tables:

> All of the physical properties [provided in Subpart 2] are considered typical. They are neither average nor minimum. Thermal–physical properties such as thermal expansion, thermal conductivity, and thermal diffusivity are affected more by alloy content than by crystal structure or heat treatment. Due to the permitted range for elements comprising alloys (specification ranges of chemical compositions), the thermal–physical properties described in [Table TE-4] and Table TCD should be considered to have an associated uncertainty of ±10%.

Materials

Descriptions of the source, form and chemistry of the four different heats of Alloy 617 characterized in these experiments are given in Table 1. Products obtained from Special Metals Corporation, now Special Metals Division of PCC Energy Group (SMC) (Heat 1) and ThyssenKrupp VDM (Heat 2) were in plate form. The material from Haynes International, Inc. (Heat 3) was 3mm-thick sheet with an equiaxed microstructure. The material from Oxford Alloys, Inc. (Heat 4) was weld metal deposited using the gas tungsten arc process using weld wire of Alloy 617 composition meeting specification SFA-5.14; the composition given in Table 1 is from the vendor certification of the weld wire composition. Heats 1, 2 and 3 were provided in the solution-annealed condition, consisting of holding at 2150°F (1175°C) followed by rapid cooling to room temperature, according to SB166 and SB168. Heat 4 (weld wire) was provided in the as-welded condition.

Quality

Physical properties of Alloy 617 reported by the Idaho National Laboratory (INL) through the Next Generation Nuclear Plant (NGNP) or Advanced Reactor Technologies (ART) programs were determined under an NQA-1 quality program. Details of the quality program implementation are given in INL document PLN-2690 "Idaho National Laboratory Advanced Reactor Technologies Technology Development Office Quality Assurance Program Plan".

Page intentionally left blank

Table 1. Source and chemical composition of the Alloy 617 materials (weight percent).

Heat ID	Source	Form	Ni	Cr	Co	Mo	Fe	Mn	Al	C	Cu	Si	S	Ti	B
	ASME		44.5 min	20.0-24.0	10.0-15.0	8.0-10.0	3.0 max	1.0 max	0.8-1.5	0.05-0.15	0.5 max	1.0 max	0.015 max	0.6 max	0.006 max
1	VDM	plate	54.1	22.2	11.6	8.6	1.6	0.1	1.1	0.05	0.04	0.1	<0.002	0.4	<0.001
2	SMC	plate	53.59	21.91	11.42	9.78	1.69	0.11	0.96	0.08	NR	0.12	0.001	0.34	0.002
3	Haynes	sheet	54.08	22.00	11.80	9.37	1.10	0.05	1.01	0.080	0.04	0.05	<0.002	0.41	0.002
4	Oxford	weld wire	53.91	22.41	11.49	8.98	1.37	0.11	1.10	0.089	0.04	0.04	0.001	0.34	NR

NR – not reported

Page intentionally left blank

TE — THERMAL EXPANSION

Thermal expansion of the four heats of Alloy 617 was measured at INL using a Netzsch dilatometer over the temperature range 25 to 1000°C.[1] Testing was performed according to ASTM E228,[2] implementing a more repeatable reference temperature of 30°C rather than the recommended 25°C. Measured $\Delta l/l_0$ values are given in Appendix I. It can be seen in Figure 1 that the values are similar for the four materials. A third-order polynomial passing through 0 at 20°C was fit to the data. The polynomial expression for $\Delta l/l_0$ in SI units was used to calculate the corresponding $\Delta l/l_0$ values in customary units.

The equation for thermal expansion in customary units is:

$$\frac{\Delta l}{l_0} = 3.974308E-10\ T_F{}^3 + 7.773689E-07\ T_F{}^2 + 8.296749E-03\ T_F - 5.678985E-01$$

where $\Delta l/l_0$ is in units of in./(100 ft) and T_F is the temperature in °F. The equation for thermal expansion in SI units is:

$$\frac{\Delta l}{l_0} = 1.931514E-09 T_C{}^3 + 2.201910E-06\ T_C{}^2 + 1.252158E-02\ T_C - 2.513279E-01$$

where $\Delta l/l_0$ is in units of mm/m and T_C is the temperature in °C.
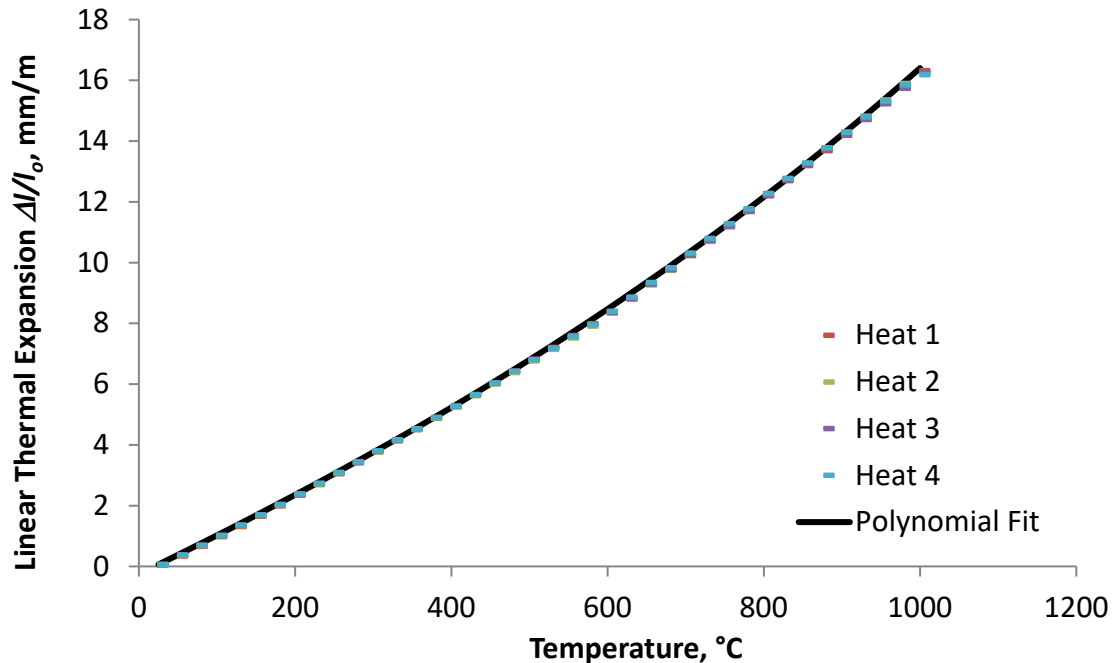
Figure 1. Change in length/initial length (mm/m) for four heats of Alloy 617, modeled with a third-order polynomial fit passing through (20°C, 0).

No Alloy 617 thermal expansion data have been found in the literature for comparison. However, ASME Code Section II, Part D Table TE-4 does include values for similar nickel-based solid-solution alloys. In Figure 2 the measured $\Delta l/l_0$ values[1] are compared to values from Table TE-4 for Haynes 230 and Hastelloy X. It can be seen that the values are comparable.
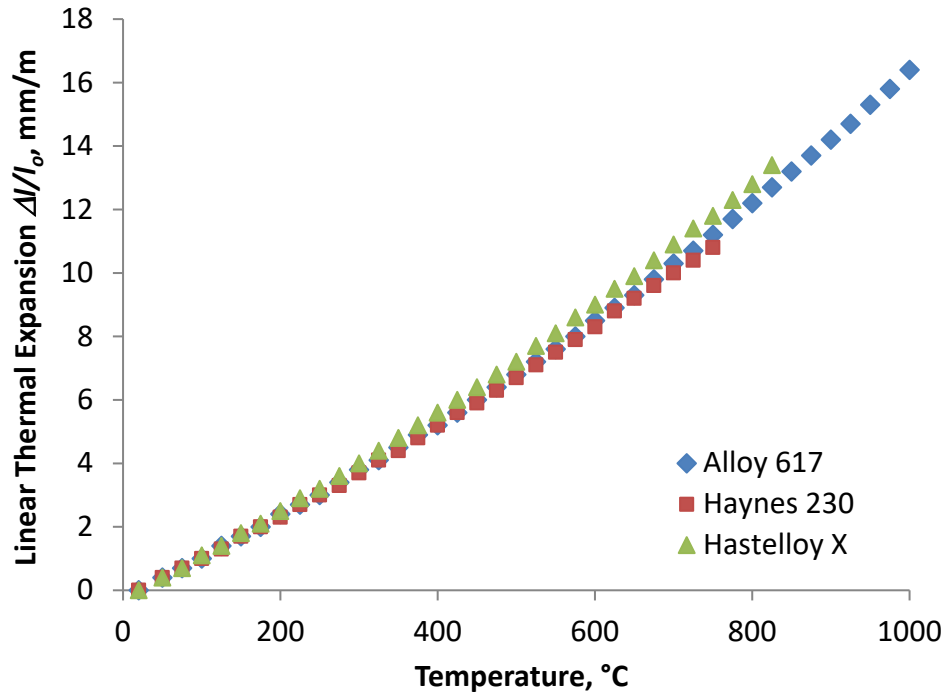
Figure 2. Alloy 617 $\Delta l/l_0$ behavior calculated from the polynomial fit to experimental data compared to Code values for similar Ni-based solid-solution alloys.

Mean Coefficient of Thermal Expansion (CTE) values from 20°C (70°F) were calculated by dividing the $\Delta l/l_0$ values from the polynomial fit by $T_C-20°C$ (or $T_F-68°F$, the conversion of 20°C). There are two older sets of comparable mean CTE values: vendor datasheets that appear to have been determined by Huntington Alloys (SMC)[3] during development of the alloy, and the draft ASME Alloy 617 Code Case submitted in 1992, although the origin of the data in that draft Code Case is not clear. A comparison of measured values[1] and historical values is shown in Figure 3. For this comparison, only values for customary units are shown, since it is believed that the original experiments were carried out using customary units and the method for subsequent conversion to SI units is not specified.
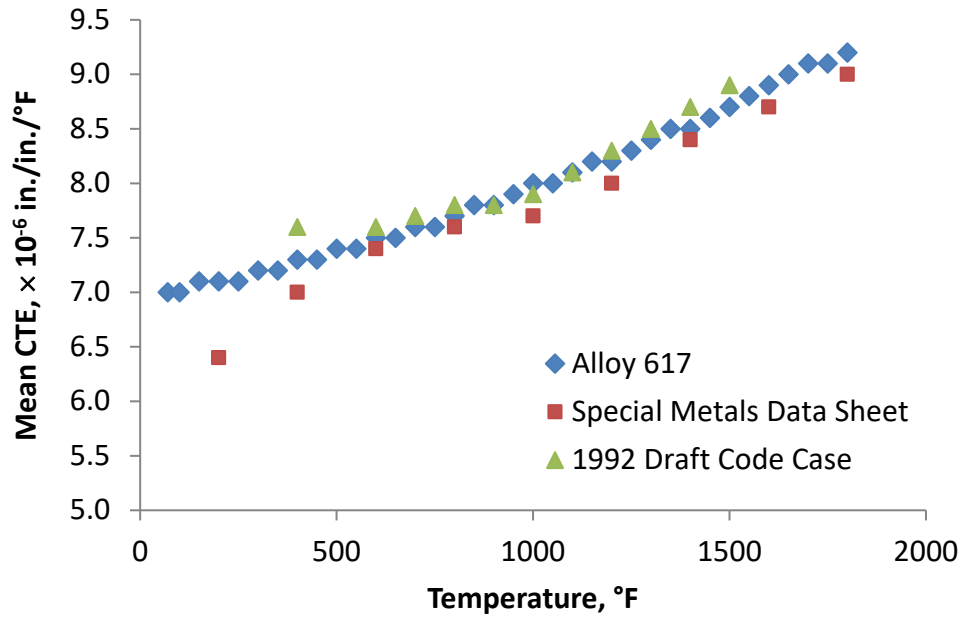
Figure 3. Mean CTE (linear expansion from 70°F to temperature of interest) for experiments compared to values from vendor datasheet and from 1992 draft Alloy 617 Code Case.

The instantaneous CTE was calculated using the derivative of the polynomial fit to the $\Delta l/l_0$ data from 20–1000°C (70–1800°F). Instantaneous CTE data for this alloy have not been found in the literature. Figure 4 shows instantaneous CTE values calculated from the fit to data shown in Figure 1 compared to ASME Code Section II, Part D Table TE-4 values for two similar Ni-based solid-solution alloys in SI units. The agreement is quite good.
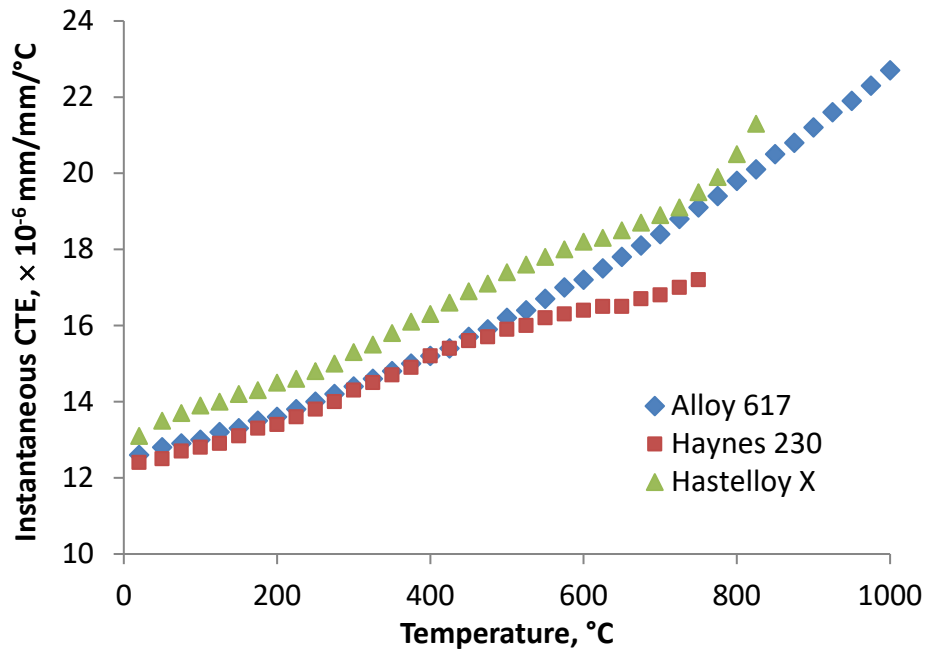
Figure 4. Instantaneous CTE for current experiments using fit to data shown in Figure 1 compared to Code values for two similar Ni-based solid-solution alloys.

TCD — THERMAL CONDUCTIVITY AND THERMAL DIFFUSIVITY

Thermal diffusivity was measured at INL for the four Alloy 617 heats (Table 1) from 20 to 1000°C using a Netzsch laser flash system,[1] following ASTM E2585.[4] The experimental values are given in Appendix II and shown in Figure 5. The local maximum in the region of 750°C appears to be the result of Ni-Cr clustering.[1] Because of this deviation from monotonic behavior, a two-piece third-order polynomial fit is used to describe the experimental data. The fitting technique requires the two polynomials to be equivalent at the breaking point of 700°C. The polynomial fit to the diffusivity data in SI units was used to calculate the values in customary units. The equation describing the thermal diffusivity in customary units is given by:

$Diffusivity * 10\char`^6$

$$= \begin{cases} 1.582634E-11\,T_F{}^3 - 3.288719E-08\,T_F{}^2 + 8.494502E-05\,T_F + 1.059727E-01 & T_F \leq 1292°F \\ -3.169467E-10\,T_F{}^3 + 1.616931E-06\,T_F{}^2 - 2.685705E-03\,T_F + 1.649358E+00 & T_F > 1292°F \end{cases}$$

where diffusivity is in units of ft²/hr and T_F is the temperature in °F. The equation for thermal diffusivity in SI units is given by:

$Diffusivity * 10\char`^6$

$$= \begin{cases} 2.381911E-09\,T_C{}^3 - 2.622753E-06\,T_C{}^2 + 3.850314E-03\,T_C + 2.804066E+00 & T_C \leq 700°C \\ -4.770140E-08\,T_C{}^3 + 1.326520E-04\,T_C{}^2 - 1.199934E-01\,T_C + 4.038859E+01 & T_C > 700°C \end{cases}$$

where diffusivity is in units of m²/s and T_C is the temperature in °C.
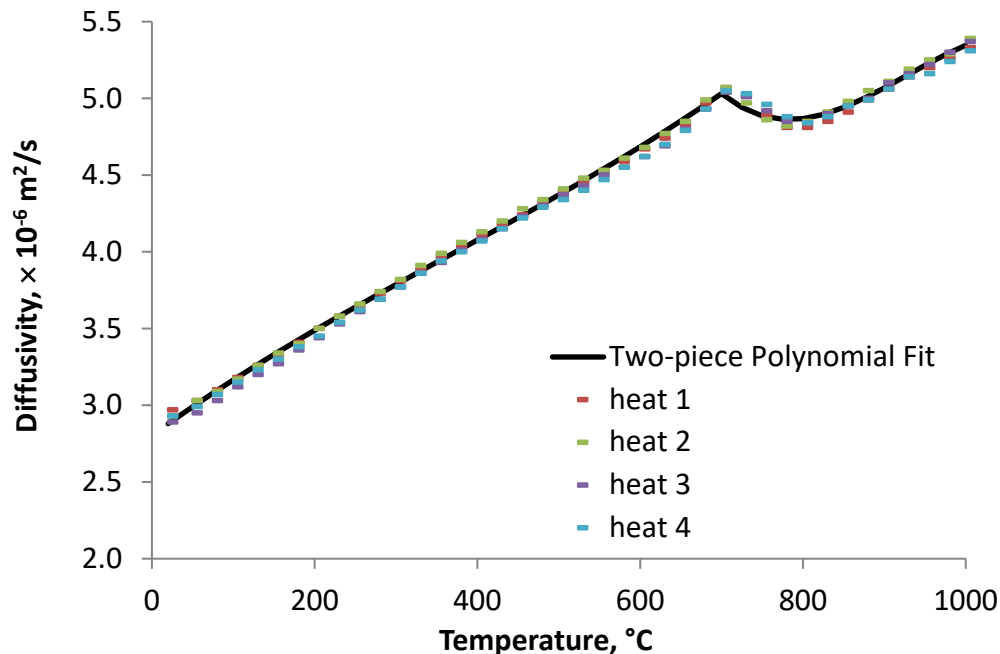
Figure 5. Thermal diffusivity for four heats of Alloy 617 showing two-piece cubic fit.

The heat capacity of the four Alloy 617 heats was measured at INL using a Netzsch calorimeter according to ASTM E1269,[5] and the average heat capacity of the four specimens was calculated at each temperature.[1] The thermal conductivity was calculated as the product of the diffusivity (from the above two-piece polynomial), the average heat capacity, and the temperature corrected density.

The temperature corrected density can be calculated from the density and the coefficient of thermal expansion. In practice, experimental data for thermal expansion was not acquired for temperatures less than room temperature (~22°C), so the first measured value was reported at 25°C. The temperature adjusted density, ρ_T, is calculated as

$$\rho_T = \rho_0 \left(\frac{1}{(1+(mean\ CTE*(T_C-25)))} \right)^3$$

where ρ_0 is 8360 kg/m³, the value for Alloy 617 from ASME Code Section II Part D Table PRD, T_C is temperature in °C, and *mean CTE* is given in Appendix I and calculated as described above.

Fitting the thermal conductivity required a three piece second-order polynomial. The fitting technique requires the three polynomials to be equivalent at the breaking points of 550 and 700°C. The polynomial fit of the conductivity in SI units was used to calculate the values in customary units. Conductivity values calculated for Alloy 617 from the polynomial fit and from the product are given in Appendix III, along with the measured and average heat capacity, and the temperature corrected density. The equation describing the thermal conductivity in customary units is given by:

$$Conductivity$$
$$= \begin{cases} -1.117326E-06\ T_F{}^2 + 6.781195E-03\ T_F + 5.590050E+00 & T_F \leq 1022°F \\[2mm] -5.758185E-05\ T_F{}^2 + 1.462698E-01\ T_F - 7.799099E+01 & 1022 < T_F \leq 1292°F \\[2mm] 1.426307E-05\ T_F{}^2 - 4.119446E-02\ T_F + 4.428466E+01 & T_F > 1292°F \end{cases}$$

where conductivity is in units of BTU/(hr·ft·°F) and T_F is the temperature in °F. The equation for thermal conductivity in SI units is given by:

$$Conductivity$$
$$= \begin{cases} -6.265498E-06\ T_C{}^2 + 2.090284E-02\ T_C + 1.004848E+01 & T_C \leq 550°C \\[2mm] -3.228949E-04\ T_C{}^2 + 4.441969E-01\ T_C - 1.269828E+02 & 550 < T_C \leq 700°C \\[2mm] 7.998132E-05\ T_C{}^2 - 1.254903E-01\ T_C + 7.438879E+01 & T_C > 700°C \end{cases}$$

where conductivity is in units of W/(m·°C) and T_C is the temperature in °C.

Thermal conductivity is shown in Figure 6 in SI units along with data from the SMC vendor datasheet[3] for comparison. The SMC vendor datasheet[3] was the only source of historical information on thermal conductivity available in the literature specifically for Alloy 617, and notes that thermal conductivity was calculated from electrical resistivity. It is not clear if the difference in calculation method is the sole reason why the vendor data do not include the perturbation from monotonic behavior in the region of 750°C. The heat capacity also exhibits a deviation from monotonic behavior, but over a slightly different temperature range compared to that for the thermal diffusivity. As a result, the temperature range of non-monotonic behavior shown by the thermal conductivity extends over approximately 200°C. Although the deviation is not shown in the vendor datasheet for Alloy 617[3] or in Section II, Part D for the other nickel solid solutions, the magnitude of the local peak in conductivity is nearly 20% compared to a monotonic curve, and the local peak lies within the temperature range where it is anticipated that Alloy 617 will be used for nuclear heat exchanger design.
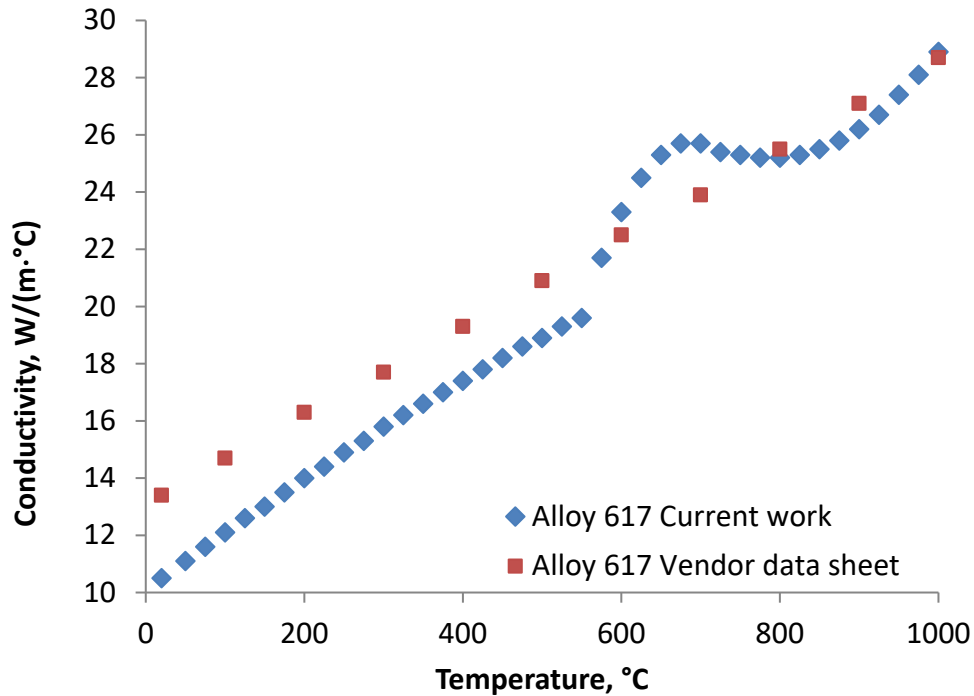
Figure 6. Thermal conductivity for Alloy 617 showing a three-piece fit to data calculated from thermal diffusivity and heat capacity compared to data from Alloy 617 vendor datasheet calculated from electrical resistivity.

REFERENCES

[1] B. H. Rabin, W. D. Swank and R. N. Wright, "Thermophysical Properties of Alloy 617 from 25 to 1000°C", *Nuclear Engineering and Design Journal,* Vol. 262, 2013, p. 72.

[2] ASTM E228, "Standard Test Method for linear Thermal Expansion of solid materials with a Push-Rod Dilatometer," ASTM International.

[3] INCONEL® Alloy 617 Datasheet, Special Metals Corp., Publication No. SMC-029 Huntington, WV, 2005.

[4] ASTM E2585, "Standard Practice for Thermal Diffusivity by the Flash Method," ASTM International.

[5] ASTM E1269, "Standard Test Method for Determining Specific heat Capacity by Differential Scanning Calorimetry," ASTM International.

BACKGROUND
MODULUS OF ELASTICITY TABLES FOR ALLOY 617

Scope

This document provides the background/technical basis in support of the recommendation for Section II Part D, Subpart 2, Physical Properties Tables, Tables TM-4 and TM-4M, Moduli of Elasticity E of High Nickel Alloys for Given Temperatures. Alloy 617 modulus values currently appear in Table TM-4 up to 1500°F and in Table TM-4M up to 850°C. The Alloy 617 Code Case specifies use of the alloy up to 1750°F (950°C) in Section III, Division 5 for construction of high temperature nuclear components. Therefore the temperature range for elastic modulus values must be increased to accommodate the temperature limits of the Code Case.

Background

The following is extracted from Section II Part D, Subpart 2, Physical Properties Tables:

> All of the physical properties [provided in Subpart 2] are considered typical. They are neither average nor minimum…

> Moduli of elasticity and Poisson's ratio are also typical values, but the values of modulus of elasticity, shown as a function of temperature in [Table TM-4], tend to be closer to average values since their temperature dependency is factored against an "average" room temperature value.

Data Sources and Materials

Descriptions of the source, form and chemistry of the two different heats of Alloy 617 characterized in these experiments are given in Table 1. Material was obtained from ThyssenKrupp VDM in 37-mm thick plate and 51-mm diameter rod form. Both product forms were provided in the solution-annealed condition, consisting of holding at 2150°F (1175°C) followed by rapid cooling to room temperature, according to standards SB166 and SB168.

TM — MODULUS OF ELASTICITY

The basis for increasing the temperature range of elastic modulus values is twofold: extrapolation of the elastic modulus values currently in the ASME Code, and confirmation from experimental measurement. The current ASME Code values, the extrapolated values for the Code Case and the experimental results are shown in Figure 1 and tabulated in Appendix IV.

The elastic modulus values currently in Tables TM-4 and TM-4M were extrapolated to 950°C and 1800°F using a third-order polynomial fit. The equation for modulus of elasticity, E, in customary units is

$$E = -7.247802 \times 10^{-10} \, T_F^3 + 4.613058 \times 10^{-7} \, T_F^2 - 4.137668 \times 10^{-3} \, T_F + 2.935848 \times 10^1$$

where E is in units of 10^6 psi and T_F is temperature in °F. The equation for modulus of elasticity in SI units is

$$E = -2.914376 \times 10^{-8} \, T_C^3 + 8.750848 \times 10^{-6} \, T_C^2 - 5.101234 \times 10^{-2} \, T_C + 2.015110 \times 10^2$$

where E is in units of 10^3 MPa and T_C is temperature in °C.

Page intentionally left blank

Table 1. Source and chemical composition of the Alloy 617 materials (weight percent).

Heat ID	Source	Form	Ni	Cr	Co	Mo	Fe	Mn	Al	C	Cu	Si	S	Ti	B
	ASME		44.5 min	20.0-24.0	10.0-15.0	8.0-10.0	3.0 max	1.0 max	0.8-1.5	0.05-0.15	0.5 max	1.0 max	0.015 max	0.6 max	0.006 max
314626	VDM	plate	54.1	22.2	11.6	8.6	1.6	0.1	1.1	0.05	0.04	0.1	<0.002	0.4	<0.001
188155	VDM	rod	53.27	22.02	11.91	9.38	1.46	0.23	1.10	0.080	0.02	0.20	0.001	0.32	0.002

Page intentionally left blank

The two orange points in Figure 1 represent the proposed numerical values of elastic modulus for temperatures of 900 and 950°C, calculated from the polynomial fit of the Code values. Elastic modulus values in customary units (°F, psi) have also been calculated from the third-order polynomial fit. Proposed values are shown in Table TM and TM (M) of this Code Case for the entire temperature range from ambient to 1800°F and 950°C, respectively. Note that the values used up to 1500°C (850°C) are unchanged from current ASME Code Section II, Part D Table TM-4 (TM-4M) values.

The results of experiments conducted on Alloy 617 at the University of Dayton Research Center[1] were used to validate this extrapolation. The dynamic elastic modulus was determined using the resonant frequency in the flexural mode of vibration. Measurements were performed according to ASTM E1875,[2] in 5°C increments up to 1000°C on the plate and rod heats of Alloy 617 described above. Note that there are some gaps in the experimental data due to higher order modes of flexural resonant frequency observed at some temperatures; however, data in the higher temperature range supports the extrapolation. It can be seen from Figure 1 that the experimental results and the extrapolation of Table TM-4M values are in close agreement.
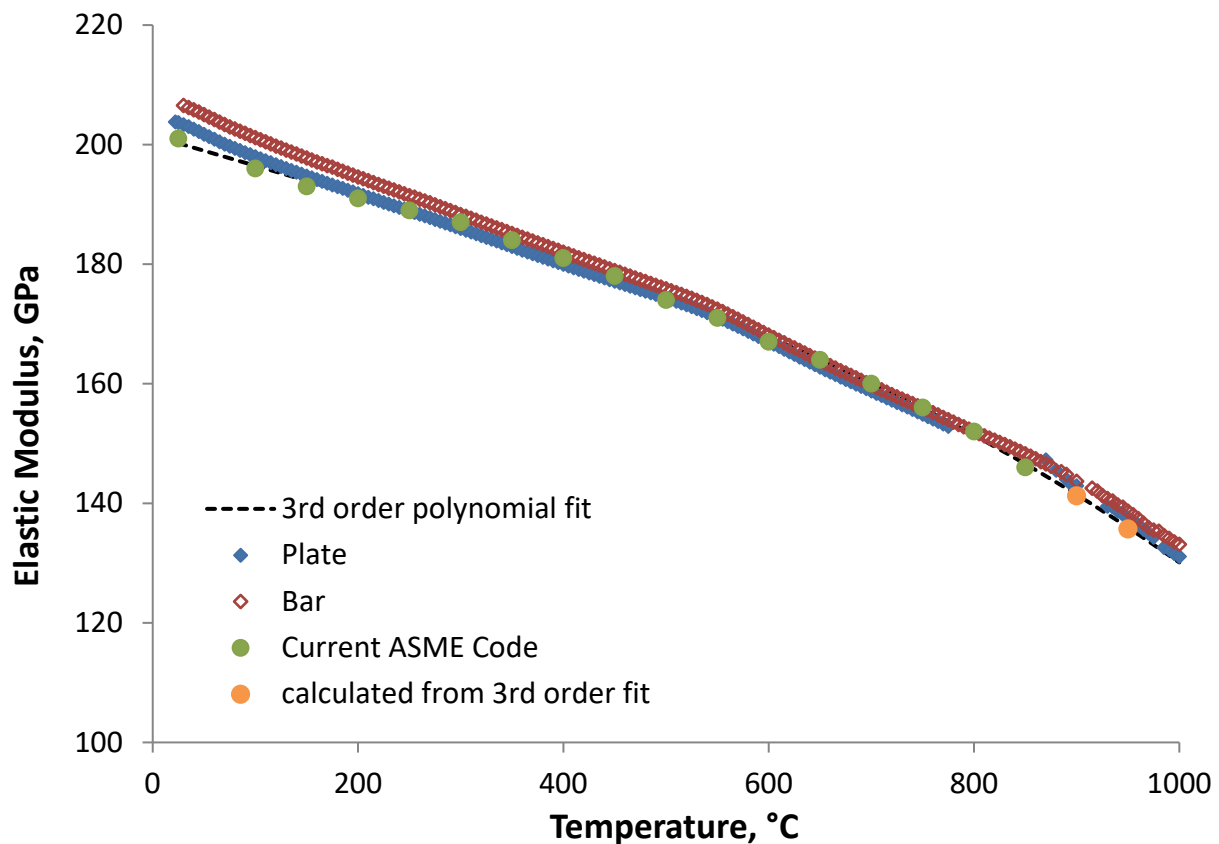
Figure 1. Elastic modulus as a function of temperature (°C) comparing resonant frequency experiments (diamonds), Code values (circles), and a third-order polynomial fit of the Code values (dashed line).

References

[1] Unpublished Research via private communication from Steven M. Goodrich, Advanced High Temperature Materials, University of Dayton Research Institute, to Barry Rabin, Idaho National Laboratory.

[2] ASTM E1875, "Standard Test Method for Dynamic Young's Modulus, Shear Modulus, and Poisson's Ratio by Sonic Resonance," ASTM International.

Page intentionally left blank

Appendix I

Data Compilation for Coefficient of Thermal Expansion of Alloy 617

Temp. T_C (°C)	Heat 1 linear $\Delta l/l_o$ (mm/m)	Heat 2 linear $\Delta l/l_o$ (mm/m)	Heat 3 linear $\Delta l/l_o$ (mm/m)	Heat 4 linear $\Delta l/l_o$ (mm/m)	-------------- polynomial fit --------------		
					linear $\Delta l/l_o$ (mm/m)	Mean $\times 10^{-6}$ (mm/mm/°C)	Instantaneous $\times 10^{-6}$ (mm/mm/°C)
25	0.05	0.06	0.06	0.06	0.1	12.6	12.6
50	0.34	0.36	0.37	0.37	0.4	12.7	12.8
75	0.66	0.68	0.69	0.69	0.7	12.7	12.9
100	0.98	1.00	1.02	1.02	1.0	12.8	13.0
125	1.31	1.33	1.35	1.36	1.4	12.9	13.2
150	1.65	1.67	1.69	1.69	1.7	12.9	13.3
175	1.99	2.01	2.03	2.04	2.0	13.0	13.5
200	2.34	2.36	2.38	2.38	2.4	13.1	13.6
225	2.69	2.71	2.73	2.73	2.7	13.2	13.8
250	3.05	3.06	3.08	3.09	3.0	13.2	14.0
275	3.41	3.41	3.43	3.45	3.4	13.3	14.2
300	3.77	3.77	3.79	3.80	3.8	13.4	14.4
325	4.14	4.13	4.16	4.17	4.1	13.5	14.6
350	4.51	4.50	4.53	4.53	4.5	13.6	14.8
375	4.88	4.87	4.90	4.90	4.9	13.7	15.0
400	5.26	5.24	5.27	5.27	5.2	13.8	15.2
425	5.64	5.62	5.65	5.65	5.6	13.9	15.4
450	6.03	6.00	6.04	6.03	6.0	14.0	15.7
475	6.42	6.38	6.42	6.42	6.4	14.1	15.9
500	6.81	6.76	6.81	6.80	6.8	14.2	16.2
525	7.20	7.14	7.20	7.19	7.2	14.3	16.4
550	7.60	7.52	7.58	7.57	7.6	14.4	16.7
575	7.99	7.90	7.96	7.96	8.0	14.5	17.0
600	8.38	8.33	8.36	8.39	8.5	14.6	17.2
625	8.81	8.79	8.81	8.86	8.9	14.7	17.5
650	9.28	9.27	9.29	9.34	9.3	14.8	17.8
675	9.76	9.74	9.77	9.83	9.8	15.0	18.1
700	10.25	10.22	10.24	10.31	10.3	15.1	18.4
725	10.73	10.70	10.72	10.79	10.7	15.2	18.8
750	11.22	11.17	11.20	11.28	11.2	15.3	19.1
775	11.71	11.67	11.69	11.77	11.7	15.5	19.4
800	12.21	12.21	12.20	12.27	12.2	15.6	19.8
825	12.70	12.74	12.73	12.77	12.7	15.7	20.1
850	13.19	13.25	13.23	13.27	13.2	15.9	20.5
875	13.68	13.77	13.73	13.78	13.7	16.0	20.8
900	14.19	14.29	14.23	14.29	14.2	16.1	21.2
925	14.71	14.82	14.73	14.80	14.7	16.3	21.6
950	15.24	15.35	15.23	15.32	15.3	16.4	21.9
975	15.77	15.89	15.74	15.85	15.8	16.6	22.3
1000	16.32		16.25	16.18	16.4	16.7	22.7

Page intentionally left blank

Appendix II

Data Compilation for Thermal Diffusivity of Alloy 617 ($10^{-6} \cdot m^2/s$)

Temp. (°C)	Heat 1 VDM	Heat 2 SMC	Heat 3 Haynes	Heat 4 Oxford	Average	Poly Fit
25	2.97	2.93	2.89	2.93	2.93	2.90
50	3.03	3.03	2.95	2.99	3.00	2.99
75	3.10	3.09	3.03	3.07	3.07	3.08
100	3.18	3.17	3.12	3.15	3.16	3.17
125	3.26	3.26	3.20	3.23	3.24	3.25
150	3.33	3.34	3.27	3.30	3.31	3.33
175	3.41	3.40	3.36	3.38	3.39	3.41
200	3.50	3.50	3.44	3.45	3.47	3.49
225	3.58	3.58	3.53	3.54	3.56	3.56
250	3.65	3.66	3.61	3.62	3.63	3.64
275	3.73	3.74	3.69	3.69	3.71	3.71
300	3.81	3.82	3.77	3.77	3.79	3.79
325	3.88	3.91	3.86	3.86	3.88	3.86
350	3.97	3.99	3.93	3.94	3.96	3.93
375	4.03	4.06	4.01	4.00	4.02	4.00
400	4.11	4.13	4.08	4.07	4.10	4.08
425	4.18	4.20	4.15	4.15	4.17	4.15
450	4.24	4.28	4.23	4.22	4.24	4.22
475	4.32	4.34	4.30	4.29	4.31	4.30
500	4.39	4.41	4.37	4.34	4.38	4.37
525	4.46	4.48	4.43	4.40	4.44	4.45
550	4.53	4.53	4.50	4.47	4.51	4.52
575	4.59	4.61	4.55	4.55	4.58	4.60
600	4.67	4.68	4.62	4.62	4.64	4.68
625	4.74	4.77	4.69	4.70	4.73	4.77
650	4.83	4.85	4.80	4.79	4.82	4.85
675	4.97	4.99	4.93	4.93	4.96	4.94
700	5.07	5.07	5.04	5.05	5.06	5.03
725	5.02	4.97	5.01	5.03	5.01	4.94
750	4.89	4.86	4.92	4.96	4.91	4.89
775	4.81	4.82	4.85	4.88	4.84	4.86
800	4.81	4.85	4.84	4.84	4.84	4.87
825	4.85	4.91	4.90	4.88	4.89	4.90
850	4.91	4.98	4.95	4.95	4.95	4.94
875	4.99	5.05	5.00	4.99	5.01	5.00
900	5.06	5.11	5.10	5.06	5.08	5.07
925	5.14	5.19	5.16	5.14	5.16	5.14
950	5.20	5.25	5.22	5.16	5.21	5.22
975	5.26	5.29	5.30	5.24	5.27	5.28
1000	5.33	5.39	5.37	5.31	5.35	5.35

Page intentionally left blank

Appendix III

Data Compilation for Heat Capacity (C_p), Density and Thermal Conductivity of Alloy 617

Temp. T_C (°C)	Heat 1 C_p (J/(g*K)	Heat 2 C_p (J/(g*K)	Heat 3 C_p (J/(g*K)	Heat 4 C_p (J/(g*K)	Avg. C_p (J/(g*K)	Density ρ_T (kg/m³)	Poly fit diffusivity ($10^{-6} \cdot m^2/s$)	Product conductivity (W/m•K)	Poly fit conductivity (W/m•K)
50	0.435	0.435	0.431	0.443	0.436	8352	2.99	10.9	11.1
75	0.450	0.452	0.446	0.452	0.450	8344	3.08	11.6	11.6
100	0.461	0.462	0.457	0.465	0.461	8336	3.17	12.2	12.1
125	0.468	0.468	0.463	0.469	0.467	8328	3.25	12.6	12.6
150	0.473	0.474	0.470	0.475	0.473	8320	3.33	13.1	13.0
175	0.479	0.480	0.475	0.480	0.479	8311	3.41	13.6	13.5
200	0.485	0.486	0.482	0.488	0.485	8303	3.49	14.1	14.0
225	0.490	0.492	0.487	0.492	0.490	8294	3.56	14.5	14.4
250	0.493	0.495	0.490	0.495	0.493	8286	3.64	14.9	14.9
275	0.497	0.499	0.494	0.498	0.497	8277	3.71	15.3	15.3
300	0.502	0.505	0.498	0.505	0.502	8268	3.79	15.7	15.8
325	0.505	0.507	0.500	0.507	0.505	8259	3.86	16.1	16.2
350	0.509	0.511	0.504	0.513	0.509	8250	3.93	16.5	16.6
375	0.514	0.518	0.508	0.516	0.514	8241	4.00	17.0	17.0
400	0.519	0.520	0.510	0.519	0.517	8232	4.08	17.4	17.4
425	0.523	0.524	0.514	0.523	0.521	8222	4.15	17.8	17.8
450	0.528	0.529	0.518	0.529	0.526	8213	4.22	18.2	18.2
475	0.529	0.530	0.517	0.526	0.525	8203	4.30	18.5	18.6
500	0.533	0.536	0.525	0.534	0.532	8193	4.37	19.0	18.9
525	0.532	0.536	0.525	0.533	0.532	8184	4.45	19.3	19.3
550	0.542	0.542	0.523	0.540	0.537	8173	4.52	19.8	19.6
575	0.569	0.578	0.535	0.568	0.562	8163	4.60	21.1	21.7
600	0.620	0.632	0.583	0.619	0.613	8153	4.68	23.4	23.3
625	0.643	0.651	0.629	0.646	0.642	8142	4.77	24.9	24.5
650	0.644	0.645	0.630	0.636	0.638	8132	4.85	25.2	25.3
675	0.639	0.643	0.626	0.635	0.636	8121	4.94	25.5	25.7
700	0.643	0.647	0.625	0.634	0.637	8110	5.03	26.0	25.7
725	0.638	0.643	0.618	0.633	0.633	8099	4.94	25.3	25.4
750	0.643	0.644	0.618	0.632	0.634	8087	4.89	25.1	25.3
775	0.645	0.652	0.632	0.635	0.641	8076	4.86	25.2	25.2
800	0.649	0.657	0.642	0.639	0.647	8064	4.87	25.4	25.2
825	0.646	0.655	0.627	0.643	0.643	8052	4.90	25.3	25.3
850	0.647	0.652	0.624	0.637	0.640	8040	4.94	25.4	25.5
875	0.648	0.658	0.628	0.643	0.644	8028	5.00	25.9	25.8
900	0.651	0.662	0.632	0.641	0.646	8015	5.07	26.3	26.2
925	0.650	0.660	0.634	0.644	0.647	8003	5.14	26.6	26.7
950	0.659	0.673	0.649	0.650	0.658	7990	5.22	27.4	27.4

Page intentionally left blank

Appendix IV

Data Compilation for Modulus of Elasticity for Alloy 617

Temp (°C)	Heat 1 plate	Heat 2 rod	ASME	poly fit*
22	203.8			
25	203.7		201	200
30	203.3	206.5		
35	203.0	206.2		
40	202.6	205.8		
45	202.2	205.5		
50	201.7	205.0		
55	201.3	204.6		
60	200.9	204.2		
65	200.5	203.8		
70	200.1	203.4		
75	199.7	203.0		
80	199.4	202.6		
85	199.0	202.2		
90	198.7	201.9		
95	198.3	201.5		
100	198.0	201.2	196	196
105	197.6	200.8		
110	197.3	200.5		
115	197.0	200.1		
120	196.6	199.8		
125	196.3	199.4		
130	196.0	199.1		
135	195.7	198.8		
140	195.4	198.4		
145	195.1	198.1		
150	194.8	197.8	193	194
155	194.5	197.4		
160	194.2	197.1		
165	193.9	196.8		
170	193.6	196.5		
175	193.3	196.2		
180	193.0	195.9		
185	192.7	195.6		
190	192.4	195.2		
195	192.1	194.9		
200	191.8	194.6	191	191
205	191.5	194.3		
210	191.2	194.0		
215	190.9	193.7		
220	190.6	193.3		
225	190.3	193.0		
230	190.1	192.7		
235	189.8	192.4		
240	189.5	192.1		
245	189.2	191.8		
250	188.9	191.5	189	189
255	188.6	191.2		
260	188.3	190.9		
265	188.1	190.6		
270	187.8	190.3		
275	187.5	189.9		
280	187.2	189.6		
285	186.9	189.3		
290	186.6	189.0		
295	186.3	188.6		
300	186.0	188.3	187	186

Temp (°C)	Heat 1 plate	Heat 2 rod	ASME	poly fit*
305	185.7	188.0		
310	185.4	187.7		
315	185.1	187.4		
320	184.8	187.0		
325	184.5	186.7		
330	184.2	186.4		
335	183.9	186.1		
340	183.6	185.8		
345	183.3	185.5		
350	182.9	185.1	184	183
355	182.6	184.8		
360	182.3	184.5		
365	182.0	184.2		
370	181.7	183.9		
375	181.4	183.6		
380	181.2	183.3		
385	180.8	182.9		
390	180.6	182.6		
395	180.3	182.3		
400	180.0	182.0	181	181
405	179.7	181.7		
410	179.4	181.4		
415	179.1	181.1		
420	178.8	180.8		
425	178.5	180.5		
430	178.3	180.2		
435	178.0	179.9		
440	177.7	179.5		
445	177.4	179.2		
450	177.1	178.9	178	178
455	176.9	178.6		
460	176.6	178.3		
465	176.3	178.0		
470	176.0	177.7		
475	175.8	177.4		
480	175.5	177.1		
485	175.2	176.8		
490	174.9	176.5		
495	174.7	176.2		
500	174.4	175.9	174	175
505	174.1	175.6		
510	173.8	175.2		
515	173.5	174.9		
520	173.2	174.6		
525	172.9	174.3		
530	172.6	173.9		
535	172.2	173.6		
540	171.9	173.3		
545	171.5	172.9		
550	171.2	172.5	171	171
555	170.8	172.1		
560	170.4	171.7		
565	170.0	171.2		
570	169.6	170.8		
575	169.2	170.3		
580	168.8	169.9		
585	168.3	169.5		
590	167.9	169.0		
595	167.5	168.6		
600	167.0	168.1	167	168
605	166.6	167.7		

Temp (°C)	Heat 1 plate	Heat 2 rod	ASME	poly fit*
610	166.2	167.3		
615	165.8	166.8		
620	165.3	166.4		
625	164.9	166.0		
630	164.5	165.6		
635	164.0	165.1		
640	163.6	164.7		
645	163.2	164.3		
650	162.8	163.9	164	164
655	162.3	163.5		
660	161.9	163.0		
665	161.5	162.6		
670	161.1	162.2		
675	160.7	161.8		
680	160.3	161.4		
685	159.9	161.0		
690	159.5	160.6		
695	159.2	160.2		
700	158.8	159.8	160	160
705	158.4	159.4		
710	158.0	159.0		
715	157.6	158.6		
720	157.2	158.2		
725	156.9	157.8		
730	156.5	157.4		
735	156.1	157.1		
740	155.7	156.7		
745	155.3	156.3		
750	154.9	155.9	156	156
755	154.5	155.6		
760	154.1	155.2		
765	153.7	154.8		
770	153.3	154.4		
775	152.9	154.0		
780		153.6		
785		153.2		
790		152.8		
795		152.4		
800		152.0	152	151
805		151.7		
810		151.3		
815		150.9		
820		150.5		
825		150.2		
830		149.8		
835		149.5		
840		149.0		
845		148.7		
850		148.3	146	147
855		147.9		
860		147.5		
865		147.0		
870	147.3	146.6		
875		146.2		
880	145.5			
885		145.3		
890	144.0	144.8		
895	143.1			
900	142.9	143.7		141
905				
910				

Temp (°C)	Heat 1 plate	Heat 2 rod	ASME	poly fit*
915		142.5		
920		142.1		
925		141.3		
930	139.5	140.8		
935	139.4	140.4		
940	138.7	139.7		
945	138.1	139.3		
950	137.5	138.7		136
955	137.0	138.1		
960	136.4	137.4		
965	135.7	136.7		
970	135.0	135.9		
975	134.3	135.5		
980		135.3		
985	132.6	134.6		
990	132.3	134.1		
995	131.6	133.5		
1000	131.1	133.1		

*Third order polynomial fit to ASME Code values

Background Document – Record No. 16-996

Contents

- Balloting Actions

- Article HBB-T-1500 Buckling and Instability
- HBB-T-1520 Buckling Limits
- HBB-T-1522 Time-Dependent Buckling

Page intentionally left blank

Alloy 617 Code Case Balloting Actions

RC #	Item	Section II and III Committees (See Color Key Below For Balloting Actions)								
16-994	Permissible base and weld materials, allowable stress values	WG-ASC	SG-ETD	SG-HTR	SG-MFE	II-SG-NFA	II-SG-SW	BPV-II		
16-995	Physical properties and extension of modulus values to higher temperatures	WG-ASC	SG-ETD	SG-HTR	SG-MFE	II-SG-NFA	II-SG-PP	BPV-II		
16-996	Temperature-time limits for NB buckling charts	WG-AM	SG-ETD	SG-HTR	SG-MFE	II-SG-EP	BPV-II	II-SG-NFA	SC-D	
16-997	Huddleston parameters, ISSCs	WG-ASC	SG-ETD	SG-HTR	II-SG-NFA	BPV-II	SC-D			
16-998	Negligible creep, Creep-Fatigue: D-diagram and EPP	WG-CFNC	SG-ETD	SG-HTR	SC-D					
16-999	EPP strain limits	WG-AM	SG-ETD	SG-HTR	SC-D					
16-1000	Fatigue design curves	WG-CFNC	WG-FS	SG-ETD	SG-HTR	SG-DM	SC-D			
16-1001	Alloy 617 Overall Code Case	WG-ASC	WG-AM	WG-CFNC	WG-FS	SG-ETD	SG-HTR	SG-MFE	SC-D	BPV-II
		BPV-III								

Color Key	Balloting Action
	For Review and Approval
	For Review and Comment

Page intentionally left blank

ARTICLE HBB-T-1500 BUCKLING AND INSTABILITY

HBB-T-1520 BUCKLING LIMITS

HBB-T-1522 Time-Dependent Buckling

Scope

This document provides the background and technical basis supporting the recommended buckling charts for Alloy 617 specified as Figures HBB-T-1522-1, HBB-T-1522-2, and HBB-T-1522-3.

Background

Section III, Division 5, HBB-T-1520 presents two options for designing a component against time independent and time dependent buckling. For either time independent or time dependent buckling a designer can perform a full instability analysis, using a factorized load for load-controlled situations. Alternatively, for time independent buckling the designer can use the buckling charts from Section III, Division 1, NB-3133. These buckling charts apply to three simple geometries: a cylinder under axial compression, a sphere under external pressure, and a cylinder under external pressure.

Instead of performing a full instability analysis the designer can skip the time-dependent buckling check if they can demonstrate that time-independent buckling will occur at a lower load and therefore govern the design. In this case the designer only needs to check for time-independent buckling against the charts in Section III, Division 1, NB-3133. To aid in this task HBB-T-1522 provides three buckling charts. These three charts correspond to the three simple geometries used in NB-3133 (a cylinder under axial compression, a sphere under external pressure, and a cylinder under external pressure). The charts delineate regions where, for these geometries, time independent buckling occurs at a lower load than time dependent buckling and therefore the designer can safely skip an explicit check for time-dependent, creep buckling.

Conceptually, the lines on the buckling charts are the conditions at which the allowable load for time-dependent creep buckling equals the allowable load for time-independent buckling. A Welding Research Council (WRC) technical report describes the process of constructing this line for the three geometries[1].

The basis of the WRC approach is an analytical solution for the elastic-plastic buckling load of each the three geometries in terms of the tangent and secant moduli of the flow curve. These moduli are functions of the applied load and so solving for the buckling limit load requires solving an implicit nonlinear equation. For time-dependent buckling the report assumes a method of isochronous curves – for time dependent buckling the method uses the same, elastic-plastic solutions but replaces the flow curve with the isochronous curve for the design life of interest. The region where the designer may skip the time-dependent buckling check is where the allowable load for time-dependent buckling, using the isochronous curves, is greater than that for time-independent buckling, using the Code hot tensile curves. At first thought it would seem that the time dependent allowable load will always be less than the allowable load for time dependent buckling as the isochronous curves tend to have lower values of tangent and secant modulus than the hot tensile curves. However, Section III, Division 5 applies a load factor of 3 for time-independent buckling but only 3/2 for time dependent buckling. Therefore, there is a large region where the time-independent allowable load governs.

The table below summarizes the equations used to determine the buckling charts for each of the three geometries. In these equations E_t is the tangent modulus of either the design hot tensile (time-independent buckling) or design isochronous (time-dependent buckling) flow curve and E_s is similarly

---

[1] Griffin, D. S. "Design Limits for Elevated-Temperature Buckling." In Welding Research Council Bulletin 443 *External Pressure: Effect of Initial Imperfections and Temperature Limits*, pp. 11-26, 1999.

the secant modulus of the appropriate flow curve. Both these quantities are functions of the equivalent stress σ_i, calculated here using the Tresca theory. For time-dependent buckling using the isochronous curves these quantities are also functions of the design life τ. The factor χ is

$$\chi = \frac{1}{2} - \left(\frac{1}{2} - v\right)\frac{E_s}{E}$$

for the Section II values of Young's modulus E and Poisson's ratio v. t/r is the thickness-to-radius aspect ratio of the vessel. Computing the tangent and secant moduli of the flow curves requires design hot tensile and isochronous stress-strain curves. These curves are defined in this Code Case for Alloy 617. Following the WRC report, the buckling calculations for Alloy 617 here use the Division 5 curves directly, which implies the buckling charts are based on an average, rather than lower bound, material response.

	σ_p	α	σ_i	F_{ti}	F_{td}
Cylinder under external pressure	$\dfrac{E_t(t/r)^2}{4(1-\mu^2)}$	1	$\dfrac{\sqrt{3}}{2}\alpha\sigma_p$	3	3/2
Sphere under external pressure	$\dfrac{(t/r)\sqrt{E_t E_s}}{\sqrt{3(1-\mu^2)}}$	1/2	$\alpha\sigma_p$	3	3/2
Cylinder under axial compression	$\dfrac{(t/r)\sqrt{E_t E_s}}{\sqrt{3(1-\mu^2)}}$	1	$\alpha\sigma_p$	3	3/2

Table of solutions for the three buckling problems.

For each geometry the region of interest is given by the equation

$$\frac{1}{F_{ti}}\alpha\sigma_p(\sigma_i, T, t/r) > \frac{1}{F_{td}}\alpha\sigma_p(\sigma_i, T, t/r, \tau)$$

which describes the region where the time independent allowable buckling load exceeds the time dependent allowable buckling load. σ_i is a function of σ_p but this still leaves three free variables: temperature (T), aspect ratio (t/r), and design life (τ). To simplify this equation to a buckling chart that can be plotted in 2D the WRC method makes simplifying assumptions for the three geometries. For the cylinder under external pressure the method fixes $\tau = 100{,}000$ hours leaving the Division 5 buckling chart for this geometry as a function of temperature and aspect ratio. For the cylinder under axial load and the sphere under external pressure the method fixes the aspect ratio $r/t = 150$ leaving the buckling chart for these cases as a function of temperature and design life. The WRC report describes the technical justification for these assumptions in detail. Both are conservative assumptions for reasonable vessel designs.

The implementation of the WRC method was verified by reproducing the current Section III, Division 5 buckling charts for 304H and 316H. Solving the reduced equations numerically, including the simplifying assumptions, produces the buckling charts proposed for Alloy 617 as part of this Code Case.

Background Document Record No. 16-997

Contents

- Balloting Actions

- HBB-T-1411 Huddleston Parameter for Multiaxial Creep Failure Criterion

- HBB-T-1800 Isochronous Stress-Strain Relations

Page intentionally left blank

Alloy 617 Code Case Balloting Actions

RC #	Item	Section II and III Committees (See Color Key Below For Balloting Actions)								
16-994	Permissible base and weld materials, allowable stress values	WG-ASC	SG-ETD	SG-HTR	SG-MFE	II-SG-NFA	II-SG-SW	BPV-II		
16-995	Physical properties and extension of modulus values to higher temperatures	WG-ASC	SG-ETD	SG-HTR	SG-MFE	II-SG-NFA	II-SG-PP	BPV-II		
16-996	Temperature-time limits for NB buckling charts	WG-AM	SG-ETD	SG-HTR	SG-MFE	II-SG-EP	BPV-II	II-SG-NFA	SC-D	
16-997	Huddleston parameters, ISSCs	WG-ASC	SG-ETD	SG-HTR	II-SG-NFA	BPV-II	SC-D			
16-998	Negligible creep, Creep-Fatigue: D-diagram and EPP	WG-CFNC	SG-ETD	SG-HTR	SC-D					
16-999	EPP strain limits	WG-AM	SG-ETD	SG-HTR	SC-D					
16-1000	Fatigue design curves	WG-CFNC	WG-FS	SG-ETD	SG-HTR	SG-DM	SC-D			
16-1001	Alloy 617 Overall Code Case	WG-ASC	WG-AM	WG-CFNC	WG-FS	SG-ETD	SG-HTR	SG-MFE	SC-D	BPV-II
		BPV-III								

Color Key	Balloting Action
	For Review and Approval
	For Review and Comment

Page intentionally left blank

BACKGROUND DOCUMENTS – R-16-997

HBB-T-1411 Huddleston Parameter for Multiaxial Creep Failure Criterion

Scope

This document provides the background/technical basis in support of the recommendation for the constant, *C*, for Alloy 617 in Subarticle HBB-T-1411.

Background

A multiaxial failure criterion for creep rupture has been developed by Huddleston.[1,2] It offers significant improvements in predicting creep rupture under multiaxial (three-dimensional) stress states over classical models such as von Mises or Tresca. The equation used to determine the equivalent stress for the inelastic analysis approach used to satisfy deformation-controlled limits in HBB-T-1411 includes a constant, *C*, which is based on Huddleston's approach. Using the symbols from HBB-T-1411, the equivalent stress for the Huddleston theory is

$$\sigma_e = \bar{\sigma} \exp\left[C \left(\frac{J_1}{S_s} - 1 \right) \right] \tag{1}$$

where J_1 is the first invariant of the stress tensor, S_s is an invariant stress parameter, and $\bar{\sigma}$ is the von Mises equivalent stress, which are defined below. Note that in Huddleston's papers, the constant, *C*, is given the label of b [1,2].

$$J_1 = \sigma_1 + \sigma_2 + \sigma_3 \tag{2}$$

$$S_s = [\sigma_1{}^2 + \sigma_2{}^2 + \sigma_3{}^2]^{1/2} \tag{3}$$

$$\bar{\sigma} = \frac{1}{\sqrt{2}} [(\sigma_1 - \sigma_2)^2 + (\sigma_2 - \sigma_3)^2 + (\sigma_3 - \sigma_1)^2]^{1/2} \tag{4}$$

where $\sigma_1, \sigma_2, \sigma_3$ are principal stresses.

In Subarticle HBB-T-1411, a value of 0.24 has been accepted for the Huddleston constant for Types 304 and 316 stainless steels, and 0 is used for alloy 800H. When *C*=0, the effective stress is equivalent to the von Mises effective stress. As *C* increases, there is a larger difference between the equivalent stress under tension vs. compression.

A "universal" value of *C*=0.24 has been recommended for austenitic stainless steels and Inconel if other specific data are not available.[1] When *C*=0.24 is used for 316 or 304, the predictions of rupture life are more accurate and also less overly-conservative. "…both von Mises and Tresca theories result in highly conservative life predictions for biaxial tension-compression stress states and also are less accurate for tension-tension stress states."[1] Specific analyses have yielded values of 0.29 for Type 304 SS,[1] 0.19 for Type 316 SS,[2] and 0.25 for Inconel 600.[3]

The biaxial isochronous stress-rupture contour for Inconel 600 is shown in Figure 1. Inconel 600 is an austenitic Ni based solid solution alloy similar to Alloy 617. As the figure shows, the Huddleston stress-rupture contour is slightly more conservative in tension (upper right quadrant) and less conservative in compression (lower left quadrant).
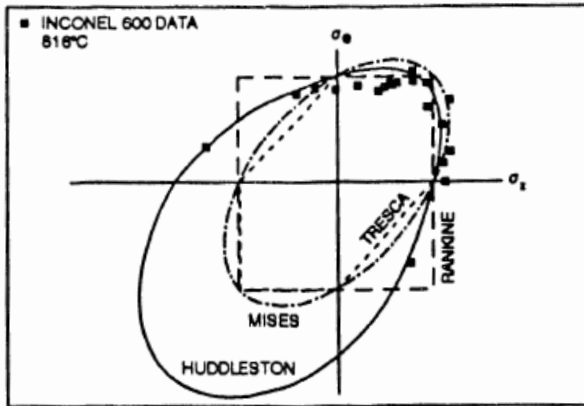
Figure 1. Biaxial isochronous stress-rupture contour for Inconel 600, showing C=0.24821.[3]

Code Case Recommendation

Inconel (Alloy 600) is a very similar Ni based solid solution alloy to Alloy 617. Huddleston recommends austenitic stainless steels and Inconel 600 use C=0.24 if alloy specific data are not available. This value is supported by calculation of C for a single compression hold creep-fatigue test (provided in detail below) indicating $C = 0.25$. Therefore, a value of C=0.24 is recommended for Alloy 617, which is consistent with the other austenitic alloys in Section III Division 5.

Calculation of Huddleston Constants Using a Single Compression Hold Creep-fatigue Test

In Section 4.5.2.2 of his 2003 report,[5] Huddleston demonstrates how to calculate the constant from a single compression hold creep-fatigue test. In the following analysis, the symbols used in HBB-T-1411 and the background documentation for HBB-T-1420-2 (C&S connect RC-16-998) will be used; in some cases these differ from symbols used within Huddleston's papers.[1, 2, 3]

A single compression hold test that was performed at 950°C, 0.3% strain range with a 3 minute hold time. Tensile-hold creep fatigue as well as low cycle fatigue (LCF) (no hold) test data is also available for this test condition [4].

Materials

Creep-fatigue has been performed at INL on specimens machined from an Alloy 617 reference material plate.[4] The 37 mm thick solution-annealed plate is from heat 314626, produced by ThyssenKrupp VDM and the composition is given in Table 1. Although the average grain size of the plate is quantified as approximately 150 μm, significant grain size inhomogeneity is present in the microstructure.

Table 1. The composition in wt% of Alloy 617.

	Ni	C	Cr	Co	Mo	Fe	Al	Ti	Si	Cu	Mn	S	B
314626	Bal.	0.05	22.2	11.6	8.6	1.6	1.1	0.4	0.1	0.04	0.1	0.002	0.001

Quality

Creep-fatigue properties of the Alloy 617 reference plate (heat 314626) reported by the Idaho National Laboratory (INL) through the Next Generation Nuclear Plant (NGNP) or Advanced Reactor Technologies (ART) programs were determined under an NQA-1 quality program. Details of the quality program implementation are given in INL document PLN-2690 "Idaho National Laboratory Advanced Reactor

Technologies Technology Development Office Quality Assurance Program Plan."

Creep-Fatigue Testing Procedure

Cylindrical cyclic test specimens [4], 0.295 in. (7.5 mm) diameter with a reduced section of 0.79 in. (20 mm) and gage length of 0.5 in. (12.7 mm), were machined from heat 314626. Low stress grinding and longitudinal polishing were used in the final machining of the reduced section to eliminate cold work and circumferential machining marks. The long axis of the specimens was aligned with the rolling direction.
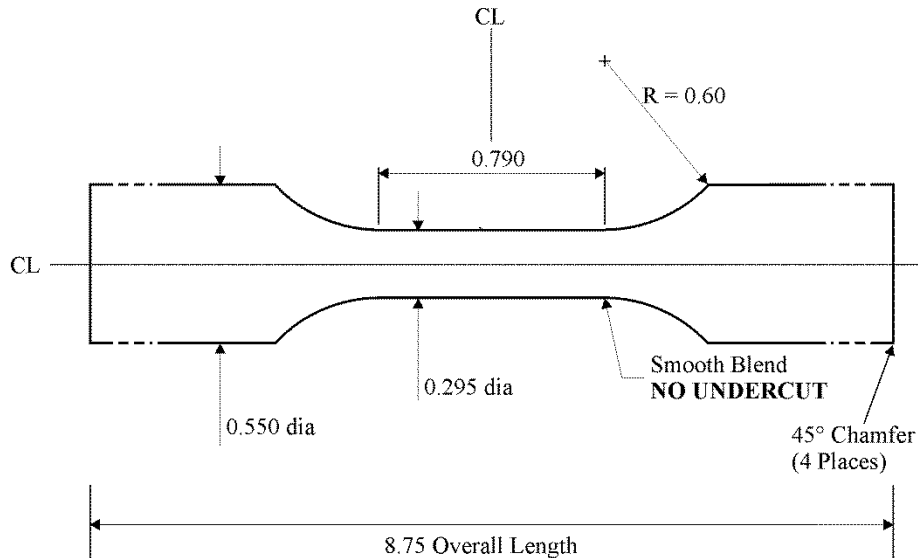
Figure 2. Specimen used for fatigue and creep-fatigue tests at 850 and 950°C.

Fully reversed strain-controlled creep-fatigue testing was conducted in air on servo-hydraulic test machines at 950°C, a total strain range of 0.3%, with a strain rate during loading and unloading of 10^{-3}/s. Multiple tests with a three minute tensile hold, as well as a single compression-hold specimen were tested using calibrated extensometers for strain determination.[8, 9,10] A schematic of the tensile-hold creep-fatigue waveform is shown in 3. Several intermediate strain cycles were applied during a limited number of initial cycles before reaching the target strain level on most of the tests, in order to prevent overshooting the target strain on the first cycle. Testing was designed to be compliant with American Society for Testing and Materials (ASTM) Standard E606.[11]

Specimens were heated either using a 3-zone resistance furnace or by radio-frequency induction. The temperature gradient was measured using a specimen with spot-welded thermocouples along the gage section, and was found to vary less than 1%. The temperature was monitored and/or controlled using either a spot-welded thermocouple on the specimen shoulder or a thermocouple loop at the center of the gage section, in conjunction with calibration curves from the temperature profile characterization. Test temperature was generally maintained within 2°C throughout the duration of the test.
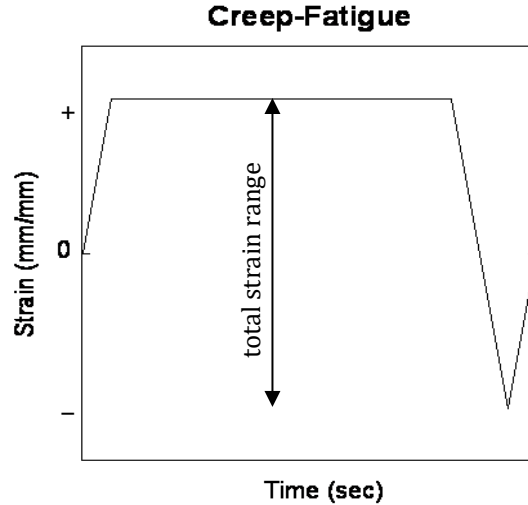
Figure 3. Schematics of the strain versus time waveforms for tensile-hold creep-fatigue.

Peak tensile and compressive load and strain and temperature were recorded for each cycle. Strain, load and temperature were recorded as a function of time for each of the first hundred cycles, and periodically thereafter, with the cycle recording frequency dependent upon the anticipated lifetime of the specimen. Cyclic stress-strain curves (hysteresis loops) and stress relaxation behavior can be plotted for the cycles where the load and strain data have been collected.

The number of cycles to failure, N_f, is determined from a plot of the ratio of peak tensile to peak compressive stress versus cycles, as originally described in Totemeier and Tian.[12] Macro-crack initiation, N_i, is defined as the point at which the stress ratio deviated from linearity; and failure, N_f, is defined as a 20% reduction in stress ratio from the point of deviation. The ratio method could not be used for the specimen that included a compressive hold so N_i and N_f were determined from the peak tensile stress curve instead, using a 25% reduction in stress from the point of deviation.

Development of Creep Damage Equations

The creep damage for the kth creep-fatigue cycle, D_k^c (Huddleston[5] uses a symbol of d_c for creep damage per cycle), can be determined by evaluating the integral

$$D_k^c = \int \left(\frac{1}{T_d}\right)_k dt \qquad [5]$$

$$D_k^c = \int_0^{t_h} \frac{dt}{T_d}$$

To perform the integration, the correlation between the rupture time, T_d (T_r in Huddleston[5]), temperature, and applied stress for Alloy 617 is required. A Larson-Miller relation is a common way to do this and for Alloy 617, a linear equation in log stress describes the creep data well.[6]

$$LMP = a_0 + a_1 log_{10}(\sigma) \qquad [6]$$

where a_0 and a_1 are the fitting parameters, σ is stress (MPa) and LMP is the Larson-Miller Parameter, defined as

$$LMP = T\left(C_{LM} + log_{10}(t)\right) \qquad [7]$$

and T is the temperature in Kelvin, C_{LM} is the Larson-miller constant, and t is time in hours. Isolating t on the left side, gives

$$log_{10}(t) = -C_{LM} + \frac{a_0}{T} + \frac{a_1}{T} log_{10}(\sigma)$$ [8]

and changing base to the natural logarithm gives

$$\frac{ln(t)}{ln(10)} = -C_{LM} + \frac{a_0}{T} + \frac{a_1}{T} \frac{ln(\sigma)}{ln(10)}$$ [9]

which can be rearranged as

$$ln(t) = -C_{LM} \, ln(10) + \frac{a_0 \, ln(10)}{T} + \frac{a_1 ln(\sigma)}{T}$$ [10]

Hence

$$t = \exp\left(-C_{LM} \, ln(10) + \frac{a_0 \, ln(10)}{T}\right) \sigma^{\left(\frac{a_1}{T}\right)}$$ [11]

or $\quad t = 10^{\left(-C_{LM} + \frac{a_0}{T}\right)} \sigma^{\left(\frac{a_1}{T}\right)}$ [12]

For the calculations that follow,[7] it is more convenient to use time in seconds for T_d, so we have:

$$T_d = 3600 * 10^{\left(-C_{LM} + \frac{a_0}{T}\right)} \sigma^{\left(\frac{a_1}{T}\right)}$$ [13]

We can rewrite Equation [13] as

$$T_d = A\sigma_e{}^m$$ [14]

where

$$A = 3600 * 10^{\left(-C_{LM} + \frac{a_0}{T}\right)}, \quad m = \frac{a_1}{T}$$ [15]

In order to integrate $\frac{1}{T_d}$ over the hold time for Equation [5], stress must be expressed as a time dependent function. This requires analysis of the stress as it relaxes during the strain hold period, which can be fit to a power-law trend curve using the following functional form:

$$\sigma = b_0(t + t_0)^{b_1}$$ [16]

where b_0, b_1, and t_0 are treated as fitting parameters, σ is stress in MPa and t and t_0 are in seconds. An example of relaxation during the creep-fatigue tensile hold is shown in Figure 4
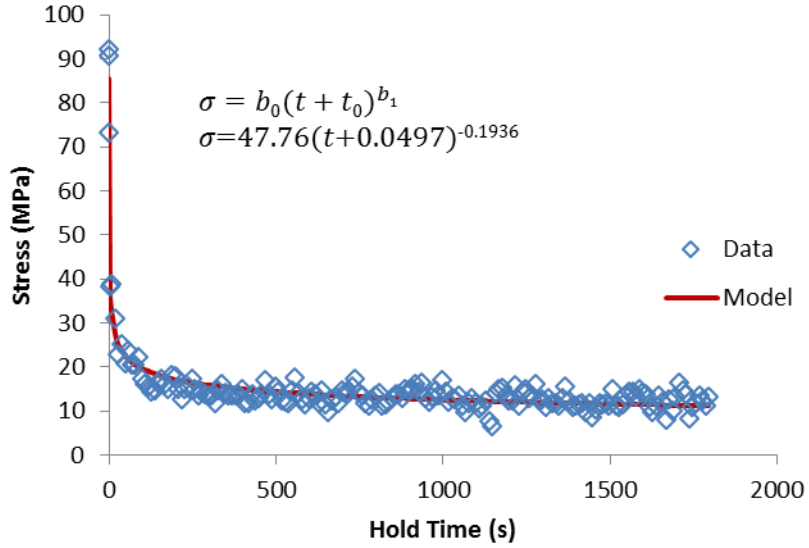
Figure 4. Example of a power law fit of the form $\sigma = b_0(t + t_0)^{b_1}$ to the stress relaxation portion of the midlife creep-fatigue cycle of an Alloy 617 specimen cycled at 950°C, 0.3% total strain, and 1800 s hold time.

Substituting Equations [14] – [16] into Equation [5] results in

$$D_k^c = \int_0^{t_h} \frac{1}{A} (b_0(t + t_0)^{b_1})^{-m} \, dt \qquad [17]$$

$$= \frac{b_0^{-m}}{A(1-b_1 m)} \left((t_h + t_0)^{1-b_1 m} - (t_0)^{1-b_1 m}\right)$$

Applying the Huddleston Model

The equivalent stress for uniaxial compression for the Huddleston theory given in Equation [1] is

$$\sigma_e = |\bar{\sigma}| \exp(-2C) \qquad [18]$$

since $\frac{J_1}{S_s} = -1$ for compression. Recall that Huddleston[5] uses a symbol of b for the constant. Substituting this into Equation [14] gives

$$T_d = A[\,|\bar{\sigma}| \exp(-2C)]^m \qquad [19]$$

The creep damage for each creep-fatigue cycle considering the Huddleston multiaxial criterion, d_c, is obtained by substituting Equation [19] into Equation [5]

$$d_c = \int_0^{t_h} \frac{dt}{A[\,|\bar{\sigma}| \exp(-2C)]^m} \qquad [20]$$

$$= \exp(2Cm) \int_0^{t_h} \frac{dt}{A|\bar{\sigma}|^m}$$

Substituting in Equation [16] gives

$$d_c = \exp(2Cm) \int_0^{t_h} \frac{dt}{A|b_0(t+t_0)^{b_1}|^m} \qquad [21]$$

$$= \exp(2Cm) \int_0^{t_h} \frac{1}{A} \left(b_0(t + t_0)^{b_1}\right)^{-m} dt$$

The integral above is defined as D_k^c in equation [17],[7] Therefore

$$d_c = D_k^c \, exp(2Cm) \tag{22}$$

The total compressive creep damage at failure, D_C, is determined by multiplying by the number of cycles to failure, N_f,

$$D_C = N_f d_c \tag{23}$$
$$= N_f \, D_k^c \, exp(2Cm)$$

The Creep-Fatigue Interaction Diagram

The creep-fatigue interaction diagram, Figure HBB-T-1420-2, proposed for Alloy 617 is reproduced in Figure 5. The bilinear curves represent the damage envelopes for each material, within which calculated damage for a design must fall. A design point must fall on or below the bilinear line. The interaction point, (F, F) is where the total fatigue damage, D_F, and total creep damage (Huddleston[5] uses a symbol of D_F for total fatigue damage), D_C, are equal. Therefor the line segments are given as

$$D_C = 1+(F–1)D_F/F \qquad \text{when } D_C \geq D_F \tag{24}$$
$$D_F = 1+(F–1)D_C/F \qquad \text{when } D_C \leq D_F \tag{25}$$
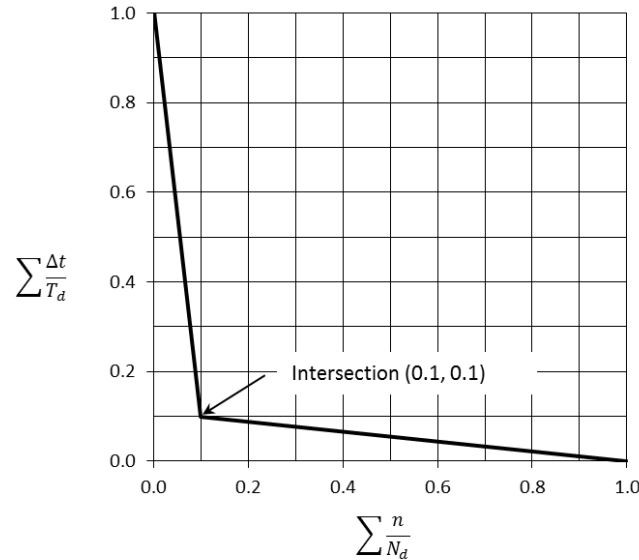
Figure 5. Creep-fatigue interaction diagram for ASME Section III, Division 5, Subsection HB, Subpart B. The coordinates of the intersections of the bilinear curves are shown in the legend.

Calculating the Huddleston Constant

In Huddleston's proposed methodology for using compressive hold creep-fatigue data [5], the same data from a single test is used to determine the intersection point on the creep-fatigue damage interction diagram. However, for this evaluation the interaction diagram has been previously established as shown above in Figure 5 based on numerous data points developed mostly from tensile hold creep-fatigue data. For this assessment of the Huddleston constant, C, the previously established interception point at (0.1, 0.1) as shown in Figure 5 is used.

The Huddleston constant, C can now be calculated. Rearranging Equation [23] in terms of C

$$C = \frac{1}{2m} \, Ln \left[\frac{D_C}{N_f D_k^c} \right] \tag{26}$$

Case 1: $d_c \leq d_n$

Rearranging Equation [25] in terms of D_C and substituting into Equation [26]

$$C = \frac{1}{2m} \, Ln \left[\frac{F(D_F - 1)}{(F-1)N_f D_k^c} \right]$$ [27]

The total fatigue damage at failure, D_F is defined as

$$D_F = N_f/N_d$$ [28]

where N_d, is the cycles to failure for LCF testing at the same temperature and strain range. The fatigue damage/cycle, d_f, is the inverse of N_d therefore

$$D_F = N_f \, d_f$$ [29]

and

$$C = \frac{1}{2m} \, Ln \left[\frac{F(Nf \, df - 1)}{(F-1)N_f D_k^c} \right]$$ [30]

Assuming an interaction point (F,F), where $F = 0.1$,[7] and using the values obtained for the compression hold creep fatigue specimen given in

Table 2, the Huddleston constant for Case 1 is 0.253. Recall that the constant Huddleston reports for Inconel 600 is 0.25. A similar process is used to determine C for Case 2 where $d_c \geq d_f$, using Equation [24], however the Huddleston constant for Case 2 is nonsensical since the logarithm of a negative value is required. Calculating d_c using Equation [22] and assuming $C = 0.253$ gives $d_c = 1.327 \times 10^{-4} \exp [2 \cdot 0.253 \cdot -4.83] = 1.19 \times 10^{-5}$, confirming $d_c \leq d_f$, so Equation [27] is appropriate.

Table 2. Values of constants and from measurements on specimen 4-1-7.

Description	Symbol	value	units
Larson-Miller constant	C	16.73049602	
Linear regression for L-M	a_0	32976.41125	
Linear regression for L-M	a_1	-5908.103107	
Stress-relaxation fit constant	b_0	86.93	MPa
Stress-relaxation fit constant	b_1	-0.3117	
Stress-relaxation fit constant	t_0	0.298	sec
LCF cycles to failure (avg)	N_d	8006	cycles
C-f cycles to failure 4-1-7	N_f	4373	cycles
Total creep damage 4-1-7	D_C	0.5805	
Total fatigue damage 4-1-7	D_F	0.5462	
Creep damage/mid cycle 4-1-7	D_k^c	1.327E-4	
Exponent defined as a_1/T in K	m	-4.83	

References

[1] R. L. Huddleston, "Assessment of an Improved Multiaxial Strength Theory Based on Creep-Rupture Data for Type 316 Stainless Steel," Journal of Pressure Vessel Technology, Vol 115, pp. 117-184, 1993.

[2] R. L. Huddleston, "An Improved Multiaxial Creep-Rupture Strength Criterion," Journal of Pressure Vessel Technology, Vol 107, pp. 421-429, 1985.

[3] R. L. Huddleston, "Assessment of an Improved Multiaxial Strength Theory Base on Creep-Rupture Data for Inconel 600," ASME Pressure Vessel & Piping, Denver, CO, July 26-30, 1993.

[4] K. Wright, L. J. Carroll, C. Cabet, T. M. Lillo, J. K. Benz, J. A. Simpson, W. R. Lloyd, J. A. Chapman, and R. N. Wright, "Characterization of elevated temperature properties of heat exchanger and steam generator alloys," Nuclear Engineering Design, Vol. 251, 2012, pp. 252–260.

[5] R. L. Huddleston, "Two-Parameter Failure Model Improves Time-Independent and Time-Dependent Failure Predictions," UCRL-TR-202300, December 2003.

[6] R. W. Swindeman and M. J. Swindeman, Analysis of Time Dependent Materials Properties Data, ASME Standards Technology, LLC, 2014.

[7] C-16-998, "Background Document – Record No. 16-998," HBB-T-1420-2 Creep-Fatigue Damage Envelope, Creep-Fatigue Interaction Analyusis.

[8] L. J. Carroll, C. Cabet, M. C. Carroll, and R. N. Wright, "The development of microstructural damage during high temperature creep–fatigue of a nickel alloy," International Journal of Fatigue, Vol. 47, 2013, pp. 115 125.

[9] M. C. Carroll, and L. J. Carroll, "Developing Dislocation Subgrain Structures and Cyclic Softening During High-Temperature Creep–Fatigue of a Nickel Alloy," Metallurgical and Materials Transactions, Vol. 44, 2013, No. 8, pp. 3592 3607.

[10] P. G. Pritchard, L. Carroll, T. Hassan, "Constitutive Modeling of High Temperature Uniaxial Responses of Alloy 617," Transactions of the American Nuclear Society, Vol 109, 2013, pp. 562-565.

[11] Standard Test Method for Strain–Controlled Fatigue Testing, ASTM E606/E606M-12, ASTM International, West Conshohocken, PA.

[12] T. Totemeier T. and Tian H., "Creep-Fatigue-Environment Interactions in Inconel 617," Materials Science and Engineering A, Vol. 468-470, 2007, p. 81-87.

Page intentionally left blank

ARTICLE HBB-T-1800 ISOCHRONOUS STRESS-STRAIN RELATIONS

Scope

This document provides the background and technical basis supporting the isochronous stress-strain curves proposed for Alloy 617 as Figures HBB-T-1800-1 through HBB-T-1800-20.

Background

Section III, Division 5, HBB-T-1800 provides average property hot tensile and isochronous stress-strain curves for use with the Nonmandatory Appendix HBB-T design rules for meeting the design limits on deformation controlled quantities. The Code provides isochronous curves covering the entire Section III, Division 5 temperature range for each material. For Alloy 617 this is 800° to 1750° F. This Code Case provides hot tensile and isochronous curves in 50° F increments, matching the practice of the current Code. Table HBB-T-1820-1 summarizes the provided temperature range and temperature increment.

The Division 5 hot tensile curves represent the average experimentally-measured tensile flow curves for the material. The isochronous curves can be read as the average stress to accumulate some amount of total strain over some period of time. The experimental data underlying the design hot tensile curves are a series of elevated temperature tensile tests. The data underlying the isochronous curves are the tensile tests plus elevated temperature creep tests.

In order to provide design information at uniformly spaced, densely packed intervals of temperature, strain, and time the processed used to create the current Code curves first fits a material model to the available tensile and creep data and then uses that model to generate hot tensile and isochronous curves. The Code curves for the current Class A materials[1][2] are based on an additive, history-independent decomposition of the total strain into elastic, time-independent plastic, and time-dependent creep parts:

$$\varepsilon = \varepsilon_e + \varepsilon_p + \varepsilon_c.$$

The hot tensile curves are the outcome of this model when $\varepsilon_c = 0$, i.e. when $t = 0$, whereas the isochronous curves are the output of the model for some fixed, non-zero time.

The elastic strain is calculated using the Section II, temperature dependent values of Young's modulus for Alloy 617

$$\varepsilon_e = \frac{\sigma}{E}.$$

Based on experimentation with different standard plasticity models, the plastic response of Alloy 617 was divided into two regions based on temperature. At low temperatures, below 750° C, the composite model uses a Ramberg-Osgood model for the plastic strain to capture the experimentally-observed smooth transition from elastic to work hardening plastic behavior. Above this temperature the model uses a Voce form to capture a quick transition to a nearly perfectly-plastic response. The composite model for the plastic strain is then

---

[1] Blackburn, L. "Isochronous Stress-Strain Curves for Austenitic Stainless Steels." In *The Generation of Isochronous Stress-Strain Curves*, pp. 15-48, 1972.
[2] Swindeman, R. W. "Construction of isochronous stress-strain curves for 9Cr-1Mo-V steel." *Advances in Life Prediction Methodology* 391, pp. 95-100, 1999.

$$\varepsilon_p = \begin{cases} \begin{cases} 0 & \sigma \le \sigma_0 \\ K\left(\dfrac{\sigma - \sigma_0}{\sigma_0}\right)^n & \sigma > \sigma_0 \end{cases} & T \le 750°\text{C} \\[2em] \begin{cases} 0 & \sigma \le \sigma_1 \\ \dfrac{1}{\delta}\ln\left(1 - \dfrac{\sigma - \sigma_1}{\sigma_p - \sigma_1}\right) & \sigma > \sigma_1 \end{cases} & T > 750°\text{C} \end{cases}$$

The temperature-dependent model parameters are σ_0, K, and n below 750° C and σ_1, δ, and σ_p above 750° C.

Elevated temperature tension tests conducted at Idaho National Laboratory (INL) on a single heat of Alloy 617 plate were used to calibrate these parameters. Tension tests results are available at 425° C and at 50° C intervals from 450° to 950° C. For most temperatures a single test was used to calibrate the model coefficients. However, at several critical temperatures multiple tests were run to ensure experimental variability did not affect the final model coefficients.

The figures below compare the INL experimental data (black) to the hot tensile curves calculated using the calibrated model. The parameters were calibrated to the data using nonlinear least squares regression. In all cases the model hot tensile curves pass through the average experimental flow curve.
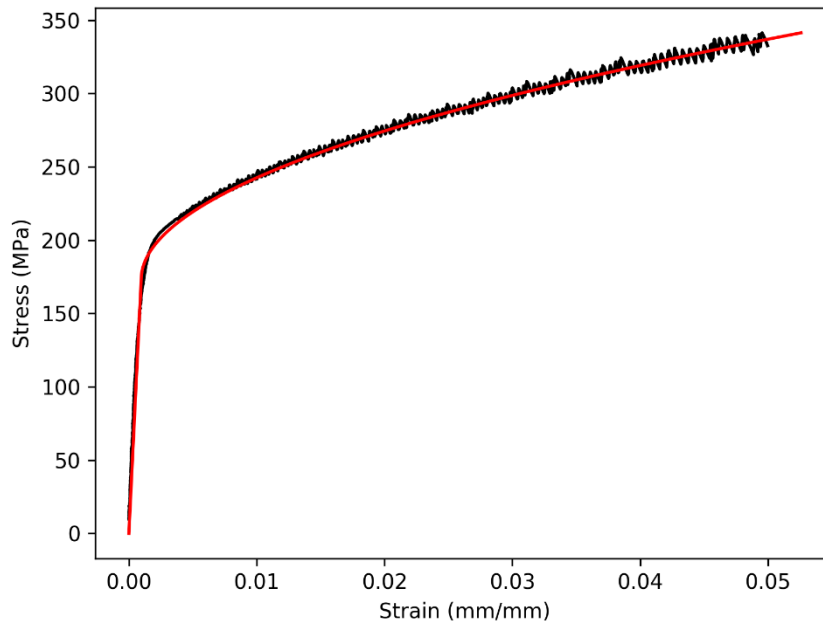
Comparison between INL experimental data (black) and model hot tensile curve (red) at 425° C.
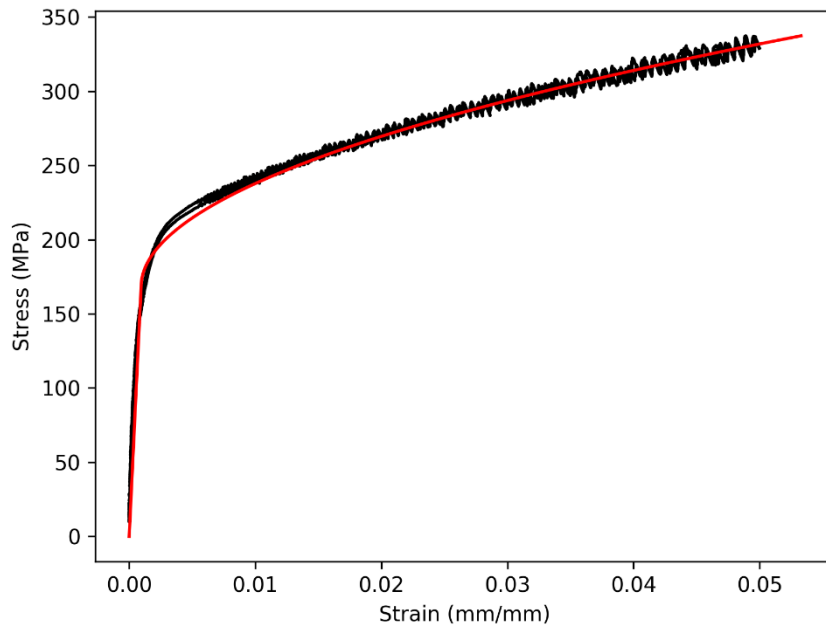
Comparison between INL experimental data (black) and model hot tensile curve (red) at 450° C.
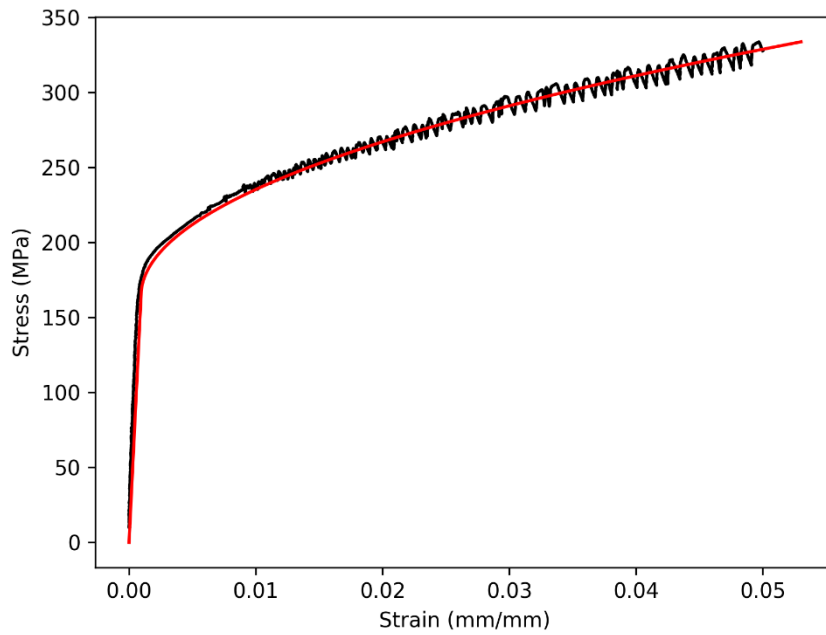
Comparison between INL experimental data (black) and model hot tensile curve (red) at 500° C.
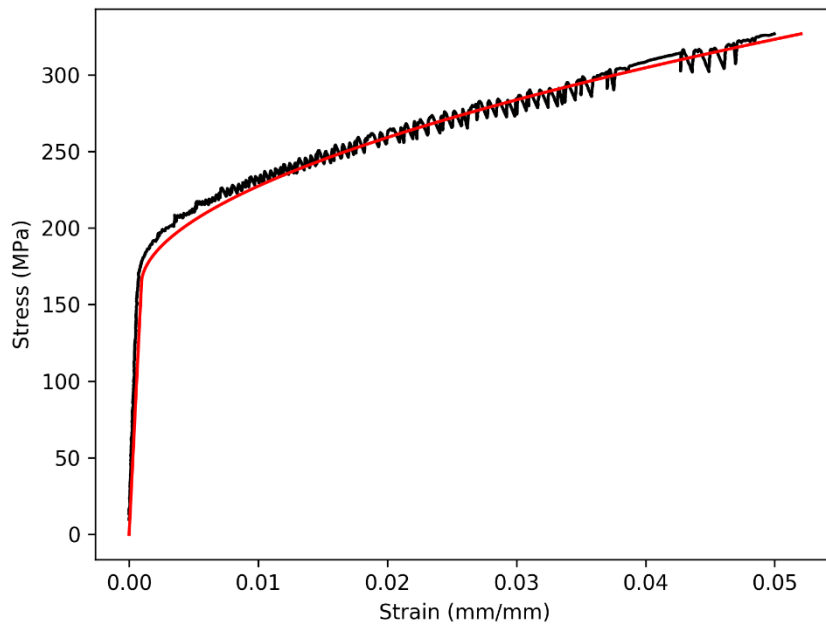
Comparison between INL experimental data (black) and model hot tensile curve (red) at 550° C.
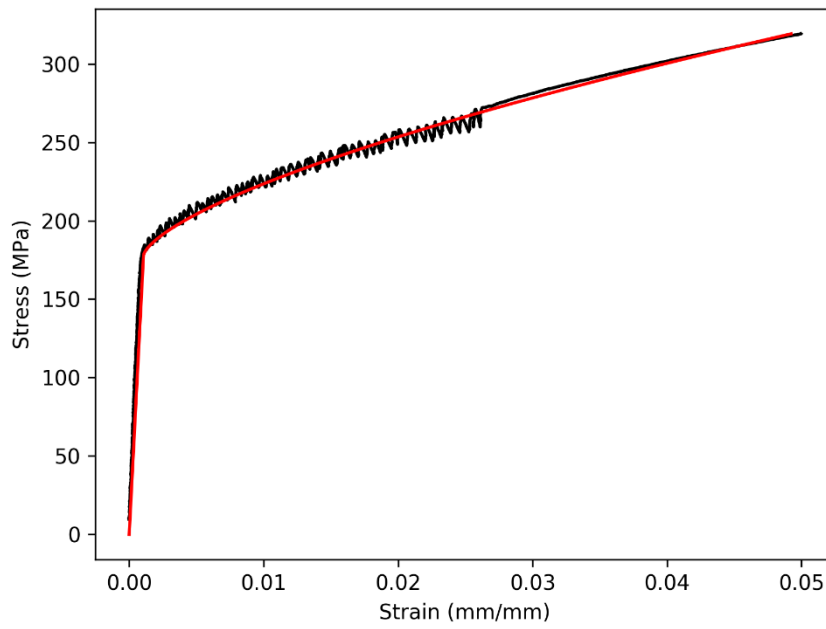
Comparison between INL experimental data (black) and model hot tensile curve (red) at 600° C.
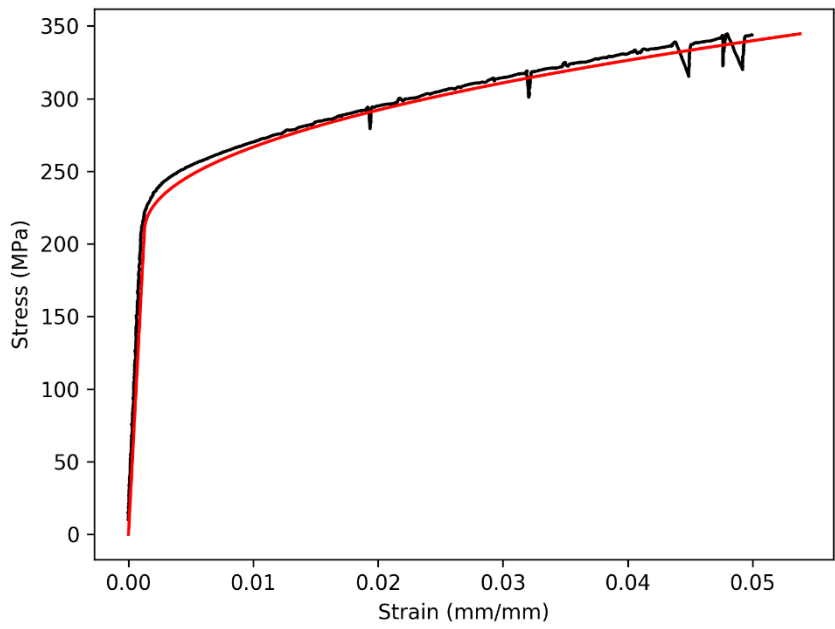
Comparison between INL experimental data (black) and model hot tensile curve (red) at 650° C.
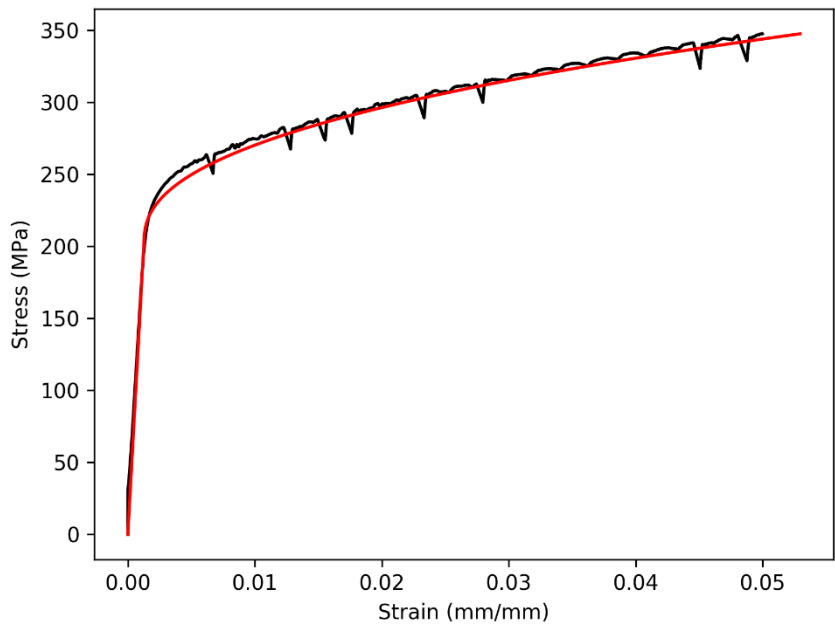
Comparison between INL experimental data (black) and model hot tensile curve (red) at 700° C.
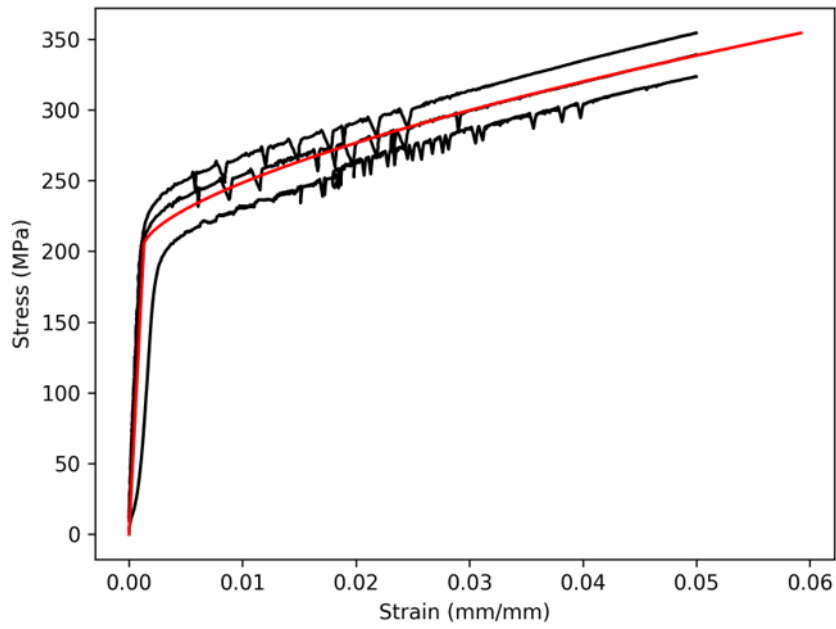
Comparison between INL experimental data (black) and model hot tensile curve (red) at 750° C.
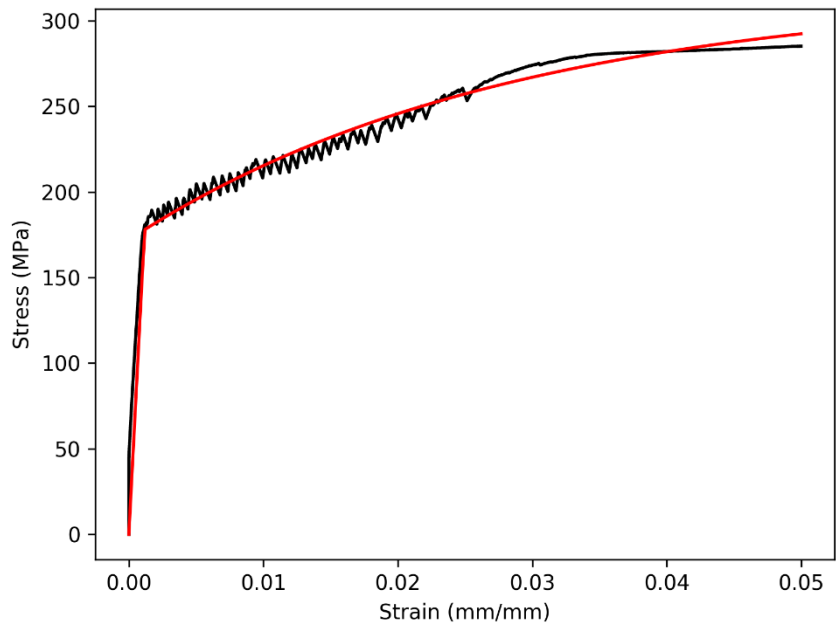
Comparison between INL experimental data (black) and model hot tensile curve (red) at 800° C.
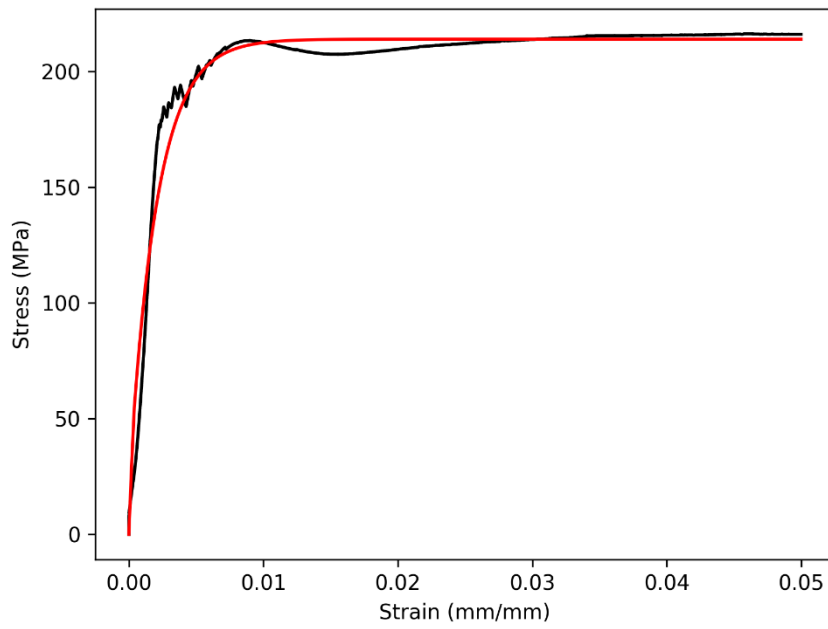
Comparison between INL experimental data (black) and model hot tensile curve (red) at 850° C.
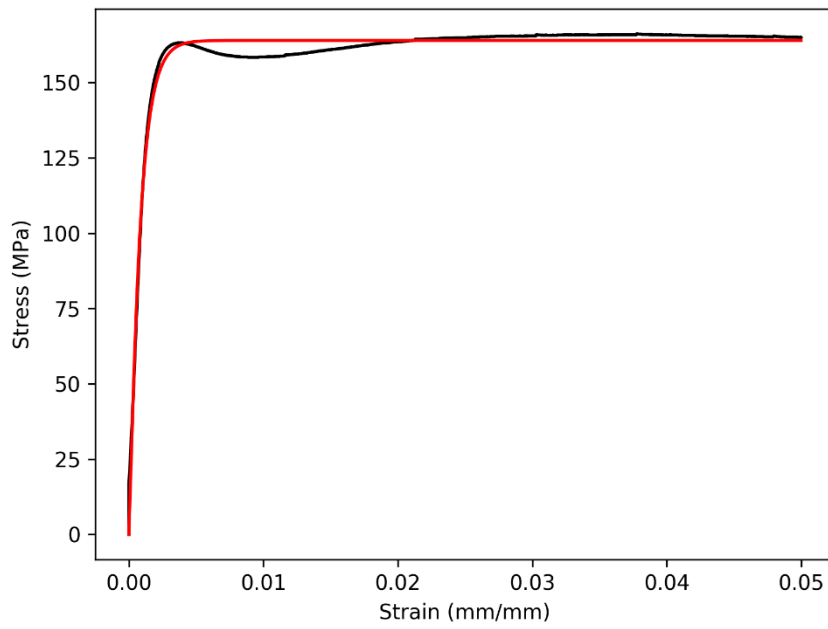
Comparison between INL experimental data (black) and model hot tensile curve (red) at 900° C.
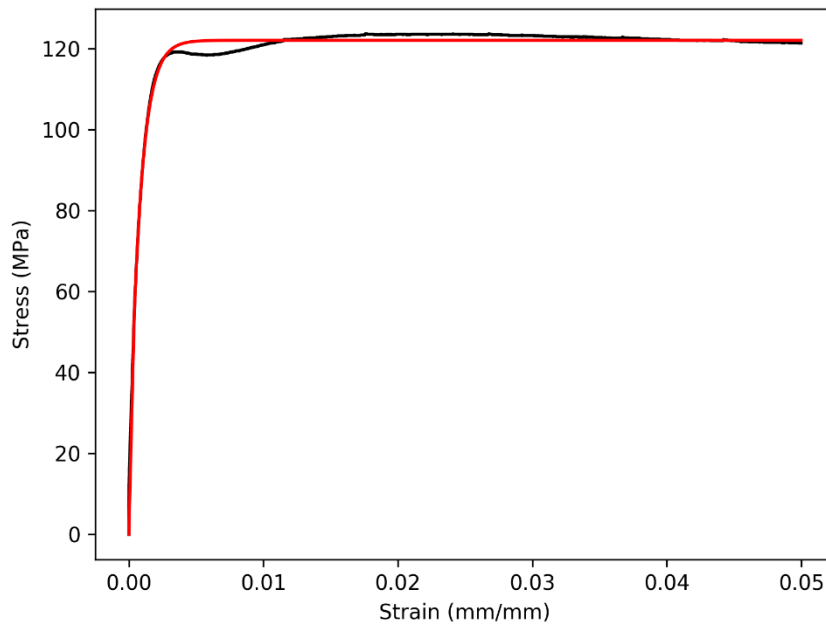
Comparison between INL experimental data (black) and model hot tensile curve (red) at 950° C.

The tension test data shows a marked transition from work hardening behavior below 750° C to a nearly perfectly plastic response a t and above 850° C. This change in behavior coincides with a region of serrated plastic flow and a metallurgical change in the alloy. This phenomenon is described in greater detail below in the section describing the model for creep deformation. The composite model for the plastic strain empirically captures this transition by switching from the Ramberg-Osgood to the Voce flow model.

Previous models used to create Division 5 design hot tensile curves have attempted to normalize the curves based on the Code values of S_y. Because S_y is not an average material property, these previous models empirically adjust the Code S_y to approximate the true average material yield stress, often simply by dividing by 80%. This ad hoc adjustment is unlikely to produce more representative curves than simply averaging experimental flow curves, as was done for the present model. As such, no normalization was attempted and the proposed model for plastic strain directly adopts the parameters calibrated to the INL tests. Furthermore, there is no way to consistently normalize the creep data used to calibrate the time-dependent portion of the model for the isochronous curves. Much of the creep data was collected from creep tests on the same heat of material used in the INL tension tests. As such, it is at least consistent to use unormalized models calibrated to this data for both the hot tensile and isochronous curves.

The INL experiments cover the full temperature range for Alloy 617 in Division 5, from 425° to 950° C. The parameters for the plastic strain model should be interpolated linearly in between INL test temperatures. The calibrated material properties in the table below then fully define the model for plastic strain.

T (°C)	σ_0 (MPa)	K (-)	n (-)	σ_1 (MPa)	σ_p (MPa)	δ (-)
425	175	0.056	1.96			
450	170	0.053	1.97			
500	166	0.050	2.01			
550	165	0.052	1.84			
600	178	0.067	1.50			
650	209	0.13	2.13			
700	206	0.12	2.29			
750	205	0.093	1.55	228	522	9.70
800				178	317	35.5
850				50	214	482
900				51	164	1250
950				54	122	1240

Parameters for the composite model for ε_p.

This leaves the model for the time-dependent creep strain ε_c. Ideally, this model would be calibrated to a wide variety of full, experimentally measured creep curves. However, for Alloy 617 only a limited number of full creep curves are available from INL experiments on the same batch of material used for the elevated temperature tension tests. To supplement these creep curves, this Code Case has collated simplified creep metrics from a variety of data sources. These simplified measures, for example time to 1% creep strain as a function of stress and temperature, have been used to set the time dependent allowable stress S_{mt}.

Division 5 design isochronous curves only provide data out to 2.2% total strain. At most, this represents about 2% creep strain. A very simple creep model is capable of representing the INL creep curves over this limited range of strains. The model for the time-dependent strain adopted here is

$$\varepsilon_c = \dot{\varepsilon}_c(T, \sigma)t$$

where $\dot{\varepsilon}_c$ is some constant, average creep rate, which is a function of temperature and stress. Where full creep curves are available this average creep rate should be taken as the average rate over the first 2% increment of creep strain. The model developed here further assumes that this average rate over the first 2% of creep strain is approximately equal to average rate over the first 1% of creep strain. This allows the model to use the time-to-1% data for calibration.

The time-to-1% data was converted to an average rate by dividing 1% creep strain by the time. The full creep curve data was converted to a plot of creep strain rate versus creep strain and averaged over the first 1% to produce a similar mean rate. This process produces a database relating the average creep rate over the first 1% of creep strain to the applied stress and temperature. A model must be developed for this average creep rate in order to interpolate the data to all the conditions required to generate the design isochronous curves.

The Alloy 617 creep model adopts a form developed by Kocks[3] and Mecking[4]. Their model posits a linear relation between the log-normalized material flow stress

$$\log\frac{\sigma}{\mu},$$

where μ is the material flow stress, and the normalized activation energy

$$\frac{kT}{\mu b^3}\ln\frac{\dot{\varepsilon}_0}{\dot{\varepsilon}}$$

where k is the Boltzmann constant, T is absolute temperature, b is a characteristic Burgers vector, and $\dot{\varepsilon}_0$ is some reference strain rate. If this log-linear relation exists, the Kocks-Mecking model can be converted into a model for the deformation strain rate as a function of the linear fit slope A and intercept B

$$\dot{\varepsilon} = \dot{\varepsilon}_0 e^{B\mu b^3/(AkT)}\left(\frac{\sigma}{\mu}\right)^{-\mu b^3/(AkT)}.$$

The following figure plots the available Alloy 617 creep data using the average rate to 1% creep strain as the deformation strain rate and the applied values of stress and temperature. The shear modulus values are those implied by the isotropic, temperature dependent values of Young's modulus for Alloy 617 in Section II of the Code and the value of Poisson's ratio likewise from Section II. The experimental data was divided into several categories: average creep curve rates from INL experiments for 750°, 800°, and 900° C, the collected average time to 1% rates for $T \leq 750°$ C, and the collected average time to 1% rates for $T > 750°$ C.
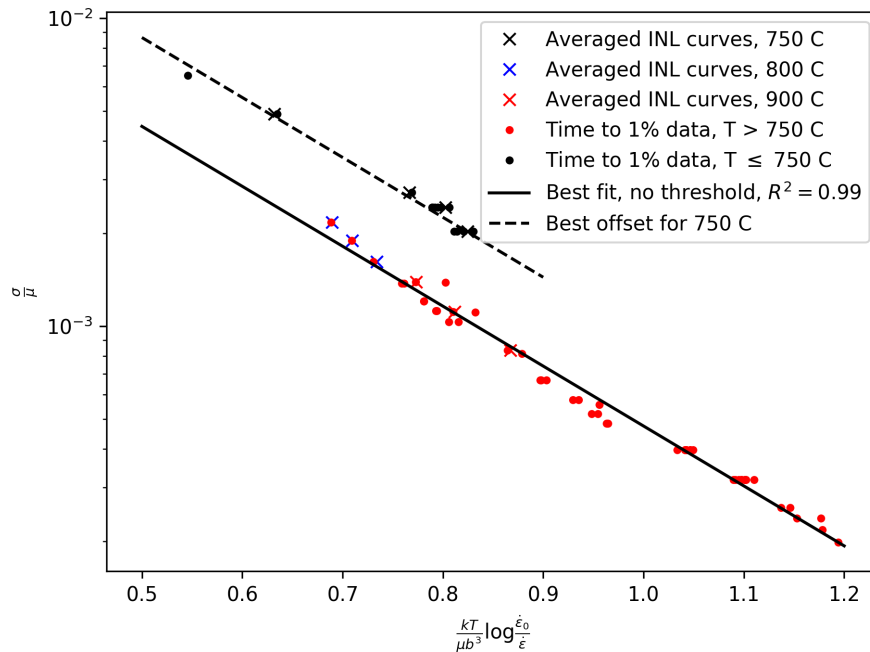
Kocks-Mecking diagram used to construct the model for time-dependent creep strain.

[3] Kocks, U. F. "Realistic constitutive relations for metal plasticity." *Materials Science and Engineering A* 317, pp. 181-187, 2001.
[4] Estrin, Y. and H. Mecking. "A unified phenomenological description of work hardening and creep based on one-parameter models." *Acta Metallurgica* 32:1, pp. 57-70, 1984.

As the figure shows, the Alloy 617 creep data nearly obeys the Kocks-Mecking form. All the data for temperatures greater than 750° C collapse to one line. The data for temperatures less than 750° C falls along a second line that shares the same slope. The only difference between the two temperature regimes is an offset or threshold stress. This implies that at 750° C and below creep strain is proportional to $\sigma - \sigma_{th}$ for some threshold stress σ_{th} rather than the stress σ directly.

Based on this diagram, the model for the creep strain adopted here is

$$
\varepsilon_c = \begin{cases} \dot{\varepsilon}_0 e^{B_1 \mu b^3/(AkT)} \left(\dfrac{\sigma}{\mu}\right)^{-\mu b^3/(AkT)} t & T \leq 775° \text{ C} \\[2ex] \dot{\varepsilon}_0 e^{B_2 \mu b^3/(AkT)} \left(\dfrac{\sigma}{\mu}\right)^{-\mu b^3/(AkT)} & T > 775° \text{ C} \end{cases}
$$

where the shift in the linear model intercept from B_1 to B_2 accommodates the threshold stress effect.

The parameters for the creep model are the reference strain rate $\dot{\varepsilon}_0$, the linear slope A, and the two linear intercepts B_1 and B_2. The Burgers vector was taken to be the Burgers vector of an edge dislocation in α-Fe and the shear modulus is given as

$$
\mu = \frac{E}{2(1 + v)}
$$

from the Section II values of the Young's modulus and Poisson's ratio. The parameters were calibrated to the experimental data plotted on the Kocks-Mecking diagram. First the data for $T \leq 750°$ C was excluded and an arbitrary reference strain rate was selected. Linear regression was used to determine the best-fit values of A and B_2 along with the correlation coefficient R^2. This process was repeated for different values of the reference strain rate to maximize the value of the correlation coefficient, i.e. achieve the best fit to the experimental data. Finally, given these optimal values of $\dot{\varepsilon}_0$ and A constrained linear regression was used to find the best-fit value of B_1 to the $T \leq 750°$ C data. The following table lists the values of the calibrated creep model parameters and the values of the physical constants that appear in the Kocks-Mecking model.

Parameter	Value
$\dot{\varepsilon}_0$	1.656e7 hrs^{-1}
A	-4.480
B_1	-2.510
B_2	-3.174
b	2.019e-7 mm
k	1.38064e-20 mJ/K

Calibrated parameters and physical constants for the Kocks-Mecking creep model.

The Kocks Mecking diagram above shows the best fit trend line for $T > 750°$ C and the shifted trend line for $T \leq 750°$ C. The correlation coefficient is $R^2 = 0.99$, which shows the model accurately captures the collated experimental data.

The temperature range requiring a threshold stress in the creep model correlates to the change in the character of the flow curves in the hot tensile model and the region of serrated flow observed in the INL tensile tests. Both the time independent plastic strain and the time dependent creep strain models capture

this metallurgical change: the plastic strain model transitions from Ramberg-Osgood to Voce at 750° C and the model for the creep strain uses a threshold stress for temperatures equal to or less than 750° C. This threshold stress effect accounts for an abrupt increase in the creep rate at temperatures above 800° C evident in the final isochronous stress-strain curves.

Threshold stresses are commonly included in creep rate models for precipitate hardened materials. For example, in the canonical power law model for the minimum creep rate:

$$\dot{\varepsilon}_{min} \propto D\frac{\mu b}{kT}\left(\frac{\sigma - \sigma_o}{\mu}\right)^n$$

We have measured the threshold stress at 750°C for the INL heat of Alloy 617. For this alloy tested at 750°C the material started the creep test in the solution annealed condition and the minimum creep rate was obtained in less than a few thousand hours. Transmission electron microscopy on the shoulder sections of the creep samples showed that significant γ' (Ni3Al,Ti) precipitation occurred during the aging associated with the creep test. TEM in the gage section showed dislocation pinning by the γ'. We showed that for these test conditions the threshold stress was 65 MPa.

The textbook explanation is that the threshold stress represents the magnitude of the stress necessary to overcome dislocation-particle interaction. Once that interaction is overcome the rate controlling mechanism is conventional climb controlled power law creep that represents the characteristics of the matrix containing the precipitates.

If we use that threshold stress and plot the results for the creep testing that has been done on the INL heat of Alloy 617 using the normalization parameter Z:

$$Z = \dot{\varepsilon}_{min}\ exp\left(\frac{Q_c}{RT}\right)$$

we get the plot below. The fact that all the test data fall on a single line indicates that they all fit dislocation control creep with a stress exponent of 5.6 and all have the same activation energy once we eliminate the effect of precipitates.
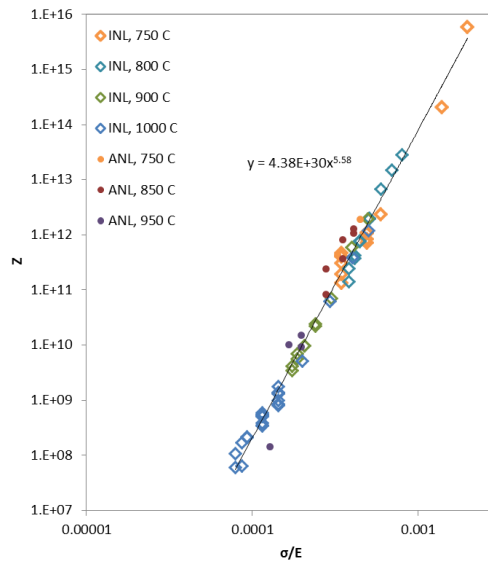
We have subsequently measured the threshold stress at 750°C for INL plate material that was furnace aged for 20,000 and 32,000 hours prior to creep testing. The measured values were 45 and 30 MPa, respectively. TEM characterization showed that the γ' precipitates had coarsened significantly during the furnace aging and were thus less effective in strengthening. The rate at which coarsening occurs will decrease with further increase in aging time so the threshold stress will continue to become smaller, albeit at a diminishing rate. So it would not be reasonable to have one correction at 750°C for threshold stress, it would be a function of the expected time at temperature. For very long times solid solution behavior is expected.

Furthermore, it is difficult to quantify the contribution from precipitation strengthening at temperatures below 750°C for solution annealed material. The driving force for γ' precipitation would likely be higher, but the kinetics for nucleation and growth to a particle size that would contribute to strengthening would be substantially reduced compared to 750°C. Shingledecker et al., showed that there was γ' precipitation at about 600°C that increased room temperature hardness, but only after aging for 64,000 hours.

There are limited creep rate data for lower temperatures (593, 650, 704 and 760°C) for some of the older Huntington and ORNL creep tests. Values of threshold stress varied substantially with heat, which may be the result of differences in chemistry, test methods (eg. soaking time before testing), minimum creep rate measurements, etc. Analysis based on equation (2), and using reported minimum creep rates, indicates threshold stresses for these heats tend to peak at 650°C. No threshold stress is indicated at 593°C for 2 of the 3 heats with creep tests at that temperature. Much lower threshold stresses were found at 760°C than that determined (by multiple methods) for the INL heat at 750°C.

In summary, test results at or below about 750°C show a particle strengthening contribution. Tests above that temperature will show solid solution behavior for thermodynamic reasons, i.e., a substantial volume fraction of γ' will not form. Below 750°C, thermodynamics may indicate that γ' should form, but the kinetics may be so slow that we will not observe precipitation effects for laboratory creep test times. This evidence all supports the incorporation of a threshold stress effect in the model for creep rate.

The hot tensile curve at 750°C exhibits rather abrupt yielding compared to those at either higher or lower temperature. Examination of the entire experimental tensile curves shows that this behavior is related to the presence of serrated flow resulting from dynamic strain aging at this temperature. It is typical for many austenitic materials to exhibit dynamic strain aging near this temperature and the phenomena is typically thought to be related to pinning and abrupt unpinning of dislocations from a solute atmosphere. Dynamic strain aging sometimes is related to a reduction in the elongation to failure in a tensile test, however, at the small strains used for the hot tensile curves in this Code Case it is not anticipated that this phenomena is relevant to the material behavior except for altering the shape of the curve at yielding.

Given the models for ε_e, ε_p, and ε_c defined here the hot tensile curves are stress/strain histories for $t = 0$ and increasing values of strain and the isochronous stress-strain curves are stress/strain histories for t fixed to some non-zero value and increasing values of strain.

Page intentionally left blank

Background Document – Record No. 16-998

Contents

- Balloting Plan
- HBB-T-1324 Test A3, r and s Factors for Negligible Creep
- HBB-T-1420-2, Creep-Fatigue Damage Diagram
  - Appendix I, Data Compilation of Fatigue and Creep-Fatigue Tests
  - Appendix II, Data Calculations for Creep-Fatigue Tests
- HBB-T-1431(e), Temperature Limits
- HBB-T-1440 Limits Using Elastic-Perfectly Plastic Analysis – Creep-Fatigue Damage

Page intentionally left blank

Alloy 617 Code Case Balloting Actions

RC #	Item	Section II and III Committees (See Color Key Below For Balloting Actions)								
16-994	Permissible base and weld materials, allowable stress values	WG-ASC	SG-ETD	SG-HTR	SG-MFE	II-SG-NFA	II-SG-SW	BPV-II		
16-995	Physical properties and extension of modulus values to higher temperatures	WG-ASC	SG-ETD	SG-HTR	SG-MFE	II-SG-NFA	II-SG-PP	BPV-II		
16-996	Temperature-time limits for NB buckling charts	WG-AM	SG-ETD	SG-HTR	SG-MFE	II-SG-EP	BPV-II	II-SG-NFA	SC-D	
16-997	Huddleston parameters, ISSCs	WG-ASC	SG-ETD	SG-HTR	II-SG-NFA	BPV-II	SC-D			
16-998	Negligible creep, Creep-Fatigue: D-diagram and EPP	WG-CFNC	SG-ETD	SG-HTR	SC-D					
16-999	EPP strain limits	WG-AM	SG-ETD	SG-HTR	SC-D					
16-1000	Fatigue design curves	WG-CFNC	WG-FS	SG-ETD	SG-HTR	SG-DM	SC-D			
16-1001	Alloy 617 Overall Code Case	WG-ASC	WG-AM	WG-CFNC	WG-FS	SG-ETD	SG-HTR	SG-MFE	SC-D	BPV-II
		BPV-III								

Color Key	Balloting Action
	For Review and Approval
	For Review and Comment

Page intentionally left blank

BACKGROUND

HBB-T-1324 Test No. A-3

Values of the *r* and *s* Parameters

Scope

This document provides the background/technical basis in support of the recommendation for the r and s Parameters of Test No. A-3 for Alloy 617 in Figure HBB-T-1324.

Background

HBB-1324 is one of the means by which the strain limits of HBB-T-1310, Limits for Inelastic Strains, are considered to have been satisfied. It is also used in HBB-T-1430, Limits Using Elastic Analysis.

Included in the rules for elastic analysis evaluation of primary plus secondary stresses are criteria for the use of the rules of Subsection NB when creep effects are not significant. The conceptual basis for this approach is to approximate the creep damage and deformation that would occur at the nominal flow stress of the material without accounting for stress relaxation. One of the criteria for the time−temperature regime of applicability of this approach is defined by insuring that a stress equal to a factor, *s*, times the minimum yield strength results in a creep damage fraction, adjusted with the factor, *r*, that doesn't exceed 0.1. The *s* factor accounts for both the difference between nominal yield and the tabulated yield, S_y, taken as a factor of 1.25, multiplied by an additional factor to account for the effects of strain hardening (or softening), usually taken as 1.2 for non−strain softening materials. The *r* factor is intended to account for the potential degradation of creep rupture strength due to strain cycling in strain softening materials such as Grade 91.

Value of the *s* Parameter

The *s* factor accounts for the difference between nominal yield and the tabulated yield, S_y, taken as a factor of 1.25, and also for the effects of strain hardening (or softening), taken as 1.2 if the material does not strain soften. Figure 1 is a plot of the peak tensile and compressive stress from Alloy 617 fatigue test at 850 and 950°C.[1] These results show that Alloy 617 does not fall into the strain softening category and the corresponding value of *s* is conservatively taken as 1.25 multiplied by 1.2, or *s* = 1.5, corresponding to the other non softening materials listed Table HBB- T- 1324.
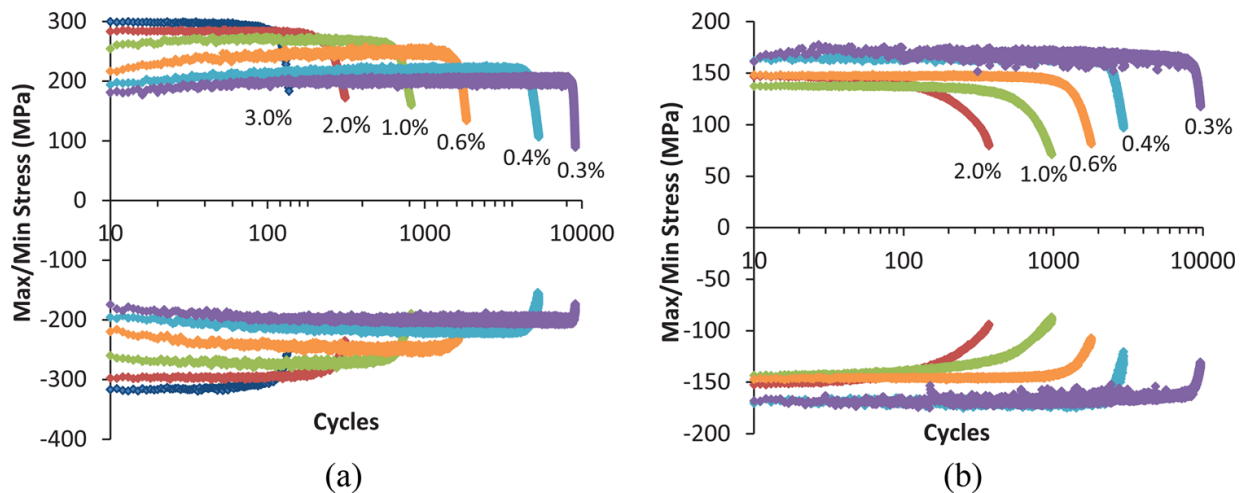

Figure 1. Peak tensile and compressive stress plotted as a function of cycle for one fatigue test specimen at each total strain range for (a) 850°C and (b) 950°C.

Value of the *r* Parameter

Alloy 617 is primarily a solid solution strengthened alloy, particularly at temperature above 750°C (some strengthening from the γ' phase has been observed in the range of 650−750°C[2,3]). In solid solution alloys, fatigue damage will be primarily manifested as development of dislocation substructures in the form of tangles or cells. Dislocation structures will rearrange into low energy arrays upon subsequent exposure to elevated temperature and are not expected to substantially affect the creep properties, since the basic strengthening mechanism is unaffected. Although there do not appear to be experiments reported for fatigue followed by creep testing for austenitic materials, it has been observed in Alloy 617 that dislocation structures developed during creep-fatigue testing with tensile holds appear qualitatively similar to those observed in uniaxial creep. This anticipated behavior in solid solution strengthened material would be in contrast to that in precipitation strengthened alloys like Grade 91, where the fatigue damage could degrade the effectiveness of the dominant strengthening mechanism. Thus, for Alloy 617 the *r* factor was taken as 1.0, similar to the other solid solution strengthened materials listed in Table HBB- T- 1324.

References

[1] J. K. Wright, L. J. Carroll, J. A. Simpson, and R. N. Wright, "Low Cycle Fatigue of Alloy 617 at 850 and 950°C," *Journal of Engineering Materials and Technology*, Vol. 135, July 2013.

[2] Q. Wu, H. Song, R. W. Swindeman, J. P. Shingledecker, and V. K. Vasudevan, "Microstructure of Long-Term Aged IN617 Ni-Base Superalloy," *Metallurgical and Materials Transactions A*, Vol. 39A, 2008, pp. 2569-2585.

[3] J. K. Benz, L. J. Carroll, J. K. Wright, R. N. Wright, and T. M. Lillo, "Threshold Stress Creep Behavior of Alloy 617 at Intermediate Temperatures," *Metallurgical and Materials Transactions A*, Vol. 45A, 2014, pp. 3010-3022.

BACKGROUND

HBB-T-1420-2

Creep-Fatigue Damage Envelope

Scope

This document provides the background/technical basis in support of the recommendation for the creep-fatigue damage envelope in Figure HBB-T-1420-2.

Background

Creep-fatigue damage is one of the most severe structural failure modes in elevated temperature design. When cyclic tests include a static hold, the cyclic life is reduced due to the creep damage accumulated during the hold time. The creep and fatigue damage are evaluated independently and the interaction is represented graphically in a creep-fatigue interaction diagram (described in detail below). Generally, the creep-fatigue damage envelope represents the average trend of the interaction between the creep damage and fatigue damage. For Alloy 617, Corum and Blass[1] had recommended a bilinear representation of the damage envelope with an intersection point of (0.1, 0.1). This document provides an assessment supporting the Corum-Blass damage envelope with new creep-fatigue data.

Materials

The majority of the fatigue and creep-fatigue testing has been performed on specimens machined from an Alloy 617 reference material plate.[2] The 37 mm thick solution-annealed plate is from heat 314626, produced by ThyssenKrupp VDM and the composition is given in Table 1. Although the average grain size of the plate is quantified as approximately 150 µm, a significant grain size inhomogeneity is present in the microstructure.

Additional creep-fatigue tests were performed on specimens machined from a 20 mm thick plate of Alloy 617 (heat XX2834UK) procured from Special Metals Corporation.[3, 4] The chemical composition of this plate is also listed in Table 1. The microstructure of the plate is heavily banded with stringers of coarse carbide precipitates and associated coarse and fine grains aligned in the rolling direction. Grains in the coarse bands are approximately 100 µm in diameter and the finer grains range from approximately 10 to 30 µm in diameter.

Table 1. The composition in wt% of Alloy 617.

	Ni	C	Cr	Co	Mo	Fe	Al	Ti	Si	Cu	Mn	S	B
314626	Bal.	0.05	22.2	11.6	8.6	1.6	1.1	0.4	0.1	0.04	0.1	0.002	0.001
XX2834UK	Bal.	0.08	21.91	11.42	9.78	1.69	0.96	0.34	0.12		0.11	0.001	0.002

Quality

Creep-fatigue properties of the Alloy 617 reference plate (heat 314626) reported by the Idaho National Laboratory (INL) through the Next Generation Nuclear Plant (NGNP) or Advanced Reactor Technologies (ART) programs were determined under an NQA-1 quality program. Details of the quality program implementation are given in INL document PLN-2690 "Idaho National Laboratory Advanced Reactor Technologies Technology Development Office Quality Assurance Program Plan". Creep-fatigue testing on heat XX2834UK predated implementation of the INL NQA-1 quality program for testing Alloy 617.

Creep-Fatigue Testing

Cylindrical cyclic test specimens (Figure 1), 0.295 in. (7.5 mm) diameter with a reduced section of 0.79 in. (20 mm) and gage length of 0.5 in. (12.7 mm), were machined from heat 314626. Low stress grinding and longitudinal polishing were used in the final machining of the reduced section to eliminate cold work and circumferential machining marks. Specimens machined from the heat XX2834UK plate and some additional specimens from the heat 314626 plate were similar to that shown in Figure 1, except with a 0.250 in. (6.4 mm) gage diameter. In all cases the long axis of the specimens was aligned with the rolling direction.
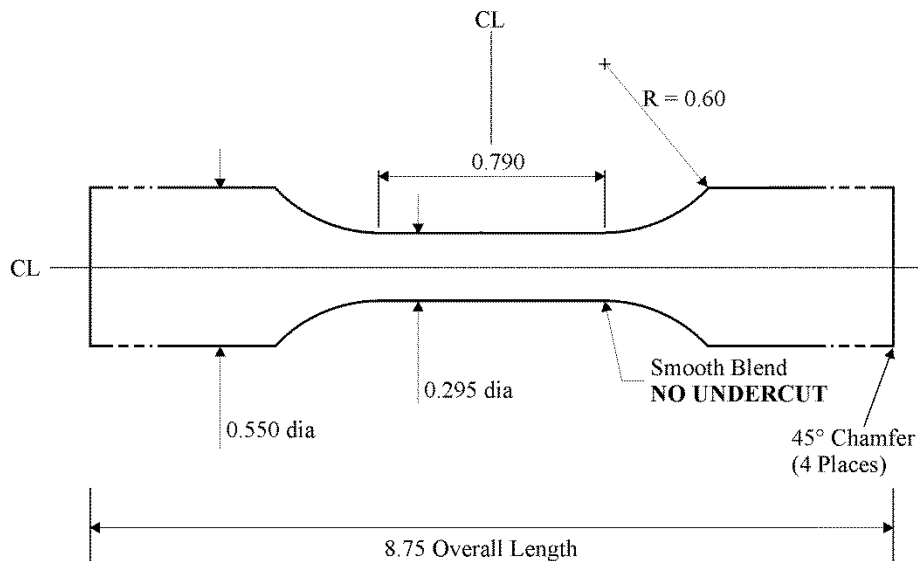
Figure 1. Specimen used for fatigue and creep-fatigue tests at 850 and 950°C.

Fully reversed, continuous low cycle fatigue (LCF) and tensile-hold creep-fatigue testing was conducted in air in on servo-hydraulic test machines. Tests were performed in strain control at total strain ranges from 0.3% to 1.0% using calibrated extensometers for strain determination. Testing was designed to be compliant with American Society for Testing and Materials (ASTM) Standard E606.[5] Tests on heat 314626 were performed at 850[6, 7] and 950°C,[7, 8, 9] while tests on heat XX2834UK were performed at 800[4] and 1000°C.[3, 4] Specimens were heated either using a 3-zone resistance furnace or by radio-frequency induction. The temperature gradient was measured using a specimen with spot-welded thermocouples along the gage section, and was found to vary less than 1%. The temperature was monitored and/or controlled using either a spot-welded thermocouple on the specimen shoulder or a thermocouple loop at the center of the gage section, in conjunction with calibration curves from the temperature profile characterization. Test temperature was generally maintained within 2°C throughout the duration of the test; a few 1% strain range specimens tested at 950°C via induction exceeded 2°C, but were all within 2.5%.

LCF testing followed a triangular waveform. The majority of creep-fatigue testing employed a tensile-hold waveform with a constant strain-controlled hold time at peak tensile strain,[6, 8] although a few tests were performed with compressive, or tensile and compressive holds.[9] Schematics of the fatigue and tensile-hold creep-fatigue waveform are shown in Figure 2. The strain rate during loading and unloading was 10^{-3}/s, except for a few tests which had a strain rate of 4×10^{-4}/s.[10] Several intermediate strain cycles

were applied during a limited number of initial cycles before reaching the target strain level on most of the tests, in order to prevent overshooting the target strain on the first cycle. The hold time duration in creep-fatigue varied from as short as 2 seconds to as long as 240 minutes. A complete matrix of conditions tested is presented in Appendix I.
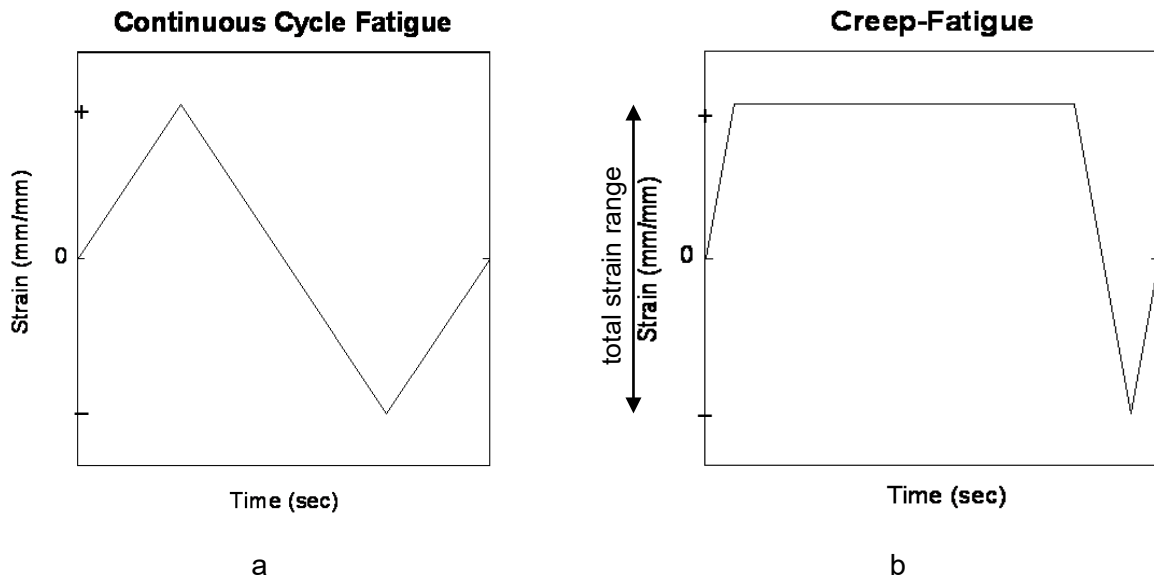

Figure 2. Schematics of the strain versus time waveforms for a) fatigue and b) tensile-hold creep-fatigue.

Peak tensile and compressive load and strain and temperature were recorded for each cycle. Strain, load and temperature were recorded as a function of time for each of the first hundred cycles, and periodically thereafter, with the cycle recording frequency dependent upon the anticipated lifetime of the specimen. Cyclic stress-strain curves (hysteresis loops) and stress relaxation behavior can be plotted for the cycles where the load and strain data have been collected.

The number of cycles to failure, N_f, is determined from a plot of the ratio of peak tensile to peak compressive stress versus cycles, as originally described in Ref. [3]. Determining the life from this ratio allows changes in peak stresses due to cyclic work hardening or softening to be distinguished from those due to crack formation and propagation. Macro-crack initiation, N_i, is defined as the point at which the stress ratio deviated from linearity; and failure, N_f, is defined as a 20% reduction in stress ratio from the point of deviation, as shown in Figure 2. Due to the rapidly-falling peak tensile force during the final crack propagation phase, N_f is not very sensitive to the exact value of load drop used to define failure or to the accuracy of the crack initiation determination. In some cases the test was stopped before a 20% reduction in stress ratio was achieved and the N_f is the last cycle of the test. These cases are indicated in the data table in Appendix I. The ratio method could not be used for the three specimens that included a compressive hold so N_i and N_f were determined from the peak tensile stress curve instead, using a 25% reduction in stress from the point of deviation.
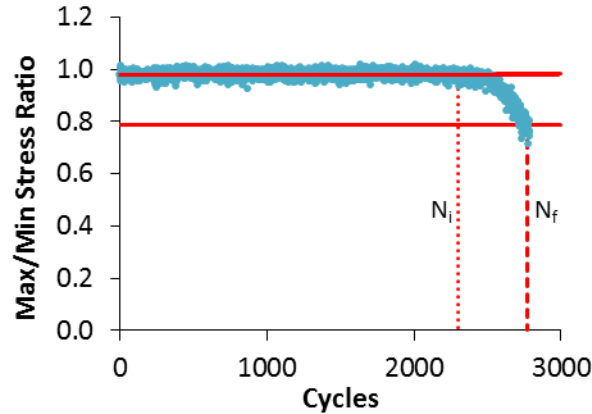
Figure 3. Illustration of failure criterion for fatigue and creep-fatigue tests.

In most cases, test termination was prior to actual specimen separation, based upon a predetermined drop in load; when the set load drop was detected, the test automatically switched to zero load and power to the heat source was shut off. In some cases, a tensile load was applied at the completion of the creep-fatigue test until complete fracture was achieved. Selected specimens were examined after testing to reveal the cracking morphology, i.e. the initiation sites and crack propagation paths. Transverse sections of the gage length were characterized using standard metallographic techniques.

Creep-Fatigue Interaction Analysis

In the ASME Code, creep-fatigue life is evaluated by a linear summation of fractions of cyclic damage and creep damage. The creep-fatigue criterion is given by:

$$\underbrace{\sum_{j}\left(\frac{n}{N_d}\right)_j}_{\text{Cyclic Damage}} + \underbrace{\sum_{k}\left(\frac{\Delta t}{T_d}\right)_k}_{\text{Creep Damage}} \leq D$$

[1]

where n and N_d are the number of cycles of type j and the allowable number of cycles of the same cycle type, respectively; and Δt and T_d are the actual time at stress level k and the allowable time at that stress level, respectively; D is the allowable combined damage fraction. Since the creep damage term is evaluated as a ratio of the actual time versus the allowable time, it is generally referred to as a time-fraction. The cyclic- and creep-damage terms on the left hand side of Equation [1] are evaluated in an uncoupled manner, and the interaction of creep and fatigue is accounted for empirically by the D term on the right side of the equation. This is represented graphically by the creep-fatigue interaction diagram, which is shown for the ASME Division 5 materials in Figure HBB-T-1420-2, reproduced here in Figure 4. The bilinear curves represent the damage envelopes for each material, within which calculated damage for a design must fall.
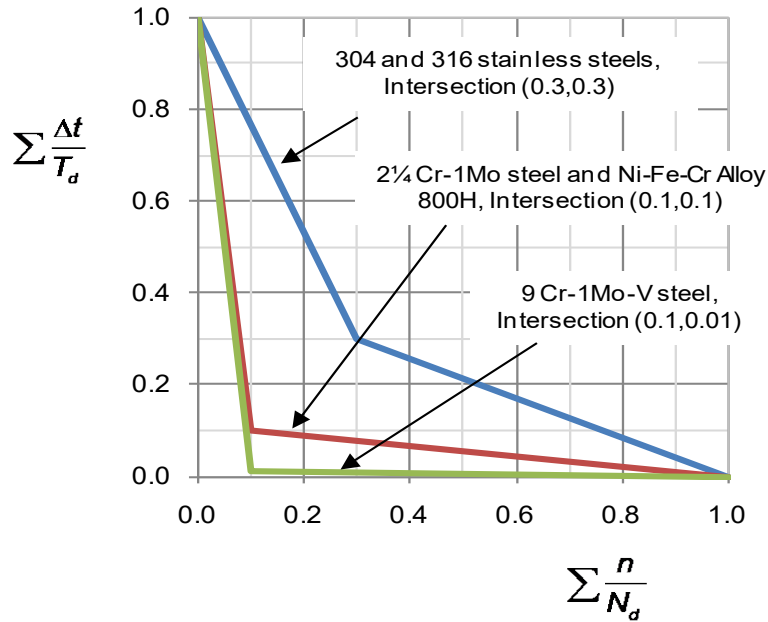
Figure 4. Creep-fatigue interaction diagram for ASME Section III, Division 5, Subsection HB, Subpart B. The coordinates of the intersections of the bilinear curves are shown in the legend.

Fatigue Damage Calculations

The fatigue damage fraction, D_F, for a creep-fatigue test is defined in terms of the ratio of the cycle to failure under the creep-fatigue condition, N_f, to the cycle to failure under continuous cycling condition, N_d, for the same product form and heat, and at the same total strain range, strain rate, and temperature as the creep-fatigue test. If data for more than one continuous cycling test for the same set of conditions were obtained, their average was used for the value of N_d, as best estimate values are to be used for establishing the envelope of the interaction curve in the D-diagram. For each creep-fatigue test, there was at least one LCF test for the same conditions. The fatigue damage calculations for each creep-fatigue test are given in Appendix II.

Creep Damage Calculations

Development of Equations

The creep damage for the kth creep-fatigue cycle, D_k^c, can be determined by evaluating the integral

$$D_k^c = \int \left(\frac{1}{T_d}\right)_k dt \tag{2}$$

over the hold time of the cycle.

To perform the integration, the correlation between the rupture time, temperature, and applied stress for the heat of Alloy 617 under consideration is required. In this analysis, a creep rupture time correlation based on all available creep rupture data for Alloy 617 was used in the creep damage evaluation. A Larson-Miller relation is a common way to do this and for Alloy 617, a linear equation in log stress describes the creep data well.[11]

$$LMP = a_0 + a_1 log_{10}(\sigma) \tag{3}$$

where a_0 and a_1 are the fitting parameters, σ is stress (MPa) and *LMP* is the Larson-Miller Parameter, defined as

$$LMP = T(C + log_{10}(t))$$ [4]

and *T* is the temperature in Kelvin, *C* is the Larson-miller constant, and *t* is time in hours.

Isolating t on the left side, we have

$$log_{10}(t) = -C + \frac{a_0}{T} + \frac{a_1}{T} log_{10}(\sigma)$$ [5]

and changing base to the natural logarithm gives

$$\frac{ln(t)}{ln(10)} = -C + \frac{a_0}{T} + \frac{a_1}{T} \frac{ln(\sigma)}{ln(10)}$$ [6]

which can be rearranged as

$$ln(t) = -C \, ln(10) + \frac{a_0 \, ln(10)}{T} + \frac{a_1 ln(\sigma)}{T}$$ [7]

Hence $\quad t = exp\left(-C \, ln(10) + \frac{a_0 \, ln(10)}{T}\right) \sigma^{\left(\frac{a_1}{T}\right)}$ [8]

or $\quad t = 10^{\left(-C+\frac{a_0}{T}\right)} \sigma^{\left(\frac{a_1}{T}\right)}$ [9]

For the calculations that follow, it is more convenient to use time in seconds for T_d, so we have:

$$T_d = 3600 * 10^{\left(-C+\frac{a_0}{T}\right)} \sigma^{\left(\frac{a_1}{T}\right)}$$ [10]

We can rewrite [10] as

$$T_d = A\sigma^m$$ [11]

where

$$A = 3600 * 10^{\left(-C+\frac{a_0}{T}\right)}, \quad m = \frac{a_1}{T}$$ [12]

The damage for a given cycle is calculated by integrating $\frac{1}{T_d}$ over the hold time. This requires analysis of the stress as it relaxes during the strain hold period, which can be fit to a power-law trend curve using the following functional form:

$$\sigma = b_0(t + t_0)^{b_1}$$ [13]

where b_0, b_1, and t_0 are treated as fitting parameters, σ is stress in MPa and *t* and t_0 are in seconds.

Substituting Equations [11] – [13] into Equation [2] results in

$$D_k^c = \int_0^{t_h} \frac{1}{A} (b_0(t + t_0)^{b_1})^{-m} \, dt$$ [14]

$$D_k^c = \frac{b_0^{-m}}{A} \frac{(t+t_0)^{1-b_1 m}}{1-b_1 m}\Bigg|_0^{t_h}$$ [15]

$$D_k^c = \frac{b_0^{-m}}{A(1-b_1 m)}\left((t_h + t_0)^{1-b_1 m} - (t_0)^{1-b_1 m}\right) \qquad [16]$$

where t_h is the stress relaxation hold time in seconds. The total creep damage accumulated during a creep-fatigue test, D_C, can then be determined by summing the creep damages calculated for all the cycles. This would require the stress relaxation for each cycle. However, such data are not collected for all the cycles during a creep-fatigue test. An approximation commonly made in calculating the total creep damage is to evaluate the creep damage for one cycle at mid-life, and then multiply this value by the total number of cycles to failure in the creep-fatigue test.

The Larson-Miller Relation

A spreadsheet developed for ASME[11] for the analysis of time-dependent materials properties was used to generate the Larson–Miller relation (Figure 4) from Section HBB-I-14.6. The data set is comprised of information from 348 creep-rupture specimens from multiple heats and product forms with known chemistry. Regression analysis for a linear fit produced values of a_0 = 32976.41125, a_1 = -5908.103107 and C = 16.73049602 according to Equations [3] and [4].
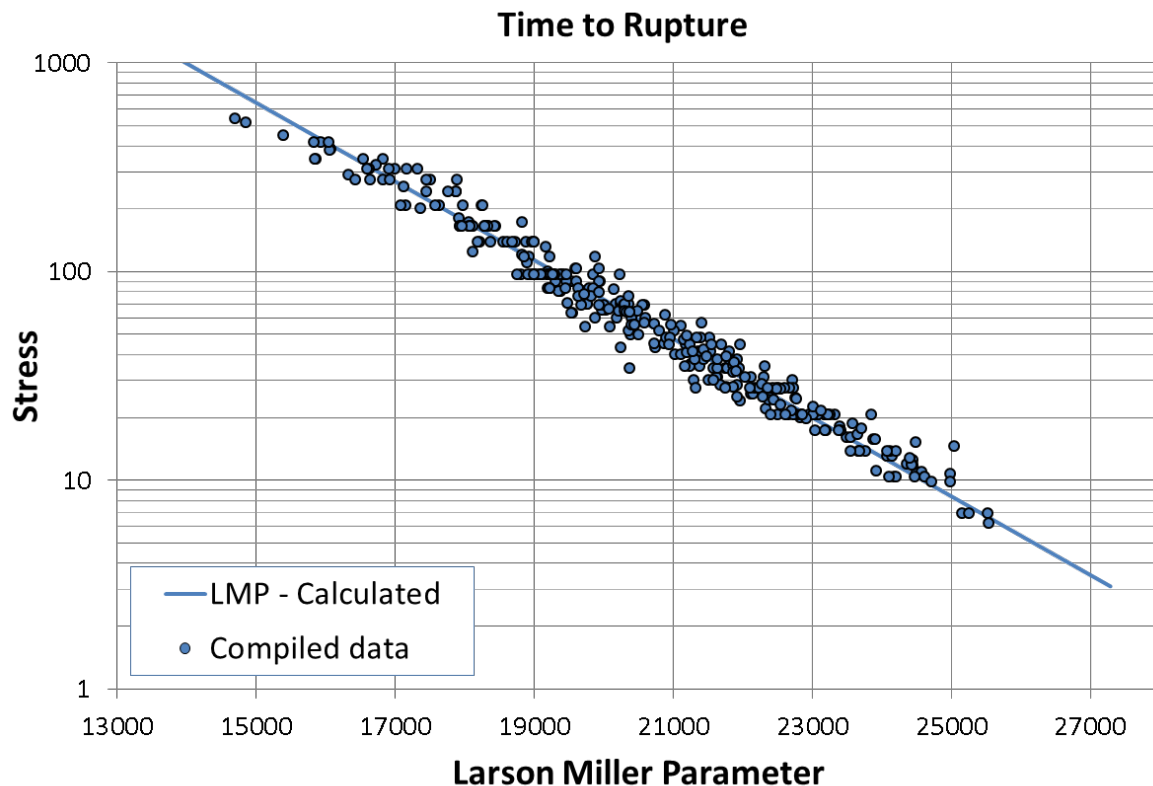

Figure 5. Larson-Miller plot with linear fit for time to creep rupture of Alloy 617.

Analysis of Stress Relaxation

The stress relaxation curves during strain hold for midlife cycles were fit to Equation [11] and the fitting parameters were determined. These parameters are used with the equations developed above to evaluate the creep damage for those selected cycles. An example of the power-law fit to midlife stress relaxation data during the strain hold period is shown in Figure 5. The stress relaxation fitting parameters for the midlife cycle of each creep-fatigue test are given in Appendix II.
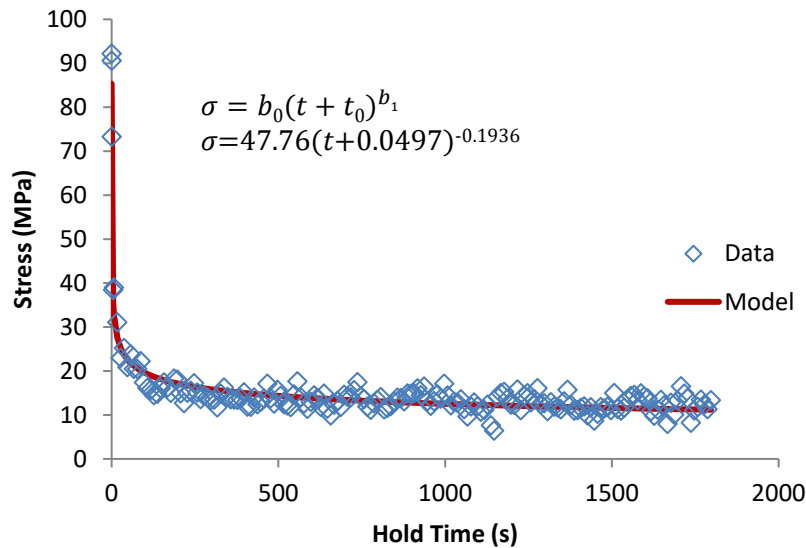
Figure 6. Example of a power law fit of the form $\sigma = b_0(t + t_0)^{b_1}$ to the stress relaxation portion of the midlife creep-fatigue cycle of an Alloy 617 specimen cycled at 950ºC, 0.3% total strain, and 1800 s hold time.

Calculation of Total Creep Damage

As mentioned above, stress relaxation data are not collected for all the cycles during a creep-fatigue test, so the creep damage of a midlife cycle is determined, and then multiplied by the total number of cycles to failure in the creep-fatigue test. The available cycle that was closest to $N_f/2$ was selected to represent the midlife cycle.

For the example shown in Figure 6, the number of cycles to failure was 4650. The creep damage for the mid-life cycle was calculated to be 2.6E-05 from Equation [16]; therefore the total creep damage is $2.60\text{E}{-}05 \times 4650 = 0.121$. The mid-life cycle creep damage and the total creep damage are given for each test in Appendix II.

This approach assumes that the creep damage at mid-life gives a reasonable assessment of the area under the creep damage curve as a function of cycles. The midlife damage estimate was checked against the cumulative damage for 12 specimens where the stress relaxation was recorded for a large number of cycles. The specimens analyzed in this way represent a variety of strain ranges, hold times and temperatures, as shown in Table 2.

Table 2. Multiple cycle cumulative creep damage analysis for selected specimens.

Specimen	Temp. (°C)	Hold Time (min)	Strain Range (%)	Cycles to Failure N_f	Fatigue Cycles to Failure N_d	fatigue damage	Cycle Used	Mid-Life Damage Estimate	Increment of Cycles Analyzed	Multiple Cycle Damage Estimate
4_1_10	850	3	0.3	1944	10010	0.194	950	0.401	50	0.354
4_2_9	850	10	0.3	2104	10010	0.210	1050	0.249	50	0.223
4_7_1	850	30	0.3	1200	10010	0.120	600	0.316	50	0.222
4_2_1	850	3	1	544	828	0.657	250	0.063	50	0.056
4_2_2	850	10	1	487	828	0.588	249	0.048	50	0.050
4_2_8	850	30	1	453	828	0.547	250	0.063	50	0.074
K-14	950	0.03	0.3	3538	8006	0.442	1751	0.617	100	0.537
B-5	950	3	0.3	3984	8006	0.498	2000	0.242	100	0.325
B-7	950	10	0.3	4096	8006	0.512	2000	0.370	100	0.415
B-8	950	30	0.3	4650	8006	0.581	2300	0.121	100	0.259
E-9	950	30	1	334	937	0.356	151	0.098	50	0.177
E-10	950	150	1	386	937	0.412	200	0.050	50	0.056

In many cases the total creep damage calculated based on the mid-life creep damage is similar to the total creep damage calculated from a summation of the creep damage from multiple cycles, as the example (4-2-9) in Figure 7 shows. In this case, the stress relaxation was analyzed for every 50th cycle. The cumulative creep damage is 0.223, and the creep damage calculated from the midlife cycle is 0.249. In other cases, the mid-life gives only an approximate estimate of the cumulative creep damage. This typically occurs because the midlife cycle used is somewhat atypical of other mid-range D_k^c values, or early cycle D_k^c values are high and are not offset by late cycle low values. Figure 8 shows an example (B-8) where both of these circumstances are evident. The cumulative creep damage in this case is 0.259, and the creep damage calculated from the midlife cycle is 0.121.
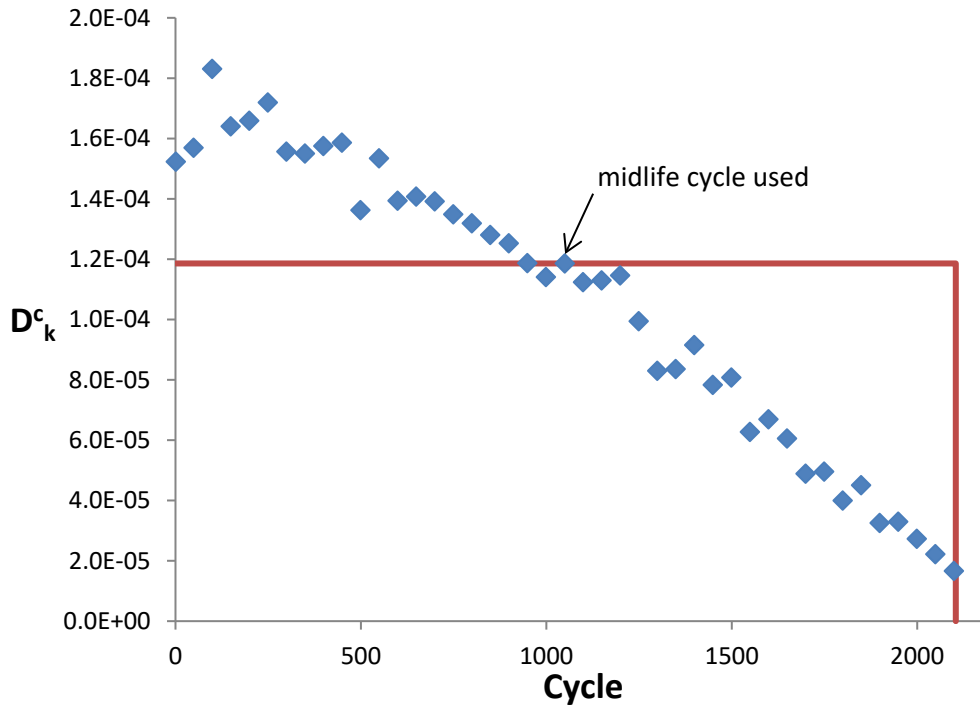
Figure 7. Example of a creep-fatigue test where the creep damage at mid-life gives a reasonable approximation for determining the area under the creep damage curve as a function of cycles.
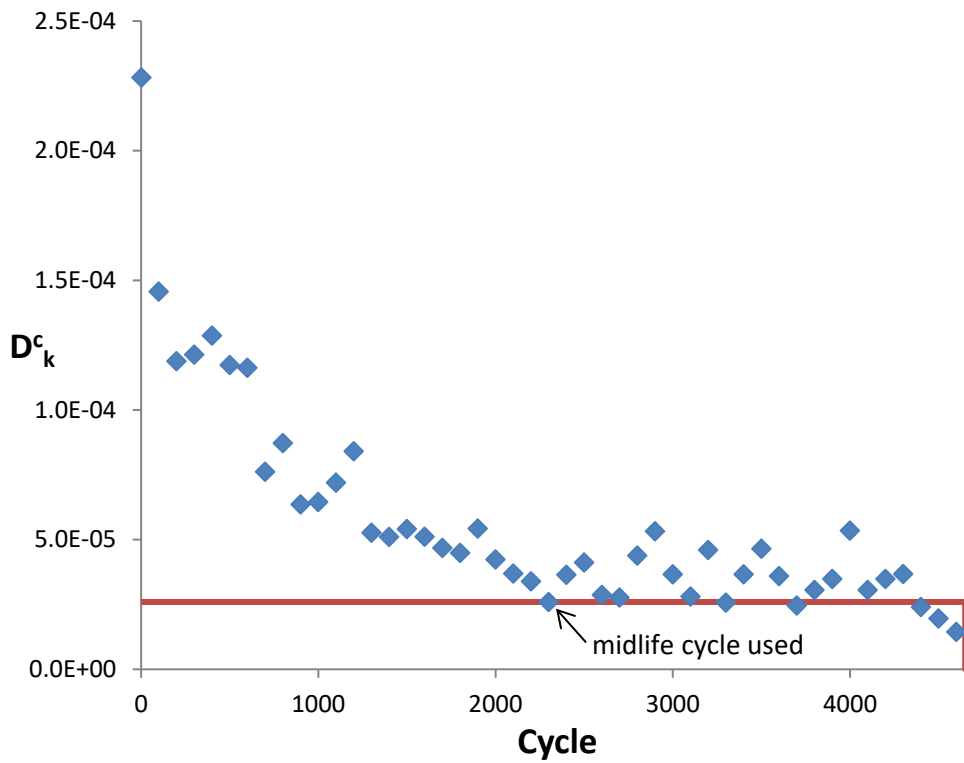

Figure 8. Example of a creep-fatigue test where the creep damage at mid-life gives a poor approximation for determining the area under the creep damage curve as a function of cycles.

The 12 cases shown in Table 2 are plotted on a creep-fatigue interaction diagram in Figure 9. In all cases the points fall near or within the proposed damage envelope proposed by Corum and Blass[1] whether the creep damage was calculated using multiple cycles recorded throughout the creep-fatigue test or only the midlife cycle. Based on Figure 9, the midlife approximation is deemed an adequate method of determining the total creep damage. The proposed intersection point of the envelope is sufficiently conservative and is supported by both methods.
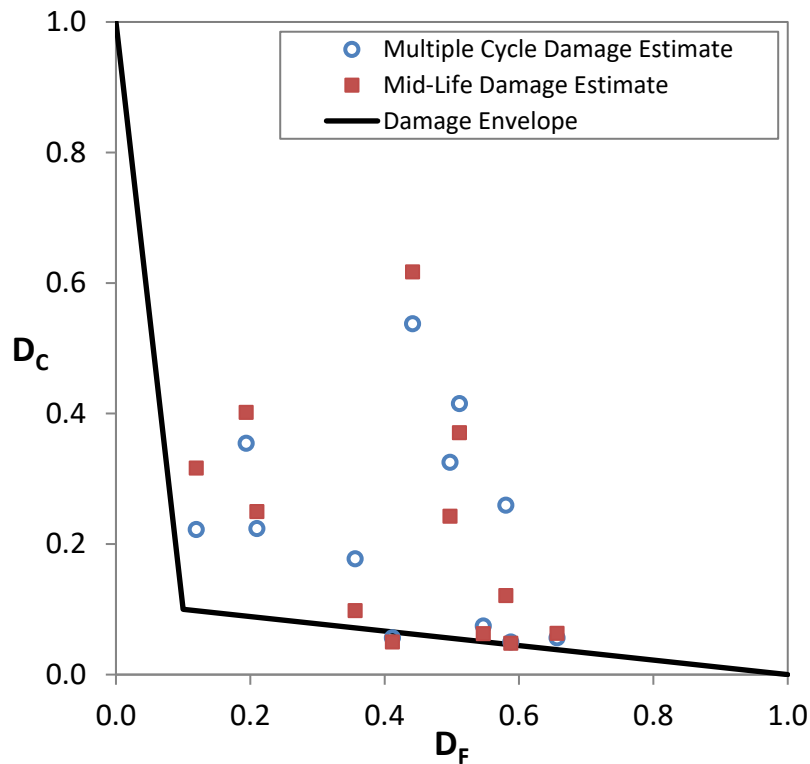

Figure 9. D-diagram comparing creep damage calculated using the midlife cycle to creep damage calculated using cycles recorded throughout the creep-fatigue test. The envelope shown has an intersection point of (0.1,0.1).

Creep-Fatigue Interaction Diagrams for Alloy 617

The calculated total creep damage and total fatigue damage for all creep-fatigue tests listed in the Appendices are shown in Figure 10. The strain rate for all tests was 10^{-3} /s unless specified otherwise in the legend, and "alternate" refers to tests that had a compressive hold or both tensile and compressive holds. The creep-fatigue damage envelope with an interaction point of (0.1, 0.1), as proposed by Corum and Blass,[1] is also shown in Figure 10. Generally, the creep-fatigue damage envelope represents the average trend of the interaction between the creep damage and fatigue damage. While the data shown in Figure 10 could support an intersection point of (0.2, 0.2), the intersection of (0.1, 0.1) is recommended to provide some added conservatism.
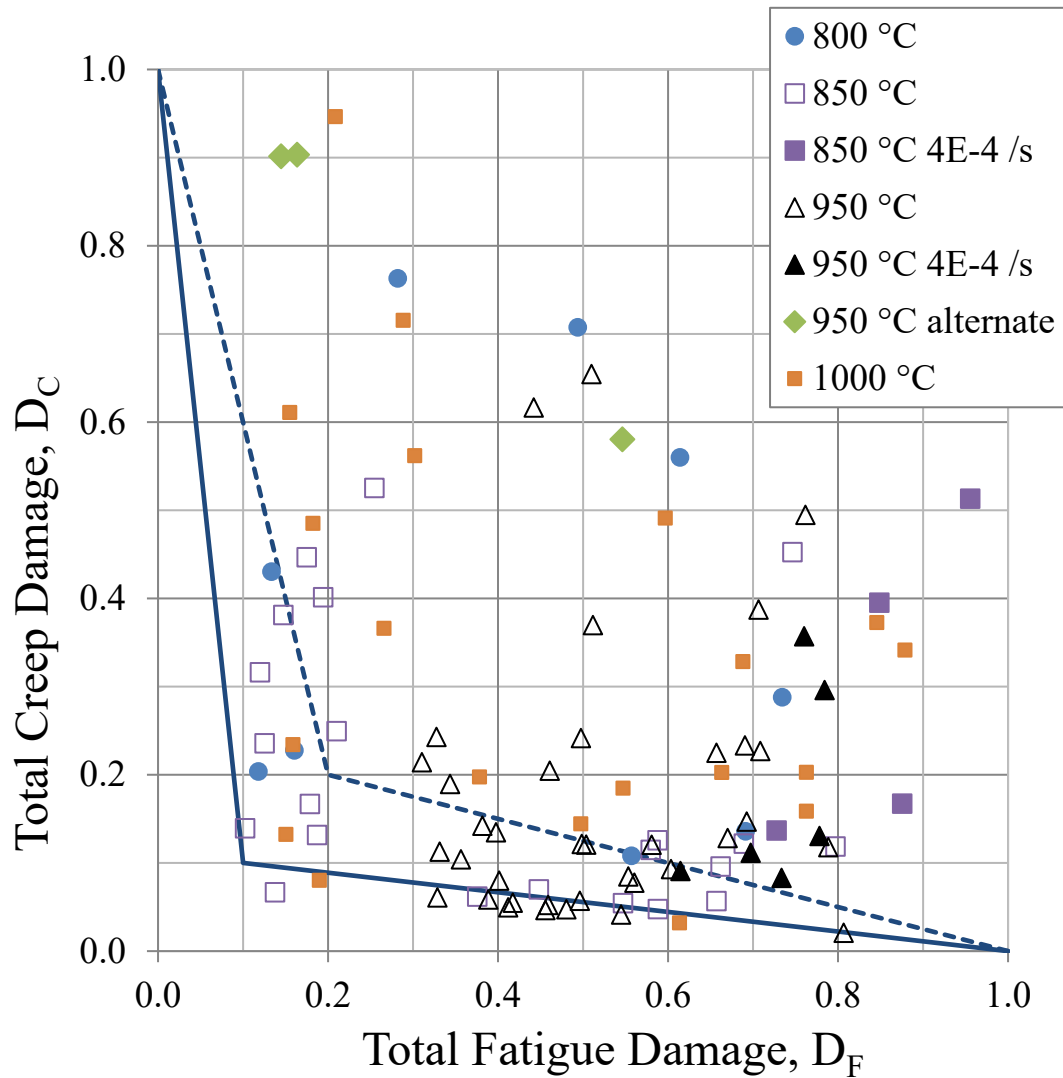
Figure 10. Creep-fatigue interaction diagram showing data for Alloy 617. The solid line represents the creep-fatigue envelope from the Draft Alloy 617 Code Case with intersection coordinates of (0.1, 0.1). An envelope with an intersection of (0.2, 0.2) is also shown for reference. The strain rate was 10^{-3} /s unless specified, and "alternate" refers to tests that included a compression hold.

References

[1] J. M. Corum and J. J. Blass, "Rules for Design of Alloy 617 Nuclear Components to Very High Temperatures," *PVP Pressure Vessel Piping Fatigue Fracture and Risk ASME*, Vol. 215, 1991, pp. 147–153.

[2] J. K. Wright, L. J. Carroll, C. Cabet, T. M. Lillo, J. K. Benz, J. A. Simpson, W. R. Lloyd, J. A. Chapman, and R. N. Wright, "Characterization of elevated temperature properties of heat exchanger and steam generator alloys," *Nuclear Engineering Design*, Vol. 251, 2012, pp. 252–260.

[3] T. Totemeier T. and Tian H., "Creep-Fatigue-Environment Interactions in Inconel 617," *Materials Science and Engineering A,* Vol. 468-470, 2007, p. 81-87.

[4] T. C. Totemeier, "High-Temperature Creep-Fatigue of Alloy 617 Base Metal and Weldments", *Proceedings of CREEP8, Eighth International Conference on Creep and Fatigue at Elevated Temperatures, San Antonio, TX, July 22-26, 2007*.

[5] Standard Test Method for Strain–Controlled Fatigue Testing, ASTM E606/E606M-12, ASTM International, West Conshohocken, PA.

[6] L. Carroll, *Progress Report on Long Hold-time Creep-fatigue of Alloy 617 at 850°C*, INL/EXT-15-35132 Rev. 1, August 2015.

[7] P. G. Pritchard, L. Carroll, T. Hassan, "Constitutive Modeling of High Temperature Uniaxial Responses of Alloy 617," Transactions of the American Nuclear Society, Vol 109, 2013, pp. 562-565.

[8] L. J. Carroll, C. Cabet, M. C. Carroll, and R. N. Wright, "The development of microstructural damage during high temperature creep–fatigue of a nickel alloy," *International Journal of Fatigue*, Vol. 47, 2013, pp. 115-125.

[9] M. C. Carroll, and L. J. Carroll, "Developing Dislocation Subgrain Structures and Cyclic Softening During High-Temperature Creep–Fatigue of a Nickel Alloy," *Metallurgical and Materials Transactions*, Vol. 44, 2013, No. 8, pp. 3592-3607.

[10] Shahriar Quayyum, Tasnim Hassan, "Constitutive Model Development for Alloy 617 Under High Temperature Multiaxial Loading," Transactions of the American Nuclear Society, Vol 109, 2013, pp. 558-561.

[11] R. W. Swindeman and M. J. Swindeman, *Analysis of Time-Dependent Materials Properties Data,* ASME Standards Technology, LLC, 2014.

Page intentionally left blank

Appendix I

Data Compilation for Fatigue and Creep-Fatigue Tests

Specimen ID	Heat ID of plate	Temp (°C)	Total Strain Range (%)	Hold Time (s)	Hold Time (min)	Strain Rate (1/s)	Hold Type†	Cycles to Initiation N_i	Cycles to Failure N_f
800-04	XX2834UK	800	0.3	0	0	1E-03	N	28300	29680
800-18	XX2834UK	800	0.3	18	0.3	1E-03	T	7600	8160
800-09	XX2834UK	800	0.3	60	1	1E-03	T	8007	8370
800-10	XX2834UK	800	0.3	60	1	1E-03	T	4000	4760
800-13	XX2834UK	800	0.3	600	10	1E-03	T	1790	3960
800-20	XX2834UK	800	0.3	600	10	1E-03	T	3050	3500
800-01	XX2834UK	800	1.0	0	0	1E-03	N	530	690
800-02	XX2834UK	800	1.0	0	0	1E-03	N	775	890
800-05	XX2834UK	800	1.0	60	1	1E-03	T	380	485
800-06	XX2834UK	800	1.0	60	1	1E-03	T	340	440
800-24	XX2834UK	800	1.0	180	3	1E-03	T	445	546
800-07	XX2834UK	800	1.0	600	10	1E-03	T	300	580
800-11	XX2834UK	800	1.0	600	10	1E-03	T	100	390
43-6	314626	850	0.3	0	0	1E-03	N	9900	10495
43-13	314626	850	0.3	0	0	1E-03	N	8500	8904
43-22	314626	850	0.3	0	0	1E-03	N	10000	10631
4-1-10	314626	850	0.3	180	3	1E-03	T	1402	1944
4-1-12	314626	850	0.3	180	3	1E-03	T	1954	2547
4-1-20	314626	850	0.3	600	10	1E-03	T	950	1475
4-1-22	314626	850	0.3	600	10	1E-03	T	1300	1750
4-2-9	314626	850	0.3	600	10	1E-03	T	1080	2104
4-7-1	314626	850	0.3	1800	30	1E-03	T	790	1200
4-7-3	314626	850	0.3	1800	30	1E-03	T	880	1255
4-7-17	314626	850	0.3	3600	60	1E-03	T	650	1025
313b-6	314626	850	0.3	7200	120	1E-03	T	800	1200
9557-1	314626	850	0.6	0	0	1E-03	N	1575	1712
9557-2	314626	850	0.6	0	0	1E-03	N	1400	1584
LCF-2	314626	850	0.6	0	0	1E-03	N	1175	1,423
LCF-3	314626	850	0.6	0	0	1E-03	N	1850	2,139*
9557-5	314626	850	0.6	60	1	1E-03	T	1000	1,182
9557-6	314626	850	0.6	60	1	1E-03	T	840	994
LCF-10	314626	850	0.6	60	1	1E-03	T	920	1,008*
LCF-11	314626	850	0.6	60	1	1E-03	T	980	1,280*
9557-3	314626	850	0.6	0	0	4E-04	N	1190	1394
LCF-4	314626	850	0.6	0	0	4E-04	N	1395	1633*
LCF-5	314626	850	0.6	0	0	4E-04	N	1690	1886*
9557-7	314626	850	0.6	60	1	4E-04	T	940	1434
9557-8	314626	850	0.6	60	1	4E-04	T	920	1192
LCF-12	314626	850	0.6	60	1	4E-04	T	1200	1565*
LCF-13	314626	850	0.6	60	1	4E-04	T	1100	1390*
416-7	314626	850	1.0	0	0	1E-03	N	660	821*
416-9	314626	850	1.0	0	0	1E-03	N	620	850
416-22	314626	850	1.0	0	0	1E-03	N	680	813*
4-2-1	314626	850	1.0	180	3	1E-03	T	258	544
4-2-4	314626	850	1.0	180	3	1E-03	T	393	660
4-2-2	314626	850	1.0	600	10	1E-03	T	308	487
4-2-5	314626	850	1.0	600	10	1E-03	T	388	548
4-2-7	314626	850	1.0	1800	30	1E-03	T	185	371
4-2-8	314626	850	1.0	1800	30	1E-03	T	310	453
4-7-15	314626	850	1.0	7200	120	1E-03	T	132	148
4-7-16	314626	850	1.0	7200	120	1E-03	T	240	311*
4-7-18	314626	850	1.0	14400	240	1E-03	T	102	114*
4-7-19	314626	850	1.0	14400	240	1E-03	T	132	155*

Specimen ID	Heat ID of plate	Temp (°C)	Total Strain Range (%)	Hold Time (s)	Hold Time (min)	Strain Rate (1/s)	Hold Type†	Cycles to Initiation N_i	Cycles to Failure N_f
A-20	314626	950	0.3	0	0	1E-03	N	8639	9641*
B-1	314626	950	0.3	0	0	1E-03	N	5033	5867*
B-3	314626	950	0.3	0	0	1E-03	N	8139	9054*
F-12	314626	950	0.3	0	0	1E-03	N	6377	7133
315-16	314626	950	0.3	0	0	1E-03	N	7863	8333
K-11	314626	950	0.3	2	0.033	1E-03	T	3200	4083
K-14	314626	950	0.3	2	0.033	1E-03	T	3250	3538
F-14	314626	950	0.3	180	3	1E-03	T	3889	4486
B-5	314626	950	0.3	180	3	1E-03	T	2600	3984
B-6	314626	950	0.3	180	3	1E-03	T	1944	2485
B-7	314626	950	0.3	600	10	1E-03	T	3583	4096
A-22	314626	950	0.3	600	10	1E-03	T	3569	4430
B-9	314626	950	0.3	600	10	1E-03	T	2183	2623
F-15	314626	950	0.3	600	10	1E-03	T	3736	4361
B-11	314626	950	0.3	1800	30	1E-03	T	4194	4832*
B-8	314626	950	0.3	1800	30	1E-03	T	4375	4650
43-14	314626	950	0.3	1800	30	1E-03	T	2508	2653*
4-1-7	314626	950	0.3	180	3	1E-03	C		4373
4-1-5	314626	950	0.3	90+90	1.5+1.5	1E-03	T & C		1310
4-1-3	314626	950	0.3	360+360	6+6	1E-03	T & C		1159
RT-68	314626	950	0.4	0	0	1E-03	N	2040	2378
RT-70	314626	950	0.4	60	1	1E-03	T	840	1680
RT-69	314626	950	0.4	0	0	4E-04	N	1800	2326
RT-71	314626	950	0.4	60	1	4E-04	T	920	1768
B-13	314626	950	0.6	0	0	1E-03	N	783	1722
B-14	314626	950	0.6	0	0	1E-03	N	762	1390
B-15	314626	950	0.6	0	0	1E-03	N	826	1480
RT-8	314626	950	0.6	0	0	1E-03	N	780	1342
RT-64	314626	950	0.6	0	0	1E-03	N	1000	1295
RT-17	314626	950	0.6	0	0	1E-03	N	1050	1432
LCF-6	314626	950	0.6	0	0	1E-03	N	1100	1266
LCF-7	314626	950	0.6	0	0	1E-03	N	1000	1085*
RT-12	314626	950	0.6	60	1	1E-03	T	620	1085
RT-16	314626	950	0.6	60	1	1E-03	T	460	953
RT-66	314626	950	0.6	60	1	1E-03	T	400	975
LCF-15	314626	950	0.6	60	1	1E-03	T	590	904*
LCF-18	314626	950	0.6	60	1	1E-03	T	450	1048*
A-23	314626	950	0.6	180	3	1E-03	T	450	950*
B-16	314626	950	0.6	180	3	1E-03	T	297	922
B-18	314626	950	0.6	600	10	1E-03	T	402	686
B-19	314626	950	0.6	600	10	1E-03	T	416	634*
A-14	314626	950	0.6	600	10	1E-03	T	312	547
B-21	314626	950	0.6	1800	30	1E-03	T	367	661
F-13	314626	950	0.6	1800	30	1E-03	T	860	1110*
416-18	314626	950	0.6	1800	30	1E-03	T	410	525
RT-65	314626	950	0.6	0	0	4E-04	N	1000	1498
RT-9	314626	950	0.6	0	0	4E-04	N	960	1254
RT-11	314626	950	0.6	0	0	4E-04	N	1040	1233
LCF-8	314626	950	0.6	0	0	4E-04	N	980	1229*
LCF-9	314626	950	0.6	0	0	4E-04	N	1100	1506*
RT-13	314626	950	0.6	60	1	4E-04	T	520	826
RT-15	314626	950	0.6	60	1	4E-04	T	520	986*
RT-67	314626	950	0.6	60	1	4E-04	T	480	1046
LCF-16	314626	950	0.6	60	1	4E-04	T	660	1054*
LCF-17	314626	950	0.6	60	1	4E-04	T	740	937*
315-1	314626	950	1.0	0	0	1E-03	N	593	963
E-11	314626	950	1.0	0	0	1E-03	N	666	972
E-12	314626	950	1.0	0	0	1E-03	N	447	916
E-13	314626	950	1.0	0	0	1E-03	N	561	897*

Specimen ID	Heat ID of plate	Temp (°C)	Total Strain Range (%)	Hold Time (s)	Hold Time (min)	Strain Rate (1/s)	Hold Type†	Cycles to Initiation N_i	Cycles to Failure N_f
K-12	314626	950	1.0	2	0.033	1E-03	T	280	820
K-13	314626	950	1.0	2	0.033	1E-03	T	330	790
A-6	314626	950	1.0	180	3	1E-03	T	165	376
F-5	314626	950	1.0	180	3	1E-03	T	172	465
B-12	314626	950	1.0	180	3	1E-03	T	330	472*
A-13	314626	950	1.0	600	10	1E-03	T	148	308
F-4	314626	950	1.0	600	10	1E-03	T	145	391
E-1	314626	950	1.0	600	10	1E-03	T	308	427
E-8	314626	950	1.0	600	10	1E-03	T	311	430
E-6	314626	950	1.0	1800	30	1E-03	T	217	322
E-7	314626	950	1.0	1800	30	1E-03	T	271	364
E-9	314626	950	1.0	1800	30	1E-03	T	226	334
E-10	314626	950	1.0	9000	150	1E-03	T	268	386
1000-06	XX2834UK	1000	0.3	0	0	1E-03	N	12700	13610
1000-06R	XX2834UK	1000	0.3	0	0	1E-03	N	12880	12930
1000-12	XX2834UK	1000	0.3	18	0.3	1E-03	T	1560	2060
1000-13	XX2834UK	1000	0.3	18	0.3	1E-03	T	2200	2770
1000-14	XX2834UK	1000	0.3	18	0.3	1E-03	T	2020	2420
1000-07	XX2834UK	1000	0.3	60	1	1E-03	T	3300	3830
1000-28	XX2834UK	1000	0.3	60	1	1E-03	T	4330	5020
1000-08	XX2834UK	1000	0.3	180	3	1E-03	T	3330	4010
1000-08R	XX2834UK	1000	0.3	180	3	1E-03	T	3100	3530
1000-09	XX2834UK	1000	0.3	600	10	1E-03	T	2130	2520
1000-18B	XX2834UK	1000	0.3	600	10	1E-03	T	1500	2110
1000-23	XX2834UK	1000	0.3	1800	30	1E-03	T	1580	2000
1000-01	XX2834UK	1000	1.0	0	0	1E-03	N	240	525
1000-01R	XX2834UK	1000	1.0	0	0	1E-03	N	195	680
1000-11	XX2834UK	1000	1.0	18	0.3	1E-03	T	145	530
1000-11R	XX2834UK	1000	1.0	18	0.3	1E-03	T	165	510
1000-02	XX2834UK	1000	1.0	60	1	1E-03	T	185	415
1000-21	XX2834UK	1000	1.0	60	1	1E-03	T	135	370
1000-03	XX2834UK	1000	1.0	180	3	1E-03	T	175	360
1000-03R	XX2834UK	1000	1.0	180	3	1E-03	T	150	330
1000-04	XX2834UK	1000	1.0	600	10	1E-03	T	160	400
1000-15	XX2834UK	1000	1.0	600	10	1E-03	T	130	300
1000-05	XX2834UK	1000	1.0	1800	30	1E-03	T	220	460
1000-17	XX2834UK	1000	1.0	1800	30	1E-03	T	360	460

†N ≡ no hold

T ≡ tensile hold

C ≡ compressive hold

*Test stopped before 20% reduction in stress ratio. N_f given is last cycle of test.

Page intentionally left blank

Appendix II
Damage Calculations for Creep-Fatigue Tests

Creep Damage Calculations

Specimen ID	Temp (°C) T	Total Strain Range (%)	Hold Time (s) t_h	Strain Rate (1/s)	Cycles to Failure N_f	Cycle used for Midlife N_{mid}	b_0	b_1	t_0	$A=3600*10^{-C+a_0/T}$	$m=a_1/T$	$1-b_1\,m$	Mid-life Creep Damage $D_k{}^c$	Creep Damage Fraction D_C
800-18	800	0.3	18	1E-03	8160	4100	1.7083E+02	-1.1423E-01	1.0006E+00	3.619E+17	-5.5061	0.3710	2.895E-05	0.236
800-09	800	0.3	60	1E-03	8370	4200	1.8873E+02	-1.0351E-01	3.9161E+00	3.619E+17	-5.5061	0.4300	9.118E-05	0.763
800-10	800	0.3	60	1E-03	4760	2400	1.8716E+02	-1.5220E-01	1.6510E+00	3.619E+17	-5.5061	0.1620	4.786E-05	0.228
800-13	800	0.3	600	1E-03	3960	2000	1.7166E+02	-1.2460E-01	2.4754E+00	3.619E+17	-5.5061	0.3139	1.087E-04	0.431
800-20	800	0.3	600	1E-03	3500	1753	1.7287E+02	-1.5405E-01	2.0370E+00	3.619E+17	-5.5061	0.1518	5.826E-05	0.204
800-05	800	1.0	60	1E-03	485	240	3.3846E+02	-1.8370E-01	3.9629E-01	3.619E+17	-5.5061	-0.0115	1.155E-03	0.560
800-06	800	1.0	60	1E-03	440	220	2.7224E+02	-2.2942E-01	4.1959E-01	3.619E+17	-5.5061	-0.2632	2.458E-04	0.108
800-24	800	1.0	180	1E-03	546	270	2.6230E+02	-2.1022E-01	4.7778E-01	3.619E+17	-5.5061	-0.1575	2.490E-04	0.136
800-07	800	1.0	600	1E-03	580	289	2.7782E+02	-1.9377E-01	3.4838E-01	3.619E+17	-5.5061	-0.0669	4.967E-04	0.288
800-11	800	1.0	600	1E-03	390	200	3.4495E+02	-1.8078E-01	6.1023E-01	3.619E+17	-5.5061	0.0046	1.814E-03	0.708
4-1-10	850	0.3	180	1E-03	1944	950	2.3536E+02	-2.6719E-01	4.3119E+00	1.550E+16	-5.2609	-0.4057	2.065E-04	0.401
4-1-12	850	0.3	180	1E-03	2547	1250	2.0730E+02	-2.4264E-01	2.1325E+00	1.550E+16	-5.2609	-0.2765	2.062E-04	0.525
4-1-20	850	0.3	600	1E-03	1475	749	1.6827E+02	-1.8099E-01	7.3258E-01	1.550E+16	-5.2609	0.0478	2.585E-04	0.381
4-1-22	850	0.3	600	1E-03	1750	899	1.8631E+02	-2.0777E-01	1.3788E+00	1.550E+16	-5.2609	-0.0931	2.553E-04	0.447
4-2-9	850	0.3	600	1E-03	2104	1050	1.7075E+02	-2.3626E-01	9.3830E-01	1.550E+16	-5.2609	-0.2429	1.186E-04	0.249
4-7-1	850	0.3	1800	1E-03	1200	600	2.0285E+02	-2.3324E-01	1.9689E+00	1.550E+16	-5.2609	-0.2271	2.635E-04	0.316
4-7-3	850	0.3	1800	1E-03	1255	649	1.7934E+02	-2.2287E-01	1.1718E+00	1.550E+16	-5.2609	-0.1725	1.878E-04	0.236
4-7-17	850	0.3	3600	1E-03	1025	507	1.7382E+02	-2.3112E-01	1.4925E+00	1.550E+16	-5.2609	-0.2159	1.360E-04	0.139
9557-5	850	0.6	60	1E-03	1182	600	1.6368E+02	-2.2757E-01	4.8234E-01	1.550E+16	-5.2609	-0.1972	1.031E-04	0.122
9557-6	850	0.6	60	1E-03	994	500	1.6235E+02	-2.4031E-01	2.4488E-01	1.550E+16	-5.2609	-0.2642	1.156E-04	0.115
LCF-10	850	0.6	60	1E-03	1008	500	1.4104E+02	-1.4149E-01	3.1488E-02	1.550E+16	-5.2609	0.2556	1.248E-04	0.126
LCF-11	850	0.6	60	1E-03	1280	600	2.4302E+02	-2.7102E-01	1.5515E+00	1.550E+16	-5.2609	-0.4258	3.535E-04	0.452
9557-7	850	0.6	60	4E-04	1434	720	1.8464E+02	-2.7738E-01	7.4669E-01	1.550E+16	-5.2609	-0.4593	1.167E-04	0.167
9557-8	850	0.6	60	4E-04	1192	596	1.7540E+02	-2.5869E-01	5.6130E-01	1.550E+16	-5.2609	-0.3610	1.148E-04	0.137
LCF-12	850	0.6	60	4E-04	1565	800	2.2399E+02	-2.4706E-01	1.1880E+00	1.550E+16	-5.2609	-0.2998	3.279E-04	0.513
LCF-13	850	0.6	60	4E-04	1390	700	2.2563E+02	-2.6146E-01	1.3187E+00	1.550E+16	-5.2609	-0.3755	2.844E-04	0.395
4-2-1	850	1.0	180	1E-03	544	250	1.9291E+02	-3.2597E-01	7.4134E-01	1.550E+16	-5.2609	-0.7149	1.156E-04	0.063
4-2-4	850	1.0	180	1E-03	660	349	1.8294E+02	-2.4670E-01	4.6847E-01	1.550E+16	-5.2609	-0.2978	1.798E-04	0.119
4-2-2	850	1.0	600	1E-03	487	249	1.8342E+02	-3.1767E-01	6.9914E-01	1.550E+16	-5.2609	-0.6712	9.782E-05	0.048
4-2-5	850	1.0	600	1E-03	548	250	1.7852E+02	-2.4447E-01	4.3590E-01	1.550E+16	-5.2609	-0.2861	1.753E-04	0.096
4-2-7	850	1.0	1800	1E-03	371	185	1.6202E+02	-2.1090E-01	1.8704E-01	1.550E+16	-5.2609	-0.1096	1.889E-04	0.070
4-2-8	850	1.0	1800	1E-03	453	249	1.6041E+02	-2.2745E-01	2.8333E-01	1.550E+16	-5.2609	-0.1966	1.380E-04	0.063
4-7-15	850	1.0	7200	1E-03	148	74	2.1619E+02	-1.9663E-01	2.4285E-01	1.550E+16	-5.2609	-0.0345	1.128E-03	0.167
4-7-16	850	1.0	7200	1E-03	311	151	1.4028E+02	-1.7417E-01	6.3979E-02	1.550E+16	-5.2609	0.0837	1.991E-04	0.062
4-7-18	850	1.0	14400	1E-03	114	57	1.5171E+02	-1.5321E-01	2.7185E-02	1.550E+16	-5.2609	0.1940	5.857E-04	0.067
4-7-19	850	1.0	14400	1E-03	155	77	2.0913E+02	-2.0383E-01	3.0060E-01	1.550E+16	-5.2609	-0.0724	8.496E-04	0.132

Specimen ID	Temp (°C)	Total Strain Range (%)	Hold Time (s)	Strain Rate (1/s)	Cycles to Failure	Cycle used for Midlife	Stress Relaxation Fitting Parameters				$m=a_1/T$	$1-b_1 m$	Mid-life Creep Damage	Creep Damage Fraction
	T		t_h		N_f	N_{mid}	b_0	b_1	t_0	$A=3600*10^{-C+a_0/T}$			$D_k{}^c$	D_C
K-11	950	0.3	2	1E-03	4083	2049	1.0203E+02	-3.3572E-01	3.9010E-01	6.155E+13	-4.8308	-0.6218	1.603E-04	0.655
K-14	950	0.3	2	1E-03	3538	1750	1.0398E+02	-3.3260E-01	3.9233E-01	6.155E+13	-4.8308	-0.6067	1.743E-04	0.617
F-14	950	0.3	180	1E-03	4486	2200	5.5031E+01	-3.0644E-01	2.1763E-01	6.155E+13	-4.8308	-0.4804	1.731E-05	0.078
B-5	950	0.3	180	1E-03	3984	2000	7.3674E+01	-3.2347E-01	2.7738E-01	6.155E+13	-4.8308	-0.5626	6.066E-05	0.242
B-6	950	0.3	180	1E-03	2485	1200	7.3894E+01	-2.6415E-01	1.7593E-01	6.155E+13	-4.8308	-0.2760	8.621E-05	0.214
B-7	950	0.3	600	1E-03	4096	2000	7.6779E+01	-2.8151E-01	2.4332E-01	6.155E+13	-4.8308	-0.3599	9.031E-05	0.370
A-22	950	0.3	600	1E-03	4430	2200	4.9695E+01	-2.3351E-01	7.0771E-02	6.155E+13	-4.8308	-0.1280	1.912E-05	0.085
B-9	950	0.3	600	1E-03	2623	1300	7.1679E+01	-2.3859E-01	1.5901E-01	6.155E+13	-4.8308	-0.1526	9.260E-05	0.243
F-15	950	0.3	600	1E-03	4361	2200	4.6572E+01	-2.8465E-01	1.5522E-01	6.155E+13	-4.8308	-0.3751	9.514E-06	0.041
B-11	950	0.3	1800	1E-03	4832	2400	5.6153E+01	-2.8848E-01	2.5782E-01	6.155E+13	-4.8308	-0.3936	1.926E-05	0.093
B-8	950	0.3	1800	1E-03	4650	2300	4.7755E+01	-1.9358E-01	4.9747E-02	6.155E+13	-4.8308	0.0648	2.596E-05	0.121
43-14	950	0.3	1800	1E-03	2653	1350	6.2704E+01	-2.7363E-01	1.5051E-01	6.155E+13	-4.8308	-0.3218	4.250E-05	0.113
RT-70	950	0.4	60	1E-03	1680	800	9.8594E+01	-3.0749E-01	3.1745E-01	6.155E+13	-4.8308	-0.4854	2.306E-04	0.387
RT-71	950	0.4	60	4E-04	1768	900	1.0576E+02	-3.0907E-01	7.5058E-01	6.155E+13	-4.8308	-0.4931	2.020E-04	0.357
RT-12	950	0.6	60	1E-03	1085	500	7.9067E+01	-2.4818E-01	2.2525E-01	6.155E+13	-4.8308	-0.1989	1.087E-04	0.118
RT-16	950	0.6	60	1E-03	953	500	8.5852E+01	-2.4855E-01	2.6331E-01	6.155E+13	-4.8308	-0.2007	1.542E-04	0.147
RT-66	950	0.6	60	1E-03	975	480	9.6535E+01	-2.7333E-01	3.0989E-01	6.155E+13	-4.8308	-0.3204	2.328E-04	0.227
LCF-15	950	0.6	60	1E-03	904	400	1.1450E+02	-3.3330E-01	8.0500E-01	6.155E+13	-4.8308	-0.6101	2.490E-04	0.225
LCF-18	950	0.6	60	1E-03	1048	500	1.3299E+02	-3.3459E-01	9.0328E-01	6.155E+13	-4.8308	-0.6163	4.722E-04	0.495
A-23	950	0.6	180	1E-03	950	480	9.2266E+01	-2.5638E-01	2.1110E-01	6.155E+13	-4.8308	-0.2385	2.456E-04	0.233
B-16	950	0.6	180	1E-03	922	462	7.6555E+01	-2.2381E-01	9.8978E-02	6.155E+13	-4.8308	-0.0812	1.390E-04	0.128
B-18	950	0.6	600	1E-03	686	350	7.9158E+01	-2.2273E-01	1.2086E-01	6.155E+13	-4.8308	-0.0760	1.773E-04	0.122
B-19	950	0.6	600	1E-03	634	301	8.9013E+01	-2.1914E-01	1.1931E-01	6.155E+13	-4.8308	-0.0586	3.227E-04	0.205
A-14	950	0.6	600	1E-03	547	251	8.0953E+01	-2.0347E-01	8.4710E-02	6.155E+13	-4.8308	0.0171	2.464E-04	0.135
B-21	950	0.6	1800	1E-03	661	350	6.6646E+01	-2.3916E-01	1.2826E-01	6.155E+13	-4.8308	-0.1553	7.186E-05	0.048
F-13	950	0.6	1800	1E-03	1110	560	5.2594E+01	-2.6800E-01	1.4423E-01	6.155E+13	-4.8308	-0.2946	1.883E-05	0.021
416-18	950	0.6	1800	1E-03	525	251	8.4958E+01	-2.3032E-01	7.9762E-02	6.155E+13	-4.8308	-0.1126	2.708E-04	0.142
RT-13	950	0.6	60	4E-04	826	400	8.5734E+01	-2.7015E-01	5.0241E-01	6.155E+13	-4.8308	-0.3050	1.101E-04	0.091
RT-15	950	0.6	60	4E-04	986	500	7.9591E+01	-2.4993E-01	5.4586E-01	6.155E+13	-4.8308	-0.2074	8.432E-05	0.083
RT-67	950	0.6	60	4E-04	1046	500	8.2622E+01	-2.5912E-01	2.5036E-01	6.155E+13	-4.8308	-0.2517	1.249E-04	0.131
LCF-16	950	0.6	60	4E-04	1054	500	1.0338E+02	-2.6095E-01	5.2974E-01	6.155E+13	-4.8308	-0.2606	2.809E-04	0.296
LCF-17	950	0.6	60	4E-04	937	500	8.2159E+01	-2.4004E-01	3.5773E-01	6.155E+13	-4.8308	-0.1596	1.190E-04	0.112
K-12	950	1.0	2	1E-03	820	399	9.0269E+01	-3.1180E-01	3.4543E-01	6.155E+13	-4.8308	-0.5062	9.545E-05	0.078
K-13	950	1.0	2	1E-03	790	399	8.3173E+01	-2.7604E-01	2.6191E-01	6.155E+13	-4.8308	-0.3335	7.356E-05	0.058
A-6	950	1.0	180	1E-03	376	200	8.4696E+01	-2.2010E-01	1.6086E-01	6.155E+13	-4.8308	-0.0633	2.126E-04	0.080
F-5	950	1.0	180	1E-03	465	250	7.7588E+01	-2.3963E-01	1.6657E-01	6.155E+13	-4.8308	-0.1576	1.229E-04	0.057
B-12	950	1.0	180	1E-03	472	250	8.9677E+01	-2.3431E-01	1.6264E-01	6.155E+13	-4.8308	-0.1319	2.559E-04	0.121
A-13	950	1.0	600	1E-03	308	151	7.8228E+01	-2.0553E-01	1.1623E-01	6.155E+13	-4.8308	0.0071	1.976E-04	0.061
F-4	950	1.0	600	1E-03	391	200	7.4604E+01	-2.1934E-01	1.0245E-01	6.155E+13	-4.8308	-0.0596	1.404E-04	0.055
E-1	950	1.0	600	1E-03	427	201	7.8010E+01	-2.5273E-01	2.8884E-01	6.155E+13	-4.8308	-0.2209	1.090E-04	0.047
E-8	950	1.0	600	1E-03	430	201	7.4950E+01	-2.2824E-01	1.7864E-01	6.155E+13	-4.8308	-0.1026	1.217E-04	0.052
E-6	950	1.0	1800	1E-03	322	151	9.2513E+01	-1.9466E-01	1.1115E-01	6.155E+13	-4.8308	0.0597	5.890E-04	0.190
E-7	950	1.0	1800	1E-03	364	200	8.3562E+01	-2.4843E-01	3.2594E-01	6.155E+13	-4.8308	-0.2001	1.609E-04	0.059
E-9	950	1.0	1800	1E-03	334	151	7.9680E+01	-1.9462E-01	8.2963E-02	6.155E+13	-4.8308	0.0370	2.928E-04	0.098
E-10	950	1.0	9000	1E-03	386	200	8.5416E+01	-2.7656E-01	4.6763E-01	6.155E+13	-4.8308	-0.3360	1.288E-04	0.050

Specimen ID	Temp (°C) T	Total Strain Range (%)	Hold Time (s) t_h	Strain Rate (1/s)	Cycles to Failure N_f	Cycle used for Midlife N_{mid}	Stress Relaxation Fitting Parameters b_0	b_1	t_0	$A=3600*10^{-C+a0/T}$	$m=a_1/T$	$1-b_1\,m$	Mid-life Creep Damage D_k^c	Creep Damage Fraction D_C
1000-12	1000	0.3	18	1E-03	2060	999	6.7275E+01	-3.2313E-01	1.2274E-01	5.373E+12	-4.6410	-0.4997	2.965E-04	0.611
1000-13	1000	0.3	18	1E-03	2770	999	7.7928E+01	-3.6839E-01	3.1079E-01	5.373E+12	-4.6410	-0.7097	3.416E-04	0.946
1000-14	1000	0.3	18	1E-03	2420	1000	6.6076E+01	-3.5050E-01	2.2126E-01	5.373E+12	-4.6410	-0.6267	2.004E-04	0.485
1000-07	1000	0.3	60	1E-03	3830	999	6.4481E+01	-3.3160E-01	2.1760E-01	5.373E+12	-4.6410	-0.5390	1.868E-04	0.715
1000-28	1000	0.3	60	1E-03	5020	2500	4.8212E+01	-3.5655E-01	2.9920E-01	5.373E+12	-4.6410	-0.6548	3.933E-05	0.197
1000-08	1000	0.3	180	1E-03	4010	999	5.9547E+01	-3.0534E-01	2.0594E-01	5.373E+12	-4.6410	-0.4171	1.401E-04	0.562
1000-08R	1000	0.3	180	1E-03	3530	1800	5.6830E+01	-3.0733E-01	2.4612E-01	5.373E+12	-4.6410	-0.4263	1.037E-04	0.366
1000-09	1000	0.3	600	1E-03	2520	1300	4.2064E+01	-3.2368E-01	1.5658E-01	5.373E+12	-4.6410	-0.5022	3.184E-05	0.080
1000-18B	1000	0.3	600	1E-03	2110	1055	5.8213E+01	-3.3148E-01	2.5268E-01	5.373E+12	-4.6410	-0.5384	1.110E-04	0.234
1000-23	1000	0.3	1800	1E-03	2000	1000	5.2184E+01	-3.2082E-01	2.7457E-01	5.373E+12	-4.6410	-0.4889	6.609E-05	0.132
1000-11	1000	1.0	18	1E-03	530	265	8.6838E+01	-2.8481E-01	2.7668E-01	5.373E+12	-4.6410	-0.3218	6.439E-04	0.341
1000-11R	1000	1.0	18	1E-03	510	255	9.1634E+01	-3.0022E-01	3.4039E-01	5.373E+12	-4.6410	-0.3933	7.304E-04	0.373
1000-02	1000	1.0	60	1E-03	415	207	8.8045E+01	-2.7758E-01	2.6750E-01	5.373E+12	-4.6410	-0.2883	7.912E-04	0.329
1000-21	1000	1.0	60	1E-03	370	190	5.2120E+01	-2.8076E-01	1.4450E-01	5.373E+12	-4.6410	-0.3030	8.618E-05	0.032
1000-03	1000	1.0	180	1E-03	360	180	7.9407E+01	-1.7304E-01	6.4196E-02	5.373E+12	-4.6410	0.1969	1.364E-03	0.491
1000-03R	1000	1.0	180	1E-03	330	165	7.5384E+01	-2.4925E-01	1.4290E-01	5.373E+12	-4.6410	-0.1568	5.595E-04	0.185
1000-04	1000	1.0	600	1E-03	400	200	7.4542E+01	-2.5977E-01	1.8766E-01	5.373E+12	-4.6410	-0.2056	5.062E-04	0.202
1000-15	1000	1.0	600	1E-03	300	200	6.7832E+01	-2.2171E-01	1.0412E-01	5.373E+12	-4.6410	-0.0290	4.810E-04	0.144
1000-05	1000	1.0	1800	1E-03	460	230	8.1542E+01	-3.4057E-01	5.2084E-01	5.373E+12	-4.6410	-0.5806	3.446E-04	0.159
1000-17	1000	1.0	1800	1E-03	460	200	7.2131E+01	-2.6059E-01	2.0913E-01	5.373E+12	-4.6410	-0.2094	4.407E-04	0.203

Creep Damage Calculations for Tests with Compressive Holds

Specimen ID	Hold Type[†]	Temp (°C)	Total Strain Range (%)	Hold Time (s) t_h	Strain Rate (1/s)	Cycles to Failure N_f	Cycle used for Midlife N_{mid}	Stress Relaxation Fitting Parameters b_0	b_1	t_0	$A=3600*10^{-C+a0/T}$	$m=a_1/T$	$1-b_1\,m$	Creep Damage/ Cycle D_k^c	Creep Damage Fraction D_C
4-1-7	C	950	0.3	180	1E-03	4373	2190	8.6929E+01	-3.1171E-01	2.9803E-01	6.155E+13	-4.8308	-0.5058	1.327E-04	**0.58**
4-1-5	T	950	0.3	90	1E-03	1310	650	1.1183E+02	-3.4952E-01	3.9482E-01	6.155E+13	-4.8308	-0.6885	3.439E-04	0.45
	C	950	0.3	90	1E-03	1310	650	1.0265E+02	-2.9902E-01	2.2190E-01	6.155E+13	-4.8308	-0.4445	3.457E-04	0.45
	T & C	950	0.3	180	1E-03	1310	650								**0.90**
4-1-3	T	950	0.3	360	1E-03	1159	583	1.0337E+02	-2.9066E-01	2.3799E-01	6.155E+13	-4.8308	-0.4041	3.666E-04	0.42
	C	950	0.3	360	1E-03	1159	583	1.0489E+02	-2.8825E-01	2.1786E-01	6.155E+13	-4.8308	-0.3925	4.112E-04	0.48
	T & C	950	0.3	720	1E-03	1159	583								**0.90**

[†] T ≡ tensile hold
C ≡ compressive hold
T & C ≡ tensile & compressive holds

Page intentionally left blank

Fatigue Damage Calculations

Specimen ID	Temp (°C)	Total Strain Range (%)	Hold Time (s)	Strain Rate (1/s)	Cycles to Failure	Average Fatigue Life	Fatigue Damage Fraction
			t_h		N_f	N_d	D_F
800-18	800	0.3	18	1E-03	8160	29680	0.275
800-09	800	0.3	60	1E-03	8370	29680	0.282
800-10	800	0.3	60	1E-03	4760	29680	0.160
800-13	800	0.3	600	1E-03	3960	29680	0.133
800-20	800	0.3	600	1E-03	3500	29680	0.118
800-05	800	1.0	60	1E-03	485	790	0.614
800-06	800	1.0	60	1E-03	440	790	0.557
800-24	800	1.0	180	1E-03	546	790	0.691
800-07	800	1.0	600	1E-03	580	790	0.734
800-11	800	1.0	600	1E-03	390	790	0.494
4-1-10	850	0.3	180	1E-03	1944	10010	0.194
4-1-12	850	0.3	180	1E-03	2547	10010	0.254
4-1-20	850	0.3	600	1E-03	1475	10010	0.147
4-1-22	850	0.3	600	1E-03	1750	10010	0.175
4-2-9	850	0.3	600	1E-03	2104	10010	0.210
4-7-1	850	0.3	1800	1E-03	1200	10010	0.120
4-7-3	850	0.3	1800	1E-03	1255	10010	0.125
4-7-17	850	0.3	3600	1E-03	1025	10010	0.102
9557-5	850	0.6	60	1E-03	1,182	1715	0.689
9557-6	850	0.6	60	1E-03	994	1715	0.580
LCF-10	850	0.6	60	1E-03	1,008	1715	0.588
LCF-11	850	0.6	60	1E-03	1,280	1715	0.746
9557-7	850	0.6	60	4E-04	1434	1638	0.875
9557-8	850	0.6	60	4E-04	1192	1638	0.728
LCF-12	850	0.6	60	4E-04	1565	1638	0.955
LCF-13	850	0.6	60	4E-04	1390	1638	0.849
4-2-1	850	1.0	180	1E-03	544	828	0.657
4-2-4	850	1.0	180	1E-03	660	828	0.797
4-2-2	850	1.0	600	1E-03	487	828	0.588
4-2-5	850	1.0	600	1E-03	548	828	0.662
4-2-7	850	1.0	1800	1E-03	371	828	0.448
4-2-8	850	1.0	1800	1E-03	453	828	0.547
4-7-15	850	1.0	7200	1E-03	148	828	0.179
4-7-16	850	1.0	7200	1E-03	311	828	0.376
4-7-18	850	1.0	14400	1E-03	114	828	0.138
4-7-19	850	1.0	14400	1E-03	155	828	0.187
K-11	950	0.3	2	1E-03	4083	8006	0.510
K-14	950	0.3	2	1E-03	3538	8006	0.442
F-14	950	0.3	180	1E-03	4486	8006	0.560
B-5	950	0.3	180	1E-03	3984	8006	0.498
B-6	950	0.3	180	1E-03	2485	8006	0.310
4-1-7	950	0.3	180*	1E-03	4373	8006	0.546
4-1-5	950	0.3	90+90[†]	1E-03	1310	8006	0.164
B-7	950	0.3	600	1E-03	4096	8006	0.512
A-22	950	0.3	600	1E-03	4430	8006	0.553
B-9	950	0.3	600	1E-03	2623	8006	0.328
F-15	950	0.3	600	1E-03	4361	8006	0.545
4-1-3	950	0.3	360+360[†]	1E-03	1159	8006	0.145
B-11	950	0.3	1800	1E-03	4832	8006	0.604
B-8	950	0.3	1800	1E-03	4650	8006	0.581
43-14	950	0.3	1800	1E-03	2653	8006	0.331
RT-70	950	0.4	60	1E-03	1680	2378	0.706
RT-71	950	0.4	60	4E-04	1768	2326	0.760
RT-12	950	0.6	60	1E-03	1085	1376	0.789
RT-16	950	0.6	60	1E-03	953	1376	0.693

Specimen ID	Temp (°C)	Total Strain Range (%)	Hold Time (s) t_h	Strain Rate (1/s)	Cycles to Failure N_f	Average Fatigue Life N_d	Fatigue Damage Fraction D_F
RT-66	950	0.6	60	1E-03	975	1376	0.709
LCF-15	950	0.6	60	1E-03	904	1376	0.657
LCF-18	950	0.6	60	1E-03	1048	1376	0.762
A-23	950	0.6	180	1E-03	950	1376	0.690
B-16	950	0.6	180	1E-03	922	1376	0.670
B-18	950	0.6	600	1E-03	686	1376	0.499
B-19	950	0.6	600	1E-03	634	1376	0.461
A-14	950	0.6	600	1E-03	547	1376	0.398
B-21	950	0.6	1800	1E-03	661	1376	0.480
F-13	950	0.6	1800	1E-03	1110	1376	0.807
416-18	950	0.6	1800	1E-03	525	1376	0.382
RT-13	950	0.6	60	4E-04	826	1344	0.615
RT-15	950	0.6	60	4E-04	986	1344	0.734
RT-67	950	0.6	60	4E-04	1046	1344	0.778
LCF-16	950	0.6	60	4E-04	1054	1344	0.784
LCF-17	950	0.6	60	4E-04	937	1344	0.697
K-12	950	1.0	2	1E-03	820	937	0.875
K-13	950	1.0	2	1E-03	790	937	0.843
A-6	950	1.0	180	1E-03	376	937	0.401
F-5	950	1.0	180	1E-03	465	937	0.496
B-12	950	1.0	180	1E-03	472	937	0.504
A-13	950	1.0	600	1E-03	308	937	0.329
F-4	950	1.0	600	1E-03	391	937	0.417
E-1	950	1.0	600	1E-03	427	937	0.456
E-8	950	1.0	600	1E-03	430	937	0.459
E-6	950	1.0	1800	1E-03	322	937	0.344
E-7	950	1.0	1800	1E-03	364	937	0.388
E-9	950	1.0	1800	1E-03	334	937	0.356
E-10	950	1.0	9000	1E-03	386	937	0.412
1000-12	1000	0.3	18	1E-03	2060	13270	0.155
1000-13	1000	0.3	18	1E-03	2770	13270	0.209
1000-14	1000	0.3	18	1E-03	2420	13270	0.182
1000-07	1000	0.3	60	1E-03	3830	13270	0.289
1000-28	1000	0.3	60	1E-03	5020	13270	0.378
1000-08	1000	0.3	180	1E-03	4010	13270	0.302
1000-08R	1000	0.3	180	1E-03	3530	13270	0.266
1000-09	1000	0.3	600	1E-03	2520	13270	0.190
1000-18B	1000	0.3	600	1E-03	2110	13270	0.159
1000-23	1000	0.3	1800	1E-03	2000	13270	0.151
1000-11	1000	1.0	18	1E-03	530	603	0.879
1000-11R	1000	1.0	18	1E-03	510	603	0.846
1000-02	1000	1.0	60	1E-03	415	603	0.688
1000-21	1000	1.0	60	1E-03	370	603	0.614
1000-03	1000	1.0	180	1E-03	360	603	0.597
1000-03R	1000	1.0	180	1E-03	330	603	0.547
1000-04	1000	1.0	600	1E-03	400	603	0.663
1000-15	1000	1.0	600	1E-03	300	603	0.498
1000-05	1000	1.0	1800	1E-03	460	603	0.763
1000-17	1000	1.0	1800	1E-03	460	603	0.763

[*] compressive hold
[†] tensile & compressive holds

BACKGROUND

HBB-T-1431(e) TEMPERATURE LIMITS

The current rules in Subsection HB, Subpart B for the evaluation of strain limits and creep-fatigue damage using simplified methods based on elastic analysis have been deemed inappropriate for Alloy 617 at temperatures above 1200°F (Corum 1991). Although the restriction specifically focuses on strain limits, satisfaction of the simplified rules for strain limits is a prerequisite for satisfaction of the current rules for creep fatigue evaluation. Specifically, a change in behavior of Alloy 617 above 1200°F is cited as the principal reason. Below 1200°F Alloy 617 behaves similar to the other Subsection HB materials whose behavior has been well studied and the rules verified. Applicable changes above 1200°F are cited as: "(1) lack of a clear distinction between time independent (elastic-plastic) and time dependent (creep) behavior, (2) high dependence of flow stresses on strain rate, and (3) softening with time, temperature and strain. However, the simplified methods in Subsection HB are based on time and rate independent, or train hardening, idealizations of material behavior." These behavioral changes are equally applicable to the current creep-fatigue evaluation rules.

References

Corum, J.M., and Blass, J.J., (1991), Rules for Design of Alloy 617 Nuclear Components to Very High Temperatures, ASME PVP Vol. 215, p.147, American Society of Mechanical Engineers, New York, NY.

Page intentionally left blank

BACKGROUND

HBB-T-1440 LIMITS USING ELASTIC-PERFECTLY PLASTIC ANALYSIS

CREEP-FATIGUE DAMAGE

Background

High temperature design methods employ a group of simplified analysis methods whose objective is to show compliance with code criteria for allowable stress, strain and creep-fatigue limits. "Simplified methods" refers to analysis methods that do not require the use of comprehensive full inelastic constitutive equations. An advantage of Elastic-perfectly plastic (EPP) simplified analysis methods is that they have been shown to demonstrate compliance with code strain and creep-fatigue limits without the use of stress classification procedures.

Application of EPP to Cyclic Loading and Strain Limits

Consider the application of EPP methods to address cyclic loading. The use of EPP methods for assessment of strain limits and creep-fatigue has been justified by detailed proofs [1] and by intuitive arguments. These proofs have been supplemented with experimental data, inelastic analyses and example problems as reported in [1], [2], [3] and [4]. Details on previous applications for cyclic loading are also given in [5], [6] and [7]. A summary of the EPP methods is scheduled for PVP 2016 [8]. The application of the EPP methodology to 304H and 316H stainless steel in Code Cases N-861 [9] and N-862 [10] for strain limits and creep fatigue, respectively, is the same as currently proposed for Alloy 617.

The detailed proofs are based on consideration of the work and energy dissipation rates over and throughout the volume of the structure as augmented by the observation that decreasing the yield stress for a given bounding solution will not reduce the deformation. The latter point provides the bridge between time independent cyclic plastic analyses and full visco-plastic behavior. Thus, a viable rapid cyclic solution, where "rapid cycle" describes the case with no consideration of stress relaxation during the cycle, represents an acceptable design. The rapid cycle solution is that determined from the EPP analysis with the associated yield stress identified as the "pseudo yield stress". The pseudo yield stress is that for which the EPP analysis must demonstrate shakedown to ensure compliance throughout the structure with the selected limit.

The strain limits are, thus, guaranteed by a ratcheting analysis with the pseudo yield stress defined by the stress to cause the target inelastic strain in a selected time. It may be shown, for example, that if an EPP cyclic analysis with a material pseudo yield stress defined by x% inelastic strain in say 300,000 hours does not give ratcheting, then the steady cyclic strain accumulation in 300,000 hours will be less than x%. However, there is the potential for additional straining due to redistribution effects from elastic follow-up, redundancy etc. that are required to set up the steady cyclic state. This additional strain is represented by the plastic strain, p%, from the shakedown analysis using the pseudo yield strength based on x%. Thus, it is required that the analysis plastic strain p% at one point anywhere in every cross-section satisfies x% + p% ≤ 1%. This guarantees a continuous core with not more than 1% accumulated inelastic strain. There are similar requirements for all points in the structure and for welds for their respective limits.

The calculation of creep damage in a cyclic creep-fatigue assessment is based on similar arguments. The difference is that the strain limits calculation deals with deformations over the limiting section in the structure and cyclic creep damage is calculated at a critical point. For this case, the pseudo yield stress is the stress to cause creep damage = 1 in a selected time, as a function of temperature. The EPP analysis

looks for shakedown (elastic) behavior to show that cyclic creep damage is less than 1. The selected time may then be used in a time fraction, creep damage calculation. The fatigue damage is based on the total, elastic plus inelastic, strain ranges from the elastic shakedown analysis. The combined creep and fatigue damage is then evaluated using the allowable creep-fatigue damage envelope.

Summary

In summary, the general property relied on in these simplified calculations is the conservatism of the rapid cycle solution. Rapid cycles accumulate more strain and damage than cycles defined by the same loads but with a hold time. The EPP analyses reflect the rapid cycle solutions, which are physically realistic.

Also included in the rules based on EPP analysis is new guidance on evaluation of Service level C conditions. Because Level C events are not expected, are limited in number, and require shutdown and inspection for damage and repair, Level C events are permitted to be evaluated separately and not combined with Levels A and B as is the current requirement.

References

1. Wang, Y., Jetter, R. I., Baird, S. T., Pu, C. and Sham, T.-L. (2015a): "Report on FY15 Alloy 617 SMT Creep-Fatigue Test Results" ORNL/TM-2015/300, Oak Ridge National Laboratory, Oak Ridge, TN., http://info.ornl.gov/sites/publications/Files/Pub56336.pdf

2. Wang, Y., Jetter, R. I., Baird, S. T., Pu, C. and Sham, T.-L. (2015b), "Report on FY15 Two-Bar Thermal Ratcheting Test Results" ORNL/TM-2015/284, Oak Ridge National Laboratory, Oak Ridge, TN. http://info.ornl.gov/sites/publications/Files/Pub56202.pdf

3. ASME C&S CONNECT, Record # 14-1445, "EPP Strain Limit Code Case for 304 and 316 Stainless Steel."

4. ASME C&S CONNECT, Record # 14-1446, "EPP Creep-Fatigue Code Case for 304 and 316 Stainless Steel."

5. Carter, P., (2005), "Analysis of cyclic creep and rupture. Part 1: Bounding Theorems and Cyclic Reference Stresses," Int. J Press & Piping, Vol. 82, pp. 15-26.

6. Carter, P., Jetter, R., Sham, T.-L., (2012a), "Application of Elastic-Perfectly Plastic Cyclic Analysis to Assessment of Creep Strain", PVP 2012 – 78082, American Society of Mechanical Engineers, New York, NY.

7. Carter, P., Jetter, R., Sham, T.-L., (2012b), "Application of Shakedown Analysis to Evaluation of Creep-Fatigue Limits", PVP 2012-78083, American Society of Mechanical Engineers, New York, NY.

8. Carter, P., Sham, T-L., Jetter, R, (2016), "Overview of Proposed High Temperature Design Code Cases", PVP 2016 – 63559, American Society of Mechanical Engineers, New York, NY.

9. Code Case N-861, "Satisfaction of Strain limits for Division 5 Class A Components at Elevated Temperature Service Using Elastic-Perfectly Plastic Analysis."

10. Code Case N-862, "Calculation of Creep-Fatigue for Division 5 Class A Components at Elevated Temperature Service Using Elastic-Perfectly Plastic Analysis.

Page intentionally left blank

Background Document – Record No. 16-999

Contents

- Balloting Actions
- HBB-T-1340 Satisfaction of Strain Limits Using Elastic-Perfectly Plastic Analysis

Page intentionally left blank

Alloy 617 Code Case Balloting Actions

RC #	Item	Section II and III Committees (See Color Key Below For Balloting Actions)								
16-994	Permissible base and weld materials, allowable stress values	WG-ASC	SG-ETD	SG-HTR	SG-MFE	II-SG-NFA	II-SG-SW	BPV-II		
16-995	Physical properties and extension of modulus values to higher temperatures	WG-ASC	SG-ETD	SG-HTR	SG-MFE	II-SG-NFA	II-SG-PP	BPV-II		
16-996	Temperature-time limits for NB buckling charts	WG-AM	SG-ETD	SG-HTR	SG-MFE	II-SG-EP	BPV-II	II-SG-NFA	SC-D	
16-997	Huddleston parameters, ISSCs	WG-ASC	SG-ETD	SG-HTR	II-SG-NFA	BPV-II	SC-D			
16-998	Negligible creep, Creep-Fatigue: D-diagram and EPP	WG-CFNC	SG-ETD	SG-HTR	SC-D					
16-999	EPP strain limits	WG-AM	SG-ETD	SG-HTR	SC-D					
16-1000	Fatigue design curves	WG-CFNC	WG-FS	SG-ETD	SG-HTR	SG-DM	SC-D			
16-1001	Alloy 617 Overall Code Case	WG-ASC	WG-AM	WG-CFNC	WG-FS	SG-ETD	SG-HTR	SG-MFE	SC-D	BPV-II
		BPV-III								

Color Key	Balloting Action
	For Review and Approval
	For Review and Comment

Page intentionally left blank

HBB-T-1340   SATISFACTION OF STRAIN LIMITS USING ELASTIC-PERFECTLY PLASTIC ANALYSIS

Background

High temperature design methods employ a group of simplified analysis methods whose objective is to show compliance with code criteria for allowable stress, strain and creep-fatigue limits. "Simplified methods" refers to analysis methods that do not require the use of comprehensive full inelastic constitutive equations. An advantage of Elastic-perfectly plastic (EPP) simplified analysis methods is that they have been shown to demonstrate compliance with code strain and creep-fatigue limits without the use of stress classification procedures.

Application of EPP to Cyclic Loading and Strain Limits

Consider the application of EPP methods to address cyclic loading. The use of EPP methods for assessment of strain limits and creep-fatigue has been justified by detailed proofs [1] and by intuitive arguments. These proofs have been supplemented with experimental data, inelastic analyses and example problems as reported in [1], [2], [3] and [4]. Details on previous applications for cyclic loading are also given in [5], [6] and [7]. A summary of the EPP methods is scheduled for PVP 2016 [8]. The application of the EPP methodology to 304H and 316H stainless steel in Code Cases N-861 [9] and N-862 [10] for strain limits and creep fatigue, respectively, is the same as currently proposed for Alloy 617.

The detailed proofs are based on consideration of the work and energy dissipation rates over and throughout the volume of the structure as augmented by the observation that decreasing the yield stress for a given bounding solution will not reduce the deformation. The latter point provides the bridge between time independent cyclic plastic analyses and full visco-plastic behavior. Thus, a viable rapid cyclic solution, where "rapid cycle" describes the case with no consideration of stress relaxation during the cycle, represents an acceptable design. The rapid cycle solution is that determined from the EPP analysis with the associated yield stress identified as the "pseudo yield stress". The pseudo yield stress is that for which the EPP analysis must demonstrate shakedown to ensure compliance throughout the structure with the selected limit.

The strain limits are, thus, guaranteed by a ratcheting analysis with the pseudo yield stress defined by the stress to cause the target inelastic strain in a selected time. It may be shown, for example, that if an EPP cyclic analysis with a material pseudo yield stress defined by x% inelastic strain in say 300,000 hours does not give ratcheting, then the steady cyclic strain accumulation in 300,000 hours will be less than x%. However, there is the potential for additional straining due to redistribution effects from elastic follow-up, redundancy etc. that are required to set up the steady cyclic state. This additional strain is represented by the plastic strain, p%, from the shakedown analysis using the pseudo yield strength based on x%. Thus, it is required that the analysis plastic strain p% at one point anywhere in every cross-section satisfies x% + p% ≤ 1%. This guarantees a continuous core with not more than 1% accumulated inelastic strain. There are similar requirements for all points in the structure and for welds for their respective limits.

The calculation of creep damage in a cyclic creep-fatigue assessment is based on similar arguments. The difference is that the strain limits calculation deals with deformations over the limiting section in the structure and cyclic creep damage is calculated at a critical point. For this case, the pseudo yield stress is the stress to cause creep damage = 1 in a selected time, as a function of temperature. The EPP analysis looks for shakedown (elastic) behavior to show that cyclic creep damage is less than 1.The selected time may then be used in a time fraction, creep damage calculation. The fatigue damage is based on the total, elastic plus inelastic, strain ranges from the elastic shakedown analysis. The combined creep and fatigue damage is then evaluated using the allowable creep-fatigue damage envelope.

Summary

In summary, the general property relied on in these simplified calculations is the conservatism of the rapid cycle solution. Rapid cycles accumulate more strain and damage than cycles defined by the same loads but with a hold time. The EPP analyses reflect the rapid cycle solutions, which are physically realistic.

Also included in the rules based on EPP analysis is new guidance on evaluation of Service level C conditions. Because Level C events are not expected, are limited in number, and require shutdown and inspection for damage and repair, Level C events are permitted to be evaluated separately and not combined with Levels A and B as is the current requirement.

References

1. Wang, Y., Jetter, R. I., Baird, S. T., Pu, C. and Sham, T.-L. (2015a): "Report on FY15 Alloy 617 SMT Creep-Fatigue Test Results" ORNL/TM-2015/300, Oak Ridge National Laboratory, Oak Ridge, TN., http://info.ornl.gov/sites/publications/Files/Pub56336.pdf

2. Wang, Y., Jetter, R. I., Baird, S. T., Pu, C. and Sham, T.-L. (2015b), "Report on FY15 Two-Bar Thermal Ratcheting Test Results" ORNL/TM-2015/284, Oak Ridge National Laboratory, Oak Ridge, TN. http://info.ornl.gov/sites/publications/Files/Pub56202.pdf

3. ASME C&S CONNECT, Record # 14-1445, "EPP Strain Limit Code Case for 304 and 316 Stainless Steel."

4. ASME C&S CONNECT, Record # 14-1446, "EPP Creep-Fatigue Code Case for 304 and 316 Stainless Steel."

5. Carter, P., (2005), "Analysis of cyclic creep and rupture. Part 1: Bounding Theorems and Cyclic Reference Stresses," Int. J Press & Piping, Vol. 82, pp. 15-26.

6. Carter, P., Jetter, R., Sham, T.-L., (2012a), "Application of Elastic-Perfectly Plastic Cyclic Analysis to Assessment of Creep Strain", PVP 2012 – 78082, American Society of Mechanical Engineers, New York, NY.

7. Carter, P., Jetter, R., Sham, T.-L., (2012b), "Application of Shakedown Analysis to Evaluation of Creep-Fatigue Limits", PVP 2012-78083, American Society of Mechanical Engineers, New York, NY.

8. Carter, P., Sham, T-L., Jetter, R, (2016), "Overview of Proposed High Temperature Design Code Cases", PVP 2016 – 63559, American Society of Mechanical Engineers, New York, NY.

9. Code Case N-861, "Satisfaction of Strain limits for Division 5 Class A Components at Elevated Temperature Service Using Elastic-Perfectly Plastic Analysis."

10. Code Case N-862, "Calculation of Creep-Fatigue for Division 5 Class A Components at Elevated Temperature Service Using Elastic-Perfectly Plastic Analysis.

Background Document – Record No. 16-1000

Contents

- Balloting Actions
- HBB-T-1420-1 Design Fatigue Strain Range, ϵ_t, for Alloy 617

Page intentionally left blank

Alloy 617 Code Case Balloting Actions

RC #	Item	Section II and III Committees (See Color Key Below For Balloting Actions)								
16-994	Permissible base and weld materials, allowable stress values	WG-ASC	SG-ETD	SG-HTR	SG-MFE	II-SG-NFA	II-SG-SW	BPV-II		
16-995	Physical properties and extension of modulus values to higher temperatures	WG-ASC	SG-ETD	SG-HTR	SG-MFE	II-SG-NFA	II-SG-PP	BPV-II		
16-996	Temperature-time limits for NB buckling charts	WG-AM	SG-ETD	SG-HTR	SG-MFE	II-SG-EP	BPV-II	II-SG-NFA	SC-D	
16-997	Huddleston parameters, ISSCs	WG-ASC	SG-ETD	SG-HTR	II-SG-NFA	BPV-II	SC-D			
16-998	Negligible creep, Creep-Fatigue: D-diagram and EPP	WG-CFNC	SG-ETD	SG-HTR	SC-D					
16-999	EPP strain limits	WG-AM	SG-ETD	SG-HTR	SC-D					
16-1000	Fatigue design curves	WG-CFNC	WG-FS	SG-ETD	SG-HTR	SG-DM	SC-D			
16-1001	Alloy 617 Overall Code Case	WG-ASC	WG-AM	WG-CFNC	WG-FS	SG-ETD	SG-HTR	SG-MFE	SC-D	BPV-II
		BPV-III								

Color Key	Balloting Action
	For Review and Approval
	For Review and Comment

Page intentionally left blank

HBB-T-1420-1 DESIGN FATIGUE STRAIN RANGE, ϵ_t, FOR ALLOY 617

Scope

This document provides the background/technical basis in support of the recommendation for the design fatigue strain range for Alloy 617 in Figure HBB-T-1420-1F.

Background

The design fatigue curves are used in the Creep-Fatigue Evaluation presented in HBB-T-1400 and in the determination of Creep-Fatigue Reduction Factors (within Special Strain Requirements at Welds) in HBB-T-1715.

Data Sources

Fatigue data for Alloy 617 was compiled for the Alloy 617 draft Code Case developed in the late 1980s and presented by Yukawa.[1] Yukawa compiled data from numerous sources, including Oak Ridge National Laboratory, General Atomics, General Electric, German and Japanese sources.[2-7] Fatigue tests were conducted in air, axially loaded, and generally conformed to ASTM E466 and E606. Most testing was done at a nominal rate of 4E−03 /s. Data obtained from bending or on thin sheet were excluded from this data set. The data compiled by Yukawa is reproduced in Appendix I. Recent fatigue data have been contributed by Idaho National Laboratory (INL)[8] and are tabulated in Appendices II–IV.

Materials

Recent fatigue testing has been performed at INL on specimens machined from an Alloy 617 reference material plate.[9] The 37 mm thick solution-annealed plate is from heat 314626, produced by ThyssenKrupp VDM and the composition is given in Table 1. Although the average grain size of the plate is quantified as approximately 150 µm, significant grain size inhomogeneity is present in the microstructure.

Table 1. The composition in wt% of Alloy 617.

	Ni	C	Cr	Co	Mo	Fe	Al	Ti	Si	Cu	Mn	S	B
314626	Bal.	0.05	22.2	11.6	8.6	1.6	1.1	0.4	0.1	0.04	0.1	0.002	0.001

Quality

Fatigue properties of the Alloy 617 reference plate (heat 314626) reported by the Idaho National Laboratory (INL) through the Next Generation Nuclear Plant (NGNP) or Advanced Reactor Technologies (ART) programs were determined under an NQA-1 quality program. Details of the quality program implementation are given in INL document PLN-2690 "Idaho National Laboratory Advanced Reactor Technologies Technology Development Office Quality Assurance Program Plan".

Fatigue Testing

Cylindrical cyclic test specimens (Figure 1), 0.295 in. (7.5 mm) diameter with a reduced section of 0.79 in. (20 mm) and gage length of 0.5 in. (12.7 mm), were machined from heat 314626. Low stress grinding and longitudinal polishing were used in the final machining of the reduced section to eliminate cold work and circumferential machining marks. The long axis of the specimens was aligned with the rolling direction.
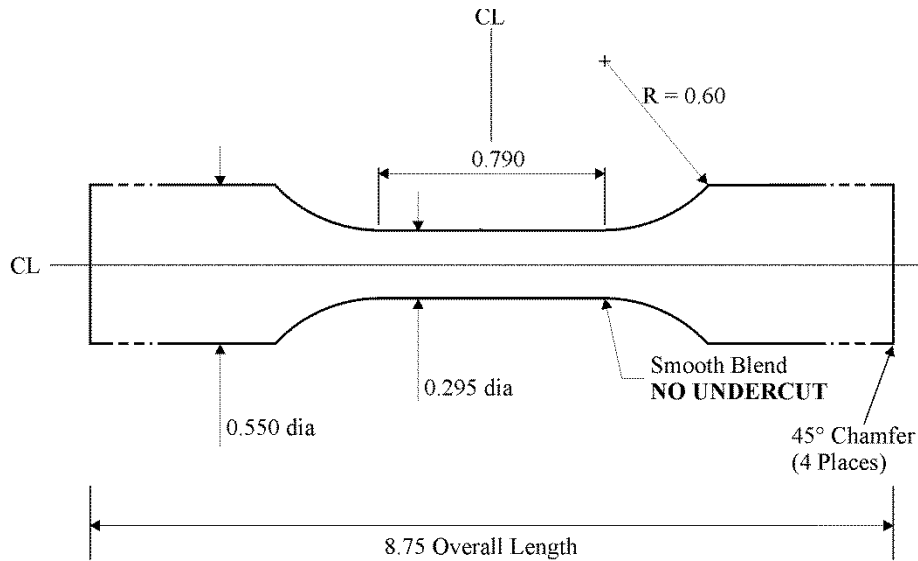
Figure 1. Specimen used for fatigue tests at INL.

Fully reversed, continuous low cycle fatigue (LCF) testing was conducted in air on servo-hydraulic test machines in strain control using calibrated extensometers for strain determination. LCF testing followed a triangular waveform with a strain rate during loading and unloading of 10^{-3}/s. A few tests were also run at a strain rate of 10^{-4}/s. Tests were performed at nominal total strain ranges from 0.3% to 2.0% at 427°C, from 0.2% to 2.0% at 850°C and from 0.3% to 3.0% at 950°C.[8] Two specimens were also tested at room temperature and nominal strain ranges of 0.42 and 0.80%. Testing was designed to be compliant with American Society for Testing and Materials (ASTM) Standard E606.[10] Specimens were heated either using a 3-zone resistance furnace or by radio-frequency induction. The temperature gradient was measured using a specimen with spot-welded thermocouples along the gage section, and was found to vary less than 1%. The temperature was monitored and/or controlled using either a spot-welded thermocouple on the specimen shoulder or a thermocouple loop at the center of the gage section, in conjunction with calibration curves from the temperature profile characterization. Test temperature was generally maintained within 2°C throughout the duration of the test; higher strain range specimens tested at 950°C via induction exceeded 2°C, but were all within 2.5%.

Maximum mean stress testing was performed at 550°C and strain ranges of 0.36 and 0.48% according to recommended methods.[11] For each condition, a baseline test with zero mean stress and a maximum mean stress test were performed. Because the tests were run in strain control, the actual mean stresses were limited by the range of the extensometer, ±2.2%. For the 0.36% test the maximum mean stress was calculated to be about 293 MPa, a stress of 283 MPa was targeted, corresponding to 3.36% strain according to a 550°C tensile test. The 3.36% tensile strain applied to the fatigue test, resulting in 278 MPa. The test was then cycled ±0.18% about a mean tensile strain of 3.365%. The 0.48% maximum mean stress test experienced a tensile strain of 3.257%, corresponding to a stress of 260 MPa prior to cycling ±0.24%. For both the 0.36 and 0.48% strain range tests, the mean stress drops dramatically from the stress obtained upon loading, even in the very first cycle, and the tests had average mean stress levels of 23 and 9 MPa, respectively.

The number of cycles to failure, N_f, is determined from a plot of the ratio of peak tensile to peak compressive stress versus cycles.[12] Determining the life from this ratio allows changes in peak stresses due to cyclic work hardening or softening to be distinguished from those due to crack formation and propagation. Macro-crack initiation, N_i, is defined as the point at which the stress ratio deviated from linearity; and failure, N_f, is defined as a 20% reduction in stress ratio from the point of deviation, as

shown in Figure 2. Due to the rapidly-falling peak tensile force during the final crack propagation phase, N_f is not very sensitive to the exact value of load drop used to define failure or to the accuracy of the crack initiation determination. In some cases the test was stopped before a 20% reduction in stress ratio was achieved and the N_f is the last cycle of the test. These cases are indicated in the data table shown in Appendices II and IV. In most cases, test termination was prior to actual specimen separation, based upon a predetermined drop in load; when the set load drop was detected, the test automatically switched to zero load and power to the heat source was shut off.
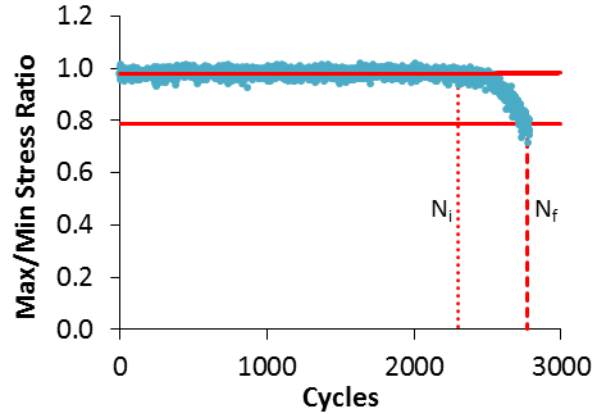
Figure 2. Illustration of failure criterion for fatigue tests.

Peak tensile and compressive load and strain and temperature were recorded for each cycle. Strain, load and temperature were recorded as a function of time for each of the first hundred cycles, and periodically thereafter, with the cycle recording frequency dependent upon the anticipated lifetime of the specimen. Cyclic stress-strain curves (hysteresis loops) can be plotted for the cycles where the load and strain data have been collected. The inelastic strain range for each specimen was determined from the width of a hysteresis loop at zero stress using a cycle at or near mid-life ($N_f/2$), as shown in Figure 3. The elastic strain range was determined by difference according to

$$\Delta\varepsilon_t = \Delta\varepsilon_i + \Delta\varepsilon_e \qquad [1]$$

where $\Delta\varepsilon_t$ is the total strain range, $\Delta\varepsilon_e$ is the elastic strain range, and $\Delta\varepsilon_i$ is the inelastic strain range. Elastic and inelastic strain ranges are used to calculate the elevated temperature design fatigue curves.
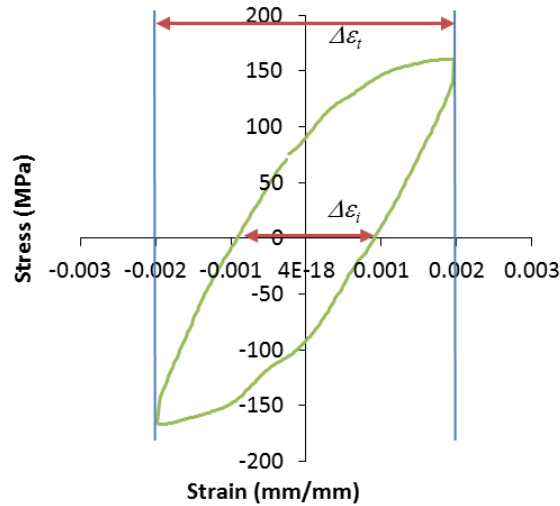
Figure 3. Inelastic strain determination from the width of a mid-life hysteresis loop. Example shown is from a specimen tested at 950°C and a total strain range of 0.4%.

Design fatigue Curves

Lower Temperature Design Curve

Design fatigue curve I-9.5 for nickel-chromium-molybdenum-iron alloys for temperatures not exceeding 425°C/800°F from ASME Code Section III, Mandatory Appendix I is compared to fatigue testing on Alloy 617 at 427°C and at room temperature (Appendix III) in Figure 4. Design fatigue curve I-9.5 has been approved for Alloy 617 by C&S Connect Record number 15-2762 by ASME Section III Subgroup Design Methods, Working Group Fatigue Strength. It has also been approved as part of the Alloy 617 Code Case for Section III, Division 5, Subsection HB, Subpart A, (i.e. Class A Metallic Pressure Boundary Components for Low Temperature Service) by the Board of Nuclear Codes and Standards.
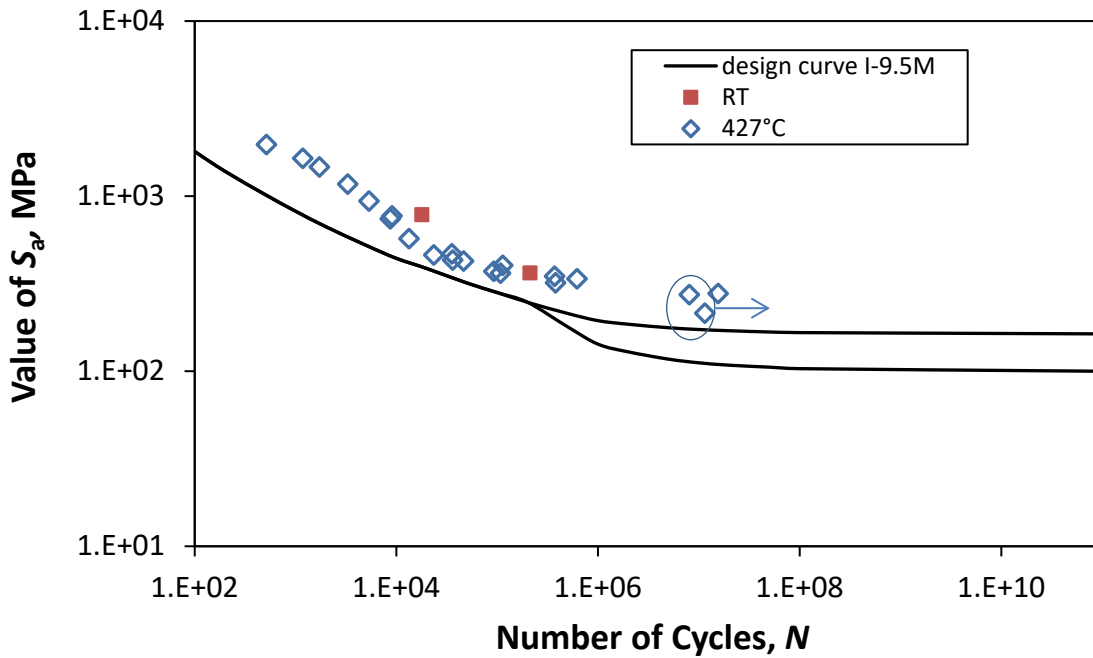
Figure 4. Design fatigue curve I-9.5M from ASME Code Section III, Appendix I, shown with fatigue data for Alloy 617. Circled symbols indicate tests that were suspended. A modulus value of 195E+03 MPa was used to calculate S_a for the data according to the footnote for Figure I-9.5M.

Elevated Temperature Design Curves

Fatigue test data from testing at the INL (Appendix II), described above, are in good agreement with the Yukawa data tested at similar strain rates and temperatures (Appendix I), as shown in Figure 5. Additional sources of data not included in the Yukawa compilation are also plotted in Figure 5.[13–15]
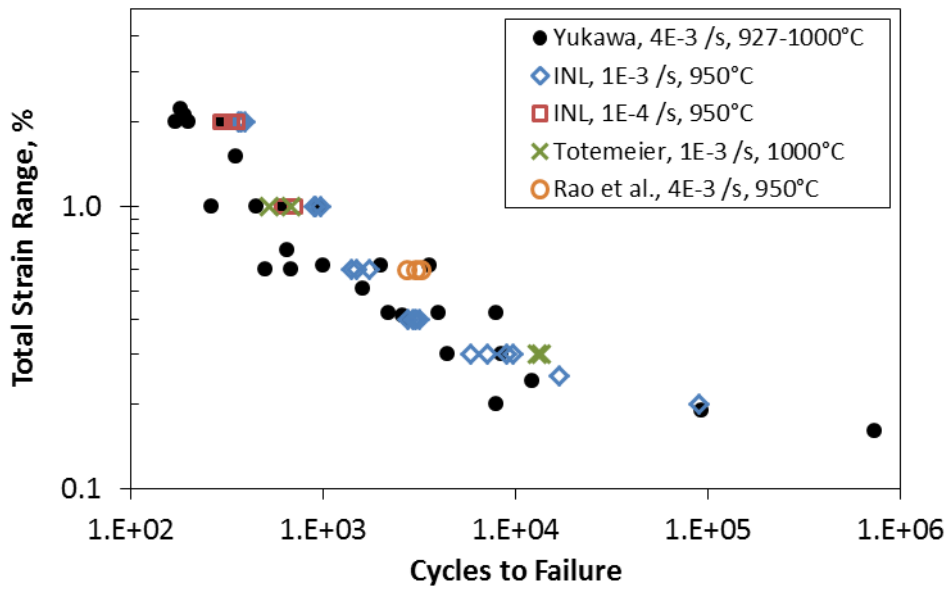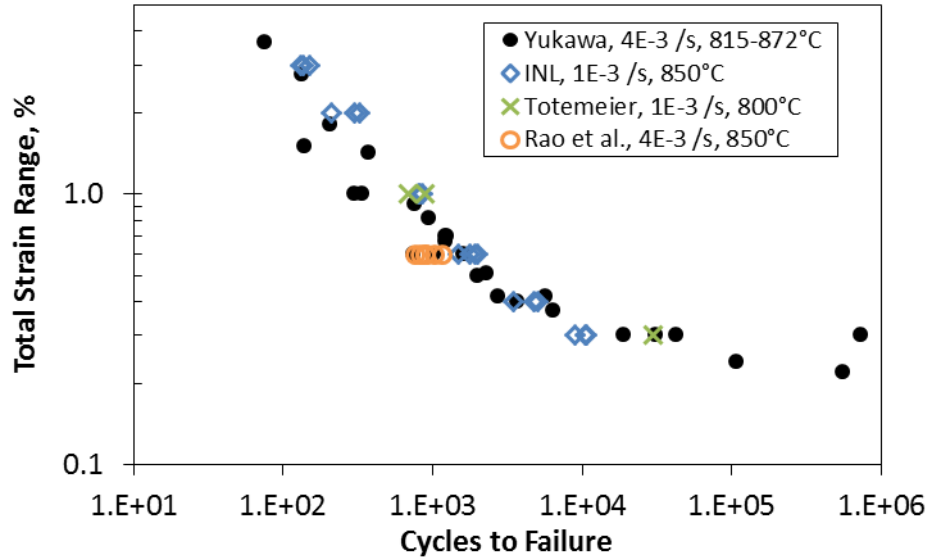
Figure 5. Comparison of recent fatigue data generated at 850 and 950°C to previous data compiled by Yukawa and additional data for Alloy 617 from tests at similar temperatures and strain rates.

Fatigue data were analyzed using the generalized equation from ASTM E606 with modified notation, presented by Yukawa[1]

$$\Delta\varepsilon_t = A(N_f)^a + B(N_f)^b \qquad [2]$$

where the first term is inelastic strain and the second term is elastic strain, N_f is the number of cycles to failure, and $A, a, B, b,$ are fitting parameters. Not all fatigue data used by Yukawa could be separated into their elastic and inelastic components. Where the stress range was reported, the elastic strains were calculated as:

$$\Delta\varepsilon_e = \Delta\sigma/E \qquad [3]$$

where $\Delta\sigma$ is the stress range and E is the elastic modulus. The E used was not reported, but by dividing the reported stress ranges by the elastic strain ranges it appears that temperature dependent values of E were used that are consistent with values reported in the SMC datasheet,[16] as shown in Figure 6. Moduli values reported in Section II of the ASME B&PV Code are shown for comparison. Inelastic strains were determined from Equation [1].
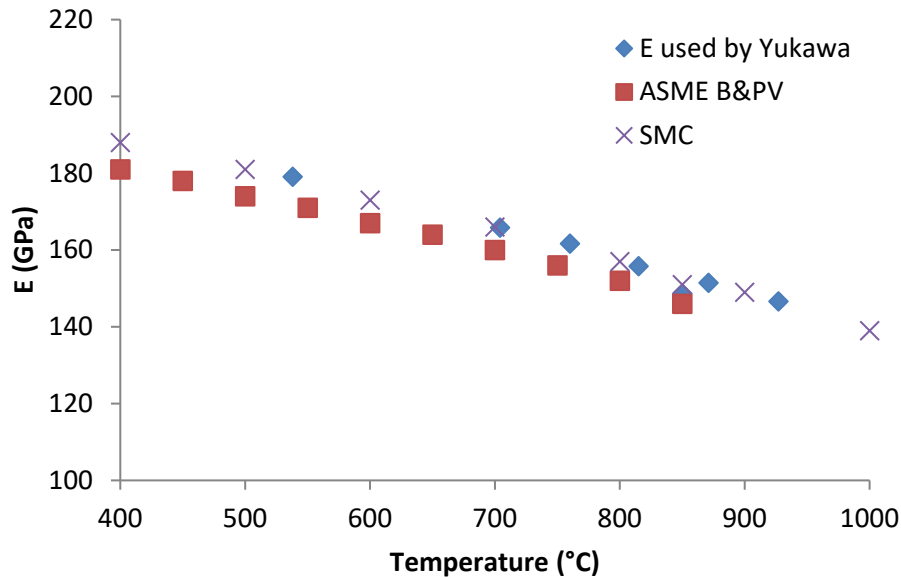
Figure 6. Analysis of elastic modulus values used by Yukawa. Values reported by SMC and in Section II of the ASME B&PV Code are shown for comparison.

The elastic and inelastic strain components of the combined data set (Yukawa compiled data + INL data) are plotted as a function of N_f. The inelastic strain range data, shown in Figure 7, are not dependent on temperature; the data can be represented by a single line. The coefficients of A and a from Equation [2] are 112.46 and −0.80, respectively.

However the elastic strain range data were found to cluster into three temperature dependent groups of 1000–1300°F (538–704°C), >1300–1600°F (>704–871°C), and >1600–1800°F (>871–982°C) as found by Yukawa[1] and are shown in Figure 8. These temperature ranges will henceforth be referred to and labeled by their maximum Fahrenheit use temperature, as they are in Figures HBB-T-1420-1 in ASME B&PV Section III, Division 5, Subsection HB, Subpart B. The coefficients of B and b from Equation [2] are shown on the figure and also in Table 2.
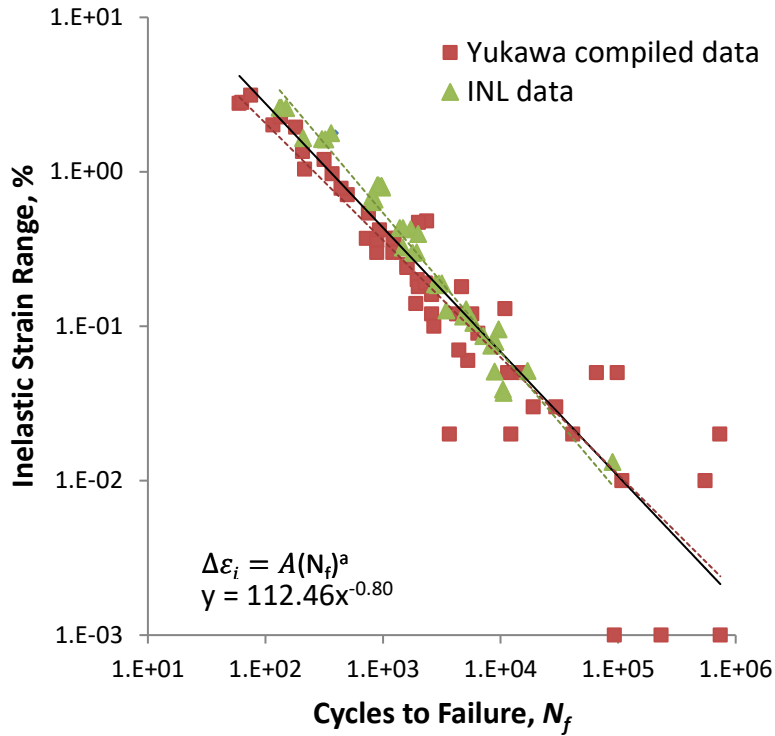
Figure 7. Inelastic strain as a function of cycles to failure for all INL fatigue data and fatigue data compiled by Yukawa for which stress range was reported.
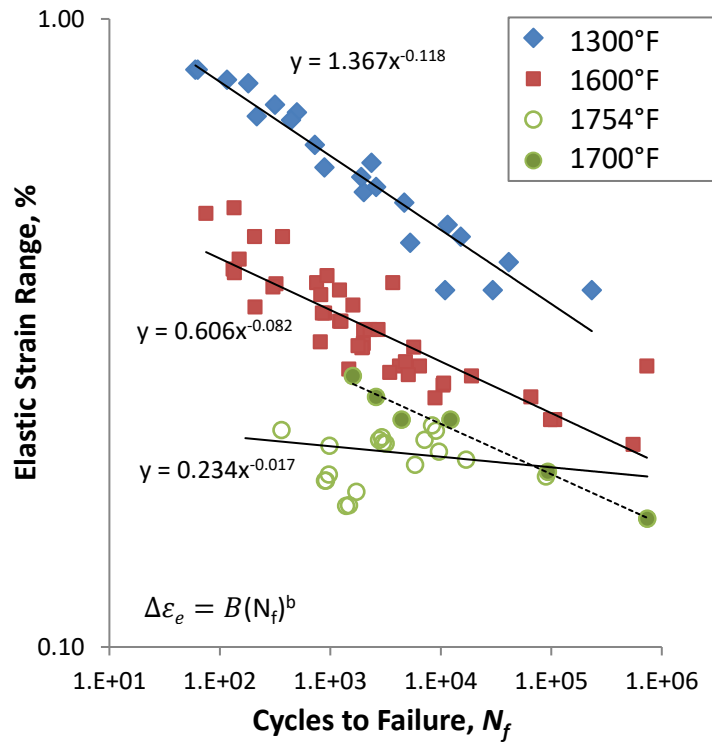
Figure 8. Elastic strain as a function of cycles to failure for all INL fatigue data and fatigue data compiled by Yukawa for which stress range was reported, showing temperature dependence.

Table 2. Elastic strain coefficients determined by regression fit to power-law equations.

label	T(°F)	T(°C)	B	b
1300°F	1000–1300°F	538−704°C	1.367	−0.118
1600°F	>1300–1600°F	>704−871°C	0.606	−0.082
1750°F	>1600–1750°F	>871−982°C	0.234	−0.017

The addition of the INL data set produces only a slight change in the inelastic relationship, as can be seen by comparing the red dotted line for the Yukawa data to the black line for all data in Figure 7. The elastic relationship for the 1300°F temperature range in Figure 8 and Table 2 is the same as that presented by Yukawa and the 1600°F elastic strain relationship of the intermediate temperature range differs slightly.

Although the six 1700°F data points from Yukawa (filled green circles and dotted line in Figure 8) have a similar slope to the lower temperature lines, the 1754°F data has little to no dependence on N_f. At 1754°F there is essentially no work hardening; peak stress, which correlates with elastic strain according to Equation [3], does not increase with increasing strain range. This has also been reported for 1832°F (1000°C).[13] The low b value obtained from the 1750°F combined data set (shown as a solid black line through the green data points in Figure 8) produces a design fatigue curve which would intersect the 1600°F curve at high cycles, which is not reasonable.

As an alternative, the slope for the elastic fit of the 1750°F line was set by extrapolating the slopes determined for the 1300 and 1600°F lines as shown in Figure 9. This results in a slope of −0.064 rather than −0.017. The linear regression of the elastic strain range is repeated with a slope of −0.064, resulting in a modified version of Figure 8, which is shown in Figure 10.
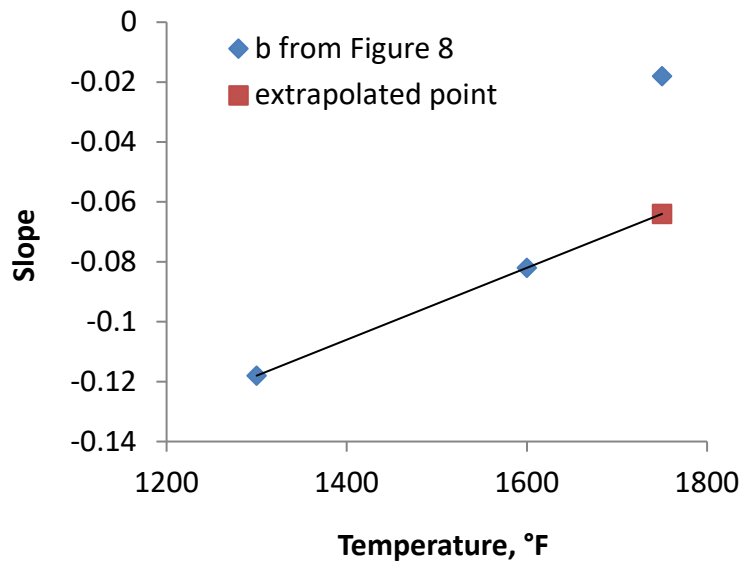
Figure 9. Determination of slope for 1750°F elastic fit by extrapolation of the 1300 and 1600°F slopes.
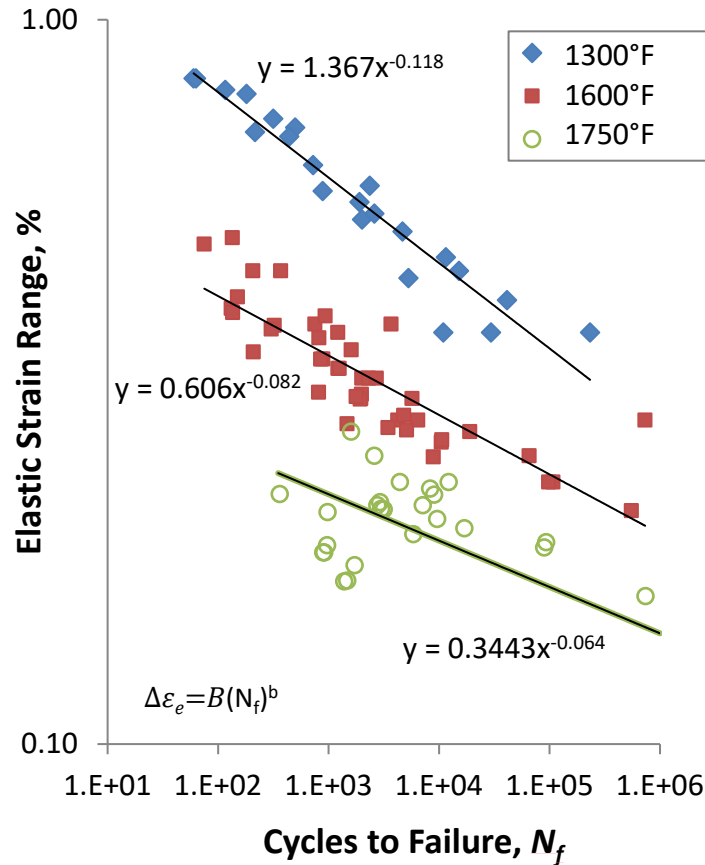
Figure 10. Elastic strain as a function of cycles to failure using the extrapolated slope shown in Figure 9 for the 1750°F line.

Multiaxial effects, including Poisson's ratio, are included in the design procedure, so the Poisson's correction[17] applied by Yukawa is not required.

In Appendix I to Section III, the design fatigue curve I-9.2 for the 300 series stainless steels and Ni-Cr-Fe alloys (including Alloy 800H) now reflects the use of a factor of 2 on the stress and 12 on cycles to failure. This modification was made based on a re-analysis of the Type 304 and 316 data in NUREG/CR-6909. All of the remaining curves in the Appendix to Section III, and all of the Section III Division 5 design fatigue curves retain the factors of 2 and 20. The fatigue data, curve fit, and 2 and 20 construction curves for creating the 1600°F design curve are shown in Figure 11. In ASME B&PV Section III, Division 5, HBB-T-1420, the design fatigue curves presented for some of the materials are smooth (304 and 316 SS), and others display cusps (2 ¼ Cr – 1 Mo Steel and alloy 800H, as shown in Figure 12). The smoothing process results in additional conservatism, particularly in the range of 10^2-10^4 cycles. The Alloy 617 elevated temperature design fatigue curves will be plotted to a maximum of 10^6 allowable cycles, without smoothing and using factors of 2 and 20, consistent with the low temperature curve from I-9.5 and the other Division 5 curves in HBB-T-1420.
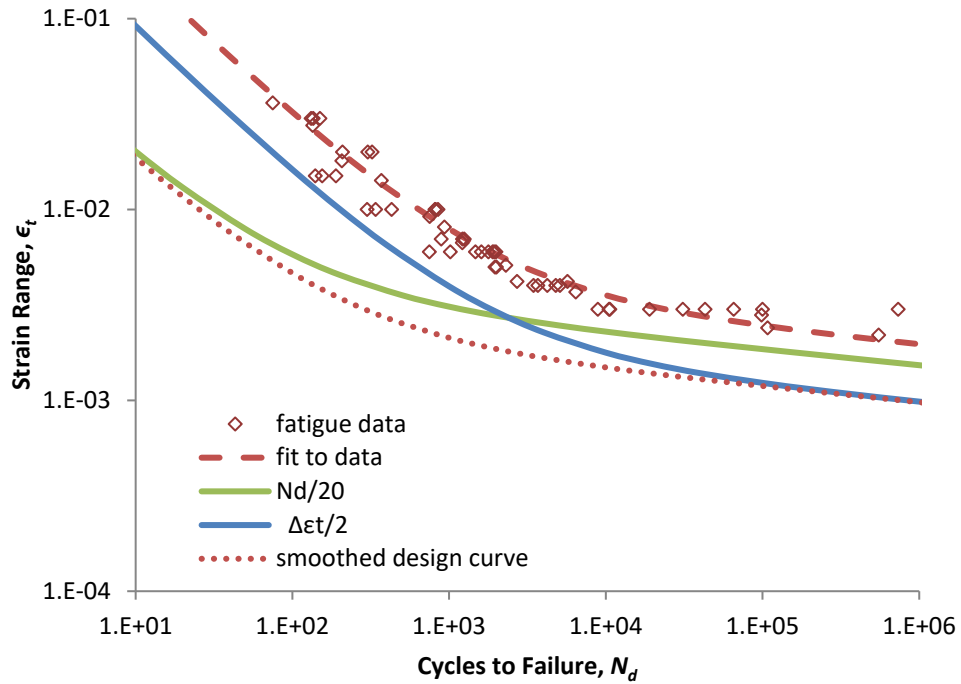
Figure 11. Fatigue data, curve fit, and construction curves used to construct the 1600°F design fatigue curve, along with an example of a smooth design curve.
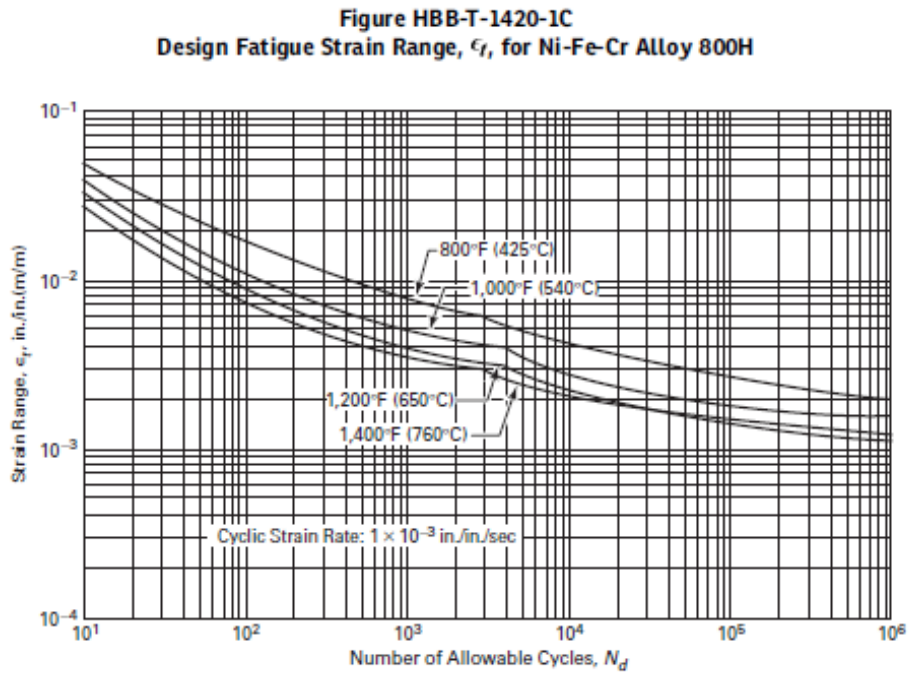
Figure 12. Design fatigue curves for Alloy 800H from the ASME B&PV Code Section III.

339

Design fatigue curve I-9.5 includes a maximum mean stress correction calculated based on the modified Goodman diagram.[2,18] At the highest temperatures, the material is not expected to sustain a significant mean stress because of rapid stress relaxation.[19] To assess the need for a mean stress correction in the temperature range of 1000-1300°F, maximum mean stress testing was performed at 1022°F (550°C) and strain ranges of 0.36 and 0.48% (Appendix IV). The baseline and mean stress tests are plotted with the fit to the fatigue data from 1000 and 1300°F (538 and 704°C). For both strain ranges tested, the maximum mean stress test does have a shorter life, but all four tests fall above the fit to the zero-mean-stress fatigue data. As a result, no maximum mean stress correction is included for the 1300°F design curve.
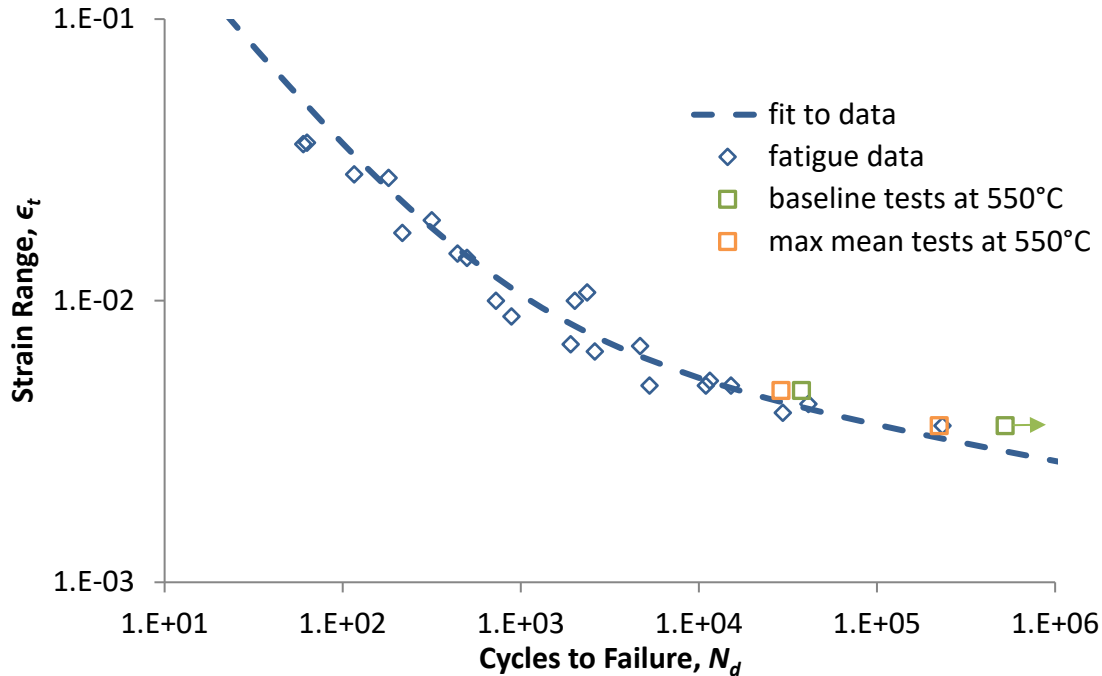
Figure 13. The baseline and mean stress tests for strain ranges of 0.36 and 0.48% and 550°C are plotted with the fatigue data for 538 and 704°C. The arrow on the 0.36% baseline test indicates that it did not fail, but was suspended at 524,319 cycles.

Figure HBB-T-1420-1F

In order to plot the elevated temperature design fatigue curves with curve I-9.5, the latter must be converted from S_a stress to ϵ_t strain range. This was done by multiplying S_i by 2, to convert stress into stress range, and dividing by 195 GPa, the elastic modulus noted on curve I-9.5M.

The design fatigue curves for all temperatures are shown together in Figure 14.
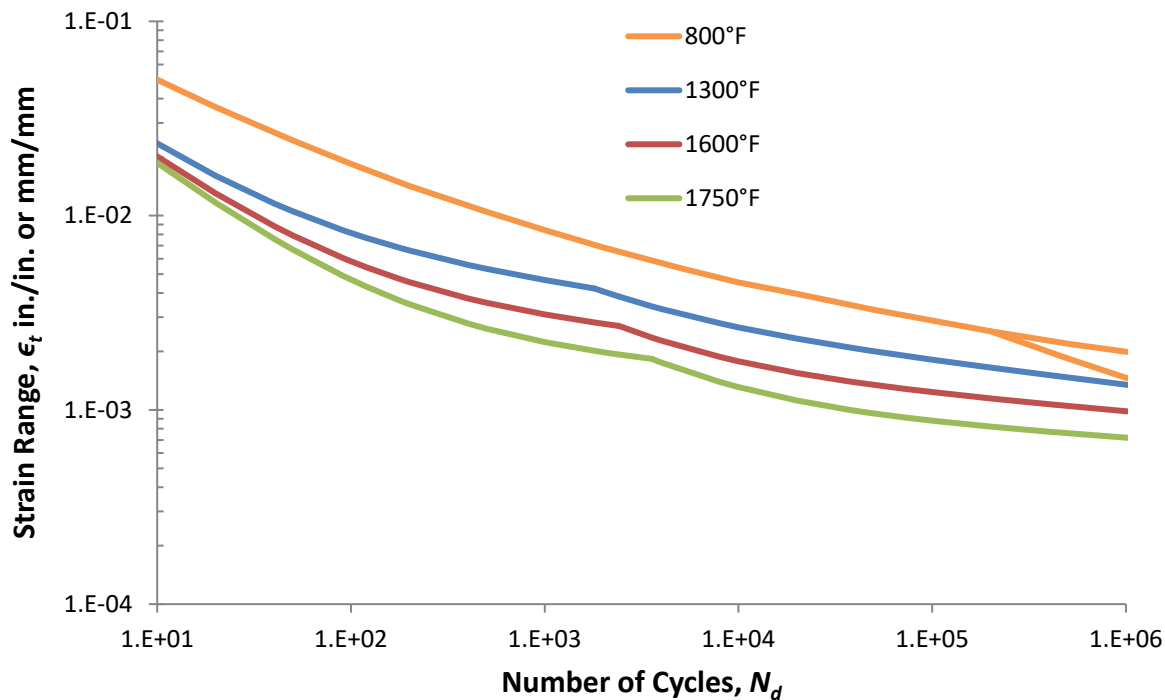
Figure 14. Comparison of elevated temperature design curves to Division 5 (temperatures not exceeding 425°C or 800°F) to proposed design curve I-9.5 for Alloy 617.

References

[1] S. Yukawa, "Elevated Temperature Fatigue Design Curves for Ni-Cr-Co-Mo Alloy 617," *1st JSME/ASME Joint International Conference on Nuclear Engineering, Tokyo, Japan, 1991.*

[2] J. P. Strizak, C. R. Brinkman, M. K. Booker, and P. L. Rittenhouse (Oak Ridge National Laboratory), "The Influence of Temperature, Environment, and Thermal Aging on the Continuous Cycle Fatigue Behavior of Hastelloy X and Inconel 617," ORNL/TH-8130, April 1982.

[3] J. L. Kase (General Atomics Co.), "Low Cycle Fatigue Data for Inconel 617," Document No. 904668, March 1980.

[4] H. P. Meurer, H. Breitling, and E. D. Grosser, "Low Cycle Fatigue Behavior of High Temperature Alloys in HTR-Helium," *Behavior of High Temperature Alloys in Aggressive Environments*, London: The Metals Society, 1980, pp. 1005-1015.

[5] Project Staff (General Electric Co.), "Advanced Gas Cooled Nuclear Reactor Materials Evaluation and Development Program," Final Report for Period Sept. 1976 to Sept. 1982, Report DOE-ET-34202-80, May 15, 1983.

[6] M. Kitagawa, J. Hamanaka, T. Umeda, T. Goto, Y. Saiga, M. Ohnami, and T. Udoguchi, "A New Design Code for 1.5 MWt Helium Heat Exchanger," in *Proceedings of the 5th International Conference on Structural Mechanics in Reactor Technology, Berlin, Germany*, Vol. F, 1979.

[7] H. Hattori, M. Kitagawa, and A. Ohtomo, "Effect of Grain Size on High Temperature Low-Cycle Fatigue Properties of Inconel 617," (in Japanese) *Transactions of the Iron and Steel Institute of Japan*, Vol. 68, No. 16, Dec. 1982, pp. 121-130.

[8] J. K. Wright, L. J. Carroll, J. A. Simpson, and R. N. Wright, "Low Cycle Fatigue of Alloy 617 at 850 and 950°C," *Journal of Engineering Materials and Technology*, Vol. 135, July 2013.

[9] J. K. Wright, L. J. Carroll, C. Cabet, T. M. Lillo, J. K. Benz, J. A. Simpson, W. R. Lloyd, J. A. Chapman, and R. N. Wright, "Characterization of elevated temperature properties of heat exchanger and steam generator alloys," *Nuclear Engineering Design*, Vol. 251, 2012, pp. 252–260.

[10] Standard Test Method for Strain–Controlled Fatigue Testing, ASTM E606/E606M-12, ASTM International, West Conshohocken, PA.

[11] Jones and O'Donnell, "Recommended Test Procedure for Fatigue Testing of Metallic Materials Below the Creep Range, Revision 4" Prepared by Subgroup on Fatigue Strength, ASME Boiler and Pressure Vessel Committee.

[12] T. Totemeier and Tian H., "Creep-Fatigue-Environment Interactions in Inconel 617," *Materials Science and Engineering A,* Vol. 468-470, 2007, p. 81-87.

[13] T. C. Totemeier, "High-Temperature Creep-Fatigue of Alloy 617 Base Metal and Weldments", *Proceedings of CREEP8, Eighth International Conference on Creep and Fatigue at Elevated Temperatures, San Antonio, TX, July 22-26, 2007.*

[14] K.B.S. Rao, H.P. Meurer and H. Schuster, "Creep-fatigue interaction of Inconel 617 at 950ºC in simulated nuclear reactor helium," *Materials Science and Engineering A,* Vol. 104, 1988, pp. 37-51.

[15] K.B.S. Rao, H. Schiffers, H. Schuster and H. Nickel, "Influence of Time and Temperature Dependent Processes on Strain Controlled Low Cycle Fatigue Behavior of Alloy 617," *Metallurgical Transactions A,* Vol. 19A, 1988, pp. 359-371.

[16] INCONEL® Alloy 617 Datasheet, Special Metals Corp., Publication No. SMC-029 Huntington, WV, 2005.

[17] S. S. Manson, Thermal Stress and Low Cycle Fatigue, McGraw-Hill, 1966, pp. 165-170.

[18] B. F. Langer, "Design of Pressure Vessels for Low-Cycle Fatigue," *Journal of Basic Engineering*, September 1962, pp. 389-402.

[19] J. K. Wright, L. J. Carroll, T.-L. Sham, N. J. Lybeck and R. N. Wright, "Determination of the Creep-fatigue Interaction Diagram for Alloy 617," *Proceedings of the ASME 2016 Pressure Vessels and Piping Conference PVP2016*, Vancouver, British Columbia, Canada, July 17-21, 2016.

Appendix I

Tabulated Elevated Temperature Fatigue Data Reproduced from Yukawa

Source in Yukawa*	Temp (°C)	Temp (°F)	Total Strain Range (%)	N_f, Cycles to Failure	Elastic Strain Range (%)	Plastic Strain Range (%)
2	538	1000	3.60	60	0.83	2.77
2	538	1000	2.73	181	0.79	1.94
2	538	1000	1.93	316	0.73	1.20
2	538	1000	1.42	498	0.71	0.71
2	538	1000	1.07	2357	0.59	0.48
2	538	1000	1.00	2009	0.53	0.47
2	538	1000	0.69	4672	0.51	0.18
2	538	1000	0.52	11520	0.47	0.05
2	538	1000	0.50	10929	0.37	0.13
2	538	1000	0.43	41180	0.41	0.02
2	704	1300	3.64	63	0.83	2.81
2	704	1300	2.81	116	0.80	2.01
2	704	1300	1.74	216	0.70	1.04
2	704	1300	1.47	441	0.69	0.78
2	704	1300	0.88	886	0.58	0.30
2	704	1300	0.66	2600	0.54	0.12
2	704	1300	0.50	15142	0.45	0.05
3,4	704	1300	1.00	724	0.63	0.37
3,4	704	1300	0.70	1905	0.56	0.14
3,4	704	1300	0.50	5283	0.44	0.06
3,4	704	1300	0.40	29550	0.37	0.03
3,4	704	1300	0.36	232901	0.37	0.00
3,4	704	1300	0.30		0.29	0.01
5	750	1382	1.50	155		
5	750	1382	1.50	190		
5	750	1382	1.00	430		
5	750	1382	0.60	1900		
5	750	1382	0.30	100000		
3,4	760	1400	0.70	891	0.34	0.36
3,4	760	1400	0.50	1963	0.30	0.20
3,4	760	1400	0.40	4240	0.28	0.12
3,4	760	1400	0.30	65551	0.25	0.05
3,4	760	1400	0.28	98615	0.23	0.05
3,4	815	1500	0.70	1220	0.33	0.37
3,4	815	1500	0.50	2006	0.32	0.18
3,4	815	1500	0.37	6431	0.28	0.09
3,4	815	1500	0.30	19024	0.27	0.03
3,4	815	1500	0.24	107784	0.23	0.01
3,4	815	1500	0.22	551352	0.21	0.01
5	850	1562	1.50	140		
5	850	1562	1.00	300		
5	850	1562	1.00	340		
5	850	1562	0.60	750		
5	850	1562	0.60	1020		
5	850	1562	0.30	31000		
5	850	1562	0.30	43000		
6	850	1562	0.70	1250	0.33	0.37
6	850	1562	0.40	3685	0.38	0.02
6	850	1562	0.30	734000	0.28	0.02
2	871	1600	3.62	75	0.49	3.13
2	871	1600	2.76	135	0.50	2.26
2	871	1600	1.80	207	0.45	1.35
2	871	1600	1.42	370	0.45	0.97
2	871	1600	0.92	753	0.38	0.54
2	871	1600	0.81	935	0.39	0.42

Source in Yukawa*	Temp (°C)	Temp (°F)	Total Strain Range (%)	N_f, Cycles to Failure	Elastic Strain Range (%)	Plastic Strain Range (%)
2	871	1600	0.67	1216	0.37	0.30
2	871	1600	0.60	1608	0.35	0.25
2	871	1600	0.51	2304	0.32	0.19
2	871	1600	0.42	2715	0.32	0.10
2	871	1600	0.42	5700	0.30	0.12
3,4	927	1700	0.51	1600	0.27	0.24
3,4	927	1700	0.41	2600	0.25	0.16
3,4	927	1700	0.30	4424	0.23	0.07
3,4	927	1700	0.24	12246	0.23	0.02
3,4	927	1700	0.19	93198	0.19	0.001
3,4	927	1700	0.16	740713	0.16	0.001
5	950	1742	1.00	260		
5	950	1742	0.60	500		
5	950	1742	0.60	680		
5	950	1742	0.30	8500		
7	1000	1832	2.20	180		
7	1000	1832	2.10	190		
7	1000	1832	1.50	350		
7	1000	1832	0.70	650		
7	1000	1832	0.40	2800		
7	1000	1832	0.20	8000		
8	1000	1832	2.00	300		
8	1000	1832	1.00	950		
8	1000	1832	0.62	3600		
8	1000	1832	0.42	8000		
8	1000	1832	2.00	200		
8	1000	1832	1.00	625		
8	1000	1832	0.62	2000		
8	1000	1832	0.42	4000		
8	1000	1832	2.00	170		
8	1000	1832	1.00	450		
8	1000	1832	0.62	1000		
8	1000	1832	0.42	2200		

*Source is the reference number from S. Yukawa, "Elevated Temperature Fatigue Design Curves for Ni-Cr-Co-Mo Alloy 617," *1st JSME/ASME Joint International Conference on Nuclear Engineering, Tokyo, Japan, 1991*.

2. J. P. Strizak, C. R. Brinkman, M. K. Booker, and P. L. Rittenhouse (Oak Ridge National Laboratory), "The Influence of Temperature, Environment, and Thermal Aging on the Continuous Cycle Fatigue Behavior of Hastelloy X and Inconel 617," ORNL/TH-8130, April 1982.

3. J. L. Kase (General Atomics Co.), "Low Cycle Fatigue Data for Inconel 617," Document No. 904668, March 1980.

4. J. L. Kase (General Atomics Co.), private communication to T. K. Odegaard (General Electric Co.), June 2 and 7, 1983.

5. H. P. Meurer, H. Breitling, and E. D. Grosser, "Low Cycle Fatigue Behavior of High Temperature Alloys in HTR-Helium," *Behavior of High Temperature Alloys in Aggressive Environments*, London: The Metals Society, 1980, pp. 1005-1015.

6. Project Staff (General Electric Co.), "Advanced Gas Cooled Nuclear Reactor Materials Evaluation and Development Program," Final Report for Period Sept. 1976 to Sept. 1982, Report DOE-ET-34202-80, May 15, 1983.

7. M. Kitagawa, J. Hamanaka, T. Umeda, T. Goto, Y. Saiga, M. Ohnami, and T. Udoguchi, "A New Design Code for 1.5 MWt Helium Heat Exchanger," in *Proceedings of the 5th International Conference on Structural Mechanics in Reactor Technology, Berlin, Germany*, Vol. F, 1979.

8. H. Hattori, M. Kitagawa, and A. Ohtomo, "Effect of Grain Size on High Temperature Low-Cycle Fatigue Properties of Inconel 617," (in Japanese) *Transactions of the Iron and Steel Institute of Japan*, Vol. 68, No. 16, Dec. 1982, pp. 121-130.

Appendix II

Tabulated Elevated Temperature Fatigue Data from Idaho National Laboratory

Specimen ID	Temp (°C)	Temp (°F)	Strain Rate (s⁻¹)	Nominal Total Strain Range (%)	N_f, Cycles to Failure	Mid Cycle Elastic Strain Range (%)	Mid Cycle Inelastic Strain Range (%)
43-6	850	1562	1E-03	0.30	10495	0.26	0.039
43-13	850	1562	1E-03	0.30	8904	0.25	0.051
43-22	850	1562	1E-03	0.30	10631	0.26	0.037
4-1-1	850	1562	1E-03	0.40	3462	0.27	0.127
416-15	850	1562	1E-03	0.40	4800	0.28	0.116
416-20	850	1562	1E-03	0.40	5100	0.27	0.129
416-3	850	1562	1E-03	0.60	1993	0.30**	0.396
416-4	850	1562	1E-03	0.60	1939	0.30	0.301
416-5	850	1562	1E-03	0.60	1475	0.28	0.323
416-8	850	1562	1E-03	0.60	1785	0.30	0.298
416-7	850	1562	1E-03	1.00	821*	0.36	0.636
416-9	850	1562	1E-03	1.00	850	0.34	0.660
416-22	850	1562	1E-03	1.00	813*	0.31	0.694
416-10	850	1562	1E-03	2.00	323	0.38	1.622
416-11	850	1562	1E-03	2.00	303	0.37	1.626
416-21	850	1562	1E-03	2.00	209	0.35	1.652
416-12	850	1562	1E-03	3.00	132*	0.40	2.601
416-14	850	1562	1E-03	3.00	150	0.41	2.586
416-19	850	1562	1E-03	3.00	136*	0.39	2.606
43-10	950	1742	1E-03	0.20	89700	0.19	0.013
E-22	950	1742	1E-03	0.25	16970	0.20	0.051
315-16	950	1742	1E-03	0.30	8333	0.23	0.075
A-20	950	1742	1E-03	0.30	9641*	0.20	0.096
B-1	950	1742	1E-03	0.30	5867*	0.19	0.105
B-3	950	1742	1E-03	0.30	9054*	0.22	0.079
F-12	950	1742	1E-03	0.30	7133	0.21	0.086
43-5	950	1742	1E-03	0.40	3168	0.21	0.189
43-9	950	1742	1E-03	0.40	2932	0.22	0.184
43-16	950	1742	1E-03	0.40	2769	0.21	0.186
43-20	950	1742	1E-03	0.40	2995	0.21	0.189
B-13	950	1742	1E-03	0.60	1722	0.18	0.424
B-14	950	1742	1E-03	0.60	1390	0.17	0.432
B-15	950	1742	1E-03	0.60	1480	0.17	0.432
315-1	950	1742	1E-03	1.00	963	0.21	0.791
E-11	950	1742	1E-03	1.00	972	0.19	0.812
E-12	950	1742	1E-03	1.00	916	0.18	0.816
E-13	950	1742	1E-03	1.00	897*	0.18	0.816
E-28	950	1742	1E-03	2.00	362	0.22	1.779
J-1	950	1742	1E-03	2.00	371	0.21	1.785
J-5	950	1742	1E-03	2.00	393	0.22	1.784
43-3	950	1742	1E-04	1.00	715	0.17	0.831
43-8	950	1742	1E-04	1.00	710*	0.16	0.836
J-2	950	1742	1E-04	2.00	290	0.16	1.843
J-4	950	1742	1E-04	2.00	355	0.15	1.855
J-6	950	1742	1E-04	2.00	327	0.15	1.849

* Test stopped before 20% reduction in stress ratio. N_f given is last cycle of test.

**This value was adjusted because the actual total strain range for the mid cycle was 0.70

Page intentionally left blank

Appendix III

Tabulated Fatigue Data from Idaho National Laboratory for Comparison to Design Fatigue Curve I-9.5

Specimen ID	Temp (°C)	Temp (°F)	Strain Rate (s⁻¹)	Nominal Total Strain Range (%)	Measured Total Strain Range (%)	N_f, Cycles to Failure	$S_a=0.5(\Delta\varepsilon_t)E$† (MPa)	Mid Cycle Maximum Stress (MPa)
4-2-24	427	800	1E-03	0.29	0.29	15529632	277.88	297.4
4-2-14	427	800	1E-03	0.30	0.22	11475111*	214.50	–
4-2-19	427	800	1E-03	0.36	0.28	8052622*	273.98	–
K-23	427	800	1E-03	0.40	0.33	379500	319.80	335.2
K-27	427	800	1E-03	0.42	0.35	620000	337.35	355.1
4-2-21	427	800	1E-03	0.42	0.41	113600	402.68	393.5
K-25	427	800	1E-03	0.43	0.36	371000	349.05	350.6
K-28	427	800	1E-03	0.44	0.37	108000	362.70	355.4
K-24	427	800	1E-03	0.45	0.38	92536	372.45	358.4
J-28	427	800	1E-03	0.50	0.47	23527	461.18	353.5
K-21	427	800	1E-03	0.50	0.44	46494	426.08	370.7
K-22	427	800	1E-03	0.50	0.44	36200	430.95	366.8
4-2-20	427	800	1E-03	0.50	0.48	35637	468.00	367.2
4-2-22	427	800	1E-03	0.60	0.59	13351	571.35	423.4
4_2_12	427	800	1E-03	0.80	0.79	9087	771.23	462.1
K-19	427	800	1E-03	0.80	0.76	8709	742.95	460.1
4-2-15	427	800	1E-03	1.00	0.96	5356	937.95	488.0
4_2_11	427	800	1E-03	1.20	1.20	3294	1170.98	508.3
4_2_10	427	800	1E-03	1.50	1.51	1726	1467.38	547.1
4-2-16	427	800	1E-03	1.70	1.69	1182	1644.83	571.2
4_2_13	427	800	1E-03	2.00	2.02	516	1969.50	594.2
4-2-18	RT	RT	1E-03	0.42	0.36	212401	346.13	329.3
4-2-17	RT	RT	1E-03	0.80	0.80	17989	780.00	436.4

† E = 195E+03 MPa according to Figure I-9.5M

* Test was suspended at this cycle. Specimen did not fail.

Page intentionally left blank

Appendix IV

Maximum Mean Stress Testing from Idaho National Laboratory

Specimen ID	Temp (°C)	Temp (°F)	Strain Rate (s⁻¹)	Nominal Total Strain Range (%)	Mean Strain (%)	Preload (MPa)	N_f, Cycles to Failure
313b-7	550	1022	1E-03	0.36	0	0	524,319*
313b-8	550	1022	1E-03	0.36	3.365	278	223,626**
313b-9	550	1022	1E-03	0.48	0	0	37,700
48-1	550	1022	1E-03	0.48	3.257	260	28,884**

* Test was suspended at this cycle. Specimen did not fail.

** N_f given is last cycle of test.

Page intentionally left blank

Background Document – Record No. 16-1001

Contents

- Abridged Background for Overall Alloy 617 Code Case

Page intentionally left blank

BACKGROUND FOR DRAFT CODE CASE: USE OF ALLOY 617 (UNS N06617) FOR CLASS A ELEVATED TEMPERATURE SERVICE CONSTRUCTION

INTRODUCTION

The ASME Task Group on Alloy 617 Qualification is requesting an ASME Boiler and Pressure Vessel, Section III, Division 5 Code Case for Alloy 617 (UNS N06617) 52Ni-22Cr-13Co-9Mo to allow construction of components conforming to the requirements of Section III, Division 5, Subsection HB, Subpart B "Elevated Temperature Service" for service when Service Loading temperatures exceed the temperature limits established in Subsection HA, Subpart A.

Labeling in this document follows that of corresponding labeled paragraphs of the Alloy 617 Code Case. Labeling also follows that of Section III, Division 5, Subsection HB, Subpart B "Elevated Temperature Service" except where additional or new requirements have resulted in new numbered paragraphs of the Code Case. Values for mechanical and physical properties have been determined for Alloy 617 and are detailed in this technical justification, following the numbering of Section II, Part D.

The background information provided herein supporting Record No. 16-1001 is a summary of more detailed information provided for the specific topic of interest under its own record number.

ARTICLE HBB-2000
MATERIAL

HBB-2100

HBB-2160   DETERIORATION OF MATERIAL IN SERVICE

The language with respect to the currently allowed Code materials has been carried over into this section of the Code Case. Note that the proposed aging factor for Alloy 617 is 1.0 which means that the effects of thermal aging do not significantly impact its yield and ultimate strength, and time independent allowable stress values.

Detailed background documentation and the data package can be found in RC-16-994.

ARTICLE HBB-3000
DESIGN

HBB-3200   DESIGN BY ANALYSIS

HBB-3210   DESIGN CRITERIA

HBB-3212 *(d)*   Basis for Determining Stress, Strain, and Deformation Quantities, and
HBB-3214   Stress Analysis
   HBB-3214.2   Inelastic Analysis

The use of unified, or viscoplastic constitutive material models appropriately accounts for the lack of independence between plasticity and creep as discussed in Corum and Blass.[1]

HBB-3220   DESIGN RULES AND LIMITS FOR LOAD-CONTROLLED STRESSES IN STRUCTURES OTHER THAN BOLTS

HBB-3225   Level D Service Limits
HBB-3225-1   Tensile Strength Values, S_u

The New Material Data Analysis (NDMA) Excel spreadsheet for time-independent material properties[2] was used to analyze tensile data for T > 525°C. At T ≤ 525°C the current ASME Code values from Section II, Part D, Table U were used as input.

Tensile strength values from the curve fit are only used above 525°C.

Tensile strength values (S_u) from Section II, Part D, Table U for Alloy 617 have been used up to 1000°F (525°C), rather than the curve fit.

Detailed background documentation and the data package can be found in RC-16-994.

HBB-3225-2   Tensile and Yield Strength Reduction Factor Due to Long Time Prior Elevated Temperature Service

ASME Code Section III, Division 5, Subsection HB, Subpart B Table HBB-3225-2 lists tensile and yield strength factors due to long time prior elevated temperature service. Although "long time" is not defined, a reduction factor is required for service at and above a given temperature for the three austenitic materials permitted in Subsection HB, Subpart B.

Room temperature yield and ultimate tensile strengths for Alloy 617 aged at temperatures up to 800°C actually increase slightly after aging in the range of 100 to 10,000 hours. Measurements on material aged at 871°C for times up to 20,000 hours indicate there may be a small decrease in tensile strength. Above 871°C long aging time data are not available, however room temperature tensile properties are essentially unchanged after aging for 100 and 1000 hours at 1000°C. The constant room temperature strengths up to 1000°C and the T-T-T diagram for this material[3] both indicate that it is highly unlikely that a new aging phenomenon is operative at this temperature compared to those at lower temperature. In some cases ductility is decreased after aging, however all specimens had total elongations of at least 20%. Yield and tensile strength measured at the aging temperature are about the same or higher for the aged material for all aging/test temperatures.

It is proposed that the Table HBB-3225-2 values for Alloy 617 be listed as 1.0 for yield strength reduction factor and tensile reduction factor for temperatures ≥800°C (1475°F) up to and including 950°C (1750°F).

Detailed background documentation and the data package can be found in RC-16-994.

ARTICLE HBB-4000
FABRICATION AND INSTALLATION

HBB-4200

HB-4210

HBB-4212   Effects of Forming and Bending Processes

ASME Code Section III, Division 5, Subsection HB, Subpart B allows use of only three austenitic structural materials, Type 304 and 316 stainless steel, and Alloy 800H. Section III, Division 5, does not require a post-fabrication heat treatment for materials that have experienced strains of 5% or less. It is reasonable to assume that the limits on Alloy 617 would be similar to those for Alloy 800H. Cold work

alters the creep rupture behavior of Alloy 617 for strains as low as 5%. For the desired 100,000 hour life for temperatures up to 950ºC, limiting the fabrication strain in components which are given a post-fabrication solution treatment to less than 5% is recommended. This limited amount of allowed cold work allows incidental deformation associated with fit-up and installation without deleterious effect on properties.

For fabrication strains greater than 5%, a post-fabrication solution heat treatment of 1150°C for 20 minutes/25 mm of thickness or 10 minutes, whichever is greater, is currently required in ASME Code Section VIII, Division 1. This requirement is also adopted for this Code Case. This heat treatment will likely recrystallize the material and allow grain growth that is required for creep-rupture resistance.

Detailed background documentation can be found in RC-16-994.

HBB-4800   RELAXATION CRACKING

Relaxation cracking is a mode of delayed intergranular failure defined in Section II, Part D, Appendix A, Subsection A-206. Relaxation cracking in Alloy 617 is usually observed in association with welds or in cold worked material, but is also observed in solution annealed material. It is most prevalent from 550 to 700°C. It occurs after extended periods of exposure (typically on the order of one to two years) in the range where carbide precipitation occurs and/or the ordered γ' (Ni$_3$Al) phase forms. It is recommended that components that will see service between 500 and 780°C be given a heat treatment of three hours at 980°C to eliminate relaxation cracking. This recommendation applies regardless of whether the material is in a welded or solution annealed condition. This heat treatment must be performed after the post-fabrication solution annealing if post-fabrication heat treatment was also required.

Detailed background documentation can be found in RC-16-994.

MANDATORY APPENDIX HBB-I-14
TABLES AND FIGURES

HBB-I-14.1

HBB-I-14.1(a)   PERMISSIBLE BASE MATERIALS FOR STRUCTURES OTHER THAN BOLTING

All of the specifications that are allowed represent wrought and solution annealed material. The properties that have been used in developing this Code Case are representative of this material condition. The solution treatment required by these specifications results in a large grain size (typically greater than 150µm), that contributes to the creep resistance of the alloy. The minimum thickness specified in the note to Table HBB-I-14.1(a) was agreed upon to ensure that a sufficient number of grains were contained through the thickness of the material, and as a consequence that material selected for construction is well represented by the bulk properties used in developing allowable stresses for this Code Case.

Detailed background documentation can be found in RC-16-994.

HBB-I-14.1(b)   PERMISSIBLE WELD MATERIALS

Only one filler material, ERNiCrCoMo-1, is allowed in ASME Code Section IX for gas tungsten arc welding Alloy 617, as called out in specification SFA-5.14.

Detailed background documentation can be found in RC-16-994.

HBB-I-14.2 S_o – MAXIMUM ALLOWABLE STRESS INTENSITY FOR DESIGN CONDITION CALCULATIONS

S_o values correspond to the S values given in ASME Code Section II, Part D, Subpart 1, Table 1B. The SI version of Table 1B only includes values up to 900°C, but additional values are given in Note G29 that were used to interpolate the values for 925 and 950°C.

Detailed background documentation can be found in RC-16-994.

HBB-I-14.3 S_{mt} – ALLOWABLE STRESS INTENSITY VALUES

S_{mt}, the allowable limit of general primary membrane stress intensity is the lower of two stress intensity values, S_m (time-independent) and S_t (time-dependent).

At each temperature, S_m is the lowest of the stress intensity values obtained from the time–independent strength criteria given in ASME Code Section II, Part D, Table 2-100(a).

S_t is presented in detail in Section HBB-I-14.4.

Detailed background documentation can be found in RC-16-994.

HBB-I-14.4 S_t – ALLOWABLE STRESS INTENSITY VALUES (TIME-DEPENDENT)

S_t is defined as the lesser of three quantities: 100% of the average stress required to obtain a total (elastic, plastic, primary and secondary creep) strain of 1%, 67% of the minimum stress to cause rupture, and 80% of the minimum stress to cause the initiation of tertiary creep. This is achieved by using the Larson-Miller plots to all acceptable creep data. A spreadsheet developed for ASME for the analysis of time-dependent materials properties[4] was used to generate the L-M plots.

Time to 1% Strain

The strain to 1% criterion is used to limit the overall deformation of a component.

A Larson-Miller plot was created using time to 1% total strain measured during creep tests and used to determine stress at 1% strain. The stress at 1% plastic + elastic strain must be obtained from the hot tensile curves. The average hot tensile curves are plotted along with isochronous stress-strain curves in Section NBB-T-1800 of this Code Case. The total stress at a strain of 1% will be the minimum of the elastic/plastic stress from the hot tensile curves and the stress from the 1% Larson-Miller plot for a given temperature.

Time to Onset of Tertiary Creep

ASME adopted the tertiary creep criterion after it was observed experimentally that internally-pressurized tubes of austenitic stainless steel leaked due to creep damage at times less than those predicted using analysis based on uniaxial rupture data. In the absence of extensive experimental tube failure data over a range of relevant temperatures, this criterion was developed based on the logic that the onset of tertiary creep during uniaxial testing of austenitic stainless steels is associated with extensive creep induced cavitation. Eliminating tertiary creep, and the associated cavitation, was presumed to represent a conservative indirect limit to minimize the potential for premature failure of tubes under multi-axial loading. For many temperatures and stresses, Alloy 617 exhibits extensive tertiary creep prior to rupture, without evidence of measurable cavitation. This has raised questions regarding the validity of the tertiary creep criterion for the S_t value for Alloy 617 as well as some other alloys that exhibit similar creep behavior. S_t would be increased over a wide range of time and temperatures by eliminating the tertiary creep criterion.

A Larson-Miller plot was also created using time to onset of tertiary creep for creep tests where it is available or can be reasonably determined. The recommended method of determining the onset of tertiary creep uses a 0.2% strain offset from the minimum creep rate, and was used where possible. If a tabulated value was reported, it was included even if it was not offset, as these values are more conservative than the offset values. The minimum stress is needed rather than the average, defined as a line displaced 1.65 standard error of estimate (*SEE*) in log time from the average curve; 80% of this minimum stress is used for the tertiary creep criterion.

Stress-Rupture

The strain to rupture criterion is used to limit the failure of a component. The calculation of minimum stress to rupture, S_r, is discussed in Section HBB-I-14.6. The stress-rupture criterion is defined as 67% of S_r.

Determining S_t

To determine S_t the minimum of the three criteria is determined for each time/temperature combination. While the tertiary creep criterion governs the creep behavior in most cases; the 1% total strain criterion is governing when the behavior is primarily plastic (little or no creep).

Detailed background documentation and the data package can be found in RC-16-994.

HBB-I-14.5 S_y – YIELD STRENGTH VALUES

The NDMA Excel spreadsheet for time-independent material properties[2] was used to analyze yield strength data for T > 525°C. At T ≤ 525°C the ASME Code values from Section II, Part D, Table Y-1 were used as input.

Yield strength values from the curve fit are only used above 525°C.

Yield strength values (S_y) from Section II, Part D, Table Y-1 for Alloy 617 have been used up to 1000°F (525°C), rather than the curve fit.

Detailed background documentation and the data package can be found in RC-16-994.

HBB-I-14.6 S_r – MINIMUM STRESS-TO-RUPTURE

A spreadsheet developed for ASME for the analysis of time-dependent materials properties[4] was used to generate a Larson-Miller stress to rupture plot.

In order to produce the S_r table required for the Code Case, the *LMP* is calculated for each time and temperature increment. The minimum stress is needed which is determined by creating a line that is displaced 1.65 standard error of estimate (*SEE*) in log time from the average stress-to-rupture curve.

The S_r value calculated from the *LMP* can exceed the ultimate strength of the material, which is not physically possible, so an upper bound on the S_r that is controlled by the tensile strength, S_u. At temperatures above room temperature, values of S_u tend toward and average or expected value. Since S_r is the minimum stress to rupture, the upper bound has been set at $S_u/1.1$ to represent a minimum tensile stress (although not in a statistical sense). S_u can be found for Alloy 617 in Table U of ASME Code Section II, Part D up to 525°C. Higher temperature values for materials approved for use in elevated temperature nuclear applications appear in Table NBB-3225-1 of the Alloy 617 Code Case.

Detailed background documentation and the data package can be found in RC-16-994.

HBB-I-14.10   STRESS RUPTURE FACTORS FOR WELDED ALLOY 617

The weldment stress reduction factor, SRF, is defined as Stress$_{weld}$/Stress$_{base}$, where Stress$_{weld}$ is the applied stress which causes creep rupture in time t, and Stress$_{base}$ is the rupture stress of base metal in

the same time and at the same temperature. An average base metal rupture stress is calculated for the time to rupture of the weldment using the Larson–Miller relation for Alloy 617 creep-rupture data from Section HBB-I-14.6. The result is one data point for the SRF of each weldment creep test.

A factor of 1 adequately described the experimentally determined behavior for GTAW weldments up to 850°C. At a temperature of 850° and above, a factor of 0.85 is a more conservative representation of the experimental data.

Detailed background documentation and the data package can be found in RC-16-994.

HBB-I-14.11   PERMISSIBLE MATERIALS FOR BOLTING

No bolting is permitted for Alloy 617.

NONMANDATORY APPENDIX HBB-T
RULES FOR STRAIN, DEFORMATION, AND FATIGUE LIMITS AT ELEVATED TEMPERATURES

HBB-T-1300   DEFORMATION AND STRAIN LIMITS FOR STRUCTURAL INTEGRITY

HBB-T-1320   SATISFACTION OF STRAIN LIMITS USING ELASTIC ANALYSIS

HBB-T-1321   General Requirements

(e) The restriction on applicability of HBB-T-1321, -1322 and -1323 to 1200°F (650°C) and below is based on a paper by Corum and Blass[1] which deemed that the rules based on the results of elastic analysis were not applicable to Alloy 617 above 1200°F due to the difficulty in defining a yield strength and separating plasticity and creep at higher temperatures.

HBB-T-1323   Test No. A-2

The temperature at which $S_m = S_t$ at 100,000 hours is 588.7°C at 145 MPa, where S_m and S_t. are determined as described in Sections HBB-I-14.3 and HBB-I-14.4, respectively.

Detailed background documentation can be found in RC 16-998.

HBB-T-1324   Test No. A-3

Included in the rules for elastic analysis evaluation of primary plus secondary stresses are criteria for the use of the rules of Subsection NB when creep effects are not significant. The conceptual basis for this approach is to approximate the creep damage and deformation that would occur at the nominal flow stress of the material without accounting for stress relaxation. One of the criteria for the time−temperature regime of applicability of this approach is defined by insuring that a stress equal to a factor, *s*, times the minimum yield strength results in a creep damage fraction, adjusted with the factor, *r*, that doesn't exceed 0.1. The *r* factor is intended to account for the potential degradation of creep rupture strength due to strain cycling in strain softening materials such as Grade 91. The *s* factor accounts for the difference between nominal yield and the tabulated yield, S_y, taken as a factor of 1.25, and also for the effects of strain hardening (or softening), taken as 1.2 if the material does not strain soften. Alloy 617 does not strain soften so the *s* factor is 1.5, the product of 1.25 and 1.2, and the *r* factor is 1.0.

Detailed background documentation can be found in RC 16-998.

HBB-T-1330   SATISFACTION OF STRAIN LIMITS USING SIMPLIFIED INELASTIC ANALYSIS

HBB-T-1331*(i)*   **General Requirements,**
HBB-T-1332*(e)*   **Test Nos. B-1 and B-2, and**
HBB-T-1333*(d)*   **Test No. B-3**

The restriction on applicability of these subparagraphs to 1200°F (650°C) and below is based on a paper by Corum and Blass[1] which deemed that the rules based on the results of elastic analysis were not applicable to Alloy 617 above 1200°F due to the difficulty in defining a yield strength and separating plasticity and creep at higher temperatures.

HBB-T-1340   SATISFACTION OF STRAIN LIMITS USING ELASTIC-PERFECTLY PLASTIC ANALYSIS

High temperature design methods employ a group of simplified analysis methods whose objective is to show compliance with code criteria for allowable stress, strain and creep-fatigue limits. "Simplified methods" refers to analysis methods that do not require the use of comprehensive full inelastic constitutive equations. An advantage of Elastic-perfectly plastic (EPP) simplified analysis methods is that they have been shown to demonstrate compliance with code strain and creep-fatigue limits without the use of stress classification procedures.

Consider the application of EPP methods to address cyclic loading. The use of EPP methods for assessment of strain limits and creep-fatigue has been justified by detailed proofs and by intuitive arguments. These proofs have been supplemented with experimental data, inelastic analyses and example problems. The application of the EPP methodology to 304H and 316H stainless steel in Code Cases N-861 for strain limits is the same as currently proposed for Alloy 617.

The detailed proofs are based on consideration of the work and energy dissipation rates over and throughout the volume of the structure as augmented by the observation that decreasing the yield stress for a given bounding solution will not reduce the deformation. The latter point provides the bridge between time independent cyclic plastic analyses and full visco-plastic behavior. Thus, a viable rapid cyclic solution, where "rapid cycle" describes the case with no consideration of stress relaxation during the cycle, represents an acceptable design. The rapid cycle solution is that determined from the EPP analysis with the associated yield stress identified as the "pseudo yield stress". The pseudo yield stress is that for which the EPP analysis must demonstrate shakedown to ensure compliance throughout the structure with the selected limit.

The strain limits are, thus, guaranteed by a ratcheting analysis with the pseudo yield stress defined by the stress to cause the target inelastic strain in a selected time. It may be shown, for example, that if an EPP cyclic analysis with a material pseudo yield stress defined by x% inelastic strain in 300,000 hours does not give ratcheting, then the steady cyclic strain accumulation in 300,000 hours will be less than x%. However, there is the potential for additional straining due to redistribution effects from elastic follow-up, redundancy etc. that are required to set up the steady cyclic state. This additional strain is represented by the plastic strain, p%, from the shakedown analysis using the pseudo yield strength based on x%. Thus, it is required that the analysis plastic strain p% at one point anywhere in every cross-section satisfies x% + p% ≤ 1%. This guarantees a continuous core with not more than 1% accumulated inelastic strain. There are similar requirements for all points in the structure and for welds for their respective limits.

Also included in the rules based on EPP analysis is new guidance on evaluation of Service level C conditions. Because Level C events are not expected, are limited in number, and require shutdown and inspection for damage and repair, Level C events are permitted to be evaluated separately and not combined with Levels A and B as is the current requirement.

More detailed background information may be obtained in RC No's. 16-999 and 14-1445

HBB-T-1400   CREEP‑FATIGUE EVALUATION

HBB-T-1410   GENERAL REQUIREMENTS

HBB-T-1411 Huddleston Parameter for Multiaxial Creep Failure Criterion

A multiaxial failure criterion for creep rupture has been developed by Huddleston which offers significant improvements in predicting creep rupture under multiaxial (three-dimensional) stress states over classical models such as von Mises or Tresca. The equation used to determine the equivalent stress for the inelastic analysis approach used to satisfy deformation-controlled limits in HBB-T-1411 includes a constant, C, which is based on Huddleston's approach. Using the symbols from HBB-T-1411, the equivalent stress for the Huddleston theory is

$$\sigma_e = \bar{\sigma} \exp\left[C\left(\frac{J_1}{S_s} - 1\right)\right] \tag{1}$$

where J_1 is the first invariant of the stress tensor, S_s is an invariant stress parameter, and $\bar{\sigma}$ is the von Mises equivalent stress.

In Subarticle HBB-T-1411, a value of 0.24 has been accepted for the Huddleston constant for Types 304 and 316 stainless steels, and 0 is used for alloy 800H. When C=0, the effective stress is equivalent to the von Mises effective stress. As C increases, there is a larger difference between the equivalent stress under tension vs. compression.

A "universal" value of C=0.24 has been recommended for austenitic stainless steels and Inconel if other specific data are not available.[1] When C=0.24 is used for 316 or 304, the predictions of rupture life are more accurate and also less overly-conservative. Specific analyses have yielded values of 0.29 for Type 304 SS,[1] 0.19 for Type 316 SS,[2] and 0.25 for Inconel 600.[3]

Inconel (Alloy 600) is a very similar Ni based solid solution alloy to Alloy 617. Huddleston recommends austenitic stainless steels and Inconel 600 use C=0.24 if alloy specific data are not available. This value is also supported by calculation of C for a single compression hold creep-fatigue test indicating $C = 0.25$. Therefore, a value of C=0.24 is recommended for Alloy 617, which is consistent with the other austenitic alloys in Section III Division 5.

More detailed information may be obtained in RC 16-997

HBB-T-1411*(d)* Damage Equation

A value of $C = 0.24$ is recommended for Alloy 617, which is consistent with the other austenitic alloys in Section III Division 5. Multiaxial creep rupture data for Inconel 600 supports this value, which is a solid solution nickel based alloy similar to Alloy 617.

HBB-T-1420   LIMITS USING INELASTIC ANALYSIS

HBB-T-1420-1   Design Fatigue Strain Range, ϵ_t, for Alloy 617

Design fatigue curve I-9.5 for nickel-chromium-molybdenum-iron alloys for temperatures not exceeding 425°C/800°F from ASME Code Section III, Mandatory Appendix I is supported by 427°C and room temperature fatigue data and has been approved for Alloy 617.

Elevated temperature fatigue data for Alloy 617 was compiled from numerous sources and presented by Yukawa.[5] Recent fatigue data have been contributed by Idaho National Laboratory (INL)[6] to create the combined the data set.

The elastic and inelastic strain components were independently analyzed and used to fit the fatigue data using

$$\Delta \varepsilon_t = A(N_f)^a + B(N_f)^b \qquad [2]$$

where the first term is inelastic strain and the second term is elastic strain, N_f is the number of cycles to failure, and $A, a, B, b,$ are fitting parameters. The inelastic data were not temperature dependent and a fit to the data set resulted in A and a values of 112.46 and −0.80, respectively. The elastic data were found to cluster into three temperature dependent groups of 1000–1300°F (538–704°C), >1300–1600°F (>704–871°C), and >1600–1750°F (>871–950°C). These temperature ranges will henceforth be referred to and labeled by their maximum Fahrenheit use temperature. The values used for the elastic fitting parameters are given in Table 1.

Table 1. Elastic strain coefficients used to develop design fatigue curves.

T(°F)	B	b
1300°F	1.367	−0.118
1600°F	0.606	−0.082
1750°F	0.234	−0.064

The design fatigue curves are obtained by dividing the stress by a factor of 2 and the cyclic life by a factor of 20 and using the minimum value at each cycle. The design fatigue curves display cusps where the 2 and 20 construction curves meet. The curves are plotted to a maximum of 10^6 allowable cycles, consistent with the other design fatigue curves in HBB-T-1420.

Design fatigue curve I-9.5 includes a maximum mean stress correction. At the highest temperatures, the material is not expected to sustain a significant mean stress because of rapid stress relaxation. To assess the need for a mean stress correction in the temperature range of 1000-1300°F, limited maximum mean stress testing was performed at 1022°F (550°C). The maximum mean stress had only a minor effect on fatigue life and as a result, no maximum mean stress correction is included for the 1300°F design curve.

In order to plot the elevated temperature design fatigue curves with curve I-9.5, the latter must be converted from S_a stress to ϵ_t strain range. This was done by multiplying S_i by 2, to convert stress into stress range, and dividing by 195 GPa, the elastic modulus noted on curve I-9.5M.

Detailed background documentation and the data package can be found in RC-16-1000.

HBB-T-1420-2   Creep-Fatigue Damage Envelope

In the ASME Code, creep-fatigue life is evaluated by a linear summation of fractions of cyclic damage and creep damage. The creep-fatigue criterion is given by:

$$\underbrace{\sum_j \left(\frac{n}{N_d}\right)_j}_{\text{Cyclic Damage}} + \underbrace{\sum_k \left(\frac{\Delta t}{T_d}\right)_k}_{\text{Creep Damage}} \leq D \qquad (3)$$

where n and N_d are the number of cycles of type j and the allowable number of cycles of the same cycle type, respectively; and Δt and T_d are the actual time at stress level k and the allowable time at that stress level, respectively; D is the allowable combined damage fraction. Since the creep damage term is

evaluated as a ratio of the actual time versus the allowable time, it is generally referred to as time-fraction. The cyclic- and creep-damage terms on the left hand side of Equation (10) are evaluated in an uncoupled manner, and the interaction of creep and fatigue is accounted for empirically by the D term on the right side of the equation. This can be represented graphically by the creep-fatigue interaction diagram.

Fatigue Damage Calculations

The fatigue damage fraction, D^t, for a creep-fatigue test is defined in terms of the ratio of the cycle to failure, n, under creep-fatigue condition to the cycle to failure, N_d, under continuous cycling condition for the same product form and heat, and at the same total strain range and temperature, as the creep-fatigue test.

Creep Damage Calculations

The creep damage for the kth creep-fatigue cycle, D_k^c, can be determined by evaluating the integral

$$D_k^c = \int_{hold\ time} \left(\frac{1}{T_d}\right)_k dt$$

(4)

over the hold time of the cycle. To perform the integration, the correlation between the rupture time, temperature, and applied stress for the heat of Alloy 617 under consideration is required. The Larson-Miller relation for creep rupture data used for this purpose is described in detail in Sections HBB-I-14. 6.

The total creep damage accumulated during a creep-fatigue test can then be determined by summing the creep damages calculated for all the cycles. An approximation commonly made is to evaluate the creep damage for one cycle at mid-life, and then multiply this value by the total number of cycles to failure in the creep-fatigue test. The available cycle that is closest to the midlife is selected and the stress relaxation during the strain hold is evaluated for that cycle.

Proposed Creep-Fatigue Interaction Diagram

A point is generated on the creep-fatigue interaction diagram for each creep-fatigue test. The diagram is intended to represent average material behavior. An intersection point for a linear summation of creep and fatigue damage at (0.1, 0.1) is a reasonable representation of Alloy 617 behavior.

Detailed background documentation and the data package can be found in RC-16-998.

HBB-T-1430   LIMITS USING ELASTIC ANALYSIS

HBB-T-1431(e) General Requirements

The restriction on applicability to 1200°F (650°C) and below is based on a paper by Corum and Blass[1] which deemed that the rules based on the results of elastic analysis were not applicable to Alloy 617 above 1200°F due to the difficulty in defining a yield strength and separating plasticity and creep at higher temperatures.

HBB-T-1440   LIMITS USING ELASTIC-PERFECTLY PLASTIC   ANALYSIS – CREEP-FATIGUE DAMAGE

High temperature design methods employ a group of simplified analysis methods whose objective is to show compliance with code criteria for allowable stress, strain and creep-fatigue limits. "Simplified methods" refers to analysis methods that do not require the use of comprehensive full inelastic constitutive equations. An advantage of elastic-perfectly plastic (EPP) simplified analysis methods is that they have been shown to demonstrate compliance with code strain and creep-fatigue limits without the use of stress classification procedures.

Consider the application of EPP methods to address cyclic loading. The use of EPP methods for assessment of strain limits and creep-fatigue has been justified by detailed proofs and by intuitive arguments. These proofs have been supplemented with experimental data, inelastic analyses and example problems. The application of the EPP methodology to 304H and 316H stainless steel in Code Case N-862 for creep fatigue is the same as currently proposed for Alloy 617.

The detailed proofs are based on consideration of the work and energy dissipation rates over and throughout the volume of the structure as augmented by the observation that decreasing the yield stress for a given bounding solution will not reduce the deformation. The latter point provides the bridge between time independent cyclic plastic analyses and full visco-plastic behavior. Thus, a viable rapid cyclic solution, where "rapid cycle" describes the case with no consideration of stress relaxation during the cycle, represents an acceptable design. The rapid cycle solution is that determined from the EPP analysis with the associated yield stress identified as the "pseudo yield stress". The pseudo yield stress is that for which the EPP analysis must demonstrate shakedown to ensure compliance throughout the structure with the selected limit.

The calculation of creep damage in a cyclic creep-fatigue assessment is calculated at a critical point. For this case, the pseudo yield stress is the stress to cause creep damage = 1 in a selected time, as a function of temperature. The EPP analysis looks for shakedown (elastic) behavior to show that cyclic creep damage is less than 1. The selected time may then be used in a time fraction, creep damage calculation. The fatigue damage is based on the total elastic plus inelastic, strain ranges from the elastic shakedown analysis. The combined creep and fatigue damage is then evaluated using the allowable creep-fatigue damage envelope

Also included in the rules based on EPP analysis is new guidance on evaluation of Service level C conditions. Because Level C events are not expected, are limited in number, and require shutdown and inspection for damage and repair, Level C events are permitted to be evaluated separately and not combined with Levels A and B as is the current requirement.

More detailed background information may be obtained in RC No's. 16-998 and 14-1446

HBB-T-1500   BUCKLING AND INSTABILITY

HBB-T-1520   BUCKLING LIMITS

HBB-T-1522   Time-Dependent Buckling

This document provides the background and technical basis supporting the recommended buckling charts for Alloy 617 specified as Figures HBB-T-1522-1, HBB-T-1522-2, and HBB-T-1522-3. Section III, Division 5, HBB-T-1520 presents two options for designing a component against time independent and time dependent buckling. For either time independent or time dependent buckling a designer can perform a full instability analysis, using a factorized load for load-controlled situations. Alternatively, for time independent buckling the designer can use the buckling charts referenced in Section III, Division 1, NB-3133. These buckling charts apply to three simple geometries: a cylinder under axial compression, a sphere under external pressure, and a cylinder under external pressure.

Instead of performing a full instability analysis the designer can skip the time-dependent buckling check if time-independent buckling will occur at a lower load and therefore govern the design. In this case the designer only needs to check for time-independent buckling against the charts referenced in Section III, Division 1, NB-3133. To aid in this task HBB-T-1522 provides three buckling charts. These three charts correspond to the three simple geometries used in NB-3133 (a cylinder under axial compression, a sphere under external pressure, and a cylinder under external pressure). The charts delineate regions where, for these geometries, time independent buckling occurs at a lower load than time

dependent buckling and therefore the designer can safely skip an explicit check for time-dependent, creep buckling.

Conceptually, the lines on the buckling charts are the conditions at which the allowable load for time-dependent creep buckling equals the allowable load for time-independent buckling. A Welding Research Council (WRC) technical report describes the process of constructing this line for the three geometries[a].

The basis of the WRC approach is an analytical solution for the elastic-plastic buckling load of each the three geometries in terms of the tangent and secant moduli of the flow curve. These moduli are functions of the applied load and so solving for the buckling limit load requires solving an implicit nonlinear equation. For time-dependent buckling the report assumes a method of isochronous curves – for time dependent buckling the method uses the same, elastic-plastic solutions but replaces the flow curve with the isochronous curve for the design life of interest. The region where the designer may skip the time-dependent buckling check is where the allowable load for time-dependent buckling, using the isochronous curves, is greater than that for time-independent buckling, using the Code hot tensile curves. At first thought it would seem that the time dependent allowable load will always be less than the allowable load for time dependent buckling as the isochronous curves tend to have lower values of tangent and secant modulus than the hot tensile curves. However, Section III, Division 5 applies a load factor of 3 for time-independent buckling but only 3/2 for time dependent buckling. Therefore, there is a large region where the time-independent allowable load governs.

The implementation of the WRC method was verified by reproducing the current Section III, Division 5 buckling charts for 304H and 316H. Solving the reduced equations numerically, including the simplifying assumptions, produces the buckling charts proposed for Alloy 617 as part of this Code Case.

Detailed background documentation and data will be found in RC-16-996.

HBB-T-1800   ISOCHRONOUS STRESS‑STRAIN RELATIONS

Section III, Division 5, HBB-T-1800 provides average property hot tensile and isochronous stress-strain curves for use with the Nonmandatory Appendix HBB-T design rules for meeting the design limits on deformation controlled quantities. The Code provides isochronous curves covering the entire Section III, Division 5 temperature range for each material. For Alloy 617 this is 800° to 1750° F. This Code Case provides hot tensile and isochronous curves in 50° F increments, matching the practice of the current Code. Table HBB-T-1820-1 summarizes the provided temperature range and temperature increment.

The Division 5 hot tensile curves represent the average experimentally-measured tensile flow curves for the material. The isochronous curves can be read as the average stress to accumulate some amount of total strain over some period of time. The experimental data underlying the design hot tensile curves are a series of elevated temperature tensile tests. The data underlying the isochronous curves are the tensile tests plus elevated temperature creep tests.

In order to provide design information at uniformly spaced, densely packed intervals of temperature, strain, and time the processed used to create the current Code curves first fits a material model to the available tensile and creep data and then uses that model to generate hot tensile and isochronous curves. The Code curves for the current Class A materials[bc] are based on an additive, history-independent decomposition of the total strain into elastic, time-independent plastic, and time-dependent creep parts:

[a] Griffin, D. S. "Design Limits for Elevated-Temperature Buckling." In Welding Research Council Bulletin 443 *External Pressure: Effect of Initial Imperfections and Temperature Limits*, pp. 11-26, 1999.

[b] Blackburn, L. "Isochronous Stress-Strain Curves for Austenitic Stainless Steels." In *The Generation of Isochronous Stress-Strain Curves*, pp. 15-48, 1972.

$$\varepsilon = \varepsilon_e + \varepsilon_p + \varepsilon_c.$$

The hot tensile curves are the outcome of this model when $\varepsilon_c = 0$, i.e. when $t = 0$, whereas the isochronous curves are the output of the model for some fixed, non-zero time.

The elastic strain is calculated using the Section II, temperature dependent values of Young's modulus for Alloy 617

$$\varepsilon_e = \frac{\sigma}{E}.$$

Based on experimentation with different standard plasticity models, the plastic response of Alloy 617 was divided into two regions based on temperature. At low temperatures, below 750° C, the composite model uses a Ramberg-Osgood model for the plastic strain to capture the experimentally-observed smooth transition from elastic to work hardening plastic behavior. Above this temperature the model uses a Voce form to capture a quick transition to a nearly perfectly-plastic response.

Elevated temperature tension tests conducted at Idaho National Laboratory (INL) on a single heat of Alloy 617 plate were used to calibrate the model parameters. Tension tests results are available at 425° C and at 50° C intervals from 450° to 950° C. For most temperatures a single test was used to calibrate the model coefficients. However, at several critical temperatures multiple tests were run to ensure experimental variability did not affect the final model coefficients.

The tension test data shows a marked transition from work hardening behavior below 750° C to a nearly perfectly plastic response a t and above 850° C. This change in behavior coincides with a region of serrated plastic flow and a metallurgical change in the alloy. This phenomenon is described in greater detail below in the section describing the model for creep deformation. The composite model for the plastic strain empirically captures this transition by switching from the Ramberg-Osgood to the Voce flow model.

This leaves the model for the time-dependent creep strain ε_c. Ideally, this model would be calibrated to a wide variety of full, experimentally measured creep curves. However, for Alloy 617 only a limited number of full creep curves are available from INL experiments on the same batch of material used for the elevated temperature tension tests. To supplement these creep curves, this Code Case has collated simplified creep metrics from a variety of data sources. These simplified measures, for example time to 1% creep strain as a function of stress and temperature, have been used to set the time dependent allowable stress S_{mt} .

Division 5 design isochronous curves only provide data out to 2.2% total strain. At most, this represents about 2% creep strain. A very simple creep model is capable of representing the INL creep curves over this limited range of strains. The model for the time-dependent strain adopted here is

$$\varepsilon_c = \dot{\varepsilon}_c(T, \sigma)t$$

where $\dot{\varepsilon}_c$ is some constant, average creep rate, which is a function of temperature and stress. Where full creep curves are available this average creep rate should be taken as the average rate over the first 2% increment of creep strain. The model developed further assumes that this average rate over the first 2% of creep strain is approximately equal to average rate over the first 1% of creep strain. This allows the model to use the time-to-1% data for calibration.

The time-to-1% data was converted to an average rate by dividing 1% creep strain by the time. The full creep curve data was converted to a plot of creep strain rate versus creep strain and averaged over the first 1% to produce a similar mean rate. This process produces a database relating the average creep rate over the first 1% of creep strain to the applied stress and temperature.

[c] Swindeman, R. W. "Construction of isochronous stress-strain curves for 9Cr-1Mo-V steel." *Advances in Life Prediction Methodology* 391, pp. 95-100, 1999.

The Alloy 617 creep model adopts a form developed by Kocks[d] and Mecking[e]. The experimental data was divided into several categories: average creep curve rates from INL experiments for 750°, 750°, and 750° C, the collected average time to 1% rates for $T \leq 750°$ C, and the collected average time to 1% rates for $T > 750°$ C. The Alloy 617 creep data nearly obeys the Kocks-Mecking form. All the data for temperatures greater than 750° C collapse to one line. The data for temperatures less than 750° C falls along a second line that shares the same slope. The only difference between the two temperature regimes is an offset or threshold stress. This implies that at 750° C and below creep strain is proportional to $\sigma - \sigma_{th}$ for some threshold stress σ_{th} rather than the stress σ directly.

The textbook explanation is that the threshold stress represents the magnitude of the stress necessary to overcome dislocation-particle interaction. Once that interaction is overcome the rate controlling mechanism is conventional climb controlled power law creep that represents the characteristics of the matrix containing the precipitates.

In summary, test results at or below about 750°C show a particle strengthening contribution. Tests above that temperature will show solid solution behavior for thermodynamic reasons, i.e., a substantial volume fraction of γ' will not form. Below 750°C, thermodynamics may indicate that γ' should form, but the kinetics may be so slow that we will not observe precipitation effects for laboratory creep test times. This evidence all supports the incorporation of a threshold stress effect in the model for creep rate.

The hot tensile curve at 750°C exhibits rather abrupt yielding compared to those at either higher or lower temperature. Examination of the entire experimental tensile curves shows that this behavior is related to the presence of serrated flow resulting from dynamic strain aging at this temperature. It is typical for many austenitic materials to exhibit dynamic strain aging near this temperature and the phenomena is typically thought to be related to pinning and abrupt unpinning of dislocations from a solute atmosphere. Dynamic strain aging sometimes is related to a reduction in the elongation to failure in a tensile test, however, at the small strains used for the hot tensile curves in this Code Case it is not anticipated that this phenomena is relevant to the material behavior except for altering the shape of the curve at yielding.

Given the models for ε_e, ε_p, and ε_c defined here the hot tensile curves are stress/strain histories for $t = 0$ and increasing values of strain and the isochronous stress-strain curves are stress/strain histories for t fixed to some non-zero value and increasing values of strain.

Detailed background documentation and the data package will be found in RC-16-997.

HBB-T-1820   MATERIALS AND TEMPERATURE LIMITS

The maximum temperature and the temperature increment where the isochronous stress-strain curves are presented graphically are given in Table HBB-T-1820-1.

PHYSICAL PROPERTY TABLES

TE — THERMAL EXPANSION

Thermal expansion, $\Delta l/l_0$, of four heats of Alloy 617 was measured using a Netzsch dilatometer over the temperature range 20 to 1000°C.[7] The values are similar for the four materials, and the data are well represented by a third-order polynomial fit.

---

[d] Kocks, U. F. "Realistic constitutive relations for metal plasticity." *Materials Science and Engineering A* 317, pp. 181-187, 2001.

[e] Estrin, Y. and H. Mecking. "A unified phenomenological description of work hardening and creep based on one-parameter models." *Acta Metallurgica* 32:1, pp. 57-70, 1984.

Mean Coefficient of Thermal Expansion (CTE) values from 20°C (70°F) were calculated from the $\Delta l/l_0$ polynomial fit. The instantaneous CTE was calculated using the derivative of the polynomial fit to the $\Delta l/l_0$ data from 20–1000°C (70–1800°F).

Detailed background documentation and the data package can be found in RC-16-995.

TCD — THERMAL CONDUCTIVITY AND THERMAL DIFFUSIVITY

Thermal diffusivity was measured for the same four Alloy 617 heats noted in Section TE, from 20 to 1000°C using a Netzsch laser flash system.[7] A two-piece third-order polynomial fit is used to describe the experimental data due to a deviation from monotonic behavior in the region of 750°C.

The heat capacity of the four Alloy 617 heats was measured using a Netzsch calorimeter, and the temperature corrected density can be calculated from the ASME Code Section II, Part D Table PRD density and the thermal expansion data. The thermal conductivity is the product of the diffusivity, temperature corrected density, and heat capacity. Like thermal diffusivity, fitting the thermal conductivity required a three piece second-order polynomial.

The heat capacity also exhibits a deviation from monotonic behavior, but over a slightly different temperature range compared to that for the thermal diffusivity. As a result, the temperature range of non-monotonic behavior shown by the thermal conductivity extends over approximately 200°C. The magnitude of the local peak in conductivity is nearly 20% compared to a monotonic curve, and the local peak lies within the temperature range where it is anticipated that Alloy 617 will be used for nuclear heat exchanger design.

Detailed background documentation and the data package can be found in RC-16-995.

TM — MODULUS OF ELASTICITY

Extension of Elastic Modulus Values from Section II, Part D to Higher Temperature

Elastic modulus values for Alloy 617 are currently included in Section II, Part D of the ASME Code (Table TM-4 and TM-4M) for temperatures up to 1500°F (850°C). The temperature range for elastic modulus values must be increased to accommodate the temperature limits of this Code Case and allow use of this alloy for design in high temperature gas-cooled nuclear reactors.

The elastic modulus values currently in Table TM-4 were extrapolated to 1000°C using a third-order polynomial fit to the tabulated values. Experiments[8] on two heats of Alloy 617 were carried out to determine the dynamic elastic modulus as a function of temperature using the resonant frequency in the flexural mode of vibration in order to validate this extrapolation. The experimental results and the extrapolation of Table TM-4 values are in close agreement.

Proposed values are shown in Table TM of this Code Case for the entire temperature range from ambient to 1800°F and 1000°C. Note that the values used up to 1500°C (850°C) are unchanged from current ASME Code Section II, Part D Table TM-4 (TM-4M) values.

Detailed background documentation and the data package can be found in RC-16-995.

REFERENCE

[1] J. M. Corum and J. J. Blass, "Rules for Design of Alloy 617 Nuclear Components to Very High Temperatures," ASME PVP Vol. 215, American Society of Mechanical Engineers, New York, NY, 1991, p.147.

[2] R. W. Swindeman and M. J. Swindeman, *Analysis of Time-Independent Materials Properties Data,* ASME Standards Technology, LLC, 2009.

[3] Q. Wu, H. Song, R. W. Swindeman, J. P. Shingledecker, and V. K. Vasudevan, "Microstructure of Long-Term Aged IN617 Ni-Base Superalloy," *Metallurgical Transactions*, Vol. 39A, 2008, pp. 2569-2585.

[4] R. W. Swindeman and M. J. Swindeman, *Analysis of Time-Dependent Materials Properties Data,* ASME Standards Technology, LLC, 2014.

[5] S. Yukawa, "Elevated Temperature Fatigue Design Curves for Ni-Cr-Co-Mo Alloy 617," *1st JSME/ASME Joint International Conference on Nuclear Engineering, Tokyo, Japan, 1991.*

[6] J. K. Wright, L. J. Carroll, J. A. Simpson, and R. N. Wright, "Low Cycle Fatigue of Alloy 617 at 850 and 950°C," *Journal of Engineering Materials and Technology*, Vol. 135, July 2013.

[7] B. H. Rabin, W. D. Swank and R. N. Wright, "Thermophysical Properties of Alloy 617 from 25 to 1000°C", *Nuclear Engineering and Design Journal,* Vol. 262, 2013, p. 72.

[8] Idaho National Laboratory, Advanced Reactor Technologies program, unpublished research.